THE USE OF HIGH RESOLUTION GEOPHYSICS FOR THE INVESTIGATION OF SUBMERGED PALAEO-GLACIOMARINE ENVIRONMENTS

Justin K. Dix

A Thesis Submitted for the Degree of PhD
at the
University of St Andrews

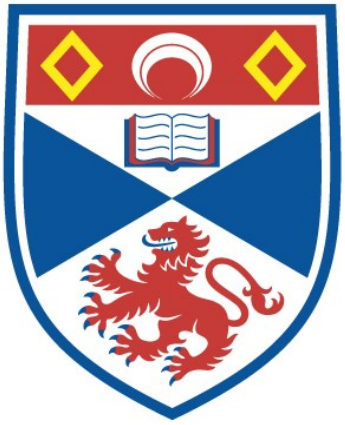

1996

UNIVERSITY OF ST ANDREWS

The Use of High Resolution Geophysics for the Investigation of Submerged Palaeo-glaciomarine Environments

by

Justin K. Dix

Submitted in partial fulfilment for the degree of Doctor of Philosophy
Department of Geology and Geography, Faculty of Science,
University of St. Andrews

Submitted in August 1995

ProQuest LLC.
789 East Eisenhower Parkway
P.O. Box 1346
Ann Arbor, MI 48106 – 1346

(i) I, Justin K. Dix, hereby certify that this thesis, which is approximately 85,000 words in length, has been written by me, that it is the record of work carried out by me and that it has not been submitted in any previous application for a higher degree.

date 31/8/95 signature of candidate .....

(ii) I was admitted as a research student in October 1989 and as a candidate for the degree of Ph.D. in October 1989; the higher study for which this is a record was carried out in the University of St. Andrews between 1989 and 1993.

date 31/8/95 signature of candidate .....

(iii) I hereby certify that the candidate has fulfilled the conditions of the Resolution and Regulations appropriate for the degree of Ph.D. in the University of St.Andrews and that the candidate is qualified to submit this thesis in application for that degree.

date 31.8.95 signature of supervisor .....

In submitting this thesis to the University of St. Andrews I understand that I am giving permission for it to be made available for use in accordance with the regulations of the University Library for the time being in force, subject to any copyright vested in the work not being affected thereby. I also understand that the title and abstract will be published, and that a copy of the work may be made and supplied to any bona fide library or research worker.

date 31/8/95 signature of candidate .....

ABSTRACT

A multi-disciplinary, high resolution, geophysical investigation of a Scottish Sea loch has facilitated both the reconstruction of a detailed late Quaternary para-stratigraphic model and the critical assessment of the acquisition and analytical methodologies most appropriate for the study of submerged palaeo-glaciomarine environments. Loch Ainort, situated on the eastern coast of the Isle of Skye, has been surveyed using a 192 kHz echosounder, a 400 kHz side scan sonar and a 3.5 kHz sub-bottom profiler. Lithological calibration was provided by the analysis of both *in situ* core data and extant terrestrial data sets.

It is proposed that for the effective reconstruction of these and any other nearshore palaeo-environments a multi-disciplinary geophysical approach is essential. The critical control on success is the adherence, during interpretation, to a single unifying seismo-analytical framework. The seismo-stratigraphical analysis technique has been adapted for high-resolution work in order to provide this rigid framework. Objective descriptive analysis of the seismic traces provides a "seismic para-stratigraphy" which when combined with lithological data is used to construct a "composite para-stratigraphy". This is a process based, litho-stratigraphic interpretation that, by virtue of the detailed spatial extent afforded it by geophysical data, can be placed in a wider environmental context.

The composite para-stratigraphy for the Loch Ainort basin is dominated by Loch Lomond Stadial glacial activity. Terminal and readvance limits are identified at several localities within the basin. Variable morphological styles of the glacial sequences show that deglaciation occurred in two distinct, climatically controlled, phases. The first marked by a fluctuating ice margin and the second by uninterrupted retreat and *in situ* ice stagnation. Sub-aerially induced debris flows occur during the initial paraglacial phase but stabilisation of exposed slopes restricts this input and rapid sedimentation of fines from sediment-rich meltwaters becomes dominant. Modern fjordic sedimentation develops after the disappearance of glacier ice.

I dedicate this thesis to my father

"..... signs and the signs of signs are used only when we are lacking things."

Brother William of Baskerville (1327).

CONTENTS

FIGURES

Chapter 1:

Chapter 2:

Chapter 3:

Chapter 4:

Chapter 5:

Chapter 6:

Chapter 7:

TABLES

Chapter 1:

Chapter 3:

Chapter 4:

Chapter 5:

Acknowledgements

Due to the drawn out circumstances under which this thesis has been produced, there are a large number of people who I must thank for their help and support. First and foremost I will forever be indebted to the patience, encouragement and continually deserved abuse of Dr. Rob Duck, without whom I would never have got where I will be tomorrow. Equally, I must thank my other two supervisors Professor J. McManus and Professor C.K. Ballantyne for their help with this work. I must also thank the support of the St Andrews technical staff for help over the years, particularly, Ian Lorimer, Angus Calder, Andy Mackie and Colin Cameron.

Over the last two years I must also thank many of the members of staff of the Department of Oceanography, Geology and Geography at the University of Southampton who have bent over backwards to ensure that I do finally complete. In particular I must mention my "benefactor", Professor M.B. Collins, my collaborators Dr. Jon Bull and Dr. Anthony Long (there's no stopping us now!!!) and eternal prompts Dr's. Boxall, Kemp, Richards, Robinson and Statham (yes - I have finished).

On a personal level I must thank the following: Debbie (*nee* Kemp-McCarthy) without whom I would never have followed this path too.....? Mark Errington always a role model, but you can now call me Doctor (Give us a job). Mike McDonald and Dave "Trubshawe" Lowry, how low can one go? Dougie, Steve and Dave for giving me an extra year of my youth. Stu Allison, for being the one person who was always in a more depressed state than I was. Simon Wathen, Jon Seedhouse, Ricky Yarr, Donald Herd and the Hammers Football team for providing amusing asides. Karen Barr, for putting up with my coldness for so long - I am truly sorry. Rob Rolph, for always being a real brick in a tight corner.

At Southampton I am indebted to the following; Paul Riddy, Robin Edwards, Rory Quinn, Gary Momber and Dave Roberts for helping out during those last frantic moments. To Huw

"fat-boy" Powell (the proto-happy clapper - oh so dated), Bruce "Bosnia" Tomlinson (she almost ditched me last night!), Simon "jingly" Webster (its just not the same without hand signals), Alan Tappin and Ian Hall (for generating more vitriol than I could ever imagine possible) and the now sadly defunct Les Enfants D'Or. To Dr Rachel "media star" Mills (are you sure I do not know more about you than you do), Jenny "nice junction" Pike (thanks for everything) and Sarah (here's to being rich and famous). I would also like to thank Craig, Ruth and aarron joe for allowing the yuppy interloper to stress out in there home.

Finally I would like to thank my family (Ma, Pa and chuck), I will never be able to express my gratitude for your love, moral and financial support and lets not forget the large doses of emotional blackmail dealt out.

CHAPTER 1

1. INTRODUCTION

High resolution seismic surveys have frequently been employed as a means of identifying former ice limits in a variety of submerged environments (*eg.* continental shelves, fjords and lakes). The majority of marine investigations have been focused on the construction of seismic para-stratigraphies[1] for the offshore zone from sub-bottom profiles (*eg.* Canals *et al.*, 1988; Wingfield, 1990). Offshore research has been further restricted to large scale studies of the continental shelves, with the emphasis being placed on the reconstruction of the major Pleistocene ice sheets (*eg.* King, 1969, Scotian Shelf; Stoker, 1988, NW UK Continental margin; Holtedahl, 1989 Norwegian Shelf). All of these studies tend to deal with the identification of remnant features that are 10s to 100s of km in length and with a current bathymetric relief of several 10s of m. Calibration is conventionally provided by either pre-existing, randomly distributed isolate, borehole data or coarsely gridded surface sampling strategies (*eg.* King, 1969; Gilbert, 1985; Aarseth *et al.*, 1989).

A combination of water depth (100s m) and more importantly the accumulation of thick para- and post-glacial sedimentary deposits (10s to 100s m) enforce the use of low frequency seismic profiling systems *eg.* Sparker, Boomer (See Section 2.3.3.). Although the use of these systems enables penetration of a complete surficial para-stratigraphy (*ie.* sea-bed to rockhead) the corresponding loss of resolution (See Section 2.3.3.3.) has resulted in significant interpretational problems being encountered.

The establishment of effective and most importantly spatially transferable seismic para-stratigraphies has also been hampered by the lack of an adequately consistent nomenclature for seismic signature description (See Section 1.2.1.). This is compounded by the ubiquitous bad habit of mixing seismic facies identification with environmental interpretation (See Sections 1.2.1. and 1.2.2.) and so engendering an inductive rather than a deductive approach to seismo-stratigraphically based palaeo-environmental reconstructions.

[1] Defined as a series of units "... identified by objective criteria which reflect some aspect of lithology, in this case seismic signature which reflects acoustic properties." (Boulton *et al.*, 1981) - See Section 6.2..

In addition to sub-bottom profiling systems, high frequency non-penetrative echo-sounders (See Section 2.3.3.1. and Chapter 4) and side-scan sonars (See Section 2.3.3.2. and Chapter 5) are commonly deployed as part of multi-disciplinary geophysical investigations (*eg.* King, 1969; Bishop and Jones, 1979; Forbes *et al.*, 1991). However, data from these devices are frequently overlooked and used purely to provide background descriptions of current sea-bed morphology and/or composition (*eg.* Bishop and Jones, 1979). Quite logically it is assumed that, as the majority of glacially related stratigraphy will be buried beneath a large post-glacial sedimentary pile, these non-penetrative techniques will yield little useful information. Consequently, side scan sonar in particular has been restricted to the investigation of active glacial environments (*eg.* Prior *et al.*, 1981; Prior and Bornhold, 1989; Carlson *et al.*, 1992).

Acquisition of high resolution, spatially extensive data from nearshore environments has consistently been restricted to modern cold climate (currently or recently glaciated), fjordic, coastlines such as western Norway, Alaska and Antarctica (*eg.* Aarseth *et al.*, 1989; Carlson, 1989; Griffith and Anderson, 1989; Larsen *et al.*, 1991). However, these surveys are again frequently characterised by the acquisition of shallow penetration sub-bottom profile data over a large area, by either a low density survey grid or individual long profiles (*eg.* Orheim, 1988). This is because the majority of surveys are either constructed for the identification specific features (*eg.* Aarseth, 1987 - Outwash deltas; Aarseth *et al.*, 1989 - Submarine slides; Larsen *et al.*, 1991 - De Geer Moraines) or conversely the production of simple spatially extensive palaeo-environmental models (*eg.* Gilbert, 1985; Holtedahl, 1989; Forbes *et al.*, 1991). For nearshore geophysical studies calibration is again provided by isolate borehole and surface sample data, but due to their close proximity to land, terrestrial sites provide a useful additional stratigraphic control (*eg.* Larsen *et al.*, 1991; Carlson *et al.*, 1992).

In Scotland the environmental reconstruction of ancient glaciated terrestrial regimes has been the focus for a larger number of scientists since the turn of the Century (*eg.* Ballantyne, Benn, Boulton, Clough and Harker, Peach *et al.*, Sissons, Sugden, Sutherland).

Of particular interest has been the readvance glaciers of the Loch Lomond Stadial, a period of climatic deterioration between *c.* 11-10 ka BP. A combined research effort has led to the identification and detailed reconstruction of a mainland ice-field centred on Rannoch Moor and a smaller but discrete ice-field focused on central Skye (See Section 3.2.2.2.). A multi-disciplinary approach to research has also attempted to constrain the dramatic fluctuations in climate that occurred at this time and in particular the response of this system to extremely rapid climatic amelioration at the end of the stadial (*eg.* Walker *et al.*, 1988; Ballantyne, 1989; Walker and Lowe, 1990; Benn *et al.*, 1992). However, there is a significant discrepancy between the volume of work conducted on-land and research aimed at investigating the palaeo-glaciomarine environments of this period.

An exception to this oversight was the work of Boulton *et al.* (1981) who attempted to produce a seismic para-stratigraphy (sub-bottom profile data alone) for a small area on the western Invernesshire coastline. However, despite being in close proximity to terrestrial control, the emphasis of this paper was placed on trying to fit their results into a pre-existing seismic para-stratigraphy for the north-western seaboard of the Scottish Highlands (Binns *et al.*, 1974a. and b.; Bishop and Jones, 1979), rather than developing our understanding of the Loch Lomond Stadial palaeo-environment.

It is therefore the aim of this project to assess the use of an integrated, multi-instrument geophysical programme to investigating ancient, submerged, nearshore glaciated systems. The study is based on the western seaboard of the Scottish Highlands, where the limits of well-established glacial events (the Wester Ross, *c.* 13.5 - 13 ka BP and Loch Lomond Readvances) are well documented from terrestrial evidence, which places them across the mouths of fjords and within the nearshore zone.

To emphasise the proposed importance of marine geophysics to the understanding of ancient glaciated environments, a complete palaeo-environmental reconstruction of the chosen field site will be attempted based on both onshore and offshore datasets. Finally, the seismic para-stratigraphy created for the field area, and based up on both non-penetrative

and penetrative datasets, will be used to reappraise the present para-seismostratigraphy proposed for the western seaboard of north-west Scotland (Davies *et al.*, 1984, Long, 1991).

1.1. OBJECTIVES

Having outlined the broad aims of the project, it is necessary to present the specific objectives of this piece of research:

i) To reconstruct, using multi-disciplinary geophysical techniques, a nearshore glaciomarine environment associated with a terrestrially well constrained Lateglacial Readvance tidewater glacier, on the western seaboard of the Scottish Highlands.

ii) To use the evidence from ***i***) to critically assess the use of a range of high-resolution geophysical techniques for the reconstruction of ancient, nearshore, submerged glaciomarine environments.

iii) To construct a seismic para-stratigraphy (based on all three seismic reflection techniques) for the chosen survey areas and to attempt to correlate this with the extant seismic para-stratigraphies developed for the western seaboard of the Scottish Highlands.

1.2. BACKGROUND RESEARCH

To fully comprehend the research presented within this thesis, it is necessary to place it in the context of pre-existing published and un-published data. As has been described in the opening paragraphs of this introductory chapter there are many related topics that could be discussed (*eg.* comprehensive reviews of seismic investigations of a variety of glaciated sub-

aqueous environments). However, in the interest of brevity only short summaries of; the development of a unified framework for the description of sub-bottom profiles (Seismo-stratigraphic analysis: See Section 1.2.1.); and the previously constructed seismic para-stratigraphies of the western seaboard of the Scottish Highlands (See Section 1.2.2.), are presented here.

1.2.1. SEISMO-STRATIGRAPHIC ANALYSIS: A HISTORY

Since the late 1950's the structure and morphology of submerged surfaces has been investigated by seismic reflection techniques. Interpretation of seismic reflection profiles is conventionally based up on seismo-stratigraphical analysis which is described as "....the analyses of reflection sequences as the seismic expression of lithologically-distinct depositional sequences" (Kearey and Brooks, 1991). The main aim of seismo-stratigraphical analysis is to create a seismic para-stratigraphy which can then be integrated with the equivalent litho-stratigraphy to ultimately create a comprehensive palaeo-environmental model.

The principle debate within the subject of seismo-stratigraphical analysis has been the establishment of a standard nomenclature with which to describe the basic components of a seismic profile. Over the last thirty years there has been a wide variety of terms cited, from the "sub-bottom units" of King (1969), to the "Formations" of Lineback *et al.* (1971), Binns *et al.* (1974a and b.), Bishop (1975) and Bishop and Jones (1977) and to the "Acoustic Units" of Jansen (1976). This evident lack of a unifying framework for seismo-stratigraphic analysis in the early work, resulted in the publication of numerous studies which contained non-comparable data., thus the impact of this research was considerably reduced.

The pioneering breakthrough in seismo-stratigraphic analysis came with the work of Vail and Mitchum (*eg.* Vail and Mitchum, 1977; Mitchum *et al.*, 1977a and b; Mitchum and Vail,

1977). They applied for the first time the principles of sequence stratigraphy[2] to the interpretation of seismic reflection profiles. This new approach involved; first, seismic sequence analysis (See Section 6.2.3.), whereby the record is subdivided into large scale components or "Seismic Sequences"; secondly, further subdivision of these sequences, by seismic facies analysis (See Section 6.2.4.), into genetically related reflectors or "Seismic Facies Units", to create a detailed seismic para-stratigraphy (See Sections 6.4. and 8.4.); and finally, the correlation of the developed seismic para-stratigraphy with a global, process based, stratigraphy (*ie.* large scale sea-level fluctuation).

This technique was originally applied to low frequency profiles run for petroleum exploration purposes, but has since been successfully transposed to high frequency, high resolution seismic profiles (*eg.* Landmesser *et al.*, 1982 (Great Lakes); Bellaiche *et al.*, 1986 (Rhone fan); Canals *et al.*, 1988 (Ebro delta); Aarseth *et al.*, 1989 (Norwegian fjords); Hequette and Hill, 1989 (Beaufort Sea); Mullins *et al.*, 1990 (Kalamalka Lake, British Columbia)). Unfortunately, despite using the framework offered by the earlier researchers, the terminology "Seismic Sequence" and "Seismic Facies Unit" still has not been universally applied. For instance terms such as "Layer" (*eg.* Finckh *et al.*, 1984; Ben Avraham *et al.*, 1986), "Member" (Davies *et al.*, 1984) and "Type" (eg. Johnson, 1980; Wingfield, 1990) have been used where the previously proposed terminology would have sufficed.

However, despite the definition of seismo-stratigraphic analysis being "....the analyses of reflection sequences as the seismic expression of lithologically-distinct depositional sequences" (Kearey and Brooks, 1991), it is important to recognise that in reality it is not possible to directly correlate reflector type with an actual litho-stratigraphy. This is because both the point of reflection of an acoustic pulse does not necessarily correspond with a lithological boundary (See Section 2.3.3.) and that the limitations of the resolution of the profiling systems are incapable of identifying meso- and micro-scale lithological variations (See full discussion in Section 2.3.3.). This is particularly important when one considers the frequent mixing of seismic reflector descriptions with generic terms (*eg.* Jansen (1976)

[2] Developed by Sloss (1963).

ultimately gave his "units" the status of "deposits" (*eg.* Witch Deposits, Hills Deposits) or described purely with genetic terms (*eg.* tidal sand ridge, channel fill)). It is therefore important to recognise that generic and process terms should only be used during the final creation of a palaeo-environmental model, when the individual workers can draw on data from both seismic para-stratigraphies and litho-stratigraphies of an area.

1.2.2. SEISMIC PARA-STRATIGRAPHIES FROM THE WESTERN SEABOARD OF THE SCOTTISH HIGHLANDS

Over the last twenty years attempts have been made by several authors (Binns *et al.*, 1974a and b.; Bishop, 1975, Bishop, 1977, Bishop and Jones, 1979; Boulton *et al.*, 1981; Davies *et al.*, 1984: See Sections 1.2.2.1., 1.2.2.2., 1.2.2.3. and 1.2.2.4. respectively) to construct a seismic para-stratigraphy for the inner continental shelf of the western seaboard of the Scottish Highlands. Data have primarily been acquired by high resolution Sparker and Pinger systems, which achieve maximum penetration of 300 m and 40 m respectively (Davies *et al.*, 1984). Lithological calibration of the seismic profiles has been provided by sporadic borehole and surface sample data obtained and collated by the Continental Shelf Unit of the British Geological Survey (B.G.S.), Edinburgh, formerly known as the Institute of Geological Sciences (I.G.S.). By the analysis (lithological and micropalaeontological) and integration of these multi-disciplinary datasets, all of these authors also attempted to provide a broad palaeo-environmental reconstruction of the Quaternary history of this area.

1.2.2.1. Seismic Para-stratigraphy of Binns *et al.* (1974a. and b.).

Binns *et al.* (1974a. and b.) identified four seismic sequences[3] within the Sea of Hebrides (East of 08° 00' W: See Figure 1.1). A series of 5 boreholes provided both a lithological control and a source of additional information necessary for a basic palaeo-environmental reconstruction. A summary of the seismic para-stratigraphy is presented in Table 1.1..

[3] In the original text these were termed "Formations". For a full discussion of standardisation of seismostratigraphic nomenclature see Section 1.2.1.

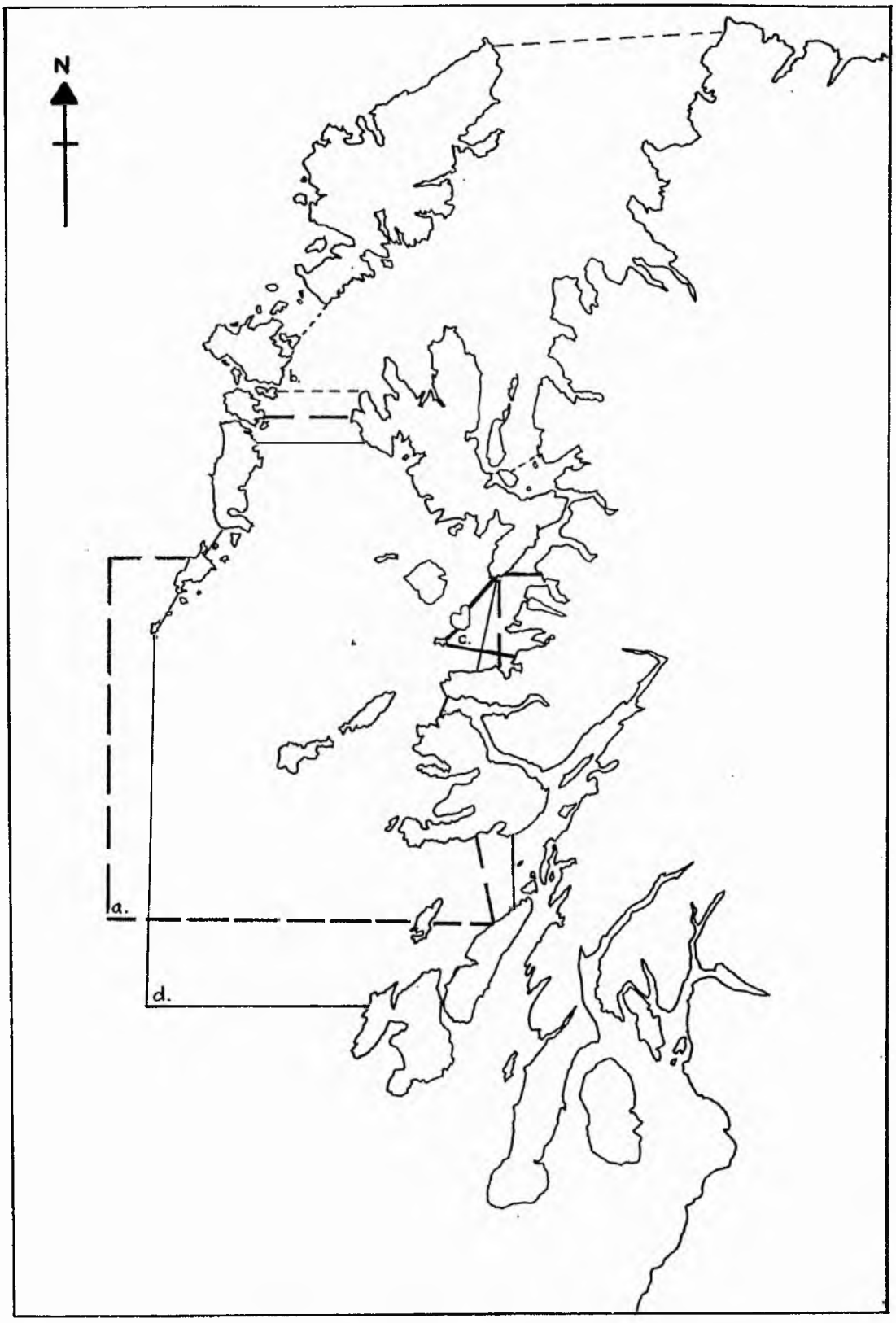

Figure 1.1. Previous seismic surveys completed on the western seaboard of Scotland. Authors and dates of data acquisition are as follows: a.) Binns *et al.* (pre-1973), b.) Bishop and Jones (1969 to 1973), c.) Boulton *et al.* (July, 1976) and d.) Davies *et al.* (1972 to 1982).

Although the seismic interpretation of Binns *et al.* cannot be questioned, the chrono-stratigraphic interpretation established was generally inductive, being based on inference to the then current theories of late Quaternary glacial to inter-glacial fluctuations and a single radiocarbon date (8.68 ka. BP), obtained from the upper part of Seismic Sequence 3. Despite the constraints of limited, independent chrono-stratigraphic data, Binns *et al.* suggest that the sequences they had identified were produced by the diachronous retreat (and minor readvance) of the Late Devensian ice sheet.

Seismic Sequence	*Seismic Signature*	*Lithological Correlative*	*Environment*
4	Not Described	Thin layer (0.5 - 2 m) of Muddy sands, sandy Muds and Sand.	Modern sediments with a spatial distribution controlled by bathymetry and local hydrodynamic conditions.
3	Closely spaced horizontal reflectors which fade laterally. In the outer part of the basin reflectors fill shallow depressions in the erosive upper surface of Sequence 2.	Poorly sorted sandy Muds, medium sands and occasional pebble grade clasts. No correlative of the horizontal reflectors were identified. Faunal content: a) Warm water forms. (-30 m to -28 m); b) Cold water foraminifera (-26 m to -14 m); c) Warm water forams - 10 m to surface.	This sequence represents the transition from a warm (Allerød Stadial) to a cold (Loch Lomond Stadial) to a warm (Holocene) climate. Sedimentation pattern dominated by high inputs from fluvioglacial activity and distal glaciomarine processes related to the advance and retreat of Loch Lomond Ice.
2	Acoustically transparent with widely spaced reflectors, an erosive upper surface and an unconformable lower boundary with a bedrock reflector.	Poorly sorted sandy Muds variable quantities of granule to pebble grade lithic fragments. Marine dinoflagellate cyst assemblages present.	Proximal glaciomarine sedimentation related to the retreating Devensian [*sic*] ice sheet. Possible submarine flow tills present.
1	Occasional hummocky upper surface, but commonly impedance contrast between Sequence 1 and 2 too low to provide a reflective surface.	Till.	Deposited in a Devensian [*sic*] sub-glacial environment.
	Single strong irregular reflector - no penetration.	Bedrock.	Glaciated, over-deepened trenches common, due to polycyclic glaciation. In outer shelf dips gently and uniformly westwards.

Table 1.1. A summary of the seismic para-stratigraphy of Binns *et al.* (1974a. and b.).

Simply, this seismic sequence represents subglacial till/diamicton deposited beneath the Late Devensian maximum ice sheet [Dimlington Ice Sheet: See Section 3.2.2.1. for full discussion]. The unconformably overlying Seismic Sequence 2 represent proximal glaciomarine sedimentation in front of the retreating mainland ice sheet. Seismic Sequence 3 represents the dominant sequence of this para-stratigraphy and the micropalaeontological evidence it has yielded suggests it represents the transition of full marine to distal glaciomarine and finally a return to full marine conditions, in response to the advance and retreat of the Loch Lomond Readvance glaciers (See Section 3.2.2.2. for full discussion). Finally, Seismic Sequence 4 is interpreted as being a thin veneer of modern sediments.

1.2.2.2. Seismic Para-stratigraphy of Bishop and Jones (1979)

Bishop and Jones (1979; See also Bishop, 1975 and 1977) analysed seismic profiles (Sparker, Pinger and Side Scan Sonar) and borehole data from the Skye-Shiant platform to the north of the Binns *et al.* field area (See Figure 1.1 and Section 1.2.2.1.). The seismic para-stratigraphy generated by Bishop and Jones was structured to fit into that of Binns *et al.* (1974a. and b.), with the identification of 4 equivalent seismic sequences (See Table 1.2.: Overleaf)[2]. However, as can be seen by the comparison of the two seismic para-stratigraphies (Table 1.1. *vs.* Table 1.2.) Bishop and Jones had significant difficulty in constructing a strict chronological order for the North Minch area.

In particular, they identified a problem with the chrono-stratigraphic relationship between Seismic Sequences 1 and 3. To the north-west of the area Seismic Sequence 1 tills are interpreted as passing both laterally and lying unconformably on the supposed chronologically higher Seismic Sequence 3. In the latter case this "Sub-unit 3" has a strong unconformable upper bounding reflector with Seismic Sequence 1. Instead of attempting to re-define the para-stratigraphy to account for this contradiction, they prefered to explain these obvious discrepancies in terms of lateral facies variation whilst still retaining the orignal nomenclature. Environmentally, they account for these spatial variations through the complex interplay between "peri-glacial" [marine?] and "fluvio-glacial" processes.

Seismic Sequence	*Seismic Signature*	*Lithological Correlative*	*Environment*
4	Not Described	Thin layer (0.5 - 2 m) of Muddy sands, sandy Muds and Sand.	Modern sediments with a spatial distribution controlled by bathymetry and local hydrodynamic conditions.
3	Closely spaced horizontal reflectors which fade laterally. In the outer part of the basin reflectors fill shallow depressions in the erosive [*sic*] upper surface of sequence 2.	Poorly sorted sandy Muds, medium sands and occasional pebble grade clasts. No correlative of the horizontal reflectors were identified.	Represents the combination of peri-glacial [paraglacial?] activity in front of a retreating ice front and fluvio-glacial deposition beneath a wet based glacier [sub-aerial processes].
2	A generally structureless sequence with widely spaced reflectors. A single strong, laterally continuous reflector is frequently identified in the middle of this sequence. The sequnece has an erosive [*sic*] upper surface and an unconformable lower surface with both bedrock reflector and Seismic Sequence 1.	Poorly sorted sandy Muds variable quantities of granule to pebble grade lithic fragments.	Postulated as being Lateglacial, glaciomarine flow till deposited beneath a floating glacier tongue. The sequence having been laid down after slumping of foreset tills on the steep sediment face under the glacier "buoyancy line". Widely spaced reflectors thought to be gravel or sand horizons.
1	A fine jumbled and hummocky internal texture with an uneven upper surface. Unconformably overlays strong basal bedrock reflector or unassigned seismic sequence described below.	Till.	Lateglacial Sub-glacial till deposits which have undergone strong horizontal shear beneath the ice. This process pushes and rolls the till forwards toward the buoyancy line.
"Sub-Unit 3"	Continuous horizontal to sub-horizontal reflectors unconformably draped over a prominent single strong reflector.	Not sampled	Unknown.
	Single strong irregular reflector - no penetration.	Bedrock.	Glaciated, over-deepened trenches common, due to polycyclic glaciation. Identifies the largest basins in the Inner Sound and the Sound of Raasay.

Table 1.2. A summary of the seismic para-stratigraphy after Bishop (1977) and Bishop & Jones (1979).

Although a point not to be laboured in this discussion it is worth re-emphasising the necessity for a universal nomenclature for both seismo-stratigraphic analysis and cold environment processes. For instance, Bishop & Jones misinterpret the original environmental reconstruction work of Binns *et al.* "Formation 3 sediments are considered to have been deposited at some distance from the ice front (compare with the 'periglacial marine' sediments of southern Alaska)." vs "... Binns *et al.* hold it to be of peri-glacial origin, laid down a short distance from a retreating ice front.". Although this may appear to be a pedantic observation on the part of this author, the implications of such a misinterpretation are significant. They effectively hypothesise that an inferred periglacial origin for Seismic Sequence 3 deposits taken form the Skye/Shiant Platform and the Shiant East Bank lends credence to their interpretation of these areas as being sub-aerially exposed during the Lateglacial and early Holocene.

1.2.2.3. Seismic Para-stratigraphy of Boulton *et al.* (1981)

The third seismic para-stratigraphy to be constructed for this area was that of Boulton *et al.* (1981). These workers undertook Sparker surveys inshore of the peninsula of Sleat and the islands of Eigg and Muck, and within the sea-lochs of Nevis and Ailort (See Figure 1.1). Again lithological control, in the form of borehole data, was obtained from the B.G.S.. However, in order to increase the reliability of the calibration between the seismic profiles and the core data a single seismic line was run directly over Borehole 71/10. From the analysis and interpretation of these data Boulton *et al.* constructed a five-fold seismic para-stratigraphy to which they assigned a site specific seismo-stratigraphic nomenclature (See Table 1.3.: Overleaf).

As with the chrono-stratigraphy presented by *Binns et al.* (1974a. and b.: See Section 1.2.2.1.) and reaffirmed by Bishop and Jones (1979: See Section 1.2.2.2.), Boulton *et al.* have interpreted their sequence as representing deposition and erosion since the last glacial maximum (Dimlington Stadial). These age constraints are again based on minimal chronological data, in fact the only date they quote is the single radiocarbon date of Binns

Seismic Sequence	*Seismo-Stratigraphy*	*Seismic Signature*	*Lithological Correlative*	*Environment*
3	Arisaig Formation (Within loch equivalent is the Nevis Formation)	Closely spaced weak reflectors frequently obscured by acoustic blanking (thought to be the result of biogenic gasification). In troughs and depressions of the outer shelf these reflectors exhibits non-parallelism, thickening towards the centre of the basins. Within lochs reflectors exhibit catenary bedding. Where large bodies occur they have distinct convex upper boundary. Prominent unconformable lower boundary	On upper surfaces thin lenses of fine muddy Sand, surficial coarse shelly Sands and gravels Olive-grey to dark green-grey Mud with isolated pebbles and shell fragments. Occasional green-grey sandy Mud and muddy Sand.	Upper surfaces represent early Flandrian marine deposits. Remainder of sequence represents high density fluvio-glacial discharge from retreating glaciers, which deposits sediments in low points in the contemporaneous sea bed topography. Within lochs this sequence represents progressive infill of the larger basins.
4	-	Closely spaced, irregular, strong reflectors infill basins in underlying transgressive boundary. Localised in lochs with no lateral equivalent on shelf.	Not sampled.	Proximal glaciomarine outwash.
-	Mallaig Formation	Large masses and occasional discrete ridges. This sequence has a strong surface reflection, numerous hyperbolic reflectors but no internal coherency.	Diamicton	Large volumes of basal diamicton found within lee of rock bars and several locals within the lochs. Possibly push moraines formed by the deformation of pre-existing tills during a readvance.
2b	Muck Formation	Coherent, closely spaced weak parallel reflectors. Prominent unconformable upper surface.	Dark blue-grey/ dark-grey/ black Mud and sandy Muds with isolated pebbles and shells.	Full marine deposition.
2a		Strong well spaced coherent parallel reflectors draped over substratum.		Paraglacial glaciomarine sedimentation that grades into full marine.
1	Minch Formation	Lenticular body with strong surface reflector, many hyperbolic reflectors but no internal coherency.	Boulder clay/diamicton.	Subglacial till deposited by Dimlington Stadial ice sheet.

Table 1.3. Summary of the para-stratigraphy constructed by Boulton *et al.* (1981) for western Inverness-shire.

et al., obtained from the upper part of their Seismic Sequence 3 (See Above). However, unlike the previous authors the close proximity of the Boulton *et al.* survey area to catalogued terrestrial data has enabled them to more effectively constrain their chrono-stratigraphic interpretations.

As can be seen in Table 1.3. the basic format of the Boulton *et al.* seismic para-stratigraphy corresponds to the four-fold division of the previous workers. At the base of the sequence they identify lenticular bodies of "boulder clay/diamicton" (Seismic Sequence 1: Minch Fm.) which is interpreted as being deposited under the Dimlington Stadial ice sheet. This inference is based purely on the identification of a radiocarbon dated till unit on the Island of Lewis (100 km to the north-west). This single date (27.55 ka BP; After von Weymarn & Edwards, 1973) is used to substantiate the westward advance of a major ice body from the mainland, overriding the Outer Hebrides some time after 27 ka BP.

Unconformably draped over this till or bedrock are fine grained sediments (Muds and sandy Muds) of Seismic Sequence 2, the Muck Formation. This sequence is found to the west of the sea lochs and is interpreted as representing a period of uninterrupted sedimentation during the deglaciation of the Dimlington Ice Sheet and the Loch Lomond Readvance (For a discussion of the influence of this event see below). The presence of discrete pebble and shell fragments toward the base of this sequence was presumed to represent deposition in a proximal to increasingly distal glaciomarine environment. In fact the change in seismic facies style defined by the "sub-units" 2a and 2b (See Table 1.3.) is interpreted as representing the gradation between glacially influenced marine deposition and "normal" marine conditions.

From its acoustic signature (comparable to that of the Minch Fm.) the Mallaig Fm. is interpreted as a till/diamicton, however, an alternative hypothesis is put forward for its timing and origin. This Formation is localised, occurring only on the eastern flanks and summit of the bedrock bar at the mouth of Loch Nevis and as discrete ridges at both the mouth of Loch Ailort and at numerous sites within Loch Nevis. Boulton *et al.* interpret these

large masses as either representing local thickening (> 40 m in places) of the pre-existing Minch Fm. tills during a readvance phase or as enhanced sub-glacial deposition during a still-stand phase of the retreating Dimlington Stadial ice sheet. An examination of a series of sub-aerially exposed moraines at a similar location in the Loch Morar basin (situated between these two lochs) and Loch Shiel confirmed a maximal Readvance origin, originally proposed by Peacock (1970). Further detailed analysis, by Boulton *et al.*, of their form and internal structure suggested they were in fact push-moraines, which had not been overridden and so did represent a maximum Readvance position. Having satisfied themselves with the correlation between the deposits of the Mallaig Fm. and these sub-aerial push-moraines they subsequently assigned a Loch Lomond Readvance age for these features (Again the original dates for the terrestrial moraines were based on inferences made by Peacock, 1970 and Sissons, 1974a).

Seismic Sequence 4 (No site specific nomenclature assigned) is locally found within depressions in the irregular upper surface of the Mallaig Fm. at the mouth of Loch Nevis. Having been identified as being discrete from the Mallaig Fm. Boulton *et al.*, suggest it may represent proximal glaciomarine sedimentation being deposited in front of a now receding Loch Lomond valley glacier. These authors do offer an alternative mode of formation for Seismic Sequence 4, as a recent sediment redeposited by the rapid tidal currents that are present over this moraine. However, as they earlier describe the same sequence as being overlain by the Nevis Formation (A lateral equivalent of the older Arisaig Fm.; See Below) the evidence for its stratigraphical significance remains equivocal. A reappraisal of the limited original traces/stylised interpretations, presented in Boulton *et al.* (1981), by this author would suggest that a stratigraphical position between the Mallaig Fm. and the Arisaig Fm. should be maintained. In the absence of either additional seismic or direct lithological evidence this author cannot comment on the environment in which the sequence was formed.

Seismic Sequence 3 (Arisaig Formation) is the stratigraphically highest sequence in the seismic para-stratigraphy of Boulton *et al.*. It predominates in the sounds to the west of the surveyed sea lochs with the Nevis Formation, representing the lateral equivalent of this

sequence within both of the sea lochs studied. The proposed lithological correlatives of this sequence (Muds and sandy Muds) are found in all the boreholes analysed. One of these boreholes yielded the ^{14}C date quoted by Binns *et al.* (1974a) from the upper part of this formation, however, Boulton *et al.* place greater emphasis on the unreliability of this date[4]. In support of this tentative age they suggest that, due to its stratigraphical position overlying inferred Loch Lomond Stadial sediments within the sea lochs an entirely Holocene age for this sequence is anticipated.

In the sounds Boulton *et al.* identify a prominent unconformable boundary between the Muck Formation and the Arisaig Formation. Again these authors have difficulty in assigning an age or duration to this major event. They attempt to temporally constrain this unconformable boundary by its relationship to the Mallaig Formation (and Seismic Sequence 4) and the two sequences which it separates. Due to the absence of this sequence within the sea loch, a Holocene age for the overlying Arisaig Fm., the evident change in sedimentation styles it represents (*ie.* from extensive erosion to deposition) and the inability to place such dramatic changes within the perceived Holocene environments, Boulton *et al.* suggest it represents sea bed erosion by strong density currents emanating from Loch Lomond Readvance glaciers.

Boulton *et al.* again identify that this progression from; true marine warm inter-stadial conditions of the upper part of the Muck Fm. to cold water stadial conditions with the development of Readvance glaciers at the prominent unconformable boundary and then ultimately a return to warm water non-glacially influenced marine sedimentation is reflected in the micro-palaeontological record of the area (See Table 1.1). The up core variability of microfaunal assemblages within borehole 71/9 and 71/10 (Harland and Hughes, in the appendices of Binns *et al.* 1974b.), shows a warm water assemblage at depth, a rapid decline to cold water assemblages immediately beneath the inferred unconformity and above this boundary a return to warm water assemblages.

[4] The disseminated core material analysed from this core actually yielded a date of 9961 ± 250 yr. BP. but because of re-worked Mesozoic material this was corrected to 8680 yr. BP. quoted by Binns *et al.* (1974a).

Finally these authors posed but failed to satisfactorily answer the question of, to what extent Holocene deposition was sourced from either land-derived material or the re-suspension of pre-existing marine/glaciomarine sediments. They tentatively suggest that the basin thickening reflectors typifying the Arisaig Fm. deposits in the sounds, are the result of cyclical sedimentation and resuspension. By comparison a predominantly land derived source for deposits within the lochs is postulated. This hypothesis is supported by the increase in acoustic blanking/masking of the Arisaig Fm. in a shoreward direction. This is because the blanking effect is attributed to increased gas production which is in turn believed to be related to the sediments having a relatively higher organic content, due to large volumes of biogenic material being washed in from nearby land areas.

Having recognised the similarities between the seismic signatures of Binns *et al.* (1974a. and b.: See Section 1.2.2.1.) and those they described, Boulton *et al.* attempted to correlate the two para-stratigraphies (See Table 1.4.: Overleaf).

Despite the continued reference to the previously established seismic para-stratigraphy throughout the Boulton *et al.* text and the use of much of the earlier data in their construction of their own para-stratigraphy, the latter authors fail to justify their correlation between the two para-stratigraphies. In particular, they do not explain why they choose to correlate the boundary between the Muck Fm. and the Arisaig Fm.[5] with some arbitrary point within Binns *et al.*'s Seismic Sequence 3.

Boulton *et al.* suggest that the 4 sequences identified by Binns *et al.* were based primarily on borehole data "...as their seismic resolution of the Quaternary sequence was relatively poor.", as compared to their own sub-division which was primarily based on "...the gross spatial relationships [of each sequence]". However, this does not account for the similarity between the seismic signature descriptions presented by the two sets of authors (See Table 1.1. *vs* 1.3.). A comparison of these signatures suggests that a more realistic hypothesis

[5] It was not necessary to discuss the significance of the Mallaig Fm. and "Seismic Unit 4" from the Boulton *et al.* para-stratigraphy as there spatial extent was limited to within loch localities whilst the Binns *et al* data was restricted to the outer shelf.

would be a direct correlation between Seismic Sequence 2 and the Muck Fm. and between Seismic Sequence 3 and the Arisaig Fm. In particular the identification of a prominent unconformable boundary in both cases and the infilling, by the respective upper sequences, of depressions in the lower sequences is a strong argument for correlation. This comparison does produce a slight mis-match between the style of reflectors within the two lower sequences; "widely spaced reflectors" (Seismic Sequence 2) *vs* "closely spaced reflectors (Muck Fm. - Upper Part). However, Boulton *et al.* do describe the unconformable boundary as being transgressive and deeply incised, in places cutting all the way down to bedrock. The form of this boundary would allow the Arisaig Fm. to lie directly on the lower part of the Muck Fm. ("strong well spaced coherent reflectors") which does possess an equivalent seismic signature to Binns *et al.* Seismic Sequence 2. In order to resolve this interpretative discrepancy either a reappraisal of all pre-existing data must be undertaken or a new survey instigated.

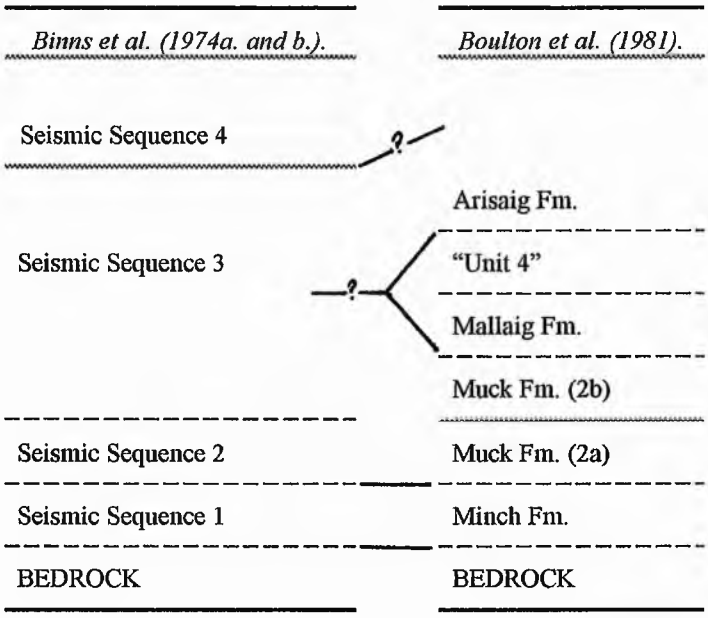

Table 1.4. Boulton *et al.*'s (1981) correlation of their seismic para-stratigraphy with that of Binns *et al.* (1974a. and b.).

1.2.2.4. Seismic para-stratigraphy of Davies *et al.* (1984)

The most recent attempt at defining a seismic para-stratigraphy for the western sea-board has been by Davies *et al.* (1984). These authors consulted several thousands of kilometres of single channel analogue seismic reflection profiles, using both multi-electrode Sparker and Pinger sources, acquired from a total of eleven cruises undertaken between 1972 and 1982. Calibration with lithological material was again provided by a series of key B.G.S. boreholes. In addition to constructing their own seismic para-stratigraphy they also presented critical reviews of previous workers attempts. A summary of their seismic para-stratigraphy is presented in Table 1.5.[6] (See Page 20). Davies *et al.* attempt to chrono-stratigraphically constrain their seismic para-stratigraphy based on three lines of evidence:

i) Analysis of dinoflagellates from the base of borehole 81/10 (Skerryvore Fm.) identified an assemblage dominated by *Achomosphaera andalouense* which is indicative of a pre-Devensian age (Harland pers. comm.; Davies *et al.*, 1984).

ii) The apparently ubiquitous radiocarbon dates obtained from borehole 71/9, one from 6 m below seabed (9.961 ± 0.2 ka BP.) and the other 30 m below the sea bed (16.47 ± 0.3 ka BP.) which give a Late Devensian to Holocene age for this part of the sequence (Jura Fm.). Davies *et al.* recognise that these dates represent maximal values[7] and in fact they do not quote the lower readjusted value presented by Binns *et al.* (See Section 1.2.2.1.: 8.68 ka BP.). They do, however, reaffirm a basic Late Devensian to Holocene chrono-stratigraphy based on the micropalaeontological fluctuations also described by Binns *et al.* (See Section 1.2.2.1.). Davies *et al.* attempt to support this hypothesis by stating that "Micropalaeontological evidence from other BGS boreholes (71/10, 72/6, 72/9, 73/25, 78/1) also reveals climatic phases which can be identified within the standard Late Devensian-Holocene framework (Gregory, Harland, pers. comm.).", but the nature of the supporting evidence is not given.

---

[6] For clarity the term Formation (Fm.) has again been retained from the original seismic para-stratigraphy of Davies *et al.* (1984).

[7] The dubious nature of these dates due to the inferred presence of reworked Mesozoic material has been discussed in Section 12.2.3..

iii) They assume that the major unconformity between the Barra Fm. and the sequences beneath could only have been produced by direct glacial action. This interpretation is based purely on the spatial extent, the "freshness" and the state of preservation of this surface only a "few" metres beneath the sea bed/Late Devensian-Holocene Jura Fm..

From this supposedly constrained framework they propose that the lowest sequence, the Skerryvore Fm., represents climatic deterioration during the latter stages of a pre-Devensian interglacial/interstadial period. This interpretation is based on its stratigraphical position below a till layer (Malin Fm.), which by inference from assumption *iii*) (See Above) must represent a pre-Devensian glaciation and the presence of a pre-Devensian dinoflagellate association (*i*)). Davies *et al.* extend this inference to the point at which they create the "Malin Glaciation" to account for both the Malin A and B Fms. Despite no absolute age constraints they logically place the overlying Canna Fm. into their pre-Devensian chrono-stratigraphic cycle of glacial to interglacial fluctuations. This sequence representing complex distal glaciomarine deposition in front of the retreating Malin ice sheet.

The Stanton Fm. lies directly beneath the major unconformable boundary described in *iii*). Their interpretation of this sequence in the Malin sea suggests that there was no substantial period of sedimentation between deposition of this Fm. and its subsequent erosion. From this hypothesis they suggest a Lower and/or Middle Devensian age for this formation, it being deposited from calving ice from an uneven glacier front centred over the Inner Hebrides/mainland. Again even with the absence of effective chrono-stratigraphic control they suggest the beginning of this event to correlate with Isotopic Stage "5/4" at approximately 75 kaBP[8].

[8] Presumably equivalent to oxygen isotope stage 5a/4 at 74 ka BP. (Dawson, 1992).

Seismo-Stratigraphy	*Seismic Member*	*Seismic Signature*	*Lithological Correlatives*	*Environment*
Lorne		Thin sequence with an unconformable lower boundary.	Sands	Present day shelf processes.
Jura	Sleat	Thin poorly developed sequence. Acoustically transparent with unconformable lower boundary. A series of thin overlapping point source reflectors, occur over large vertical distance in the Jura Fm.	Muds and Silts.	Due to limited evidence correlation with specific climatic events was not attempted. Micropalaeontological evidence suggests the base of the Jura Fm. pre-dates the Loch Lomond Readvance. Based on the contrast in seismic signature between the Barra and Jura Fm a date of 13.5 ka BP is given to this lower boundary. The top of the sequence is placed somewhere in the Holocene. A Loch Lomond Readvance age is tentatively given to the point source layers.
	Arisaig	Thick acoustically transparent sequence.	Muds and Silts.	
	Rhum	Thin, strong closely spaced horizontal to inclined reflectors. This sequence has conformable lower and upper boundaries.	Muds and Silts.	
	Muck	Thick acoustically transparent with a weak background signal. Unconformable lower boundary.	Muds and Silts.	
Barra		Acoustically transparent with a low seismic background signal. Occasionally short randomly spaced internal reflectors. Unconformable upper and lower boundaries	Silty Clays with dropstones.	Complex glaciomarine environment typified by high accumulation rates. Deposited following ice-front recession during the Late Devensian.
Hebrides		Thin sequence of diffraction hyperbolae covering an extensive unconformable lower boundary.	No direct borehole evidence.	Major erosive boundary cut during the Late Devensian Glacial Maximum. With thin cover of till.
Stanton	Stanton B	Wedges into its lateral equivalent Stanton A. Commonly acoustically transparent. Variable strength background signal with decreasing backscatter level towards mainland. Occasional short internal reflectors.	Silty Clays with dropstones.	Rapid and complex ice-proximal glaciomarine sedimentation in front of grounded glaciers centred over Inner Hebrides and Mainland. Stiff glaciomarine deposits with intercalated till.
	Stanton A	Well stratified with parallel strata of medium [*sic*] thickness draped over irregularities in unconformable lower boundary. Occasional point source diffraction hyperbolae.	Silty Clays with dropstones.	Complex distal glaciomarine deposition from suspension fall out in quite water environments. Stadial conditions implied.
Canna		Low internal backscatter level/acoustically transparent. Occasional short, discontinuous, randomly spaced reflectors. Unconformable boundaries.	Sands, Silts and Clays with numerous cobbles and boulders.	Rapidly deposited glaciomarine sediments possibly tills which accumulated under stadial conditions.
Malin	Malin B	Low backscatter level parallel sub-horizontal reflectors. In isolated pockets within/adjacent to Malin A.	No borehole control. Well sorted and well stratified sediments	Fluvio-glacial/proglacial lake sediments.
	Malin A	High internal backscatter level, confused, short and jumbled reflectors. Point hyperbolae prevalent. Uneven hummocky top. Unconformable base.	Diamicton	Spatially extensive glacial till deposited by the Pre-Devensian Malin glaciation.
Skerryvore		Low internal backscatter level with a structureless base and an upper facies with feint parallel bedding and occasional point source reflectors.	Silty Clays with isolated boulders towards the upper surface.	Interstadial to interglacial transition from temperate marine to distal glaciomarine in front of advancing ice.

Table 1.5. The Seismic Para-stratigraphy constructed by Davies *et al.* (1984).

The Hebrides Fm. is believed to represent a spatially restricted thin remnant till which lies on top of the "Late Devensian" unconformable boundary. The restricted distribution of this

sequence is accounted for by reference to ice sheet models (Boulton, 1974 and Boulton and Jones, 1975). These models suggest that under the high sliding velocities anticipated under thin temperate ice invoked for the Dimlington Stadial ice sheet, active erosion would remove any sub-glacial till present. The Barra Fm. directly overlies the "Late Devensian" unconformable boundary and the spatially restricted glacial deposits of the Hebrides Fm. and so is interpreted as representing rapid Late Devensian sedimentation following ice front retreat and associated sea-level rise.

The micropalaeontological evidence described in *ii*) and Section 1.2.2.1. suggests the base of the Jura Fm. predates the Loch Lomond Readvance. Davies *et al.* suggest that the distinct change in seismic signature between the Barra and Jura Fm. can be correlated with the retreat of polar waters from the vicinity of the British Isles at approximately 13.5 ka BP. boundary (Ruddiman and McIntyre, 1973; Ruddiman *et al.*, 1977) [13 ka BP.][9]. Although they do not give any indication of the processes responsible for the unconformable nature of this boundary. These authors go on to use this correlation to give a tentative date for the base of this sequence as being at 13.5 ka BP. [13 ka BP.] which is at variance with the radiocarbon date (16.47 ka BP. ± 0.3) taken directly from the base of the Jura Fm.. Davies *et al.* prefer the inferred younger date, again invoking the presence of reworked Mesozoic carbon as being responsible for the discrepancy between these two dates.

The transition from the Lateglacial to the Holocene is not identified within the proposed Davies *et al.* seismic para-stratigraphy. No correlation between the defined seismic sequences and "Members" with the warm water - cold water - warm water transitions identified from the micropalaeontological evidence has been made. Davies *et al.* do identify "...extensive cobble 'pavements', which have developed over a considerable vertical and horizontal distance within the Jura formation..." at the mouth of the Firth of Lorne and interpret these as being the product of intense glaciomarine sedimentation during the Loch Lomond Stadial. However, Davies *et al.* do not discuss where the pavements actually lie

[9] The oceanic/atmospheric polar fronts were actually believed to be in the vicinity at 13 ka BP. (See Section 3.2.2.1.).

within the seismic para-stratigraphy and so these cannot be built into their final chrono-stratigraphic model. Finally, the Lorne Fm. which is restricted to the edge of bare rock platforms, takes the form of thin "sandwaves" which presumably are forming under present conditions.

Having constructed their own seismic para-stratigraphy, Davies *et al.* critically compared their own work with that of the previous authors discussed in Sections 1.2.2.1., 1.2.2.2. and 1.2.2.3.. They considered the Binns *et al.* hypothesis, that all their sequences are of a purely Late Devensian origin (See Section 1.2.2.1.), to be significantly flawed. Following a reappraisal of the original seismic and lithological data used by Binns *et al.*, Davies *et al.* suggest that "... their seismic formation 1 is equivalent to the Malin formation [A pre-Devensian till deposit] while their formation 1 [lithological], as logged in coastal boreholes, is probably Devensian...". Having identified these inconsistencies in the Binns *et al.* chrono-stratigraphy, they also attempted to correlate the Binns *et al.* seismic para-stratigraphy with their own and hence redefine the palaeo-environmental history of the area (See Table 1.6.:Overleaf). However, their correlation is presented without published justification and, at the same time, fails to address the implications of this new interpretation.

Justification is particularly required for the correlation of Seismic Sequence 2 with a significant section (Canna Fm., Stanton Fm., Hebrides Fm. and the Barra Fm.; See Table 1.5.) of the Davies *et al.* para-stratigraphy. As can be seen from Table 1.1., Seismic Sequence 2 represents an acoustically transparent sequence with widely spaced reflectors, an "erosive" upper surface and an unconformable lower boundary with bedrock. By comparison their proposed seismo-stratigraphic equivalents (See Table 1.6.:Overleaf) to the south-west, represent a variety of different seismic signatures; from the acoustically transparent with short randomly spaced reflectors (Barra Fm. and Canna Fm.); to the well stratified with isolated point hyperbolae (Stanton Fm.); and to the chaotic diffraction hyperbolae (Hebrides Fm.). Further a total of three unconformable boundaries are identified within this sequence, the most prominent being the major bounding unconformity at the base of the Hebrides/Barra Fms., which is interpreted as a major erosion surface cut by a Late

Devensian ice sheet [Dimlington Stadial Ice]. It is therefore evident that there is a marked discrepancy between the seismic signatures of the two proposed seismic para-stratigraphic correlatives.

	Davies et al. (1984).	*Binns et al. (1974a. and b.).*
	Lorne Fm.	Seismic Sequence 4
J	Sleat Member	
U	Arisaig Member	Seismic Sequence 3
R	Rhum Member	
A	Muck Member	
	Barra Fm.	
	Hebrides/ Minch Fm.	Seismic Sequence 2
	Stanton Fm.	
	Canna Fm.	
	Malin Fm.	Seismic Sequence 1
	Skerryvore Fm.	
	BEDROCK	BEDROCK

Table 1.6. Davies et al.'s (1984) correlation of their seismic para-stratigraphy with that of Binns *et al.* (1974a. and b.).

This discrepancy between correlatives is further emphasised when the thickness of the two para-stratigraphies are compared. A maximum thickness of ~ 30 m is recorded for Seismic Sequence 2, which is significantly smaller than the maximum thickness of 110 m for the equivalent Davies *et al.* sequence. Such a contrast does not totally invalidate the correlation, as a lateral thickening of the sequence to the south-west is feasible, particularly considering the irregular topography of the pre-Devensian surface on which it is deposited. In fact in B.G.S. borehole 81/10, located in the Skerryvore trough, the maximum thickness of these sequences (Stanton and Canna Fms. present) is reduced to only 30 m. However, this re-examination of all the published evidence emphasises the equivocal nature of this correlation.

Davies *et al.* again critically assessed the contribution of Bishop and Jones (1979: See Section 1.2.2.2.) to developing a para-stratigraphy for the North Minch area. However, they failed to offer any constructive contribution based on this work, concluding that "New data might enable a stratigraphy comparable to that given in this paper [Davies *et al.*, 1984] to be erected for the North Minch". Observations of Bishop and Jones do, however, add credence to the Davies *et al.* reinterpretation of the Binns *et al.* para-stratigraphy.

Firstly they identified the presence of a strong major reflector within Seismic Sequence 2 and in profiles from the northern end of the Stornoway basin to the mouth of the Inner Sound (See Table 1.2.). This boundary separates two acoustically transparent layers with infrequent, laterally persistent widely spaced internal reflectors. It is plausible that this reflector represents the major erosion surface that separates the Barra Fm. from the Stanton and Canna Fms. Considering the dearth of seismic reflector equivalents identified between Seismic Sequence 2 and the Davies *et al.* sequence, this particularly strong reflector represents the only corroborative evidence for the correlation to date. Further if the interpretation of this single reflector as the main erosion surface is upheld, its presence in profiles that include Seismic Sequence 1 at depth, would support the inference of Davies *et al.* that this sequence was deposited during an earlier (pre-Devensian) glacial event.

Finally the stratigraphical position (beneath Seismic Sequence 1) and seismic signature (continuous horizontal to sub-horizontal reflectors unconformably draped over a prominent single strong reflector) of "sub-unit 3" enables a tentative correlation with the Skerryvore Fm. of Davies *et al.* (See Table 1.6.). Such an interpretation would again provide further evidence to support the re-constructed chrono-stratigraphy of Davies *et al.*

Evidently the re-interpretation of the chrono-stratigraphy of both Binns *et al.* and Bishop and Jones, and in particular the extension of the proposed time-scale from a restricted Late Devensian to Holocene sequence to a more extensive pre-Devensian to Holocene stratigraphy, should have repercussive implications on the para-stratigraphy of Boulton *et al.*. However, Table 1.7. (Overleaf) shows that Davies *et al.* retain a Late Devensian age for

the Minch Fm. correlating it with their own Hebrides Fm.. Unfortunately these authors again fail to justify this correlation making it difficult to critically assess its validity. Further, Davies *et al.* also attempt to correlate the individual Members of their Jura Fm. with part of the Boulton *et al.* seismic para-stratigraphy. Detailed analysis of this work also leads to the identification of significant, unaccounted for discrepancies. In particular Davies *et al.* attempt to correlate their Muck Member, described as a "Thick acoustically transparent unit.." with the Boulton *et al.* Muck Fm. (2a) described as a "unit" composed of "Strong well spaced coherent parallel reflectors draped over the substratum.". This simple description begs for a more detailed explanation for their correlation but none is given.

Davies *et al.* also fail to adequately account for their conversion of the unconformable boundary between the Muck Fm. and the Arisaig Fm. described by Boulton *et al.* to a conformable boundary between their equivalent Arisaig and Rhum Members. They do state that "After careful analysis of both Sparker and Pinger records from the area between Skye and Ardnamurchan, it is concluded that the apparent downcutting is in reality a function of both sediment compaction and extensive draping over a rugged rockhead.", however, they fail to present any pictorial evidence to support this important assertion. Although this author could not directly view the original data of either Boulton *et al.* or Davies *et al.*, the nature of this important boundary still remains equivocal, particular as the authors of the Boulton *et al.* paper are still confident of their original interpretation (Jarvis, 1994 *pers. comm.*).

Confidence in the Davies *et al.* paper is further questioned by their inability to be consistent with their seismic facies and sequence descriptions. In particular they give contradictory descriptions of the seismic signatures of the Jura Formation: firstly it is described as being ".....generally well stratified with close, parallel horizontal reflectors,...". Conversely, they later describe the components of the Jura Fm. as: "The basal unit, Member A, is thick acoustically transparent and is characterised by a weak background signal." and "This [Member A] grades conformably into member B which is comparatively thin with strong closely spaced reflectors." [Note similarity with description of general Jura Fm., the

only difference is the lack of an unconformable lower boundary] "Member C is thick and acoustically transparent. Member D is thin poorly developed acoustically transparent and lies unconformably on the other Units.". Again these major contradictions could potentially be explained by lateral seismic facies variations, however, no spatial information on these variations is actually described so this hypothesis could not be supported.

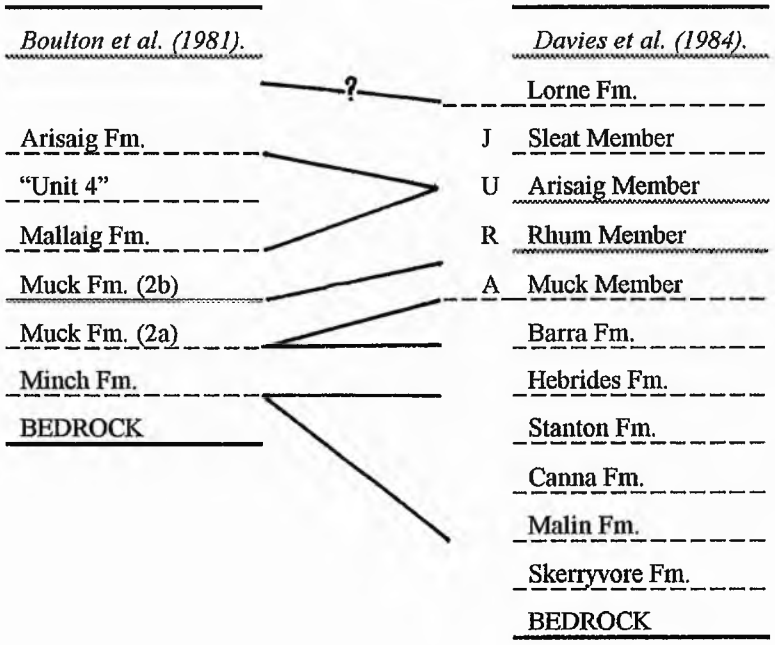

Table 1.7. Davies *et al.*'s (1984) correlation of their seismic para-stratigraphy with that of Boulton *et al.* (1981).

1.3. CONCLUSIONS

It is evident from the discussions in Sections 1.2.1. and 1.2.2. that their are still significant problems in the use of seismo-stratigraphic analysis for the interpretation of ancient submerged environments. In particular the lack of a unified framework, or in recent cases the lack of adherence to this framework, significantly reduces the ability of later workers to fruitfully integrate previous work with their own. The discussions presented in Section

1.2.2., especially those in Section 1.2.2.4., also emphasise the importance of justifying environmental interpretations based wholly, or in part, on seismic data. Without the presentation of substantiating evidence it is impossible to place any scientific credibility up on their deductions. It is therefore hoped to present in this thesis a fully substantiated and reproducible seismic para-stratigraphy, based on a variety of seismic datasets (both non-penetrative and penetrative: See Chapters 4,5 and 6) acquired for the chosen field area. This in turn will be correlated with relevant terrestrial (See Chapter 3) and sedimentological data (See Chapter 7) to construct a simple palaeo-environmental model and composite para-stratigraphy (See Chapter 8).

CHAPTER 2

2. FIELD METHODOLOGY

2.1. INTRODUCTION

This chapter deals with all aspects of the field techniques employed during this project. It covers the rationale behind the site location of the geophysical survey, including both practical and academic considerations (Section 2.2.). Details of all vessels used during fieldwork are given, as well as an assessment of their performance during these tasks. The methods of position fixing employed in association with the geophysical survey techniques are described (Section 2.3.).

A brief summary is given of the basic principles of seismic reflection, followed by descriptions of the individual techniques (echosounder, side scan sonar and sub-bottom profiler) and their respective applications (Section 2.3.3.). Analysis and interpretation of information gained from these surveys has been consciously omitted from this section and is dealt with separately in Chapters 4, 5, 6 and 8. The final part of the field methodology addressed is the retrieval of sediment samples by gravity coring of the field area (Section 2.4.), the analysis and interpretation of these data being presented in Chapters 7 and 8.

2.2. SITE LOCATION

In accordance with the initial proposals of the project, the broad constraint on site location to the western seaboard of Scotland is derived from the occurrence of well established terrestrial limits of late Quaternary glacial readvance events along this coastline (See Figure. 2.1.).

An initial reconnaissance visit was undertaken, in order to identify a suitable off-shore site for data collection. A set of criteria for each sea loch had to be fulfilled, in order to provide optimum efficiency for geophysical surveying. This was especially important

Figure 2.1. Limits of the Loch Lomond and Wester Ross Readcvances in North-West Scotland (After Robinson and Ballantyne, 1979; Sissons, 1981a; Sissons and Dawson, 1981; and Bennett, 1994)

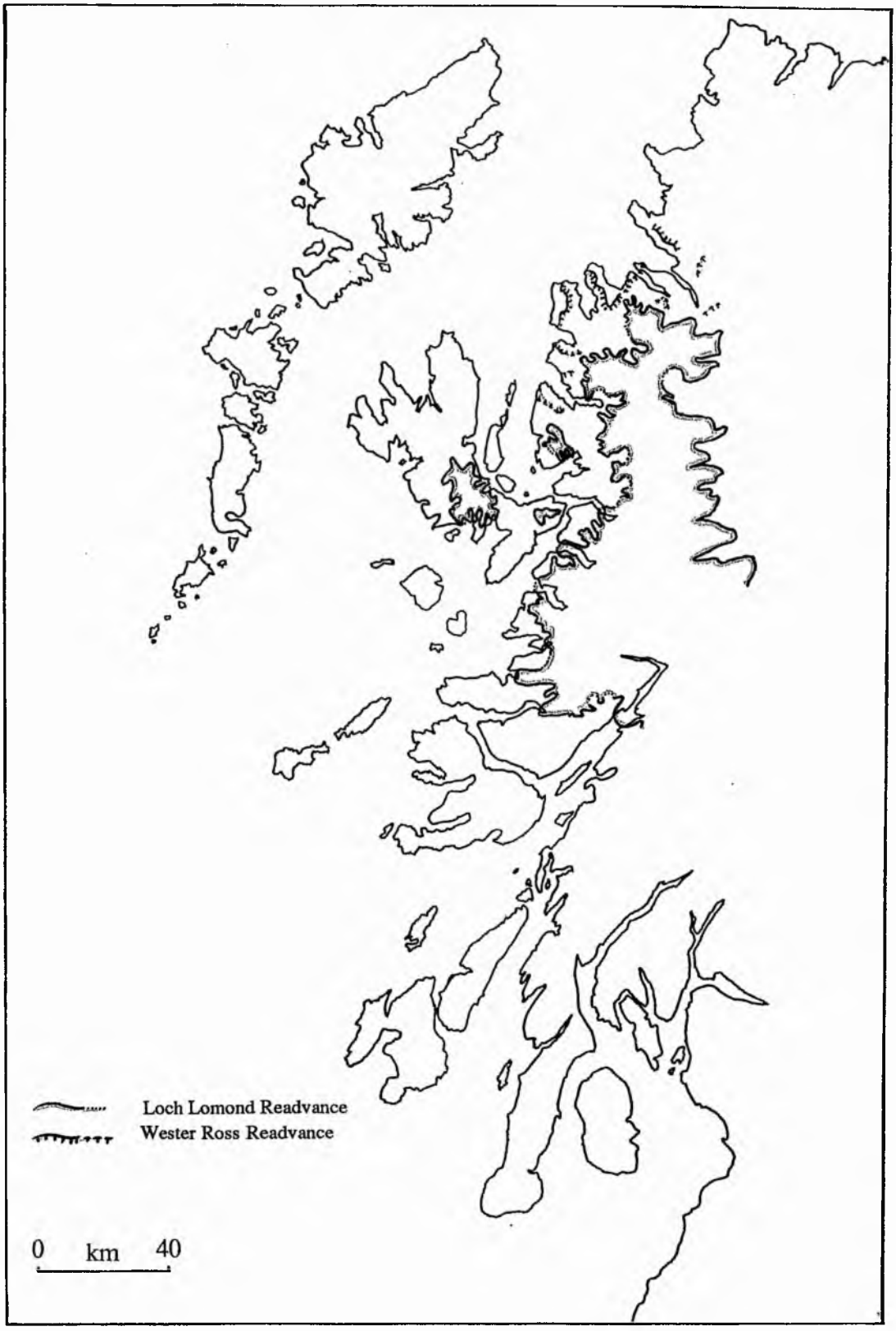

considering the distance of the field areas from St.Andrews, and the temporal and financial logistics of setting up a multi-disciplinary study.

The primary consideration for site location is the ease of boat access to the water body, with preference given to lochs that possess functional slipways or piers. Such entry points have to be easily accessible to the general public or by prior arrangement with the owners. These access points should ideally be serviceable at all stages of the tide so as not to unduly restrict survey runs to specific tidal states.

Due to an insurance restriction on the survey vessel (a 5.5 m dory: See Section 2.3.1.), such that it cannot be used for survey work in wind conditions greater than Force 4 (8 ms^{-1}), it is necessary to locate areas that possess the calmest possible water conditions. The orientation of each loch and the configuration of the surrounding topography must also be considered as they significantly affect the degree of protection offered against the prevailing southerly to westerly winds. These latter two factors thus dictate the maximum size of fetch at each locality, the fetch being the unobstructed distance of sea over which wind may blow. The height of wind-generated waves is directly proportional to the fetch (Bearman, 1989), and so true open sea areas (i.e. those with the greatest fetch) are to be avoided as they tend to have the most unpredictable wave conditions.

After taking into consideration all of the logistical parameters involved in offshore fieldwork, the final choice of field location was based on the extent of onshore mapping of any glacial limits. As can be seen in Figure 2.1, limits for the Loch Lomond and Wester Ross Readvances[1] restricted the possible survey areas to Loch Ewe and all sites south. The southern limit of interest was defined by the work of Boulton *et al.* (1981) who surveyed the area from Loch Nevis to Loch Ailort. It was not deemed necessary to duplicate previous work. The Isle of Skye, however, was considered a worthy target particularly in view of the recent reassessment of the onshore Loch Lomond glacial limits by Ballantyne (1989) and Benn (1990).

[1] A review of the Loch Lomond Readvance literature for the selected area can be seen in Chapter 3.

Applying the criteria, as defined above, the following lochs (Grid References given in square brackets) were assessed for their suitability for study (See also Figure 2.1.):

Loch Ewe [NG180880]: Several access points are available, via a jetty at Naast on the western shore and jetties at Aird Point and Tournaig on the eastern shore. The narrow neck at the mouth of the loch and its north-south orientation provides protection from severe conditions throughout. However, the previously defined Wester Ross glacial limits suggest that the off-shore limit is outwith the loch and so in open water (Robinson & Ballantyne, 1979; Sissons, 1981a; Sissons & Dawson, 1981). Thus, the primary survey area is exposed to a fetch of over 50 km and unpredictable sea conditions are to be anticipated.

Loch Gairloch [NG170870]: Access is via a slipway at Gairloch village. The open mouth, east-west orientation and a fetch in excess of 70 km all suggest impractical survey conditions for a small boat. In addition, the off-shore Wester Ross limit is again believed to be in the more exposed open sea area at the loch mouth water (Robinson & Ballantyne, 1979; Sissons, 1981a; Sissons & Dawson, 1981).

Loch Torridon [NG170860] & Upper Loch Torridon [NG180850]: Several access points are present along both the northern and southern shores, with two slipways at Shieldaig, a jetty at Torridon (to which it would be difficult to return the boat at high and low water so restricting surveys to the mid-tide/mid-tide period) and a sheltered pebbly beach at Inveralligin from which a boat could be launched. The north-west - south-east orientation, the peninsula of Applecross to the south-west, and the narrowing of the shores between the outer and upper lochs, all provide for a sheltered locality. Possible Wester Ross limits have been identified both on the northern shore of Torridon and on the northern part of Applecross, but they suggest that the off-shore limits are in the exposed Inner Sound to the west of the loch mouth (Sissons, 1981a).

Loch Kishorn [NG180830]: Onshore mapping suggests that neither Wester Ross nor Loch Lomond limits are present in this area. This water body was therefore not reconnoitred.

Loch Carron [NG190830]: Onshore mapping suggests that neither Wester Ross nor Loch Lomond limits are present in this area. This water body was therefore not reconnoitred.

Loch Duich [NG880250]: This water body affords access to Loch Long to the south and Loch Alsh to the west. Two slipways were identified at Dornie at the head of Loch Duich, with a further two at a fish farm at Letterfearn on the south-western shore. Permission to use all slipways was obtained. The north-west - south-east orientation, the surrounding mountainous topography (no area less than 400 m) and the location of the Isle of Skye to the west, all provide excellent protection from the prevailing winds. Owing to extensive afforestation, the Loch Lomond limit is ill defined in this area, but recent work does suggests that a Loch Lomond glacier front was located in the vicinity of Dornie at the mouth of Loch Duich (J.Tate, 1992 *pers. comm.*).

Loch Hourn [NG180800]: Despite the east-west orientation, the sheltered conditions, short fetch and possible Loch Lomond ice limits on both shores (Boulton *et al.*, 1981), Loch Hourn had to be disregarded due to its inaccessibility by road. This is particularly important as the survey vessel has to be towed to any chosen site.

Loch Sligachan [Skye - NG150830]: A slipway adjacent to the jetty for the Balmeanach ferry; gives possible access to the loch but there may be a problem during summer months due to competing ferry services. The loch's location on the eastern coastline of southern Skye provides it with excellent protection from wind induced waves due to the presence of the Cuillin Hills to the south-west. Loch Lomond limits are well defined on both shores with the suggested off-shore limit of the Sligachan and Glamaig glaciers occurring in the relatively sheltered waters between the Narrows of Raasay and Caol Mòr (Ballantyne, 1988, 1989, 1990; Benn 1989, 1990; Benn *et al.*, 1992).

Loch Ainort [Skye - NG150820] & Loch na Cairidh [NG150820]: Three possible slipways are present, on the south-western shore at a Marine Harvest fish farm. Permission to use any of these was granted. Probable water conditions are similar to those at Loch Sligachan, as Loch Ainort is also protected by the presence of the Cuillin Hills. Lochs Ainort and Cairidh are also sheltered to the north-east and the north by the

island of Scalpay only 1 km off the coastline. Again, on land limits of the Ainort glacier are well defined on both shores (Ballantyne, 1988, 1989, 1990; Benn 1989, 1990; Benn *et al.*, 1992).

Loch Slapin [Skye - NG150810]: An adequate slipway exists at a fish farm on the western shore. Permission to use this was obtained. Loch Slapin is protected from westerly winds by the southern margin of the Cuillin Hills. However, the north-south orientation of this loch makes it vulnerable to southerly winds with a possible fetch of over 200 km. No substantial barrier exists between this part of Skye and southern Ireland. Consequently, severe sea conditions might be anticipated. The on land glacial limits are well defined and suggest that the Slapin glacier front terminated near the head of the loch (Ballantyne, 1988, 1989, 1990; Benn 1989, 1990; Benn *et al.*, 1992).

Loch Scavaig [Skye - NG140810]: A possible entry point to this water body exists at Elgol but the slipway is very narrow making entry difficult. The only protection from westerly winds is provided by the island of Soay, whilst the open nature of the north-south orientated loch leave it fully exposed to the North Atlantic. Again this would suggest that, at the very least, weather and sea conditions would be unpredictable. On land glacial limits suggest that both the Coruisk and Creitheach glaciers would have terminated near the mouth of Loch Scavaig (Ballantyne, 1988, 1989, 1990).

Having assessed the relative merits and limitations of each loch for the project's requirements, Loch Ainort was chosen from the above list as being the most suitable area for study. This loch possessed a large, high resolution onland database with well defined limits on both shores (See Section 3.2.). Therefore it would represent a good test case of the effectiveness of geophysical techniques in identifying and hopefully supplementing sub-aerial data.

2.3. SURVEYING TECHNIQUES

Once the locality for this project had been chosen, a series of high-resolution seismic profiling surveys were carried out on the loch. Section 2.3.3. deals with all aspects of these off-shore surveys, from the logistics of operation to the rationale behind the individual geophysical operations.

2.3.1. SURVEY VESSELS.

All of the geophysical surveys were undertaken from the 5.5 m dory, R.V. Mya (See Figure 2.2.). The size of this vessel made it ideal for such survey work as it was sufficiently portable to be easily transported by trailer, both between St. Andrews and the field areas, and between individual sites. Its size also made it sufficiently flexible to be launched under difficult conditions and at poorly defined landing sites if required. All traverses were carried out at a speed of 3.5 knots (1.75 ms^{-1}), over the ground, regardless of sea conditions with each traverse extending inshore to a water depth of 2 m. As described previously this vessel has strict working conditions (See Section 2.2.); which is not only to comply with insurance regulations but also to provide optimum conditions for seismic reflection profiling. In order to obtain good geophysical data the vessel must be stable in all working sea states. This is particularly important for the echosounder and sub-bottom profile surveys (See Section 2.3.3.1 and 2.3.3.3.) as these two instruments were directly affixed to the ships hull and were therefore sensitive to the pitch and heave of the vessel.

Due to the size of coring equipment used (See Section 2.4.) it was necessary to employ a much larger vessel with a winch capacity of greater than 500 kg. This part of the survey work was carried out from the 29 m, coastal tug, the Carron Highlander (See Figure 2.3.). This provided a stable off-shore platform (irrespective of the sheltered sea conditions) with a working deck area of 67 m^2 and a winch and boom arm system capable of accommodating the weight of the coring equipment.

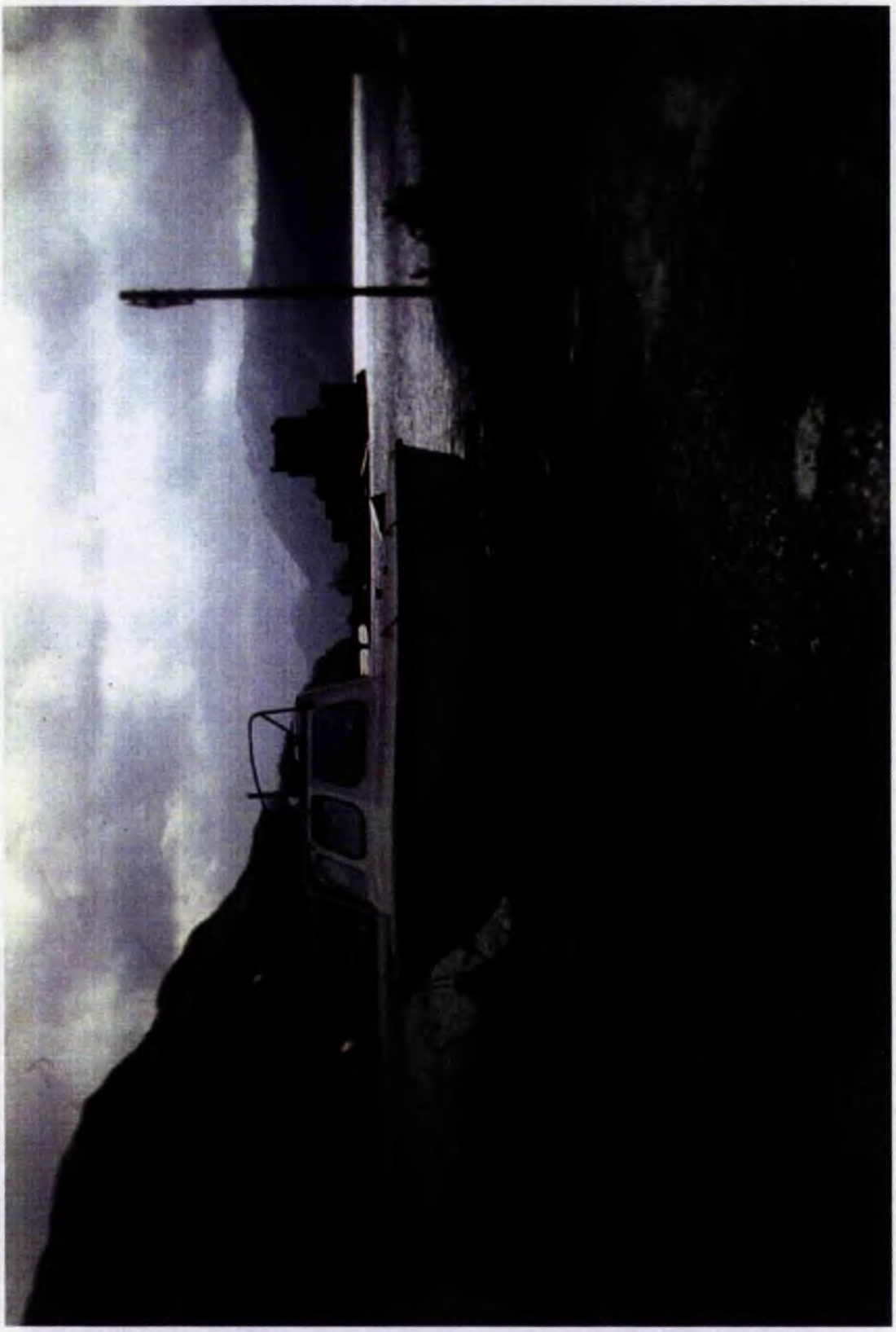

Figure 2.2. The geophysical survey vessel, the R.V. Mya.

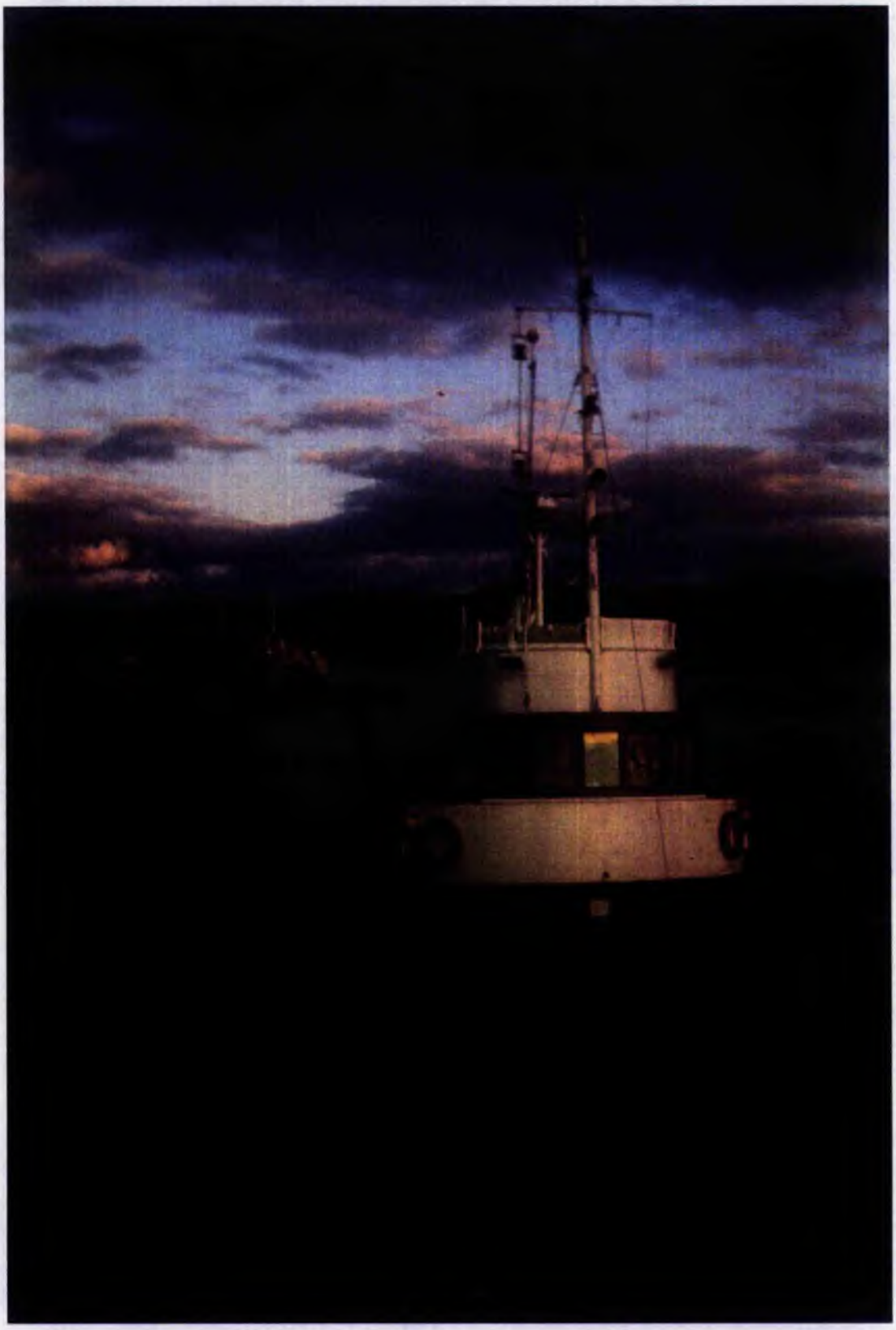

Figure 2.3. The survey vessel, the Carron Highlander.

2.3.2. POSITION FIXING.

For off-shore survey work to be of any significance, it is essential that one's location on the water body is accurately known at all times. To achieve this primary requirement a number of different techniques were used to locate the traverse lines run during each survey. It was not possible to use one consistent method of position fixing throughout this project due to both variable and impractical working conditions and the unavailability of equipment. It is, therefore, necessary to always be aware of the corresponding errors of each method during data analysis. A description of each method of navigational control employed is given below.

2.3.2.1. Traversing.

On Loch Ainort, it was necessary on occasion to navigate by compass traverses between known end points, defined on 1:10,560 scale Ordnance Survey maps. The accuracy of this method depends on visibility and sea conditions during each survey. On each survey day that this particular system was used, both visibility and sea conditions were excellent. Consequently, it is believed that the maximum positioning error in the centre of the sea loch was 40 m. This compares favourably to errors of 30 - 100 m, within sea lochs, cited by Boulton *et al.* (1981) for a similar operation.

2.3.2.2. GPS Receiver - Magellan© NAV 1000 Plus.

The Magellan© Global Positioning System is based on obtaining information, transferred by telemetry, from a satellite constellation. The constellation comprises 21 satellites and 3 working spares moving in six orbital planes. To obtain a fix, the receiver takes information from a minimum of three satellites (the greater the number of satellites it interrogates the greater the accuracy of the position). The data string emitted from each satellite includes ephemeris information (i.e. the orbit of the satellite) and the time of transmission of each string. Knowing the time of transmission, the time of reception of each signal from the satellites and the 'GPS speed of light', the receiver is then able to calculate the distance to the satellite. Using the calculated distance and the orbital

Figure 2.4. The Magellan© Hand Held Global Positioning System.

position of each satellite, the receiver determines a position fix in degrees and minutes of latitude and longitude.

Accuracy of this GPS system varies with constellation geometry, but it is suggested by the manufacturers, that an accuracy of ± 50 m or better is typical. The system can potentially provide sub-metre accuracy. However, the American Military developers have integrated a random error generator into the system known as Selective Availability. This produces both orbital and transmission time errors, at different update rates, so preventing its use by either industrial or foreign military groups. For optimum accuracy the appropriate map datum (See Section 4.2.), from a total of eleven stored in its memory, must be programmed into the Magellan© SETUP mode prior to use. For greater speed and continuity of plotting, a "navigator's Yeoman" was then used to locate each position fix on a 1:10,560 scale base map.

The surveys conducted using this equipment were carried out during the immediate aftermath of the "Gulf War". At this time increased military activity led to the downgrading of the random error of this system such that accuracy was improved to a level of ± 15 m at any locality (I.E. Lorimer, 1991 *pers. comm.).* The Magellan© unit is a recent acquisition and, therefore, has been used only on the later survey expeditions.

The Magellan© GPS system is a hand held unit, making it easily transportable and convenient to use especially in restricted working conditions (See Figure 2.4.). For continuous operation (effectively a reading every three seconds), which is essential during small scale survey work, the Magellan© can be connected to a standard 12 volts DC battery. During periods of improved accuracy, this GPS equipment is ideal for position fixing in confined inshore waters, particularly when used from smaller vessels and when survey time is limited.

2.3.3. SEISMIC REFLECTION TECHNIQUES.

All of the geophysical techniques described in this section are founded on the same basic principles of seismic reflection. The technique operates by an acoustic wave being produced from a point source, the time interval is then recorded for this wave to reach a reflecting surface and return to a point at or near the original source. This interval is known as the two-way travel time (**t**) which is related to depth (**D**) by the simple equation :

$$D = 0.5V_p \times t \qquad \textit{Equation 2.1)}$$

In this equation V_p represents the compressional velocity of the transmitting medium, this quantity being determined by the values of the bulk modulus (**k**), the shear modulus (**n**) and the density (ρ) of the medium via the relationship:

$$V_p = (k + 4/3n)/\rho \qquad \textit{Equation 2.2)}$$

The value of V_p therefore varies between different rock and sediment types, with the simple relationship that hard rigid rock materials have relatively high compressional velocities where as soft plastic rocks have low compressional velocities. Further, the general empirical rule applies that compressional velocity increases in step with increased density in similar rock types.

If an acoustic wave encounters a boundary between two mediums of differing properties the energy of the incident wave is partitioned into transmitted and reflected waves. The relative proportions of the energy transmitted to each of these waves is determined by the contrast in acoustic impedance (**Z**) across the interface. Acoustic impedance is the product of the compressional velocity (V_p) and the density (ρ) of a medium:

$$Z = \rho \times V_p \qquad \textit{Equation 2.3)}$$

Simply the greater the impedance contrast the greater proportion of the energy is apportioned to the reflected pulse and hence the stronger the returning signal. The partition of the incident wave can be expressed by the Reflection Coefficient (**R**) which is the ratio of the of the amplitude of the reflected wave ($\mathbf{A_1}$) to the amplitude of the original incident wave ($\mathbf{A_0}$). (See Figure 2.5):

$$\mathbf{R = A_1/A_0} \qquad \textit{Equation 2.4)}$$

For a normally incident wave this equation can also be expressed in terms of compressional velocity and density (*i.e.* acoustic impedance) from Zoeppritz's equation (Telford *et al.*, 1976):

$$\mathbf{R = \rho_2 Vp_2 - \rho_1 Vp_1 / \rho_2 Vp_2 + \rho_1 Vp_1} \qquad \textit{Equation 2.5)}$$

Values of **R** from this equation will range between -1 and 1; if **R** = 0 the incident energy is entirely transmitted *i.e.* there is no impedance contrast across the boundary, even if the compressional velocity and density of the two layers are different. If **R** = -1 or 1 all the incident energy is reflected this commonly occurs at the air/water interface where **R** = -0.9995 (Kearey & Brooks, 1991). Commonly values for **R** fall between ± 0.2 with the majority of the energy being transmitted. It is, however, important to understand that boundaries of strong impedance contrast need not necessarily correspond with lithological boundaries. In particular, subsurface density may vary with the liquid or gas content of a material, or indeed the degree of compaction of the sediment (Landmesser *et al.*, 1982; Davies *et al.*, 1984; Hequette and Hill, 1989; N.G.T. Fannin, 1990 *pers. comm.*).

The degree of penetration, through a medium, achieved by an acoustic wave is proportional to the rate of energy loss. This is in turn dependent on:

i) Geometrical spreading; as the wave propagates its original energy ($\mathbf{E_0}$) becomes distributed over a sphere of expanding radius. The amount of energy contained within a unit area of this sphere ($\mathbf{E_{UA}}$) can be expressed by:

Figure 2.5. Diagram Showing the Reflected and Transmitted components of an Incident Wave Striking a Boundary of High Acoustic Impedance Contrast

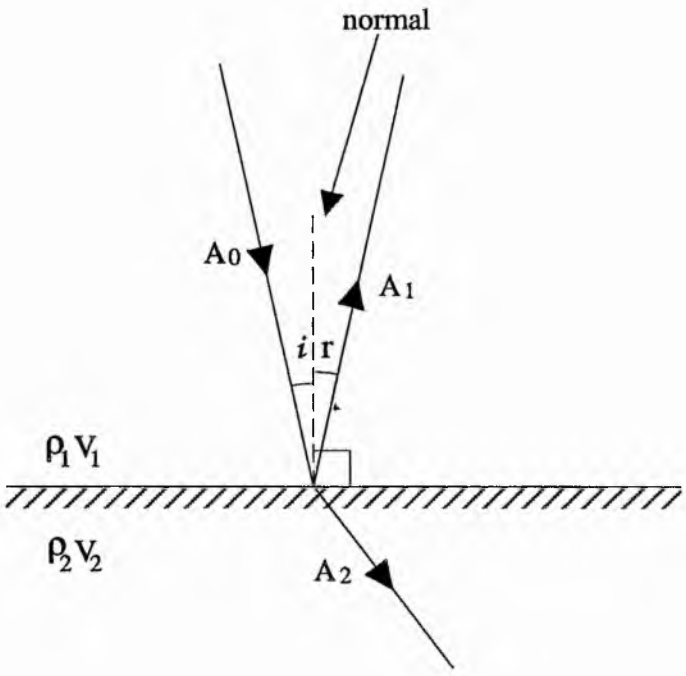

From Zoeppritz's equation we can calculate a value for the Reflection Coefficient (R) :

Assuming :

$$\rho_2 V_2 > \rho_1 V_1$$

then :

$$1 > R \geq O$$

therefore :

The majority of the orginal energy (A_0) is reflected (A_1)

Note : Energy is represented by the amplitude (A) of the individual wave components

$$E_{UA} = E_0/4\pi r^2 \qquad \textit{Equation 2.6)}$$

Consequently the energy of an individual ray will be reduced relative to r^{-2}.

ii) Internal friction losses; as energy is gradually absorbed into the medium by internal friction losses, even if an acoustic wave passed through a homogeneous medium it would still eventually disappear. The proportion of energy lost during the passage of a pulse over a single wavelength can be expressed as the absorption coefficient (α) which is measured in decibels per wavelength. The absorption coefficient can be quantitatively related to energy dissipation by:

$$\alpha = 27.3/(E_0/E_1)\ \text{dB}/\lambda \qquad \textit{Equation 2.7)}$$

Where E_0 = original energy transmitted and E_1 = energy dissipated (After McQuillin & Ardus, 1977). Common values of absorption coefficients vary between 0.25 and 0.75 dB/λ and the higher the α value the more rapidly, in terms of time and distance, the wave is attenuated.

iii) Frequency; simply lower frequency acoustic pulses achieve greater penetration than higher frequency acoustic pulses assuming the wave is travelling through a medium with constant **Vp** and α values. This is due to the fact that, as sound waves pass through successive layers, higher frequency pulses are absorbed more effectively than lower frequency ones. For example consider two waves, with frequencies (*f*) of 10 Hz and 100 Hz respectively, which are transmitted through a medium in which **Vp** = 2000 ms-1 and α = 0.5 dB/λ. The wavelength (λ) of the pulse can be calculated from the basic equation:

$$\mathbf{Vp} = f\lambda \qquad \textit{Equation 2.8)}$$

The 100 Hz wave (λ = 20 m) will be attenuated due to absorption by 5 dB over 200 m. The 10 Hz (λ =200 m) by comparison will only be attenuated by 0.5 dB over the same distance. The consequences of this frequency related attenuation are even more dramatic when you consider that the decibel scale is in fact logarithmic such that a:

$$\textbf{1 dB attenuation} = 20.\log_{10} (A_A/A_0) \qquad \textit{Equation 2.9)}$$

Where A_A = attenuated amplitude and A_0 = original amplitude, consequently an attenuation of 5 dB is equivalent to a reduction in amplitude of 50%; compared to only a 10% reduction for a 0.5 dB attenuation.

2.3.3.1. Echosounder.

For precise bathymetric surveying the Lowrance X-15^M Grayline recorder (See Figure 2.6.), with a LHT-108A transducer, was employed from the R.V. Mya. This particular model transmits and receives, from a single transducer, an acoustic pulse with a frequency of a 192 kHz. By using average figures, for acoustic absorption (0.5 dB/λ) and compressional velocity (2000 ms^{-1}), for a saturated unconsolidated sediment (After McQuillin and Ardus, 1977), a theoretical pulse wavelength of 0.01 m can be calculated from ***Equation 2.8)*** (See Section 2.3.3.). It therefore follows that the acoustic pulse will be attenuated at a rate of 50 dB/m. Since all the geophysical instruments described here are capable of resolving to $\lambda/2$ (McQuillin and Ardus, 1977), the Lowrance X-15^M can therefore theoretically identify features with minimum dimensions of 0.005 m, in a vertical plane. Equally, the rapid attenuation of the acoustic pulse makes for negligible penetration of even the most low density sediment, such that for these conditions an acoustic reduction of 40 dB occurs within 0.8 m of the surface[2].

The LHT-108A transducer is mounted within the hull of the survey vessel, the pulse being shot vertically downwards through a specially thinned section, so as to reduce any significant refraction errors as the pulse travels to and from the sea-bed. The transducer produces a pulse with an 8° cone angle, which results in the acoustic energy being concentrated in a small circular area on the sea bed (the radius of this circle being dependant on the water depth). However, the size of the area from which the receiver will actually identify reflected rays is proportionally smaller than the original insonified area. This sphere of reflection is known as the Fresnel zone and it is the width of this

[2] An attenuation of 40 dB is equivalent to a reduction in amplitude of the seismic wave to a hundredth of its original value.

Figure 2.6. The Lowrance X-15^{M} Grayline recorder.

zone which represents the absolute limit of horizontal resolution (Keary and Brooks, 1991). The diameter of the Fresnel Zone (w) is dependent on the frequency of the source pulse (described in terms of its λ, assuming either a constant or average velocity value) and the depth of the reflecting interface (**d**), such that:

$$w = (2d\lambda) \quad \text{Where } d \gg \lambda \qquad \textit{Equation 2.10)}$$

Consequently, a 192 kHz pulse (λ = 0.008 m; Calculated for an average velocity of sound through water of 1500 ms^{-1}) with a cone angle of 8° shooting on to a horizontal surface 35 m beneath the transducer would insonify a sphere of diameter 4.9 m. By comparison, the Fresnel zone for the same system would have a diameter of approximately 0.75 m. The system therefore has a horizontal resolution of 0.08 - 0.8 m (in water depths ranging from 5 - 50 m), a value significantly larger than the theoretical vertical resolution quoted earlier (0.005 m).

The pulse width of the system is automatically controlled by the echosounder, its variation depending on the setting of the lower depth limits. For the majority of the surveys the initial transmitted pulse width varied between 160 and 200 μs. These short pulse widths facilitate high-resolution along-track records, as the shorter the width of the pulse the greater the number of potential pulses that can be produced per second. In turn, the greater the number of pulses hitting a single target per second the larger the data set available for each target.

The echosounder system does not provide direct measurement of depth, but calculates a value from the recorded two-way travel time (See Section 2.3.3., ***Equation 2.1)***). The resulting dry paper trace is a permanent, two-dimensional profile of the depth changes along any one particular traverse (See Figure 2.7.). The paper speed of the Lowrance recorder is set at maximum for all surveys, in order to achieve optimum trace definition. All depths are recorded in metres, with the actual figures displayed representing the distance from the transducer to the sea-bed. Consequently, for bathymetric analysis, all values obtained must be corrected for both tidal variation and the depth of the transducer beneath the water surface (See Section 4.2.4.). This system was used extensively on the

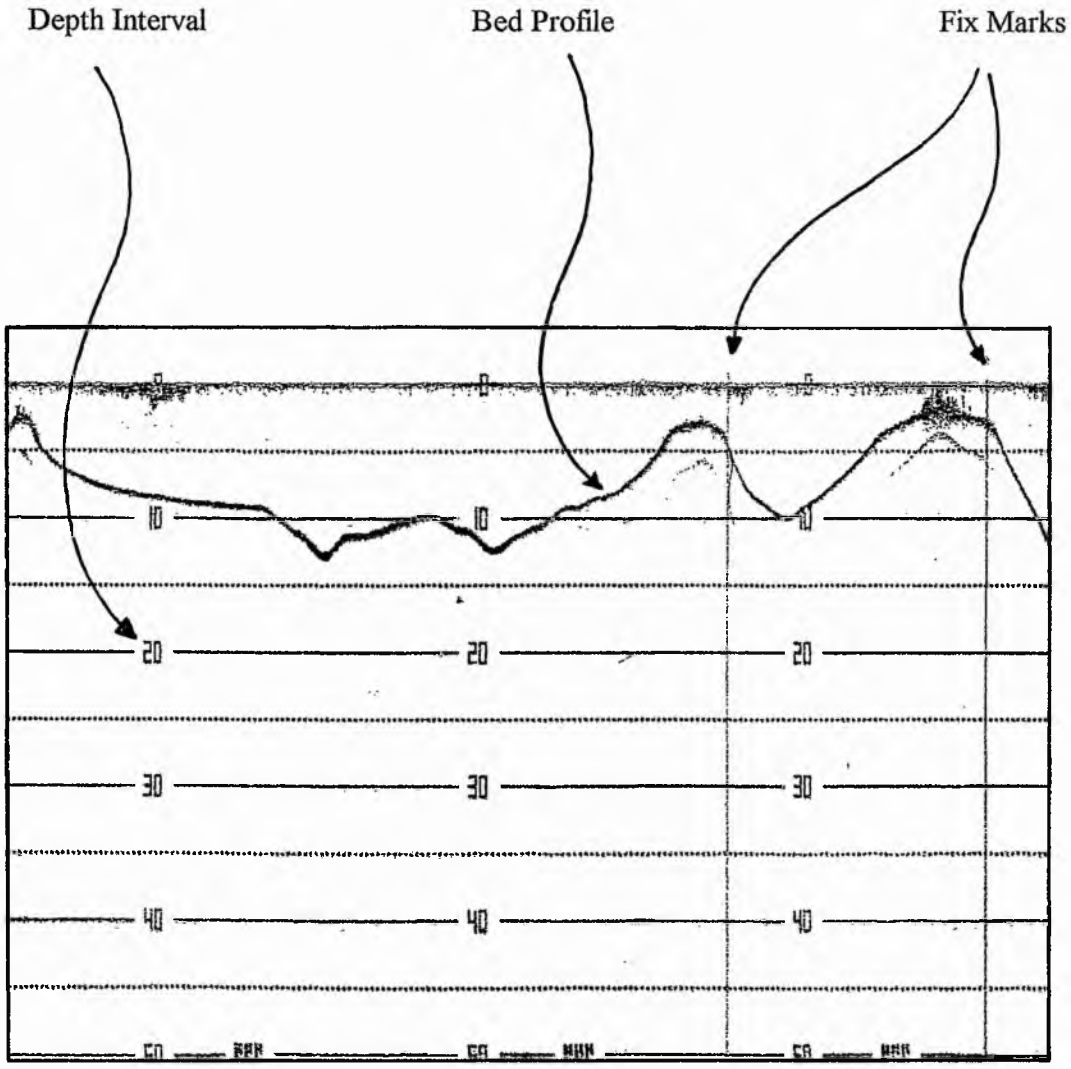

Figure 2.7.Typical two-dimensional dry paper, echosounder trace.

loch, commonly in conjunction with the pinger sub-bottom profiler (See Section 2.3.3.3.), with a total of 92.1 km of echosounder traverse lines being run.

2.3.3.2. Side Scan Sonar.

A Klein Hydroscan (Model 401) 400 kHz side scan sonar system was used as the second geophysical technique in this investigation (See Figure 2.8.), with a total of 25 km of seismic lines being shot. This technique possesses intrinsic differences from the other two systems, in that the dual-channelled transducer takes the form of a stream lined towfish deployed at distance from the survey vessel (See Figure 2.9.). From port and starboard channels, the transducer sends out pulses with large vertical beam angles (160°) but narrow horizontal beam angles (0.75°). The vertical beam is angled 10° down from the horizontal, so that the majority of the source energy is directed toward the sea floor.

This geometric configuration (See Figure 2.10.) builds up an image by laying down successive scans of the sonar on a wet paper recorder to produce a composite sepia picture, or sonograph. As a result, rather than providing individual depth or thickness values, as with the two previous techniques, an apparent three-dimensional acoustic image of the bed is produced with slant range coverage of 150 m/channel (*i.e.* 300 m total swath width). This wide ranging image results in records being produced for almost the entire loch (a total of 7.5 km^2) after only a limited number of traverse runs. The side scan system used was also capable of scanning at ranges of 75 and 300 m/channel . The 150 m/channel range was adopted as a compromise between resolution (See below) and the speed of survey completion.

The high frequency (400 kHz) and short pulse width (100 μs) signals used in all surveys again make for a high resolution seismic imaging system. The nomenclature of resolution for the side scan sonar is different to the two-dimensional techniques described in Sections 2.3.3.1. and 2.3.3.3.. Resolution is described for both a transverse ($\mathbf{R_T}$) and a range (**Rv**) dimension. The transverse resolution represents the minimum distance between two targets, parallel to the line of travel, such that the targets can be recorded on the sonograph as separate objects. This is equivalent to the intersection of the

Figure 2.8. The recording unit of the Klein Hydroscan (Model 401) 400 kHz side scan sonar system.

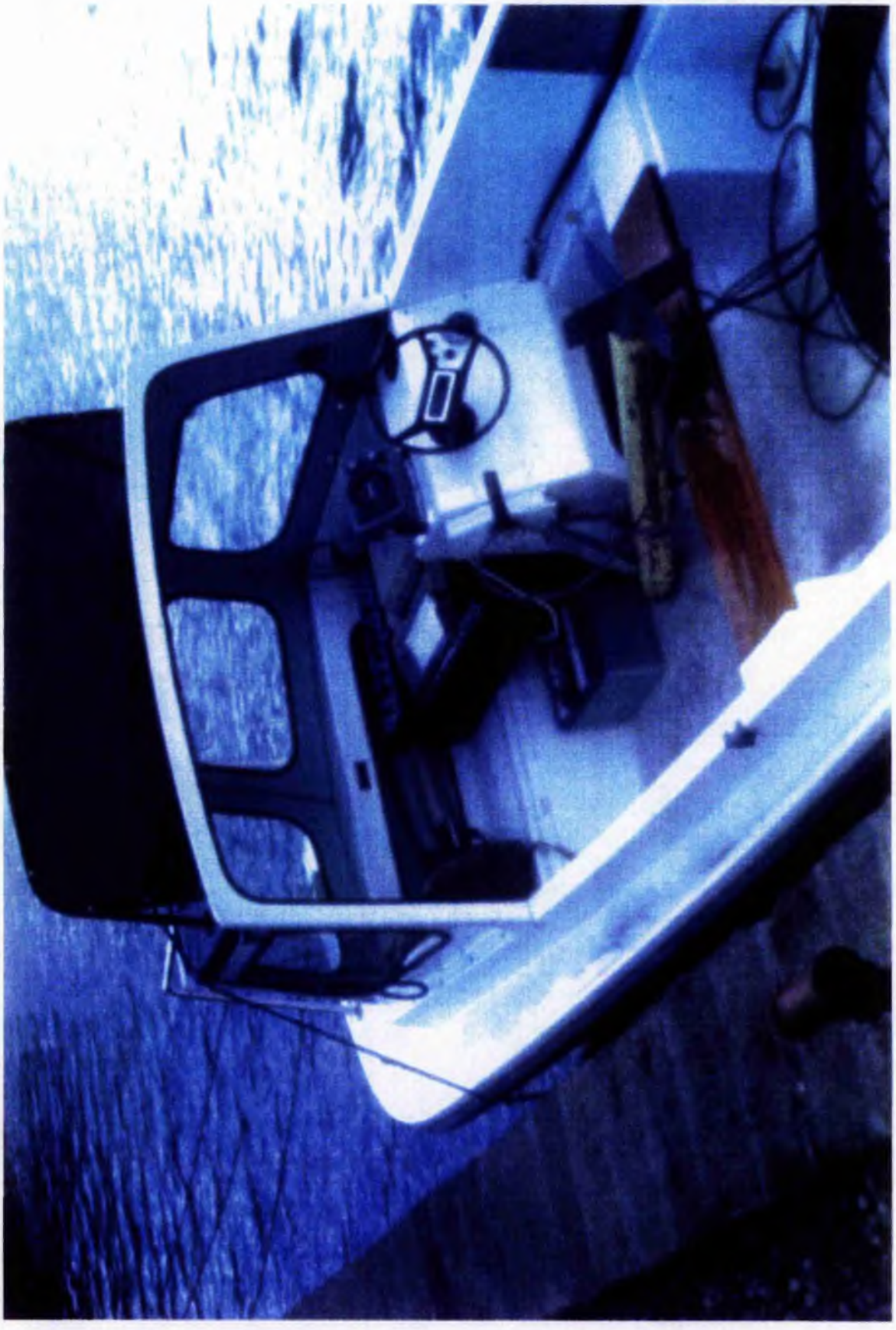

Figure 2.9. The dual-channelled side scan transducer in the form of a stream lined towfish.

Figure 2.10. Sketch Diagrams to Show the Wide Vertical and Narrow Beam Configuration for the Side Scan Sonar

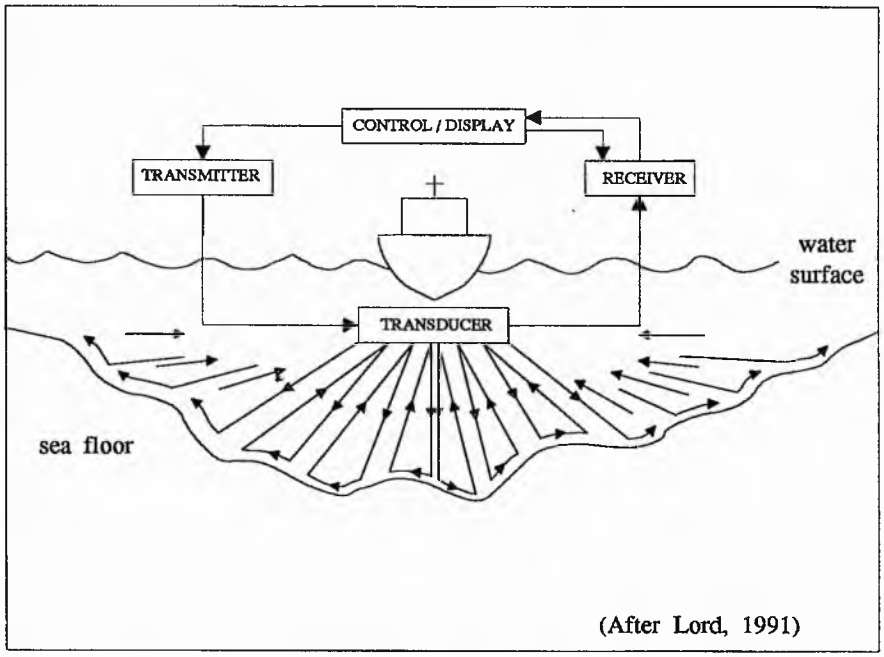

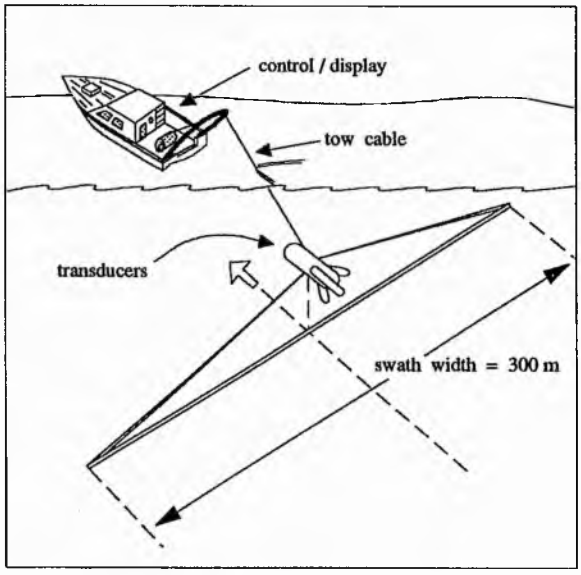

horizontal beam width of the pulse with any point on the sea bed and is equivalent to the Fresnel Zone described in Section 2.3.3.1. (***Equation 2.10)***). The transverse resolution can be calculated as follows:

$$R_T = \sin B_{HA} \times R \qquad \textit{Equation 2.11)}$$

Where B_{HA} = Horizontal Beam Angle and R = range to target. For example, at the maximum range used during this survey (150 m), R_T = 1.96 m. As the range decreases the beam width decreases and the transverse resolution will improve such that, at a range value of only 5 m, the R_T value is only 0.07 m.

The range resolution (R_V) represents the minimum distance between two objects perpendicular to the line of travel which can be recorded on the trace as separate objects. The minimum separation detectable depends up on the pulse width and the speed of sound through water:

$$R_V = P_W \times V_{pw} \qquad \textit{Equation 2.12)}$$

Equation 2.12) therefore defines the area of insonification and thus the maximum R_V, so for the Klein Hydroscan with; P_W = 100 μs, V_{PW} = 1500 ms^{-1} theoretical R_V = 0.0015 m. These values of R_T and R_V represent theoretical limits for resolution and actual detectability is a different concept with the primary control being the actual dimensions of the sonograph.

Assuming a minimum spacing of 0.5 mm on the sonograph is required to plot two objects separately, the limit of detection in a perpendicular direction will be 1/250 of the range scale, as the width of the trace per channel is 125 mm. So for a maximum range value of 150 m/channel the real range resolution (R_{RV}) is re-calculated as:

$$R_{RV} = 150/250 = 0.6 \text{ m} \qquad \textit{Equation 2.13)}$$

As the original sonographs record the along track dimensions in survey time they have to be post processed in order to obtain true distance values in metres (See Section 5.2.4.

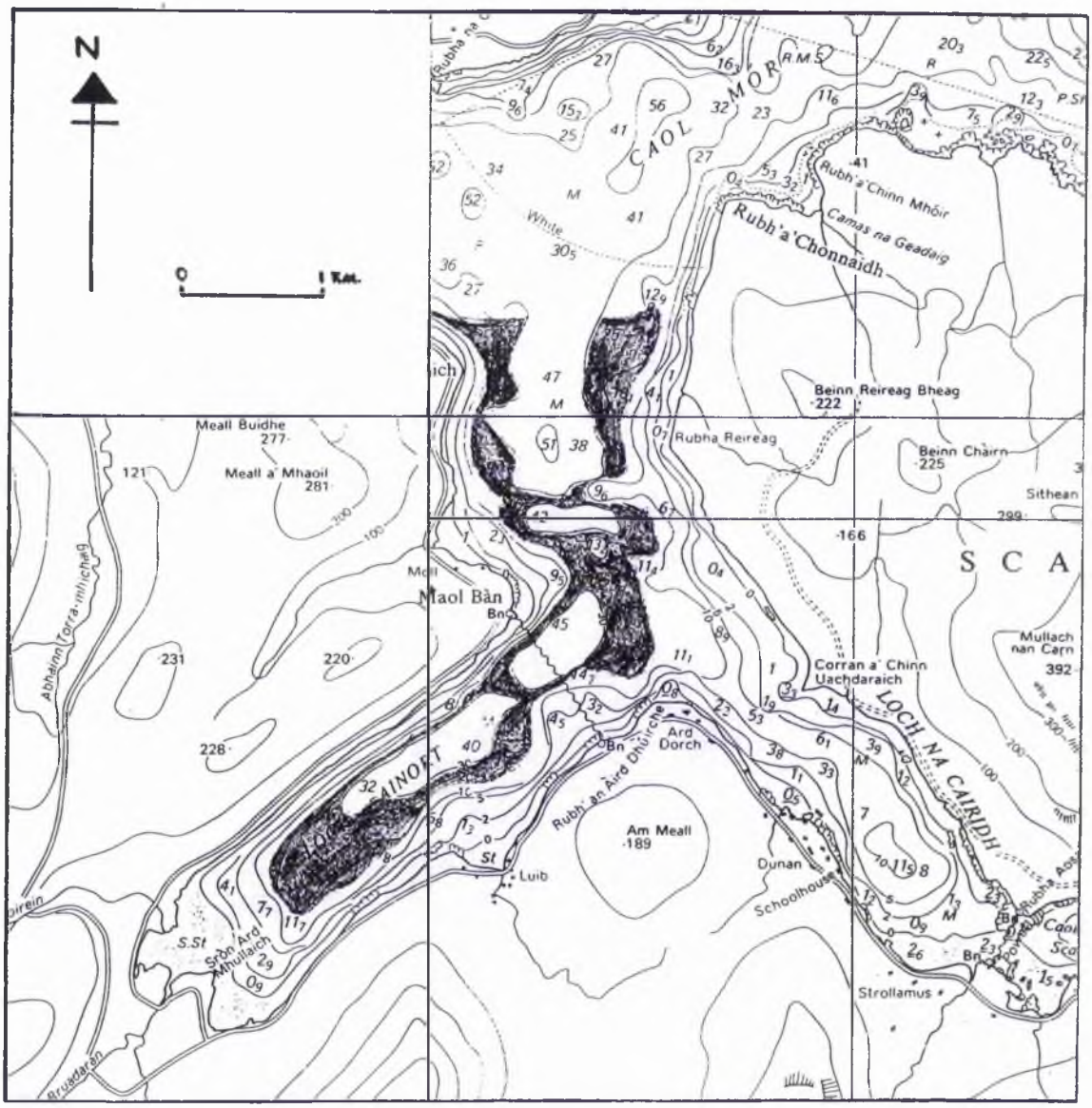

Figure 2.11. The area of optimum resolution conditions for the side scan sonar survey in Loch Ainort.

and 5.2.6.). Consequently, the true metric distance represented by any one minute interval will be determined by the speed of the vessel over the ground and the paper speed of the Klein recorder. Assuming a constant paper speed throughout the survey such that a minute interval on the trace represents 100, an average survey speed of 3.5 knots (1.75 ms^{-1}; 105 $m.min^{-1}$) is maintained and the minimum spacing between objects on the sonograph is again 0.5 mm, the real transverse resolution ($\mathbf{R_{RT}}$) can be recalculated as:

$$\mathbf{R_{RT} = 105/200 = 0.525\ m} \qquad \textit{Equation 2.14)}$$

As described above, as the beam width increases away from the fish, this new value for transverse resolution ($\mathbf{R_{RT}}$) will only be valid for the first 40 m (in a direction perpendicular to the fish) after which it will be exceeded by the theoretical value ($\mathbf{R_T}$) calculated for the system. As will be discussed in greater detail in Section 5.2.4. if the survey speed increases, resolution will decrease, with the $\mathbf{R_{RT}}$ value exceeding that of $\mathbf{R_T}$ for the entire width of the sonograph at an approximate survey speed of 13 knots (6.5 ms^{-1}).

In operation the fish should be suspended at an optimum height above the bed of approximately 10 - 20% of the selected scanning range (Williams, 1982). At the 150 m/channel range this would be equivalent to towing depths 15 - 30 m above the bed. Due to the irregular topography of the floor of Loch Ainort it was impractical to continually alter the depth of the fish, so the transducer was towed at a consistent distance of 2 m from the transom of the boat and at a depth of 1.5 m. Consequently, optimum resolution conditions were restricted (See Figure 2.11.: the shaded area represents optimum conditions). However, the sonographs that were obtained from the area are of a very good quality. Due to extensive acoustic interference and actual spatial considerations on board the survey vessel it is regarded as inadvisable to simultaneously operate the side scan sonar with either the echosounder or the sub-bottom profiling equipment.

2.3.3.3. Sub-bottom Profiler (Pinger).

Continuous sub-bottom profiles were obtained by means of a GIFFT-ORE 3.5 kHz pinger system. The acoustic signal is transmitted and received from a "two-pot" piezoelectric transducer suspended underwater, at a depth of approximately 0.75 m, from the transom of the survey vessel (See Figure 2.12.). The transducer is orientated such that the signal is directed vertically downwards, in order to receive a "true" undistorted image of the sea-bed. This device produces a focused beam with a cone angle of 30° and a pulse width of 500 μs. The transducer is connected to a wet paper GIFFT recorder (See Figure 2.13.) which produces a two-dimensional, permanent sepia trace (See Figure 2.14.).

Applying the same figures for acoustic absorption (α) and compressional velocity ($\mathbf{V_p}$), used to show the operational parameters of the echosounder (See 2.3.3.1.), theoretical pulse wavelength and acoustic attenuation values can be calculated. These are respectively 0.57 m and 0.875 dB/m. Consequently, it is possible to calculate the depth at which a 40 dB reduction of the acoustic pulse is achieved. Under these conditions this occurs at a depth of 45 m. It is therefore evident that, although resolution is reduced such that objects with a minimum vertical dimension of only 0.30 m can be identified, penetration of sub-surface units is possible. Comparison of this value with the theoretical vertical resolution calculated for the high-frequency echosounder (0.005 m; Section 2.3.3.1.) emphasises the trade-off between decreasing resolution and increasing penetration.

Similarly applying ***Equation 2.10***), derived in Section 2.3.3.1., it is also possible to compare insonified and Fresnel zone widths for any pre-defined system geometry. For these calculations an averaged velocity value for the complete water - sediment column has to be estimated, *e.g.* $\mathbf{V_p} = 1750\ ms^{-1}$. Again as in Section 2.3.3.1. we can calculate on the basis of 35 m between transducer and reflecting interface. However, on this occasion this distance represents a reflection from a horizontal sub-surface layer at 15 m depth, beneath a 20 m water column. For this set of parameters the insonified sphere would have a diameter of 18 m and a Fresnel zone diameter of 5.9 m. Comparison of the Fresnel diameter (*w*) for the two systems (0.75 m *vs* 5.9 m) again shows a significant

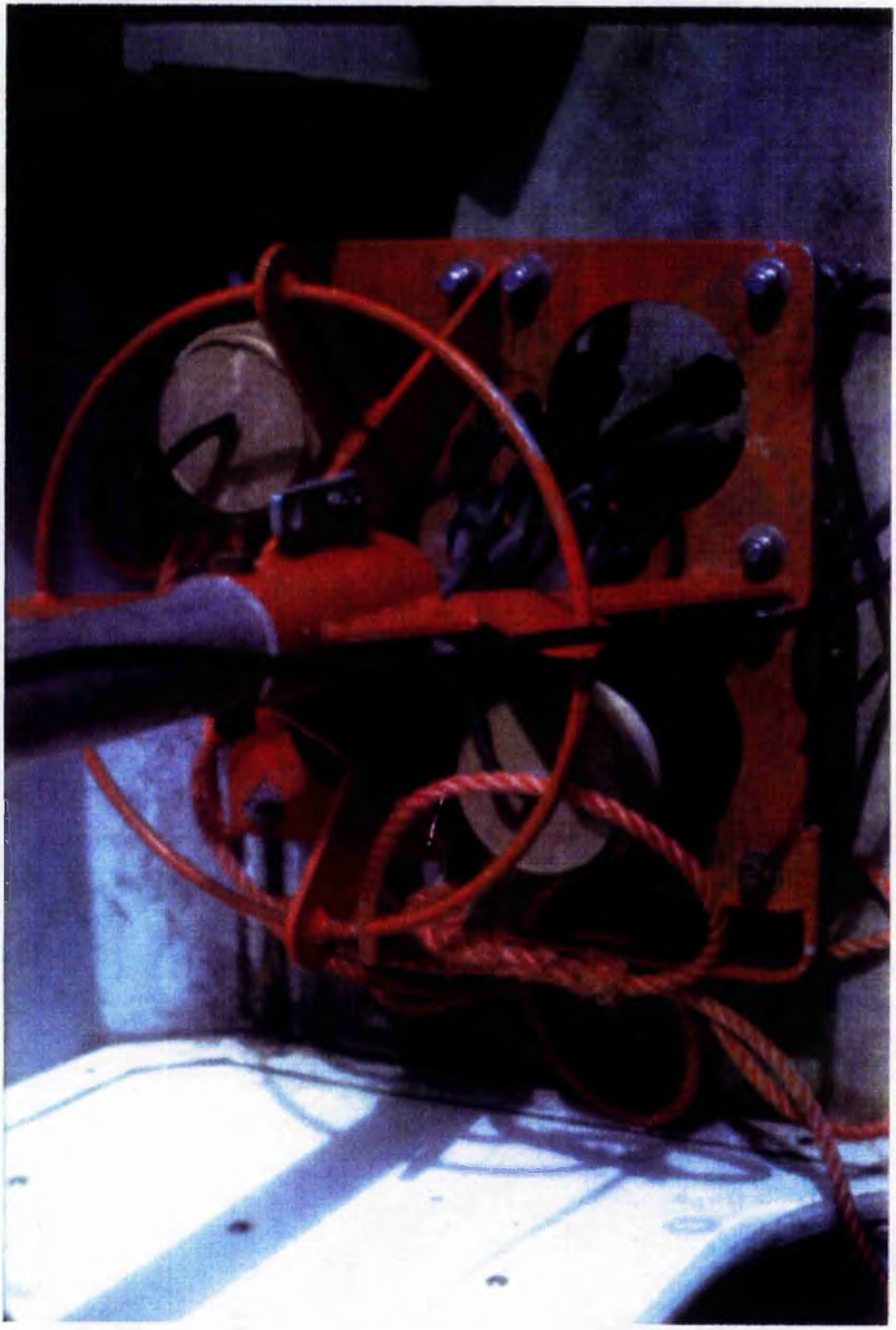

Figure 2.12. The two-pot piezoelectric transducer used during the GIFFT-ORE 3.5 kHz pinger surveys

Figure 2.13. The GIFFT wet paper recorder in operation.

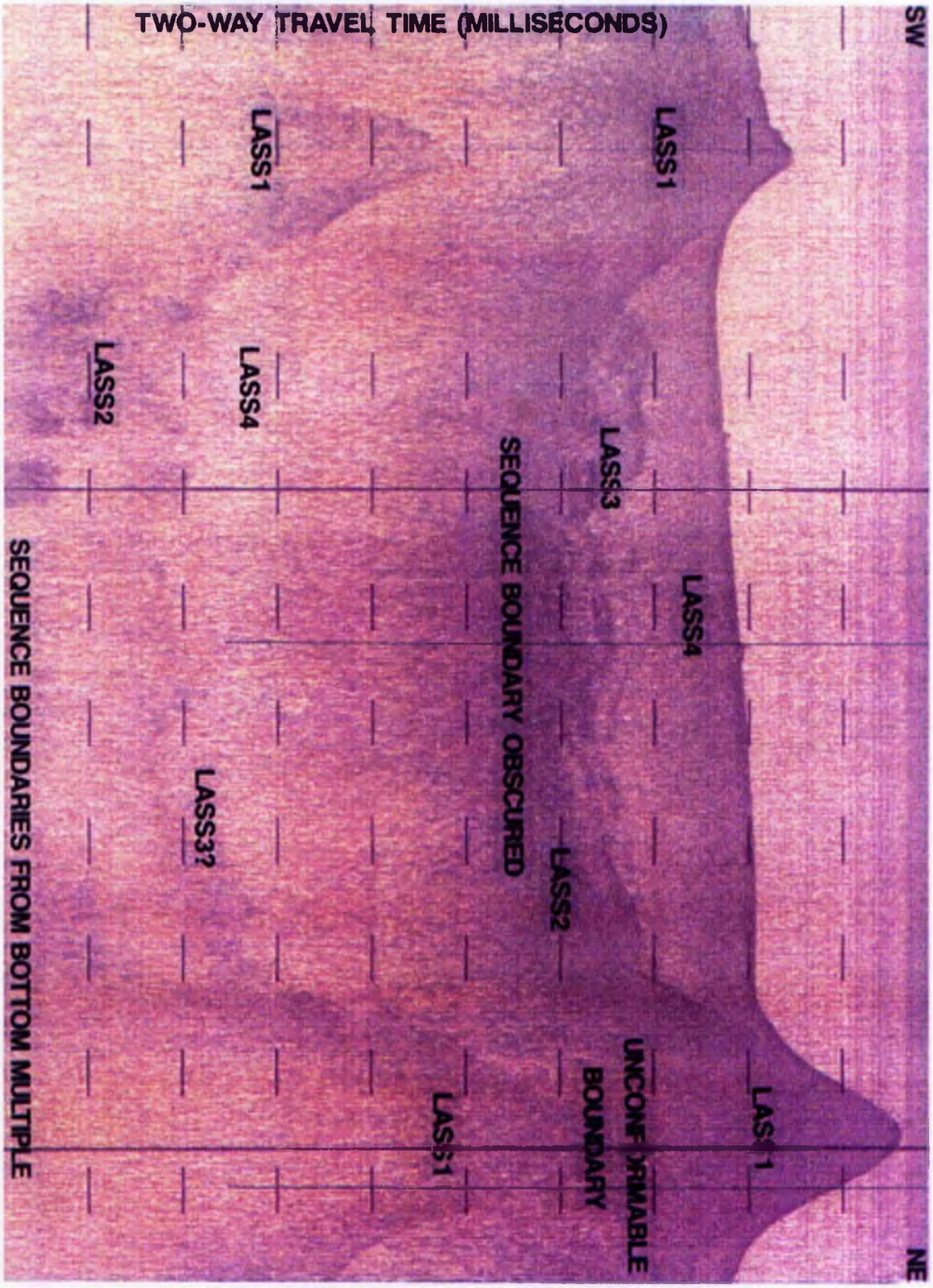

Figure 2.14. A typical two-dimensional permanent sepia pinger trace (A10).

reduction in resolution, but in the horizontal plane. The reduction of the horizontal resolution is further accentuated by the longer pulse width, and corresponding decrease in pulses produced per second, of this system

Again this system does not display direct measurement of depth and penetration, but a vertical scale that represents two-way travel time in milliseconds (See Figure 2.14.). Unlike the echosounder there is no easy conversion to depths in metres as the velocity value for each depth increment may be continually changing according to the nature of the sub-bottom deposits. As a result, all figures quoted in this text are given in milliseconds, unless otherwise stated. True depth sections are only given following comparisons of the seismic stratigraphy derived from the pinger traces with velocity analysis of the cored stratigraphic sections. A total of 79 km of pinger traverse lines were run within Loch Ainort.

2.4. CORING.

In order to provide a lithological control for the interpretations made from the different geophysical techniques described in Section 2.3.3., it is necessary to obtain surface and sub-surface samples from the loch floors. In Loch Ainort this was achieved by the use of a gravity corer. Ideally gravity corers "... should be avoided or cores from them treated with caution for physical property studies or any works which require precise data on the depths of boundaries within the sediment." (Weaver and Schultheiss, 1990). Such corers are also incapable of penetrating and recovering more than a few centimetres of sediment with a grain size greater than 125 μm, as well as being notorious for destroying original sedimentary structures and causing massive internal displacements (Sly, 1981). However, Weaver and Schultheiss (1990) do suggest that such corers represent an inexpensive and simple method of sediment retrieval. In addition they are considered as being capable of taking high-quality cores from the upper few metres of the sea floor, subject to the two main sampling errors. Mis-sampling may occur due to either sediment plugging within the core barrel or repenetration caused by the vertical oscillation of the ship's boom arm

(Weaver & Schultheiss, 1983). Both of these errors result in the shortening of the sedimentary record they sample. Little or no shortening occurring in the top 0.5 m but this increases with the length of the core recovered (Weaver & Schultheiss, op. cit.). Despite these reservations, due to financial considerations and the unavailability of other BGS apparatus, a 300 kg gravity corer was employed from the Carron Highlander (See Section 2.3.1.).

The 300 kg lead weight is fitted with interchangeable 3 m and 1.8 m core barrels, which contain plastic liners for retention of the sediment core and a 6 cm diameter cutting head. A single passage "finger-catcher" is placed within the core barrel, sandwiched between the plastic liner and the cutting head, in order to retain the sediment within the barrel (See Figure 2.15.). The entire apparatus was operated from a 500 kg capacity boom arm (See Figure 2.16.). The corer was initially lowered in a controlled manner to a depth of approximately 10 m above the loch floor, this position being identified from echosounder traces which were recorded throughout this operation. At this depth, the corer was left suspended for between 2 and 5 minutes in order to further stabilise the system and so again limit the degree of oscillation of the barrel about the vertical. The corer was then released and allowed to free-fall for the remaining distance. This 10 m height represents the minimum condition at which the weight may reach its terminal velocity. Consequently, this reduces the possibility of excessive oscillation of the corer, which is anticipated during long free-fall drops (Sly, 1981). The corer was returned to the surface by means of a hydraulic winch, and the liner and any sediment removed from the barrel. On occasion, over-penetration of the corer was such that material was actually retained on the surface of the core weight or conversely penetration was insufficient for the material to be retained within a core barrel. In both cases this material was kept and described as "surface sediment samples". However, the exact depth from which these samples came is unknown.

From a total of 21 pre-determined sites, material was retrieved from 19. Sediment was collected in the form of 14 cores and 7 surface sediment samples, one surface sample duplicating the corresponding core site (See Figure 2.17.). Navigational control was again provided by the Magellan© GPS system (See Section 2.3.2.2.). The individual cores were

Figure 2.15. A Sketch Diagram to Show Cutting Head - Catcher - Core Barrel Relationship for the 300 kg Gravity Corer

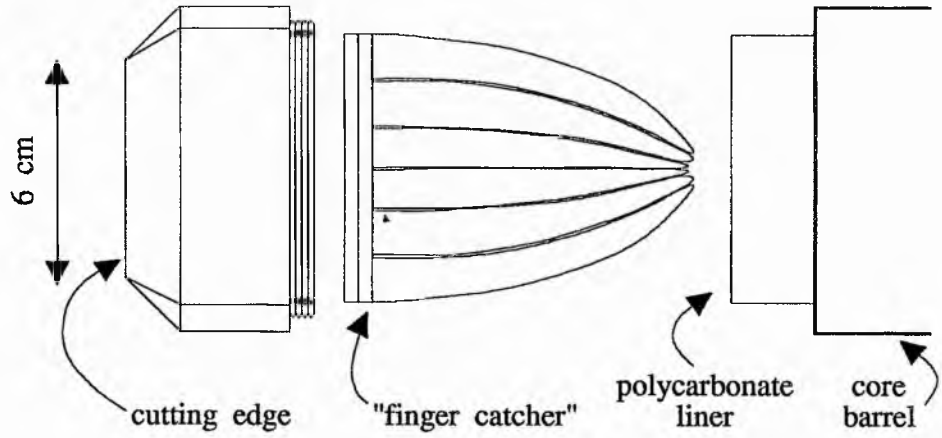

Figure 2.16. The entire coring apparatus operated from the 500 kg capacity boom arm from the Carron Highlander.

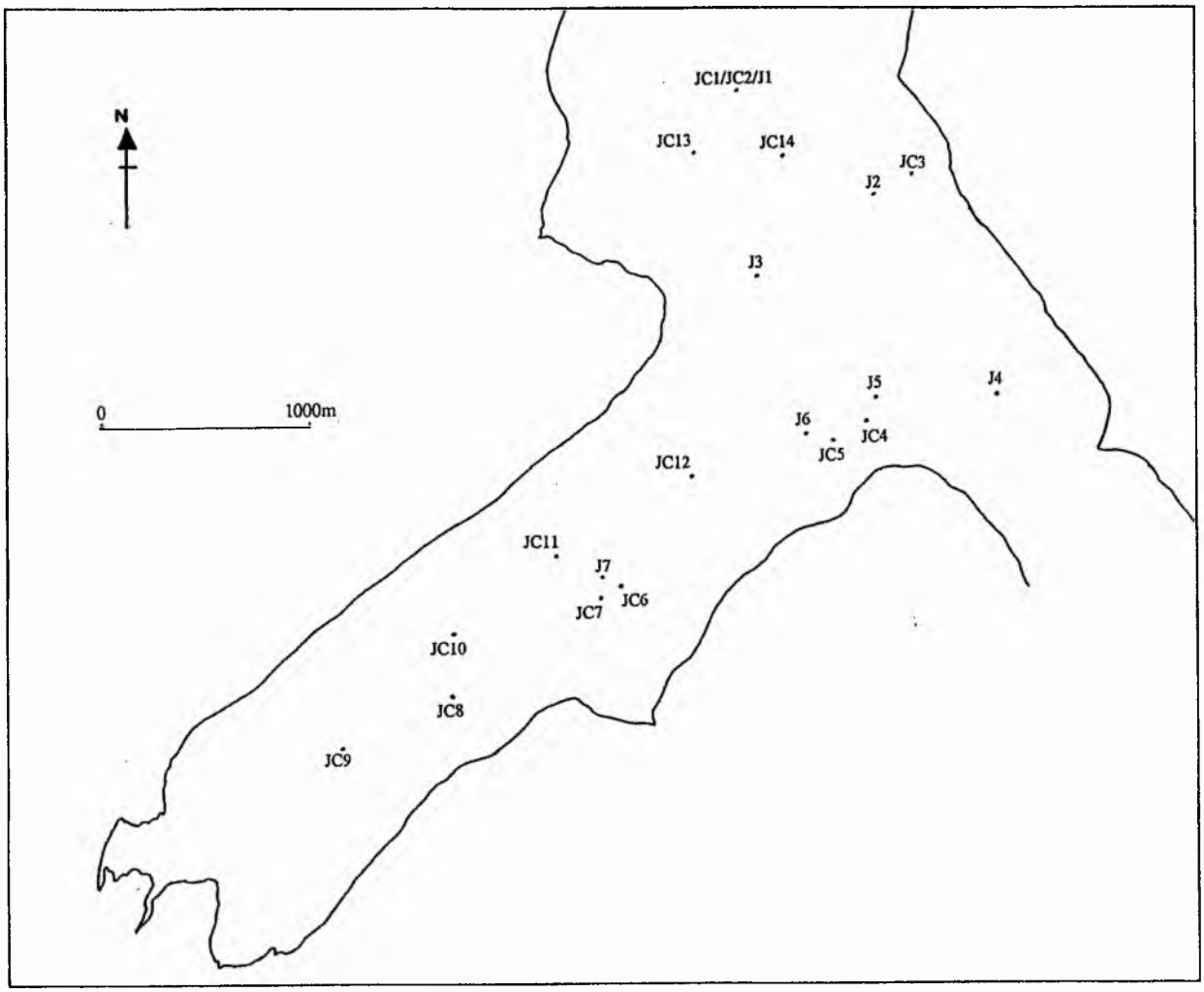

Figure 2.17. The nineteen sites from which core material (prefix JC) and surface sediment samples (prefix J) were acquired. Both within and outwith loch sites were chosen to provide calibration of the primary seismic facies units identified from the geophysical surveys (See Chapters 5 and 6).

contained within the liners by a sequence of wet rags, plastic caps and heavy duty tape, in order to prevent excessive water loss during transport. On immediate return to St. Andrews all the sealed cores were placed in a cold store, which is maintained at a constant temperature of 5°C.

CHAPTER 3

3. CATCHMENTS AND BASINS

3.1. INTRODUCTION

The nature of the catchment and basin area adjacent to any water body under investigation provides an essential physical structure with which any offshore, palaeo-environmental reconstruction must interface. Any offshore study using remote sensing techniques (even when correlated with sediment samples) can provide information for only the broadest of environmental interpretations, due to the lack of any *in situ* data. By contrast, onland reconstructions, whilst still at the mercy of personal interpretation, are based on *visible* physical evidence. It is logical to conclude that, assuming a rigorous scientific approach is employed to onland investigations, such data can provide reasonable, albeit not infallible, primary models. Therefore, it is most important to refer to these models, in order to assess the plausibility of their own reconstructions. At the same time, however, offshore workers must be careful not to let any pre-existing models unnecessarily prejudice their own final interpretations. Thus Chapter 3 gives brief geological and geomorphological summaries which together provide a primary model for the Loch Ainort study area.

3.2. LOCH AINORT

Loch Ainort is situated on the eastern coast of the Isle of Skye (57°00' - 57°42'N; 5°58'-6°47'W), the largest island of the Inner Hebrides group, which lie off the western seaboard of Scotland (See Figure 3.1a). The loch, from head to mouth, is 4.25 km long and has a maximum width, at the mouth, of 1.2 km. The loch trends north-eastwards and opens out into an unnamed basin confined to the east by the Island of Scalpay (See Figure 3.1b). This basin, and hence Loch Ainort, have open connections to the Inner Sound (the major channel separating Skye and the mainland) via the Sound of Raasay and Caol Mòr in the north and via

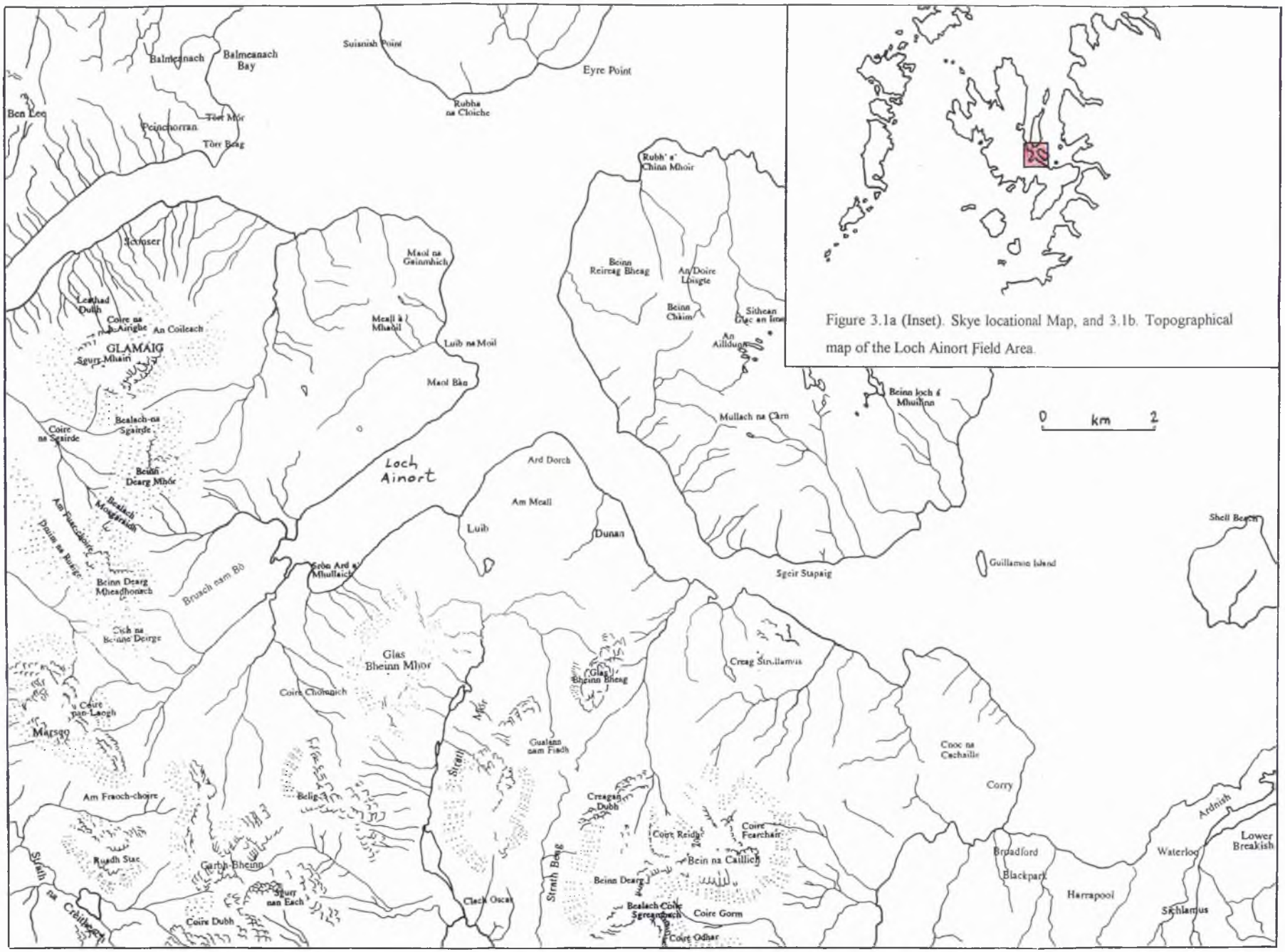

Figure 3.1a (Inset). Skye locational Map, and 3.1b. Topographical map of the Loch Ainort Field Area.

Loch na Cairidh in the south[1]. The loch and these adjacent waters function as a receptor basin for the small Ainort catchment, which covers a total area of 27 km². However, the waters of Loch na Cairidh and the unnamed deep also receive input from Coire Mòr and the slopes of Meall a' Mhaoil to the north (3 km²), from Garbh-allt and Allt Strollamus to the south (7 km²) and the majority of the western coast of Scalpay (6 km²). The geomorphological nature of the surrounding land mass is controlled by the underlying geology and the effects of numerous glacial episodes.

3.2.1. GEOLOGY

The geology of the Loch Ainort area is characterised by rocks belonging to two volcanic centres and a regional linear dyke swarm, both of which have been created by activity related to magmatism in the British Tertiary Igneous Province[2]. These two centres, the Western and Eastern Red Hills (See Sections 3.2.1.2. and 3.2.1.3. respectively), are represented by a suite of acidic, basic and hybridised igneous rocks which have been intruded into a sequence of Pre-Tertiary lithologies (See Section 3.2.1.1.). These two centres of volcanic activity were predated by two other subvolcanic centres, the basic/ultrabasic Cuillin Complex and the acidic Srath na Creitheach Centre, which lie to the west of the field area. The central intrusive activity occurred over a protracted period (*c.* 5 m.y.) between *c.* 60-55 Ma yr BP, in response to the initiation of rifting in the North Atlantic Ocean.

The associated extrusive plateau lava pile (See Section 3.2.1.4.) covers a large portion of northern Skye (albeit fragments are found in southern Skye including the field area), with eruption commencing at *c.* 59 Ma BP and continuing, intermittently, over a long period of time. The Skye dyke swarm (See Section 3.2.1.4.) developed during the formation of the lava pile and the intrusive centres, its orientation being controlled by the regional stress fields set up during this period of igneous activity. For the swarm as a whole, the maximum compressive stress was horizontal and parallel to the swarm (a north-west to south-east

---

[1] The size of the channel connecting Loch na Cairidh with the Inner Sound (Caolas Scalpay) fluctuates with the state of the tide. However, a through flow of water is retained at all times.

[2] Alternatively termed the Thulean (North Atlantic) igneous province.

orientation) with minimum stresses acting perpendicular to this direction. The remnants of magmatism and volcanic activity which occurred in this part of central and southern Skye, represent a failed attempt at rifting and ocean floor spreading. However, separation of the continental crust finally occurred 500-1000 km further west of the Scottish mainland. The volcanic centres of the British Tertiary Igneous Province therefore moved laterally away from the area of active mantle up welling and, as a result, volcanism ceased.

A large number of different authors have worked on all aspects of the geological history of the Isle of Skye. An excellent synthesis of this work has been written by Bell & Harris (1986) and it is from this text that this summary of the Loch Ainort area has been taken, unless otherwise referenced.

3.2.1.1. Pre-Tertiary Lithologies.

The country rocks into which the volcanic centres of the Western and Eastern Red Hills were intruded have only fragmentary exposure within the Loch Ainort field area. Of the exposures that do exist, these are dominated by sediments of a pre-Tertiary age. The only materials of a non-sedimentary nature are seen in minor outcrops of deformed, steeply dipping, banded Lewisian gneisses exposed at Creagan Dubh on the northern slopes of Beinn Dearg Mhór (See Figure 3.2). This inlier of gneiss has a faulted contact to the north-west against Jurassic strata and is unconformably overlain by basic lavas of Lower Tertiary age.

Pre-Tertiary sediments within the catchment area are confined to outcrops around Strollamus, the northern shores of Maol na Gainmich and the island of Scalpay. These sequences are represented by a variety of lithologies, of Torridonian, Jurassic and Cretaceous age. Lower Torridonian strata of the Diabaig Formation dominate, outcropping in the area between Maol na Gainmich and Sconser on the mainland, and throughout the island of Scalpay (See Figure 3.2). These sequences consist of fine-bedded sandstones and arkoses with subordinate siltstones and coarse sandstones, with overall dips for these units ranging between 20° and 50° to the east and north. Internal structures, where present, are in the form of crossbeds, dewatering structures and visibly obvious magnetite rich-layers.

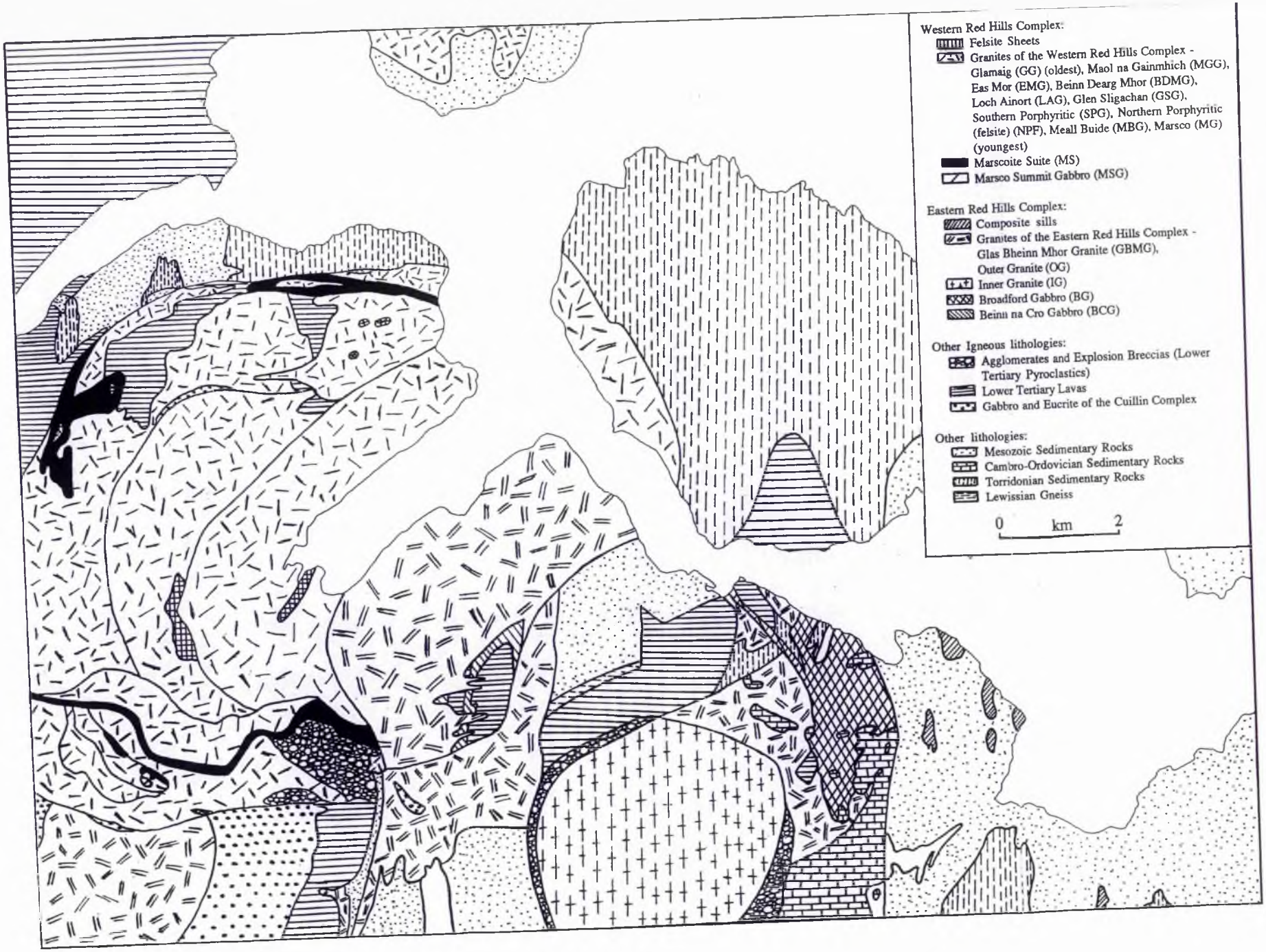
Western Red Hills Complex:
Felsite Sheets
Granites of the Western Red Hills Complex - Glamaig (GG) (oldest), Maol na Gainmhich (MGG), Eas Mor (EMG), Beinn Dearg Mhor (BDMG), Loch Ainort (LAG), Glen Sligachan (GSG), Southern Porphyritic (SPG), Northern Porphyritic (felsite) (NPF), Meall Buide (MBG), Marsco (MG) (youngest)
Marscoite Suite (MS)
Marsco Summit Gabbro (MSG)
Eastern Red Hills Complex:
Composite sills
Granites of the Eastern Red Hills Complex - Glas Bheinn Mhor Granite (GBMG), Outer Granite (OG)
Inner Granite (IG)
Broadford Gabbro (BG)
Beinn na Cro Gabbro (BCG)
Other Igneous lithologies:
Agglomerates and Explosion Breccias (Lower Tertiary Pyroclastics)
Lower Tertiary Lavas
Gabbro and Eucrite of the Cuillin Complex
Other lithologies:
Mesozoic Sedimentary Rocks
Cambro-Ordovician Sedimentary Rocks
Torridonian Sedimentary Rocks
Lewissian Gneiss
0 km 2

Exposures of Jurassic sediments also have a restricted distribution, cropping out around Strollamus and on the southern shore of Scalpay, between Rubha Aosail Sligneach and Sgeir Stapaig (See Figure 3.2). The majority of these sediments are members of the Berreraig Sandstone Formation and the Great Estuarine Group, which are both of Middle Jurassic age (U.Toarcian to U.Bathonian). The Berreraig Sandstone Formation consists of calcareous sandstones interbedded with siltstones and shales rich in calcareous concretions. By comparison the Great Estuarine Group in this area is represented by indurated black shales interbedded with thin blue limestones, the sequence dipping 40° - 50° to the south-east. Between Allt Apoldoire and Allt Eoghainn on the mainland and at the exposures on Scalpay, small outcrops of Upper Jurassic and Upper Cretaceous sediments are located (See Figure 3.2). Highly fractured and indurated rocks of the Staffin Shale Formation, dipping at *c.* 20° to the north-east, are overlain by calcareous sandstones and chalk of Cenomanian - Maestrichtian age.

All of the Jurassic units have undergone thermal metamorphism associated with the intrusion of the deep seated magmatic chambers that fed the Tertiary volcanic centres. As a result the sandstones, calcareous sandstones and limestones of the Berreraig Sandstone Formation have been metamorphosed to quartzites and calc-silicate bearing marbles. This episode of thermal metamorphism is also responsible for the baking and fracturing of the fine grained sediments of the Great Estuarine Group and the Staffin Shale Formation.

3.2.1.2. Western Red Hills Centre.

The Western Red Hills Centre occupies the majority of the ground to the north and west of Loch Ainort, including the summits of Glamaig, Beinn Dearg Mhór, Beinn Dearg Mheadhonach, Marsco and the northern slopes of Belig and Garbh-bheinn. This centre covers a total area of 35 km^2 and is dominated by annular acid intrusions of granite, granophyre and felsite. In addition to the acidic components, early basic fractionates (Marsco Summit Gabbro) and a variety of hybridised rocks (Marscoite Suite) are also present.

Intusive Event	*Rock Type*	*Locality*
Dyke	Dolerites and aplites. See Section 3.2.1.4.	See Section 3.2.1.4.
Marsco Granite (MG)	Plagiophyric fayalite ferohedenbergite granitess and granophyres.	Outcrops on south and west side of Marsco.
Meall Buidhe Granite (MBG)	Plagiophyric ferohedenbergite amphibole microgranites and granophyres.	Intruded into Marscoite suite, cropping out between Meall Buidhe and Abhainn Torra-mhichaig.
North Porphyritic Felsite (NPF)	Porphyritic felsites	Crops out to the south of Meall Buidhe covering an area of 2 km^2
Marscoite Suite (MS)	Marscoite, ferrodiorite, glamaigite, felsite and andesite.	Out crops as a discontinuous ring dyke from Marsco to Coire Choinnich. As an inclined sheet south-west of Glamaig. As an intrusion between Meall Buidhe and Abhainn Torra-mhichaig. On the Moll shore as a steep ring-dyke
South Porphyritic Granite (SPG)	Porphyritic felsites, microgranites and granophyres.	Exposed in a broad tract to the north of Marsco, between Mam à Phobuill and Allt à Mheadoin. Also crops out on the slopes of Marsco to the south of the Marscoite intrusion.
Glen Sligachan Granite (GSG)	Alkali feldsparphyric fayalite microgranite.	Has a limited outcrop on the north-west side of Marsco in Harker's Gully.
Loch Ainort Granite (LAG)	Alkali feldsparphyric fayalite ferohedenbergite granophyres.	A roughly L-shaped out crop on the low ground around the head of Loch Ainort, between Maol Ban and Coire Choinnich.
Beinn Dearg Mhor Granite (BDMG)	Alkali feldsparphyric fayalite ferohedenbergite granophyres.	Outcrops on Beinn dearg Mhor, Beinn Dearg Mheadhonach and Ciche na Beinne Deirge.
Eas Mhor Granite (EMG)	Alkali feldsparphyric amphibole granophyres.	Outcrops on the north-west slopes of Glamaig.
Maol na Gainmich Granite (MGG)	Arfevedsonite granites.	Crops out north of Loch Ainort between Ceann a' Chreagain and the coast.. Also outcrops on the south-west coast of Scalpay.
Glamaig Granite (GG)	Plagiophyric hastingsite biotite granites and granophyres.	Covers a broad tract from Glamaig to Marsco.
Marsco Summit Gabbro (MSG)	Olivine gabbro (altered).	Caps the summit of Marsco.
Belig & Meall a' Mhaoil Vents	Polymitic agglomerates.	Northern slopes of Belig and the summit of Meall a' Mhaoil.

Table 3.1.: The intrusive events, characteristic rock types and geographical distribution of the Western Red Hills Centre. Intrusive events young upwards with abbreviations corresponding to Figure 3.2. (After: Bell, 1976; Bell and Harris, 1986).

Due to this wide compositional variety and the complexity of its intrusive history, the rocks of the Western Red Hills Centre are summarised in Table 3.1.(See Previous Page). To the north and west the rocks of this centre intrude into a variable sequence of Pre-Tertiary sedimentary lithologies (See Section 3.2.1.1.). To the south and south west they cut the outer margins of the pre-existing Cuillin Complex and the Srath na Creitheach Centre (See Section 3.2.1.). To the east these rocks are truncated by the first of the Eastern Red Hills acid intrusions, the Glas Bheinn Mhór Granite (See Section 3.2.1.3.).

3.2.1.3. Eastern Red Hills Centre

The Eastern Red Hills Centre is the last of the four recognised sites of subvolcanic activity to be found on Skye. The centre occupies the ground between Loch Ainort in the north-west and Heast in the south and includes the topographical highs of Glas Bheinn Mhòr, Beinn na Cro, Glas Bheinn Bheag and the triple ridge of Beinn na Caillich, Beinn Dearg Mhór and Beinn Dearg Bheag. It covers a total area of 40 km^2 and is dominated by a series annular acid intrusions centred on the Inner Granite around Beinn na Caillich. As with the intrusion history of the Western Red Hills Centre the main period of acid activity was preceded by the intrusion of basic, unlayered gabbros (represented in the field area by the Beinn na Cro Gabbro). Unlike the Western Red Hills Centre these two events were pre-dated by a hybrid intrusion, the Kilchrist Ring-dyke. However, these rocks have a restricted outcrop being confined to the south of this centre and outside the Loch Ainort field area (See Section 3.2.1.).

Emplacement of the three subvolcanic granites was followed by the suite of composite sills and dykes, which outcrop in a large arc cutting across the area. The radius of this arc is cofocal with the centre of the Inner Granite suggesting that there is a close spatial and possibly genetic relationship between the composite intrusions and the granites. Again the intrusive history of this centre has been tabulated (See Table 3.2.) in order to provide a simplified catalogue of events.

Inrusive Events	*Rock Types*	*Locality*
Dykes	Dolerites, pitchstones, felsites and peridotites. See Section 3.2.1.4.	See Section 3.2.1.4.
Composite Sills and Dykes	Granophyre, felsite and basalt.	Out crops over a 15 km arc from Rubha Suisnish to Rubha na Sgianadin (outwith the field area) continuing through Scalpay to Loch Sligachan.
Inner Granite (IG)	Amphibole, biotite granites and granophyres plus felsites.	Outcrops on three prominent summits of Beinn na Caillich, Beinn Dearg Mhor and Beinn Dearg Bheag. Its circular outline is truncated to the north-west by a prominent fault.
Outer Granite (OG)	Amphibole, biotite granites and granophyres plus felsites.	Outcrop an arcuate belt that runs from Beinn na Cro to Beinn an Dubhaich, Beinn na Caillich and Creag Strollamus.
Glas Bheinn Mhor Granite (GBMG)	Amphibole, biotite granites and granophyres, plus felsites.	From Sron Ard a' Mhullaich at the head of L. Ainort to the col between Belig and Glas Bheinn Mhor. Detail of easterly extent unclear but covers Glas Bheinn Mhor and Am Meall.
Broadford Gabbro (BG)	Altered gabbros.	Outwith field area.
Beinn na Cro Gabbro (BCG)	Olivine gabbros and eucrites.	Limited to a series of layered intrusions along the north-south trending ridge of Beinn na Cro.
Kilchrist Hybrid Ring-dyke (KH)	Acid-basic mixed magmas.	Outwith field area.

Table 3.2.: The intrusive events, characteristic rock types and geographical distribution of the Eastern Red Hills Centre. Intrusive events young upwards with abbreviations corresponding to Figure 3.2 (After: Bell, 1976; Bell and Harris, 1986).

3.2.1.4. Minor Extrusions and Intrusions.

The Tertiary plateau lavas of Northern Skye cover a total area of 1300 km^2 and, prior to Late Tertiary and Pleistocene erosion, they are believed to have had a total thickness in excess of 1200 m (Anderson and Dunham, 1966). The southerly limit of the plateau lava outcrops extends to Glen Drynoch, to the north-west of the study area (See Figure 3.1b). Remnants of these lavas do, however, exist within the Loch Ainort area at several localities. At Creagan

Dubh the lavas rest unconformably on Lewisian Gneiss (See Section 3.2.1.1. and Figure 3.2) and have representative members of both the Skye Main Lava Series[3] and tholeiitic types (Bell, 1984). Outcrops of basaltic lava are also found at Creag Strollamus, covering the low lying ground around Loch Cùil na Creig and extending south-westwards to Allt na Teangaidh and the Creagan Dubh outcrops (See Figure 3.2). This section is also traceable across Caolas Scalpay onto the southern shores of Scalpay, east of Sgeir Stapaig. Finally, on Glamaig and Meallan a Bhealaich Bhric in the north and at Beinn na Cro in the south, basaltic lavas are found capping these topographical highs (775 m, 150 m and 400 m respectively - See Figure 3.1b).The elevated positions of these three localities are considered to be in response to the intrusion of the later granites.

The basalts identified at all of these localities have undergone both extensive hydrothermal and metamorphic (greenschist facies) alteration, which manifests itself as intense fracturing and veining of the lavas with secondary epidote and chlorite. Further, in association with many of these lava fragments are intercalated sediments. These fluviatile, polymictic, conglomerates are matrix supported with sub-angular to rounded clasts composed of Torridonian sandstones, Jurassic sandstones, limestones and shales, and Lower Tertiary basalts and dolerites. Individual clasts range in size from 0.1 to 0.5 m, whilst clast concentrations define crude sedimentary layering inclined 15°- 20° eastward.

On the northern slopes of Belig and on the summit of Meall a' Mhaoil, small exposures of matrix supported, polymictic, agglomerates are found (See Figure 3.2). The clasts have a subangular to rounded shape and a size range of 0.5 to 1 m. Dominant clast compositions are of granite, gabbro, eucrite, basalt, peridotite, trachyte, gneiss and dolerite, with minor amounts of sedimentary material. These deposits of the Belig and Meall a Mhaoil vents, post-date the majority of the cone sheets associated with the Cuillin complex and represent the earliest activity in the Western Red Hills complex (See Section 3.2.1.2.).

In addition to the intrusion of the Western and Eastern Red Hills, Tertiary igneous activity is also represented on Skye by a major concentration of linear dykes. The main orientation of

---

[3] Skye Main Lava Series = olivine basalts, hawaiites, mugearites, benmorites and trachytes.

these parallel/sub-parallel dykes is north-north-west to south-south-east (Speight *et al.*, 1982). Localised variations in orientation do occur in response to changes in dip and strike of the country rocks and the presence of pre-existing tectonic structures. These dykes are predominantly olivine-dolerites and tholeiites, which typically stand proud of the rocks into which they have been intruded. Such preferential erosion results in an irregular topography, particularly where the dykes occur in large numbers (Bell and Harris, 1986).

The Skye Tertiary dyke swarm can be further subdivided into a series of subswarms, which represent areas of localised high dilation. These subswarms are separated from the main zone of dyke intrusion by intervening areas of low dyke concentration. One of these subswarms, the Scalpay subswarm, is located in the eastern half of the Loch Ainort field area, with the western half of the area being located in the zone of low dyke concentration. This belt of high dilation passes through Raasay, Scalpay and continues south-eastward on to the mainland (See Figure 3.1b). It is suggested that this subswarm may extend even further inland to become colinear with the Glen Brittle subswarm (Speight *et al*, 1982). The dilation axis of the Scalpay subswarm is perpendicular to the main swarm with the predominant orientation of dykes in this area being north-east to south-west. Speight *et al.* (1982) further suggest that the Scalpay subswarm is probably the result of lateral flushing from the same magma sources which produced the volcanic centres (See Section 3.2.1.2. and 3.2.1.3.).

3.2.2. QUATERNARY GEOLOGY

The glacial history of the Isle of Skye and in particular the effects of the most recent glacial phase, the Loch Lomond Readvance (*c.* 11-10 ka BP), has been comprehensively researched in recent years (Walker *et al.*, 1988; Ballantyne, 1988, 1989, 1990; Benn 1989, 1990; Benn *et al.*, 1992). Consequently, this summary of the landforms and sediments produced by the glaciation of the Loch Ainort basin, relies heavily on the work of these authors. However, acknowledgement should also be given to the large body of work compiled prior to these most recent studies (Clough and Harker, 1904; Peach *et al.*, 1910; Sissons, 1977). As the work of the present author concentrates on the effects of the Loch Lomond Readvance, only a brief discussion of the earlier episodes of glacial activity will be made.

3.2.2.1. Pre- and Late Devensian Glaciations

Research on the Quaternary offshore stratigraphy of the western Scottish shelf indicates that the Isle of Skye has been subjected to at least three glaciations during this period (Davies *et al.*, 1984; Bowen and Sykes, 1988). It is clearly evident that the fjordic topography exhibited by both the island's coast line and the remainder of the west coast seaboard, could not be attributable to a single, localised, readvance episode. Loch Ainort itself represents a glacially overdeepened valley, which follows the contact between the Western and Eastern Red Hills Tertiary volcanic centres (See Sections 3.2.1.). The extent of glacial activity in this area, is further emphasised by the number of large scale erosion features present on the island; *eg.* corries, breaches, troughs and rock basins. In particular, the apparent discrepancy between the volume of the corries and the amount of material making up the Loch Lomond Readvance moraines within them, implies that these features are the product of multiple episodes rather than a single episode of erosion (Benn, 1991a).

In addition to the erosional evidence, the extent of Quaternary sedimentation also implies the occurrence of more than one glaciation. On average, 150 m of sedimentary fill is found in the Mesozoic and Tertiary basins which exist within this part of the continental shelf (Davies *et al.*, 1984). The majority of this sequence is believed to have been deposited under glacial or stadial conditions (Davies *et al.*, op. cit.). Onland evidence of pre-Loch Lomond glacial activity on Skye is restricted to medium and small scale landforms that formed during the Dimlington Stadial (26-13 ka BP; Rose, 1985), the main glacial episode of the Late Devensian in Britain. These landforms are predominantly subglacial in origin and include a series of arcuate moraines in the Kyleakin Hills, irregular ice-stagnation topography in Glen Brittle and at Strollamus, and the Strollamus boulder moraine (Walker *et al.*, 1988; Ballantyne 1988; Benn, 1990,1991a).

The form and flow direction of ice during this period has been further established by the analysis of striae and erratic distribution (Harker, 1901; Clough and Harker, 1904; Peach *et al.*, 1910). It is generally accepted that ice moved west from the mainland and encroached on the Kyleakin Hills, in the south (Ballantyne, 1989). The presence of an independent ice cap centred on the Cuillins, Bla'Bheinn and the Red Hills caused the deflection of the mainland ice sheet both to the north and south (Harker, 1901; See Figure 3.3.). However, the actual

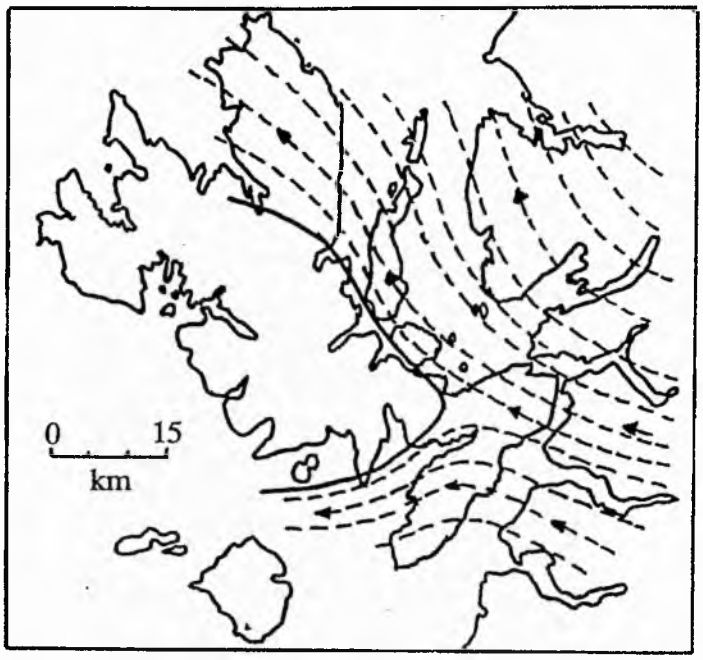

Figure 3.3.The Late Devensian Mainland Ice, its progression and deflection around Skye (After Benn, 1991).

pattern of development of the Skye ice mass is poorly understood, and it can only be assumed that it resembled that of the Loch Lomond Readvance ice cap (See Below). If this is a true analogue for glacier growth during this period it implies that the Skye icefield reached a significant size (> 155 km^2) before becoming confluent with mainland ice (Ballantyne and Benn, 1991).

The northern margin of this ice sheet has been shown to have been confluent with the radially flowing Skye ice cap, the boundary being approximately parallel to the present day coastline. This position has been inferred from the contrast between the abundance of mainland erratics on Scalpay and Raasay and their relative absence on Skye (they are restricted to the coastline below the marine limit; Ballantyne and Benn, op. cit.). The location of this margin has further been demonstrated by the interpretation of the Strollamus boulder moraine as a medial moraine formed between these two ice masses (Benn, 1990). The presence of this feature and the abundance of north-westerly oriented striae at this locality further constrains the confluence margin. It is probable that the confluent margin passed into the field area, crossing the mouth of Loch Ainort (See Figure 3.1b). Farther to the north, evidence of Dimlington Stadial ice is recorded on the Moll peninsula in the form of north-west oriented roche moutonées, erratic boulders and rare striae. Boulder lithologies confirm that mainland ice was also confluent at this locality with ice flowing from the vicinity of Marsco and Garbh bheinn. However, the actual point of confluence is still not clear (Benn *pers. comm.*, 1992).

The consensus of opinion suggests that this Dimlington Stadial ice sheet reached its maximum southerly extent in Britain at *c.* 18 ka BP (Sissons, 1981b). Although there is evidence to suggest that the maximum extent of Scottish Highland ice occurred prior to this (Sutherland, 1984: See Figure 3.4.). It is now recognised that the southward spread of polar water and the displacement of the warm waters of the North Atlantic drift were a major control on the glaciation of the British Isles. The importance of these large scale water movements is two fold; first the distribution of water in the world's oceans has a primary effect on global heat distribution, and secondly the boundary between polar and subtropical waters (the ocean polar front - See Below) is an important influence on atmospheric circulation.

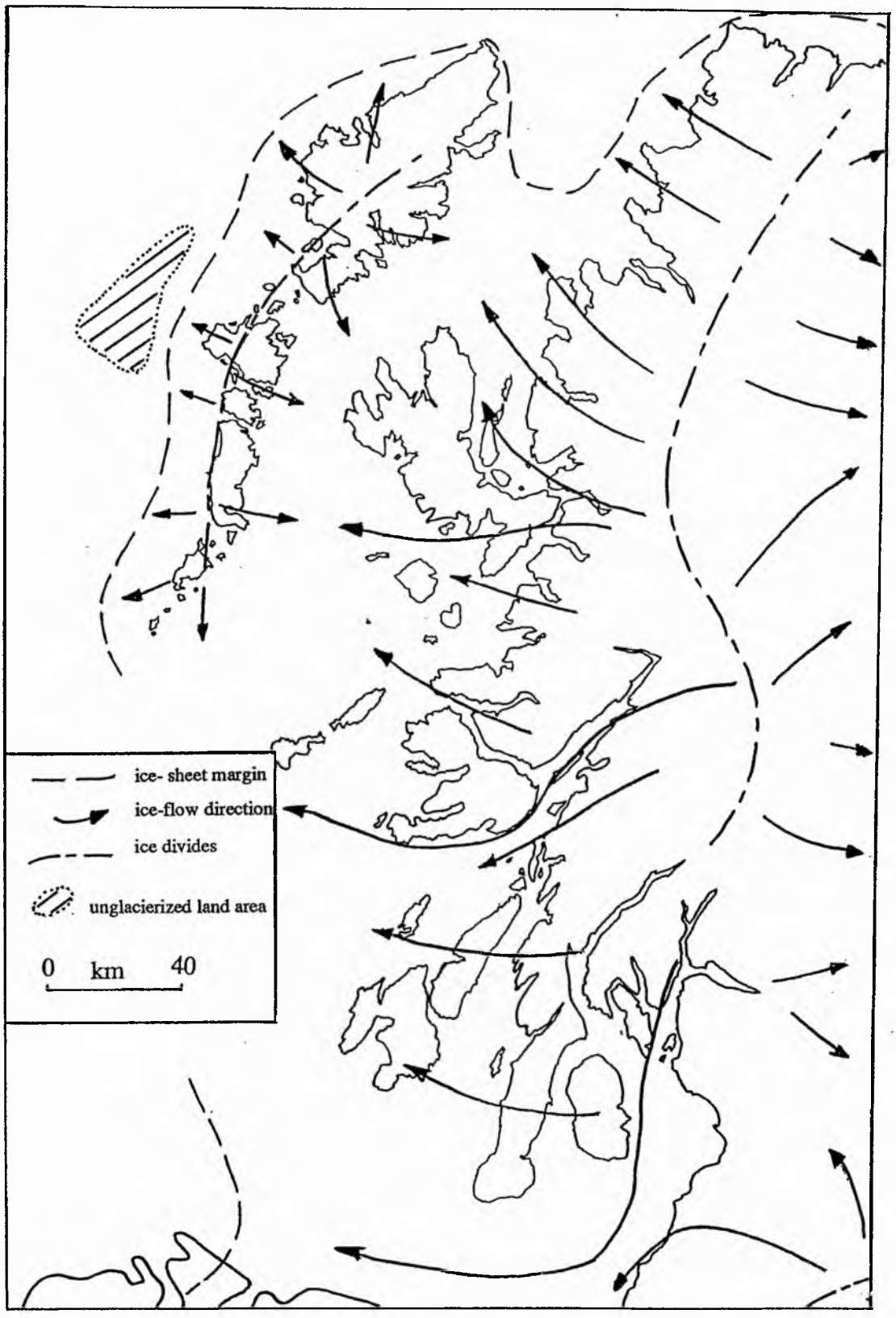

Figure 3.4. The Dimlington Stadial Ice Sheet for North-West Scotland (After Sutherland, 1984).

Ocean circulation is driven predominantly by density gradients formed partially by cooling and partially by salt enrichment. These density induced currents produce a global pattern of oceanic circulation, with the high latitude sources creating dense currents that sink and migrate to low latitudes. In order to counterbalance the volume loss incurred by this process, lower density surface waters flow from lower latitudes towards the source areas. The currents of this conveyor belt system (in this case the North Atlantic Conveyor Belt - NACB) transfer heat from low latitudes and release it at high latitudes. The production of the NACB today supplements the yearly insolation value of the North Atlantic by 25% (Broecker and Denton, 1989) with the majority of this heat being carried on to the European continent (Rind *et al.*, 1986). So, whilst the NACB is in operation, the additional heat supplied to high latitudes in the northern hemisphere is sufficient to keep high northern latitude winters relatively mild and so prevent the build up of large areas of land and sea ice.

Duplessy *et al.* (1988) and Boyle and Keigwin (1987) have been able to demonstrate that the strong outflow of North Atlantic waters was absent during glacial periods. Further, CLIMAP (1981) have estimated that surface temperatures of the North Atlantic were significantly reduced during these periods. These two points imply that the NACB was either non-existent or had significantly weakened at this time. If this was so, Europe would no longer be in receipt of its annual heat bonus, thus promoting the intensification and persistence of colder conditions and ultimately the build up of ice sheets.

The boundary at which mixing of cold, ice-laden polar waters and warmer, ice-free temperate waters occurs, is represented by a steep thermal gradient known as the oceanic polar front. As polar waters migrated southwards during the stadial, the oceanic polar front was correspondingly displaced to a latitude around Northern Spain (Ruddiman and McIntyre, 1981). This boundary is of critical importance as it acts as a major determinant for the position of the atmospheric polar front. In turn it has been shown, from general circulation models, that enhanced cyclone production (*ie.* snow-bearing depression tracks) parallels these boundaries (Dawson, 1992). The movement of the atmospheric polar front southwards was further aided by the development of permanent high pressure zones over the large continental ice sheets of the Northern Hemisphere. The development of these stable anticyclones forced the complete reorganisation of the mid-latitude cyclones. As a result the principal supply of

precipitation to these ice sheets would have been located along their southern margins (Dawson, op. cit.). In addition to controlling the position of the atmospheric polar front, the oscillation of large oceanic water bodies would also have been an important control on the amount of moisture available for precipitation on the European continent. Sea-ice cover, being well developed during glacial periods, may significantly reduce the flux of moisture to the atmosphere and so potentially hinder the accumulation of snow on any adjacent ice body.

Deglaciation of this last major event was a complicated time transgressive process which started between *c.* 14 ka BP (Mix and Ruddiman, 1985) and 13.5 ka BP (Duplessy *et al.*, 1981; Atkinson *et al.*, 1987), climatic conditions ameliorating as the oceanic and atmospheric polar fronts receded northwards. For the majority of the deglacial phase a large part of Britain was surrounded by polar water. Deglaciation was therefore predominantly controlled by precipitation starvation (Lowe and Walker, 1984), iceberg calving and marine downdraw (Ruddiman and McIntyre, 1981) rather than simple temperature variation. Consequently, by the time these fronts lay off western Ireland (13 ka BP; Ruddiman *et al.*, 1977), the still extensive Northern Hemisphere ice sheets were already relatively thin.

Subsequently, the polar ocean and atmospheric fronts reached a position between Iceland and Greenland (Ruddiman and McIntyre, 1981), so enabling the reinstatement of the NACB to its pre-glacial level and, as a result, the increase in insolation received by continental Europe. By 12.5 ka BP the climate of Britain had reached a level similar to that of the present day, with maximum summer temperatures reaching between *c.* 15°C in Scotland (Bishop and Coope, 1977) and 17°C in England and Wales (Atkinson *et al.*, 1987). This increase in temperature and the replacement of the polar waters, that surrounded Britain prior to 13 ka BP, by warmer temperate waters suggests that the remainder of the ice-sheet would have melted rapidly (Sissons, 1979a). It is probable, therefore, that the majority of Britain became ice-free by 12.5 ka BP. There is, however, indirect evidence to suggest that ice lasted throughout the Lateglacial interstadial in the Western Highlands. Peacock (1970) argued that the glaciers of the Loch Lomond Stadial (See Section 3.2.2.2.) were too large to have accumulated during this short period of climatic deterioration. Further, Manley (1949, 1971) proposed that mean summer temperatures of only *c.* 2°C below present values, over a period of several decades, were capable of sustaining small glaciers. If the mean July temperatures of

2.3°C below present values, calculated by Bishop and Coope (1977), and the lower sea temperature levels of Peacock (1981) are accepted it may therefore be inferred that total deglaciation in the North-West Highlands did not occur (Sutherland, 1984).

3.2.2.2. The Loch Lomond Readvance

The period of Lateglacial climatic amelioration experienced by the British Isles was dramatically interrupted by a return to arctic conditions during the Younger Dryas, (locally referred to, as well as within this thesis, as the Loch Lomond Stadial; 11.01 +/- 0.17 ka BP to 10.39 +/-0.13 ka BP; Bard *et al.*, 1987). Cooling began from *c.* 11.8 ka BP with mean winter temperatures falling by more than 10°C in a thousand years (Walker and Lowe, 1990). Ballantyne (1989) calculated a stadial mean July sea-level temperature of *c.* 6°C, a figure that is considered consistent with temperatures for the English Lake District (7.5°C; Sissons, 1979b), the Western Grampians (7°C; Sissons, 1980) and lowland Britain (a minimum of 10.5°C; Atkinson *et al.*, 1987)[4]. Independent coleopteran data indicates that winter temperatures ranged from -15°C to -20°C (Atkinson *et al.*, op. cit.), values which are corroborated by the periglacial evidence of Ballantyne (1984).

In addition to the data pertaining to a climatic deterioration over the North Atlantic at this time, independent field evidence from Skye enabled the identification and relative dating of the development of a major icefield during the Loch Lomond Stadial. It had long been established that there had been a readvance of locally nourished glaciers on Skye. Ballantyne (1989) has provided the basis for the current reconstruction, with minor amendments being suggested by Benn (1990; See Figure 3.5.). The results of these studies indicate the existence of: the large Cuillin Icefield (155 km²); nine or possibly ten corrie glaciers adjacent to the main icefield[5]; a small icefield within the Kyleakin Hills at the south-eastern margin of the island (*c.* 10 km²) and two small corrie glaciers on the east of the Trotternish Escarpment in the north of the Island. The presence of fluted moraines and large areas of striated and abraded bedrock within

[4] Taking into consideration latitudinal differences.

[5] The limit of the Fionn Choire Glacier is equivocal and may represent either an independent glacier or alternatively an extension of the Cuillin icefield at this juncture. (For Discussion See Ballentyne *et al.*, 1991).

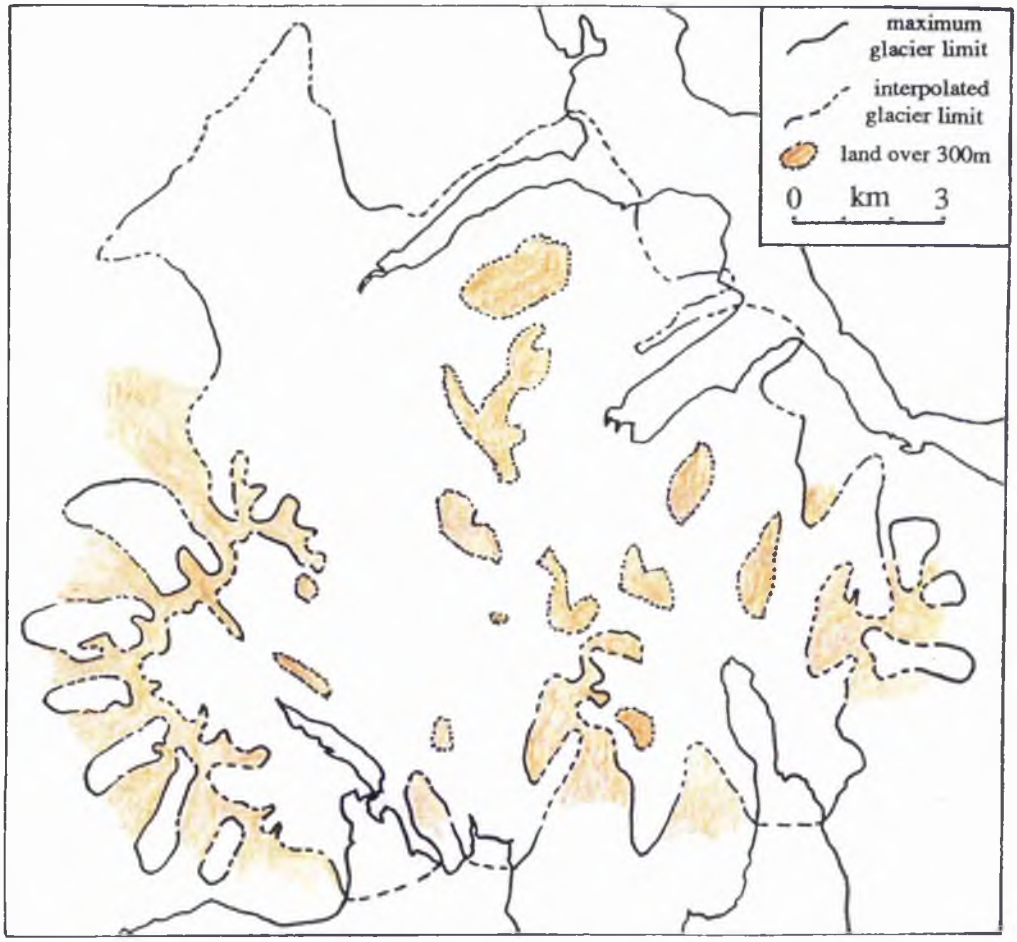

Figure 3.5. The Loch Lomond Readvance Ice Complex of Skye (After Benn *et al.*, 1992).

the limits of the Loch Lomond Readvance ice on Skye provides strong evidence that these glaciers were temperate throughout.

The Loch Ainort basin was occupied by an easterly extension of ice from the main Cuillin icefield, the Ainort Glacier (See Figure 3.5.). The northern limit of the glacier is represented by a drift bench and moraine ridges that descend eastward along the slopes of Leathad Chrithinn. Prior to reaching sea level this limit becomes indistinct. However, Benn (1990) suggests that this margin may be represented by an intertidal spit, of possible reworked glacigenic sediments (sands and gravels), that has developed off Maol Bàn. To the south of the loch, on the slopes of Glas Bheinn Mhòr, another drift bench descends eastward at a comparable level to that on the northern shore, but is absent on the slopes due south of Luib. A chain of moraines continues along the western slopes of Am Meall, with a small group of moraines marking a proposed glacier terminus approximately 100 m due south of Rubh' an Àird Duirche (Benn, 1990). This chain coincides with the northern termination of the Strollamus boulder train (See Above), already identified as relating to Dimlington ice sheet deglaciation (Ballantyne, 1988).

On the north-eastern slopes of Glas Bheinn Mhòr and within the lower parts of Srath Mòr (See Figure 3.6), moraine evidence implies that ice of the Srath Mòr Glacier became confluent with Loch Ainort ice at this locality. It is also worth noting that an extension of the Srath Mòr glacier spread north-eastward across the col between Am Meall and Glas Bheinn Bheag. Although this body of ice did not reach the shoreline, it is probable that glacial debris will have reached Loch na Cairidh from this locality via the Garbh-allt. Similarly, the Srath Beag Glacier farther south (See Figure 3.5) terminated landward of Loch na Cairidh, but may still have fed material into it via the Allt Strollamus. To the north of Loch Ainort another glacier occupied the valley of Coire Mòr during the Loch Lomond glacial maximum, this again being well defined by the pattern of moraines and drift limits. The evidence suggests that the "Moll Glacier" terminated just offshore, but the precise location of its terminus is not known. This glacier would have been another source of glacial debris entering the waters of the unnamed deep.

Onland evidence suggests that, at its maximal extent, the Loch Ainort glacier represented 3.023 km^3 of ice, occupying an area of 19.72 km^2 (Ballantyne, 1989). These figures are

calculated using the method described in Ballantyne (op. cit.), which requires the use of an inferred tidewater maximum limit, located at an arbitrary point offshore. Although its location is partially constrained by the absence of any Loch Lomond glacial activity on the corresponding shores of Scalpay, this limit must be considered subjective. Further ice volumes were calculated using minimum altitude values estimated from the relevant Admiralty chart. It should be noted that such methodology assumes the marine palaeosurface over which the glacier advance corresponds to that of the present day. Similarly, ice volumes and areas have been calculated for the Srath Mòr Glacier (0.851 km^3; 6.3 km^2), the Srath Beag Glacier (0.215 km^3; 4.15 km^2)[6] and the Glamaig-Moll Glacier (0.636 km^3; 8.22 km^2)[7].

Having established the existence of a post-Dimlington readvance phase these same workers were able to establish its age (Walker *et al.*, 1988). Dating was achieved by three independent methods; first, the restriction of in-situ frost shattered bedrock to outside the mapped readvance limits indicates a Loch Lomond Stadial age. If the areas within the limits had been exposed to the extreme climatic conditions of the Stadial, it is probable that uncovered bedrock would have experienced at least limited frost weathering. Secondly, the absence of high-level (> 15 m OD) Lateglacial raised shorelines within the established limits suggest that this event occurred during a period when sea level dropped from that of the Lateglacial to an altitude below that attained by Flandrian seas (See Section 3.2.2.3). Finally, pollen analysis and radiocarbon dating of cores, taken from filled enclosed basins both within and without the limits, further constrain the age of this event. Sites outside the limits yielded a complete sequence of Lateglacial and Flandrian sediments, whilst only a Flandrian sequence was recovered from those inside the limits, a result strongly indicative of a Loch Lomond Stadial age.

For the early accumulation phase of this stadial, Sissons (1980) has calculated an annual precipitation rate for the west of Scotland of 2700 mm yr^{-1}. Glacier dimensions, and more importantly the pattern of Equilibrium Line Altitudes (ELAs) across the Cuillin Icefield, imply that the majority of this precipitation fell from predominantly southerly *snow-bearing* winds

---

[6] This figure must be considered an over estimate, if one accepts the revised Srath Beag limit of Benn (1990).

[7] Only one figure has been quoted as the two glaciers could not be adequately subdivided at their source.

(Ballantyne, 1989). Further detailed analysis of ELAs by Ballantyne (op. cit.) has also been able to identify a significant contribution by westerly and south-westerly *snow-blowing* winds. This information supports the suggestion that, for Scotland as a whole, the principal Loch Lomond snowfalls were associated with southerly air streams that preceded the tracks of warm or occluded fronts (Sissons, 1979a). In addition, these data are also consistent with the assertion that south-westerly winds were also prevalent for the majority of upland Britain (Sissons, 1980; Ballantyne, 1989). The control on the location of these *snow-bearing* air streams was once again related to the migrating ocean and atmospheric polar fronts. Precipitation was associated with the passage of these fronts through the latitude of North-West Scotland. However, at the point of full stadial conditions the polar front once again resided at a latitude of approximately 35°N and, as a result, Scotland was cut of from its main conduit of precipitation. This situation would have been further exacerbated by the associated extension of sea-ice southwards, so again reducing the flux of moisture to the accumulation area. This climatic configuration, together with the identification of dust concentrations in ice cores, has enabled Dansgaard *et al.* (1989) to imply that, at times of full glacial conditions, stormy but very arid conditions prevailed.

Bard *et al.* (1987) suggest that the retreat of the fronts northwards, was effectively an instantaneous movement, completed in less than 400 years. In particular, evidence from South Greenland ice cores (Dansgaard *et al.*, 1989) suggests that climatic amelioration occurred in less than 20 years, with a 7°C warming being completed within *c.* 50 years. Evidence from coleopteran data in Britain (Atkinson *et al.*, 1987) also suggests a rapid rise in temperature, albeit not as marked (1.7°C per century to 2.6°C per century). However, for the Loch Lomond ice-field on Skye, geomorphological mapping and pollen-stratigraphic correlations suggest that the initial stage of retreat was actually well advanced prior to this marked temperature increase (Benn *et al.*, 1992). This phase of retreat was actually in response to the decline in effective precipitation initiated during the height of the stadial. These authors are also able to infer that it was only the final stages of deglaciation that were in response to the proposed temperature increase.

Within the glacial maximum limits of the Loch Ainort and associated glaciers, the pattern of moraine distribution suggests that deglaciation actually occurred in two distinct phases,

Deglacial Phases I and II. In all the areas covered by Loch Lomond Readvance ice, lateral and frontal moraines are confined to the lower parts of corries and valleys. By contrast, the upper parts of these glacial basins are characterised by areas of lodgement till, ice-scoured bedrock and longitudinally oriented formations (fluted moraines and boulder trains). The distribution of lateral and frontal moraines is believed to have developed during the initial stages of deglaciation, a time of glacial retreat interrupted by periods of readvance and/or stillstands (Deglacial Phase I). However, the latter stages of deglaciation are characterised by uninterrupted retreat (Deglacial Phase II), inferred from the lack of reorientation of longitudinal features deposited at the glacial maximum. Where bodies of ice became isolated from the remaining high altitude source areas (*eg.* Srath Mór) *in situ* ice stagnation occurred.

In Loch Ainort itself, the actual pattern of this proposed two phase form of retreat is incomplete, the relatively steep valley slopes having been subjected to both paraglacial and postglacial reworking. However, at least four sub-parallel benches and moraine chains can still be identified, which have been interpreted as ice-marginal landforms (Benn, 1990). The uppermost feature marks the glacial maximum position and those at lower altitudes mark the subsequent retreat stages of Deglacial Phase I. The presence of retreat moraine chains are, however, much more clearly developed in the lower parts of Coire Mòr and northern Srath Beag (An Slugan). The evidence for the more rapid Deglacial Phase II is much clearer within the Loch Ainort basin. There is little evidence of moraine orientation within the area, which is characterised by numerous isolated mounds and hummocks. The exceptions are occasional fluted moraines located in the upper reaches of the valley and oriented parallel to the valley and secondly, concentrations of longitudinal moraines trending parallel with the two well developed axial erratic trains (The Marsco Epigranite Erratic Train and the Eucrite Erratic Train; See Figure 3.6.).

Examination of exposures from the slopes above Loch Ainort suggests that there was significant reworking of glacial debris both during and shortly after deglaciation (*ie.* during the "paraglacial" period; Church and Ryder, 1972)[8]. Such activity was particularly prevalent on

[8] Defined as the time during which processes which are non-glacial but directly conditioned by glaciation occur. The paraglacial commences at the start of deglaciation and ends on the return to the pre-glacial geological "norm" in the sub-aerial environment.

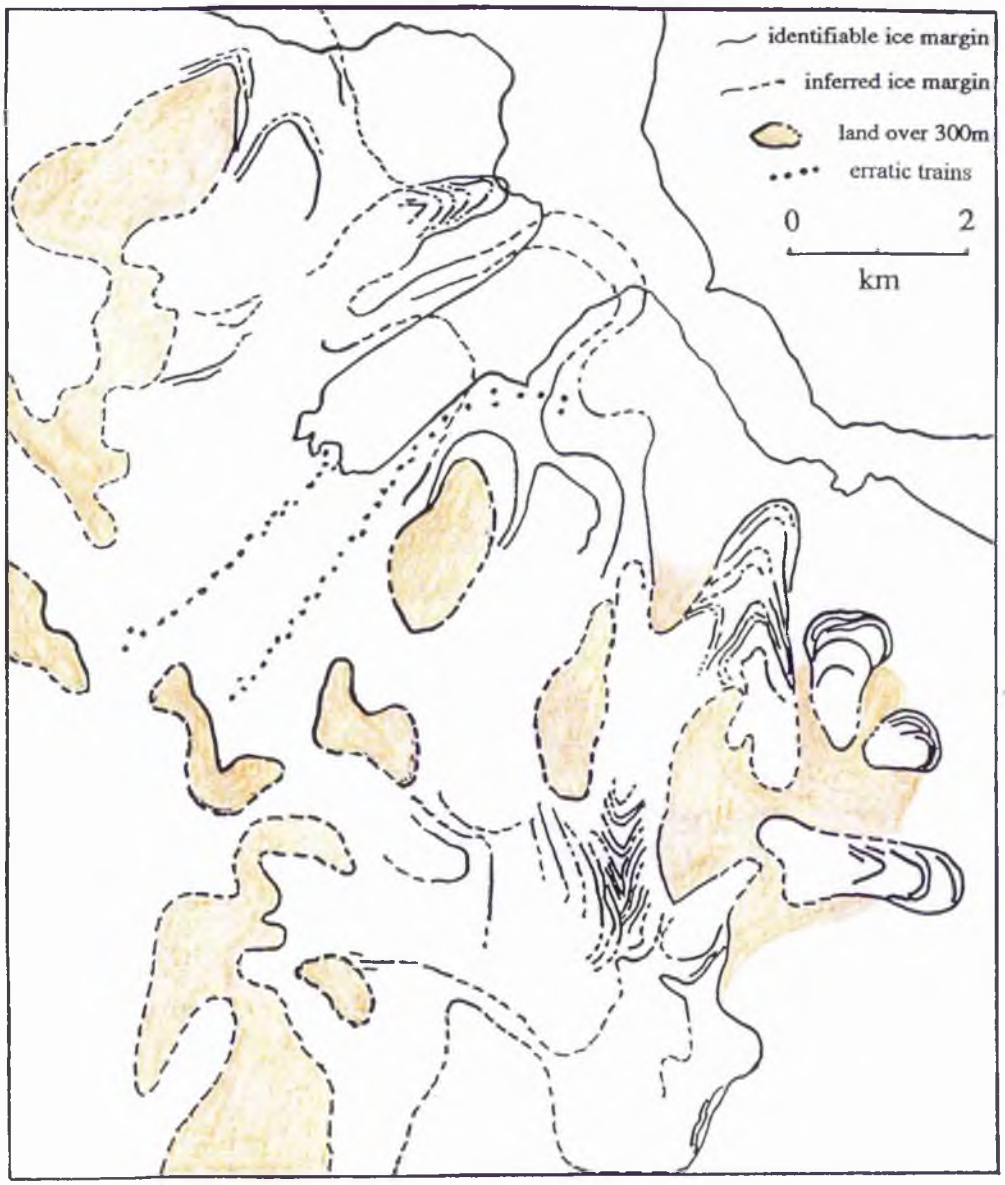

Figure 3.6. The Loch Lomond Readvance Glacier System for Loch Ainort and adjacent areas. (After Benn, 1990).

the steep slopes of Leathad Chrithinn to the north of Loch Ainort. Reworking on these slopes, and those of Glas Bheinn Mhòr to the south, was so extensive that moraine preservation only occurs on slope angles of less than 10° - 20° (the spread of values is controlled by local variations in material properties, water availability and the steepness of adjacent slopes). The principal processes operating during this period were sedimentary-gravity flows of the Types I, II and III (After Lawson, 1982 and 1988), rockfalls and landslides (Benn, 1990). The interdigitating nature of many non-glacigenic sedimentary-gravity flows and glacial diamictons, commonly with evidence of glaciotectonic deformation, implies that such activity occurred during periods of stillstands and minor readvances (*ie.* Deglacial Phase I). In fact, detailed sedimentological investigations of unaffected Loch Lomond moraines leads Benn (op. cit.) to conclude that these processes, acting on exposed Dimlington ice-sheet deposits, were the main sources for entrained glacial debris.

Benn (op. cit.) does consider the subglacial entrainment of debris to have been of local importance, but only where the underlying joint distribution and bedrock competency allowed. In addition, he also identifies the importance of glacially related fluvial activity both at ice margins, where it was intermittent and localised (*eg.* the fluted moraines described above), and in the proglacial environment where fluvial reworking of Loch Lomond sediments produced terraced sequences in parts of the valley. However, within many other exposures on these valley sides there is a total absence of structures indicative of glacial over-riding or any other form of direct glacial influence. This implies that these processes of subaerial reworking continued throughout the paraglacial, in fact being dominant up until the colonisation, and consequent stabilisation, of these slopes by vegetation. Even with the relatively thick heather and gorse cover present today, limited reworking of these slopes by both subaerial gravity flows and fluvial activity still continues.

As has been described already, the work of Ruddiman *et al.* (1977), Ruddiman and McIntyre (1981) and Bard *et al.* (1987) suggests an intimate link between climate deterioration and rapid movements of the oceanic, and therefore atmospheric, polar fronts. However, what triggered this extension of cold surface waters southwards is still unresolved (Harvey, 1989), the problem being primarily tackled by the development of increasingly complex Climatic Simulation Models (CSM's). Three main hypotheses are currently favoured

(See Harvey, op. cit. for review); first, the intrusion of a low salinity meltwater lens from ablation of continental ices sheets would result in an increase in the freezing point and stability of the ocean mixed layer. This would encourage the extensive development of sea ice leading to a large reduction of ocean-air heat flux and therefore a significant reduction in atmospheric temperatures. Second, the southward migration of icebergs into the North Atlantic from the break up of the hypothetical Arctic Ocean ice shelf, would again reduce the flux of heat from the oceans to the atmosphere. However, unless replenished, the direct influence of iceberg flooding would dissipate within 20 to 50 years.

Finally, isotope studies (Boyle and Keigwin, 1987) suggest a reduction or more probably the cessation of the NACB leading to a major reduction in the northward oceanic heat flux within this system. This may have been achieved through the influence of the previous two events. However, it is considered to be principally the result of a massive influx of glacial meltwater into the North Atlantic. Meltwater, created during the deglaciation of the Laurentide ice sheet, drained from Glacial Lake Agassiz into the Gulf of Mexico via the Mississippi River (Broecker and Denton, 1990). The retreat of the ice opened up an alternative channel to the east via the Great Lakes and the St. Lawrence River, so meltwater was diverted into the North-East Atlantic. The influx of such large volumes of fresh water significantly reduced the salt content of the ocean surface waters, reducing the density of the high latitude sources of the NACB. This reduction in density prevents the formation of southerly flowing deep ocean waters and so terminates conveyor belt circulation (Broecker and Denton, 1989). With the subsequent climatic deterioration, the Laurentide ice sheet underwent a period of readvance during which it cut off this easterly drainage route, so rediverting meltwater to the Gulf of Mexico. This enabled the re-establishment of the NACB, increasing northward oceanic heat flux and so creating rapid climate amelioration.

As a postscript to Section 3.2.2.2. it is necessary to look briefly at the validity of the chronostratigraphical time scale described above. As the reader will probably now appreciate, there are significant discrepancies in the estimates of the timings of many of the climatic changes that have occurred during the latter part of the Quaternary. Depending on which authors one cares to believe, the timing of many of the events mentioned may vary between 500 and 1000 years, a large error for a period covering only 14 ka. Considering the recent

interest in the high resolution climatic studies of the Lateglacial, it is significant that a synthesis of the timing of these events has still not been attempted (J. Harte *pers. comm.*, 1993). Reticence, on the part of Quaternary scientists, to tackle this topic is probably due to the number of major problems that would have to be overcome, including:

i) The number and variability of dating methods (*ie.* Dendrochronology, Radiocarbon dating, Tephrochronology, *etc.*) many of which are frequently not correlatable.

ii) Radiocarbon dating, that for many years has been considered the definitive dating method, is increasingly considered to be fallible. This is particularly important when considering the current desire for accurate high-resolution dates (in the order of 10s of years). When comparing dates from different authors one has to consider three main factors; first, the accuracy and precision records of the laboratories processing the samples. Secondly, the size and type of the samples themselves, which may be as diverse as individual plant fragments and foraminiferal tests to large sediment samples. Finally, one has to know the validity of the calibration curves employed, as this is of particular importance for the period discussed here. At present we have no accurate measurement of the radiocarbon content of the atmosphere during this period, a factor critical in the construction of calibration curves. All we do know is that, from a theoretical viewpoint, major fluctuations in atmospheric ^{14}C are anticipated and therefore extrapolation of known calibration curves is invalid. This theory is partially substantiated by the identification of constant radiocarbon age plateaux from Lateglacial sections (Amman and Lotter, 1989; Lowe 1991), interpreted by the authors as resulting from temporal variations of atmospheric ^{14}C. It is further suggested by Pilcher (1991), who undertook a review of all the problems cited here, that "*Until this section* (14 to 10 ka BP) *of calibration is complete it would be wise to make NO interpretation of RATES of change or ABSOLUTE ages for the Lateglacial based on radiocarbon dating.*".

iii) Although many of the figures quoted are for "*glacial events of the North Atlantic*", the actual area over which samples are taken is in excess of 107,000,000 km^2 and in many cases little consideration is given to what spatial and temporal variations may have occurred. This is particularly surprising when one considers the time transgressive nature of many of the processes in nature which we can directly observe.

iv) The link between climatic variation and glacier response, particularly over large glacial-interglacial cycles, is still poorly understood. Consequently, the correlation of dates of glacial maxima to points of significant climatic change can be difficult.

With these points in mind, it is suggested that the reader should be concerned only with the sequential nature of the climatic and physical events discussed within Section 3.2.2.2.. This rider should not be considered an excuse for the author's inability to date the period he describes, but a realisation on his part of the tasks involved in the absolute dating of glacial events, let alone the fact that this topic is well without the remit of this project.

3.2.2.3. Late Quaternary Sea Level Fluctuation

As this thesis deals with the interface between the marine and glacial regimes it is necessary to synthesise the pre-existing ancient sea level data for Loch Ainort. On Skye there is substantial evidence for an early Lateglacial marine limit and a later Main Postglacial Raised Shoreline (Sissons, 1983a). However, there is minimal direct evidence exposed on Skye's coastline, to enable the identification of a sea level contemporaneous with the Loch Lomond Readvance. Consequently, for this crucial period, it has been necessary to summarise and extrapolate information obtained from the more extensive database constructed for the Scottish mainland.

The highest beach deposits (*ie.* above *c.* +15 mOD;) is believed to represent the Lateglacial marine limit which, it is suggested, correlates with the maximum level reached by the sea during the deglaciation of the Dimlington ice sheet (See Figure 3.7.). This shoreline is represented by gravel deposits commonly in the form of raised beach terraces. It is inclined at a gradient of *c.* 0.4 m km^{-1} to the west (Walker *et al.*, 1988), with its altitude decreasing from over 30 mOD near Kyleakin to *c.* +15 mOD around Loch Harport. This gentle gradient is caused by regional differential isostatic uplift and its value correlates well with those obtained from raised beach fragments, of an inferred equivalent age, in Wester Ross (Sissons and Dawson, 1981). The limits on Skye are found predominantly on the outer parts of the coastline and around the heads of the westernmost sea lochs (See Figure 3.8.). Fragments are also found in the south-eastern extremities of the island, around Sleat and Kyleakin, suggesting that this level was maintained after mainland ice had left Skye (Benn, 1991b.).

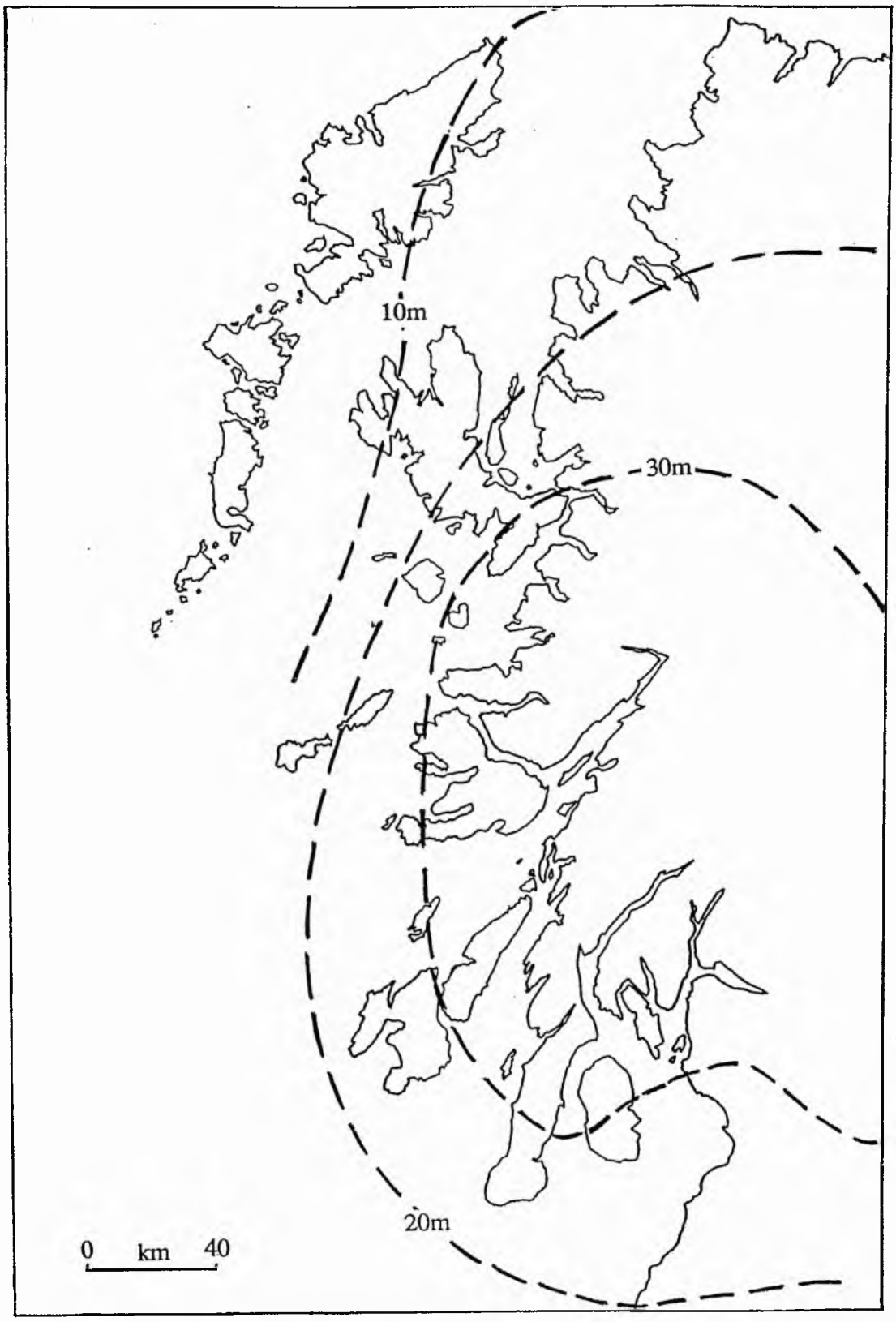

Figure 3.7. Isobase Map of the Lateglacial Marine Limit for Skye and the adjacent Mainland (After Boulton *et al.*, 1991).

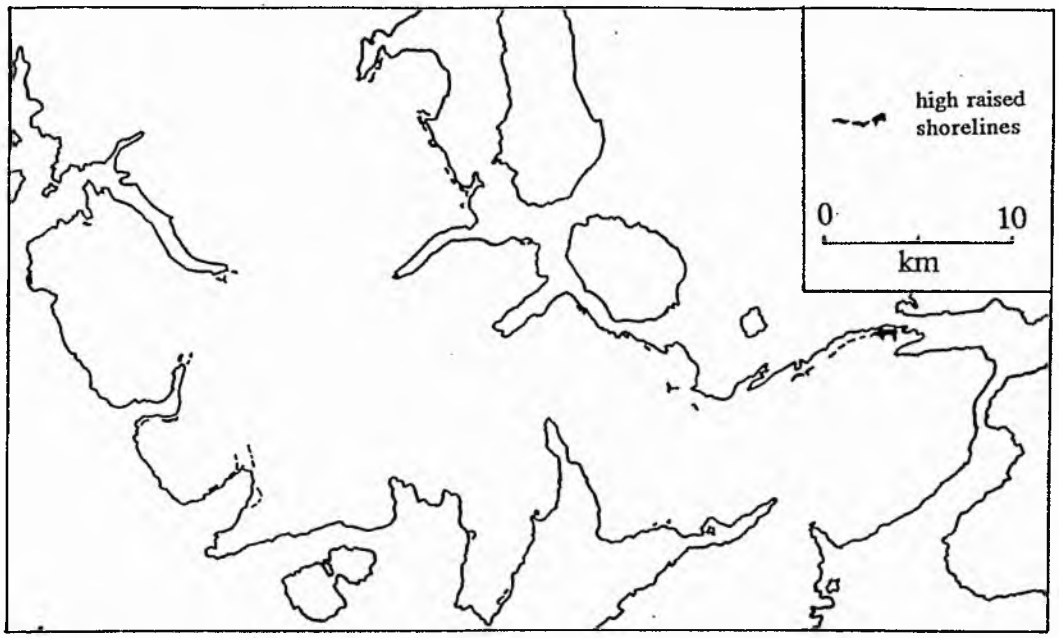

Figure 3.8. Recorded Beach Fragments of the Lateglacial Marine Limit of Skye (Walker *et al.*, 1988).

As previously suggested the majority of evidence for the altitude of sea level contemporaneous with the Loch Lomond Readvance is indirect. One primary consideration in the determination of approximate Loch Lomond Stadial sea levels is the conspicuous absence of the Lateglacial marine limit within, identifiable, Loch Lomond Glacier limits (ie. in Lochs Sligachan and Ainort). The abrupt nature of this relationship can be clearly seen around Loch Sligachan (Benn, op. cit.). One kilometre to the north of the margin of the inferred Sligachan glacier, at Braes, raised beach gravels outcrop at *c.* +30 mOD. By contrast, within the glacier margin the highest fragments of raised shorelines occur at *c.* +7 mOD (*eg.* at Peinchorran, Sconser and Sligachan). These lower raised limits are believed to be related to the Main Postglacial Raised Shoreline (Benn op. cit.; See Below). The absence of high sea level fragments suggests either a stillstand of Dimlington ice within these valleys, during which time Lateglacial sea levels fell significantly, or the removal of Lateglacial marine limit indicators by an erosive readvance event. The former hypothesis is weakened by the apparent absence of "any" ice-marginal features (Walker *et al.*, 1988) in what would have been submerged ice-proximal localities ideal for high rates of sediment accumulation. The dearth of both exposed deltaic deposits and within Loch Lomond limit Lateglacial marine fragments suggests that the maximum relative sea-level during the Readvance phase had fallen to a level at or below the altitude of the Main Postglacial Raised Shoreline.

A second line of evidence for Loch Lomond shorelines to have been at or near present day sea level rests on an alternative interpretation of a number of low (< +7 mOD) raised platform fragments. Large sections of the coasts of central and south-east Skye and in particular the Sleat and Strathaird peninsula, are characterised by raised geos, caves and stacks which are at or close to present sea level. Further, Richards (1969) identified a series of narrow platforms between Portree and Staffin at heights of +2 to +7 mOD. A number of these platforms were covered with cemented beach gravels which in turn were overlain by clay-rich, matrix supported diamictons which Richards (op. cit.) interpreted as till. Using this interpretation he went on to suggest that these platforms and associated beach deposits were of interglacial age. Although there is now some doubt on the validity of this sedimentological interpretation (Benn, 1991b), such low ice-moulded rock platforms of possible interglacial age commonly occur throughout the Hebrides (Dawson, 1980).

Arguments of Richards interpretation apart, the widespread existence of these platforms cannot be disputed. It is widely suggested that similar landforms are the result of extensive erosion during the Postglacial (McCann, 1968), and a Postglacial age would certainly correlate well with other positively identified Postglacial shoreline fragments, found around Skye, at *c.* +7 to +10 mOD (See Below). However, an alternative hypothesis for the lowest of these platform features is that they are correlatives of the Main Rock Platform (the MRP: *eg.* Sissons, 1974a; Gray, 1978) of the western coast of the mainland (Benn, 1991b). A significant body of both comparative and direct evidence suggest that the MRP represents the Loch Lomond Stadial shoreline created by a short lived (< 1000 years) period of sea-level stasis during which extensive periglacial erosion occurred (For Summary See; Sissons, 1974a; Gray, 1978; Gray and Ivanovich, 1988).

The hypothesis that the low rock platforms of Skye can be correlated with the MRP can be partially substantiated by two lines of evidence. First, the close correspondence of fragment altitudes with altitudes predicted from regional isobases for the MRP and secondly the absence of low rock platforms from within some of the glaciated valleys. Isobase maps for the MRP are well established for south-west Scotland, with the original work being conducted around the Firth of Lorne (Gray, 1974 and 1978 - See Figure 3.9.). The general elliptical pattern they describe has been verified by extensive fieldwork to both the south-east (Sound of Jura and the Firth of Clyde: Dawson, 1984) and the north-west (Ardnamurchan and Moidart: Dawson, 1988). As suggested previously within this section the westerly/south-westerly and southerly inclination of these platform fragments (gradients ranging between 0.16 $m.km^{-1}$ to 0.18 $m.km^{-1}$: *eg.* Sissons, 1974a; Dawson, 1988) is related to postglacial isostatic uplift, following the deglaciation of the Dimlington Stadial ice sheet. The general curvature of the isobases, round a centre to the north-east of the Firth of Lorne, is consistent with Late Quaternary uplift in Scotland being centred on Rannoch Moor. The uplift ellipsoid having a major axis aligned north - south over Western Scotland (Gray, 1978).

An extrapolation of the isobases north-westwards towards Skye (See Figure 3.9.) predicts MRP fragments between 0 and +5 mOD for south-east Skye descending to -5 to 0 mOD fragments for the Loch Ainort field area. However, one must consider the inaccuracy of any values extrapolated from data points in excess of 50 km away and from models that do not

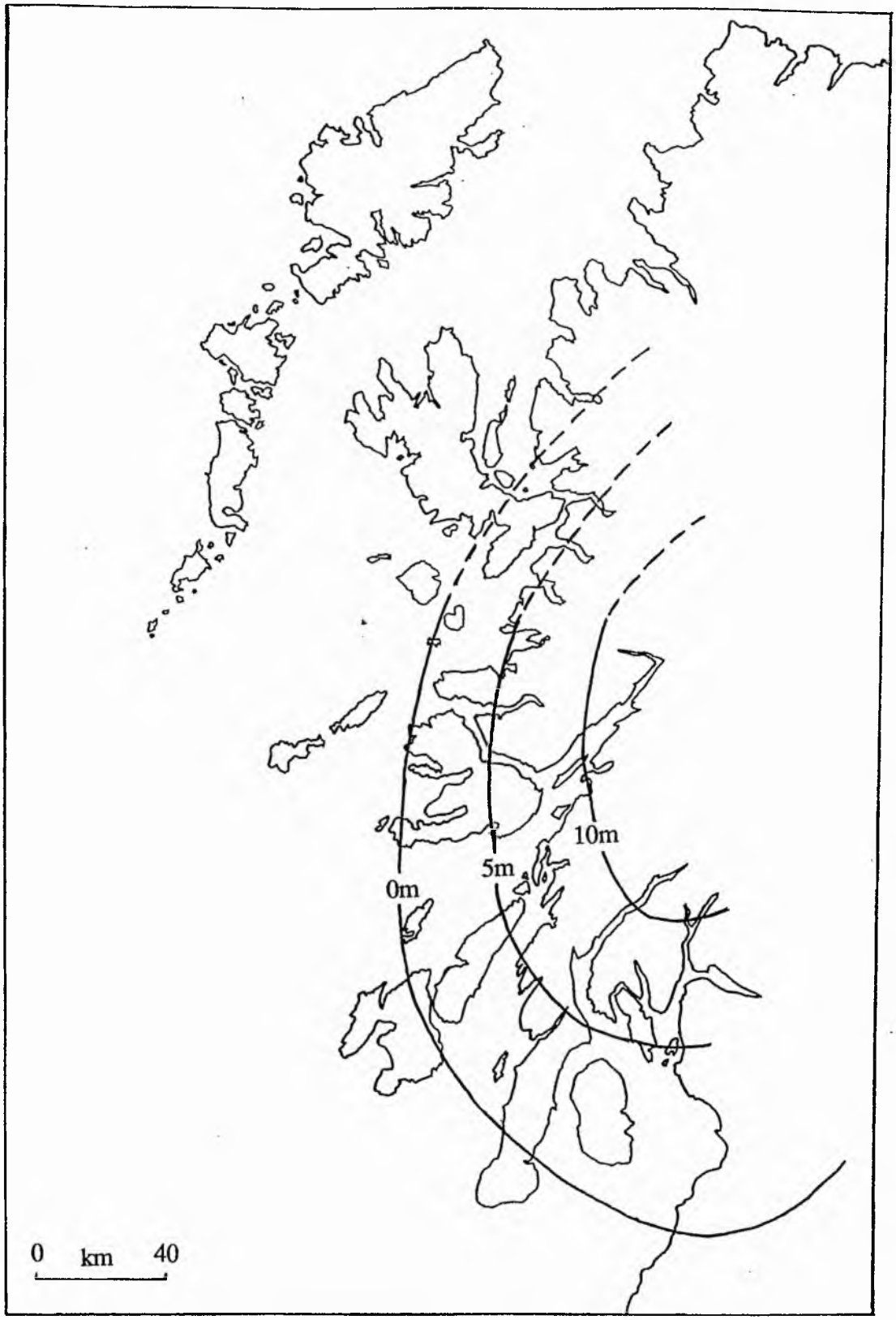

Figure 3.9. Isobase Chart of the Main Rock Platform for Skye and the adjacent mainland (After Dawson, 1984).

consider, on small (< 10 km) scales, the imperfect response of isostatic rebound. So allowing for these errors in extrapolation, the conclusion that platform fragments at or near sea level should be anticipated concurs with the interpretation of the low rock platform as a correlative with the MRP.

The second line of evidence for an MRP association with the low rock platforms of Skye, is the absence of the low platforms from within Loch Lomond limits (*eg.* Loch Sligachan, Loch Ainort and Loch Slapin: Benn, 1991b). This relationship suggests that these fragments were formed prior to or contemporaneously with the Loch Lomond Readvance and are therefore of equivalent age of the MRP. This argument requires the assumption of an, at least in part, Loch Lomond Stadial age for the MRP.

It should be noted that this assumption does pose a number of as yet unanswered questions, including, the apparent absence of the large volumes of rock debris from near shore outcrops, that would have to have been created during platform production. Secondly, despite extensive research of all theses hypothesised sea-level indicators, actual dating of the MRP and any of the other shorelines mentioned in north-west Scotland has rarely been undertaken. At the time of submission, the only actual dates recorded in the literature were uranium series disequilibrium dates taken from speleothem formation in raised caves associated with the MRP on the Island of Lismore, 90 km to the south (Gray and Ivanovich, 1988). This work generally gave dates concurrent with Loch Lomond age formation of the MRP. However, one date gives a pre-Lateglacial age which if real precludes a restricted formation of the MRP to the Loch Lomond Stadial. Using this and other evidence Gray and Ivanovich (op. cit.) suggest a polycyclic mode of formation for the MRP, albeit with a Loch Lomond Stadial component. Yet this solution does require "..a remarkable coincidence of isostatic patterns and gradients on several occasions." (Gray and Ivanovich, op. cit.).

Recent work on the biostratigraphic and lithostratigraphic analysis of isolated basins[9] to provide radiocarbon dated sea-level index points, has enabled the establishment of a Lateglacial to Holocene sea level record for Arisaig, north-west Scotland, to be constructed (Shennan *et al.*, 1994). Analysis of cores taken from 3 sites identify a rapid (maximum of 10

[9] The biostratigraphic (pollen and diatom distribution) and lithostratigraphic variations, record the isolation or connection of a proxi-coastal basin from or to the sea (*eg.* Kjemperud, 1986).

mm.yr-1) sea-level fall from +17.8 mOD at 11.8 ka BP to *c.* +5.2 mOD at 10.1 ka BP. This rapid and continuous fall, which is chronostratigraphically constrained by a series of radiocarbon dates, precludes the possibility a period of stable sea-levels during which the MRP could be formed or modified.

Approximate altitudinal values taken from the sea-level curve, constructed for Arisaig, suggest a drop in sea-level in this area from +9.3 mOD (10755 ± 90 yr BP) to +5.1 mOD (10060 ± 86 yr BP) during the Loch Lomond Stadial. Currently, this work is site specific and so isobases for Loch Lomond Stadial sea-levels cannot be constructed. However, due to the consistency of the Shennan *et al.* (1994) sea-level curve with the general sea-level trends predicted by the glacial rebound models of Lambeck (1993a and b.), tentative sea-level altitudes for the field area are proposed. Altitudinal values have been constructed by combining a gradient obtained from the Lambeck models (0.1 $m.km^{-1}$ north-north-westwards) with the absolute values of the Shennan *et al.* curve (See Above). These approximate calculations suggest a drop in sea-level in the field area from +5 mOD to + 2 mOD during the Loch Lomond Stadial.

Therefore, despite the lack of any equivocal evidence for a sea-level altitude (or altitudes) for the field area and the persitent arguments over the existence of the MRP, this author suggests that an approximate Loch Lomond sea-level of at or near that at present (± 5 m) is a reasonable assumption. Such a wide range can is justifiable when one considers both the high spring tidal range present in the area (+ 4.6 m) and that for any of the proposed shorelines, be they based on morphological or biostratigraphical parameters, it is still not known wether they represent the level of Mean High Water Springs or Highest Astronomical Tides.

As with the Lateglacial marine limit there is widespread evidence for a raised Main Postglacial Shoreline having developed on Skye. Well developed fragments can be found both within and outwith Loch Lomond glacier limits and their form depends on the local solid or drift geology and the morphology of the coastline (*eg.* is the site subject to large or small fetches). Raised features occur up to *c.* 10 mOD (Richards, 1971; Walker *et al.*, 1988), however, the tilt of the shoreline can only be estimated, at 0.07 km^{-1} north-westwards, from generalised isobases extrapolated from data collected on the mainland (Sissons, 1983b: See Figure 3.10.).

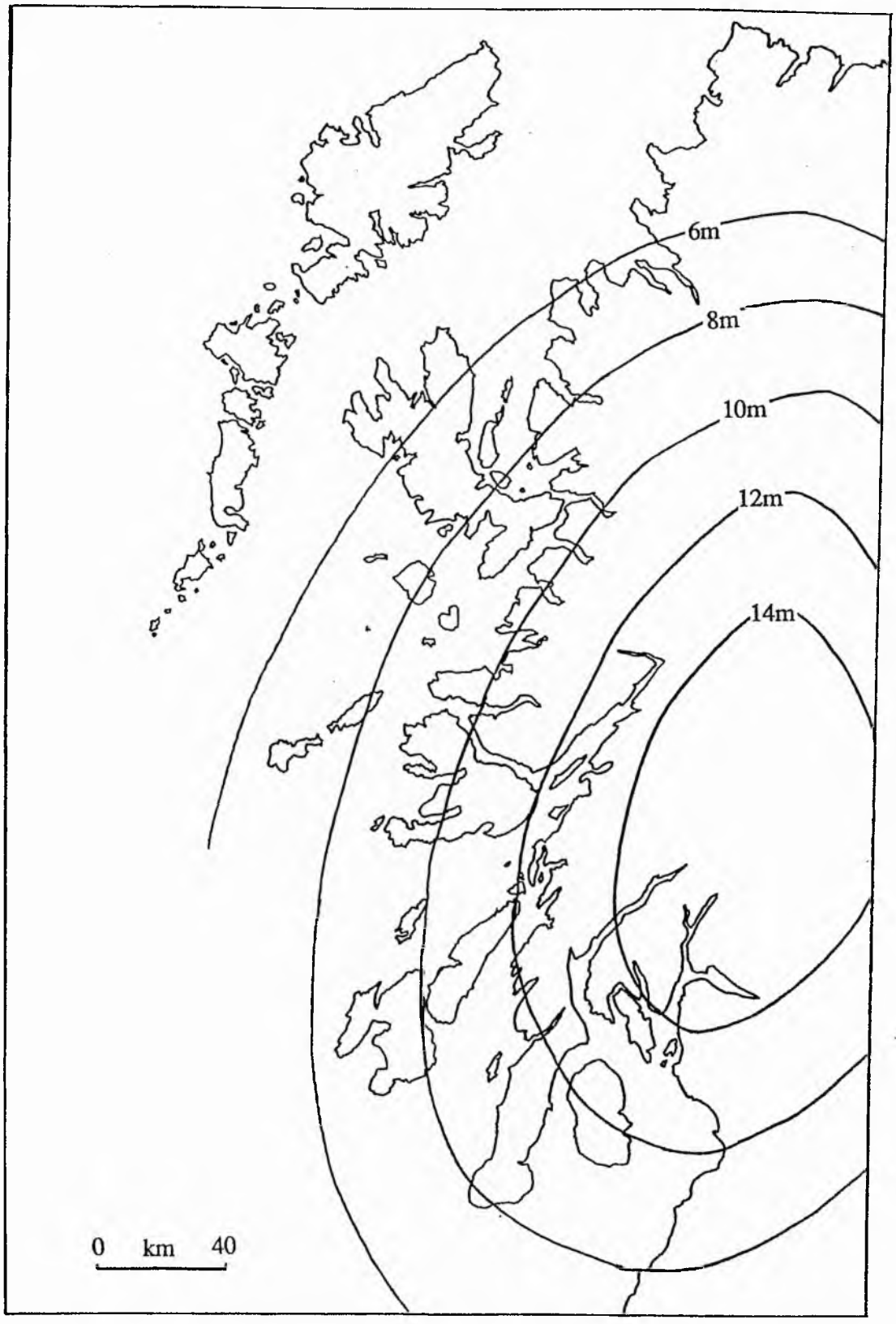

Figure 3.10. Isobase Chart of the Main Postglacial Shoreline for Skye and the adjacent Mainland (After Boulton *et al.*, 1991).

3.2.3. THE GEOMORPHOLOGY OF THE LOCH AINORT BASIN

In addition to descriptions of both the solid and surficial geology of the Loch Ainort basin presented in Sections 3.2.1. and 3.2.2., Section 3.2.3. describes the current morphology of the Loch Ainort system.

The Loch Ainort basin represents a broad valley system, with Loch Ainort itself being the marine receptor to four discrete valleys; Coire Choinnich, Coire na Seilig, Coire nam Bruadaran and the glen of the Allt Mhic Mhoirein. (See Figure 3.1b) The rivers within these valleys coalesce over an area of low ground, centred on Sròn Ard a' Mhullaich at the head of the loch, and extend offshore over a well developed inter-tidal delta plain. The hinterland of this basin rises rapidly from sea level to reach a maximum height of 806 m on the summit of Garbh-bheinn, 4 km to the south. This peak lies towards the bottom of a north-south trending ridge, the summits of which all exceed 550 m. To the east lies Belig (702 m) and Glas Bheinn Mhòr (570 m), with the summits of Marsco (736 m), Beinn Dearg Mheadhonach (651 m), Beinn Dearg Mhór (731 m) and Glamaig (775 m) located to the north. The summits are separated by broad cols which descend to a minimum height of 275 m (Màm a' Phobuill) between Marsco and Beinn Dearg Mheadhonach. Belig and Garbh-bheinn are outliers of the ultrabasic Cuillin Complex (See Sections 3.2.1., 3.2.1.4 and Figure 3.2) and, as such, their north-easterly facing corries are characterised by steep, irregular, free faces on their backwalls. These corries possess a series of immature talus slopes, which have developed during the Holocene and which record a series of rockfalls. Well developed trimlines on these same hills imply they stood as nunataks above Loch Lomond Readvance ice at least. It is unclear if they were exposed during the Dimlington Stadial glacial maximum (See Below).

By contrast, Glas Bheinn Mhòr to the north of Belig is underlain by closely jointed epigranites of the Eastern Red Hills Centre (See Section 3.2.1.3.) and, as such, is characterised by slopes with a more gentle rectilinear form. The upper slopes of this hill are generally covered by unvegetated screes and sedimentary-gravity flows, whilst the lower slopes are mantled by vegetated cover and dissected drift. To the north and west, Marsco, Beinn Dearg Mheadhonach, Beinn Dearg Mhór and Glamaig are all underlain by a variety of epigranites belonging to the Western Red Hills Centre (See Section 3.2.1.2.). Although there are spatial variations in both lithological and structural characteristics, both between these

peaks and those of the Eastern Red Hills Centre, they all share morphological similarities with Glas Bheinn Mhòr. Again the upper slopes are dominated by screes and sedimentary-gravity flows, whilst on the highest ground free faces and bedrock outcrops are not uncommon. Incipient corries are present on the east facing slopes of a number of these hills but these support only poorly developed rock walls. The only real variation to this norm is the presence of terraced, free faces cut into the basalts which cap the summit of Glamaig to the north of the area (See Section 3.2.1.4.).

To the east of Glamaig and Beinn Dearg Mhór lies the Moll peninsula, an area of undulating low ground (maximum altitude 284 m on the summit of Meall a' Mhaoil) which is separated from the major peaks by Gleann Torra-mhichaig. The underlying complex geology, which is well exposed beneath a thin veneer of primarily pre-Loch Lomond drift, is represented by only minor relief elements within a subdued lowland topography. The main feature of the Moll peninsula is the east-west trending Coire Mòr which feeds into the unnamed deep between Scalpay and the mainland. Coire Mòr is a glaciated, albeit asymmetric and V-shaped valley, which exploits the contact between well cleaved porphyritic felsite to the north and a closely jointed epigranite to the south.

Glas Bheinn Mhòr and Belig are separated from the hills farther east by the low lying (maximum altitude *c.* 25 m OD), drift covered Srath Mòr. Within it the Allt na Lùibe flows northwards toward the inter-tidal delta at Luib. Due east of Luib, is the rounded epigranite hill of Am Meall (193 m) whose boulder strewn slopes border the junction between Loch Ainort and Loch na Cairidh. Farther south the ground rises more rapidly to the more irregular peaks of Beinn na Cro (572 m) and Glas Bheinn Bheag (345 m). These hills and the cluster of peaks around Beinn na Caillich (732 m), which lie still farther south (separated by a low lying valley; Srath Beag), are also underlain by rocks of the Eastern Red Hills Centre and so again exhibit many of the characteristics ascribed to those located farther to the west. The major difference between this area and those described previously is the presence of pre-Tertiary sediments which correlate closely with the low-lying ground around Strollamus and the south-western shores of Loch na Cairidh.

The western shores of the Island of Scalpay rise more gently toward a lower range of rounded hills including, from north to south, Beinn Reireag Bheag (225 m), Beinn Chàirn

(220 m) and Mullach na Càrn (395 m). The lower drift mantled slopes lie on the extreme easterly extension of the Eastern Red Hills Centre, whilst the majority of the higher ground is underlain by competent strata belonging to the Lower Torridonian, Diabaig Formation. At the south-eastern edge of the field area to the north of the Caolas Scalpay the forested slopes have developed on indurated and metamorphosed Jurassic and Cretaceous sediments (See Section 3.2.1.1.).

3.3. THE HYDRODYNAMICS OF THE INNER SOUND AND ADJACENT AREAS.

Section 3.3. provides a brief summary of the present day hydrodynamic regime and its causes, for the Loch Ainort basin. The intention is not only to present background data for the interpretation of "modern" sedimentary processes occurring within the system (*ie.* those controlled by current climatic and oceanographic conditions) but also to act as a baseline environmental model with which to compare and contrast the reconstructed Loch Lomond Stadial palaeoenvironment. No *in situ* hydrographic data have been recorded for either area, consequently that presented here represents general interpretations for the Inner Hebrides.

Tidal motions of the British Isles are driven by the propagation of the oceanic tide over the British continental shelf (Officer, 1976). This movement produces a principally semi-diurnal tide, controlled by a minor amphidromic system centred between Scotland and Iceland, which sweeps co-tidal lines anticlockwise around the coastline of Western Britain (See Figure 3.11a - Bishop, 1977). The typical tide produced from this movement has a wavelength (λ) of approximately 1350 km. The individual component bulges and troughs of the tide develop at approximately 0.5 λ intervals ($\approx$ 675 km) a scale which would fully envelop the Inner Hebrides (Ellet and Edwards, 1983). Consequently, the tidal movement in the Inner Hebrides is predominantly controlled by the development of a smaller scale, virtual (*ie.* inland), amphidromic point centred on Islay (See Figure 3.11b).

The dominantly southwards movement of this tide into the Loch Ainort area via the Inner Sound and the Sound of Raasay produces complex oscillatory motions of the water body. By

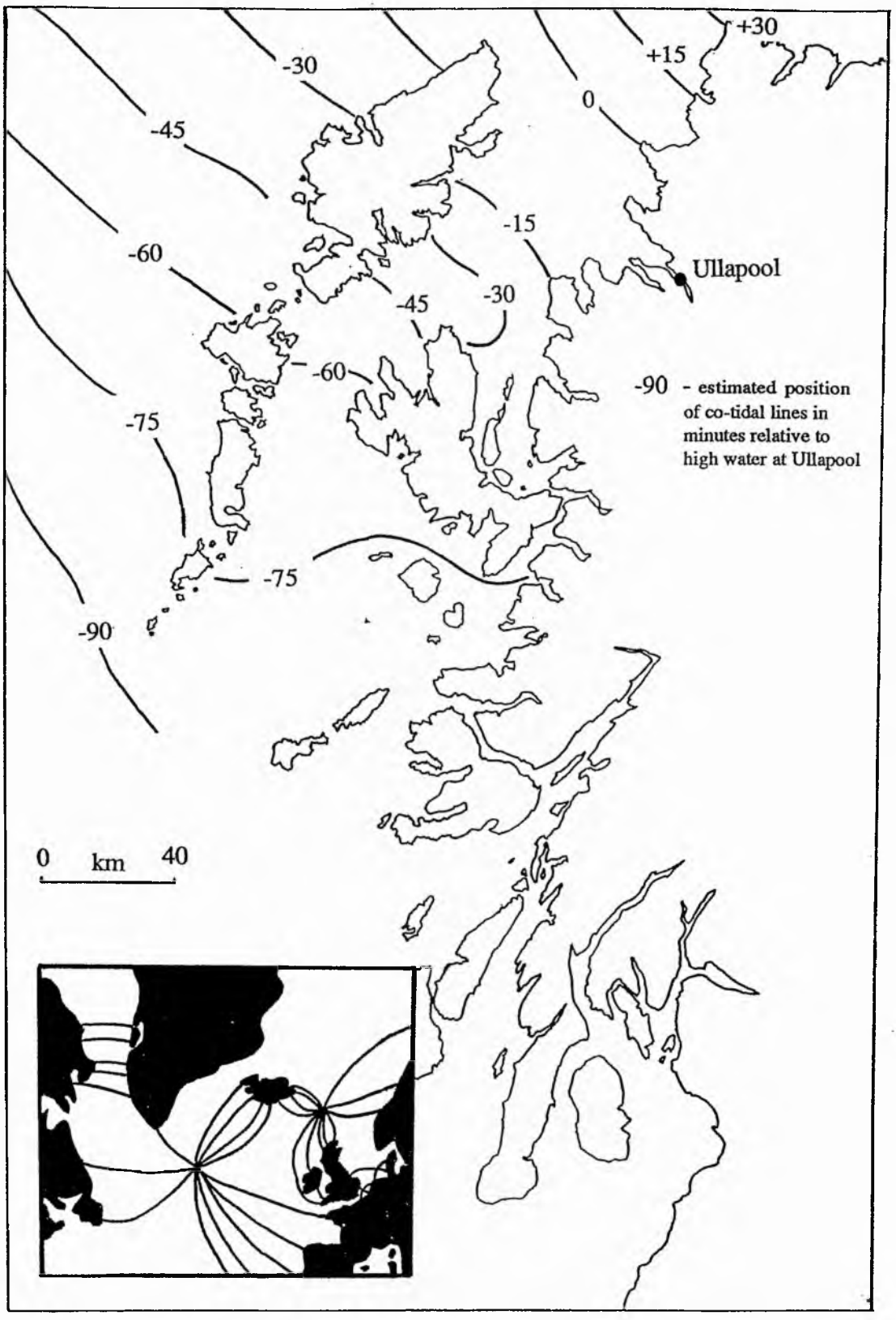

Figure 3.11. Hydrodynamic regimes of: a) the British Isles; and b) the field area (After Bishop, 1977).

applying the diagnostic criteria of Doodson and Warburg (1941)[10], Bishop (1977) identified the presence of a standing wave within the Inner Sound. Applying similar criteria[10] to the Sound of Raasay it seems plausible that a standing wave may be set up within this water body. This presumption also complies with the general characteristic of fjordic environments as described by Syvitski *et al.* (1987) such that: "The tide in fjords is predominantly a standing wave in which the sea level moves up and down synchronously.". It is therefore predicted that water movement within Loch Ainort is the result of a three way interaction. The two standing wave systems of the Inner Sound and the Sound of Raasay will enter the area via the open northerly access of Caol Mòr and the Narrows of Raasay, whilst an inferred weak component of water flows from the Sound of Sleat northwards into Loch Ainort via Kyle Akin and Caolas Scalpay.

The main component of the Inner Hebrides tidal stream passes southwards down the Inner Sound and into Loch Alsh via Kyle Akin where, due to the confining topography it changes direction and moves eastwards along Loch Alsh and into Loch Duich. However, this movement of water is complicated by the northerly passage of water from the Sound of Sleat, via Kyle Rhea and into the Loch Duich-Long-Alsh system.

For the Inner Hebrides, the coastal tidal system is characterised by a strong spring to neap range variation, with a spring tidal range approximately 4.6 m compared with a neap tidal value of approximately 1.6 m. The size of the maximum spring tidal current for the Inner Hebrides is controlled by the balance between sea surface slope forces, inertia and the Coriolis force (Ellet and Edwards, 1983). Calculations based on their equations give maximum tidal currents values of between 5 and 6 ms^{-1} for areas such as the Sound of Sleat. The strength of these currents is particularly important for the area's hydrography as they result in the vigorous mixing of incoming oceanic waters producing a near vertically homogeneous water body.

---

[10] Diagnostic features for the identification of standing waves in a short gulf: *i*)The uniform arrival of high water. *ii*) Increasing tidal range towards the head of the body. *iii*) Maximum tidal velocities occur at mid-tide.

A reduction in water depth towards shorelines and especially the more variable macro- and micro-relief of these near shore regions (See Sections 4.3.) results in the localised decrease of tidal currents, due to increased drag on the bottom of the water column. The decrease in velocity is so marked that a quote for the mean current speed over the Loch Ainort sill cross-section (0.02 ms^{-1}), by Edwards and Sharples (1991), is two orders of magnitude lower than the maximum tidal currents. However, a more representative value for the size of the tidal currents over shallow coastal regions can be calculated (After Ellet and Edwards, 1983) from:

$$\mathbf{c = [h(g/D)^{0.5}]/2} \qquad \textit{Equation 3.1)}$$

Where **c** = water velocity (ms^{-1}), **h** = maximum wave height at springs (m), **g** = acceleration due to gravity (= 9.8 ms^{-2}) and **D** = depth (m).With a maximum spring wave height for the area of 4.5 m (Ellet and Edwards, op. cit.) and an average depth of 30 m for the Loch Ainort basin, would give a maximum water velocity of 1.3 ms^{-1}.

In addition to the movement of water due to tidal ebb and flow, residual currents occur throughout the Inner Hebrides. These are related to both inshore water masses created by the large scale influx of freshwater run-off into the coastal zone (See Discussion below) and the movement of Atlantic water (*ie.* North Atlantic Drift Water) through the area. However, the latter water body is weak if not totally absent from this inner section of the western seaboard as the available information suggests it passes through the area further to the west, via the Little Minch, rather than the Sound of Sleat (Ellet and Edwards, op. cit. - See Figure 3.11b).

The interaction of oceanic waters and catchment derived fluvial waters determine the true hydrodynamic nature of the Loch Ainort system. This interconnectivity of these water bodies also provides the basis of the classic loch classification of Milne (1972: See Table 3.3.: Overleaf).

Loch Ainort has a partially silled entrance which can be defined by the 26 m contour, with the inner loch basin, this sill defines, attaining a maximum depth of -41 mOD[11]. This sill is

[11] For a full description of the bathymetry of this area see Section 4.3.1.1. and 4.3.1.2..

breached by a channel offset towards the north-western shore and which reaches a maximum depth of -44 m OD. The presence of this channel cutting through the sill will increase the exchange of water between the ocean (*ie.* water from the Minches and the Inner Sound) and the Loch Ainort basin compared to the totally enclosed 'B'-type basin (See Table 3.3.). It is evident, however, that the presence of a substantial barrier extending for over 80 % of the loch's width at this junction will still result in its oceanographic properties deviating substantially from the more oceanic conditions prevalent in the Minches and the Inner Sound (For Localities See Figure 3.11b). Consequently Milne's now apparently simple classification fails to take account of this partially silled scenario. This author therefore found it necessary to identify a new "Type A/B" category to accommodate the inferred oceanographic properties of the Loch Ainort water mass (See Table 3.3.).

LOCH TYPE	*DESCRIPTION*
A. Estuarine Sea Lochs	Deep water entrances and no sills; full penetration of salinity wedge into loch from offshore regions; typical vertical estuarine circulation; relationship between circulation and dilution depends on tidal range and fresh water run-off.
A/B. Partially Silled Sea Lochs	Partially separated from main coastal oceanic waters by incomplete sill, restricting the exchange between the saline wedge and variably diluted basin waters.
B. Fjordic Sea Lochs	Separated from main coastal oceanic waters by a single submarine barrier or sill; oceanographically termed basins.
C. Fjordic Sea Lochs	Separated from main coastal oceanic waters by double or multiple submarine barriers or sills; oceanographically termed basins.

Table 3.3. Sea Loch Classification Modified After Milne (1972).

CHAPTER 4

4. BATHYMETRY

4.1. INTRODUCTION

The importance of bathymetric charts for the comprehensive understanding of sub-aqueous environments has long been established. Many authors consider the construction and subsequent analysis of such charts particular important for the investigation of both modern and ancient glacial environments, that may be located either beneath inland, standing water bodies or at offshore localities (*eg.* Derbyshire, 1974; Gustavson, 1975; Hutchinson *et al.*, 1981; Landmesser *et al.*, 1982; Duck and McManus, 1985a and b; Lowe *et al.*, 1991).

This chapter covers the methodology of the bathymetric surveying technique used in the current research project. It also aims to describe the construction of the charts for the Loch Ainort field area. Charts 4.1. (See Backleaf) have been constructed from data retrieved from a survey conducted at the turn of the century (See Section 4.2.1.). In addition, Chart 4.2. was produced as the direct result of the manipulation of recently acquired data. This combination of data sets has enabled both the extension of the study area and, more importantly, a critical appraisal of the development of bathymetric techniques over the last hundred years. Having assessed the relative merits of each chart a detailed morphological description of the area is given.

4.2. METHODOLOGY.

Prior to acquisition of bathymetric data during the multi-geophysical investigation of Loch Ainort, the Admiralty Chart for the survey area was requested from the Ministry of Defence[1], with the intention of identifying areas requiring specific attention (See Section 4.2.1.). Copies of the original datasets for the area were obtained and converted to modern depth units and datum's to enable direct comparison between the two charts.

[1] Hydrographic Data Centre, Hydrographic Office, Ministry of Defence, Taunton, Somerset. TA1 2DN.

The current bathymetric survey of Loch Ainort was carried out using a Lowrance X-15^{M} Grayline recorder (See Section 2.3.3.1.). Navigational control was provided by Traversing (See Section 2.3.2.1.) for lines A1-A16 and B1-B14, and by the Magellan GPS receiver (See Section 2.3.2.2.) for lines C1-C13 (See Figure 4.1.). For the Magellan-controlled surveys of this area, datum was set to WGS72 (World Geodetic System - 1972 Datum). In order, for the readings to agree with the Ordnance Survey base maps, it is necessary to make a further correction to them of 0.02 minutes northward and 0.08 minutes eastward (Hall, 1989). To assess the accuracy of this navigational system two control readings were taken, one at a cable post on the north-western slopes of Am Meall [NG572288]. The second reading was taken from the south-western edge of the junction of the A850 and the Loch Ainort coastal track [NG544268]. Both of these control points plot, on a 1:10560 Ordnance survey map, within operational error (a pencil width $\leq$ 10 m).

4.2.1. ADMIRALTY CHART

The most up to date admiralty chart at the disposal of the M.o.D. for this area is a depth sounding chart produced from surveys conducted in the middle of the nineteenth century. The chart is constructed at a scale of 6 Inches to 1 Nautical Mile (1:12155), with depth given in fathoms. The chart is based on two surveys conducted under the direction of Commander James Wood R.N. (In service: 1847-1860). In 1854 he was given charge of the hydrographic survey of the Northwest coast of Scotland which included the waters of the Isle of Skye north of Loch Ainneart (Loch Ainort - surveyed in 1855) and the Sound of Sleat (Dawson, 1969).

The late nineteenth century Admiralty surveys used traverses run between known end points, with additional position fixing provided by horizontal sextant readings on known topographical stations, of which a single co-ordinate remians (See Table 4.1.). Due to the lack of actual navigational records employed during individual surveys, it is difficult to assign a positional error to the Ainort Admiralty data sets. It is generally accepted that in the hands of experienced operators horizontal sextant angles provide a positional accuracy of $\pm$ 5 m. However, comparisons of the longitude and latitude co-ordinates for the named reference station (See Table 4.1.) between the 1854 - 1855 survey and the 1968 - 1971 Ordnance

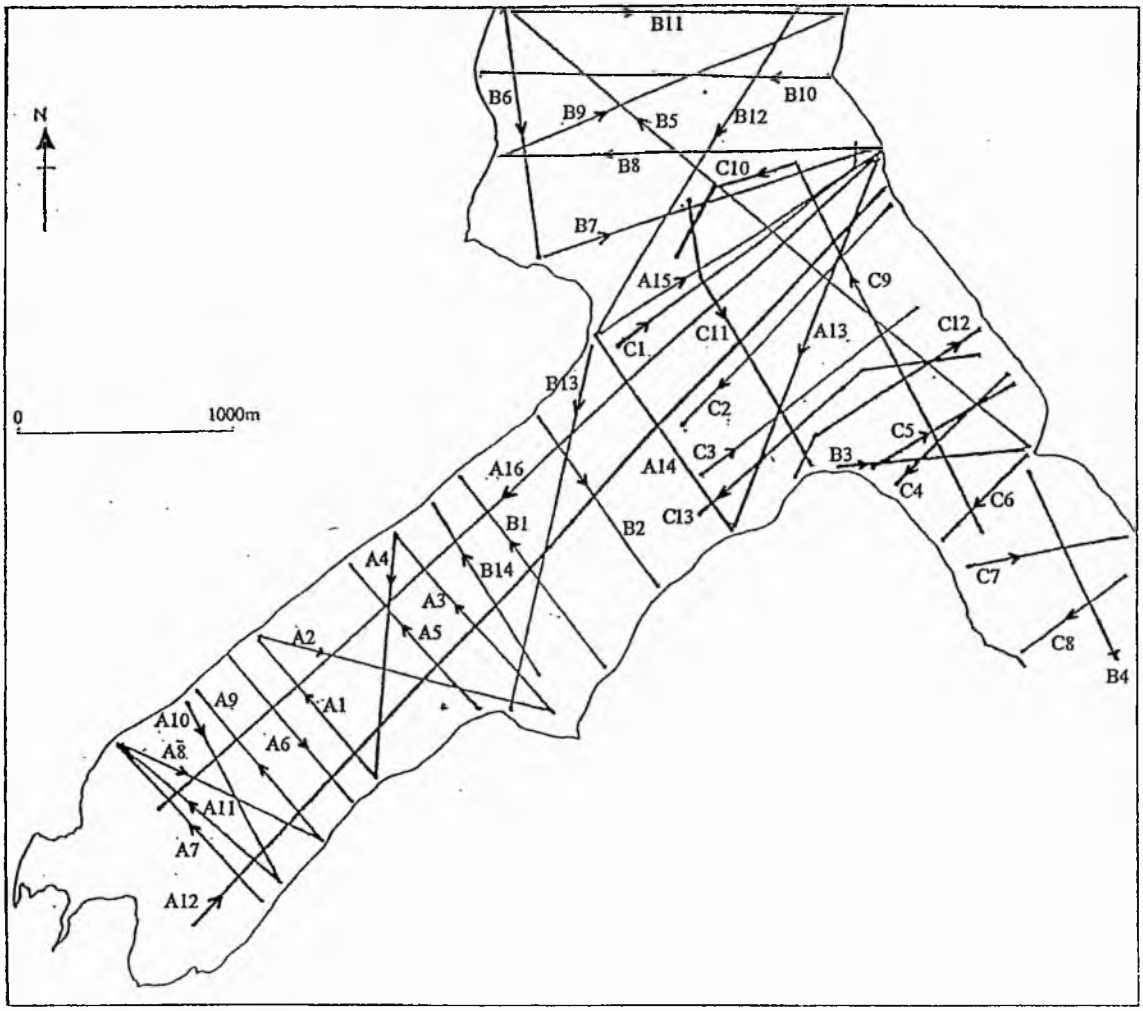

Figure 4.1. Traverse lines for the bathymetric survey of Loch Ainort.

error. Consequently where OSGB36 grid co-ordinates of geomorphological features have been given in the text they are quoted to the nearest 100 m.

The survey covers a designated area by a series of evenly spaced (*c.* 155 m) parallel traverse lines oriented at acute angles to the margin of the loch. There are no control traverses made perpendicular to the dominating traverse direction. Employing such a traverses pattern the Admiralty survey achieved a Traverse density of 7 lines/km in Loch Ainort. Depth soundings were taken between every 10 m and 130 m depending on the traverse pattern employed. All depth readings are given in fathoms and fractions of fathoms, with each sounding having been taken by the lead line technique. All soundings represent the depth at low water ordinary spring tides, having been reduced to a datum referred to as " ...a 13' mark cut inside the pier at Kyleakin, the lower part of this mark being 13' [3.96 m] above low water or zero of the ordinary spring tides.". These values were then recalculated to Ordnance Datum Newlyn to enable comparison between the Admiralty and acquired datasets.

Loch	*Reference Station (Present name in brackets)*	*Location*	*Location (OSGB36)*
Ainort	Scalpa (Mullach na Càrn)	57° 17' 27.80'' N 5° 58' 27.0'' W	Càrn (14 m WSW)

Table 4.1.: Location of the reference station for the 1855 Admiralty survey of Loch Ainort.

In order to hand contour the bathymetric chart from the depth point information it was necessary to convert the fathom readings to nearest metre values, where:

1 Fathom = 1.8288 Metres ***Equation 4.1)***

Chart 4.1. shows the results of hand contouring of the Admiralty Survey data by this author. In addition, Section 4.3.1. gives a morphological description of the area which these charts cover.

4.2.2. TRAVERSE DENSITY

For the current surveys undertaken on the loch a compromise had to be made between the density of coverage provided by the traverse lines and an expedient time frame in which to complete each survey. As has been described from many previous bathymetric surveys, increased traverse density provides greater detail from which to construct charts (McManus, 1985). However, the number of traverses that can be completed depends on the size of the water body being surveyed and the availability of equipment, time and personnel. Logically, the greatest traverse densities are possible on the smallest bodies, *eg.* a survey of Briksdal Lake, Norway (Duck and McManus, 1985a), achieved a traverse density equivalent to 530 lines/km^2 in a single day, but over an area of a mere 0.471 km^2. By comparison, a bathymetric survey of a 3.9 km^2 section of the Upper Forth Estuary (T.E.R.C., 1991) using identical equipment as that used in this project, achieved a traverse density of only 65 lines/km^2 in an intensive two week survey.

With the Loch Ainort survey occupying an area of 9 km^2, and with the constraining operational parameters inherent with a west coast survey (See Section 2.2.), it was considered impractical to attempt to acquire at these traverse densities. Therefore a traverse density of *c.* 5.5 lines/km^2 was aimed for, a value that has previously been achieved in a successful survey of the similarly sized (9.72 km^2) Loch Earn (Al-Ansari and McManus, 1980). The final traverse densities achieved was 5 lines/km^2.

In addition to considerations pertaining to the number of traverse lines acquired, it is important to consider the distribution of the lines. To aid interpolation between individual depth points a grid format (See Figure 4.2a.) is considered to be the ideal pattern, with an equal number of lines running perpendicular to each other (*eg.* Gerken, 1974). If the morphology of a survey area makes such a configuration difficult, as with the approximately rectangular form exhibited by the majority of sea lochs (*ie.* a high length:width ratio), an adapted pattern has to be used (See Figure 4.2b). Such an adapted pattern consists of a large number of "closely" spaced cross-traverses orientated parallel to the width of the loch. An element of control is brought to these lines by a smaller number of longitudinal traverses orientated parallel to the loch sides (See surveys in: Duck and McManus, 1985b). Such a configuration has been employed during the Loch Ainort survey.

Figure 4.2a. Sketch diagram showing the idealised traverse pattern for the Loch Ainort field area.

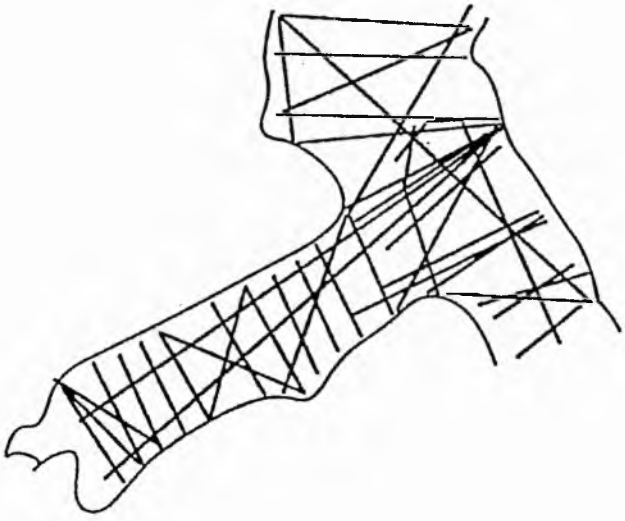

Figure 4.2b. Sketch diagram showing the adapted grid traverse pattern used in the bathymetric survey of Loch Ainort.

4.2.3. DEPTH INTERVAL

In the initial stage of chart construction it is necessary to select an appropriate depth interval at which to contour. This choice, inevitably, has to be a compromise between the maximum depth encountered, the degree of detail required, the traverse density and the accuracy of position fixing. Ideally, a contour interval of 1 m should be used in the investigation of sub-aqueous glacial environments (Lowe *et al.*, 1991), in order to identify any small scale features that may be present. Conversely plotting at depth intervals in excess of 1 m makes it increasingly difficult to identify a complex topography. When the interval exceeds 10 m, resolution becomes so poor that in these shallow nearshore environments (< 120 m) only the simplest of bathymetric charts can be constructed. However, this author suggests that a 1 m interval does have numerous operational drawbacks.

Where greater depths are encountered such a large number of contours are required that, when plotted on a reproducible scale individual contour lines merge and resolution is lost. Equally, even on surveys with a high traverse density, the actual separation between individual lines may be of the order of 10s of metres. This suggests that any aspiration towards increased resolution by using a contour interval of 1 m is restricted to only two dimensions, described by the traverse profile itself. The effective three-dimensional resolution is controlled by the largest dimension of the depth interval - traverse spacing couplet. From this it is inferred that, except in surveys with exceptionally high traverse densities (> 200 lines/km^2), the contour interval chosen should never be less than 10 m. However, to cover a survey area the size of Loch Ainort, with the minimum of 200 lines/km^2 but working at the maximum survey speed of 3.5 knots would take a minimum of 46.5 working days, a time and labour effort significantly disproportionate to the resolution possible with the data retrieved.

The problems of a 1 m depth interval are further exacerbated by the errors inherent in position fixing. Whatever form of navigational control is used during these surveys (See Section 2.3.2.) a minimum error of ± 15 m will be present. Whilst the maximum positional error may reach ± 40 m in the centre of the lochs, depending on the technique used. It is therefore considered inadvisable to choose a depth interval that is significantly lower than the accuracy of the navigational control. Having taken into consideration all the factors quoted here, a depth interval of 2 m was chosen to represent the data retrieved from the surveys

undertaken as part of this project. Although, this choice appears to contradict the operational constraints cited for such a limited survey, these problems are offset by both the shallow depths encountered and the complexity of the nearshore sea bed. It is therefore suggested that all charts constructed purely from plotted depth points should be viewed with caution.

4.2.4. TIDAL CORRECTION.

As described in Section 2.3.3.1. the Lowrance echosounder does not record true depth, but the distance from the transducer to the loch floor. For our surveys the echosounder transducer was hull mounted in a survey vessel (See Section 2.3.1.) with a draught of only 0.4 m, consequently, the transducer was measured to be 0.25 m beneath the water surface. Considering the charts were drawn with a minimum contour interval of 2 m and a maximum positional accuracy for each depth reading of at best ± 3 m, the actual distance measured from the traces was assumed to represent the distance from the water surface to the loch floor. In a tidal environment, sea level varies with the tidal cycle. Therefore in order to determine the true topographical variability of the loch floor, compensation for sea level variation with time has to be made. This is achieved by reference to the tidal curves of the area measured during the hours of operation.

Due to the absence of a tide gauge within Loch Ainort, the tidal curves (See Figure 4.3a, b and c) for the Loch Ainort bathymetric survey were constructed from measurements (given in metres relative to Admiralty Chart Datum) taken from Portree Harbour, 15 km to the north. An approximation of the tidal curve can be calculated for the area as a broad idea of the driving tidal forces are known for the area (See Section 3.3.). As suggested in Section 3.3. the tidal motions of the Inner Hebrides are driven by the propagation of the oceanic tide over the continental shelf. Such motion results in a semi-diurnal tide with a period of *c.* 12.5 hours (Ellet and Edwards, 1983), which is controlled by a minor, virtual, amphidromic system centred on Islay. The movement of this tide through the waters east of Skye, on a simplified basis, represents a standing wave from which we can infer that there is an approximate uniform arrival of high water. Consequently we can directly apply the tidal curve for Portree to the area.

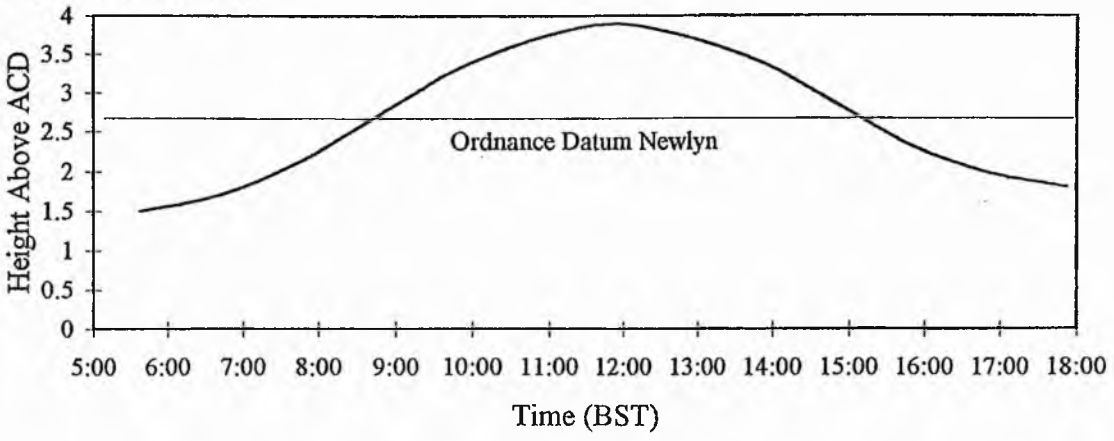

Figure 4.3a) Loch Ainort Tidal Curve: 16/05/90

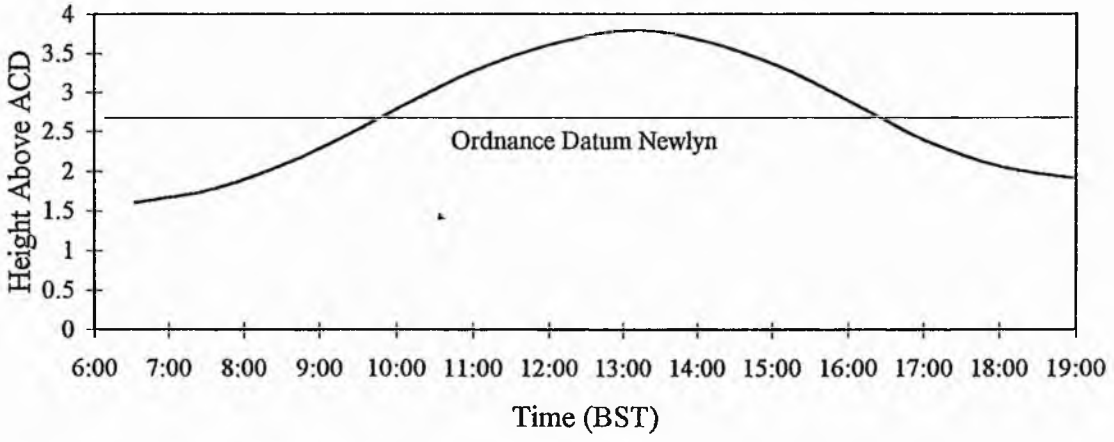

Figure 4.3b) Loch Ainort Tidal Curve: 17/05/90

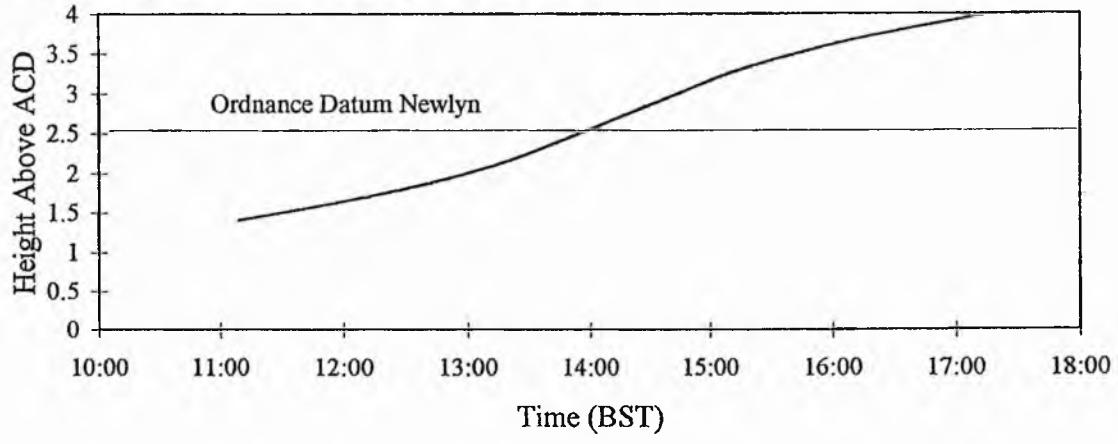

Figure 4.3c) Loch Ainort Tidal Curve: 22/05/91

Once the tidal curves had been determined relative to Admiralty Chart Datum for the Loch Ainort area during the survey periods it was then necessary to convert these measurements to Ordnance Datum, Newlyn. For Loch Ainort, Admiralty Chart datum is 2.65 m below Ordnance Datum, Newlyn. Using the reconstructed tidal curves relative to this datum, it was then possible to reduce depth data to Ordnance Datum, Newlyn, thus eradicating the sea level fluctuation error. Reduction, is a simple operation of subtracting the tidal height at time of data collection from a given depth value (Anon, 1990). Where it is necessary to describe features in relation to Mean Sea Level it is necessary to add on 2.25 m to the OD depths.

4.2.5. CHART CONSTRUCTION.

Having established the periodic variation of water level for the loch during the time of surveying, it became possible to take accurate depth measurements from the individual echograms. Using a chosen depth interval of 2 m (See Section 4.2.3.) a series of parallel lines were drawn directly on to the echograms (See Figure 4.4.), each having been corrected for the tidal variation. A perpendicular line is drawn at the point of intersection of each depth value with the uppermost reflector of the echosounder profile. These perpendicular lines represent the location along the line of traverse of each depth point and are plotted on a chart with their corresponding depth value (See Figure 4.5.). The accuracy of each position depends upon the distance between known points, be it the ends of each survey line in the case of traversed lines, or intermediate fixes where the Magellan GPS© navigation system was used (See Section 4.2.). The shorter the distance between fixed points the greater the positional accuracy of each depth point.

The individual depth points were located on 1:10560 scale maps (NG 52 NW, NG 52 NE and NG 53 SE) for the Loch Ainort. Having plotted all known depth points onto the base map, the final bathymetric chart was constructed by hand contouring. As has been discussed in Section 4.2.2. such a process requires significant interpolation between known depth points especially when considering the low traverse density of the Loch Ainort survey.

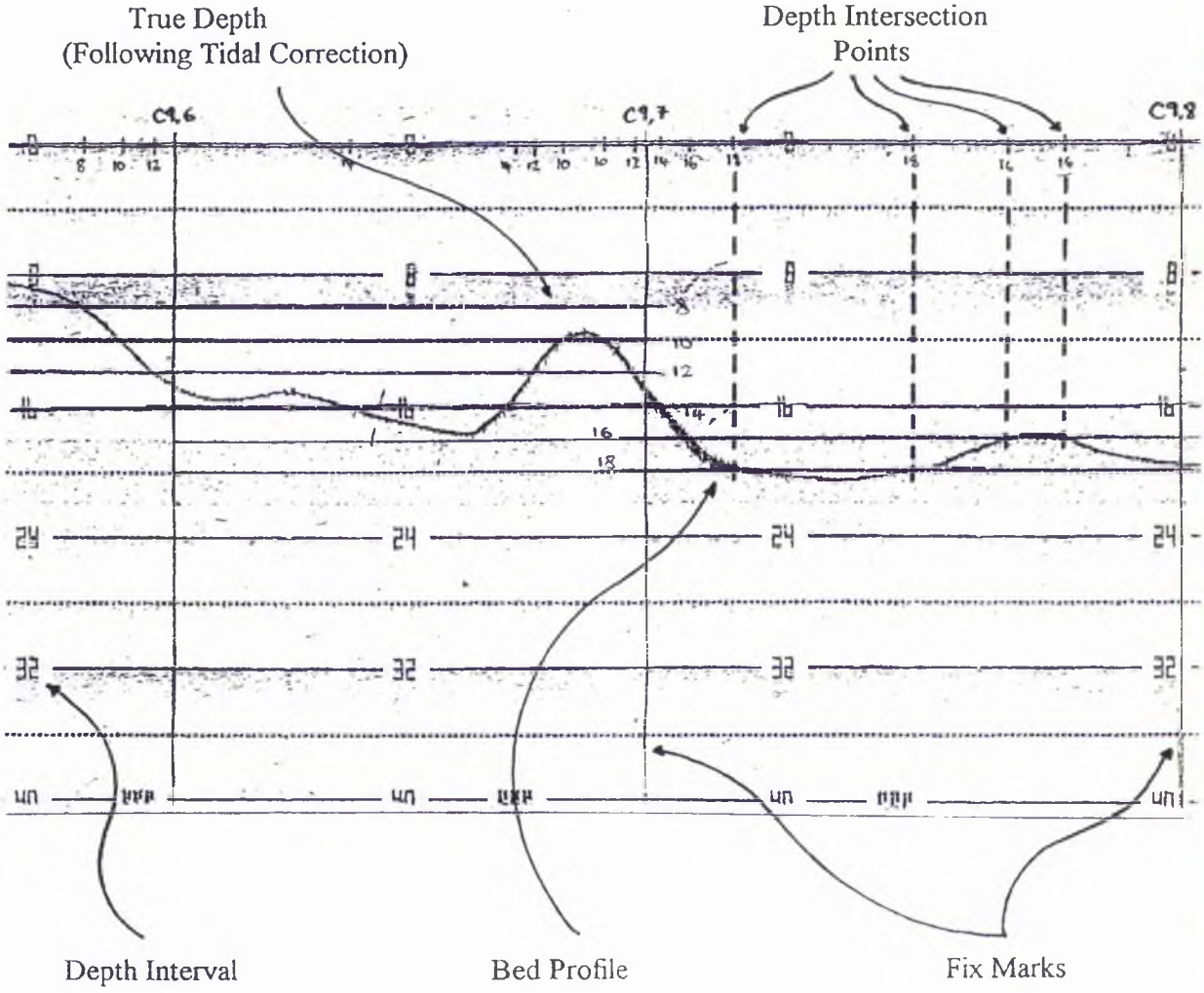

Figure 4.4. Retrieval of depth data from an echosounder trace.

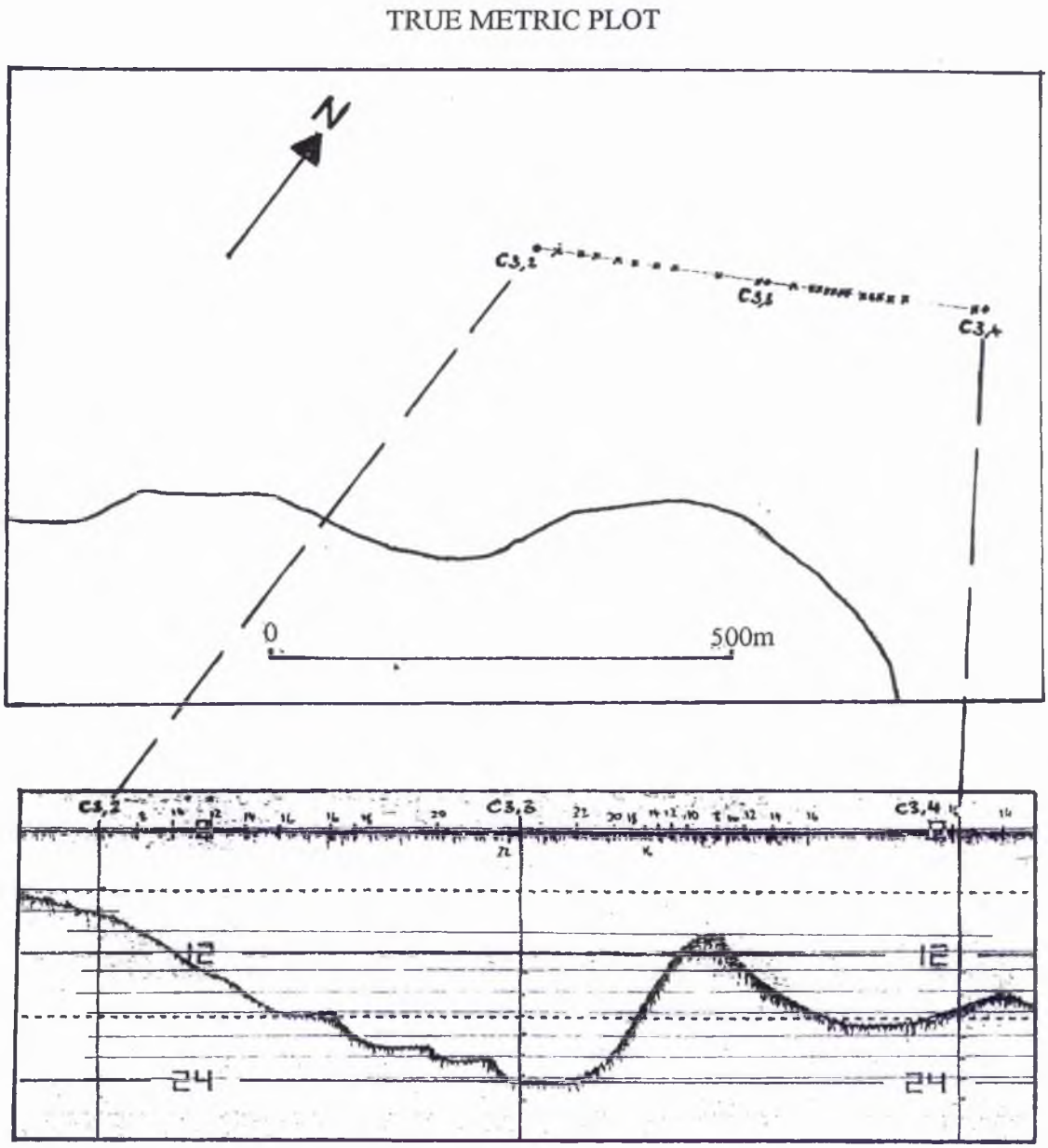

Figure 4.5. Positioning of depth points on bathymetric chart (*ie.* true metric scale).

4.3. LOCH AINORT.

For the purposes of describing its bathymetry, Loch Ainort has been divided into three discrete geographical areas, "Inner Loch Ainort", "Mouth Region" and "Unnamed Strait" (See Figure 4.6.). The boundary between the "Inner Loch Ainort and the "Mouth Region" is placed 200 m south-west of an arbitrary line drawn between Maol Bàn and Rubh' an Àird Dhuirche. The south-eastern boundary of the "Mouth Region" is again an arbitrary line drawn between Dunan and Allt Chrionaidh on Scalpay, so to include the outer part of Loch na Cairidh. The south-western shoreline of Scalpay continues to confine the "Mouth Region" to the north-east with the divide between the "Mouth Region" and the "Unnamed Strait" being represented by a line oriented due east from Mol (See Figure 4.6.).

Due to the greater traverse density and comparable positioning accuracy (potentially ± 5 m), the basic description of the loch topography is obtained from the Admiralty Chart (See Chart 4.1.) presented in Section 4.3.1.. A brief description based on the bathymetric data (See Chart 4.2.) obtained from the current surveys is presented in Section 4.3.2.. This section also attempts to compare and contrast Charts 4.1. and 4.2., to discuss the validity of non-comparable features and where appropriate amend the previous description of the loch bed.

4.3.1. ADMIRALTY CHART DATA.

As described in Section 4.2.1. the Admiralty Chart was constructed on the basis of a hydrographic survey undertaken in 1855. These data have been converted to the metric Ordnance Datum, Newlyn, and hand contoured by this author at a 2 m interval. The bathymetry of the Loch Ainort Basin is typified by a series of linear or arcuate topographical highs or as will be termed in this section ridges. For the purposes of cross-correlation with the other geophysical datasets described in Chapters 5 and 6 the individual ridges are assigned the prefix ABR, it being an acronym for Ainort Bathymetric Ridge. The descriptions presented in Section 4.3.1. are made with reference to Chart 4.1. (See Backleaf).

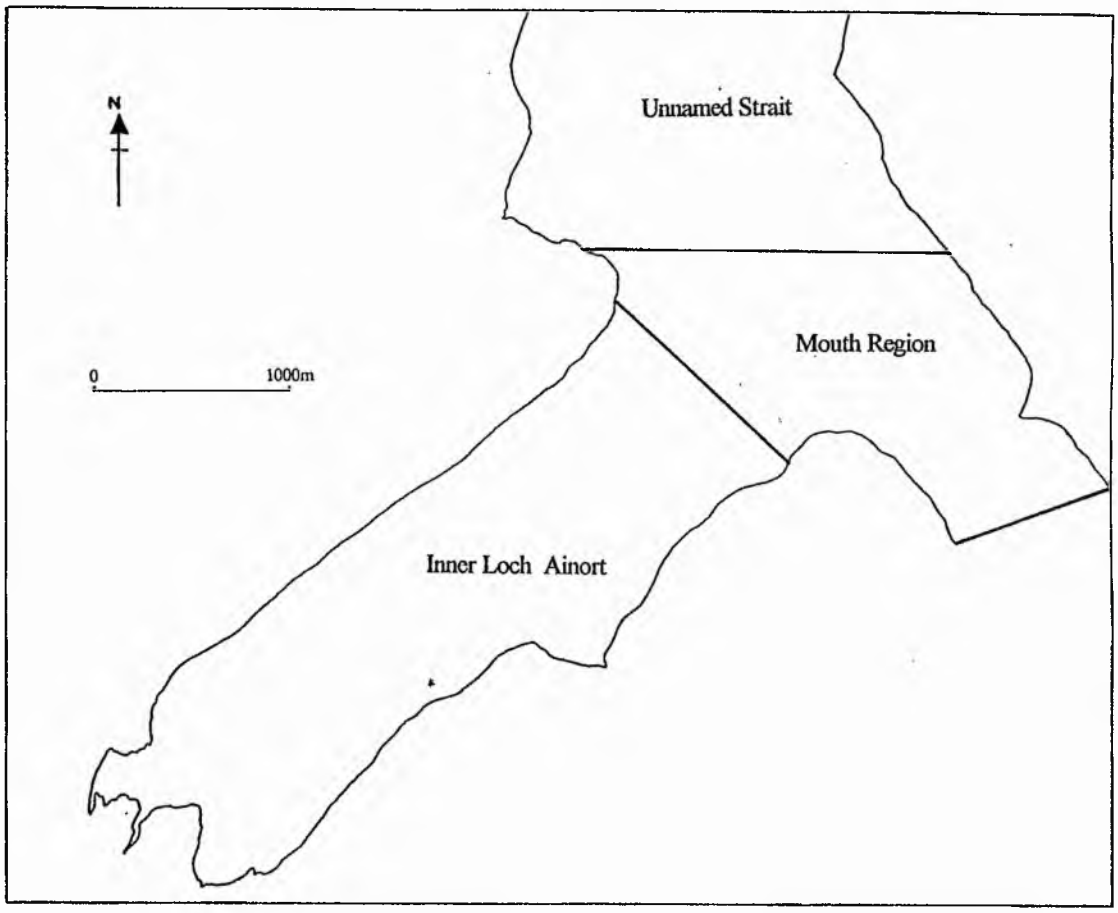

Figure 4.6. Geographical sub-divisions for use in the description of the Loch Ainort survey area.

4.3.1.1. Inner Loch Ainort.

Inner Loch Ainort (See Figure 4.6.) is characterised by an asymmetrical basin, with uniform steeper (average angle 12°) north-western slopes and more gently inclined (average angle 6°) but irregular south-eastern slopes. The deepest part (-43 mOD) of the inner loch is also offset towards the north-western shore and represents the base of a prominent shore-parallel channel defined by the -36mOD contour. The north-western margin is characterised by a shore-parallel break in slope between -4 mOD and -6 mOD. This feature defines a narrow (75 m) platform that thins in a down-loch direction and which has south-westerly gradient of 0.15°.

The relatively uniform nature of the north-western slopes are broken by two lochwards oriented ridges (ABR1 and ABR2). The first of these ridges (ABR1:[156600 829400]) is located 300 m south-west of Maol Bàn. This ridge has a relief of 12 m, between contours -22 mOD and -34 mOD, with an axial orientation of 010°. The contour configuration suggests this feature, is elongate (total length 260 m), concave to the west (down-loch) and has an asymmetric profile with an easterly inclined slope of 8° and a westerly inclined slope of 4.5°. The second ridge (ABR2: [156200 829200]) is located a further 485 m to the south-west, with its upper boundary being defined by a prominent break in slope at the -30 mOD contour. ABR2 is again elongate (total axial length 145 m) but linear and symmetrical (slope angles of 4.5° and 3°) in form. It has a relief of 6 m, between contours -30 mOD and -36 mOD, and an orientation of 165°.

Towards the head of the loch the north-western slope angles decrease as the shore-parallel channel widens from 200 m to 560 m and shallows to an averaged depth of -20 mOD. At the head of the loch 650 m to the north-east of Sròn Ard a'Mhullaich a prominent eastwardly facing slope, inclined at 7°, traverses the entire width of the loch. This slope is defined by the -10mOD and -18mOD contours and has an orientation of 174°. To the west of this slope the loch floor is inclined at a shallower angle (2.5° to the east) until becoming emergent 365 m to the north-east of Sròn Ard a'Mhullaich. This slope is broken on its southern margin by two ridges (ABR3 and ABR4). ABR3 [154700 828000] is located 790 m east of Kinloch Ainort, this ridge has an axial length of 220 m, a maximum relief of 6 m (defined by the -16 mOD and

-22 mOD contours), an orientation of 093° and an approximately symmetrical profile (northerly and southerly slopes having angles of 3.5° and 4.7° respectively).

ABR4 [155000 827500] is a east-north-easterly (075°) orientated ridge (ABR3) defined by the -12 mOD and -18 mOD contours suggesting a maximum relief of 6 m. ABR3 has an asymmetric profile with a steeper northerly facing slope (9.5°) and a gentler southerly facing slope (3.5°). ABR4 appears to have a total length of 245 m, but this is based on interpolation between only two data points so the significance of this particular feature is equivocal.

Although the south-eastern slopes have overall lower angles (average angle 6°) than those of its north-western counter-part, they have a significantly more irregular nature. Between Sròn Ard a'Mhullaich and Luib the shoreward component of these slopes are uniformly inclined at 7.5° to the north-west. A total of 250 m offshore from Aricharnach an area of broad (340 m), higher ground (-22 mOD compared to an average depth of -28 mOD) extends due north in to the loch. At the mouth of the Luib embayment the south-eastern slopes are broken by the protrusion of low-lying ground 365 m into the loch. The upper surface of this low ground is inclined by 1° north-north-westwards to a depth of -6 mOD to produce a rhomboid form. However, it is important to recognise that the angular form correlates with a single line of depth points and as such is more likely to be an artefact of the interpolation than to be of any generic significance. The slopes of this symmetrical feature are oriented to the north-west and north-east and are inclined at angles of 5.5°. This feature has a maximum relief of 20 m with a lower bounding contour of -26 mOD.

On the north-eastern limb of the Luib protrusion a poorly defined ridge (ABR5: [156600 828600]) extends 365 m due north into the loch, with an orientation of 163°. This feature has a symmetrical, arcuate profile concave down-loch. This ridge has a maximum relief of 3 m with gentle slope gradients between 1.5° and 2.5°.

A further 500 m to the north-east of this feature is another area of complex topography oriented in an overall northerly direction (340°) and extending from the lower slopes of Am Meall a total of 600 m into the loch. From a broad (460 m), rectangular, central shallow (between -8 mOD and -34 mOD) region that is inclined 0.9° to the north-north-west, two

spurs (or ridges: ABR6 and ABR7) extend further into the loch. The most prominent of these (ABR6: [156800 829100]) is a linear feature orientated at 100° with an axial length of 340 m and a maximum relief of 12 m, between -34 mOD and -22 mOD. ABR6 has an asymmetric profile with steep (15.8°) northerly facing slopes and more gently inclined southerly facing slopes (3.8°).

Ridge ABR6 actually extends from the second more poorly defined, higher altitude (between -10 mOD and -18 mOD: maximum relief 8 m), dual-ridge system (ABR7a and b: [157100 829200]). This secondary ridge has an orientation of 160°, an axial length of 350 m and a symmetric profile. The limbs of the adjoining ABR7a are, however, disproportionally developed with a well defined westerly limb (slope angle 9.3°) compared to a shorter (365 m vs 120 m) poorly developed easterly limb (slope angle 9.4°). This ridge complex, in conduction with ridge ABR1, on the north-western shore creates a partially silled entrance at the mouth of the Inner Loch. This sill is defined by the -34 mOD contour, which covers 80% of the loch width and is breached by the channel offset towards the north-western shore.

4.3.1.2. The Mouth Region.

The "Mouth Region" (See Figure 4.6.) represents the most complex topographical section of the Loch Ainort survey area. The region is characterised by an irregular ridge topography within a basin that attains a maximum depth of -48 mOD and with a maximum relief of 18 m. The deeper parts of the area are confined to a prominent channel which is a continuation of that described in the "Inner Loch" (See Section 4.3.1.1.) and which within this region turns through 90° as it opens out into the "Unnamed Strait" (See Section 4.3.1.3.) to the north. The average depth of this channel can be defined for this region by the -32 mOD contour. The maximum depth of this channel is reached at the entrance to the "Inner Loch" whilst the minimum depth of -26 mOD occurs 730 m east of Maol Bàn.

The "Mouth Region" broadly retains the asymmetric nature of the basin described in Section 4.3.1.1. with the western/north-western margins exhibiting the steepest slope angles (average 10°). Conversely the shores of Scalpay to the east and the outer part of the south-eastern shore at Rubh' an Àird Dhuirche exhibit gentler slope angles (average 2°). The shore-

parallel platform described for the "Inner Loch" area can again be defined for the western margin of the "Mouth Region". However as the platform mirrors the re-orientation of the shoreline northwards, around Maol Bàn, it widens to attain a maximum width of 255 m. The western margins of Scalpay are inclined seawards at an angle of 1.7° with the break of slope occurring between 245 m and 545 m offshore at the -10 mOD contour.

Five major ridges (ABR8, ABR9a and b, ABR10 and ABR11) can be described from this region, the first of these (ABR8: [156800 829700]) being located 300 m south-east of Maol Bàn. ABR8 is a short (axial length 170 m) linear feature, with an axial orientation of 109°, and steep (11.6°) symmetrical slopes. It has a relief of 12 m, being defined by the -38 mOD and the -26 mOD contours and appears to be spatially (albeit 4m lower) associated with ABR1 on the north-western shore of the "Inner Loch" (maximum relief 12 m, between contours -22 mOD and -34 mOD: See Section 4.3.1.1.). The second of the ridges (ABR9a: [157100 829900]) is located 360 m due east of Maol Bàn and 425 m north-east of the previously described ridge. ABR9a has an arcuate form (orientation varying between 091° and 120°), concave due south and with an asymmetric profile, the southerly facing slope being inclined at 13.4° whilst the northerly facing slopes are inclined at 6.2°. ABR9a has a maximum relief of 32 m defined by the -4 mOD and -36 mOD contours and an axial length of 415 m. To the north of this ridge the contours suggest a lower relief strongly asymmetric ridge extension (ABR9b: [157100 830100]) with an axial orientation of 075°. The gentle northerly facing slopes are inclined at 5° whilst the steeper southerly facing slopes are inclined at 10.2°. ABR9b has an axial length of 245 m and maximum relief of 14 m, defined by the -20 mOD and the -34 mOD contours.

The fourth ridge (ABR10: [157900 829300]) within this suite represents the offshore extension of the northern spur of Am Meall. ABR10 has an arcuate form, concave to the west (down loch), and extends 485 m with a variable orientation from 026° to 300°. It thins rapidly to the north from a maximum width of 300 m at Rubh' an Àird Dhuirche to an average width of 60 m at its apex. It also has a stepped longitudinal profile with a prominent plateau section (230 m x 255 m) between the -10 mOD and the -12 mOD contours. ABR10 has an average height of 14 m and again exhibits an asymmetric cross-sectional profile with steeper (7.3°) westerly facing slopes and shallower (2.7°) easterly facing slopes.

The final ridge (ABR11: [157900 829900]) to be described from within the Mouth Region is identified 890 m north of Rubh' an Àird Duirche, and extends in a westerly direction (094°) from the shallow offshore slopes of Scalpay. ABR11 has significantly different form to those described earlier with a broad (330 m) westerly margin which thins in an easterly direction attaining a minimum width of 180 m prior to merging in to the Scalpay slopes. The cross-sectional profile represents a slightly asymmetric profile (with northerly and southerly limb angles of 9.4° and 4.7° respectively) with the westerly margin of the ridge having a slope angle of 5.6°). This ridge has a maximum relief of 14 m (between the -12 mOD and the -26 mOD contours) and a maximum definable axial length of 425 m.

Although not strictly considered as being part of the "Mouth Region" a brief description of the outer part of Loch na Cairidh (the south-easterly trending basin connecting Loch Ainort to the Inner Sound: See Section 3.2.) is presented here. This thin (910 m) stretch of water represents a shallow (maximum depth -16 mOD), symmetrical, basin that merges with the main part of the Loch Ainort system to the north-west of Corran a' Chinn Uachdaraich. There is no evidence of any of the complex topography indicative of the two regions described so far being present within this area.

4.3.1.3. Unnamed Strait.

The "Unnamed Strait" (See Figure 4.6.) represents the deepest part of the Loch Ainort system with this outer basin attaining a maximum depth of -55 mOD. Unlike the remainder of the survey area described it has a symmetrical form with the offshore slopes of north-western Scalpay and of Meall à Mhaoil on the main land have average inclinations of 4.7° and 3.1° respectively. The area is also characterised by a much simpler topographic basin shape with only four ridges (ABR12, ABR13, ABR14 and ABR15), identified around the margins of this outer strait, disrupting the basic form.

The most prominent of these ridges (ABR12: [157300 830400]) occurs due north of the prominent east-west ridges described to the north of the "Mouth Region" (See Section 4.3.1.2.). This ridge has a complex longitudinal profile with an approximately horizontal (< 0.5°) upper section defined at the base by the -10 mOD contour, a steeper (9.4°) narrow (maximum width 70m) central section which again becomes an almost horizontal (< 0.7°), but

narrower (25 m) plateau between -20 mOD and -22 mOD. ABR12 finally descends to -38 mOD via a narrow ridge with a frontal ridge slope inclined at 5° to the west. The complex as a whole has a poorly developed asymmetric form with a well defined steeply dipping (9.3°) southern margin but a more poorly developed shallower northern slopes (5.6°). ABR12 has an axial length of 730 m and an overall axial orientation of 104°.

Six hundred metres to the north of ABR12 complex is a well defined thin (maximum axial width 60 m) symmetrical ridge (ABR13: [157400 831300]) with slope angles of 7.8°. ABR13 is oriented at 333°, with an axial length of 280 m and a maximum relief of 10 m (defined by the -18 mOD and -28 mOD contours). The two remaining ridges (ABR14 and ABR15) within the "Unnamed Strait" are two broad and weak features at the northern and southern margins of the Luib na Moil embayment. The most southerly of these two ridges (ABR14: [156800 830300]) is the most well defined with a slightly arcuate form (average axial orientation 056°), concave to the north. This ridge has an asymmetric profile with a steep (9.4°) northerly facing slope and a gentle (1.9°) southerly facing slope. ABR14 has a maximum relief of 12 m and an axial length of 180 m. The final ridge of this suite (ABR15: [156500 830800]) is located at the northern margin of Luib na Moil and is poorly defined for the majority of its length (axial length 440 m). ABR15 has an orientation of 109° and can be most clearly identified 630 m offshore, where it has an axial relief of 8 m (between -34 mOD and -42 mOD) and a slightly asymmetrical profile with the northerly and southerly margins having slope angles of 6.2° and 7.5° respectively.

4.3.2. BATHYMETRIC DATA

Chart 4.2. was constructed from 90.1 km of echosounder traverse lines acquired during two separate surveys on the 16/5/90, 17/5/90 and the 22/5/91. The original data was processed following the procedures described in Section 4.2.. As can be seen by visually comparing Charts 4.1. and 4.2. the morphology they both describe for the Loch Ainort basin are broadly comparable. The asymmetrical form of the inner loch is again evident with a steeper (12.5°), uniform, north-western slope and an irregular south-eastern slope with an overall gentler

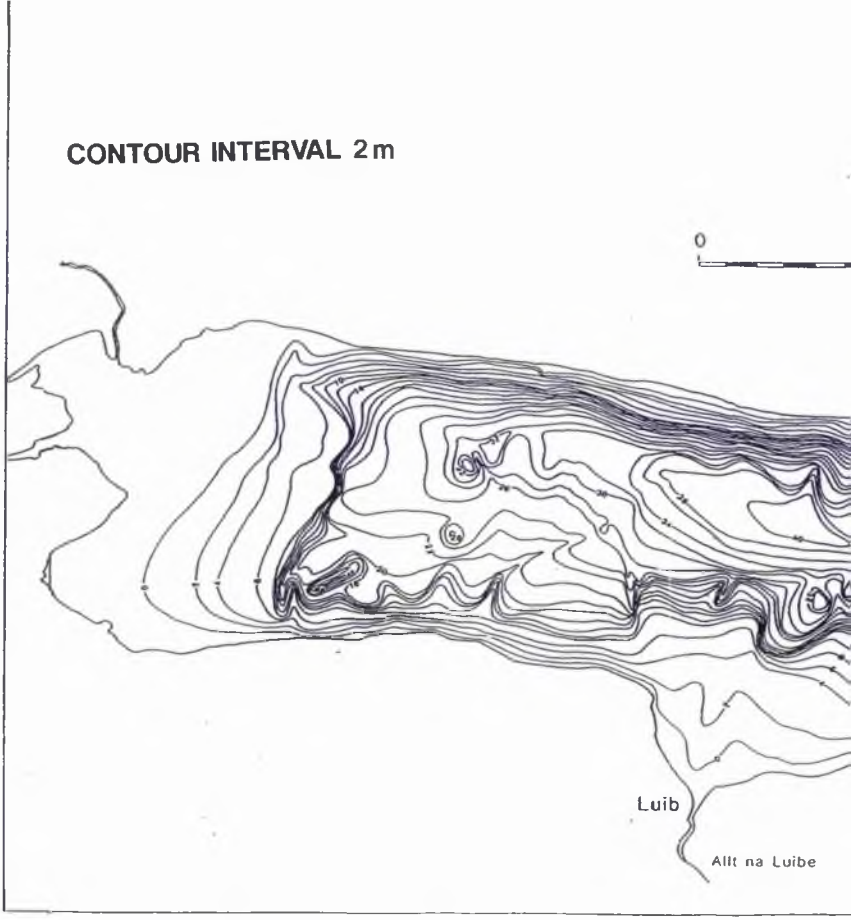

Chart 4.2. Bathymetric Chart hand contoured from echosounder data acquired during three separate surveys (16-17/05/90 and 22/05/91).

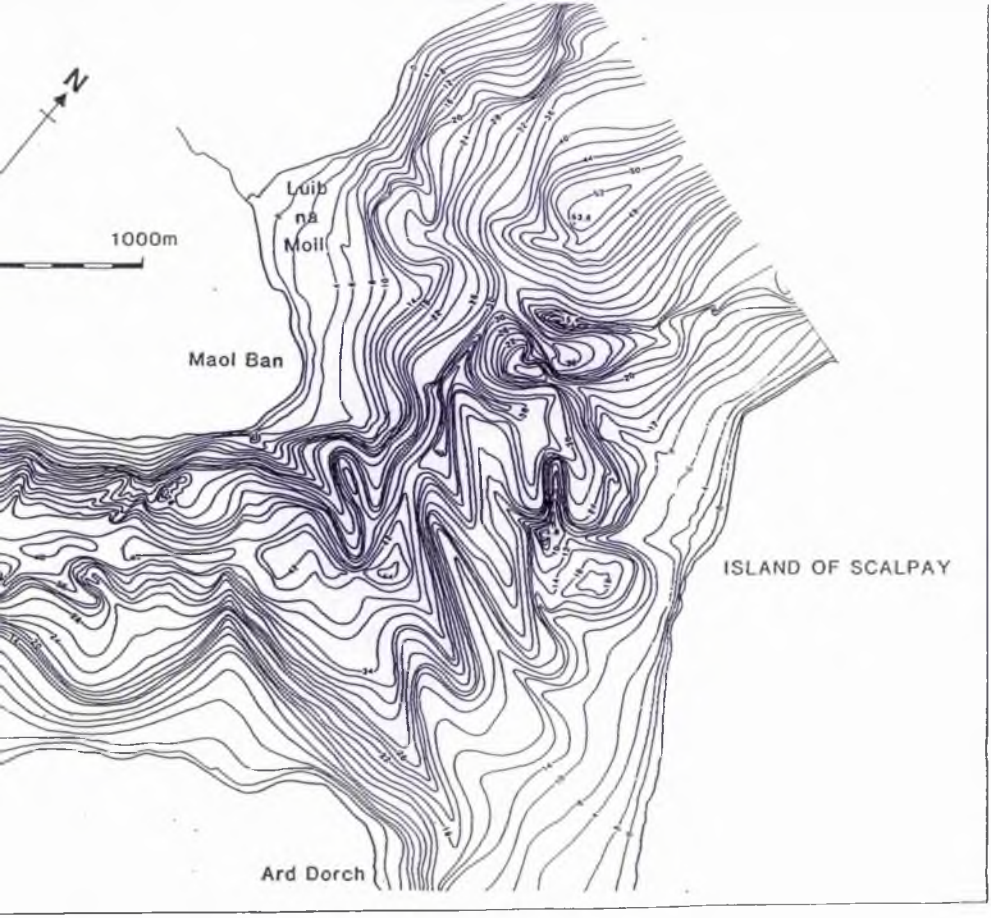
N
1000m
Loch na Moill
Maol Ban
ISLAND OF SCALPAY
Ard Dorch

(5.4°) gradient. Again the channel is offset to the north-west attaining a maximum depth of -41 mOD. Considering the inherent inaccuracy present in the construction of both of these charts the discrepancy of 1 m between the maximum depth values obtained from them should be given no genetic significance (*ie.* the product of sedimentation over the last 140 years).

The "Mouth Region" of the Loch Ainort survey area is the most topographically complex, being similarly typified by a series of interdigitised ridges and basins. However, as is discussed greater detail below the actual distribution and dimensions of ridges in this area are considerably at odds with the descriptions given from the Admiralty Chart. Finally the nature of the deep (-54 mOD) symmetrical basin of the outer "Unnamed Strait" with a small number of prominent ridges around its perimeter is in good accordance with the Admiralty Chart.

The most significant discrepancies between the two charts is the poor representation of the prominent ridges ABR1 to ABR15. On the north-western shore ABR1 and ABR2 are present and have identical dimensions, however, the irregular complex form of this representation of ABR1 (See Chart 4.2) is the result of depth inconsistencies between the intersecting lines A16, B2 and B13 (See Figure 4.7.). The upper boundary of ABR2 is again represented by the distinct break in slope at -30 mOD but has an upslope component to the -2 mOD contour. The bathymetric chart suggests that ABR2 is not in isolation with additional ridges being present to both the east and west of these features (ABR16 [156300 829300] and ABR17 [156100 829100])[2]. Ridge ABR17 in particular appears to develop at an identical level to ABR2 with no representation in the slopes above.

ABR3 has not been identified from the bathymetric chart and considering the higher density of traverse lines within this area it is surprising that there has been no corroborating evidence for this ridge. One, therefore, has to question the validity of the identification of this feature from the Admiralty Chart. ABR4 is identified on both charts with the bathymetric representation suggesting that the ridge is in fact isolate (axial length 205 m) with greater relief (10 m vs 6 m; albeit with an identical -18 mOD lower bounding contour) and a contrary orientation (024° vs 075°). The interpolation of this ridge from 4 traverse lines A8, A10, A11 and A12 on the bathymetric chart, compared to interpolation from a single depth sounding

[2] The dimensions of the additional ridges identified from the bathymetric chart are presented in Table 4.4.

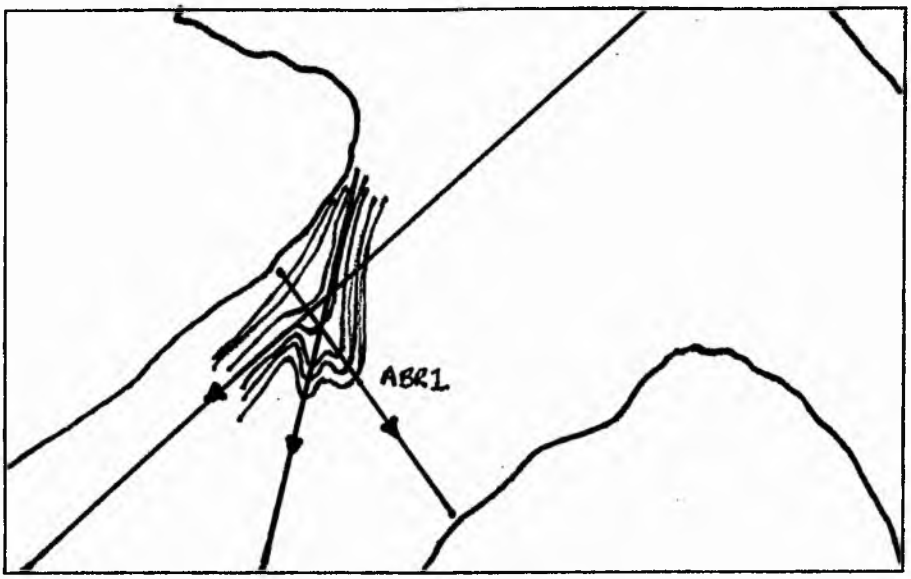

Figure 4.7. Ridge ABR1 and the intersecting lines A16, B2 and B13 from which it was constructed.

line from the Admiralty dataset suggests the former interpretation should be considered the more reliable. To the east of ABR4 three prominent ridges (ABR18 [155200 827700], ABR19 [155300 827800] and ABR20 [155400 827900]) are located on the south-eastern slopes at a locality where no features were identified from the Admiralty Chart. However, that the axis of these three ridges are coincidental with the traverse lines A9, A6 and A1 suggests they may be a product of the interpolation process thus their significance must remain equivocal.

A major discrepancy between the Admiralty and the bathymetric charts is the nature of the shallow ground and major offshore break in slope at the mouth of the Luib embayment. Albeit the morphological association of a gently sloping upper surface with a well defined frontal slope which descends to the central loch regions are present, the form and dimensions of the two representations are non-comparable. The Admiralty chart suggests a rhombic form (See Discussion in Section 4.3.1.1.) whilst the bathymetric chart identifies an arcuate feature (concave to the south-east, towards Luib) dissected by a deep (maximum depth -32 mOD) central hollow. The prominent break in slope occurs at a depth of -10 mOD (compared to -6 mOD) with a lower bounding contour of -26 mOD and a slope angle of 7.8°. Adjacent to the easterly margin of dissecting hollow is an arcuate (concave down-loch) ridge that is the spatial correlative of ABR5. However, extending from the western limb of the main ridge crest is an additional thin (40 m) symmetrical ridge (ABR21: [156500 828700]).

The ridge complex of ABR6 and ABR7 extending from the northern slopes of Am Meall is represented on the bathymetric chart but again with significant morphological and dimensional discrepancies. Unlike the broad rectangular platform described in Section 4.3.1.1. the upper slopes of ABR7 is characterised by an angular, uniformly axially inclined (4°), symmetrical ridge. Again the dependence of a single traverse line of data (A14) could be responsible for the angularity of this feature. However, the parasitic relationship of ABR6 upon ABR7 is maintained whilst the dimensions of ABR6 (See Table 4.2.: Overleaf) appear to show conformity.

Within the mouth region of the Loch Ainort basin there is significant discrepancy between the morphology described by the two charts. The central deep reaches a maximum depth of only -44 mOD a discrepancy of 4 m and albeit an equivalent spatial distribution of ridges

the morphology and dimensions of the individual ridges are at odds with the Admiralty Chart interpretation. Albeit when describing the general morphology of the loch the Admiralty Chart data has been relied up on due to the greater traverse density, where individual depth soundings are concerned it is probable that the current geophysical techniques will record depths with greater accuracy[3]. Consequently, when considering the value of individual depth soundings those from the current survey are considered the more reliable.

Ridge No.	*Axial Length (m)*	*Relief (m)*	*Bathymetric Limits (mOD)*		*Orientation (°)*	*Slope angles (°)*	
			Maximum.	*Minimum.*		*Proximal*	*Distal*
ABR6 (AC)	340	12	-34	-22	100	3.8	15.8
ABR6 (BC)	310	10	-38	-24	100	3.9	9.7

Table 4.2.: Comparison of the dimensions for ABR6 taken from the Admiralty Chart (AC) and the bathymetric chart (BC) respectively.

ABR8 is totally absent from the southern slopes of Maol Bàn, however, the equally low traverse density for this area present in both of the surveys make it impractical to determine the existence of this feature on the basis of bathymetric data alone. Ridges ABR9a and b are both present but the orientation and form ABR9b in particular shows poor correlation between the two charts (See Table 4.3).

Ridge No.	*Axial Length (m)*	*Relief (m)*	*Bathymetric Limits (mOD)*		*Orientation (°)*	*Slope Angles[4] (°)*	
			Maximum.	*Minimum.*		*Proximal*	*Distal*
ABR9b (AC)	245	14	-34	-20	075	10.2	5
ABR9b (BC)	280	24	-32	-8	136	10.3	10.5

Table 4.3. Comparison of the dimensions for ABR6 taken from the Admiralty Chart (AC) and the bathymetric chart (BC) respectively.

[3] This is not a an empirically tested deduction.
[4] The terms proximal and distal have been chosen to represent orientation relative to the head of Loch Ainort.

Ridges equivalent to ABR10 and ABR11 are present on the bathymetric chart. The stepped longitudinal profile of ABR10 is retained, as is the arcuate nature of the thin offshore segment of this ridge. However, the ridge on the bathymetric chart is concave to the north-north-east (30°), towards Scalpay. Similarly the representation of ABR11 exhibits a markedly different form with the uniform broad lochward terminating face of this ridge being dissected by a deep -36 mOD channel with a north-westerly (310°) axial orientation.

The "Unnamed Strait" also shows the same simple morphology as described from the Admiralty Chart with a wide symmetrical basin reaching the maximum depth of the survey area of -54 mOD (versus -55 mOD from Chart 1). The margins of the basin are interrupted by four prominent ridges of these there are spatial equivalents of ABR12, ABR14 and ABR15, whereas ABR13 is absent. ABR12 retains the longitudinal stepped profile extending from the Scalpay shoreline but with a wide (235 m) frontal slope similar to that described for ABR10 from the Admiralty Chart.

The arcuate (to the south-west) ridges located at the mouth of the Luib na Moil embayment ABR14 and ABR15 are both prominently marked. Despite the total absence of evidence for the existence of ABR13 an additional ridge, ABR22 [157400 830800], is identified 75 m north of ABR12. This ridge has an axial length of 470 m, a maximum height of 20 m (between -16 mOD and -36 mOD) with an axial orientation of 060°. ABR22 has the steepest slopes of any of the ridges identified within Loch Ainort, with steep (18.7°) proximal slopes and less steep (12.4°) distal slopes. However, as with ridges ABR7, 18, 19 and 20 the coincident location and orientation of the axis of ABR22 with Traverse B9 and its location at the centre of the loch where inaccuracies in traverse position would be at a maximum (See Section 2.3.2.1.) suggests one should treat the existence of this feature with caution. Conversely the high density of traverse lines acquired for the Admiralty Chart in the area of ABR13 gives strong support to its retention.

4.3.3. CONCLUSION

Bathymetric charts have been constructed from two contrasting datasets and a morphological description of the bed of Loch Ainort has been presented. From this description the basin can be split in to three broad regions; firstly an asymmetrical "Inner Loch" with a prominent channel offset towards the north-western shore. This "Inner Loch" has a partially silled entrance which is cut by the north-western channel as it deepens towards the "Mouth Region". This second geographical zone has a shallow and complex topography characterised by a series of predominantly asymmetric topographic highs (or ridges) and again cut by the north-western channel. This channel turns through 90° to finally feed in to the deep symmetrical basin of the "Unnamed Strait". In addition to the complex ridge topography of the "Mouth Region" the basic form of the entire area is disrupted by a series of these ridges. For comparative purposes with the other geophysical datasets the dimensions of all these ridge features, identified from both the Admiralty and the bathymetric charts, area are summarised in Table 4.4. (Overleaf).

In addition to Table 4.4. the distribution and axial orientation of these ridges are presented in Figure 4.8.. It should be noted that ABR3 and ABR22 have been shown on Figure 4.8. with a broken line due to the poor traverse density for these two localities. Further the location and form of ABR4 has been taken from the recently acquired bathymetric data due to the superior dataset on which it was based.

Ridge No.	*Axial Length (m)*	*Relief (m)*	*Bathymetric Limits (mOD)*		*Orientation (°)*	*Slope Angles (°)*	
			Maximum.	*Minimum.*		*Proximal*	*Distal*
ABR1	260	12	-34	-22	010	4.5	8
ABR2	145	6	-36	-30	165	4.5	3
ABR3	220	6	-22	-16	093	4.7	3.5
ABR4	245	6	-18	-12	075	9.5	3.5
ABR5	365	3	-36	-18	163	2.5	1.5
ABR6	340	12	-34	-22	100	3.8	15.8
ABR7a	350	8	-18	-10	160	9.3	9.3
ABR7b	390	8	-18	-10	170	5	3
ABR8	170	12	-38	-26	109	11.6	11.6
ABR9a	415	32	-36	-4	091/120	13.4	6.2
ABR9b	245	14	-34	-20	075	10.2	5
ABR10	485	14	-26	-12	026/300	7.3	2.7
ABR11	425	14	-26	-12	094	4.7	9.4
ABR12	730	28	-38	-10	104	9.3	5.6
ABR13	280	10	-28	-10	333	7.8	7.8
ABR14	180	14	-22	-8	056	9.4	1.9
ABR15	440	8	-42	-34	109	7.5	6.2
ABR16	200	4	-36	-6	166	6.3	4
ABR17	75	4	-38	-32	140	4	4
ABR18	95	8	-18	-10	116	6	8.6
ABR19	130	8	-18	-10	153	10.3	3.9
ABR20	155	8	-18	-10	166	18	11.5
ABR21	130	6	-28	-22	130	7.7	3.9
ABR22	470	20	-36	-16	060	18.7	12.4

Table 4.4.: Summary Table correlating the dimensions of the ridges identified from the Admiralty and Bathymetric Charts constructed for the Loch Ainort basin.

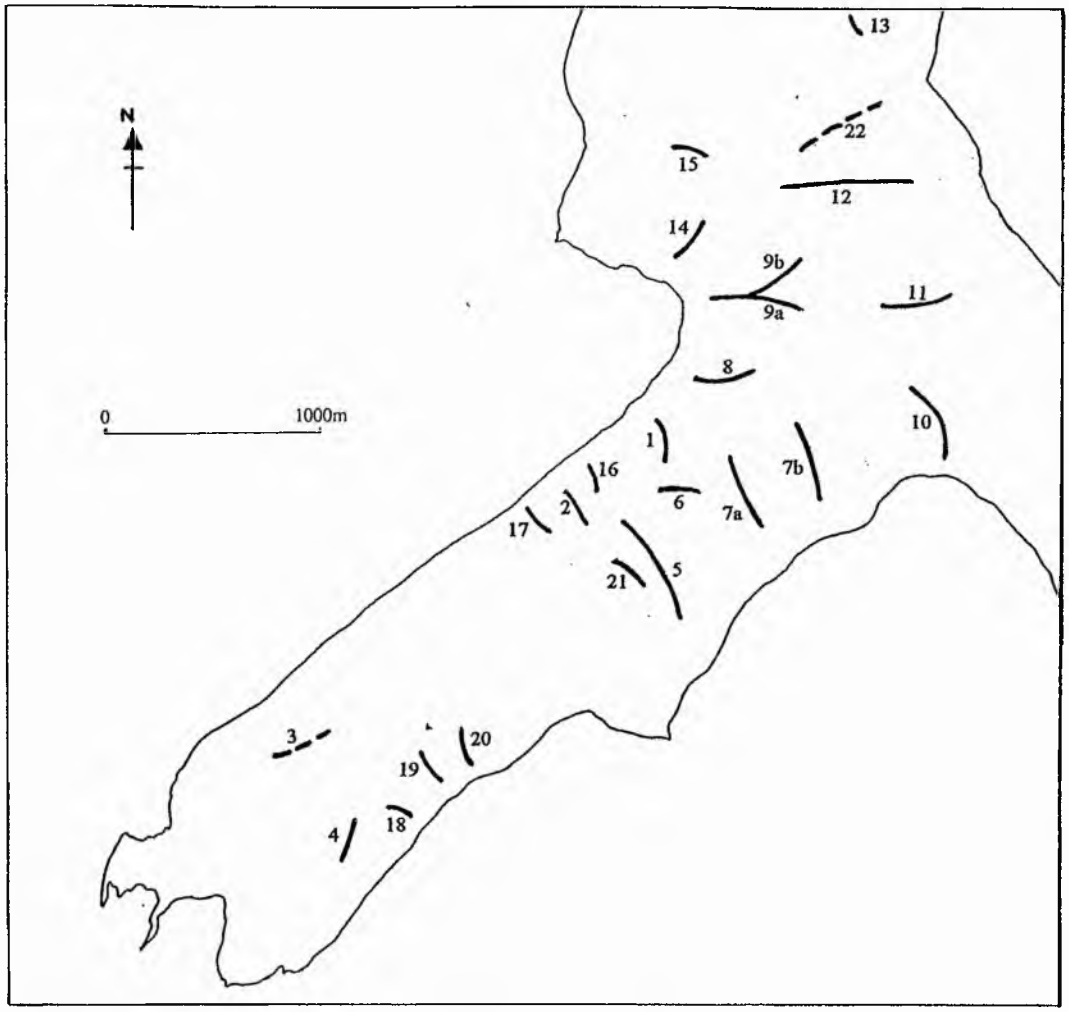

Figure 4.8. Distribution and axial orientation of ridges identified from the bathymetric charts of the Loch Ainort survey area.

CHAPTER 5

5. SIDE SCAN SONAR

5.1. INTRODUCTION

Using the Klein Hydroscan (Model 401), 400 kHz, side scan sonar system as described in Section 2.3.3.2., a total of 25 km of lines were shot within Loch Ainort and adjacent waters (See Figure 5.1a and b.). Navigational control was provided by the Magellan© GPS system (See Section 2.3.2.3.), which was set to map datum WGS72 (World Geodetic System 1972 Datum - See Section 4.2.). This chapter deals with the analysis of the traces obtained from this survey. Initially, a brief summary of the theoretical techniques of sonograph description is given, coupled with a discussion of the errors encountered during analysis. This is followed by a detailed description of the actual sonar records retrieved from Loch Ainort. A physical interpretation of the sonographs is presented as part of the complete account of the glacial history, inferred from all the techniques used, in Section 8.2..

5.2. SONOGRAPH ANALYSIS

Due to the effective three-dimensional nature of the acoustic image produced with the Klein 401 side scan sonar a distinctive set of analytical techniques must be employed when describing these sonar records. The analysis of a sonograph depends up on both a quantitative and qualitative description of the tonal intensity of each trace, with particular reference to the spatial distribution of selected "tonal groups". The variation in tonal intensity described on the trace is a function of the degree of attenuation experienced by each acoustic pulse. As each signal is transmitted it is attenuated and scattered as it passes through the water column. As the pulse strikes the loch floor further energy loss occurs, the extent of which depends primarily on inherent material and topographical effects of the bottom surface (See Section 5.2.2. and 5.2.3.). Bryant (1975) suggests that material variations change the signal strength as much as or more than any major topographical variation. A proportion of the reflected pulse will be returned to the transducer, it undergoing further energy loss during its return

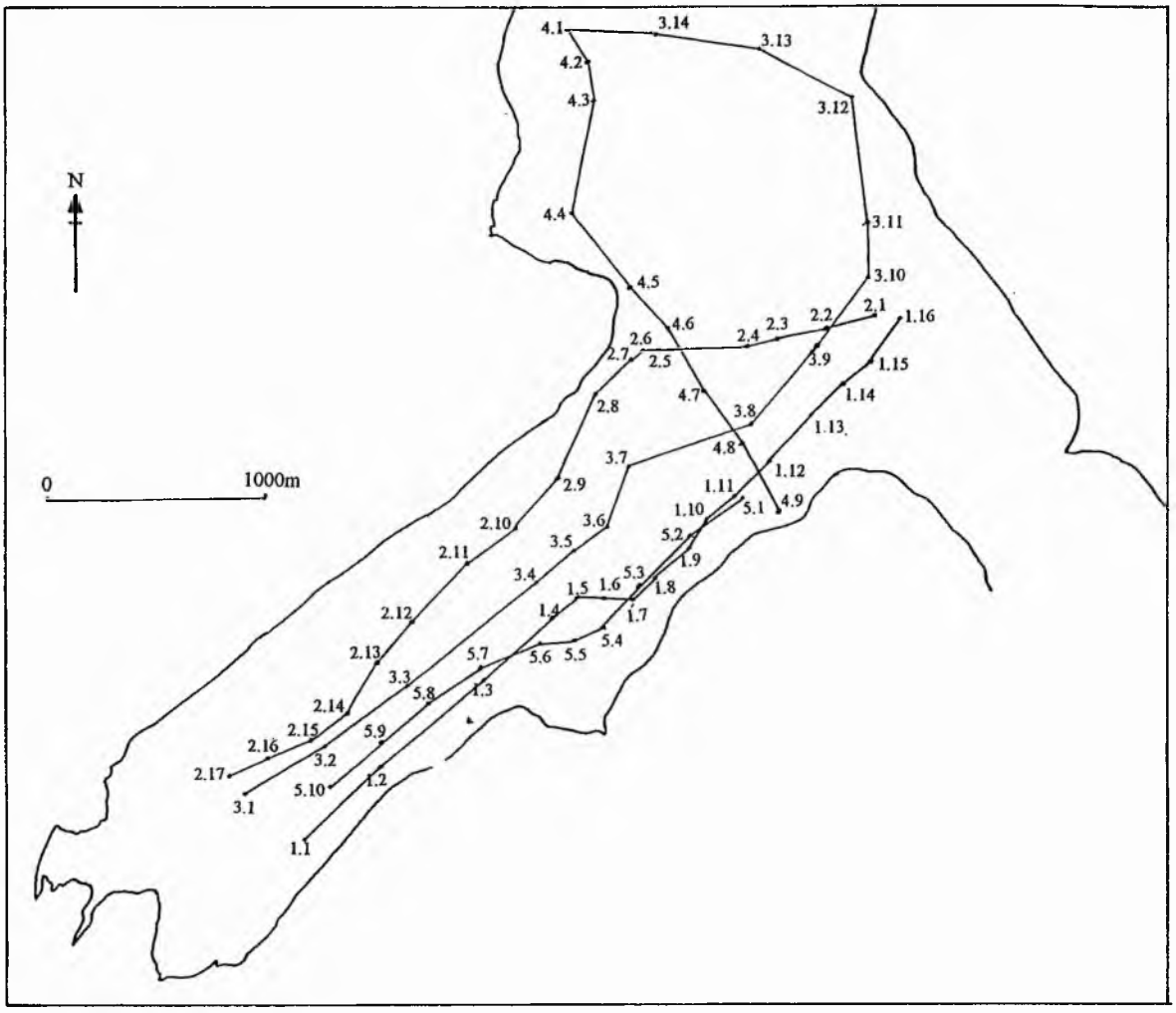

Figure 5.1a. Diagram showing side scan sonar survey lines, with fix numbers, in the Loch Ainort field area.

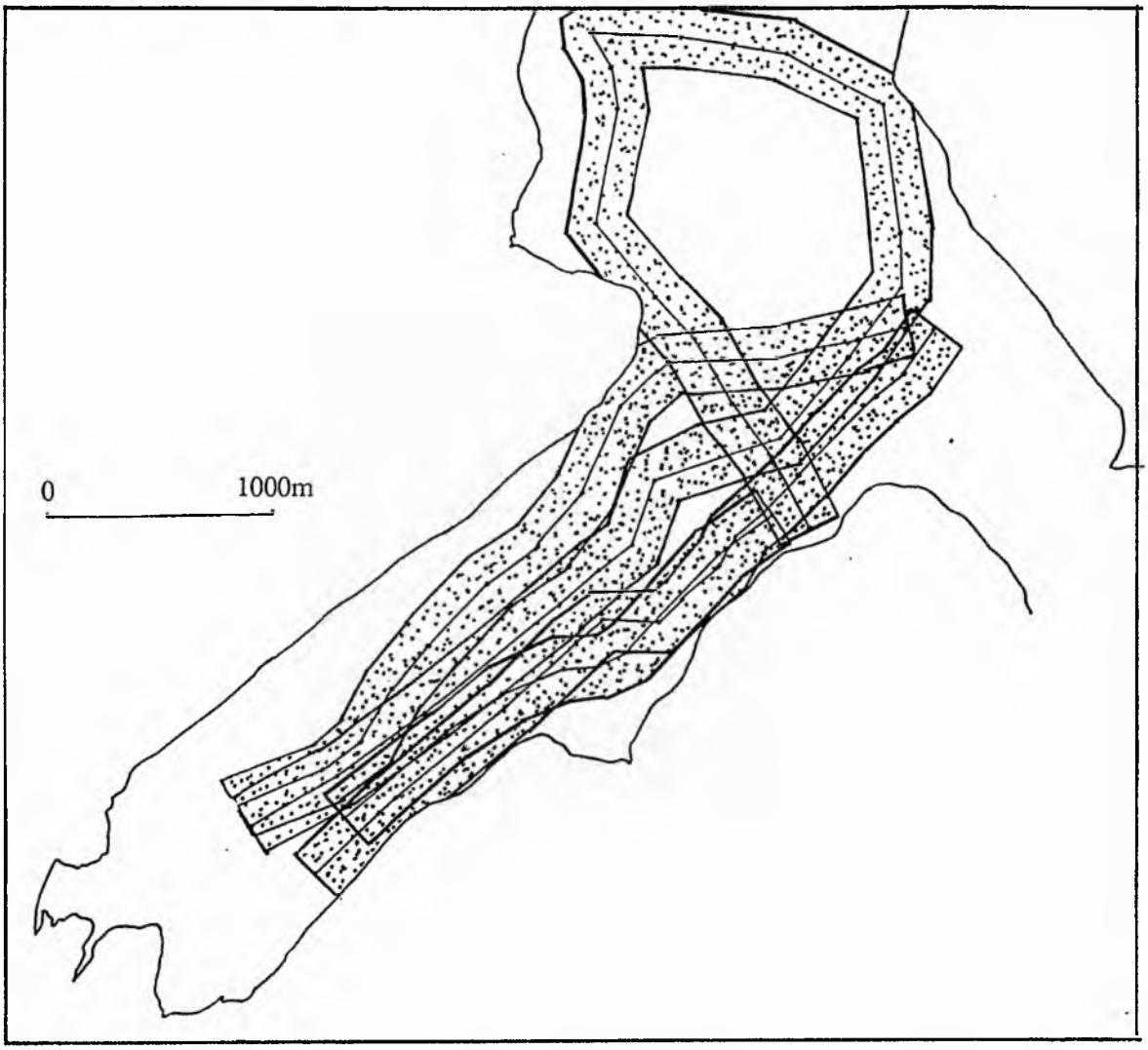

Figure 5.1b. Diagram showing side scan sonar coverage (300 m swath width) in the Loch Ainort field area.

passage through the water column. The reflected pulse is converted within the transducer into an electrical current with an amperage proportional to the intensity of the echo. The current is subsequently passed through electrosensitive paper, with the intensity of the returning signal, and therefore the strength of the current, determining the darkness of the mark made on the sonograph. This section describes both the causes of such tonal variations in more detail, and the methods used to obtain quantitative and qualitative data from them.

5.2.1. SONOGRAPH DESCRIPTION.

All of the sepia sonographs are characterised by a number of reflectors which relate to the operational properties of the system (See Figure 5.2). The occurrence of these, effectively omnipresent, marks on the trace acts as a useful guide-line to standardising the interpretation of all sonar records. As the transducer acts as both transmitter and receiver (See Section 2.3.3.2.), the transmitted acoustic pulse is recorded on the sonograph as parallel, continuous, dark lines located at the centre of the trace. These parallel lines represent the pulses sent from the port and starboard channels of the towfish transducer and as such describe the path of the fish over the loch floor. Moving outward from the centre of the trace, the next reflector to be recorded is normally from the water surface, assuming the towfish is nearer to this surface than to the loch bed (See Figure 5.3.). The presence of this echo is a consequence of the wide vertical beam angle of the transmitted pulse (See Section 2.3.3.2.). However, if the towfish is suspended such that the distance to the bottom is less than the distance to the water surface, this surface echo may be superimposed upon reflectors from the loch floor and is therefore invariably obscured. Due to the shallow tow depths used during this survey, superposition is not a problem. However, identification difficulties, due to the very shallow towing depth (1.5 m), do occur as the surface reflector merges with the central transducer lines.

As the acoustic signal continues to travel through the water column it fails to return any signal, due to the absence of any reflectors, and as a result a blank area is recorded on the sonograph. However, this area is commonly disturbed by a series of interference effects, which are generally dependant on the survey conditions (See Section 5.2.5.). Assuming that the depth to the loch floor from the fish is greater than the distance to the surface, the next

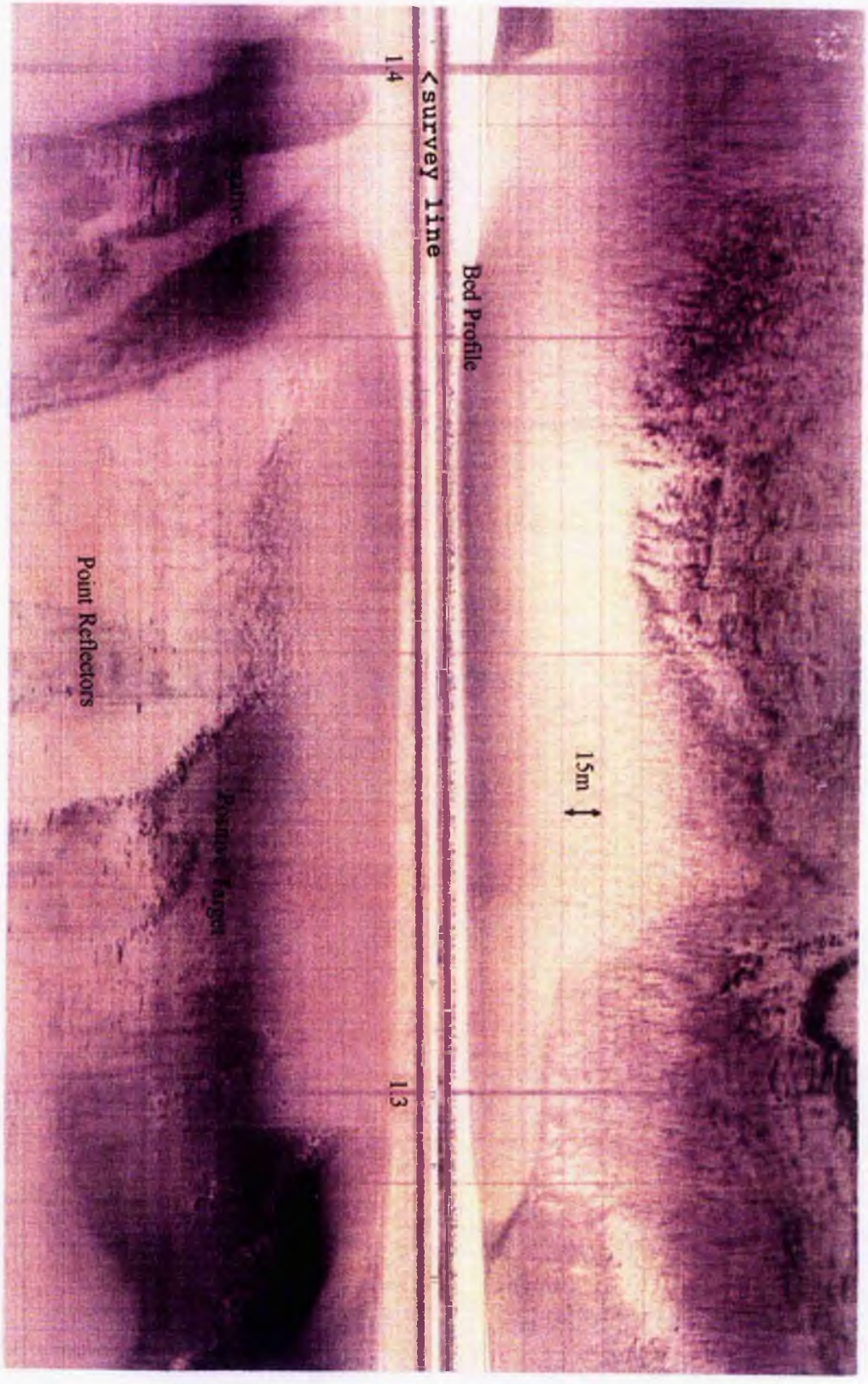

Figure 5.2. A typical sonograph trace, annotated to show principal features (Fix 1.3 - 1.4.).

Figure 5.3. Descriptive Terms Used in Side Scan Sonar Geometry

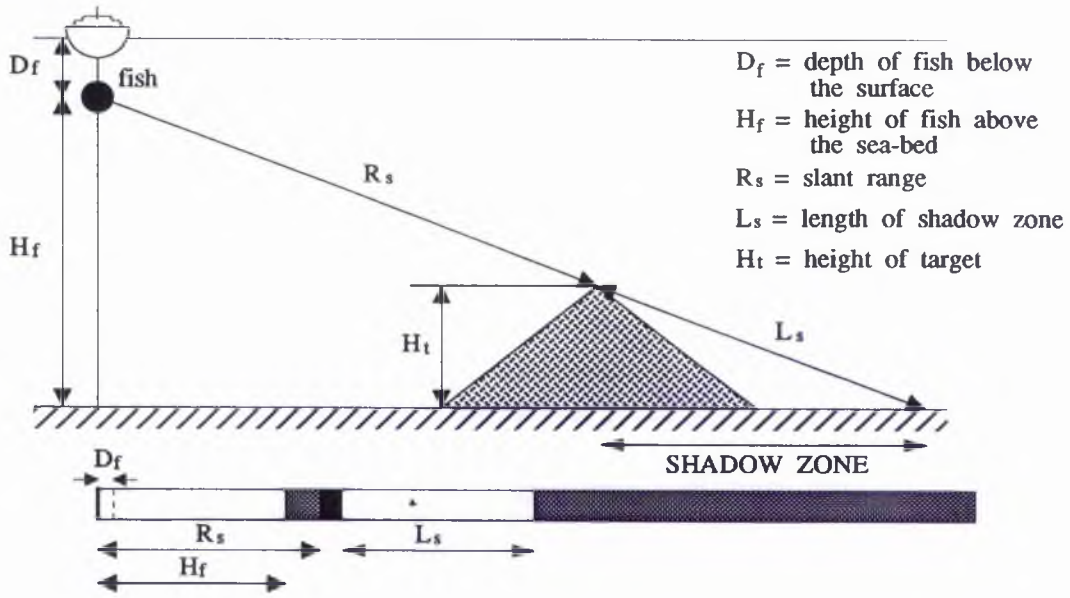

signal to be received represents the bottom echo. Due to the strong impedance contrast between the water column and the loch bed this is characteristically the strongest reflector on the trace. In fact this depth profile does not actually record the true variations in topography but the relative change in position of the fish to the loch floor. However, if profile variation was purely the result of fish movement in the water column, it would be reflected by a similar variation in the surface echo. Hence, if the surface echo remains at a constant level any changes in the bed profile can be considered "real" (Flemming, 1976).

This prominent reflector is followed by successive returns from the loch floor which build up to form the characteristic composite sonograph. As can be seen from Figure 5.3. the distance to these individual returns does not, however, represent actual horizontal distances but the "slant range" and as such must be converted if accurate measurements are required (See Section 5.2.6.). The succession of lighter lines, parallel to the central transducer record, are 15 m range marks, again these represent slant ranges not true horizontal distances. In addition to the range marks there are two sets of parallel lines that are perpendicular to the central transducer record. One set, which are generally lighter and thinner, represent two minute interval lines that are recorded automatically by the Klein Hydroscan system. The second set of lines represent "fix" marks which correspond to latitude and longitude readings taken at frequent intervals during the survey with the Magellan© GPS system. Each line is accompanied by a reference number that corresponds to the appropriate set of positional readings.

5.2.2. MATERIAL EFFECTS.

The material characteristics of the loch bed are a primary control on the degree of backscatter (bottom reverberation) experienced by each incoming pulse. Backscatter, in turn, affects the strength of the returning signal and thus the tonal intensity of the trace. If one assumed a mirror smooth surface, any input signal arriving at an angle to the bed would be reflected away from the transducer at the same angle (*ie.* specular reflection). In such a situation the sonar would only be able to identify the bottom profile (from the pulse arriving perpendicular to the surface) and any positive targets on the loch floor, with surfaces

orientated towards the sonar. In reality, the sediments or rock types of the loch bed always possess a texture related to their grain size and porosity. As such, sound may be scattered in all directions, irrespective of topographic variation, with a proportion of the signal returning to the transducer (See Figure 5.4.).

The relationships between sediment characteristics and tonal intensity are not fully understood (Williams, 1982). However, there does appear to be an empirical relationship, such that the denser and coarser the sediment the greater the reflectivity it possesses, and as a consequence the darker the tone of the image. So with a decrease of reflectivity, from bedrock through gravel and sand, to mud and silt, there is a corresponding reduction in the darkness of the sonograph (Flemming, 1976).

Williams (1982), further suggests that there is an inverse relationship between acoustic impedance and sediment porosity. So, a sediment with high porosity (*eg.* clay at 75%) has relatively low impedance and low reflectivity, and is therefore represented by a light tone. In contrast, low porosity sediments (*eg.* medium grained sands at 40%) have greater acoustic impedance and greater reflectivity and are thus characterised by darker tones. It is important to note that the porosity of a sediment is a function of grain shape, the degree of sorting, and the degree of sediment compaction (Leeder, 1982). As a result, sediments of differing sizes may have similar porosity's and therefore similar tonal shades, thus further complicating interpretation.

It is assumed that loch floor "roughness", whatever its causes, are responsible for the variation of backscatter recorded on the sonograph. However, it is important to realise that this quantity is defined as being relative to the wavelength of the incident sound pulse (Klein, 1985). As a result, higher frequency transducers, emit pulses with a shorter wavelengths, and therefore are more sensitive to bottom texture. The 400 kHz system employed during this work has a relatively short wavelength (= 0.00375 m) and as such it is regarded as being extremely sensitive to variations in bottom texture (See Section 2.3.3.3.). Klein (1985) also points out that the degree of backscatter varies with the angle of incidence, such that the shallower the angle, the weaker the backscatter will be. This property manifests itself on the trace as a progressive reduction in tonal intensity away from the fish, assuming a constant reflector type.

Figure 5.4. Principles of Specular Reflection and Backscatter

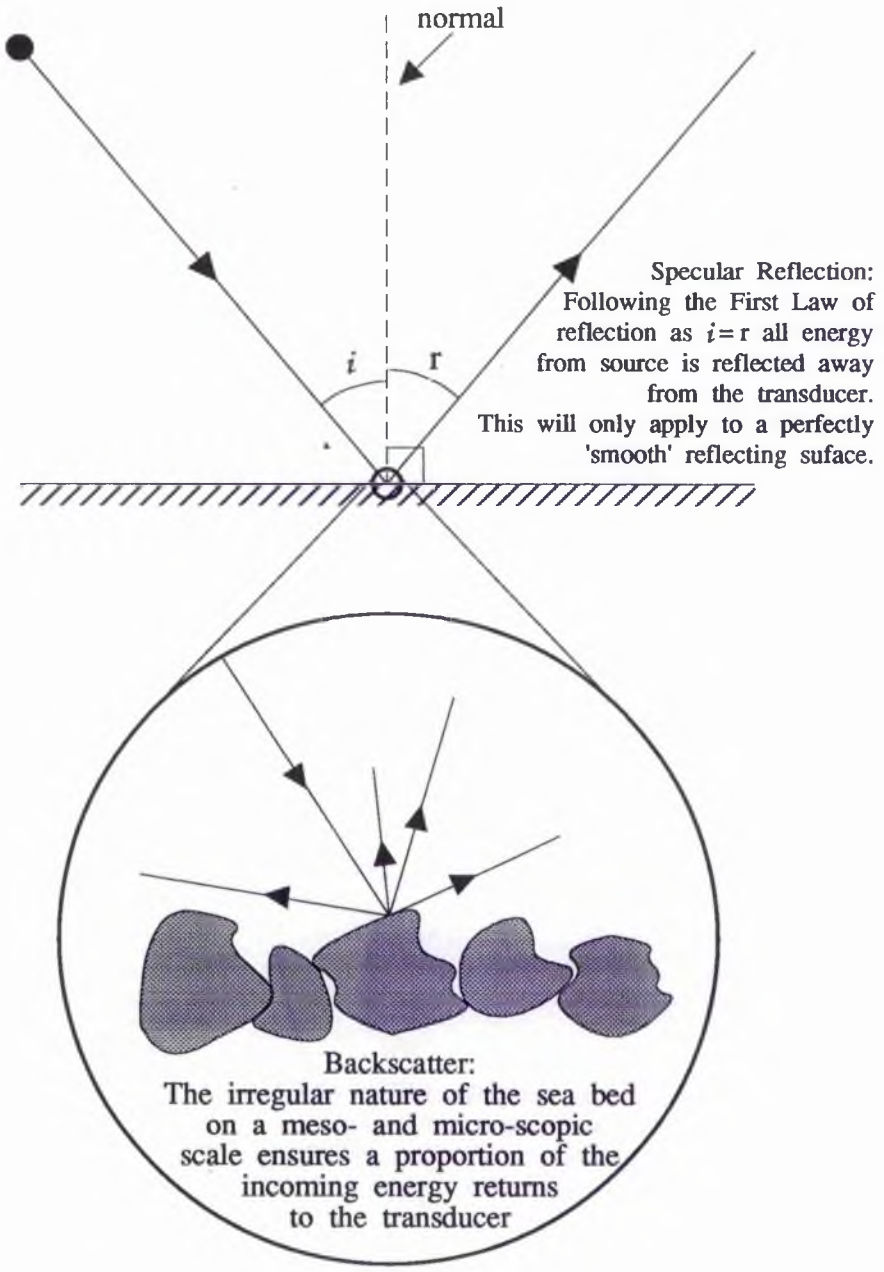

5.2.3. TOPOGRAPHIC EFFECTS

In addition to the material properties of the loch floor described in Section 5.2.2. the morphology of the surface being scanned will have an effect on the tonal variation of the trace. Any projections on the loch floor (for instance ridges, boulders and outcrops), and in particular those with slopes which face the outgoing acoustic signal, will provide a good reflecting surface. In association with these strong reflectors, acoustic shadows will appear on the trace as blank areas. These shadow zones represent parts of the survey where the pulses are prevented from striking the sea floor by the upstanding projections (See Figure 5.5a.). The couplet of strong reflector and acoustic shadow act as an integral part of both the quantitative (See Section 5.2.6.) and qualitative interpretation of sonographs. However, the shadow zones for many positive targets (See Section 5.3.3. and 5.3.4.) actually possess "colour", rather than the anticipated blank appearance (See Figure 5.5b and 5.6a). It is proposed here, that this effect may be caused by a combination of the morphology of the target and side scan geometry, rather than any variation in material or acoustic properties.

Figures 5.5a. and 5.5b. show two possible target scenarios and diagrammatic representations of their corresponding sonographs[1]. Figure 5.5a. shows a classic example of the side scan detection of a symmetrical positive target **DBE** on a horizontal sea bed. The initial part of the sonograph between **C'** and **D'** represents a uniform tonal coloration provided by the flat surface **CD**. The proximal slope of the target, **DB**, provides a prominent signal facing reflector which is represented as a very dark band (**D'B'**) on the sonar trace. This proximal slope also prevents pulses being reflected from the portion of the loch floor between points **E** and **F**. The first beam to strike the floor after the target is described by the line **ABF**, where **B** is the apex of the object. This beam configuration creates a shadow zone **BEF** that is represented on the sonograph as a blank area between **B'** and **F'**. Between **F'** and the limit of the sonar's range the image returns to a more uniform backscatter level[2]. Assuming the angle

[1] All geometrical calculations made with reference to Thompson (1931).

[2] Backscatter will show a gradational variation with range as the angle of incidence of the transmitted pulse decreases with distance from the fish (See Section 5.2.2.).

Figure 5.5a. Diagram Showing Reflection from a Positive Target and Corresponding Trace Characteristics

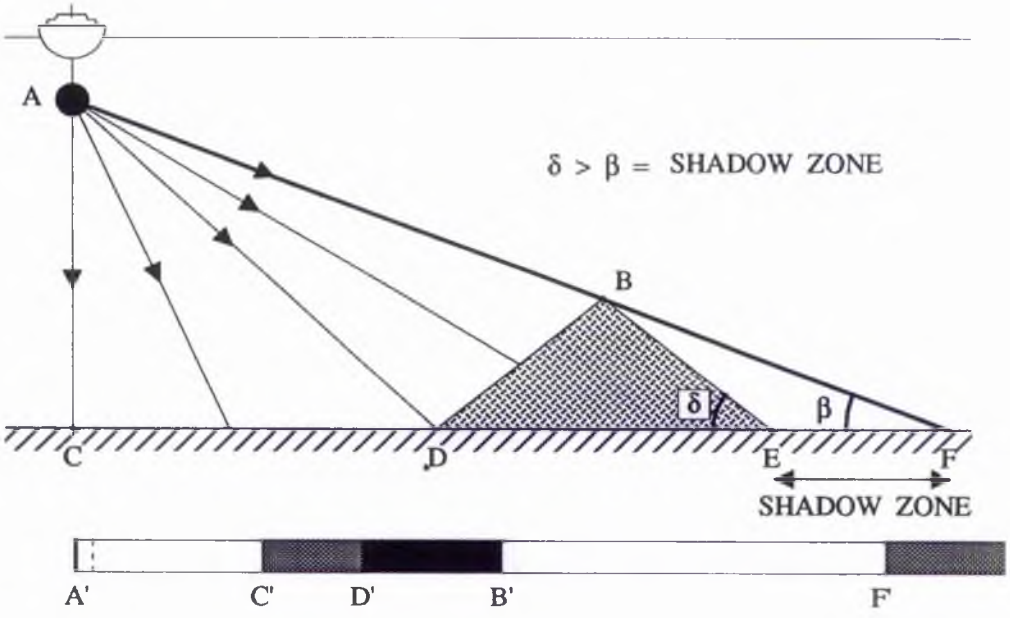

Figure 5.5b. Diagram Showing Reflection from a Positive Target with Low Tonal Colour Zone and the Corresponding Trace Characteristics

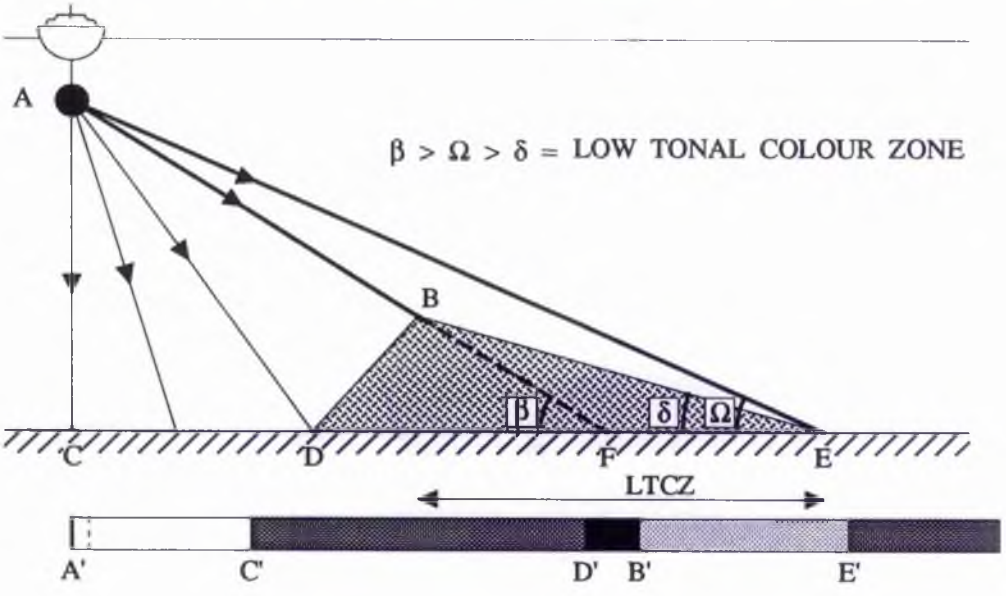

(∂) of the distal slope of the object is greater than that made by the beam **ABF** and the plain of the seabed (β), the strong reflector-shadow couplet will be maintained.

In Figure 5.5b. the uniform floor (**CD**) and proximal slope conditions (**DB**) are maintained but the angle ∂ has been decreased to a value less than that of the angle β. Under these conditions no area of the loch floor is lost to the incoming pulses and so no blank shadow zone exists. However, the angles of incidence of the incoming signals between **B** and **E** are significantly decreased due to the inclined nature of the surface presented to the sonar by the distal slope of the target. As a result of the inter-relationship between the angle of incidence and the backscatter level (See Section 5.2.2.) this geometrical configuration manifests itself on the trace as an area of low tonal coloration **B'E'**. The resulting couplet of strong reflector and low tonal colour zone (which henceforth will be referred to as the "**LTCZ**") is very similar to that of the true, reflector - shadow pair described for Figure 5.5a.

For an individual object, the angle β is simultaneously proportional to the height of the fish above the reflecting surface and inversely proportional to the distance of the object from the fish. The size of the shadow zone is in turn inversely proportional to β, therefore its size will increase with both decreasing fish height and increasing distance from the fish. As a result of this inverse relationship, at a specified distance and height dependant on the angle of the distal slope, the angle β will actually exceed that of ∂ (See Figure 5.6a.) and so a shadow zone will be replaced by an **LTCZ** (See this Section). Assuming ∂ does not exceed an angle of internal friction of 30° this substitution will occur at slant ranges of less than 20 m, 40 m and 60 m for respective fish height values of 10 m, 20 m and 30 m.

The identification of the **LTCZ** has two important implications, firstly its presence puts constraints on the angle of the distal slope and therefore target symmetry. Secondly, it puts into question any quantitative target measurements taken from such strong reflector-**LTCZ** couplets (See Section 5.2.6.). If an **LTCZ** is present it implies that the angle of the distal slope (∂) is less than the angle made by the incoming pulse **AB** (β) to the apex of the target. The angle ∂ can be further constrained by the calculation of Ω which represents the angle made by the beam **AE** which strikes the end of the **LTCZ** (See Figure 5.5b.). This value delimits a range of angles for the distal slope between 0° and Ω°. The accuracy of calculations

Figure 5.6a. Diagram Showing the Relationship between Slant Range, Fish Height and the Presence or Absence of a True Shadow Zone

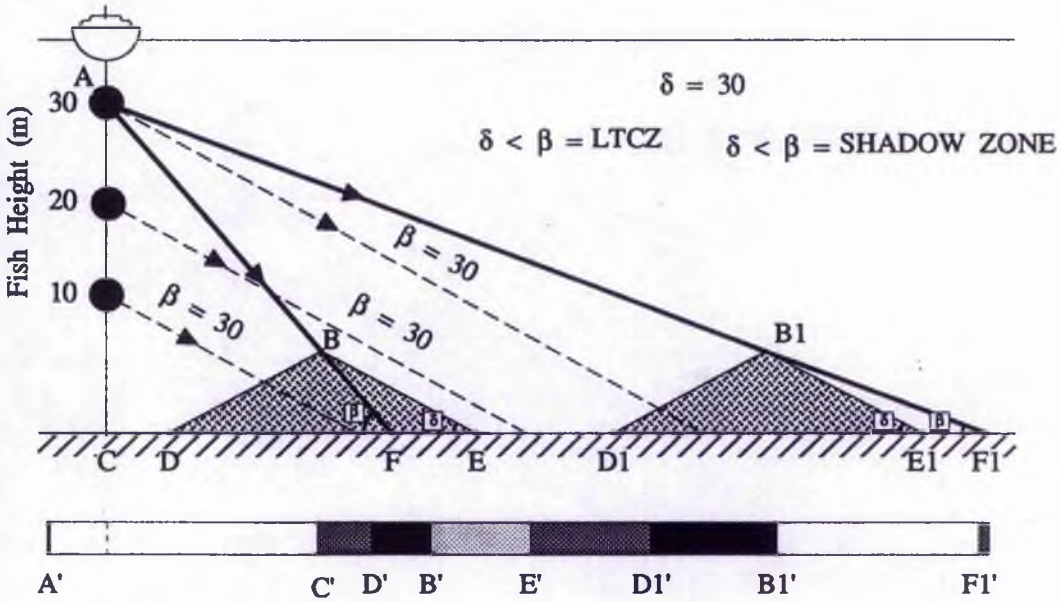

Figure 5.6b. Diagram Showing the Relationship Between True and Apparent Inclination

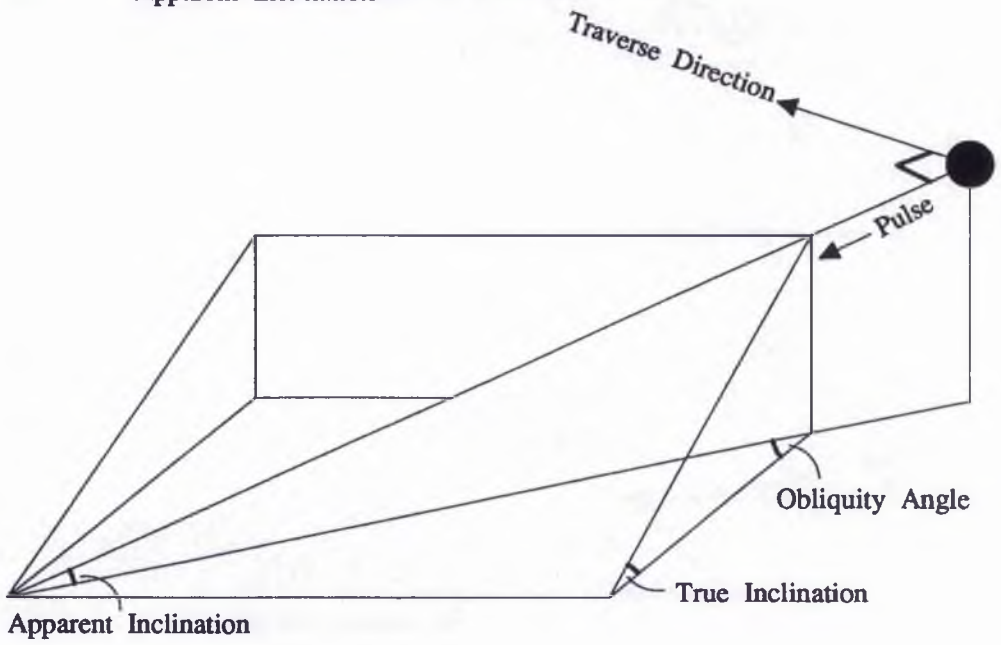

made from the range **AE** improves with either increasing distance of the object from the fish or decreasing fish height, as both these parameters cause Ω to approach 0°. This range can in turn be compared with a calculated angle for the proximal slope and therefore the target's symmetry may be deduced. It is not possible to calculate such an accurate distal slope angle range for targets with reflector-shadow couplets. Albeit, it is known in such cases that angle ∂ is greater than the angle β, the magnitude of this difference is lost within the shadow zone. Therefore the distal slope range can be constrained to between β and 90°.

In addition all the diagrammatic figures[3] in Section 5 exhibit artificial conditions, as the sonar traverses they represent all run perpendicular to the targets. Under more realistic survey conditions targets are invariably orientated at angles to the traverse line and as a result the calculated values of ∂ represent the apparent inclination of distal slopes rather than their true inclination. The relationship between true and apparent inclination is expressed as (After Lisle, 1988):

Tan (apparent inclination) = Tan (true inclination) x Cos (obliquity angle) ***Equation 5.1)***

The obliquity angle is the angle made by the incoming pulse to the strike of the positive target. The greater the obliquity angle of the pulse the greater the discrepancy between the values for true and apparent inclination (See Figure 5.6b.). As the orientation of the traverse line relative to a target is easily obtained from the sonograph it is possible to apply ***Equation 5.1)*** to determine a range of values for true inclination.

In contrast, any depression on the loch floor is represented by an acoustic shadow preceding a prominent reflector. In this scenario, the shadow is a result of the ground dropping away from the transmitted pulse and so no/minimal reflected surface is presented to it. At the trailing edge of the depression the acoustic pulse is faced with a slope orientated towards the sonar and so a strong reflection is recorded (See Figure 5.7a.). Equally following the arguments presented for positive targets (See Above) either a shadow-strong reflector or an **LTCZ**-strong reflector couplet can be imaged (See Figure 5.7b.). Which of these visual

[3] Figures 5.3., 5.5a and b., 5.6a., 5.7a and b., 5.13a - d., 5.14a and b., 5.18a and b..

Figure 5.7a. Diagram Showing Reflection from a Negative Target and Corresponding Trace Characteristics

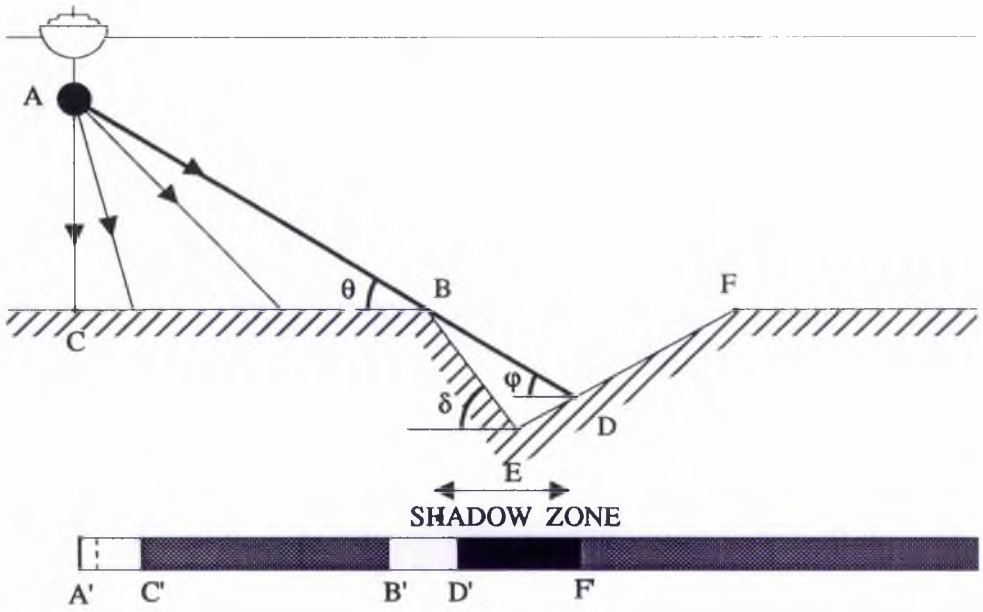

Figure 5.7b. Diagram Showing Reflection from a Negative Target with a Low Tonal Colour Zone, and the Corresponding Trace Characteristics

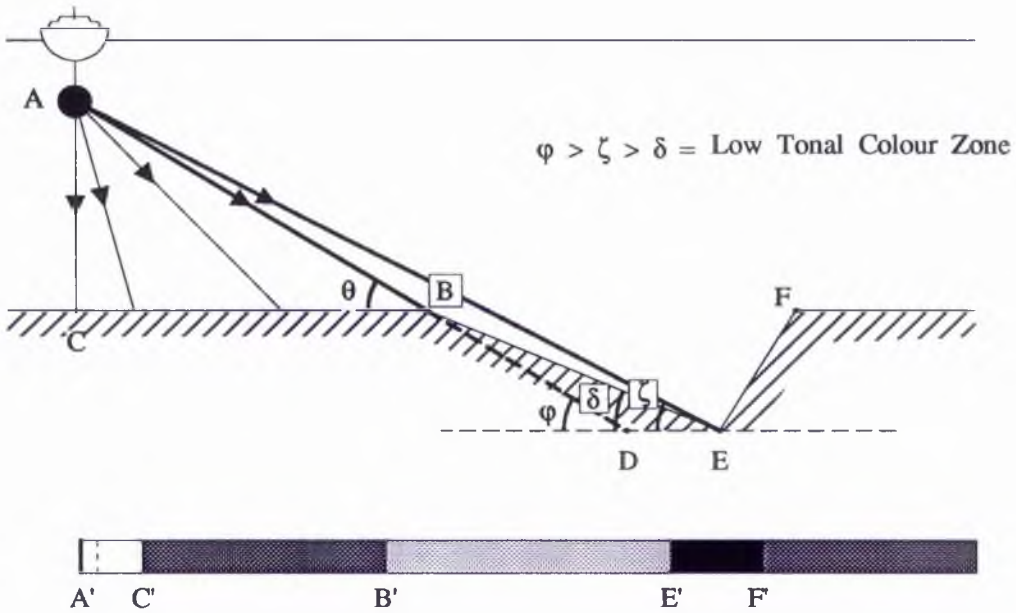

configurations occurs is controlled by the relationship between angle φ[4] and the angle δ of the proximal slope of the negative target. This geometrical relationship is identical to that described for positive targets (*ie.* the relationship between angles β and δ; Compare Figures 5.5a. and 5.5b. with 5.7a. and 5.7b.).

As identified for positive target scenarios it is also possible to use this relationship to quantitatively constrain the proximal slope angle δ. Where a shadow-strong reflector couplet is present the value of δ can be constrained between θ^{o} and 90^{o}. Due to the geometrical configuration described in Section 5.2.6., where an **LTCZ**-strong reflector is present δ can only be poorly constrained to between 0^{o} and θ^{o}. With the information available on the sonograph it is not possible to calculate the angle ξ^{o} (the negative target correlative of Ω^{o}) created by the raypath **AE**, when it strikes the bottom edge of the strong reflector zone, at the base of the depression (See Figure 5.7b.). Again these values are based up on apparent inclination ranges (See Discussion Above) so to convert to a true set of constraining values, ***Equation 5.1)*** should be applied.

By studying the nature and inter-relationship of the shadow-reflector couplet, it is possible to distinguish between man made and natural features. Characteristically, man made objects have sharp, distinct, shadows whilst those from natural objects tend to be more rounded and diffuse. This distinction is demonstrated in Figure 5.8., where the reflections from the anchor blocks holding the cages of the Marine Harvest fish farm on the northern shore of Loch Ainort are visible. These man made targets can be distinguished from the natural boulders strewn on the slopes of the southern shore.

Thus both material and topographical reflectors are capable of producing tonal variations on a sonograph, and as such it is plausible that they may produce identical sonographs. In many situations it is therefore left to the technical ability of the operator to interpret any such ambiguities. As a result a skilled operator can yield information on either the nature of the bottom material, the morphology of the bed or a combination of the two. It is further suggested by Flemming (1976) that, "..to do this accurately, he [the operator] needs

[4] The angle φ is actually represented by the angle θ. A full discussion of this relationship is given in Section 5.2.6.

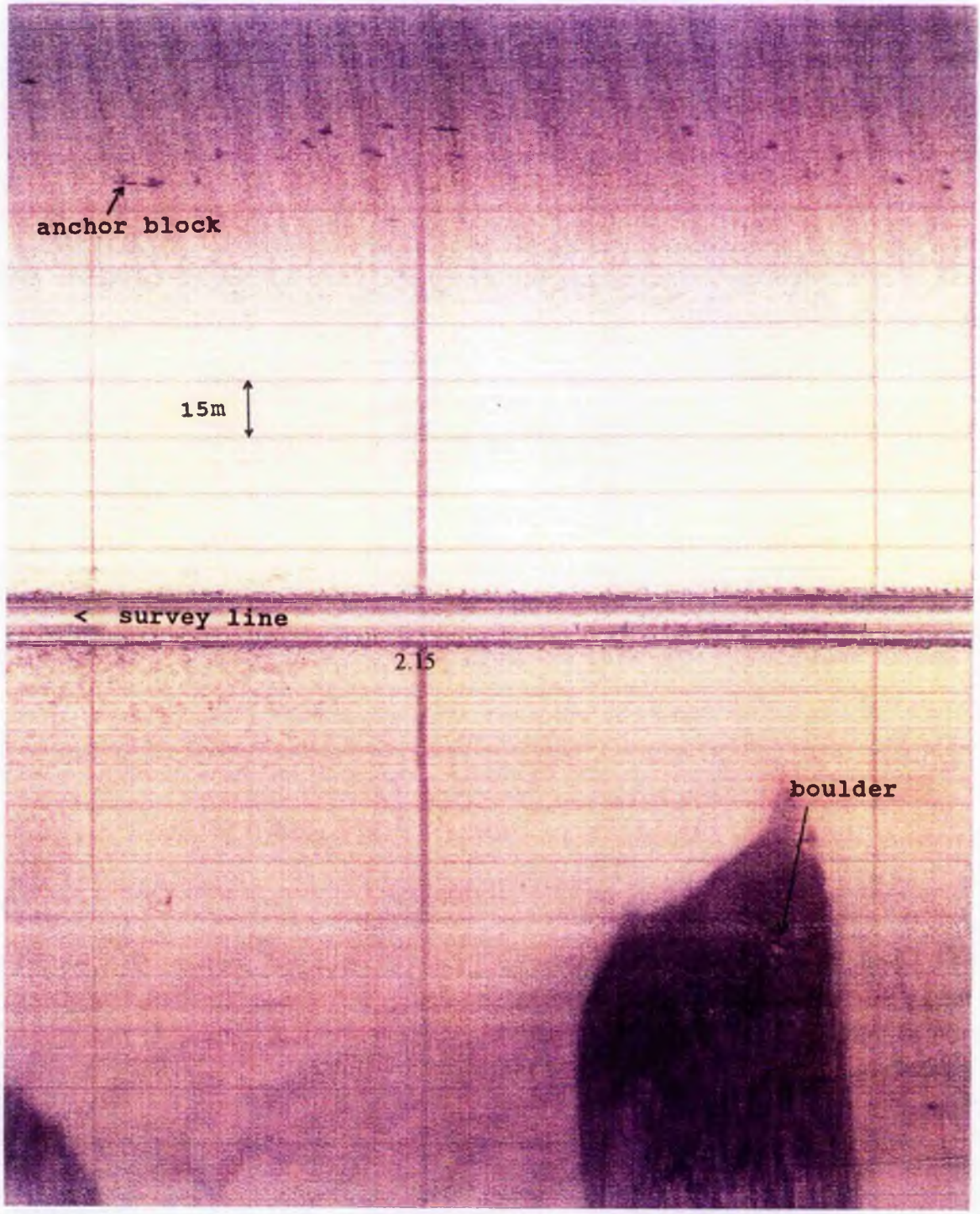

Figure 5.8. Sonograph showing the distinction between man made (anchor blocks) and natural (boulders) targets (Fix 2.14. - 2.16.).

experience and preferably first hand knowledge about the particular reflecting patterns caused by various rock types, gravels, sands, and characteristic forms associated with them such as bedding, jointing, ripple marks, sand waves *etc.*". For this project, such knowledge was acquired by reference to a catalogue of previous side scan work, both prior to and during sonograph interpretation (*eg.* Belderson *et al.*, 1972; Bryant, 1975; Flemming, 1976; Morang and McMaster, 1980; Hutchinson *et al.*, 1981; Prior *et al.*, 1981; Cook, 1982; Werner, 1982; Williams, 1982; McManus and Duck, 1983; Duck and McManus, 1985c; Klein, 1985; Carlson, 1989; Hequette and Hill, 1989; Duck and McManus, 1990; Fish and Carr, 1990).

5.2.4. DISTORTION.

Sonographs do not represent isometric maps of a surface as all features on the record are subject to a series of distortions. In particular, compression of targets parallel to the line of travel occurs, as a result of the ship's speed. At a speed of 2 knots, any target or tonal boundary will be faithfully represented on the trace. However, if this speed is exceeded both progressive shortening of objects and steepening of boundary angles is seen. All side scan surveys were conducted at a constant speed of 3.5 knots, even with this relatively small speed increase, distortion of the sonographs is a significant problem (See Figure 5.9a.). Therefore, where it has been necessary to plot isometric maps, they have been constructed with reference to distortion ellipses (After Flemming, 1976 - See Figure 5.9b.).

Lateral distortion perpendicular to the line of travel may also be a problem depending upon the height of the fish above the loch floor. If the towfish altitude is large there is a significant decrease in the amount of paper available for recording. Consequently, the true distance must be fitted into the remaining trace area so targets will be compressed in this direction. Again such a distortion is removed during the construction of isometric maps. In addition, due to the obliquity of the sonar beam, true distances do not follow a linear scale on the sonograph, with the short range intervals being compressed and the far ranges being slightly expanded. When plotting an isometric map this distortion may be removed by reference to a simple nonogram constructed after Flemming (1976).

Figure 5.9a. Distortion Effects on Some Common Shapes Parallel to the Line of Travel Caused by Various Ship Speeds (After Flemming, 1976)

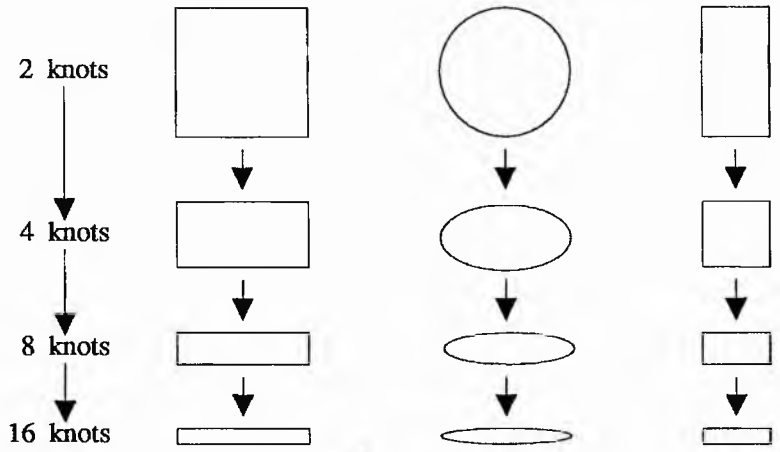

Figure 5.9b. Construction figure of Distortion ellipses With Which the Compression Effect Parallel to the Line of Travel Can be Corrected (After Flemming, 1976)

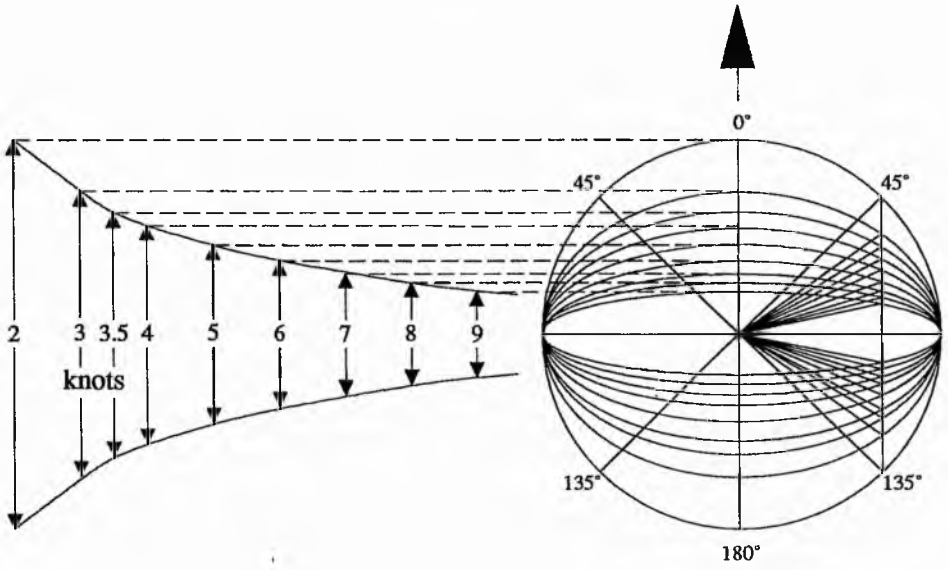

Finally, distortion parallel to the line of travel, at the outer margins of the trace may occur due to beam spreading. If two targets are separated by a distance less than the spread of the sonar beam at that range, during the period that they are being surveyed, one or other of the targets will return a signal to the sonar. This would be represented on the trace by one continuous mark, so resolution has been lost. At closer ranges the beam is narrower so this transverse resolution is significantly improved. With the system parameters of the side scan equipment used during this survey (See Section 2.3.3.2. - ***Equation 2.10***)) targets have to have a minimum separation of 1.96 m to be delimited at a 150 m (the maximum range used).

5.2.5. INTERFERENCE.

In addition to the distortion of features characteristic of all sonar traces (See Section 5.2.4.) each individual record may be obscured by a wide range of interference effects (For a comprehensive review see Klein, 1985; and Fish & Carr, 1990). Section 5.2.5. deals purely with those effects that were actually encountered during the analysis of the Loch Ainort sonographs. The recognition of any of these features, and ultimately their elimination, is a prerequisite to successful interpretation. The interference types that were observed during this survey fell into two broad categories; surface effects and acoustical noise.

Surface effects are the result of the interaction of the acoustic pulse with the water surface. In calm conditions the surface return described in Section 5.2.1. is seen as a thin, discrete line on the record. However, if either sea conditions are rough or the fish is towed too near the surface, or a combination of the two, the surface return may have a mottled appearance (See Figure 5.10.). In extreme conditions this "sea clutter" may even obscure data from the loch floor. Due to the weather restrictions enforced on any off-shore survey (See Section 2.2.) extensive sea clutter was not a problem. The shallow towing depths required for this survey (See Section 2.3.3.2.) did result in a minor, but unavoidable, degree of clutter within the water column.

Another surface effect encountered was boat wake, which is the result of the interaction of the acoustic pulse with a trail of bubbles left by the passage of a propeller. Such interference is

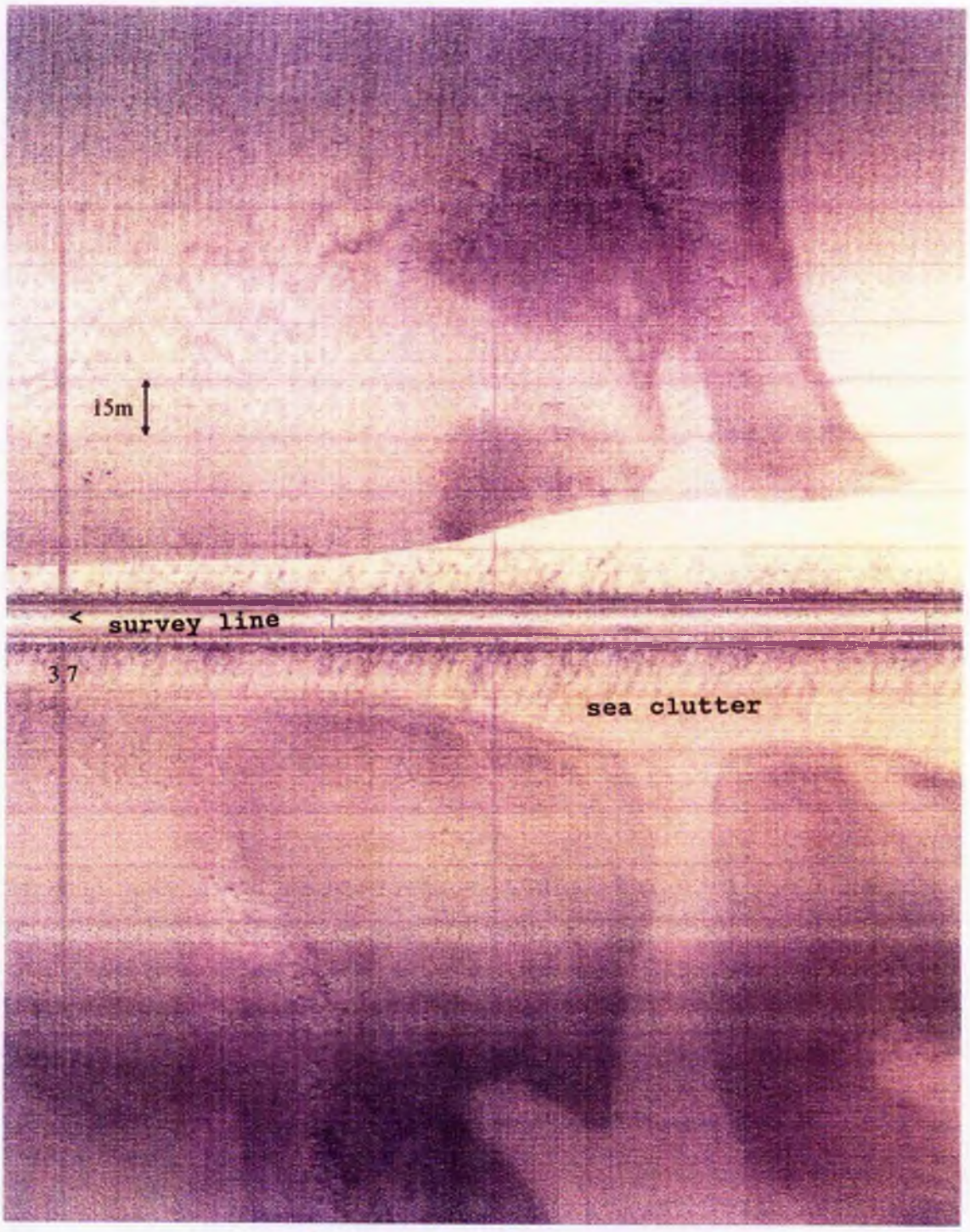

Figure 5.10. A sonograph showing sea clutter (Fix 3.7 - 3.8).

represented on the trace by a dark, "cloudlike" (Klein, 1985) zone with indistinct edges. The greater the time lapse between the formation of the wake and its interception by the pulse, the larger the area the wake covers on the record. This is the result of the gradual dispersal of the bubbles within the water column. Due to the limited boat activity on the Loch during our surveys, boat wake interference was not commonly observed. However, it was characteristically encountered when sharp turns were made during the survey, causing the towfish to intercept our own wake (See Figure 5.11.).

Acoustic noise from the water may enter the side scan system, via the transducer, having originated from sources other than the sonar itself. Again a whole series of such noises may be encountered, but during this study only one had any effect, that being echosounder interference. During the initial runs the hull mounted echosounder (See Section 2.3.3.1.) was run simultaneously with the side scan, with its transmitted pulse being detected by the towfish. This interference took the form of a regular pattern of small dark streaks moving diagonally across the outer portion of the record (See Figure 5.12.). Once identified as a source of disturbance, the echosounder was shut down during all further side scan surveys.

5.2.6. SIDE SCAN GEOMETRY.

In addition to a whole series of qualitative statements that can be deduced from sonar records it also possible to retrieve quantitative data. By the use of simple equations it is possible to calculate both the location of each target and the height to which an individual body extends above the loch floor. As mentioned throughout Section 5.2. the distance to individual points on a sonograph are not recorded as true horizontal distances, but as slant ranges. By use of Pythagoras theorem the actual horizontal distance to any point may be calculated from (See Figure 5.13a.):

$$R_h = \sqrt{R_s^2 - H_f^2} \qquad \textit{Equation 5.2)}$$

Where R_h = true horizontal distance, R_s = slant range, and H_f = fish height above the bed.

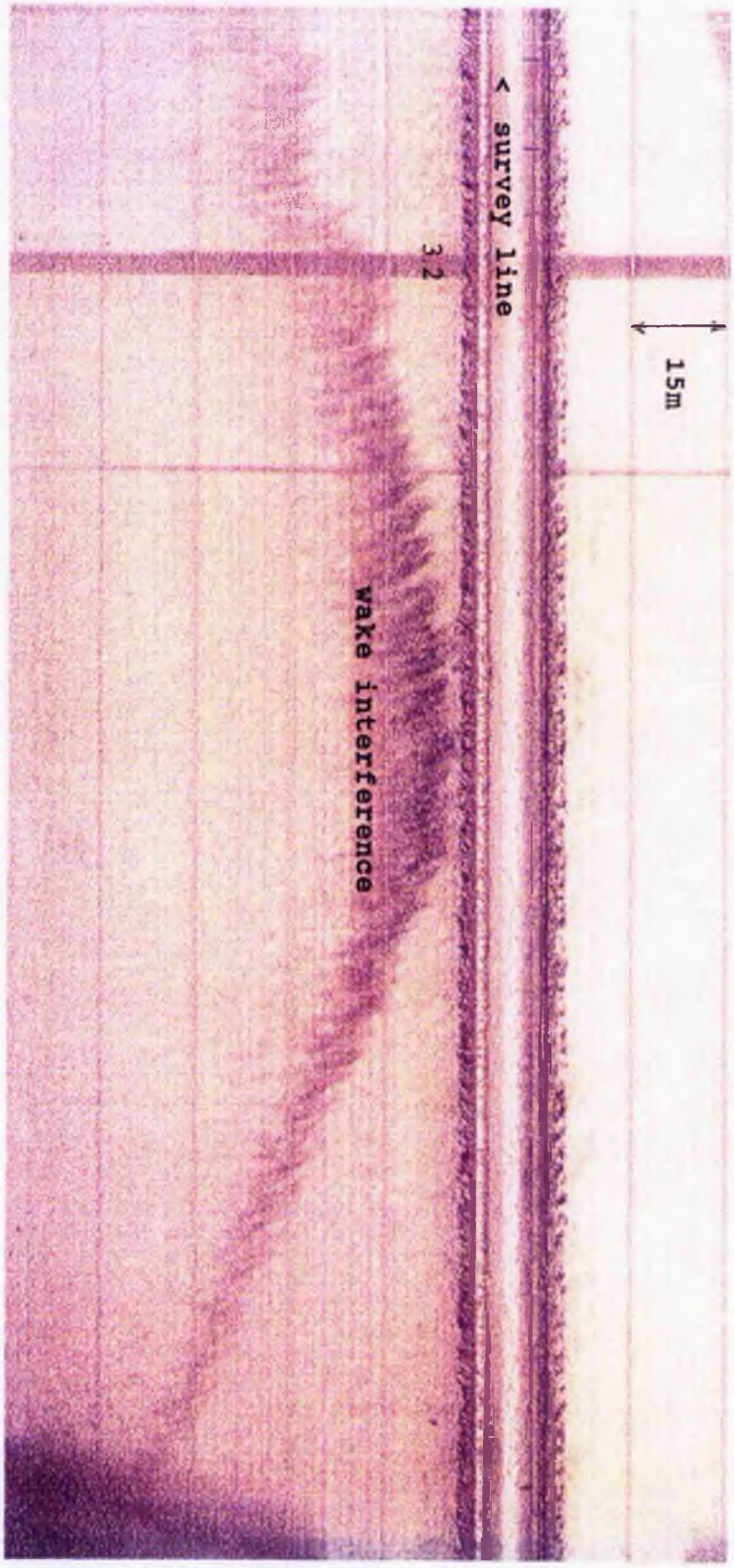

Figure 5.11. Sonograph showing wake interference (Fix 3.1 -3.2).

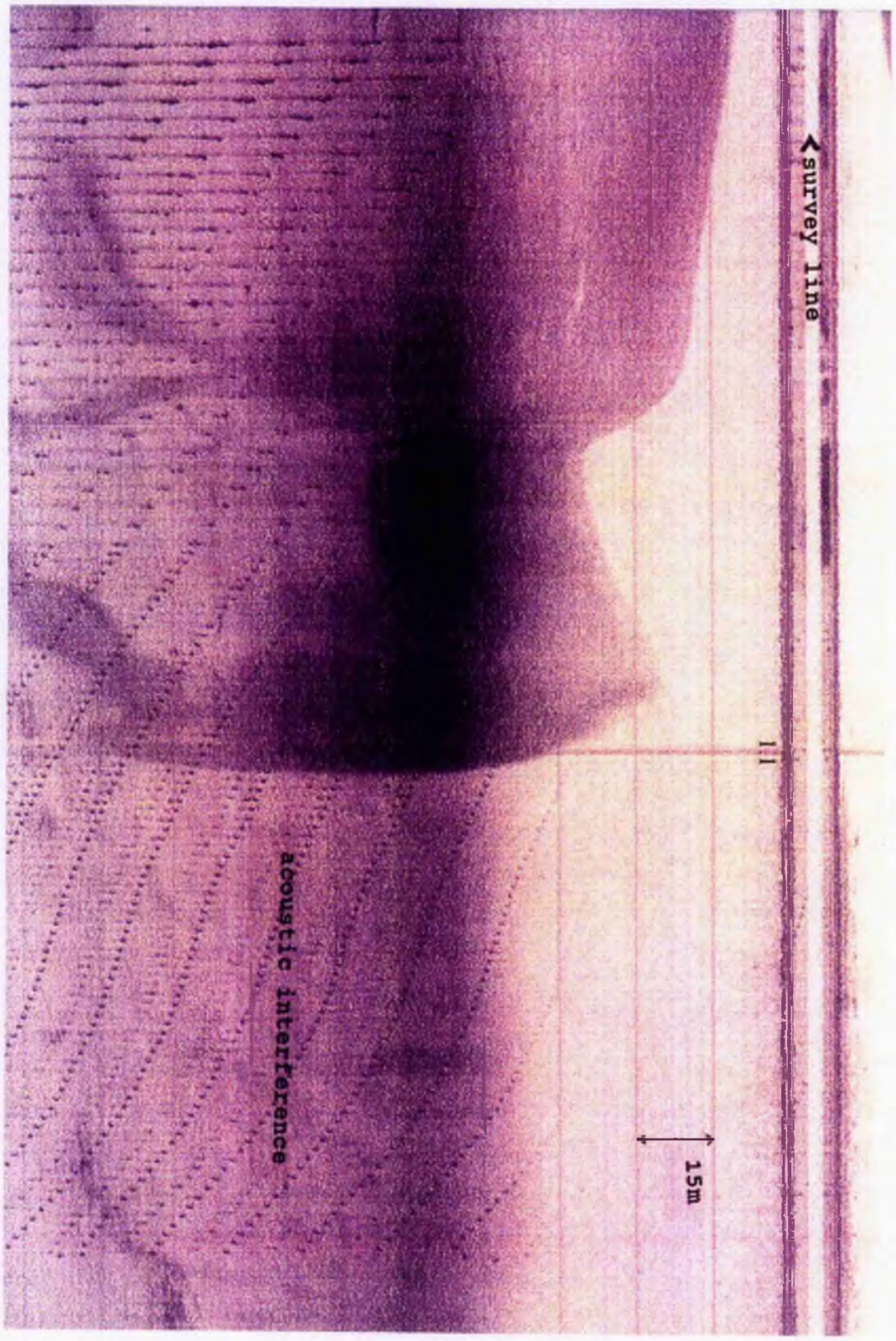

Figure 5.12. Sonograph showing acoustic interference due to the 192 kHz echosounder running simultaneously with the side scan sonar (Fix 1.1 - 1.2).

Figure 5.13a. Sketch Diagram Showing the Calculation of True Horizontal Distance of a Target From the Fish

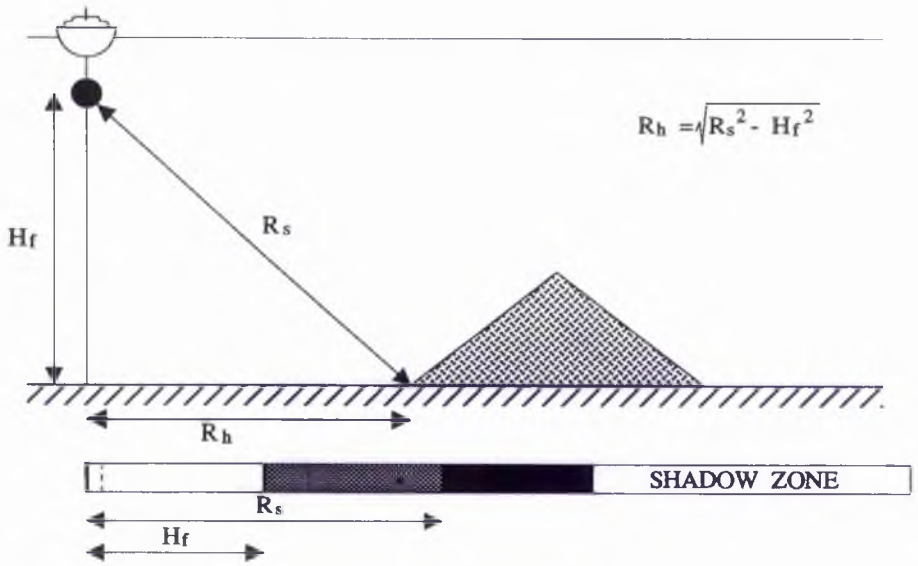

Figure 5.13b. Diagram Showing the Calculation of True Horizontal Distance to Targets on Sloping Surfaces (After Flemming, 1976)

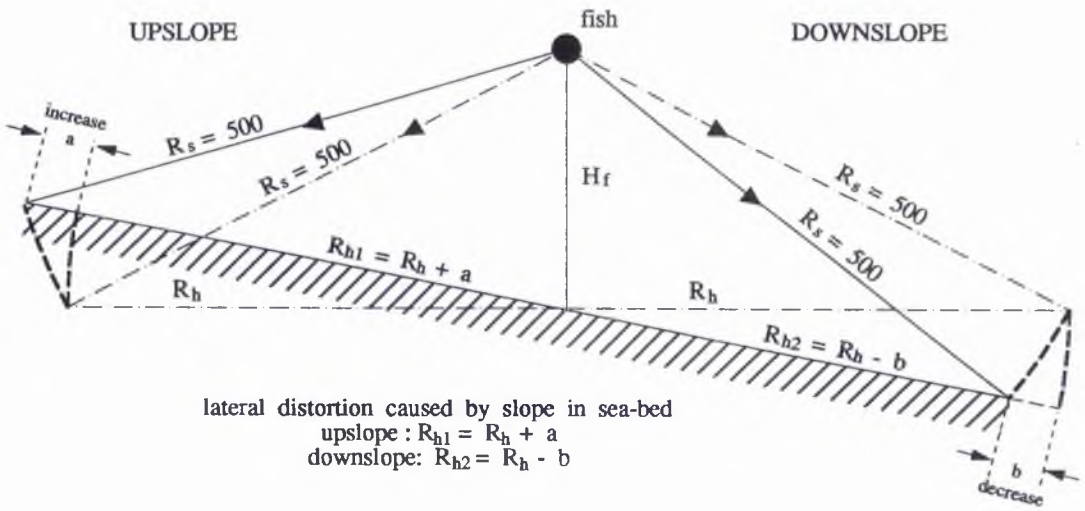

lateral distortion caused by slope in sea-bed
upslope : $R_{h1} = R_h + a$
downslope: $R_{h2} = R_h - b$

It should be taken into consideration that this value represents the true horizontal distance from the towfish to the target. To tie this value in with any position fixes taken from the boat the distance from the vessel to the fish should always be allowed for. However, the short tow length used during this survey (2 m) is well within the limits of error of the positioning equipment (See Section 2.3.2.), consequently this correction has not been applied.

These calculations are for a horizontal planar loch bed. However, the complex set of distortions caused by a sloping bed, result in the basic form expressed in ***Equation 5.2)*** to be amended (See Figure 5.13b.):

$$R_{h1} = R_h + a \; R_{h2} = R_h - b \qquad \textit{Equation 5.3)}$$

Where **a** = the incremental value of R_h, for a geometry of constant R_s intersecting with a inclining reflection surface , and **b** = the incremental value of R_h, for a geometry of constant R_s intersecting with a declining reflection surface (After Flemming (1976).

The effective result of applying these equations is that upslope distances will be increased, whilst any downslope measurements will be compressed. However, a maximum average slope angle of only 12° was encountered during this survey with average values being less than 6° (See Section 4.3.). These slope angles correspond to maximum distortions of the order of ± 14% with an average distortion of only ± 7%. Consequently, this correction has been applied only to those features found on the steepest slopes in the area.

Target height, is calculated from measurements taken from the shadow-reflector couplet. The ratio of the target height to the shadow length is equal to the ratio of the towfish height to the slant range value for the end of the shadow. From this relationship the target height can be calculated thus (See Figure 5.13c.):

$$H_t = H_f \times L_s / R_s + L_s \qquad \textit{Equation 5.4)}$$

Where H_t = height of target, H_f = height of fish above the bed, L_s = the slant length of the shadow zone, and R_s = slant range to the target.

Figure 5.13c. Diagram Showing the Calculation of Target Height Based on a Shadow - Strong reflector Couplet

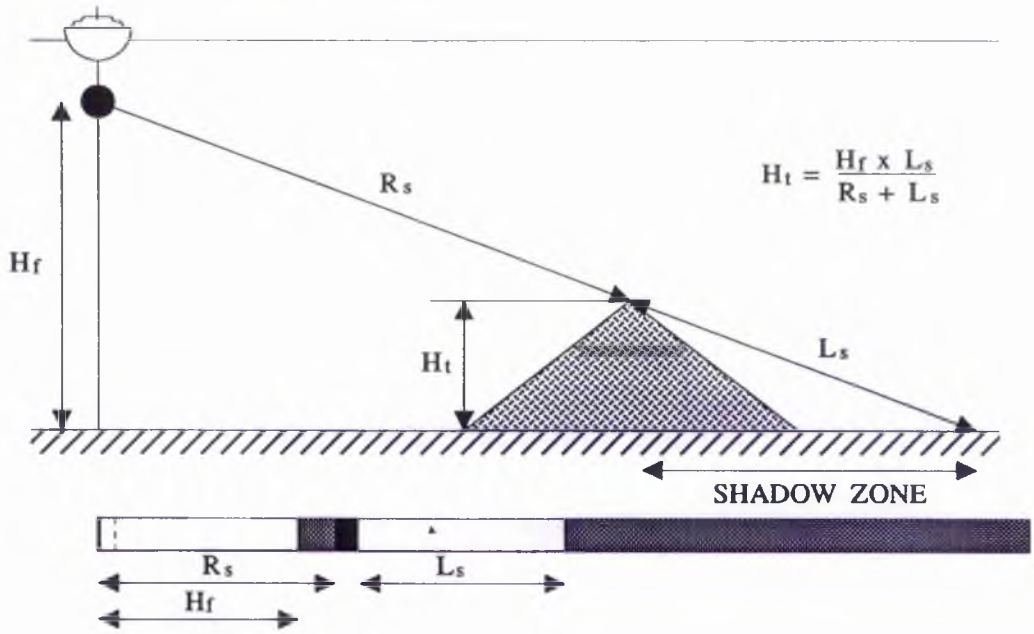

Figure 5.13d. Diagram Showing Inaccuracies with Target Height Calculation Based on an Lltcz

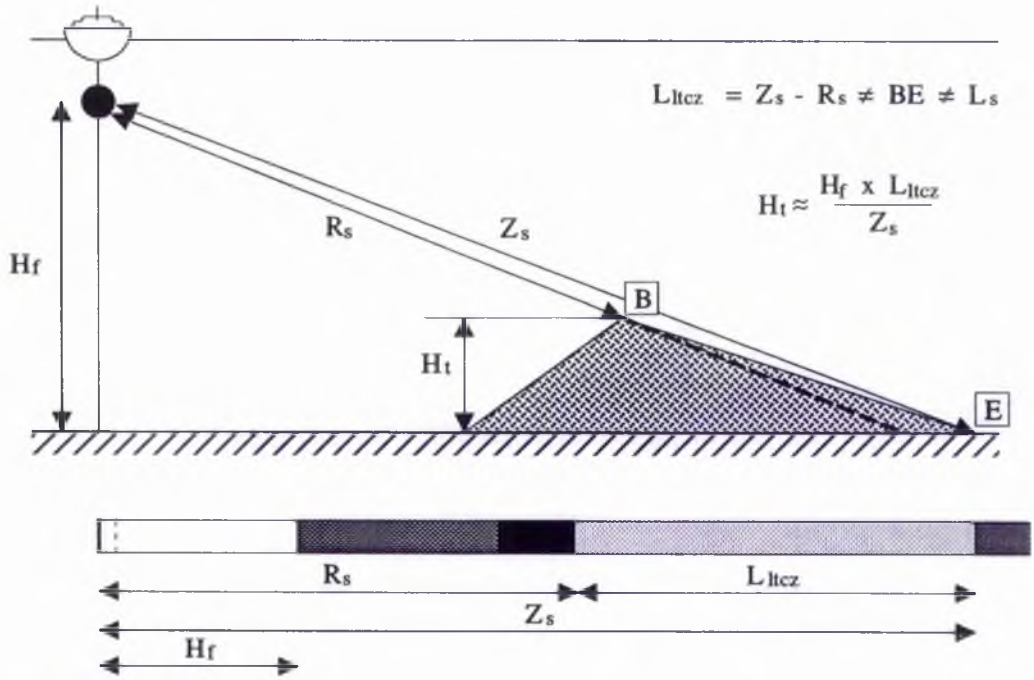

This value for target height must be considered as approximate as errors may be made in the measurement of slant ranges. It is often difficult to determine both the point at which the shadow ends and, for broad targets, the point from which the shadow is actually produced. For instance, measurements made from the trailing edge of a direct return will give shorter heights than those calculated from the leading edge. During this survey all measurements have been made from the trailing edge of any target. Irrespective of which edge the slant range values are taken, diffraction around the top of any target results in the shadow zones always being shorter than theoretically predicted. Consequently, all target heights will be slight over estimates. It should also be noted that if one or more of the parameters from ***Equations 5.2) - 5.4)*** are missing, only an estimated depth or distance value can be given. This is particularly common when surveying either at considerable depth or in a downslope direction as bottom profiles are invariably missing under such conditions. In these situations values in the text will be quoted as best estimates.

The method of target height calculation described is valid only for true, reflector-shadow couplets. If a reflector-**LTCZ** couplet is present (See Section 5.2.3.) the calculated target height ($\mathbf{H_t}$) values are invariably inaccurate as the length recorded from the sonograph, as corresponding to $\mathbf{L_s}$, is not equivalent to the length of a shadow zone. The value taken, which shall henceforth be referred to as $\mathbf{L_{ltcz}}$, is an arbitrary figure calculated as (See Figure 5.13d.):

$$\mathbf{L_{ltcz} = Z_s - R_s} \qquad \textit{Equation 5.5)}$$

Where $\mathbf{L_{ltcz}}$ = slant length of low tonal colour zone, $\mathbf{Z_s}$ = slant range to end of low tonal colour zone, and $\mathbf{R_s}$ = slant range to top of target. Substituting ***Equation 5.5)*** into ***Equation 5.4)***:

$$\mathbf{H_t \approx H_f \times L_{ltcz} / Z_s} \qquad \textit{Equation 5.6)}$$

As well as not being equal to $\mathbf{L_s}$, the length $\mathbf{L_{ltcz}}$ fails to represent the true length of the distal slope **BE** (See Figure 5.13d.). $\mathbf{L_{ltcz}}$ and therefore any calculated **Ht** values are in fact inversely proportional to the angle of the distal slope (∂), assuming both constant height and distance

from the fish. Consequently, all **Ht** values (See ***Equation 5.6)***) calculated from L_{ltcz} measurements should be treated with caution.

As discussed in Section 5.2.3., sonar traverses are seldom run perpendicular to targets but are invariably orientated at angles to the traverse line and, as a result, values of L_{ltcz} are related to the apparent inclination of the distal slope rather than the true inclination. As apparent angles are always less than true angles (See Section 5.2.3. ***Equation 1***)) the value of L_{ltcz} will be further increased relative to the true slope length, further compounding errors in any **Ht** calculations.

Similarly an estimate of the depth of negative targets can be calculated using the components of side scan geometry (See Figure 5.14a). For this geometrical configuration the angle (θ) made by the raypath **AD** ($= R_s$) striking the near edge of the negative target and the loch bed (**CD**) is equal to the angle (φ) made between the length of the shadow zone L_s (= **BD)** as it intersects the distal wall of the target. An estimate of the depth of the target (χ) can be calculated hence:

$$\sin \theta = \sin \varphi \qquad \textit{Equation 5.7)}$$

therefore:

$$H_f/R_s = \chi/L_s \qquad \textit{Equation 5.8)}$$

therefore:

$$\chi \approx H_f \times L_s/R_s \qquad \textit{Equation 5.9)}$$

As has been described for all of the quantitative values obtainable from side scan sonar traces, the depth value assigned to any negative depression can only be considered an estimate due to the geometrical assumptions on which the calculation is based. In particular it must be recognised that for a shadow-strong reflector couplet the value χ obtained can only represent a minimum depth. This is due to the constraints put on the incoming ray **ABD** by the height of the fish above the sea bed and the distance from the line of travel (See Figure 5.14a). Simply by either an increase in the value of H_f, a decrease in the slant range to the leading edge of the target (R_s) or a combination of the two, the angle φ of raypath **ABD** will approach the angle

Figure 5.14a. Diagram Showing the Calculation of Target Depth Based on Shadow - Strong Reflector Couplet

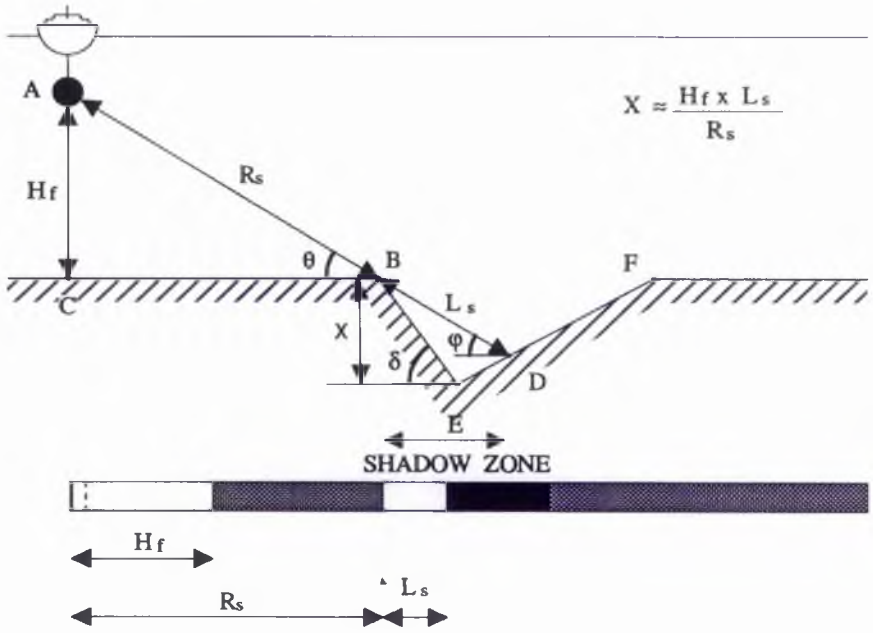

Figure 5.14b. Diagram Showing Geometric Impossibility of Calculating Target Depth on the Basis of a Low Tonal Colour Zone - Strong Reflection Couplet

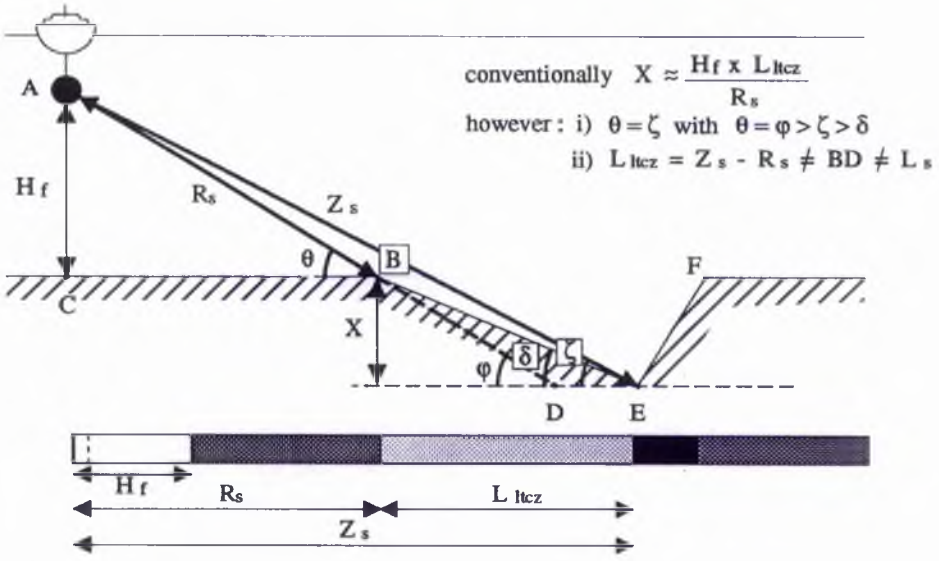

of the proximal slope (δ) and hence the better the approximation of χ to the true depth of the feature.

As can be seen in Figure 5.14b. the errors inherent in the geometry of an **LTCZ**-strong reflector couplet image make the calculation of a depth (χ) for negative targets impossible. The assumption that angle θ is equal to the angle made by the raypath **ABD** intersecting the distal slope of the depression (φ) no longer holds. In fact angle θ bears no geometric relationship with the actual angle made by the raypath **AE** which strikes the base of the depression, so forming the angle ξ. Consequently the simple relationship described in ***Equations 5.7)*** to ***5.9)*** cannot be applied. This geometrical configuration also precludes the simple substitution of $\mathbf{L}_{\text{ltcz}}$ for $\mathbf{L}_{\text{s}}$ in ***Equations 5.8)*** and ***5.9)***. As described in the discussion for positive targets this is because the $\mathbf{L}_{\text{ltcz}}$ measurement taken from the sonograph (See ***Equation 5.5)***) does not equal the required slant range value of **BD**.

Due to the geometry of the side scan system it is not possible to accurately calculate the depth from water surface to target, for objects at a distance from the traverse line. Consequently, where depths to targets have been quoted they are taken from comparison with the bathymetric chart and as such should only be considered as estimates.

5.3. LOCH AINORT: SONOGRAPH ANALYSIS.

To preserve the side scan traces in near perfect condition, so as to enable any other interested workers to verify the statements made here, features from all the sonographs were traced onto transparencies and annotated. The original traces have been stored in an opaque sealed bag to prevent fading and loss of definition. The traverses taken from Loch Ainort have been broken down into a total of 66 individual fixes corresponding to Magellan readings (See Section 5.1.). These fixes will be continually referred to in the text (they in turn can be located on Figure 5.1a.) in order to accurately locate any of the features described. To facilitate analysis, the sonographs from each survey line were divided into sections covering one, two or three of these fixes. Such a division produced

A3 size, or smaller, segments of trace from which to work. Analysis took the form of identifying individual positive and negative targets (inclusive of their shadow zones) on the transparencies, as well as plotting their location on isometric diagrams at a scale of 1:10,560. In addition, the traces were divided into zones of equal tonal quality following the relative tonal scale shown in Table 5.1.. This Table also shows the potential grain size equivalent for each tonal zone based on the scale created by Belderson *et al.* (1972). However, the descriptions given below will retain the tonal terminology with the genetic interpretation being presented in Section 8.2..

Tonal Colouration	*Material Grain Size*
Very Dark	Bedrock
Dark	Gravels
Dark/Medium	
Medium/Dark	
Medium	Sands
Medium/Light	
Light/Medium	
Light	Silts/Clays
Light/Very Light	
Very Light	

Table 5.1.: The categories of tonal colouration and the approximated corresponding material characteristics, employed during sonograph interpretation (Adapted from Belderson *et al.*, 1972).

In total 25 km of lines were shot in Loch Ainort, along five discrete survey lines (See Figure 5.1a.). Traverse 1 runs north-eastwards parallel to the south-eastern shoreline, starting from the head of the loch approximately 180 m offshore and finishing within the open waters at the mouth of the loch, 510 m west of Scalpay. Traverse 2 starts in these open waters, travels westwards across the mouth of the loch towards Maol Ban, and then turns sharply to the south-west to travel parallel to the north-western shore. Traverse 2 continues parallel to this shore but veers to 530 m offshore in order to avoid the cages of the Marine Harvest fish farm. This traverse finishes at the head of the loch. Traverse 3 follows a central route along the axis of Loch Ainort, turning due north 425 m from the coast of Scalpay to run parallel to its

western shore. On reaching Rubha Reireag, Traverse 3 turns through 90° to travel due west across the unnamed strait between Scalpay and the mainland, finishing 100 m from Maol na Gainmich. The end point of Traverse 3 also represents the start point of Traverse 4 which travels due south across the mouth of Lùib na Moil. Traverse 4 passes the point of Maol Bàn, 80 m offshore, and then follows a south-easterly course across the mouth of Loch Ainort finishing in the prominent embayment south-west of Rubh' an Àird Dhuirche. Finally, Traverse 5 effectively repeats part of Traverse 1 but is in the opposite direction. It starts 425 m from the mouth of the loch and runs south-westwards parallel to the shore, finishing in the shallow waters at the head of the loch.

For the purposes of describing the side scan sonographs, Loch Ainort has been divided into five broad geographical areas (See Figure 5.15.) following the descriptive divisions presented in Section 4.3.. Due to the detail of the geomorphic features identified from the sonographs the "Inner Loch" area (See Section 4.3.1.1.) has been further sub-divided into two shore sections and an axial zone (See Sections 5.3.1. to 5.3.3.). However, due to the nature of many of the identified targets these sub-divisions do not represent static boundaries and many features are described in more than one section. The loch is characterised by a series of linear positive targets or ridges and point reflector clusters or boulder clusters. Therefore for ease of identification the former have been numbered and prefixed with AR it being an acronym for Ainort Ridge, whilst the latter are prefixed with BC an acronym for Boulder Cluster.

For reference the location of morphological features described in Sections 5.3.1. to 5.3.5. is given in both OSGB36 co-ordinates and in relation to the minute fixes recorded directly on the side scan sonographs.

5.3.1. NORTH-WESTERN SHORE.

Confirming the information obtained from the bathymetric charts (See Section 4.3.), the side scan sonographs show that the main body of the loch has an asymmetrical cross section, with its axis offset towards the north-western shore. The south-easterly facing slopes (average angles of 12°) of this shore act as good reflectors for the incoming acoustic pulse. As a result

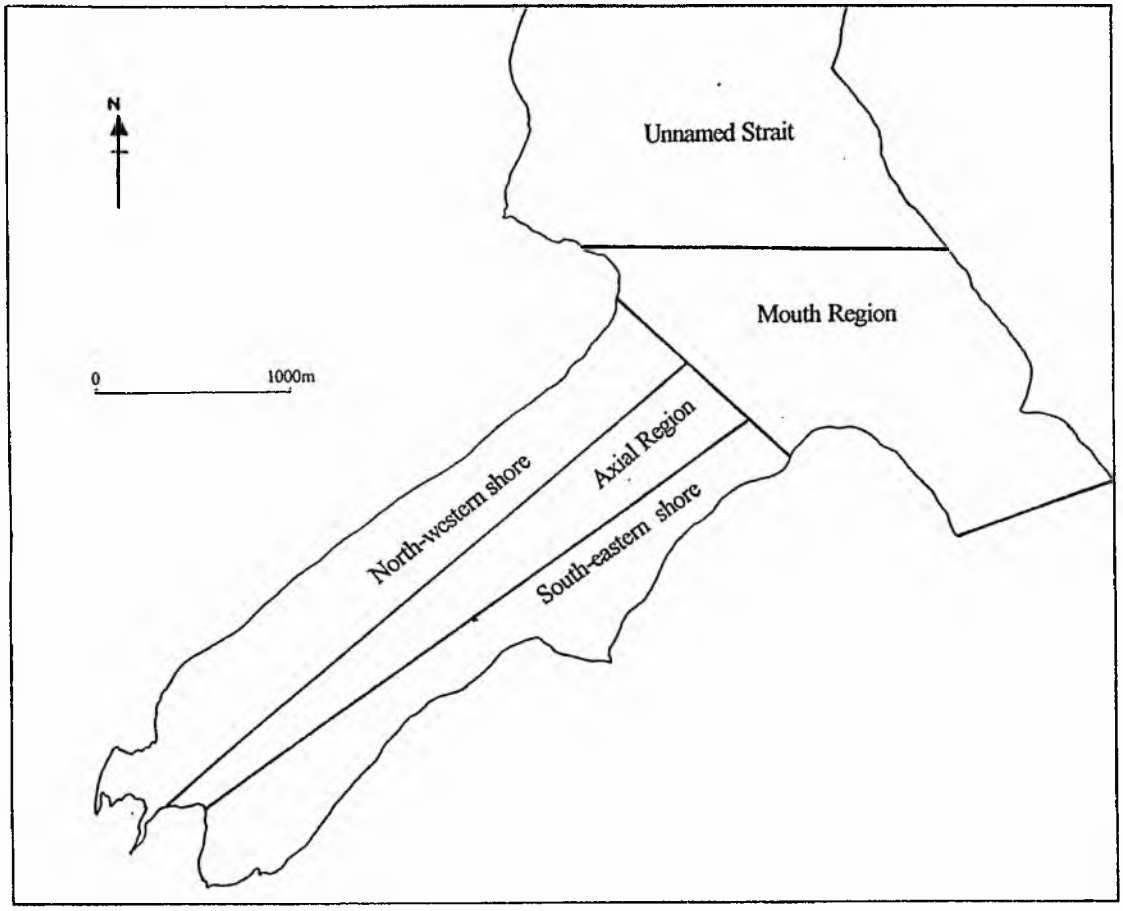

Figure 5.15. Geographical sub-divisions used for the interpretation of the side scan sonographs acquired from Loch Ainort.

these slopes are reproduced on those sonographs, in close proximity to the shore (between fixes 2.6 [156710 829700] and 2.8[156480 829500]), as "medium" to "dark" tonal areas. The continued sharp drop off from these slopes towards the centre of the loch fails to provide strong reflectors to the south-east. As a result no bottom profile is recorded between fixes 2.10 [156080 828910] and 2.16 [154870 827880], the trace being dominated by an area of no reflection. In this region, the outer portions of the sonograph do show reflectors present to the south-east, in the form of uniform areas of "medium" tonal shades which grade into this "blank" zone. Consequently, the traces from the deepest parts of this north-western channel fail to provide further significant information on the nature of these slopes.

The side scan record between fixes 2.6 [156710 829700] and 2.10 [156080 828910] is close enough to the shore, and in sufficiently shallow water, to provide some detail of the outer section of the north-western margin of Loch Ainort. At the outer edge of the trace between fix 2.7[156660 829670] and 2.8 [156480 829500] three shore-parallel benches are clearly visible at shallow depths. The central bench line represents the most prominent and continuous reflector of the three (See Figure 5.16.). The upper bench is also well defined but lacks continuity, whilst the lowermost bench is extremely disrupted and poorly represented (See Figure 5.16.). In addition, there is a fourth gentler break in slope running parallel to the shoreline between 120 and 130 m from the shore. This inclined surface extends for almost the entire length of the western margin of the loch. The offshore portion of this slope is characterised by clusters of weak "scallop" shaped features (See Figure 5.16.), with raised (3.7 m) frontal/lower segments.

A further 80 m offshore between fixes 2.8 [156480 829500] and 2.9 [156300 829310] a linear positive target (AR22) is identified (See Figure 5.16.). This ridge has a crestal orientation of 015°, and an axial length of 255 m. An associated topographical high is present on the bottom profile with a crestal relief of between 1 and 1.4 m. The ridge has a slightly asymmetrical profile with its easterly facing limb having a true ∂ range of 0° - 16° compared to an average dip of 12° for the westerly facing limb (See Section 5.2.3.). The entire ridge is encompassed by a "very dark" homogeneous tonal area. These "very dark" tonal surroundings do, however, result in the partial masking of the ridge, making identification of what is a complex target pattern difficult. The ridge is interpreted as being a single continuous

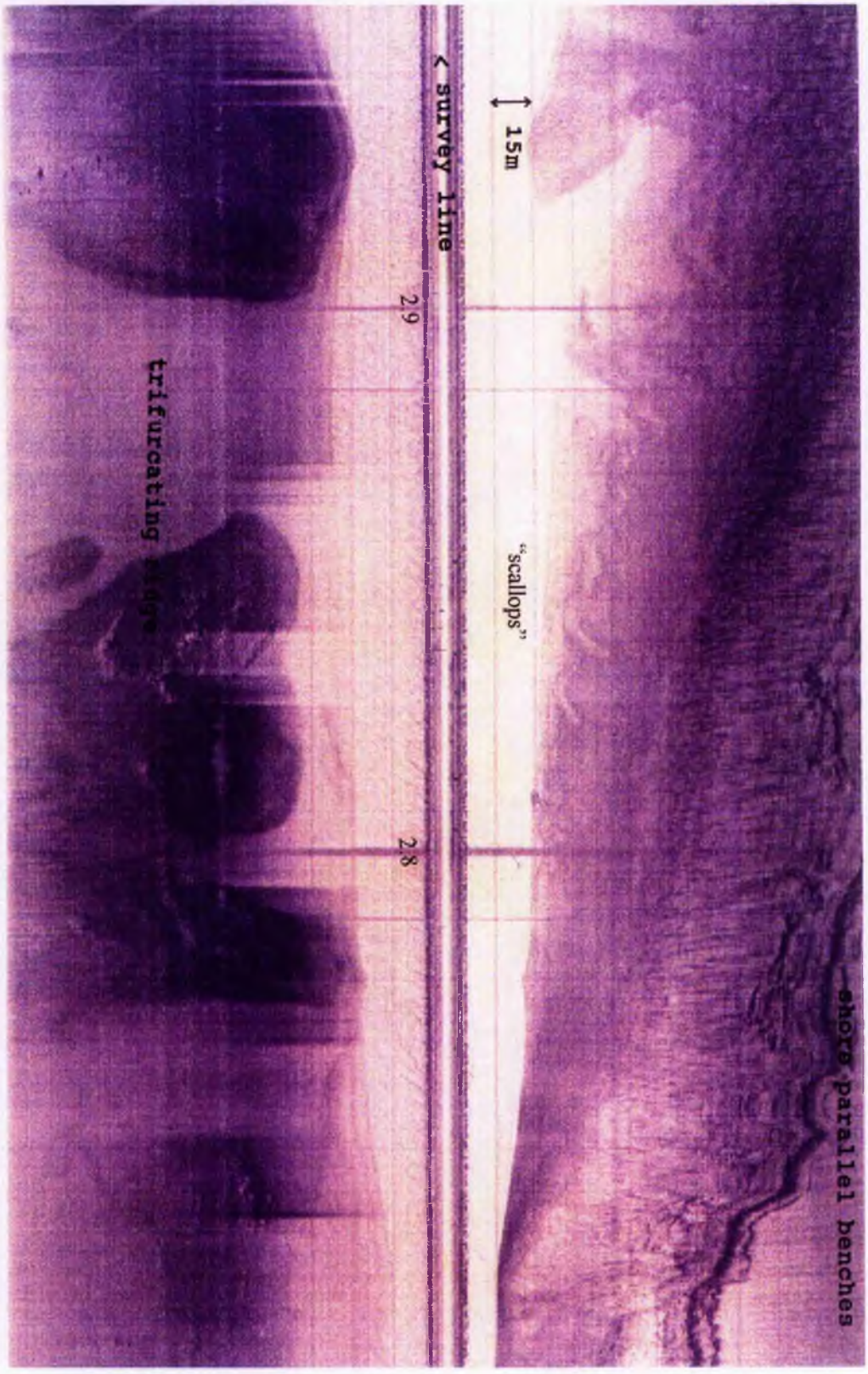

Figure 5.16. Sonograph showing shore parallel benches, weak "scallop" shaped features and trifurcating ridge from the north-western shore of Loch Ainort (Fix 2.7 - 2.9).

reflector for the majority of its length, but the reflector does appear to become disrupted at its south-westerly tip, suggesting the ridge trifurcates at this position. No clusters of point targets (boulders) are identified in association with the main section of the ridge (See Section 5.3.4), but a small group of point reflectors are located in the mouth of one of the trifurcating limbs. This is one of four ridges identified on this north-western shore but is of particular interest as it is orientated approximately perpendicular to the mean orientation (126°) of linear positive targets found in the Loch Ainort area (See Section 5.3.4.). ABR22 shows good spatial correlation with AR1 described from the bathymetry (See Table 5.2.). However, there does appear to be a significant discrepancy between the recorded dimensions (See Disscusion in Section 5.4.).

Ridge No.	*Axial Length (m)*	*Relief (m)*	*Orientation (°)*	*Slope Angles (°)* [5]	
				Proximal	*Distal*
AR22	255	1-1.4	015	12	0-16
ABR1	260	12	010	4.5	8

Table 5.2. Comparative table of bathymetric ridge ABR1 and ridge AR22 identified from the side scan sonar sonographs.

In association with ridge AR22 are two smaller linear features AR23 and AR25, which are located 30 m to the west and 75 m to the north-east respectively. AR23 [156470 829360] has an axial length of 35 m, a crestal orientation of 066° and a maximum relief of 1.2 m. **LTCZ** calculations (See Section 5.2.6.) suggest an asymmetrical profile with a very steep south-easterly slope (true ∂ range of 0° - 39°) compared to a more gentle (13°) north-westerly facing slope. The large ∂ range is probably the result of a configuration anomaly rather than a natural phenomenon (See Section 5.2.6.) as this target was located close to the bottom profile (**Zs** = 67.5 m) and at a relatively great depth (**Hf** = 32.5 m). It is therefore suggested that the actual value of ∂ is considerably less than the given range. AR25 [156630 829550] is a similar feature with an axial length of 40 m, a crestal orientation of 023° and a maximum relief of 1.1 m. Again this ridge has an asymmetric profile with a steeper

[5] As with the slopes described from both the Admiralty and bathymetric charts, the terms proximal and distal have been chosen to represent orientation relative to the head of Loch Ainort.

south-westerly slope (true ∂ range of 0° -17°) and a north-westerly slope inclined at 8°. On this ridge a small number of point reflectors are identified on its south-easterly facing slope, with a maximum height of 0.4 m (BC10).

Between fixes 2.9 [156300 829130] and 2.10 [156080 828910] a poorly defined, narrow ridge, with a crestal orientation of 108°, is identified to the north-west (AR18). This feature is associated with a marked asymmetrical rise of the bottom profile which has a relief of 12 m and a steeper (8°) south-western margin relative to the more gentle (4°) north-easterly facing slopes. In addition, an ovate "dark" tonal zone occurs to the south-west along with a well defined linear point reflector cluster at the outer margin of this "dark" tonal zone (BC6: [156350 828980]). This point reflector cluster is 65 m long by 30 m wide and contains a total of 17 individual point targets with a range of heights between 0.14 m and 1 m. It is suggested that these two features represent the north-western portion of a major, albeit discontinuous, ridge that runs across almost the entire width of the loch at this locality (See 5.3.3.). Spatially AR18 [156200 829090] coincides with ABR16 [156170 829100] but with contrasting orientations 108° and 166° respectively. Table 5.3. shows good correlation between slope angle values calculated for the two ridges but significant differences between axial lengths and relief values.

Ridge No.	*Axial Length (m)*	*Relief (m)*	*Orientation (°)*	*Slope Angles (°)*	
				Proximal	*Distal*
AR18	90	12	108	8	4
ABR16	200	4	166	6.3	4

Table 5.3. Comparative table of bathymetric ridge ABR1 and ridge AR22 identified from the side scan sonar sonographs.

Of the other three ridges (ABR2, ABR17 and ABR3) identified along the north-western shore by the bathymetric chart only two (ABR2 and ABR17) came within range of the side scan system. From the side scan traverses two additional ridges AR15 and AR11 were identified along this slope, but neither coincided with the bathymetric ridges. AR15 [156110 829050] is a short (65 m), thin, linear target with a crestal orientation of 165°. AR15 has a

crestal relief of 3 m and an asymmetrical profile with a true ∂ range of 0° - 34° for the south-western slope compared to an inclination of 21° for the north-eastern slope. AR15 has an identical orientation as ABR2 (165°) but is offset by 80 m to the north-east and has markedly different dimensions.

AR11 [155720 828760] has no bathymetric correlative it being an isolate short (42 m) ridge with an axial orientation of 011° and a low crestal relief of 0.8 m. The ridge has an asymmetric profile with a gently (2.8°) inclined easterly slope and a potentially more steeply inclined (true ∂ range 0° - 31°) western slope.

5.3.2. SOUTH-EASTERN SHORE.

The south-eastern slopes are characterised by shallower depths (less than 30 m) and overall gentler gradients (average 6°) than the north-western shoreline. Such a topographical configuration provides ideal conditions for side scan work and, as a consequence, both Traverses 1 and 5 give excellent coverage of this shore. From the outer edges of the majority of the shoreward facing traces, three sets of shore parallel benches are identified (See Figure 5.17.). These correspond closely to those described for the north-western margin of the loch (See Section 5.3.1.), with the central bench possessing the greatest degree of continuity, particularly between Luib and Rubh' an Àird Dhuirche. However, in contrast to those of the opposing shore, the uppermost bench is the weaker feature, being only discontinuously present in the innermost section of the loch (See Figure 5.17.).

The upper slopes (depths of less than 15 m) of the south-eastern margin, either side of the Luib protrusion possess the "medium" tonal colours. These surfaces have undergone extensive bedform development, with a parallel ridge and furrow topography dominating. These linear features have an average length of 19.25 m, amplitudes of up to 0.63 m, and a 020° crestal orientation, oblique to the shoreline. These ridges also have wavelengths between 4.3 m and 6 m and a Ripple Index[6] of 10.6. This bedform development is obscured towards

[6] Ripple index (RI) = Wavelength/Amplitude. (Lindholm, 1987).

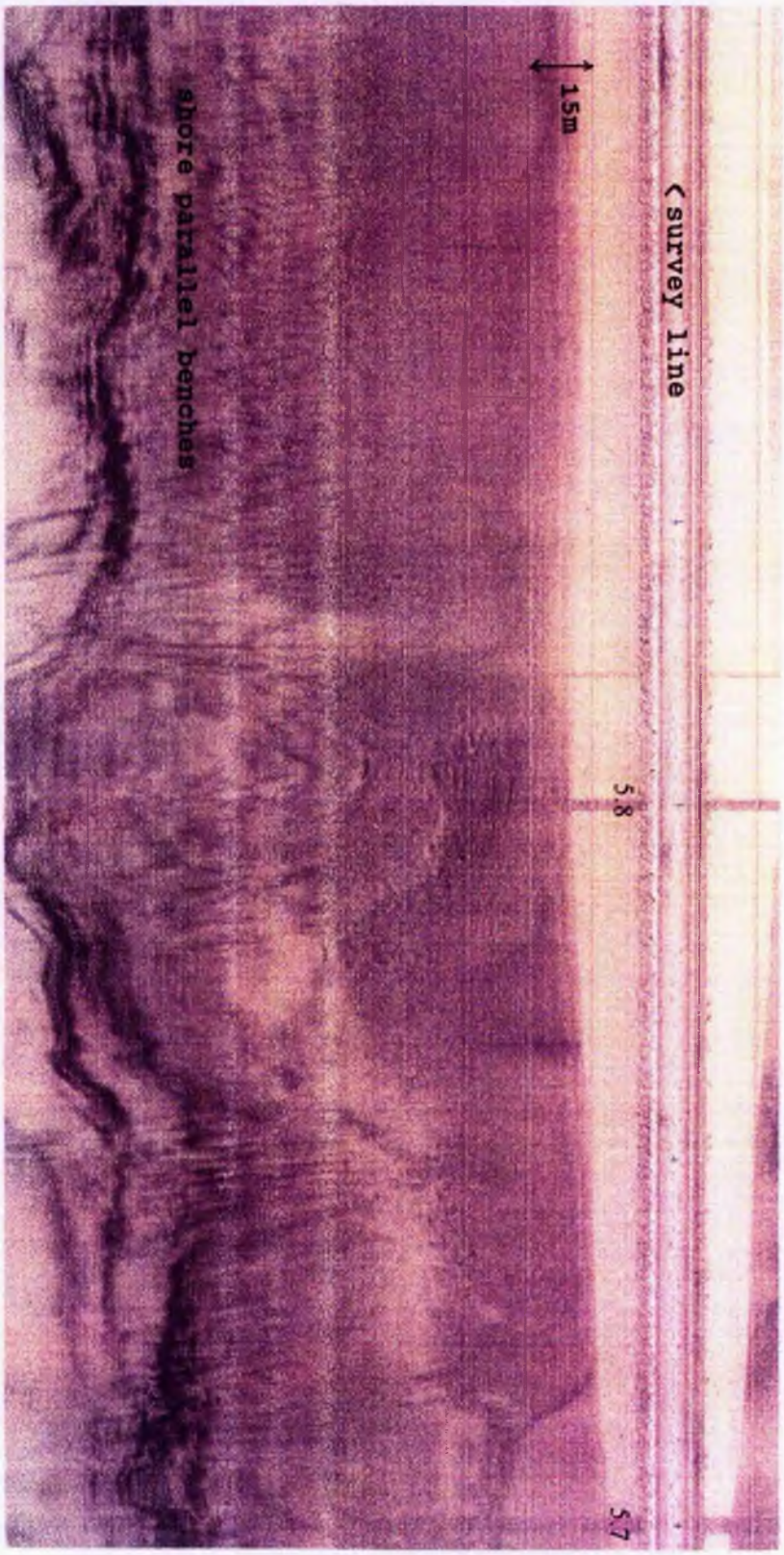

Figure 5.17. Sonograph showing shore parallel benches from the south-eastern shore of Loch Ainort (Fix 5.7 - 5.9).

the mouth of the loch by a large (265 m wide), chaotic, point reflector (average size 0.3 m) strewn fan that has developed on the north-western slopes of Am Meall between fixes 5.1 and 5.2. This fan extends 185 m offshore with its outer, arcuate, margin being deeply dissected (See Figure 5.18.).

The feature which dominates the south-eastern side of Loch Ainort is a large shallow topographical protrusion at Luib, which has previously been described from bathymetry in Section 4.3.1.1. The relevant sonographs from both Traverse 1 and 5 provide further details of the morphology of both the outer section of the top and loch-ward facing slope of this feature (See Figure 5.1b.). The gently sloping (1°) upper surface possesses a chaotic, point-reflector strewn form. To the north-east and south-west the irregular surface and lighter tonal coloration of the protrusion top contrasts sharply with the "medium" tones of these more uniform slopes. In zones where the lighter tonal material appears to dominate, a sequence of parallel, linear positive targets are present with an axial trend between 018° and 028°. These positive targets have an average axial length of 55.5 m, a wavelength of 17.4 m, an average amplitude of 0.3 m and a Ripple Index of 53.5.

The side scan traces are also able to identify the break in slope of the Luib protrusion. However, this same feature is represented differently on Traverses 1 and 5 as the sonar beams are shot at different angles to the slope. Traverse 5 runs approximately 80 m inshore of the protrusion margin and, as a result, the sonar beam travels down the frontal slope of this feature. This geometrical configuration of pulse orientation and topography causes an increase in the angle of incidence and, by the First Law of reflection, an equal increase in the angle of reflectance, so reducing the strength of the returning pulse (See Figure 5.19a). This configuration continues until a beam strikes the more gently inclined loch floor, at the base of this slope, so decreasing both the angles of incidence and reflectance and therefore increasing the strength of the returning pulse. This slope manifests itself on the trace as a blank area, with diffuse gradational boundaries, which lie between the reflectors of the protrusion top and those of the loch floor. In contrast, Traverse 1 runs 80 m offshore of the protrusion, so the slope is facing the out going acoustic pulse and as such provides an excellent reflecting surface. This configuration again results in the significant reduction of both the angles of incidence and reflectance and so increases the strength of the returning pulse (See Figure

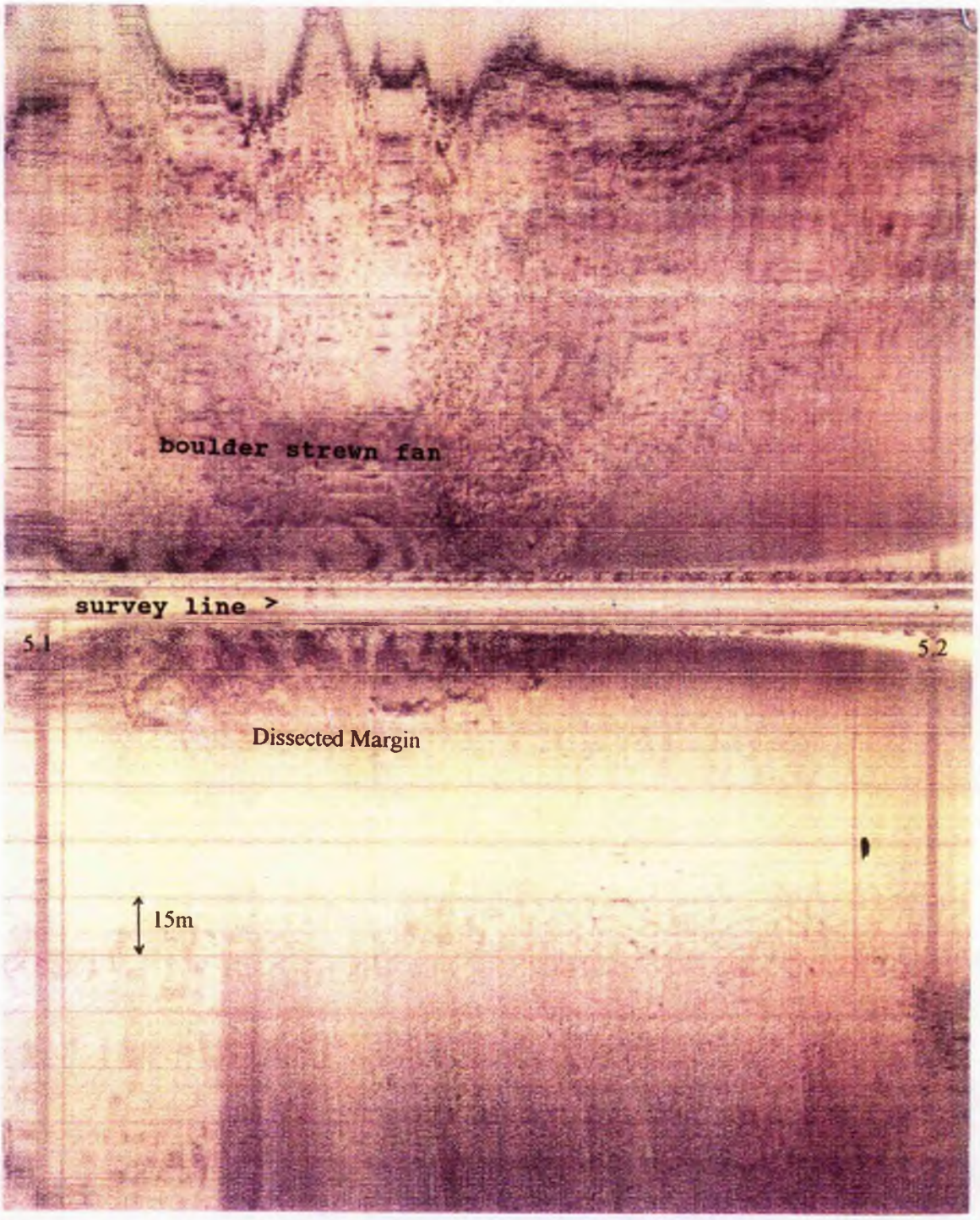

Figure 5.18. Sonograph showing large chaotic point reflector strewn fan with deeply dissected margin off the north-eastern slopes of Am Meall (Fix 5.1 - 5.2).

Figure 5.19a. Sonar Geometry for an Away Sloping Reflector

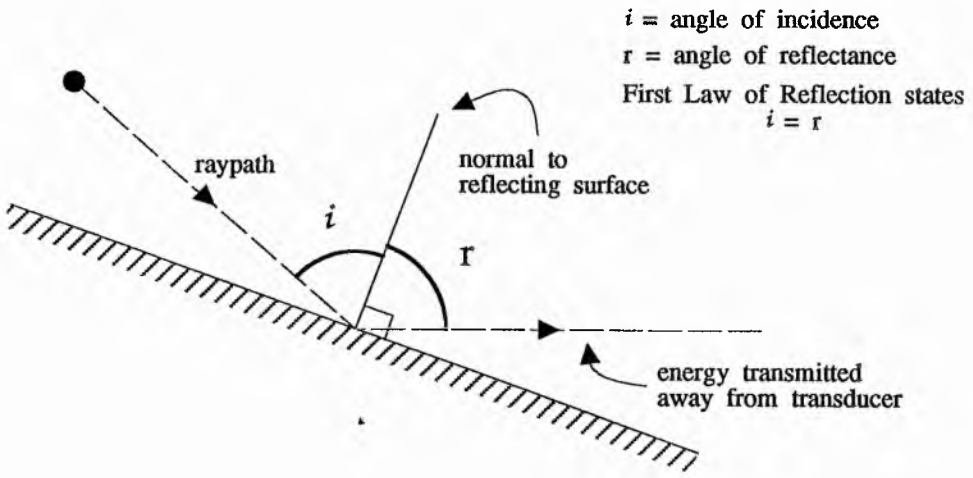

Figure 5.19b. Sonar Geometry for a Facing Reflector

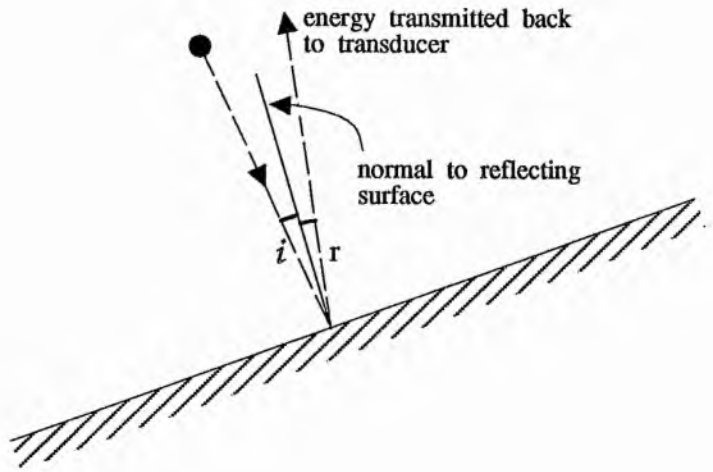

5.19b). Consequently, the top of the protrusion which continues to rise gently towards the shore is represented on the trace as a "dark" tonal band with no corresponding shadow zone.

The importance of acoustic pulse orientation to a target is further emphasised on the north-east margin of the Luib protrusion. At this locality on Traverse 1 (between fixes 1.7 and 1.8) a well developed arcuate fan is clearly visible on the gentle slopes (3°) associated with this margin of the protrusion (See Figure 5.20.). The fan has a total length of 125 m, a maximum width of 90 m and an arcuate, raised (relief of 1.4 m), frontal edge. The surface of the mid-fan area is heavily sculpted by a ridge and furrow topography (with a crestal relief of 0.7 m to 0.8 m). There is an overall progressive tonal variation down the fan, from "very dark" at the fan head through "medium" tones to "light" tones for the mid- and distal sections of the fan lobe. On Traverse 5, which was run at a less acute angle to this slope than Traverse 1, the fan does not appear on the sonographs, a marked contrast to the detail observed on Traverse 1.

The remainder of these south-eastern slopes are characterised by poorly developed targets, except for a thin curvilinear ridge complex located to the south-west of the Luib protrusion (AR6 & AR5 between fixes 5.7 [155890 828290] and 5.8.[155620 828120]). The main ridge (AR6 [155850 828110]) axis is orientated parallel to the shore at 054° with an axial length of 285 m, and an arcuate morphology concave to the north-west. This ridge has an undulating crest which ranges in height from 0.4 m to 2 m along its length. The north-westerly facing slope is inclined at 11°, whilst the angle of the south-easterly slope is lost within its shadow zone. The crest and lochward facing slopes are covered with a total of 27 individual point targets with a range of heights from 0.2 m to 1 m. At the south-western tip of AR6, is a smaller (53 m) arcuate ridge (AR5 [155630 828090]), which has an axial orientation of 027° and a south-easterly concaved form. The south-easterly slope of this ridge has a true ∂ range of 0° - 24° and a significantly gentler north-westerly slope inclined at 2°. As with the trifercating ridge described from the north-western shore, the orientation of these ridges appears to be perpendicular to the dominant 126° ridge trend (See Figure 5.21.).

The three lobes (ABR18, 19 and ABR20) and an isolated mound (ABR4) identified on these slopes to the south-west of Luib (See Section 4.3.1.1.) are not clearly identified on the

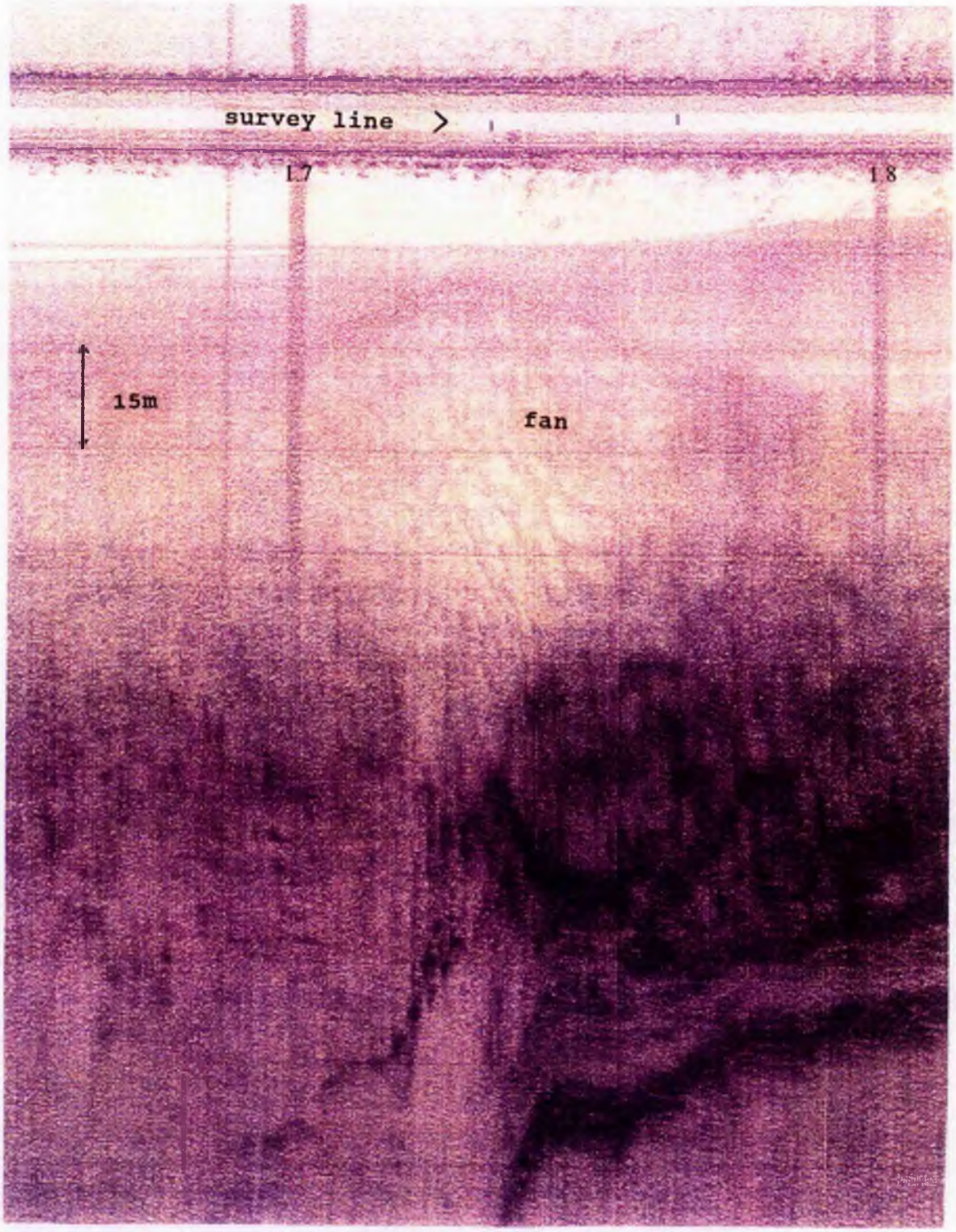

Figure 5.20. Sonograph showing a fan descending from the north-east slopes of the Luib delta (Fix 1.7 - 1.8).

Figure 5.21. An isometric diagram showing distribution of linear positive targets (ridges) and point reflector (boulder) clusters in the Loch Ainort area (Scale 1:10560). Overlay 1 - Isometric diagram (same scale) showing distribution of "dark/very dark" material reflector zones.

side scan traces of either Traverses 1 or 5. Of the three lobes only the central one has any representation on the sonographs (AR3 [155340 827880]- between fixes 5.9[155410 827980] and 5.10 [155160 827780]) but this is a relatively weak feature, consisting of an isolated topographical high on the bottom profile (with a relief of 9 m) and two associated "dark" zones on either channel. Within these two zones there is a suggestion of a linear positive target, but shadow zones are weak to absent. When the feature is transposed onto an isometric diagram it plots as a strongly concave, down loch ridge; a configuration uncommon in Loch Ainort (See Figure 5.21.). There is no evidence of this feature on sonographs from either Traverse 1 or 3. It is therefore suggested that the existence of this feature should be viewed with some scepticism. As for the isolated mound (ABR4 [155100 827600]), it was anticipated that it would only be recorded on Traverse 1 (between fixes 1.1 [154940 827600] and 1.2 [155330 827920]), yet this section of trace exhibits no such prominent feature. As this was an area where sonographs were affected by both echosounder interference and boat wake (See Section 7.2.5.) it is possible that the feature has been obscured.

5.3.3. AXIAL REGION.

The "Axial Region" is covered by sonographs from Traverse 3 (between fixes 3.1 [154870 827720] and 3.7 [156620 829180]), the port and starboard channels of Traverses 1 and 5 respectively (between fixes 1.1 [154940 827600] and 1.11 [157100 829000], 5.1 [157120 828990] and 5.10 [155160 827780]) plus an overlap with the port channel of Traverse 2 (between fixes 2.9 [156300 829130] and 2.17 [154710 827810]).

This part of the side scan survey covers the majority of the north-western channel (See Section 4.3.1.1. and 5.3.1.) and, as such, passes over the deepest waters of the inner loch. Consequently, the bottom profile is intermittent, its absence commonly occurring when the depth from the fish to loch floor exceeds 30 m. The loss of the bottom profile is always associated with a comparable loss of information at distance from the survey line. This is generally represented on the traces as uniform gradational tonal variations from "blank" to "medium" colours as the horizontal range increases. These areas of poor tonal coloration do, however, provide a marked contrast to several patches of "dark" and "very dark" tonal

shades, with no associated shadow zones, which occur throughout this sector (See Figure 5.21. Overlay 1.). In addition many more "dark" tonal patches are associated with both well defined linear positive targets (ridges) and clusters of numerous point target fields. It is this extreme variation between limited and very detailed information which characterises the "Axial Region" of Loch Ainort.

A total of fifteen individual linear to curvilinear targets are identified in the "Axial Region" and they range from small narrow features to major cross loch ridge complexes. There area three major ridge complexes (AR14, AR17 and AR24) the most prominent of which, AR17, occurs approximately mid-way between the mouth of the loch and the Luib protrusion (perpendicular to fix 2.9 [156300 829130], 3.6 [156500 828900] and 5.2[156880 828830]). The AR17 complex consists of five individual ridges (AR16, AR17, AR18, AR19 and AR20), three small point reflector fields (BC6, BC7, and BC8) and an extensive "dark" patch (See Figure 5.21. Overlay 1). It extends for a total distance of 740 m across the width of the loch, with an orientation of 102° and has an open sinuous form. However, this complex cannot be identified as a continuous feature due to both a break in coverage between Traverses 3 and 5 (See Figure 5.1b.) and a masking affect caused by the "very dark" tonal coloration between fixes 2.9 [156300 829130] and 2.10 [156080 828910].

The main ridge (AR17 [156550 828970]) has a crestal relief of between 1 m and 12 m and a crestal orientation of 091°. Where the traverse line cut directly across this ridge, the bed profile describe an asymmetric feature with steeper south-westerly facing slopes (8° compared to 2° for the north-eastern slopes). At distance from the survey line the ridge symmetry, as suggested by the nature of the **LTCZ**, has a greater degree of variability. From a total of six individual measurements the south-westerly facing slopes have an average true ∂ range of 0° - 26°. By comparison the north-easterly facing slopes have an average true ∂ range of 0° - 25°. The apparent discrepancy between the angles calculated from the bottom profile compared to those from **LTCZ** calculations is considered to be the result of these values representing a maximum range of angles rather than a precise figure (See Section 5.4.).

Of the remaining components of this complex three, AR16 [156350 828950], AR18 [156200 829090] and AR20 [156790 828900], follow the general 102° trend with crestal

orientations of 125°, 108° and 090° respectively. AR16 is offset by 20 m to the south-west of the main ridge, with an axial length of 64 m a relief of 1.1 m. This minor ridge has a south facing slope angle of 19° and a northerly inclined slope with a true ∂ range of 0° - 47°. The very large ∂ range exhibited by the northerly slope is probably highly exaggerated due to the combination of the large obliquity angle (73°) between the acoustic pulse and the true dip direction (See Section 5.2.3.), and the large **Zs** value (See Section 5.4.). AR18 is the most north-westerly component of the complex and is described in detail in Section 5.3.1.. AR20 represents the south-easterly section of the complex, with an axial length of 90 m. However, further data are unavailable due to the presence of a very weak shadow zone.

Finally, AR19 [156420 828990] is the shortest of the linear positive targets associated with this complex with an axial length of 35 m. This short feature is located 10 m to the north of the western tip of AR17 and has a crestal orientation of 030°, approximately perpendicular to the orientation of the complex as a whole. However, this feature is well defined, with a prominent **LTCZ**, a maximum relief of 5 m, and an asymmetrical profile with steep (17°) easterly facing slopes and more gently inclined western slopes (true ∂ range of 0° - 15°).

An asymmetrical distribution is also exhibited by the shape of the "very dark" tonal zone which encompasses the majority of the ridge complex (AR16, AR17, AR18, AR19 - See Figure 5.21. Overlay 1.). Overall, this zone narrows from a maximum width of 200 m at AR18 in the north-west to a minimum of 11 m at the easterly tip of AR17. However, for the entire length of AR17, the southern portion of this zone has an average width of 32 m compared to an average of 64 m on the northern margin.

Associated with both the north and south facing slopes of these ridges are numerous point reflectors, with dimensions between 0.3 m and 0.7 m. In addition to the point reflectors lying directly upon the ridge three discrete point reflector clusters are found in close proximity to the ridge complex. Two of these clusters (BC6 [156350 828980] and BC7 [156810 828890]) are thin (less than 11 m), linear features, with similar orientations (103° and 068°) to the overall 102° ridge bearing. Both of these clusters are found within "dark" to "very dark" tonal zones, which may mask shallow topographical reflectors. It is proposed that these two clusters represent extensions of the ridge complex. In fact the close proximity and similar

morphology of AR20 and BC7 suggest that they may represent the same, or part of the same, feature. These two targets have been identified from two separate traverses (5 and 1 respectively) which were run at different angles to the object. A combination of sonar beam orientation and human plotting error may account for the ± 10 m discrepancy in location. The third point reflector cluster (BC8 [156620 829000]) makes an acute angle with the main ridge, having an axial orientation of 026°. This cluster is also encompassed by a "dark" zone which appears to be an extension of the tonal zone associated with the main ridge (See Figure 5.21. Overlay 1).

The second major ridge complex (AR24 [156850 829300]) is located towards the mouth of the loch between fixes 3.7 [156620 829180] and 3.8. [157190 829330] By comparison to the multi-ridged feature described above, this major feature consists of a single ridge with a high lateral continuity. The ridge has an axial length of 405 m, a crestal orientation of 096° and a straight linear form. It has a large crestal relief with maximum values varying between 2.1 m and 5.4 m. As with many of the ridges described above it has an asymmetrical cross-section with a steeper southerly slope inclined at 13° and a more gently northerly facing slope inclined at 6°. Unlike the AR17 there is neither an associated "dark/very dark" zone nor point reflector clusters. However, there are in excess of 75 point reflectors concentrated on the axis of this ridge, with a particularly large concentration towards its easterly tip. These point reflectors have heights that range between 0.3 m and 0.7 m.

The third and final major ridge (AR14 [156300 828650]) is located at the northern margin of the Luib protrusion, perpendicular to fixes 1.5 [156350 828610], 3.4 [156180 828660] and 5.4 [156440 828410] (See Figure 5.1a.). This feature possesses a great degree of lateral continuity and again consists of a single ridge that can be traced for a distance of 470 m across the width of the loch. The ridge has a thin linear form with a predominant axial orientation of 117°. However, it does possess a marked central bulge concave down loch. At 115 m from its easterly tip it undergoes a northerly rotation to 086° becoming parallel to the north-western margin of the Luib protrusion. It also has a smaller amplitude compared with those described previously, with a crestal relief between 0.9 m and 3.6 m. It also exhibits an asymmetrical cross-section with steep south-westerly facing slopes having an average true ∂

range of 0° - 22°. On the north-easterly facing slopes gentler gradients occur which vary from 5° in the east to 12° in the west.

A number of point reflectors are again associated with this ridge, with heights ranging from 0.3 m to 1.8 m. Their distribution is, however, limited to the crestal region of the ridge. Equally, an encompassing "dark" to "very dark" tonal zone has much smaller dimensions (maximum total width of 63.5 m) than those described for AR17. This zone does possess a marked asymmetrical configuration, having an average width of 5.5 m adjacent to the south-westerly slopes compared with an average of 31.5 m for those to the north-east. The distinguishing feature of this complex is the presence of a bifurcating elongate linear hollow, that is orientated parallel to the central section of the south-western margin (See Figure 5.22.). This hollow has an average width of 32 m, an axial length of 187.5 m and a north-easterly gradient of 5°. The hollow widens to 90 m at the base of the Luib protrusion, its shape suggesting that it originates from the north-westerly facing foreslope of this protrusion, albeit no direct image is recorded from it. Comparison with the bathymetric chart (See Chart 4.3.2.) shows that this hollow has a good correlation with a large embayment identified at this part of the protrusions slope.

A further ten positive linear targets and six point target clusters (BC1-BC5 and BC9) are identified within the Axial Region of Loch Ainort. It is possible to subdivide the linear targets into two broad morphological groups; the first consists of five prominent ridges (AR4, AR8, AR9, AR12 and AR21) while the second represents four weaker, more disparate, features (AR1, AR2, AR7 and AR10). Ridges AR4, AR8, AR9 and AR12 are located to the south-west of the major AR14 ridge and run parallel to it (117°) having crestal orientations of 115°, 087°, 100° and 107° respectively.

AR12 [156150 828540] is located 180 m south-west of AR14 (between Fixes 1.4 [156220 828480] and 3.4 [156180 828660]). It is a thin, continuous, linear feature with a height of 0.2 m and a total length of 122 m. LTCZ calculations suggests that this is effectively a symmetrical feature with very gentle slope angles, 2° to the south-west compared to a north-easterly dip with a true ∂ range of 0° - 4°. This feature also acts as the sharp south-western boundary of a "very dark" zone which is bounded to the north-west by the

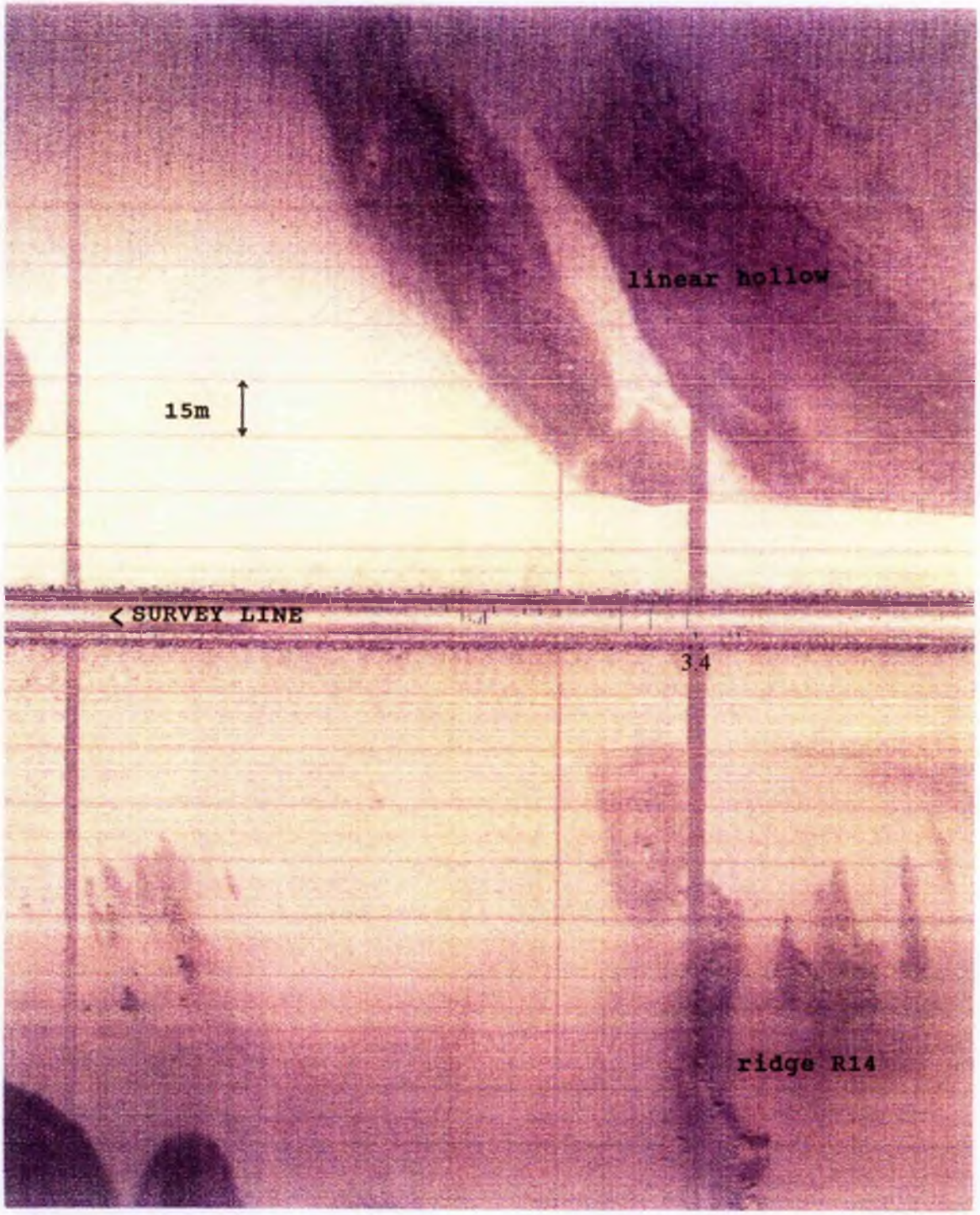

Figure 5.22. Sonograph showing AR14 and associated linear hollow (Fix 3.4).

hollow described previously. The configuration of this "dark" zone and associated shadows suggests that this represents a material variation rather than a topographical change.

Between AR12 and the next ridge (AR9) to the south-west is found a small point reflector cluster, BC2 [156070 828480]. This cluster is has an orientation of 158°, a triangular form with a total length of 65 m and a maximum width of 50 m at its north-western margin. The cluster contains 35 individual point targets with heights which range between 0.04 m and 0.06 m. This cluster is not associated with any obvious reflector-shadow couplet, but does lie in a "medium/dark" tonal area (compared to a surrounding "medium" tonal zone with uniform texture).

AR9 [156000 828470] is located a further 170 m to the south-west of AR12, midway between fixes 3.3 [155570 828210] and 3.4 [156180 828660], making an acute angle with this traverse line. It is the largest of the remaining ridges to be described in this region with an axial length of 230 m and an amplitude which varies between 0.2 m and 4.4 m. The ridge bifurcates 65 m from its south-eastern tip with the south-western branch becoming the dominant limb. The main limb has an asymmetrical profile with steep south-westerly slopes with angles varying between 8° and 27° and gently inclined north-eastern slopes, with a more uniform slope angle between 5° and 8°. This asymmetry is continued in the minor limb with gentle (true ∂ range 0° - 8°) north-eastern slopes and steeper (12°) south-western facing slopes. However, axial heights are lower on this limb reaching a maximum of 0.75 m. Associated with this ridge are a large number of point targets (heights between 0.1 m and 0.2 m), the majority of which are concentrated on the crest (44), but a significant number of targets are present on both the north-eastern (25) and south-western (18) slopes.

AR8 [155800 828300] is located 260 m south-west of AR9 at an acute angle to fixes 1.3 [155940 828330], 3.3 [155570 828210] and 5.7 [155890 828290]. This is a prominent feature identified on all three traverses as a linear positive target, 175 m long, with a maximum relief of 3 m. It has a symmetrical profile unlike those features described previously, the northerly and southerly limbs dipping at 11° and 12° respectively. The ridge is encompassed by a large "very dark" zone which has an asymmetrical distribution offset to the north-east (See Figure 5.21. Overlay 1). This zone extends 150 m in this north-easterly

direction attaining a maximum width of 105 m, whilst to the south it is limited to 20 m. Point targets are restricted to the crestal region of this ridge and a single cluster (BC1: [155900 828310]) within the "very dark" zone. BC1 contains a total of 43 point reflectors with an average size of 0.17 m. This point reflector cluster has an axial orientation of 122° and a width of 40 m at its south-eastern margin which thins to 10 m, 105 m to the north-west.

AR4 [155500 828160] is a relatively weak feature which is identified only on Traverse 1 (between fixes 1.2 [155330 827920] and 1.3 [155940 828330]) despite being in range of both Traverses 2 and 3. It is similar to AR12 having a straight, 100 m linear form, with a relief of 0.7 m and an orientation equivalent to that of AR12 (115° compared to 107°). Slope angles are again small, but exhibit an asymmetrical relationship; the steeper slopes being to the north-east (true ∂ range of 0° -15°) while the south-westerly slopes dip more gently (6°).

AR21 [156500 829130], the final ridge in this group, is located 220 m to the north-east of AR17 (between fixes 3.6 [156500 828900] and 3.7 [156620 829180]). However, it does share many of the characteristics of the ridges located in the inner loch area of the "Axial Region". This ridge has an axial length of 140 m, a maximum relief of 1.5 m and an asymmetrical profile. The steepest slopes are inclined 19° to the south-east, whilst the slopes of the north-western margin have a true ∂ range of 0° - 15°. This ridge presents a strong image in the outer portion of the sonograph where it lies within a "dark" zone. However, there is an easterly gradational decrease in both tonal intensity of the surrounding materials and the clarity of the ridge such that the target is lost. The easterly margin of the ridge is therefore inferred from the presence of point reflectors which are abundant along the ridge axis. In addition, an adjacent point reflector cluster (BC9 [156590 829150]) is identified. This feature is 80 m long, 25 m wide and contains 19 individual targets ranging in height from 0.4 m to 0.8 m. This cluster may represent a further low relief extension of AR21 but, if this were the case, it would require a 37° axial rotation of the ridge to the north. In the absence of further information at this stage, it is suggested that these two features should be considered separately.

Many of the ridges and point reflector clusters described in the central portion of the "Axial Region" (AR8, AR9, AR12, AR14, BC1 and BC2) appear to be restricted in their easterly

extent by the topographic high prograding into Luib bay. The second group of ridges is located in the innermost part of the "Axial Region", to the south-west of the Luib protrusion. They are all weakly reproduced on the sonographs and, as such, little information has been gleaned about them. AR1 [154900 827700] does have an identifiable shadow zone enabling the calculation of a crestal relief of 7.6 m and a steep (25°) north-easterly slope compared to a more gently sloping (true ∂ range 0° - 15.5°) south-westerly slope. This ridge has an axial orientation of 173° and an axial length of 58 m. AR2 ([154990 827800] between fixes 1.1 [154940 827600] and 1.2 [155330 827920]) has a crestal orientation of 020°, an axial length of 75 m but an indistinct shadow zone so no slope or height calculations can be made with any degree of accuracy. There is no associated "dark/very dark" zone, the feature occurring within an area of uniform medium tonal backscatter.

AR7 [155510 828280] (between fixes 2.12 [155580 828500] and 2.13 [155410 828320]) has a similar orientation to AR2 (018°), but is shorter with an axial length of 55 m and a maximum crestal relief of 2 m. It has an asymmetrical profile with steep (21°) north-westerly slopes compared to the more gentle south-easterly slopes, which have a true ∂ range of 0° - 17°. The ridge is located in the south-western corner of a large (150 m x 100 m) "very dark" patch (See Figure 5.21. Overlay 1) which contrasts strongly to the "light" to "medium/light" tonal coloration of the majority of the sonographs from these deeper waters (greater than 25 m).

Finally, AR10 [155780 828540] is located opposite the Luib protrusion and towards the north-west margin of the "Axial Region" (between fixes 2.11 [155860 828760] and 2.12 [155580 828500]). This positive target has a crestal orientation of 090°, an axial length of 25 m and a maximum relief of 4.7 m. The ridge has an asymmetrical profile, with the northerly slopes inclined at 37° to the north, whilst the southerly slopes have a true ∂ range of 0° - 20°. As with AR7 this ridge is located towards the south-west margin of a well defined "very dark" patch. This patch is, however, a more linear feature (165 m x 70 m) than that associated with AR7. There are no individual point reflectors associated with any of these ridges, yet this is not necessarily an indication of the absence of such point reflectors as the strong tonal coloration of the surrounding material may mask their presence.

5.3.4. THE MOUTH REGION.

The area has been comprehensively covered by the intersection of Traverses 1, 2, 3 and 4. From the 1:10560 isometric plot of both positive linear targets, or ridges (See Figure 5.21. and 5.23.) and point target clusters it is evident that this area represents the most topographically complex of the Loch Ainort region. This is further emphasised by the isometric overlay (Same scale) of "dark/very dark" material patches (See Figure 5.21: Overlay 1). A total of 22 individual ridges (AR26 to AR47) are identified within the Mouth Region. The dimensions of these features are correlated on Table 5.4 (See Overleaf), from which it is evident that they represent a sequence of very similar features. In addition to these ridges a total of 12 point target clusters (BC11 to BC22) have been identified. However, of these 12 it is suggested that at least three (BC12, BC15 and BC16) represent repetition of ridge features from two different traverses (Traverses 3 and 4) that do not overlap when plotted.

Ridge No.	*Axial Length (m)*	*Relief (m)*	*Orientation (°)*	*Slope Angles (°)*	
				Proximal	*Distal*
AR26	350	3.8	114	14	0 - 10.7
AR27	95	3.2	120	0 - 30.4	32.4
AR28	100	5.3	159	0 - 37	30.4
AR29	105	2.9	085	15.3	0 - 8.5
AR30	255	2.8	129	0 - 30.8	11.4
AR31	125	1.0	135	0 - 17.7	8.3
AR32	65	0.6	144	0 - 11.4	3.8
AR33	140	5.2	137	26.5	0 - 46.5
AR34	100	1.3	147	11.8	0 - 14.7
AR35	145	-	131	-	-
AR36	170	1.3	138	0 - 27.3	17.1
AR37	180	2.4	144	0 - 36.4	13.1
AR38	350	5.0	170	12	10.8
AR39	190	1.0	152	8.2	11.5
AR40	75	2.5	137	6.9	10.1
AR41	200	1.9	166	0 - 23.3	8.65
AR42	145	9.0	001	9.9	9.2
AR43	75	3.0	142	20.7	0- 31.3
AR44	180	4.0	135	14.6	0 - 20.5
AR45	105	2.1	159	13.4	0 - 8.9
AR46	170	0.4	151	5.6	0 - 24.5
AR47	115	1.9	137	0 - 36.4	9.1

Table 5.4. A summary table of the ridges identified within the "Mouth Region" of the Loch Ainort basin.

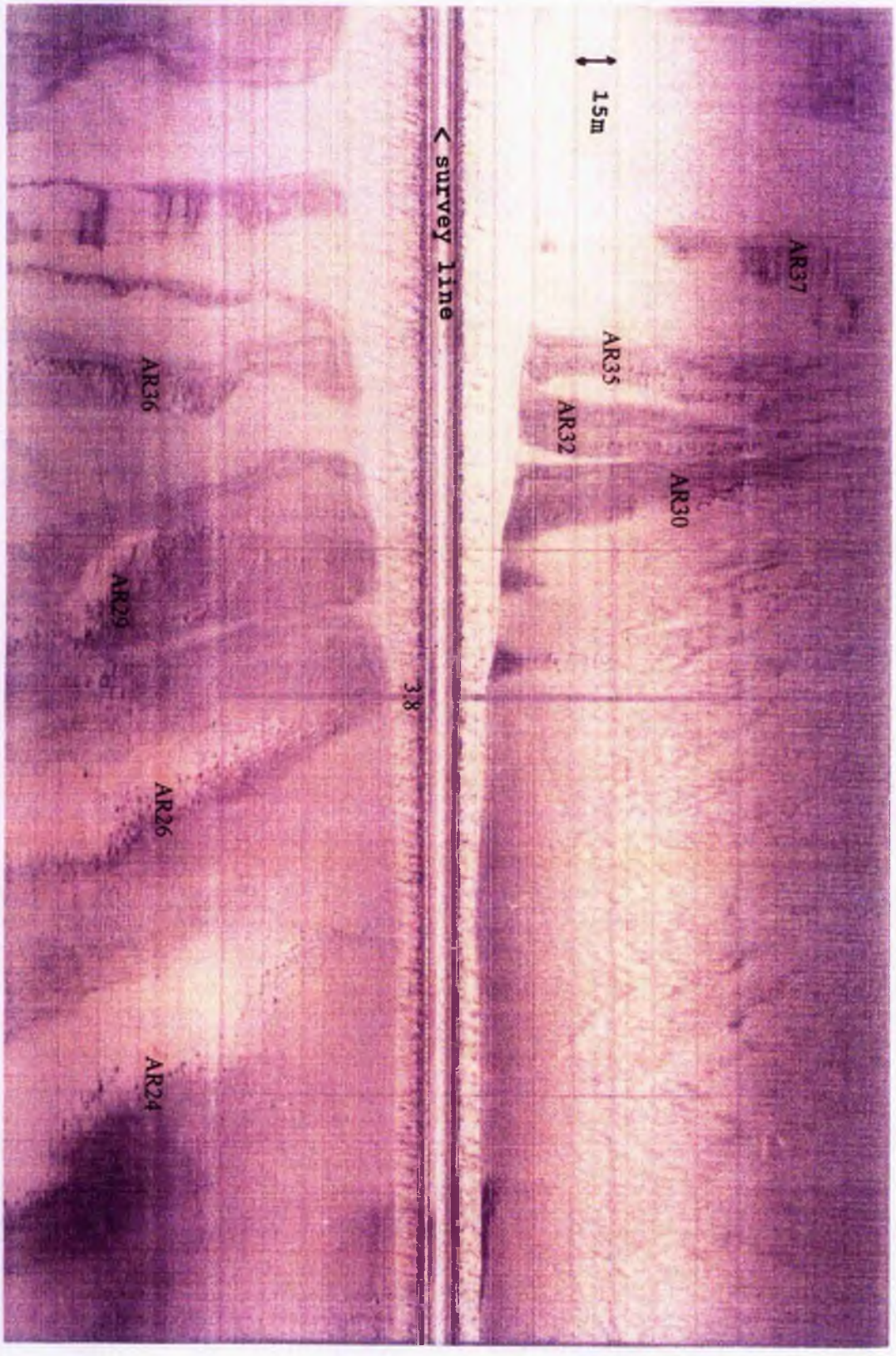

Figure 5.23. Sonograph showing a representative picture of the ridges within the "Mouth Region" (Fix 3.8).

There is an apparent concentration (10 ridges and 5 point reflector clusters in an area of 0.185 km^2) of these targets at the south-eastern margin of the mouth of Loch Ainort, adjacent to Rubh' an Àird Dhuirche. At this locality individual ridge crests have a maximum separation of 65 m. Beyond the confines of the loch, the number of targets per unit area decreases (10 ridges and 6 clusters in an area of 0.315 km^2) and the maximum separation distance of the ridges increases to 160 m. The apparent asymmetrical distribution of these ridges towards the south-eastern half of this area may be an artifact of the sonar coverage in this area. However, as is shown in Figure 5.1b. the actual area not covered by the survey is minimal particularly in between Maol Bàn and Rubh' an Àird Dhuirche; as a result this asymmetrical distribution is considered to be real.

In the north-western sector of the "Mouth Region" only two ridges have been identified from the side scan sonographs AR28 [156770 829650] and AR33 [156800 829800]. These two arcuate (down-loch) ridges have orientations of 137° and 159° and axial lengths of 100 and 140 m respectively. AR28 and AR33 have both steep proximal (true ∂ 0° - 37° and 26.5° respectively) and distal (30.4° and true ∂ 0° - 46.5° respectively) slopes and similar crestal relief's of 5.3 and 5.2 m. The spatial locations of these two ridges do coincide with the prominent bathymetric ridge ABR9a but have markedly smaller dimensions (See Table 5.5). However, the low density of traverse lines for both the Admiralty and the Bathymetric charts for the area (See Figure 5.24.) would suggest that albeit an area of low ground is present around Maol Bàn the ridges AR28 and AR33 are finer features superimposed up on a larger poorly resolved topographical high. Similarly the echosound traverses also fail to adequately cover the region to the south-east so missing the majority of the positive linear targets (AR26 to AR47). These south-eastern group of ridges coincide with the axis and western slopes of the broad, stepped, bathymetric ridge ABR10.

Ridge No.	*Axial Length (m)*	*Relief (m)*	*Orientation (°)*	*Slope Angles (°)*	
				Proximal	*Distal*
AR28	100	5.3	159	0 - 37	30.4
AR33	140	5.2	137	26.5	0 - 46.5
ABR9a	415	32	091/120	13.4	6.2

Table 5.5. Comparative table of bathymetric ridge ABR9a and ridge AR28 and AR33 identified from the side scan sonar sonographs.

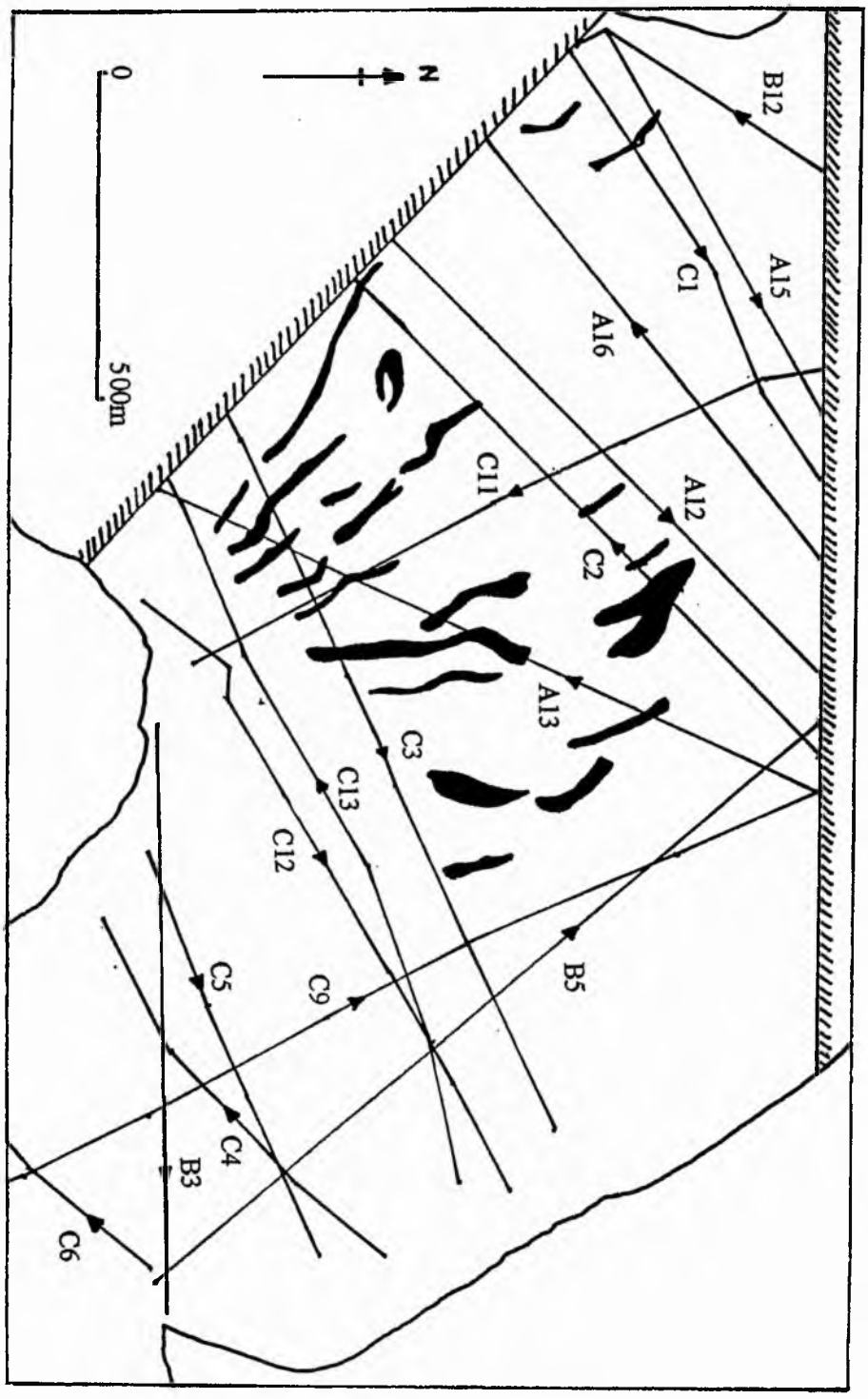

Figure 5.24. Isometric plot showing both the echosounder coverage and the positive linear target distribution in the "Mouth Region" of Loch Ainort.

There is a conspicuous absence of linear targets in the area delimited by fixes 2.4 [157190 829700], 2.5 [156790 829700], 4.6 [156840 829800] and 4.7 [156980 829520], which corresponds closely to the deep, uniform, north-westerly channel identified from bathymetry at this locality. This being one of the only positive correlations between side scan imagery and bathymetry identified in this "Mouth Region".

In association with many of the topographical targets are uniform patches of "very dark/dark" tonal coloration (See Figure 5.21. Overlay 1). The majority of these zones are in the form of a series of thin linear, interconnecting zones which encompass the corresponding linear targets. Such zones may represent localised material variations associated with ridge areas, as has been described for many of the, commonly more extensive, patches from the previous three sections. However, as has been commented on in Section 5.2.3., topographical and material reflectors are capable of producing identical tones making precise identification difficult. It is therefore suggested that the majority of these dark patches are dominantly related to topographical variation, rather than material variation. In the area defined by fixes 2.3, 2.4, 2.5, 4.6 and 4.7 occur a total of 15 of these discrete, uniform, patches. In these cases there appears to be no topographical component.

5.3.5. UNNAMED STRAIT.

The "Unnamed Strait" has not been as extensively covered as the inner loch area due to the large depths (maximum 54 m) encountered. As a result a looped traverse was taken (See Figure 5.1a. and b.), the area being covered by the sonographs of Traverses 3 (between 3.11 and 3.16) and 4 (between 4.1 and 4.5). The central area defined by the loop appeared from bathymetry to have morphological features of interest. However, it was considered that the extreme relief exhibited by these features, (in excess of 25 m) would prevent a wide swathe of the loch floor from being scanned, and therefore it was decided not to survey the area.

The western slopes of Scalpay have a uniform nature with only three identifiable, elongate, positive topographic features (AR48, AR49, and AR50). AR48 [157650 830260] is located 130 m west of fix 3.11 [157780 830230]. This is a thin, linear feature on the easterly facing

wall of a pronounced hollow (between 3.10 [157770 829990] and 3.12 [157750 830840]). The easterly facing slopes of this depression provide a good reflector and as such are represented on the trace as an area of "medium/dark" tones. The ridge has a crestal orientation of 096°, an axial length of 65 m, a maximum relief of 1.6 m and an asymmetrical profile. The steepest slopes are inclined to the south, with a true ∂ range of 0° - 33°, whilst the northern slopes dip at 23°. Five point reflectors are identified, evenly distributed, along the length of the ridge. However, shadow zones were not readily identifiable for any of these targets so heights could not be calculated.

AR49 [157750 830450] is located at the northern margin of this hollow, 65 m to the north-north-east of AR48 (between 3.11 [157780 830230] and 3.12 [157750 830840]). It is a much more prominent feature than AR48, with an axial length of 275 m and a maximum relief of 1.8 m. The ridge has a more subdued asymmetrical profile, but again with the steepest slopes inclined to the south-west at 10°, compared to a dip of 6° for the north-eastern slopes. The ridge has an open arcuate form concave to the south-west, with a tangential crestal orientation of 121° This contrasts markedly with the linear nature of the majority of the ridges described above. Unlike AR48, a large number (75) of point reflectors, ranging in height between 0.3 m and 1 m, are identified on both the slopes and the axial region of this ridge.

The final ridge located on the slopes of Scalpay's western shore is AR50 [157650 830550]. It is located a further 85 m to the north of AR49, between fixes 3.11 [157780 830230] and 3.12 [157750 830840]. The two ridges appear to be separated by a marked depression which extends from a line perpendicular to the south-easterly tip of AR50 for a distance of 55 m to the north-west. This ridge also has a slightly arcuate form (concave to the south-west), with a tangential crestal orientation of 131° and an axial length of 115 m. It has a maximum relief of 1.4 m and a symmetric profile with the slopes inclined to the north-east at 7° with the south-western slopes inclined at a true ∂ range of 0° - 6°. A large number of point reflectors are identified along the axial region of this ridge but, as with AR48, shadow zones are weak to absent so a height range cannot be given.

Spatially AR48, AR49 and AR50 coincides with the upper slopes of ABR12 described from the bathymetric charts. However, neither ridges ABR12 or ABR11 (located 800 m to the south) have any direct representation on the side scan sonographs. Again as the side scan sonar produces an image from a large area of the sea bed where as the bathymetric charts are constructed from interpolation between two-dimensional slices of data, this author suggests greater emphasis should be placed up on the former dataset. The remainder of the gently inclined (1°) slopes of Scalpay, at depths between 0 and 5 m, have a ridge and furrow topography with an average crestal orientation of 053°. These targets have axial lengths of between 17.5 and 21.5 m, average wavelengths of 4.7 m, average amplitudes of 0.35 m and a Ripple Index of 13.4.

As the traverse line turns through 90° at Rubha Reireag to cross the "Unnamed Strait", the bed profile is rapidly lost as the depths exceed 30 m. In addition the tonal coloration exhibits a gradational increase towards the outer margin of the sonograph from "very light" to "medium/dark". In the central part of this run, trending obliquely to fix 3.14 [156880 831200], is an elongate patch of "medium/dark" to "very dark" tonal quality which contrasts markedly with the surrounding light tones. The presence of such a strong reflector at these depths, and the absence of any shadow zone, suggests this represents a marked localised change in material characteristics. This patch measures 340 m by 70 m with a long axis orientation of 079°. It appears to be in close association with positive linear target AR52[7] (See Figure 5.21.: Overlay 1), which has a similar but physically unconnected "very dark" patch adjacent to its south-westerly facing slopes.

AR52 [156750 831330] is a composite feature consisting of two discrete ridges, AR52a [156740 831300] and AR52b [156780 831350], in close proximity (10 m apart). The larger of the two ridges (AR52a) occurs to the east, with a crestal orientation of 122°, an axial length of 95 m and a maximum relief of 1.1 m. It has an asymmetric profile with the north-easterly facing slopes have a true ∂ range of 0° - 23°, compared with an inclination of 15° for the south-western slope. The smaller western ridge, axial length of 30 m and a maximum relief of 0.7 m is orientated at 136°. This feature also has a similar asymmetric

[7] Calculations for AR52 (a and b) made from estimated bottom profile values.

profile with steeper north-easterly facing slopes, of true ∂ range 0° - 20°, compared to a dip of 9° to the south-west.

The slopes of the western margin of the "Unnamed Strait" possess uniform tonal gradation from "dark/medium" colours on the outer margin of the starboard channel to "medium" colours at the outer margin of the port channel. This variation represents the change in the effective angle of incidence of the beam as it travels over the inclined surface (See Section 5.3.2.). No reflector-shadow couplets are identified on the most northerly sonographs of this traverse (between fixes 4.1 and 4.3), apart from a series of large (1.3 m) positive targets clustered in a topographical depression between fixes 4.2 [156570 831100] and 4.3 [156570 830900].

Between fixes 4.3 [156570 830900] and 4.4 [156440 830370], at the mouth of Lùib na Moil, the bottom profile shows evidence of two topographical highs bounding a depression which reaches a maximum depth of 20 m. The northern high has a relief of 3.1 m and an asymmetrical profile with the southern slope inclined at 5° compared to a dip of 2° for the northern slopes. This high is connected to a very thin linear feature (AR51 [156600 830750]) with a crestal orientation of 097°and an axial length of 165 m. However, as this ridge runs almost perpendicular to the traverse line and is encompassed by an area of "dark" tonal coloration, the associated shadow is very weak so **LTCZ** calculations could not be made. This linear feature is identified, particularly in its outer reaches, from a sequence of point reflectors which appear to be intimately associated with the ridge axis. The southern high has a relief of 13.2 m and a broken northerly facing surface with a steeper lower slope (between 20 m and 10 m) inclined at 9° and a upper slope component (between 5 m and 10 m) inclined at 4°. This high is associated with a well defined, arcuate (concave to the north-west) boundary between the northerly area of "dark" tonal colouration associated with AR51 and an area of uniform "medium/light" tones. Also associated with this boundary are a number of point reflectors. These two features have a close correlation with the two arcuate ridges, ABR15 and ABR14 respectively, identified at the mouth of Lùib na Moil from the bathymetric charts (See Section 4.3.1.3.). The "dark" coloration of this area is considered to be a topographical effect caused by the beam travelling directly into the tight "jaws" of these two ridges, which provide an effectively enclosed sequence of sonar facing reflectors. The

thinner and more pronounced axial region of the northern ridge provides sufficient relief for the additional linear reflector, AR51, to be recorded. By contrast, the course taken by the towfish across the southern ridge is at a sufficient angle to record the inner sonar facing slope (including its stepped form) whilst missing the steeper south-easterly facing slope as it travels across the gentle plateau adjacent to Maol Bàn.

The remainder of Traverse 4 in this region (fixes 4.4 [156440 830370] to 4.5 [156680 830010]) continues to exhibit the uniform "medium/light" coloration of the Maol Bàn plateau area on its offshore facing, port-side channel. Within this area there is a restricted (between depths of 4 m and 7 m) development of linear topographic highs with a crestal orientation of 166°. These structures have axial lengths between 18 and 23 m, average wavelengths of 4.5 m, average amplitudes of 0.07 m and a Ripple Index of 59. The nearshore slopes shows the development of a chaotic, point reflector strewn and heavily scoured fan, which extends up to 80 m off the point of Maol Ban. This feature has a similar appearance to the disturbed area off the north-western slopes of Am Meall (See Figure 5.18.).

5.4. CONCLUSION.

From side scan sonographs obtained from Loch Ainort and the surrounding waters both qualitative and quantitative information have been determined using conventional methods of sonar interpretation. The recognition of the presence of Low Tonal Colour Zones and the development of a geometric model accounting for their occurrence has also enabled an additional level of detail to be recorded for the first time. Chapter 5 has been structured to describe the form, dimensions and distribution of reflection patterns identified on the sonographs. Comparisons have been made with features identified from the bathymetric charts and described in Section 4.3.. A palaeo-environmental interpretation of the features described from the sonograph is not attempted, this being left for the analysis of all the datasets in Section 8.2..

The loch is characterised by a series of thin, linear topographical highs or ridges which commonly have point reflector concentrations along their axis and slopes. These ridges are

commonly associated with localised "dark" tonal patches which contrasted markedly to the "medium/light" to "light" tonal coloration that typified the loch floor. Further, frequently in close association to the ridges discrete point reflector (boulder) clusters were identified.

A total of 53 ridges have been identified and documented within the survey area and their dimensions have been surmised in Table 5.6. (See Overleaf)[8]. Twenty-two of these ridges are identified within the "Mouth Region" where they have an asymmetric distribution offset towards the south-east of this geographical zone, the sonar coverage within this area suggests this distribution is real. Within Loch Ainort three major ridge complexes have been identified that traverse a minimum of half the loch's width at each locality. In addition a total of 18 isolate ridges are distributed between the marginal slopes and the deeper parts of the basin. Again there is an apparent asymmetrical distribution which sonar coverage suggests is an actual feature, except for the innermost part of the loch where there has been minimal coverage toward the north-west shore. Finally within the " Unnamed Strait" only 6 ridges were identified from the sonographs this probably being the product of the restriction of the traverse lines to marginal locations and the greater water depths.

In addition to the these topographic highs and their associated "dark" tonal patches, smaller positive topographic features (bedforms) were identified along the shallow margins of the loch again commonly associated with "medium" tones. Along both the north-western and the south-eastern margins of the inner loch shore-parallel benches have been identified being most clearly developed on both shores north-east of Luib. These benches are disrupted on the south-eastern shore by the large protruding topographical high at the mouth of Luib bay. The lochward facing slopes of this feature are clearly identified and on the north-eastern margin a detailed arcuate fan structure has been identified.

Basic spatial correlation between topographic features identified from the side scan sonographs and those determined from the bathymetric charts (See Section 4.2.) can be made. However, where detailed comparisons of the two datasets have been made, major discrepancies, particularly in their dimensions, are common.

[8] Table 5.6. (Overleaf) Summary Table correlating the dimensions of the ridges identified from the side scan sonographs interpreted for the Loch Ainort basin.

Ridge No.	*Axial Length (m)*	*Relief (m)*	*Orientation (°)*	*Slope Angles (°)*	
				Proximal	*Distal*
AR1	58	7.6	173	0 - 15.5	25
AR2	75	-	020	-	-
AR3	150	9	079/160	-	-
AR4	100	0.7	115	6	0 - 15
AR5	53	0.5	027	0 - 24	2
AR6	285	0.4 - 2	054	-	11
AR7	55	2	018	0 - 17	21
AR8	175	3	087	11	12
AR9	230	0.2 - 4.4	100	8/27	5/8
AR10	27	4.7	090	0 - 20	37
AR11	42	0.8	011	2.8	0 - 31
AR12	122	0.2	107	2	0 - 4
AR13	75	-	068	-	-
AR14	470	0.9 - 3.6	117	0 - 22	5/12
AR15	65	3	165	0 - 34	21
AR16	64	1.1	125	19	0 - 47
AR17	320	1 - 12	091	8	2
AR18	90	12	108	8	4
AR19	35	5	030	17	0 - 15
AR20	90	-	090	-	-
AR21	140	1.5	099	19	0 - 15
AR22	255	1 - 1.4	015	0 - 16	12
AR23	35	1.2	066	0 - 39	13
AR24	405	2.1 - 5.4	096	13	6
AR25	40	1.1	023	0 - 17	8
AR26	350	3.8	114	14	0 - 10.7
AR27	95	3.2	120	0 - 30.4	32.4
AR28	100	5.3	159	0 - 37	30.4
AR29	105	2.9	085	15.3	0 - 8.5
AR30	255	2.8	129	0 - 30.8	11.4
AR31	125	1.0	135	0 - 17.7	8.3
AR32	65	0.6	144	0 - 11.4	3.8
AR33	140	5.2	137	26.5	0 - 46.5
AR34	100	1.3	147	11.8	0 - 14.7
AR35	145	-	131	-	-
AR36	170	1.3	138	0 - 27.3	17.1
AR37	180	2.4	144	0 - 36.4	13.1
AR38	350	5.0	170	12	10.8
AR39	190	1.0	152	8.2	11.5
AR40	75	2.5	137	6.9	10.1
AR41	200	1.9	166	0 - 23.3	8.65
AR42	145	9.0	001	9.9	9.2
AR43	75	3.0	142	20.7	0- 31.3
AR44	180	4.0	124/147	14.6	0 - 20.5
AR45	105	2.1	159	13.4	0 - 8.9
AR46	170	0.4	151	5.6	0 - 24.5
AR47	115	1.9	137	0 - 36.4	9.1
AR48	65	1.6	096	0 - 33	23
AR49	275	1.8	121	10	6
AR50	115	1.4	131	0 - 6	7
AR51	165	-	097	-	-
AR52a	95	1.1	122	15	0-23
AR52b	30	0.7	136	9	0 - 20

CHAPTER 6

6. SUB-BOTTOM PROFILING

6.1. INTRODUCTION

Chapters 4 and 5 have discussed the type of geophysical data that can be obtained from high resolution, low penetration (*ie.* high frequency) seismic reflection equipment. Such methodologies have the potential to provide accurate and detailed information, in both a numerical and descriptive format, on the morphological, and in the case of the side scan sonar, material variations of the loch bed. However, the equipment used for these surveys gave no information on the type of unconsolidated or consolidated lithologies present beneath the loch bed. In order to effectively provide a fourth dimensional data set, "time" (*ie.* depth and type of sediment), sub-bottom profile data is required. As discussed in Sections 2.3.3. and 2.3.3.3., the sediment-water interface can be penetrated by a lower frequency acoustic pulse. Reflections, at depth, from interfaces with lower acoustic impedance contrasts can be detected and output as a simple analogue, sepia, trace. A variety of techniques are potentially available for sub-bottom data acquisition (Boomer, Sparker, Air guns, *etc.*) but for the purposes of this project a 3.5 kHz "Pinger" was chosen to provide maximum resolution from the top thirty metres of the loch bed.

As has been described in Section 1.2.1. seismic reflection profiles can be described and interpreted by seismo-stratigraphic analysis (See Section 6.2.), in order to produce a seismic para-stratigraphy for the survey area. The nomenclature used for describing the characteristics of seismic reflection profiles is based on conventional litho-stratigraphic terminology. However, it must be reiterated that reflections from materials of differing impedance contrasts need not necessarily correspond with lithological boundaries (See Section 2.3.3.3.). Consequently, Chapter 6 does not provide an environmental interpretation based on the seismic para-stratigraphy alone, this process is left for Chapter 8 where the seismic para-stratigraphy, the terrestrial data, the bathymetric and side scan data and the litho-stratigraphy can be correlated to provide a coherent environmental model.

6.2. SEISMO-STRATIGRAPHIC ANALYSIS

Having established in Section 1.2.1. that a nomenclature for seismo-stratigraphic analysis exists, albeit not universally adhered to, it is necessary to discuss the criteria by which individual and groups of reflectors are described. As described in the preliminary historical discussion the technique of seismo-stratigraphic analysis consists of three distinct phases:

i) Seismic sequence analysis (See Section 6.2.3.), whereby the record is subdivided into the largest scale units of each trace or "seismic sequences";

ii) Seismic facies analysis (See Section 6.2.4.), which sub-divides each seismic sequence into genetically related reflectors or "seismic facies units";

Phases *i*) and *ii*) are used to construct a seismic para-stratigraphy, defined as a series of units "... identified by objective criteria which reflect some aspect of lithology, in this case seismic signature which reflects acoustic properties." (Boulton *et al.*, 1981). This in turn is used for phase:

iii) For conventional, deep seismic, seismo-stratigraphic analysis, as originally proposed by Mitchum and Vail (1977), this phase represents the interpretation of the seismic para-stratigraphy by sea level analysis. When applied to high resolution profiles, seismo-stratigraphic analysis has been adapted so this phase now provides a genetic litho-stratigraphic interpretation that has a wider environmental applicability. In this study this is represented by the correlation of the developed seismic para-stratigraphy with the litho-stratigraphy (constructed from the analysis of samples taken from within the field area and, where available, data acquired from terrestrial mapping of both the solid and drift geology: See Chapters 7 and 3 respectively) to create a constrained palaeo-environmental model (See Section 8.2.).

6.2.1. PROFILE DESCRIPTION

A typical, annotated, sepia pinger profile produced by the wet paper GIFFT recorder (See Section 2.3.3.3.) is presented in Figure 6.1.. A gradated vertical scale represents the two-way travel time of the reflected pulses. The system was configured such that each trace represented a vertical two-way travel time of 125 ms (Lines A1-A16 and B1-B14) or 100 ms (Lines C1-C13) with the individual divisions representing a two-way interval of 8.33 ms and 6.67 ms respectively. The dimensions quoted in this Chapter are measured directly from this, two-way travel time (TWT), millisecond scale, conversion to depth in metres being calculated and discussed following the correlation of the seismo- and litho-stratigraphies in Section 8.2. and 8.3.. The exception to this is the conversion of bed profile dimensions to a metric scale as a velocity value of 1500 ms^{-1} is assumed.

The horizontal scale of the traces can be calculated from the perpendicular solid lines that represent the end-points for each line (or intermediate localities where appropriate). As the pinger was run simultaneously with the echosounder the positional accuracy and relevance of the surveys follows the same arguments as those discussed in Sections 2.3.2. and 4.2.. To summarise the positional data, in Loch Ainort navigational control was provided by Traversing (See Section 2.3.2.1.) for lines A1-A16 and B1-B14, and by the Magellan© GPS receiver (See Section 2.3.2.2.) for lines C1-C13 (See Figure 6.2.).

The pinger profile represents true depth from water surface to reflector, with the most prominent reflector on the trace being represented by the bottom profile. This boundary is clearly defined due to it having a high reflection coefficient R = 0.474 (Assuming $Z_{sea\ water}$ = 15.15×10^5 kgm^4s^{-1} and $Z_{sediments}$ = 42.5×10^5 kgm^4s^{-1}; See ***Equation 2.5)***, Section 2.3.3.). The presence or absence of further reflectors at depth beneath the loch bed is controlled by the degree of impedance contrast between adjacent materials.

To avoid the deterioration in quality of the individual traces they were stored, at room temperature and in permanent darkness. Detailed overlays were constructed from the original seismic profiles in order to preserve the original traces and to facilitate the interpretation of the lateral and vertical variability of "seismic sequences" and "seismic facies units".

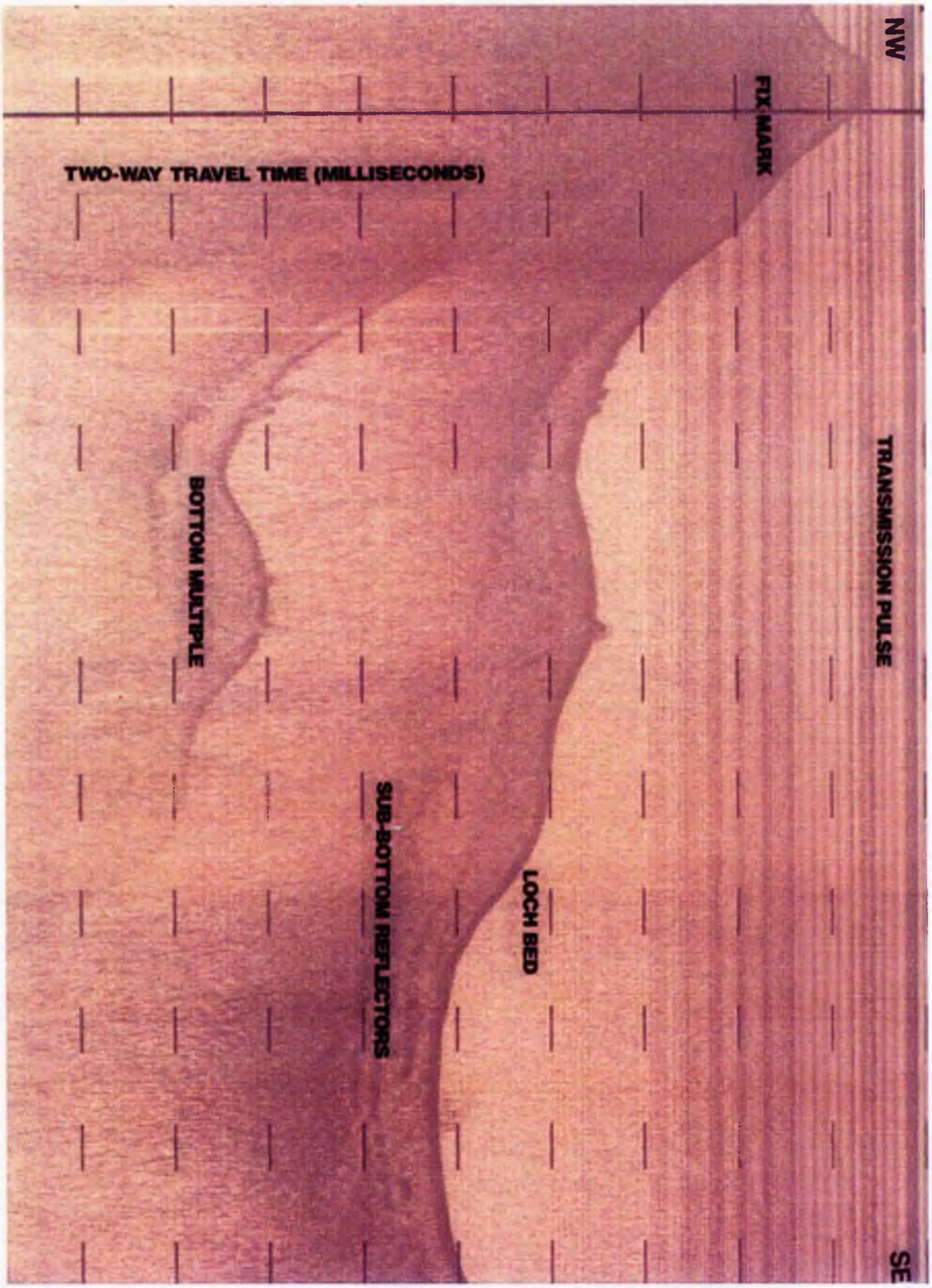

Figure 6.1. A typical sepia pinger profile produced by the wet paper GIFFT recorder, annotated to show principle features (Survey Line A10).

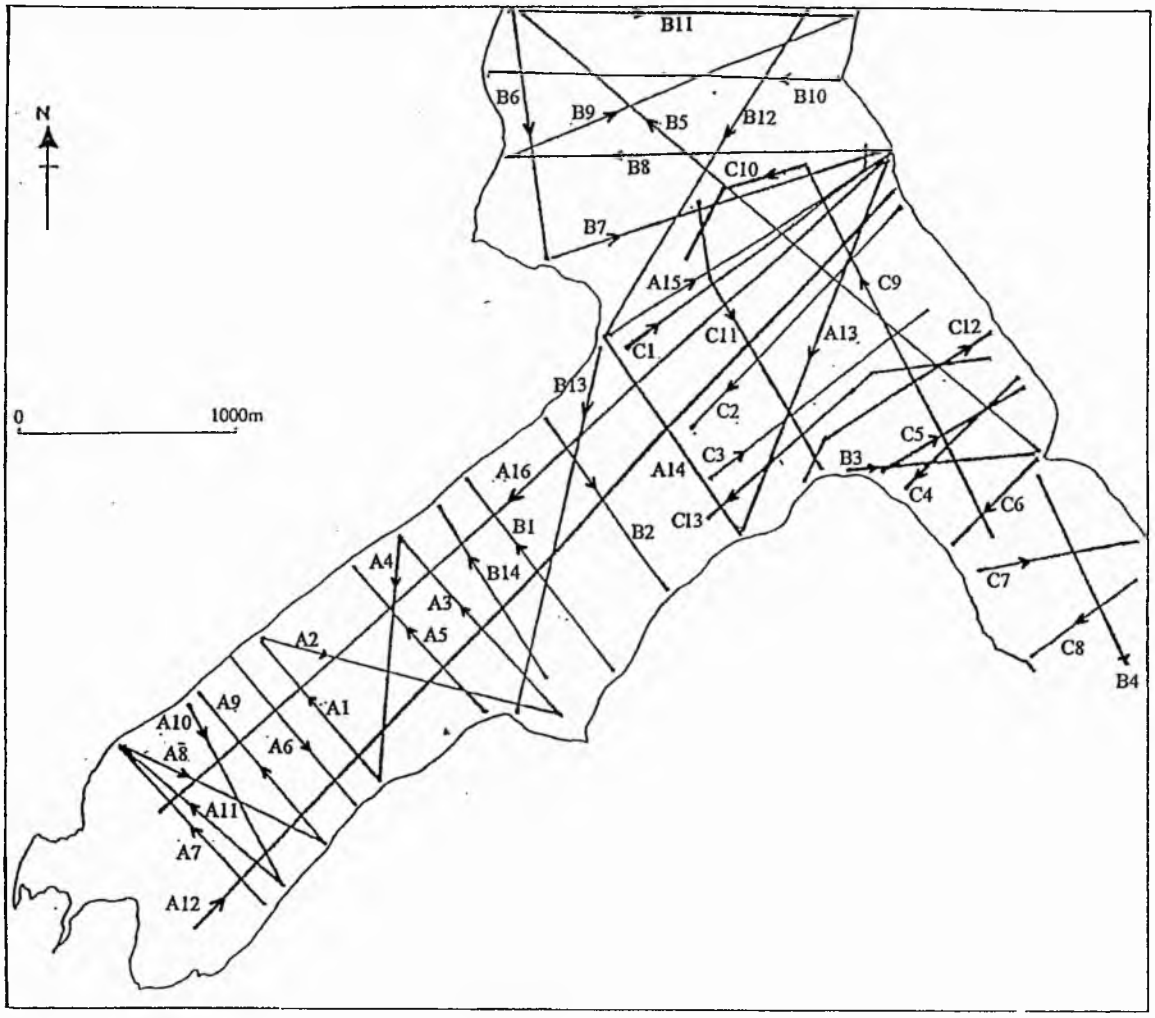

Figure 6.2. Diagram showing sub-bottom profile coverage in the Loch Ainort field area.

6.2.2. DISTORTION AND INTERFERENCE

As with the majority of geophysical techniques and particular those where it is not possible to post-process the returning acoustic signal, distortion and interference of the acoustic record is common. There are numerous distortion and interference effects that may obscure the true material reflections that the geophysicist is attempting to identify. However, this Section deals purely with those features that have been encountered during the analysis of the Loch Ainort records.

The single most important distortion effect on the, two-dimensional, sub-bottom profiles is along-track compression. As discussed in Section 5.2.4. this is the result of the vessel's speed and is exhibited in the trace in the form of shortening of the individual reflectors and steepening of their angle of inclination. Equally, if vessel speeds are excessive they will cause a reduction of the horizontal resolution of the system, as they will limit the number of pulses that can strike an individual object each second (See Discussion in Section 2.3.3.1.). As with the side scan sonar surveys a vessel speed of 3.5 knots (1.75 ms^{-1}) was retained throughout. Assuming the survey speed to be constant and by reference to the fixed navigation points, the along-track compression effect can be removed by simple proportional calculations. This is particularly important when considering the true geometry of internal reflectors present.

One of the commonest interference effects encountered in traces recorded in shallow waters (operational depths of < 50 m) are bottom, long-path, multiples. These occur where the returning signal is reflected back to the sea bed to repeat the original travel path (See Figure 6.3.). Consequently an "event" is recorded at precisely double the two-way travel time of the original reflection. This manifests itself as an identical image of the original reflecting surface but at twice the depth of the original. However, it is this regular geometric relationship of the two surfaces that enables the identification and dismissal of the multiple reflector surface. For the majority of the traces recorded in the shallow waters of Loch Ainort, a multiple reflection from the high impedance contrast boundary of the bottom profile is common. Bottom multiples should not be automatically discarded, as they can, on occasion, provide additional information on the presence or absence of internal reflectors. In localities where the profiles have a strong acoustic texture (See Section 6.2.3.) internal reflectors can be obscured. The corresponding bottom multiples of such a profile frequently

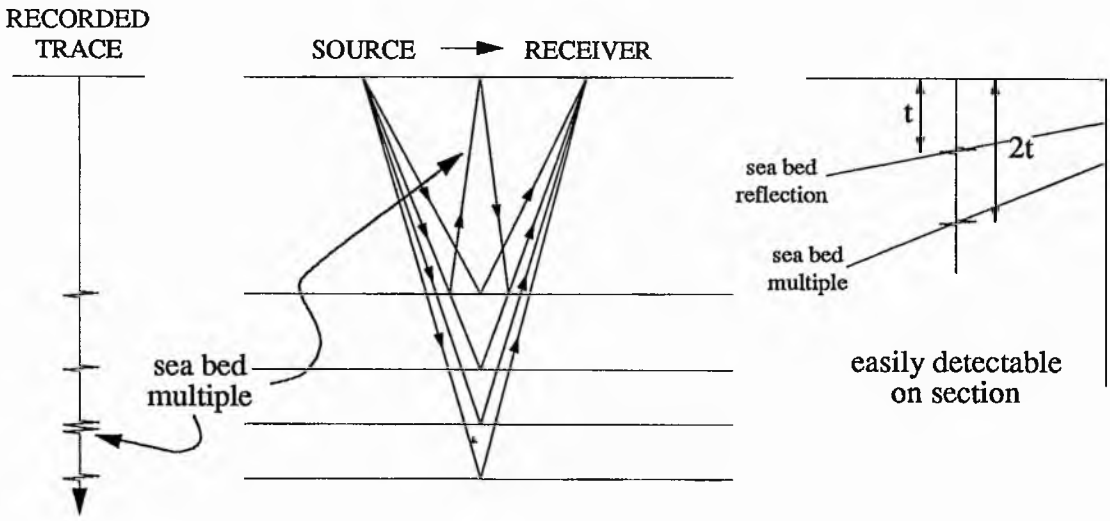

Figure 6.3. A sketch diagram showing the presence of a long-path "bottom" multiple

lose the pervasive texture of the material to reveal the presence of internal boundaries (See Section 6.3.1.).

In a similar manner to long-path multiples, short-path multiples (or "ghosts") are also frequently encountered in high-resolution shallow seismic reflection surveys. These occur where a signal is reflected from the sea-surface prior to following a normal path to the loch bed (See Figure 6.4.). These "ghost" images again mirror the loch bed topography but are located at a depth beneath the bed equal to twice the distance of the acoustic source beneath the water surface. Again it is this regular geometric relationship between the bed reflector and the "ghost" that enables the identification and dismissal of this multiple image. During this survey the shallow towing depth (0.75 m) and the constrained transmission pulse resulted in only minor interference by this type of multiple image.

As the two-pot pinger transducers were deployed from a fixed transom mount (See Section 2.3.3.3.) they were susceptible to oscillation caused by any exaggerated boat movement. Where present this movement results in the distortion of the seismic trace it can frequently be misinterpreted as topographic variation of the loch bed. However, boat movement affects the entire trace at any one point rather than the loch bed reflector alone. Consequently, due to its presence throughout the swept section, this form of distortion can be readily identified and discounted.

Finally, acoustic interference similar to that described for the side scan sonar surveys (See Section 5.2.5.) is also present in a number of the seismic profiles. In particular, "sea clutter" and electronic interference from the high frequency echosounder was identified but as described in Section 5.2.5. their form enables them to be easily discounted.

6.2.3. SEISMIC SEQUENCE ANALYSIS

The first stage in seismo-stratigraphic analysis requires the identification of the basic unit or "seismic sequence", which is defined by Mitchum *et al.* (1977) as "...a stratigraphic [*sic*] unit composed of a relatively conformable succession of genetically

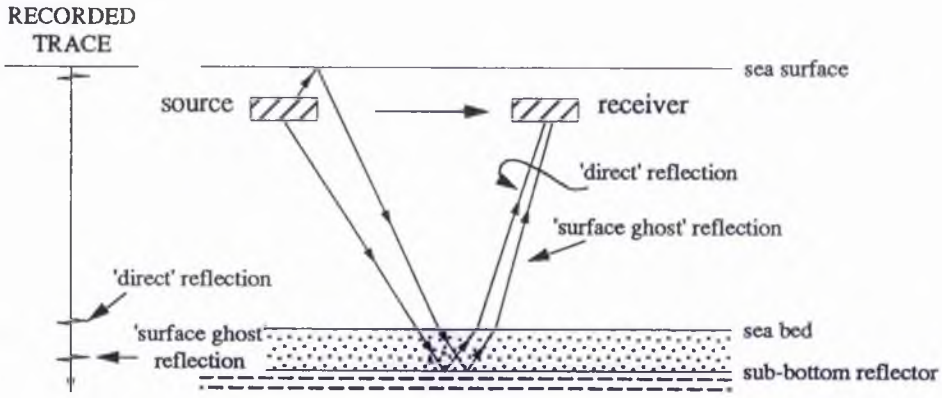

Figure 6.4. A sketch diagram showing the generation of a short-path "ghost" multiple

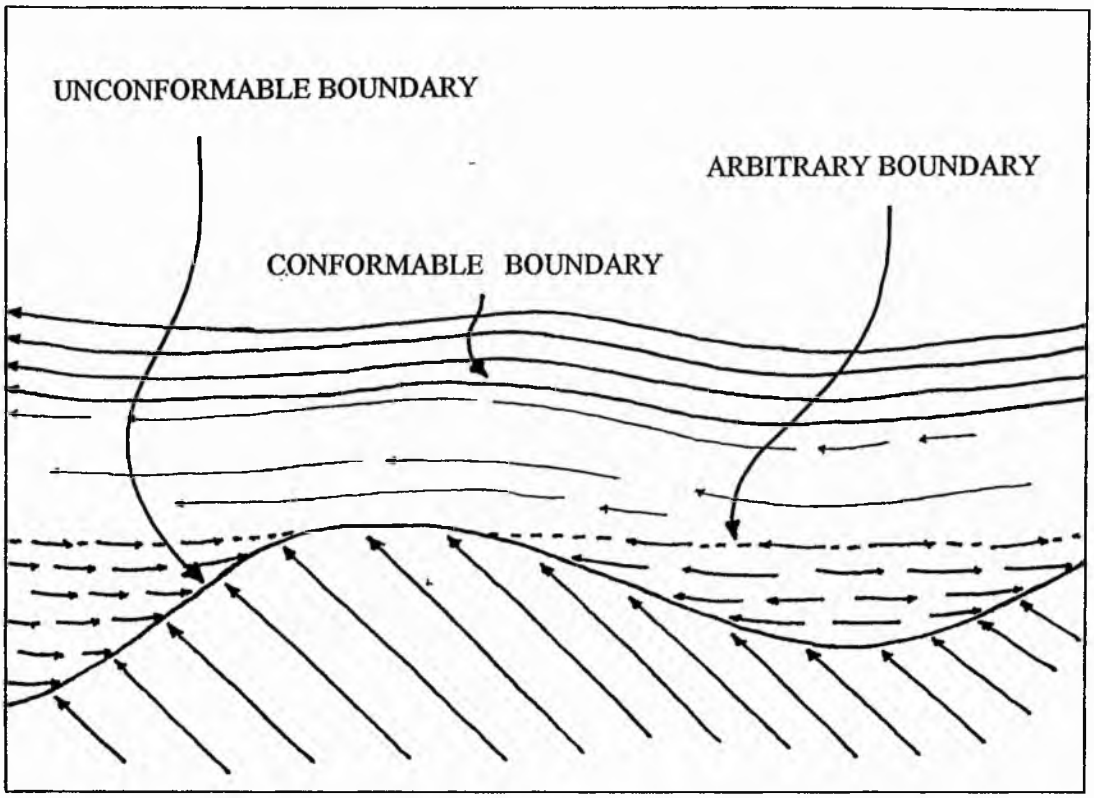

Figure 6.5. A sketch diagram showing the nature of unconformable, conformable and arbitrary sequence boundaries.

related strata [*sic*] and bounded at its top and base by unconformities or their correlative conformities". These seismic sequences can range in thickness from millimetres to thousands of metres, however, they are most commonly in the range of 10-100 m. Where a conformable boundary is present the reflectors represented by each sequence are limited by the age of the upper and lower boundaries. Where a seismic sequence boundary is unconformable the entire unit cannot necessarily be dated at any one locality. On an individual basis, however, both single reflectors and unconformable boundaries represent chrono-stratigraphic surfaces. This relationship is described by Bally (1987) as being "...perhaps the most fundamental assumption of the seismic stratigraphic method...", such that "...a seismic reflector in most cases, and for all practical purposes, is a time line.".

This procedure creates a framework based solely on an objective criterion, the physical relations of reflection termination patterns (*ie.* the acoustic representations of unconformities, disconformities and conformities). For seismic sequence analysis Ravenne (1978) identified three principal types of the external boundaries that can be used to define a seismic sequence (See Figure 6.5.):

i) The termination of a series of seismic reflections against a common reflector (an angular unconformity).

ii) The presence of a conformable reflection that bounds a particular configuration .

iii) An arbitrary boundary within the sequence when seismic parameters change gradually.

The identification of Type *i*) truncational unconformities can be further subdivided on the basis of the geometric relationship between the sequence boundary and the internal reflectors (See Table 6.1. Overleaf and Figure 6.6.):

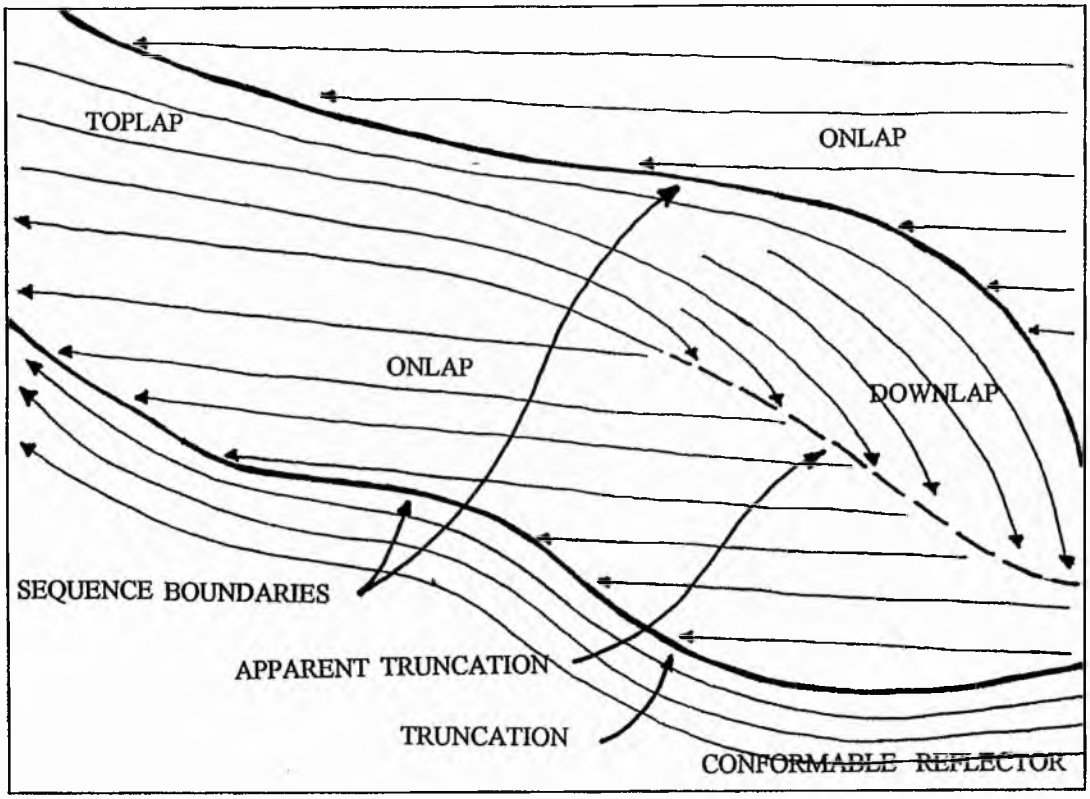

Figure 6.6. A sketch diagram showing the variety of unconformable reflector contacts.

Nomenclature		*Description*
Toplap		Reflectors terminate up dip by lapout and approach the upper boundary asymptotically.
Baselap	Onlap	Initially horizontal reflector laps out against an initially inclined surface or where an initially inclined stratum laps out up dip against a surface of greater initial inclination.
	Downlap	Initially inclined reflector terminates down dip against an initially horizontal or inclined surface.

Table 6.1.: Nomenclature and descriptions for the geometric relationship between internal reflectors and bounding surfaces (After Bally, 1987).

Differing reflection termination's at seismic sequence boundaries allow inferences to be made about the mechanism of boundary formation, assuming lithological correlation has been made and the seismic para-stratigraphy coincides with the constructed litho-stratigraphy. Truncational unconformities can result from erosion of the upper boundary of a sequence or by structural disruption through processes including faulting and gravity sliding. Conformable seismo-stratigraphic sequence boundaries may imply the separation of older strata from younger strata, but without a hiatus due to erosion or non-deposition.

In addition to describing the relationship between the internal reflectors and the bounding surface, to maximise analysis and interpretation it is essential to record in detail the boundary form. In particular it is necessary to describe the morphology of the bounding reflector and the strength of its reflection *ie.* the degree of acoustic impedance contrast it represents. Such descriptions become critical if *in situ* calibration data is not available and inferences from terrestrial mapping is required to aid interpretation.

6.2.4. SEISMIC FACIES ANALYSIS

Having established the method of delimiting the basic building blocks of seismo-stratigraphic analysis, seismic sequences, a detailed description of the lateral and vertical

variability of the internal reflectors must be provided. This is achieved by seismic facies analysis, the aim of which is "...to determine objectively all the variation of seismic parameters within an individual seismic sequence" (Vail, 1987). Thus seismic facies units have been defined as "...mappable, three dimensional units composed of groups of reflections whose parameters differ from those of adjacent facies units." (Mitchum *et al.*, 1977). A summary of the different parameters used to identify and describe seismic facies units are presented in Table 6.2..

Seismic Facies Identification Criteria
Internal backscatter
Geometry of internal reflectors
Frequency of internal reflectors
Lateral extent of internal reflectors
Continuity of internal reflectors
Dimensions (milliseconds)
Reflection amplitude
Parallelism
Presence or absence of point hyperbolae
External form and spatial association

Table 6.2. Seismic facies identification criteria.

Internal backscatter describes the pervasive acoustic texture of individual facies and is based on the same principle as that described for the backscatter terms used in the analysis of side scan sonographs (See Section 5.2.2.). Again the tonal levels of internal backscatter represent a relative scale that is constructed for each individual survey rather than a universal classification.

Where present the geometry of internal reflectors can be described by a variety of different terms that are summarised in Table 6.3. (See Overleaf). As part of the theory of seismo-stratigraphic analysis, developed by Mitchum *et al.* (1977), a series of standard "stratal configuration" terms was defined. The problem with these terms is that they are intimately associated with a pre-conceived mode of formation and in particular large scale

shelf processes driven by sea-level fluctuations. Therefore, for the analysis of high-resolution seismic profiles, this author has retained the majority of the descriptive terms used by Mitchum *et al.* (op. cit.) but has dispensed with the interpretational statements. Where the descriptive nomenclature has been deemed lacking additional terms have been suggested (See Table 6.3. Overleaf).

Following the identification criteria set out in Table 6.2 (Overleaf) it is also important to describe the frequency, lateral extent, continuity and dimensions (in two-way travel time). The reflection amplitude represents the strength of the reflecting surface that is controlled by the acoustic impedance contrast between layers (See Section 2.3.3.). The parallelism of internal reflectors is particularly useful as they provide potentially important environmental indicators if confirmed by lithological calibration. Parallel, sub-parallel and divergent reflectors can frequently be identified, the latter representing reflector morphologies generally associated with wedge shaped facies topography.

Reflections from single targets have a distinctive seismic signature, point hyperbolae (See Figure 6.7.) and are common features in shallow seismic profiles. They are the product of diffraction of the reflected ray, with the two-way reflection times of these diffracted rays to the receiver level defining the hyperbola. If arcs of circles (wavefront segments) are drawn through each reflection event it can be seen that they intersect at the actual point of diffraction. Depending upon the type of transducer or receiver configuration (*ie.* is a towed hydrophone/s deployed), speed of survey vessel and size of the insonification zone either the whole hyperbolae or just its trailing edge is recorded.

Having identified the seismic facies units within each seismic section, using the criteria presented in Table 6.2. it is also necessary to describe their external form (*ie.* the topography of the bounding surfaces), spatial distribution and inter-relationships. This again provides invaluable data for correlating the seismic para-stratigraphy with other geophysical and lithological datasets. For the interpretation of nearshore datasets the spatial distribution of each unit is particular useful for correlating the submerged with the sub-aerial models.

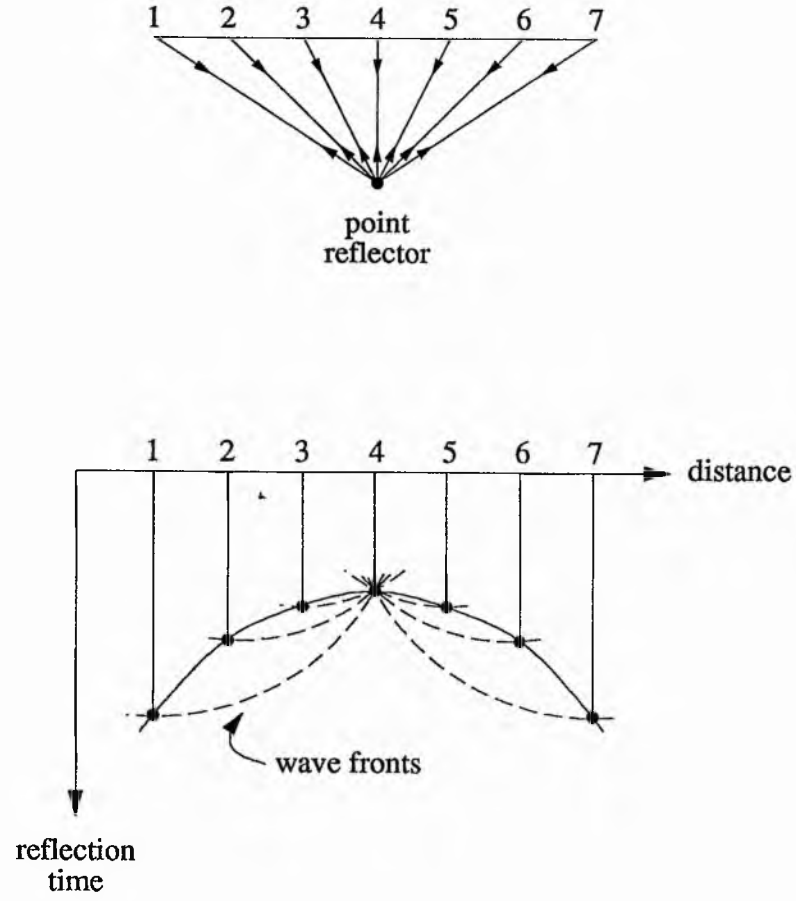

Figure 6.7. A sketch diagram showing the generation of point hyperbolae (After Kearey and Brooks, 1984)

Nomenclature		*Description*
Horizontal		
Inclined		
Prograded clinoforms	**Sigmoid clinoforms**	Laterally accreting S-shaped reflectors; topset strata horizontal/low-angled; foresets form low angle; bottomsets very low angled or horizontal strata.
	Oblique clinoforms: higher angled reflectors than sigmoid with the overall form concave upward and forward.	**Tangential oblique clinoforms:** progressive, tangential decrease in the angle of dip towards lower facies boundary
		Parallel oblique clinoforms high angles of downlap against the lower facies boundary
	Shingled clinoforms	Similar to parallel oblique differ by thinness of entire facies and very gentle angle of parallel reflectors. Termination of reflectors by toplap and downlap at very low angles.
	Hummocky/irregular clinoforms	Complete lack of lateral continuity resulting in disjointed reflection pattern.
Chaotic		Lack internal coherency often associated with individual point hyperbolae
Reflection free/ Transparent/ Acoustic blanking		Either no/very few low amplitude internal reflectors due to a low acoustic impedance contrast.

Table 6.3. Nomenclature for the description of reflection geometry (Adapted from Mitchum *et al.*, 1977).

Having completed phases 1 (Section 6.2.3.) and 2 (Section 6.2.4.) of seismo-stratigraphic interpretation a seismic para-stratigraphy for the surveyed area can be constructed. As described in the introduction to Section 6.2. the correlation of the

seismic para-stratigraphy with the other diverse datasets is discussed in Sections 8.2. and 8.3..

6.3. LOCH AINORT

Seismo-stratigraphic analysis of the 79 km of sub-bottom profiles, acquired from Loch Ainort (See Figure 6.2.), identified ten seismic facies units which could be grouped into four seismic sequences. Section 6.3. describes the nature and distribution of each of these four sequences, and their internal facies units (See Sections 6.3.1. to 6.3.4.), in ascending chrono-stratigraphical order. The complete seismic para-stratigraphy for the Loch Ainort area is presented in Section 6.4.. Where appropriate the relationship between topographic or material features identified from the sub-bottom profiles and those from the Admiralty Chart and side scan sonar datasets (See Chapters 4 and 5 respectively) are discussed. No correlation is made with the echosounder based bathymetric chart (See Chart 4.2.) as the data from which it was constructed, was acquired simultaneously with the sub-bottom data and therefore represents identical bed profiles (See Section 4.2.).

For reference within the text, the seismic sequences and seismic facies units that make up the Loch Ainort seismic para-stratigraphy, have been given the prefixes LASS and LASF respectively. Where appropriate any individual feature identified from the cross-sectional pinger profiles are located with an OSGB36 grid co-ordinate.

6.3.1. SEISMIC SEQUENCE 1: (LASS1).

Seismic sequence 1 occurs at the base of the seismic para-stratigraphy constructed for the surveyed area and as such represents the oldest sequence to be imaged. LASS1 contains two seismic facies unit (LASF1 and LASF2) which are defined purely on the basis of upper bounding sequence reflector morphology. LASF1 is the dominant facies being conspicuous in the "Mouth Region" and the "Inner Loch" (See Figure 6.8.). In the

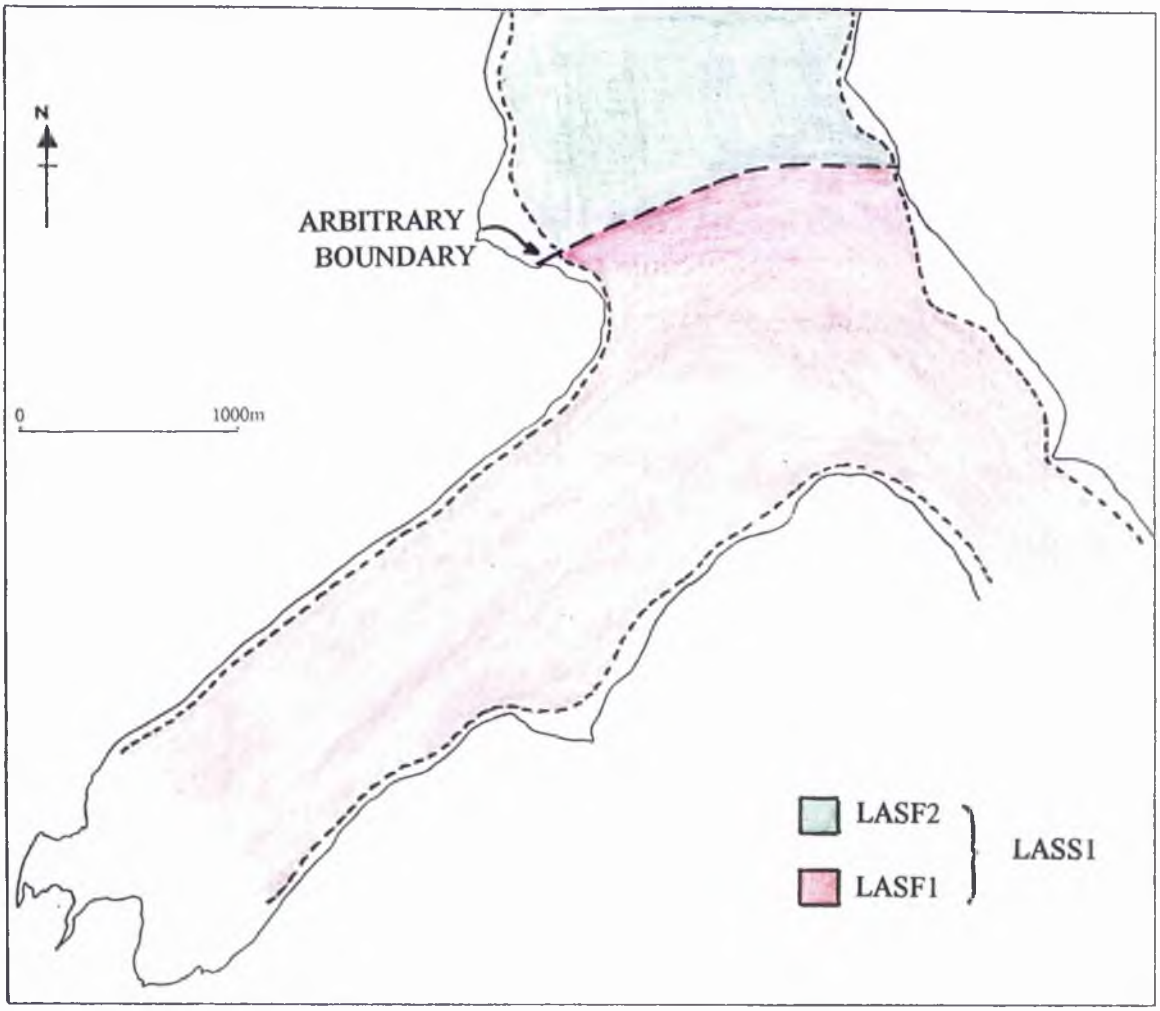

Figure 6.8. The spatial distribution of Seismic Sequence 1 (LASS1).

"Mouth Region" the upper reflector of LASF1 describes a very irregular surface, with characteristic topographic highs that attain a total maximum relief of 55.56 ms TWT (See Figure 6.9.). In this region the upper surface of LASS1 is exposed on the loch bed or beneath a thin surficial cover of LASS4 material (See Figure 6.10.).

Within the "Inner Loch", south-west of the Luib inlet, the distribution of the characteristic topographic highs becomes severely restricted (See Figure 6.8.). This is the result of a combination of factors; LASS1 developing a more subdued, albeit still irregular, relief; the gentle lochward inclination of the upper surface of LASS1 and an increase in the thickness of the overlying sequences, putting LASS1 at a depth beyond the limit of penetration of the Pinger system; and finally the similarity of the acoustic properties[1] of LASS1 and LASS2 (See Section 6.3.2.) makes the discrimination between the two sequences difficult (See Discussion Below). The exceptions to this are a small number of, partially exposed, positive relief features with a limited, asymmetric, distribution toward the south-eastern slopes of this region (See Figure 6.9.). Only four isolated topographic highs (See Section 6.3.1.1.) are located toward the north-western shoreline compared to a total of eleven toward the south-eastern shore. However, this apparent asymmetric spatial distribution is again the product of the operational constraints of the seismic system.

Where LASS2 is present the two sequences can only be defined by the identification of a prominent sequence boundary reflector within the bottom multiple (See Figure 6.11. and Section 6.3.2., Figure 6.15.). As described in Section 4.3.1.1. Inner Loch Ainort is characterised by an asymmetrical basin, with steeper north-western slopes and more gently inclined south-eastern slopes. Consequently, the shallower depths and slow drop-off rate of the south-eastern margin results in the bottom multiple residing within the 125 ms sweep time window and so discrimination of the two units is possible. Conversely, the greater depths and rapid drop-off rates on the north-western shore results in the bottom-multiples in this area being frequently beyond the 125 ms sweep time window. As a result discrimination between the two sequences in these areas, can only be achieved on the basis of upper boundary style

[1] Low acoustic impedance contrast across the LASS1 - LASS2 sequence boundary.

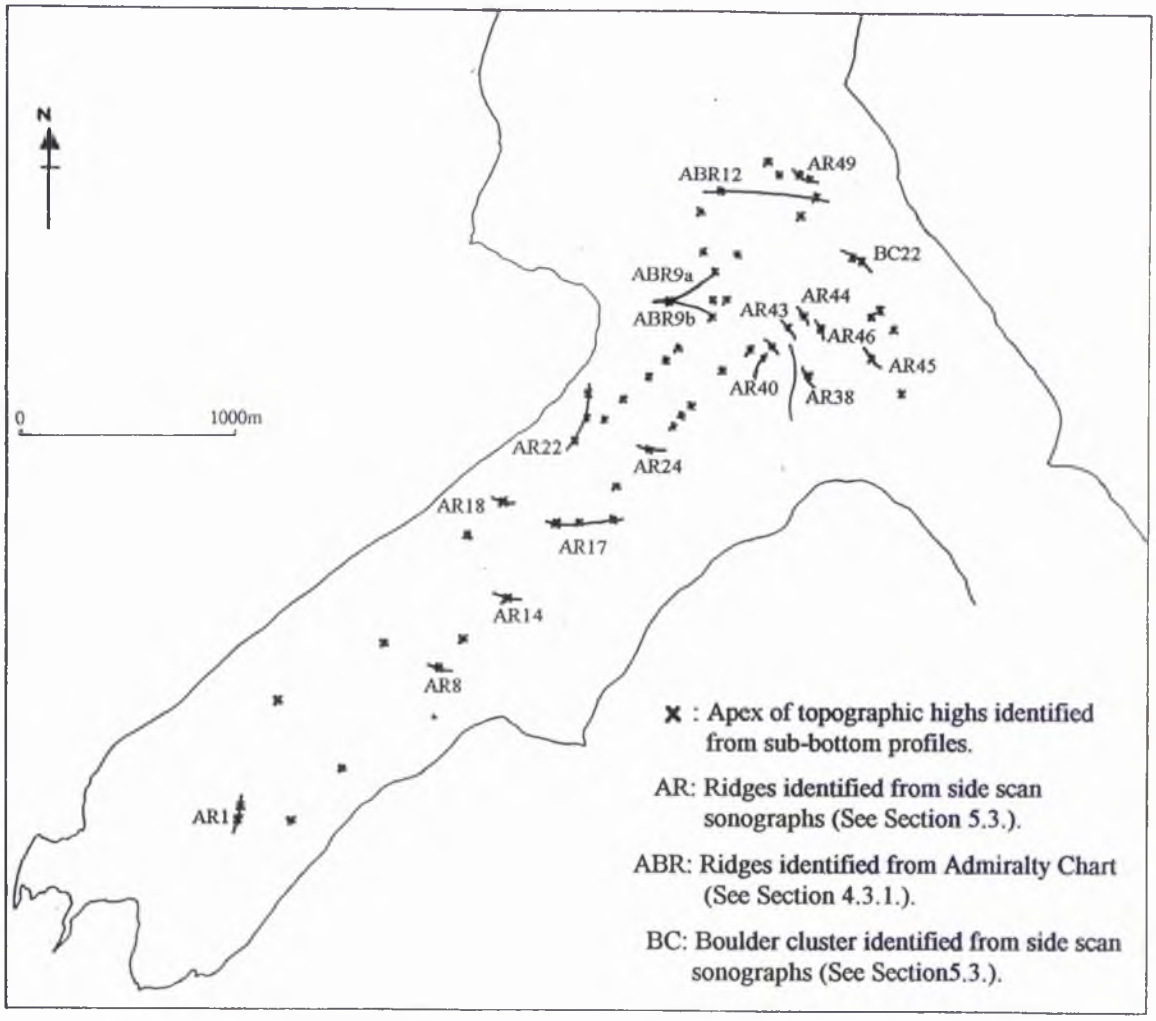

Figure 6.9. A diagram showing the distribution of LASS1 apex points throughout the survey area and their correlation with ridges and boulder clusters identified from the side scan sonographs (See Figure 5.21.) and the Admiralty Chart (See Chart 4.1.).

and so any low relief topographic highs of LASS1 may be totally obscured by LASS2 material.

In the "Unnamed Strait" LASS1 is dominated by LASF2 an identical facies to LASF1 but with an upper bounding surface that has minimal relief describing a simple basin form, which is mirrored by the present day bathymetry (See Figure 6.12.). As the lateral boundary between these two facies is based purely on a change in upper bounding reflector morphology and due to the restricted number of longitudinal survey lines that transect the two regions (only B5 and B12: See Figure 6.2.), the location of this boundary is considered to be equivocal (See Figure 6.8.).

6.3.1.1. Seismic Facies Unit 1: (LASF1).

Seismic facies unit 1 (See Figure 6.10., 6.11. and 6.12.) has a very high internal backscatter level with no discrete internal reflectors. It characteristically takes on a distinctive mottled appearance, which is interpreted as being due to the superposition of small diffraction hyperbolae, indicative of individual point reflectors (See Section 6.2.4.). Basal reflectors for this facies are absent, so a maximum recorded thickness of $\geq$ 62 ms TWT, represents a minimal estimate of the total thickness. The pronounced upper surface of LASF1 describes marked topographic highs (Maximum total relief 55.56 ms TWT) which vary from being entirely covered by the overlying seismic sequences to being totally or partially exposed on the loch bed. These topographic highs generally have asymmetric profiles with steep (Average slope angle 12°) south-westerly facing slopes and more gentle (Average slope angle 6°) north-easterly facing slopes[2]. Large point hyperbolae frequently occur at the apex's of many of these highs (See Figure 6.10.).

Figure 6.9. shows the distribution of the apex's that characterise the upper sequence boundary of LASS1 and their correlation with the ridges identified from the side scan sonographs (See Section 5.3.) and the Admiralty Chart (See Section 4.3.1.). The detail of the spatial distribution should obviously be ignored as it mirrors the location of the survey lines

[2] Unlike the slopes of the bathymetric and side scan sonar ridges (ABR and AR respectively) the terms proximal and distal have not been used to describe slope orientation of the two-dimensional positive relief features.

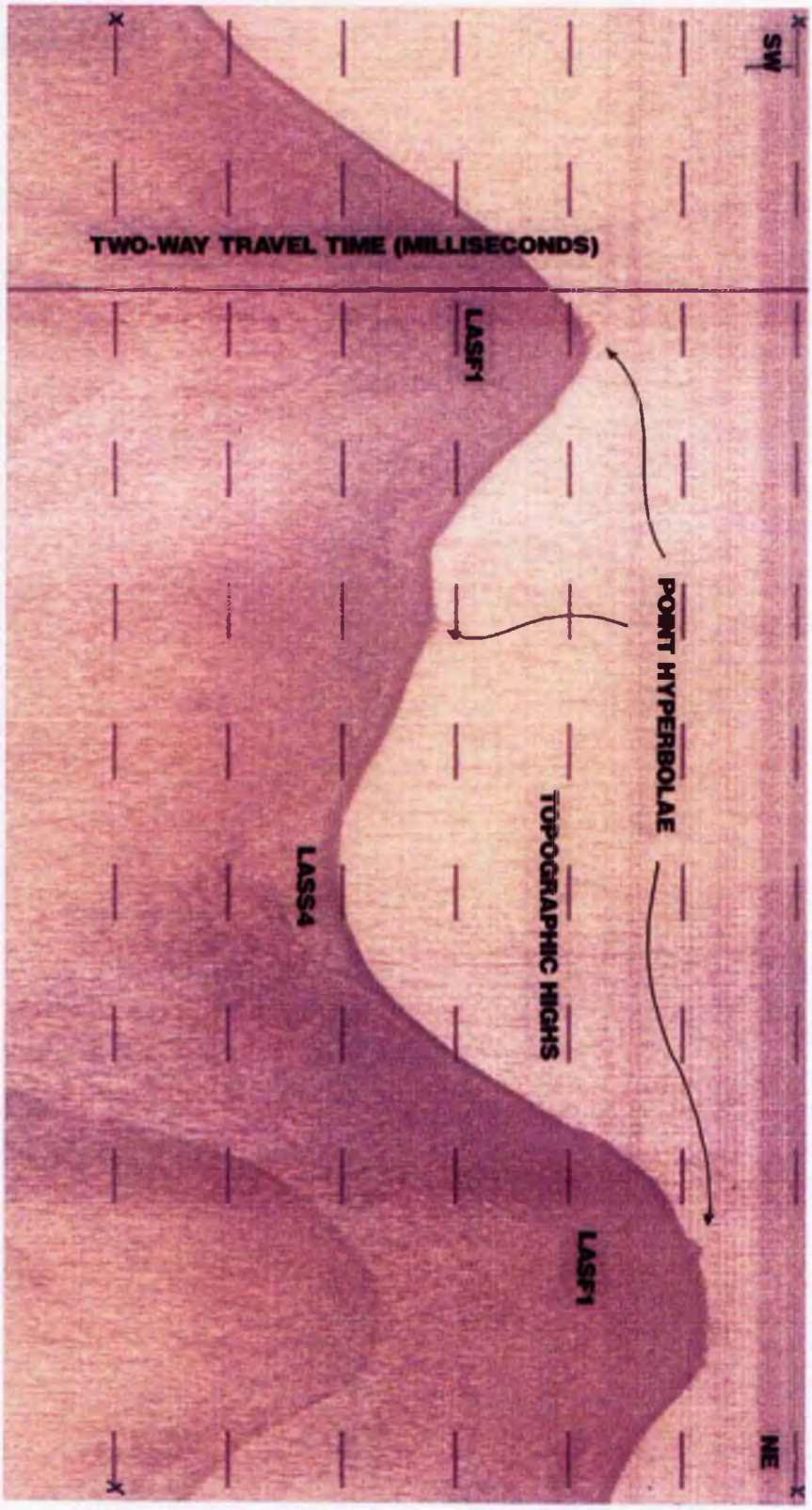

Figure 6.10. A pinger profile showing a characteristic image of LASF1 (Survey Line A12).

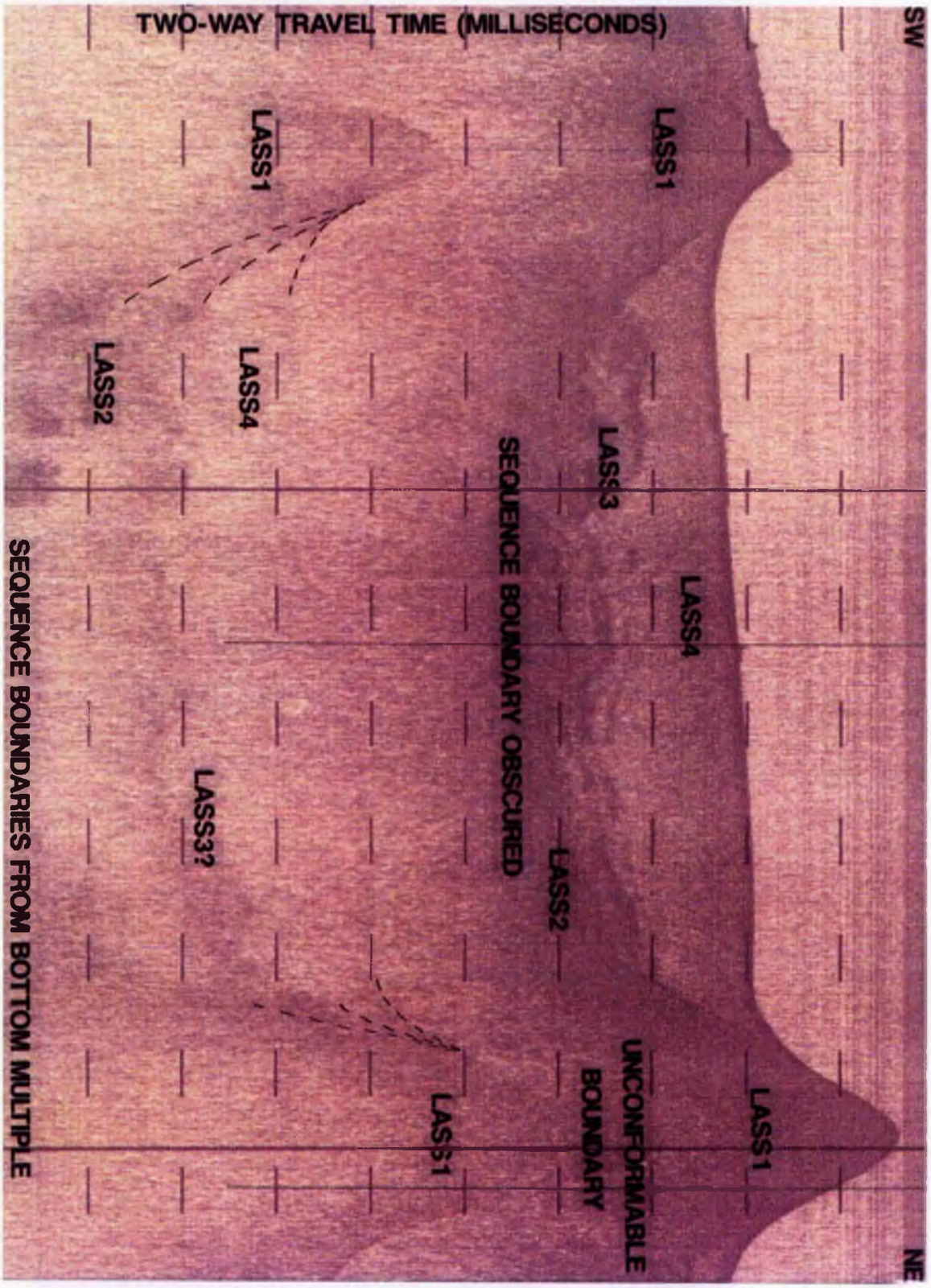

Figure 6.11. A pinger profile showing the identification of LASS1 from the bottom multiple (Survey Line A12).

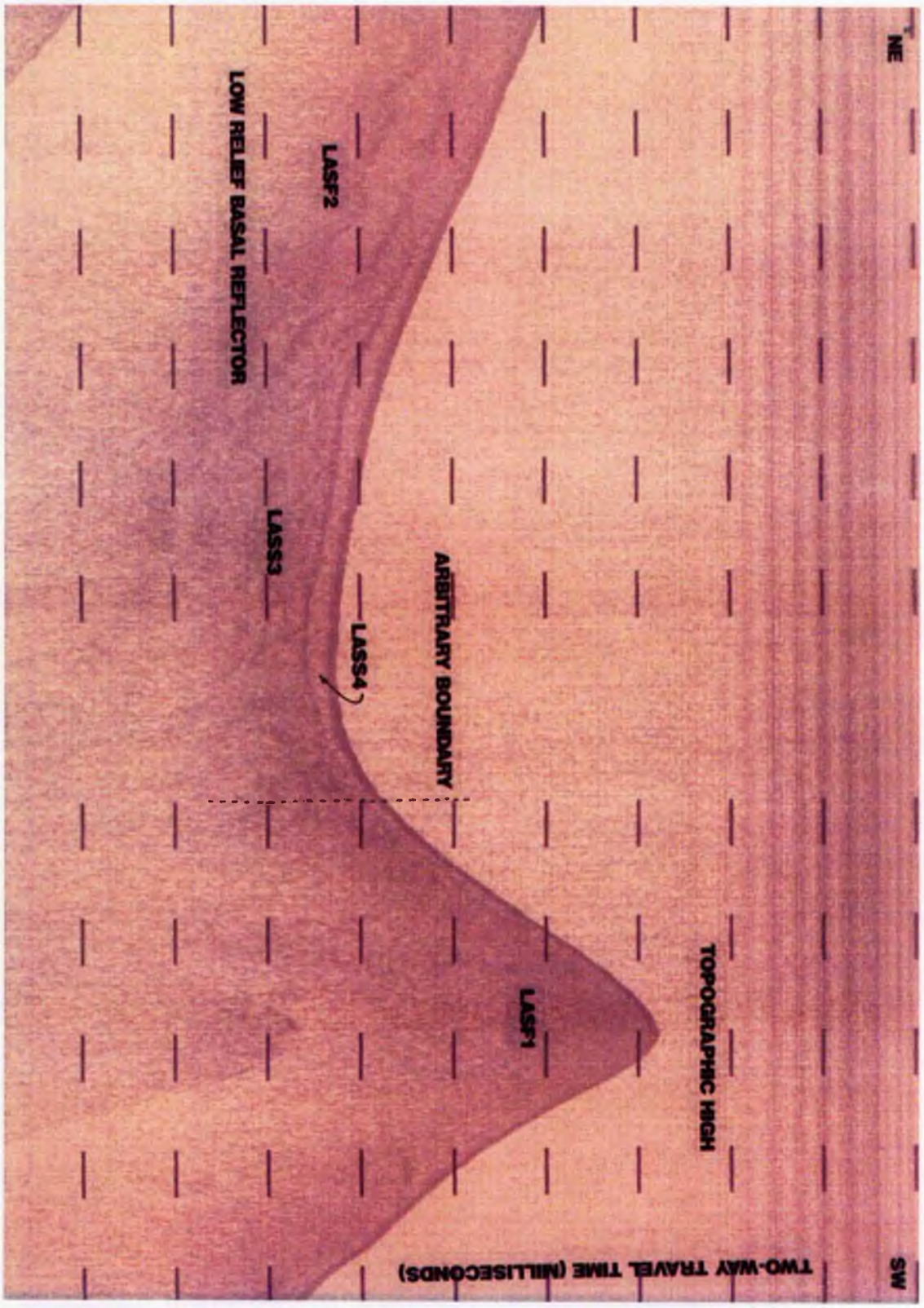

Figure 6.12. A pinger profile showing a characteristic image of LASF2 and transition with LASF1 (Survey Line B12).

within the area (See Figure 6.2. *vs* Figure 6.9.), however, the broad pattern of these points is worthy of discussion. In the "Unnamed Strait" no apex's could be identified except the central [157180 830350] major high which marks the transition between LASF1 and LASF2 (See Figure 6.12.). This is a particularly prominent feature with a maximum exposed relief of 36.11 ms TWT (27 m) and a total maximum relief of 55.56 ms TWT. This peak coincides with ABR12 [157300 830400] identified from the Admiralty Chart (4.3.1.3.) with an excellent, but chance[3], correlation between the maximum relief's recorded, 27 m vs 28 m (See Table 6.4.) respectively.

The "Mouth Region" and the north-easterly part of the "Inner Loch" contains the maximum concentration of topographic highs within the survey area (See Figure 6.9.). The majority of these features outcrop on the surface of the loch bed with a range of exposed heights from 2.78 ms TWT (2.1 m) to 33.3 ms TWT (25 m). Due to the minimal cover by the overlying seismic sequences within this region (See Sections 6.3.3. and 6.3.4.), the total relief of these positive targets is not significantly different to the exposed values, with a maximum value of only 38 ms TWT being recorded. The exceptions to this are two targets, identified from survey lines A13 and C9, which have been entirely buried by LASS4 material. The surface expression of these targets is in fact restricted to an increase in the backscatter tones and the presence of point hyperbolae. Beneath the loch bed these targets describe a total relief of 11.11 ms TWT. As can be seen in Figure 6.9. these two targets do in fact coincide with the boulder cluster (BC22) identified from the side scan sonographs. This spatial correlation and the similarity between the imaged surface expressions (high backscatter levels and presence of point hyperbolae) may suggest that a number of the other boulder clusters identified from the sonographs could represent wholly or partially buried ridges.

Out of a total of 48 topographic highs identified within this region 22 coincide with a total of 15 three-dimensional ridges[4] identified from the side scan survey (See Section 5.3.) and the Admiralty Chart (See Chart 4.1.). Table 6.4. (Overleaf) compares the maximum exposed relief values obtained from the pinger profiles with the height values obtained from the other geophysical datasets, but as discussed above the former values should be treated with caution.

[3] Due to potential errors in comparing calculations based on side scan sonographs (See Sections 5.2.3. and 5.2.6.) with a value from a single transect cutting obliquely across a three-dimensional feature.
[4] Ridges: AR14, AR17, AR18, AR22, AR24, AR38, AR40, AR43, AR44, AR45,AR46, AR49, ABR9a and b, and ABR12.

3-D Ridge Height (m)		*Sub-bottom Apex Equivalents*		*3-D Ridge Height (m)*		*Sub-bottom Apex Equivalents (m)*	
		ms TWT	*m*			*msTWT*	*m*
AR14	0.9-3.6	5.56	4.2	AR44	4	11.2	8.4
AR17	1-12	2.78:19.45: 16.67	2.1:14.6:12.5	AR45	2.1	9	6.8
AR18	12	5.56	4.2	AR46	0.4	2.5	1.9
AR22	1-1.4	2.78:5.56: 11.11	2.1:4.2: 8.3	AR49	1.8	2.78	2.1
AR24	2.1-5.4	13.89	10.4	ABR9a	32	13.89	10.4
AR38	5	22.22	16.7	ABR9b	14	25	18.75
AR40	2.5	8.33	6.2	ABR12	28	36.11	27
AR43	75	5.56	4.2				

Table 6.4. Comparison of target heights obtained from the side scan sonographs and Admiralty Charts with those calculated for the topographic highs identified from the sub-bottom profiles. Velocity conversion factor 1500 ms^{-1}.

South-west of the Luib inlet a total of only eight positive relief features (See Figure 6.9.) were confidently identified by analysis of LASS1 from both the main profile and the bottom multiple. Both asymmetric and symmetrical cross-sectional profiles are identified, where asymmetry is present the topographic highs have steep southerly facing slopes and more gently inclined northerly facing slopes. Where a concentration of LASF2 directly overlies the upper sequence boundary of LASF1, it obscures the true profile of these targets giving them an artificially lower slope angle in the main profile. The majority of these features are further partially obscured by thick (maximum thickness 32.89 ms TWT) sequences of LASS3 and LASS4 material.

On survey lines A8 and A10 a positive target, attaining a maximum exposed relief of 12.48 ms TWT (9.3 m) and a maximum total relief of 20.80 ms TWT, spatially coincides with ridge AR1 (See Section 5.3.3.). However, it should be noted that the assignment of an LASF1 composition to this target (and by inference AR1) is based on equivocal evidence. This positive target is composed of a facies with identical acoustic properties as those of LASF1[5], but exhibit a rapid gradational transition to the subdued topographic characteristics of LASS2

[5] Very high internal backscatter level with no discrete internal reflectors and a prominent irregular upper boundary.

on either slope (See Figure 6.13.). As with all the other profiles no boundary between LASF1 and LASS2 can be identified but unlike the remainder of the targets in the "Inner Loch" no bottom multiple is present on this survey line. Consequently, one has only been able to assign a LASF1 composition for this feature on the basis of its upper boundary style.

In addition to being the foundation facies to the loch floor LASF1 is also the seismic facies from which the marginal slopes of Loch Ainort are constructed. However, due to the shallow water depths at these sites, penetration is poor and basal reflectors are absent so estimates for the thickness of LASF1 at these localities cannot be made. The morphology of the shoreline mirrors the bathymetry described in Section 4.3. and in particular the plateau areas at the head of the loch, at Luib and off the northern slopes of Am Meall can all be clearly identified.

6.3.1.2. Seismic Facies Unit 2: (LASF2).

LASF2 occurs exclusively as the lowest seismo-stratigraphic unit of the "Unnamed Strait" attaining a maximum thickness of 15 ms TWT in the deepest part of this outer basin. However, due to the absence of any basal reflector this value is considered a minimum estimate. As with LASF1 this facies has a very high internal backscatter level with no discrete internal reflectors and a distinctive mottled appearance. LASF2 has a smooth, low relief, but laterally extensive, upper reflecting boundary that describes a simple U-shaped form (See Figure 6.12. and Section 6.3.3.2., Figure 6.22.). At the margins of the "Unnamed Strait" and at occasional within loch sites, LASF2 is exposed on the sea bed. Elsewhere LASF2 lies beneath a thin veneer of seismic sequences 3 and 4. The lateral transition between LASF1 and LASF2 is based on upper reflector morphology variation which can only be identified from the longitudinal transects B5 and B12 (See Figure 6.12.).

6.3.2. SEISMIC SEQUENCE 2: (LASS2).

Seismic sequence 2 is restricted to "Inner Loch" sites (See Figure 6.14.) but within this region it dominates the lower chrono-stratigraphical units, except where it unconformably overlies small exposures of seismic sequence 1 at the head of the loch. The single seismic facies units (LASF3) within LASS2 can be discriminated from the identical underlying

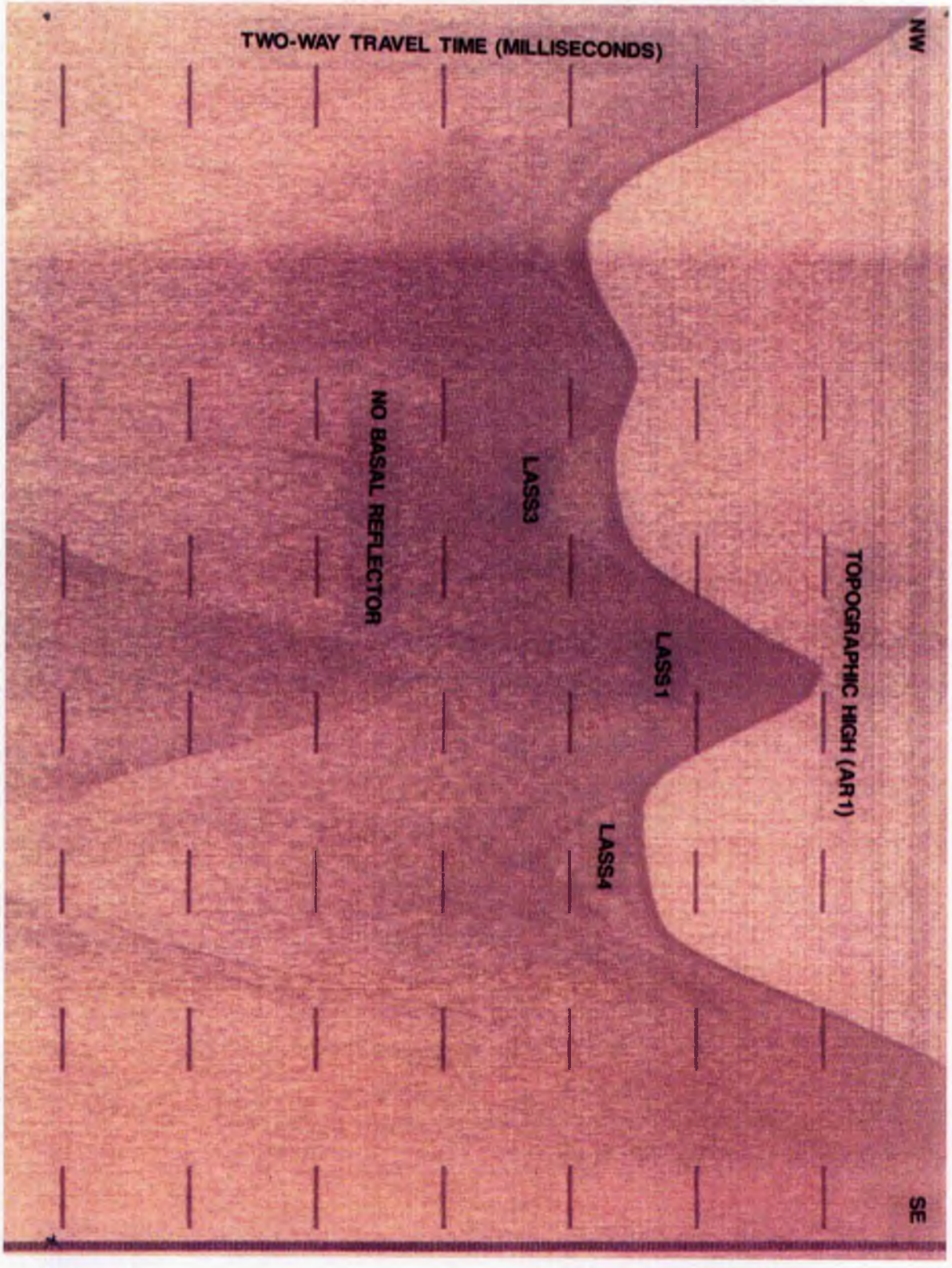

Figure 6.13. Topographic high identified from survey line A8 and coincident with AR1 idenitified from the side scan sonagraphs (See Section 5.3.3.).

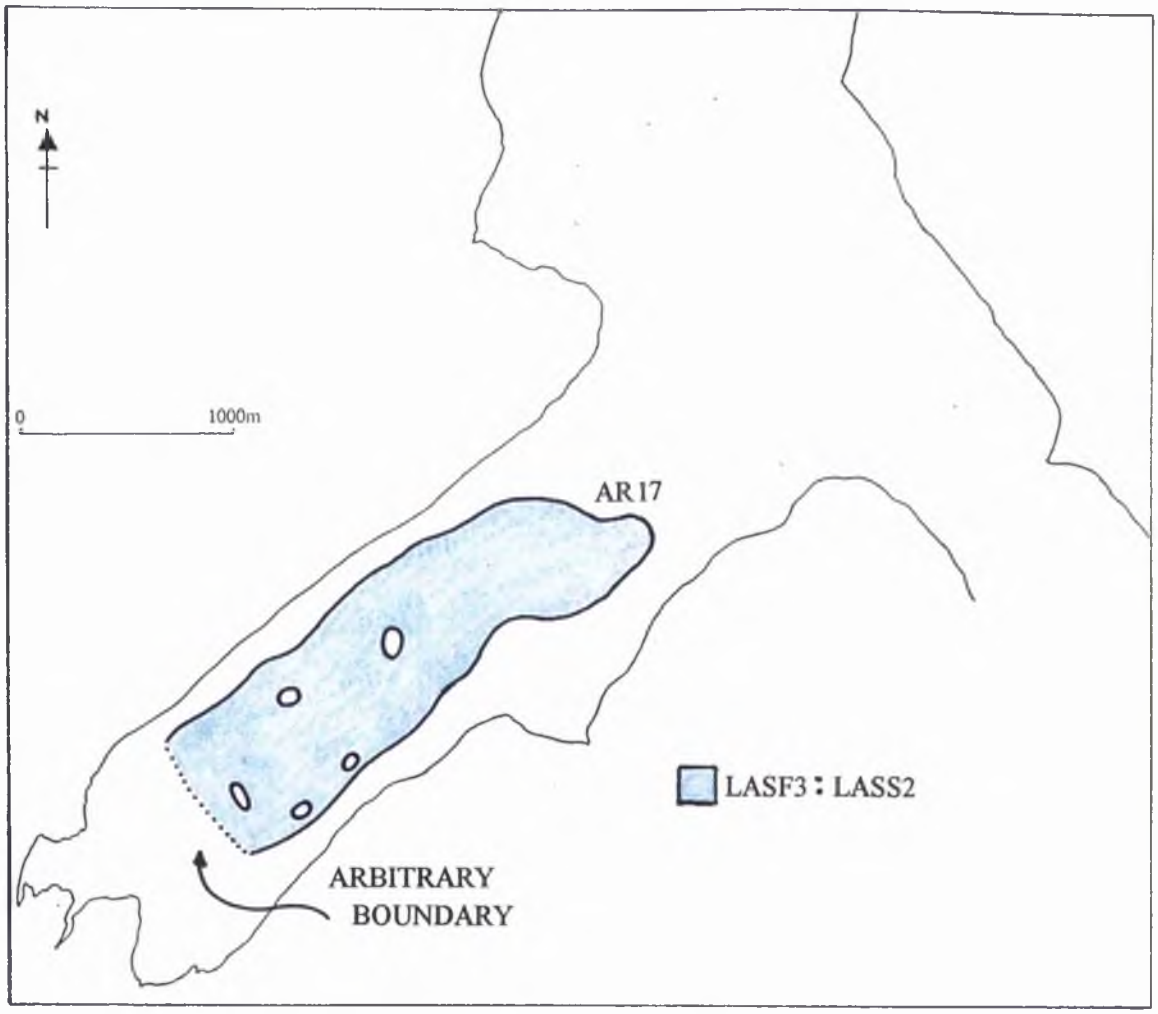

Figure 6.14. The spatial distribution of Seismic Sequence 2 (LASS2).

LASF1 by a marked change in upper boundary style and occasionally the presence of a basal reflector (See Section 6.3.1.). Where identified from the bottom multiple LASS2 has a marked unconformable lower boundary with LASS1, exhibiting onlap with this lochward inclined basal reflector (See Figure 6.15.).

The lateral thinning of LASF3 toward the north-west occurs 475 m north-east of the Luib inlet (See Full Description in Section 6.3.2.1.). However, due to the difficulty in being able to identify a basal reflector for much of this sequence, estimates of the average thickness of this facies unit are considered poor. Consequently only an approximate maximum thickness of 11.1 ms TWT for this sequence can be given. Due to the poor penetration obtained along survey lines A7 and A11 it has not been possible to identify a south-westerly boundary to this seismic sequence. As LASS1 can be clearly identified beneath the upper surface of the shallow plateau area at the head of the Loch (See Section 4.3.1.1.) an arbitrary boundary can be located between these two sites.

6.3.2.1. Seismic Facies Unit 3 (LASF3).

Seismic facies unit 3 (See Figure 6.15. and 6.16.) is characterised by a very high internal backscatter level, a mottled appearance and the absence of discrete internal reflectors. In addition, to the small point reflectors that give this mottled effect a number of singularly larger point reflectors are present and identified as large overlapping hyperbolae (See Figure 6.16.). The upper bounding reflector of this facies describes a subdued but irregular and chaotic relief. This boundary is significantly more diffuse than that described for LASF1 (See Sections 6.3.1.1.), but it can still be clearly distinguished from the seismic facies units of the overlying seismic sequences 3 and 4.

Seismic facies unit 3 is restricted to "Inner Loch" sites south-west of a transitional boundary with the underlying LASS1 (See Figure 6.17.). The irregular plan form of this boundary (See Figure 6.14.), with a slight, south-easterly located up-loch bulge, is probably attributable to the distribution of longitudinal transects within the loch (See Figure 6.2.: Survey lines A12, A16 and B13). Consequently any palaeo-environmental inferences taken from the form of this boundary should be treated with caution. The section of the longitudinal transect A12 presented in Figure 6.17. shows the transition from the low subdued topography

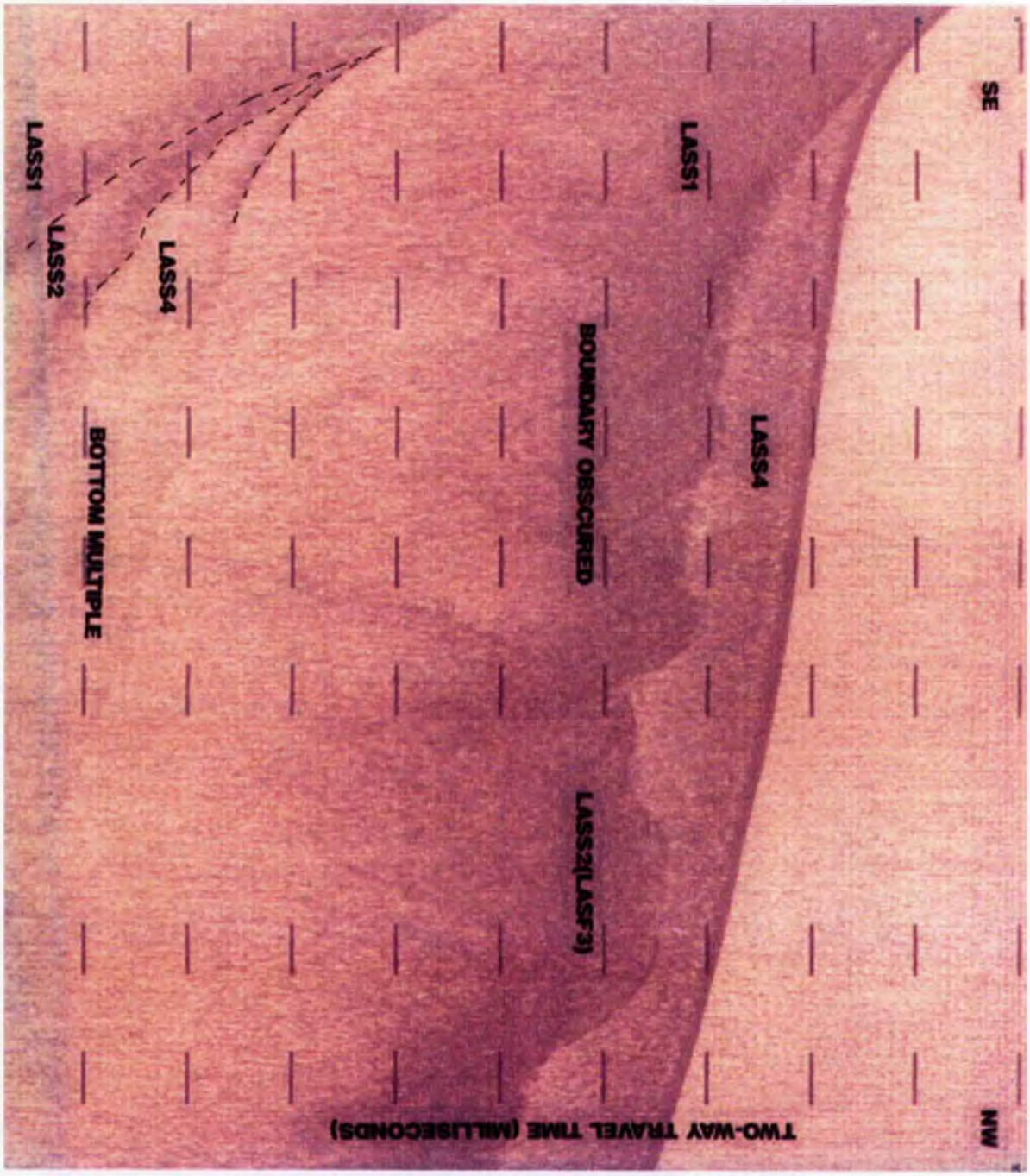

Figure 6.15. A pinger profile showing the unconformable contact between LASS1 and LASS2 (Survey Line A5).

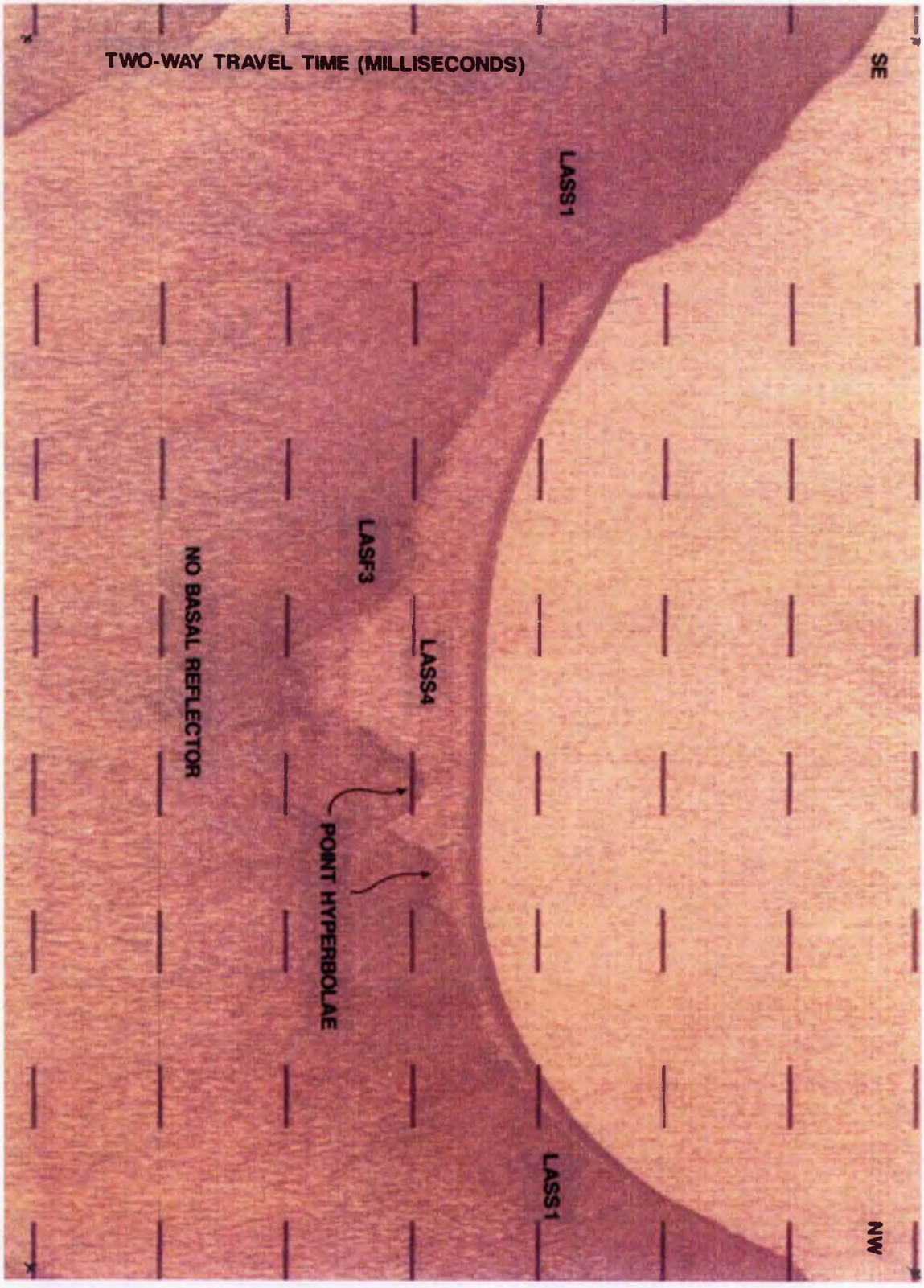

Figure 6.16. A pinger profile showing a characteristic image of LASF3 (Survey Line B14).

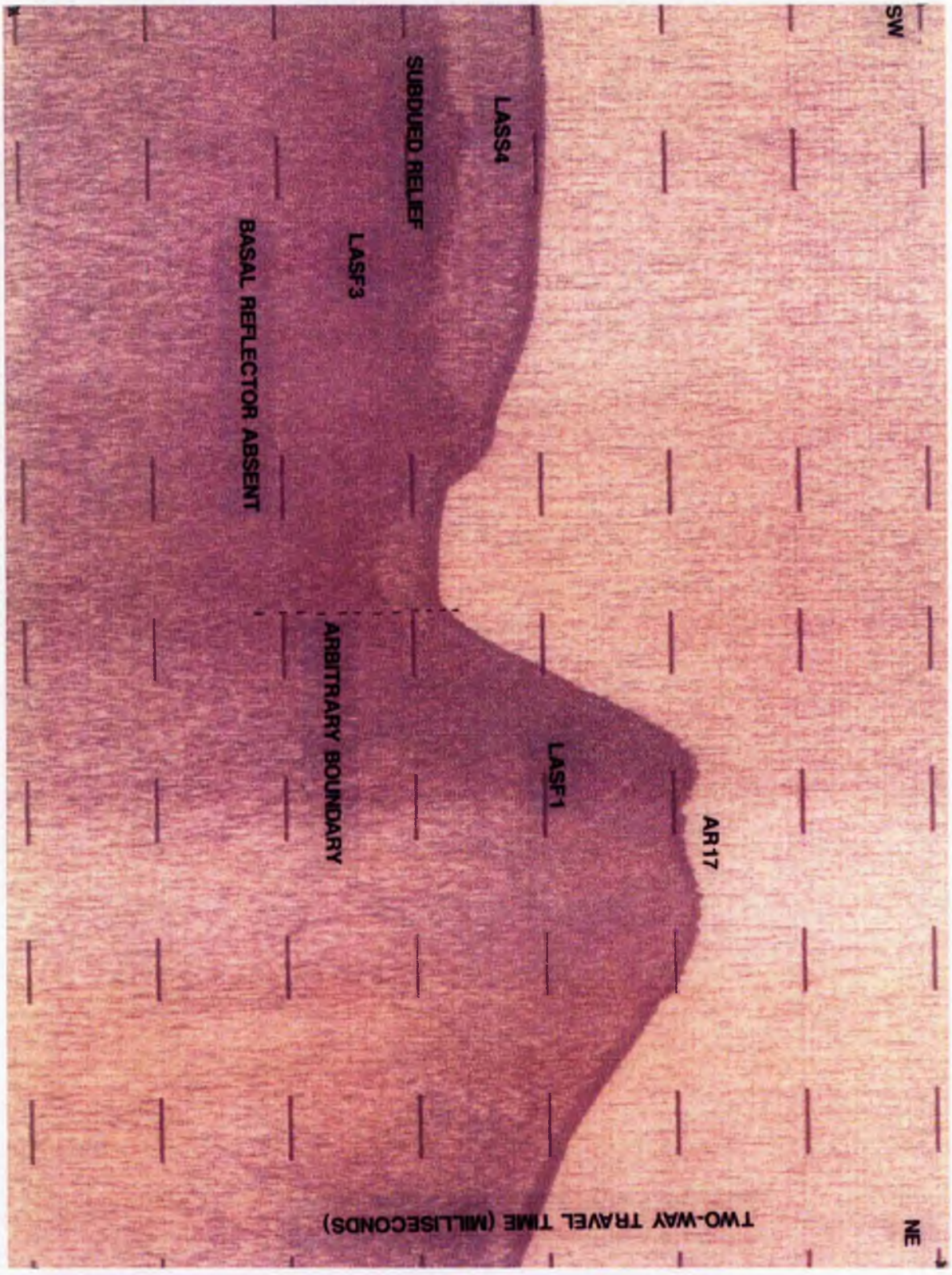

Figure 6.17. A section from pinger profile A12 showing the transition between LASF1 and LASF3. Note topographic high coincident with AR17.

of LASF3 in the south-west to the steeply inclined south-westerly facing slope of a topographic high of LASF1 ([156450 828930] Maximum exposed relief 16.67 ms (12.5 m); maximum total relief 27.7 ms TWT).

The major positive target (See Section 6.3.1.1.) which marks the north-easterly extent of LASS2[6] coincides with a ridge complex, identified from the side scan sonar images, and which is centred on AR17 ([156550 828970]: See Section 5.3.3.). This complex consists of five individual ridges, and an asymmetrically distributed "very dark" tonal zone which encompasses the majority of the ridge complex (See Figure 6.18.). There appears to be particularly good dimensional correlation between the width of the surface expression of this topographic high (160 m) with an oblique section taken along the line of A12 through the "very dark" tonal zone (175 m).

6.3.3. SEISMIC SEQUENCE 3 (LASS3).

Seismic sequence 3 contains two seismic facies, LASF4 and LASF5 (See Sections 6.3.3.1. and 6.3.3.2.) which overlie the irregular topography of the palaeo-surface described by the upper sequence boundaries of LASS1 and LASS2. The actual nature of this basal reflector changes markedly throughout the field area, its form being dependant on the sequence up on which it rests. Where present LASS3 always occupies the lowest point within the pre-existing surface, hence, LASS3 has a restricted distribution. As can be seen from the isopach map constructed for this sequence (See Figure 6.19.), LASS3 is concentrated in two main bodies, one in the "Inner Loch" and the other dominating the "Unnamed Strait".

The "Inner Loch" body has an elongate (1.9 km) form between [154900 827450] and [156150 828880] oriented along the axis of the loch and offset toward the north-western shore. This body covers a total area of 0.085 km^2, varies in width between 0.1 km and 0.365 km and attains a maximum thickness of 13.89 ms TWT. Within this body there are two locations at which LASS3 attains its maximum thickness (See Figure 6.18.). The first at the mid-point of the north-western boundary [155900 828700] and the second 0.235 km from

[6] This topographic high is also identified in survey lines A16, B2 and B13.

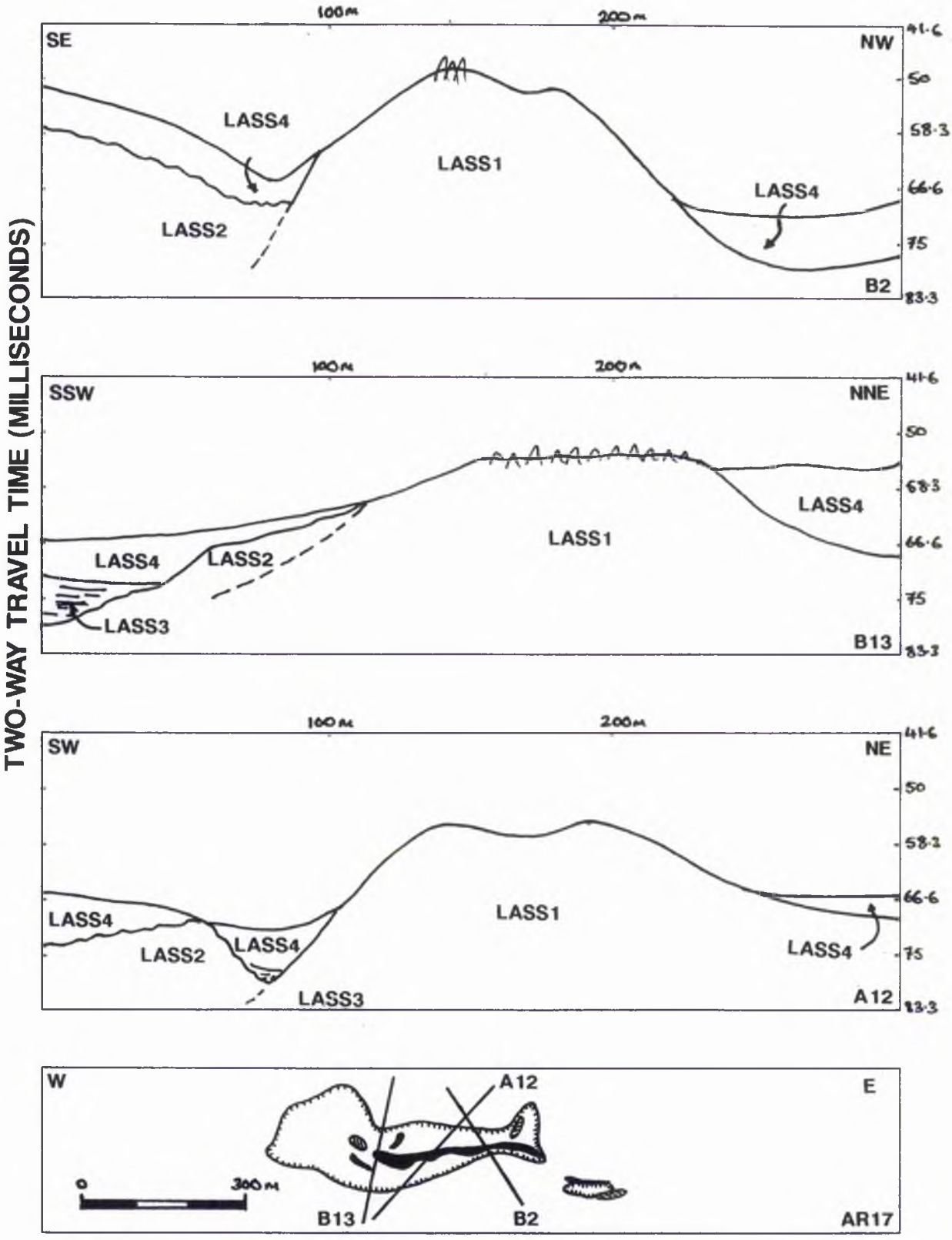

Figure 6.18. A diagram showing the dimensional comparison between the positive targets identified from A12, B2 and B13 and the ridge complex AR17.

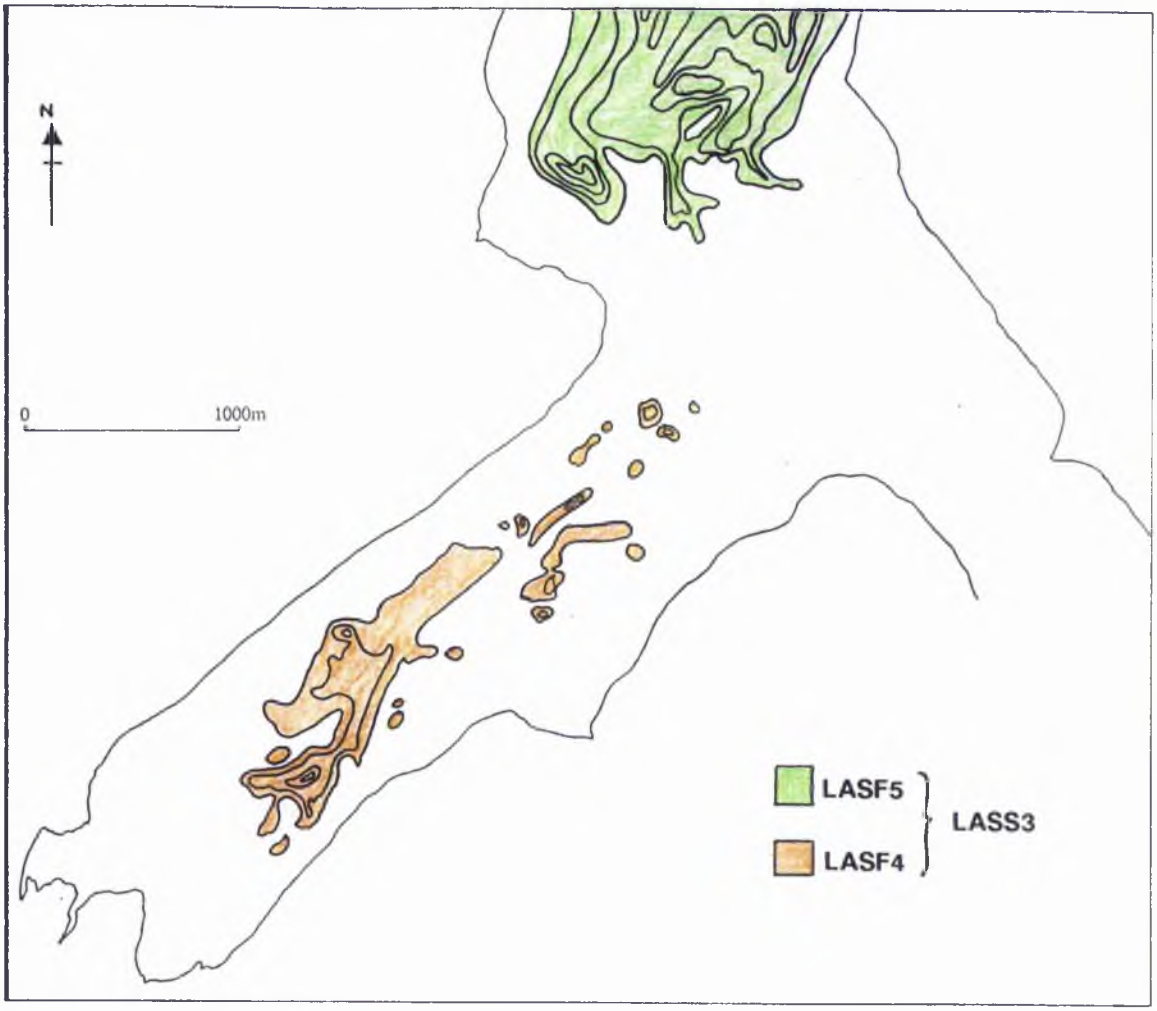

Figure 6.19. The spatial distribution of Seismic Sequence 3 (LASS3) including isopach contours in two-way travel time (Contour interval 4 milliseconds).

the south-eastern shore mid-way between Luib and Sròn Ard à Mhullaich [155100 827700]. One hundred and sixty-five metres to the north-east two smaller (0.042 km^2 and 0.026 km^2), but again elongate (0.6 km and 0.4 km) bodies of LASS3 lie at an axial position within the loch, offshore of the Luib inlet at [156300 828850] and [156400 829150] respectively. Here a maximum thickness of LASS3 of 5.56 ms TWT is attained. Around these two smaller bodies lie a series of even smaller (Average size 0.01 km^2), discrete, accumulations of LASS3 material. All of the isolate bodies identified within the "Inner Loch" are composed of LASF4.

In the "Unnamed Strait" LASS3 forms a large (1.65 km^2), thick (average thickness 11.4 ms TWT), body which is confined to the east and west by the shoreline slopes of Scalpay and Meall à Mhoil (See Figure 6.19.). To the south[7] this area of LASS3 terminates against the raised and irregular topography of the "Mouth Region". This outer zone of LASS3 attains a maximum thickness of 13.9 ms TWT towards the mouth of the Luib na Moil inlet. All of this outer body of LASS3 is composed of seismic facies unit 5.

As with the varying nature of the basal reflector of this seismic sequence, the upper bounding reflector of LASS3 with LASS4 varies in style throughout Loch Ainort. In the "Inner Loch" region an arbitrary boundary is assigned (See Section 6.3.4.) whilst in the "Unnamed Strait" the same boundary is identified by a strong, laterally continuous reflector. Unfortunately LASF4 and LASF5 never appear in the same profile making spatial correlation difficult. However, the broad similarities in facies style (See Sections 6.3.3.1. and 6.3.3.2.) and their seismo-stratigraphical position between the ubiquitous sequences LASS2 and LASS4 enables them to be assigned to the same seismic sequence.

6.3.3.1. Seismic Facies Unit 4 (LASF4).

Seismic facies unit 4 has a low to medium internal backscatter level, with thick (1.4 ms TWT) strong, discontinuous, internal reflectors of high lateral extent (See Figures 6.11., 6.20. and 6.21.). These irregular reflector packages have a horizontal to gently inclined orientation. All these bodies have unconformable onlapping contacts with the underlying sequence boundary. Where LASF4 directly overlies LASS1, north-east of the Luib inlet (See Section 6.3.1.), a strong basal reflector can be clearly identified, with the internal reflectors of this unit

[7] The northern boundary of this sequence is defined by the outermost survey line B11.

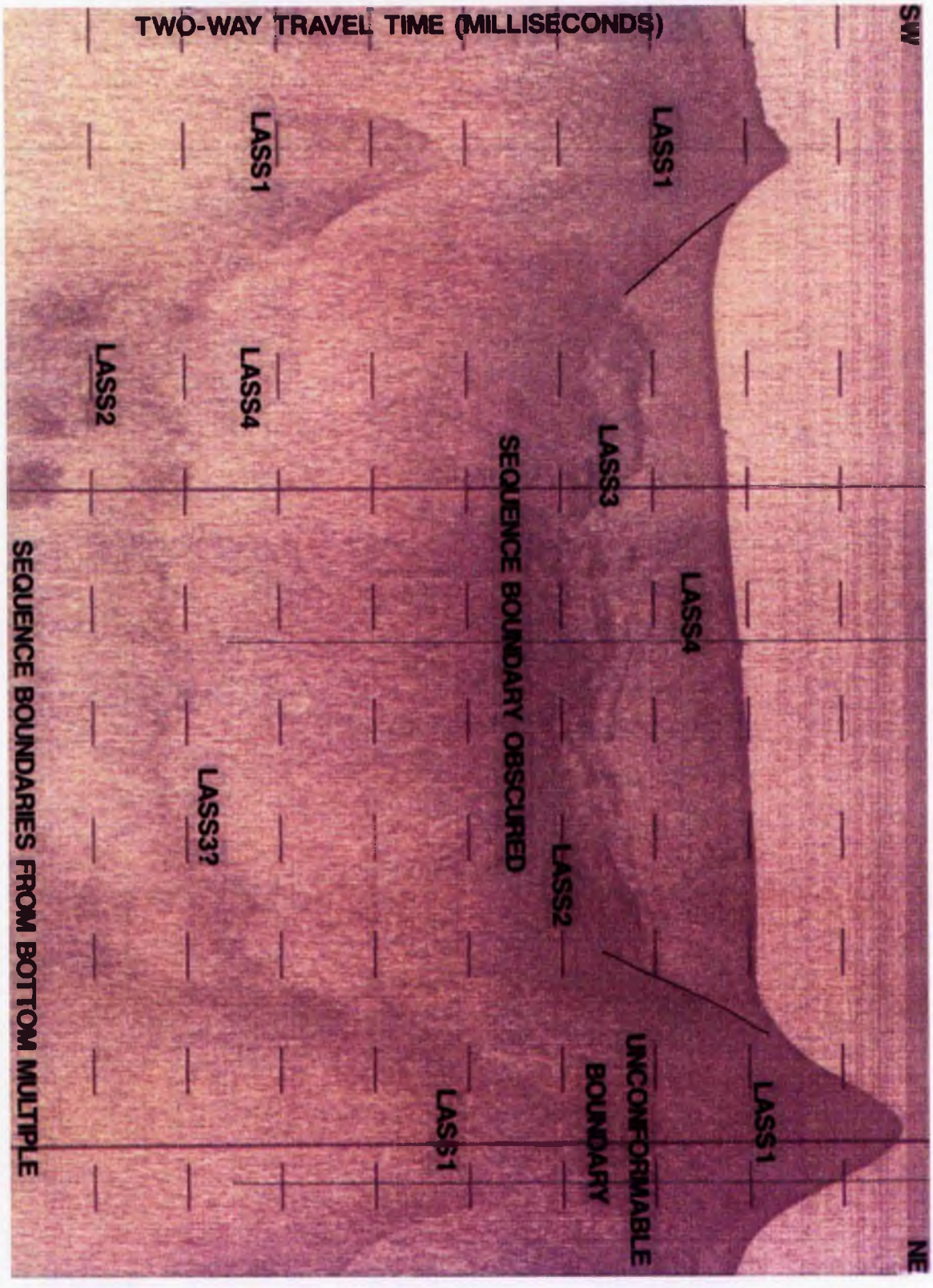

6.20. A pinger profile showing a characteristic image of LASF4 and the unconformable basal boundary with LASS1 (Survey Line A12).

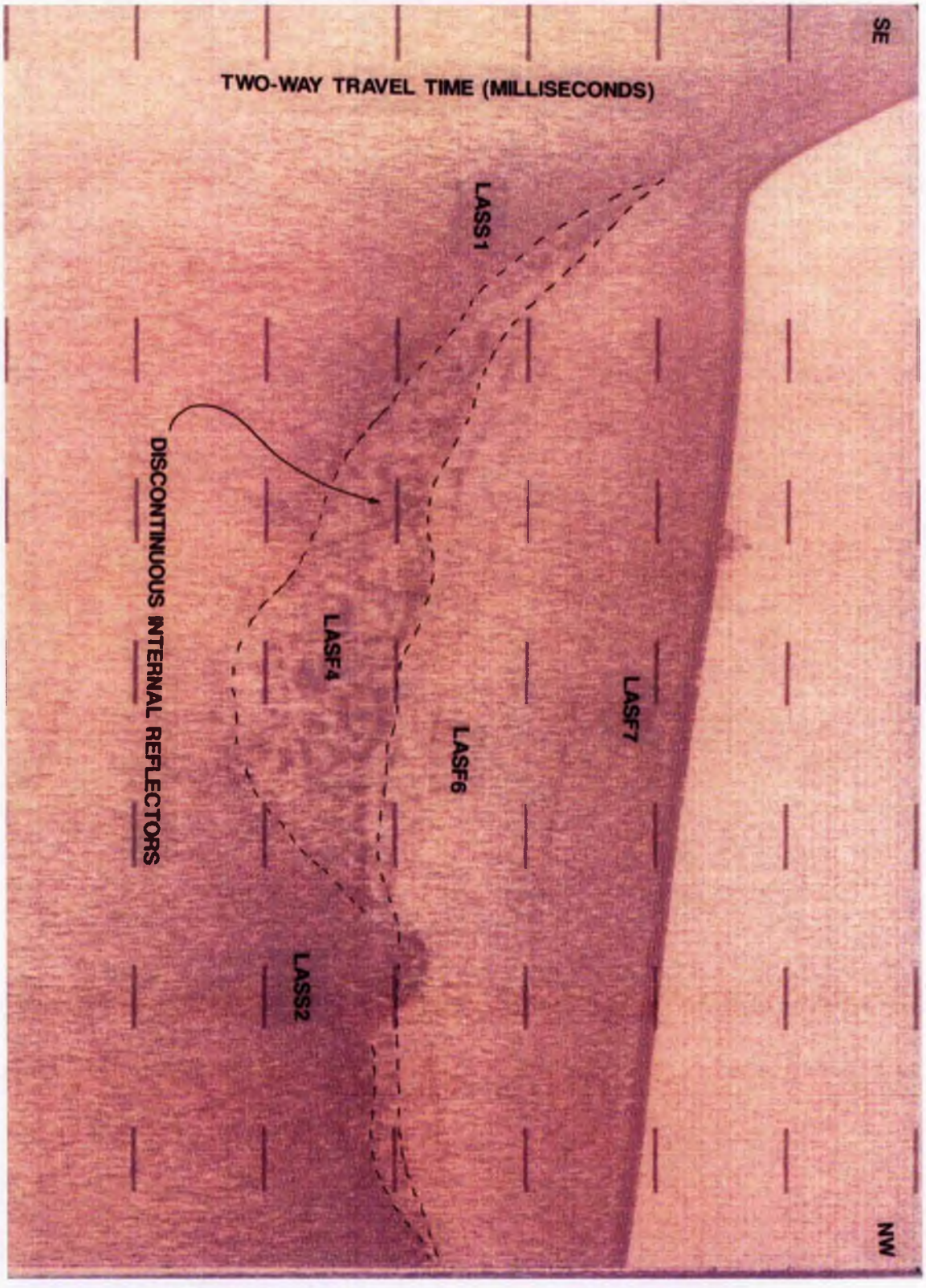

6.21. A pinger profile showing a characteristic image of LASF4 and the unconformable basal boundary with LASS2 and LASS3 (Survey Line A9).

terminating abruptly against the topographic highs that typify LASS1 (See Figures 6.11. and 6.21.). Conversely, south-west of the Luib inlet the sequence boundary between LASF4 and the underlying LASS2 is poorly defined due to the similarity between the gently undulating chaotic upper surface of LASS2 and the strong discontinuous internal reflectors of LASF4 (See Figures 6.11. and 6.21.). Consequently, the sequence boundary at these localities can only be arbitrarily defined and the unconformable nature of this contact can only be gleaned from occasional marginal sites where reflector termination's do occur (See Figure 6.21.). The upper reflector of LASF4 is arbitrarily defined being dependent on the vertical fade out of the internal reflectors. As described in Section 6.3.3., LASF4 attains a maximum thickness of 13.89 ms TWT.

6.3.3.2. Seismic Facies Unit 5 (LASF5).

Seismic facies unit 5 is similar in style to LASF4 with a medium internal backscatter level and thick (0.55 ms TWT), strong, internal reflectors. However in this facies the parallel internal reflectors have a greater lateral continuity at the base of each section (See Figure 6.12. and 6.22.). On the slightly steeper slopes of the loch margins the internal reflectors become more disrupted. In central loch localities the internal reflectors of LASF5, have an apparent conformable relationship with the underlying simple basin form of the sequence boundary with LASS1 (LASF2). However these reflectors thin out and onlap on to LASS1 at the loch margins. The most distinctive feature of LASF5 is a thin but clearly marked, gently undulating, upper reflector which separates it from LASS4 and against which the strong internal reflectors terminate (See Figure 6.22.). Within this areaLASF5 attains a maximum thickness of 13.5 ms TWT. Throughout the "Unnamed Strait" LASF5 is covered by a thin veneer (Average thickness 3.9 ms TWT) of LASS4.

6.3.4. SEISMIC SEQUENCE 4 (LASS4)

Seismic sequence 4 is the highest sequence in the seismic para-stratigraphy constructed for the Loch Ainort field area. Containing a total of five seismic facies units within its sequence boundaries, LASS4 exhibits the greatest spatial variability in seismic signature of the facies

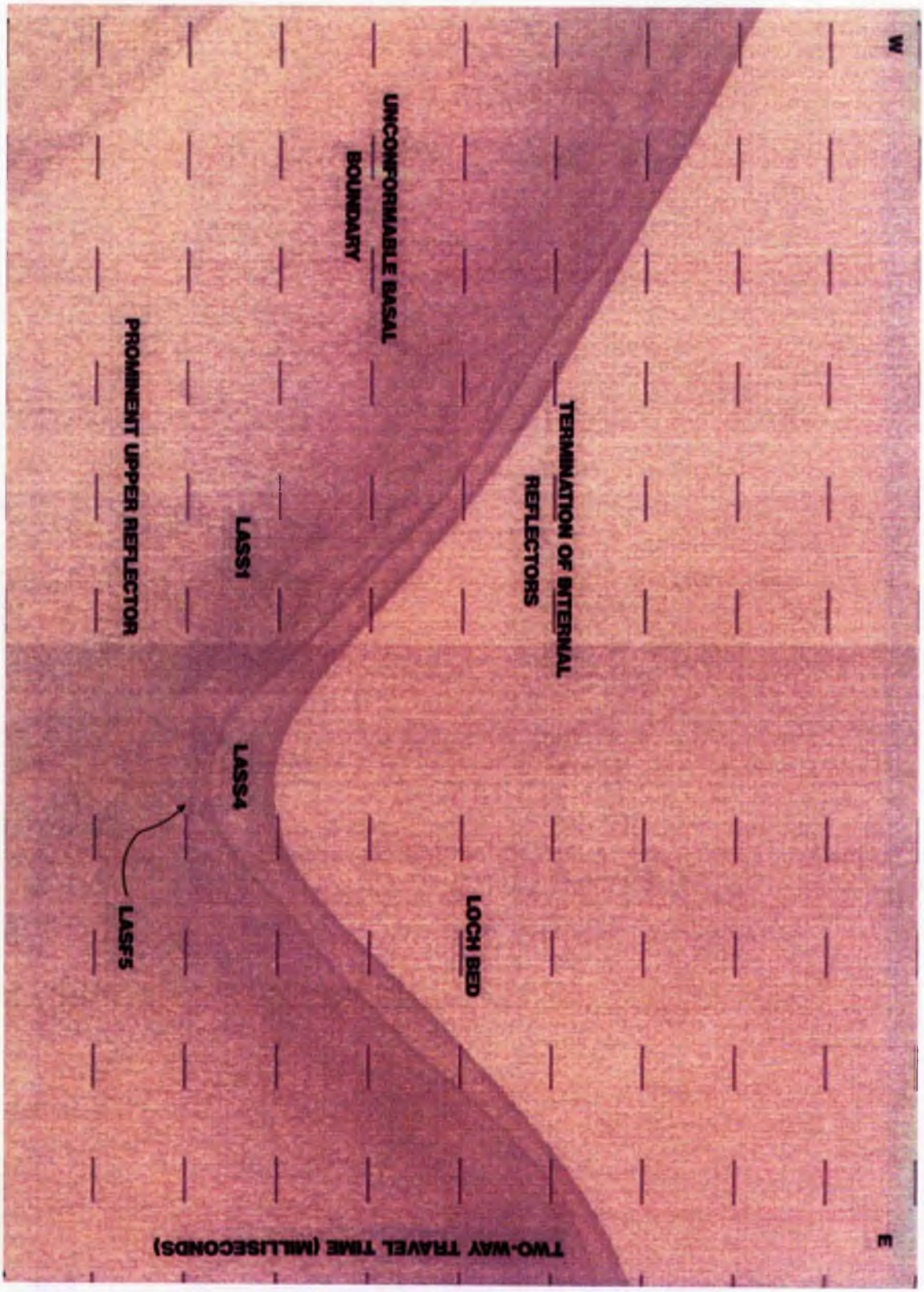

Figure 6.22. A pinger profile showing a characteristic image of LASF5 and the unconformable basal boundary with LASS1 (Survey Line B10).

identified. LASS4 is found throughout the survey area (See Figure 6.23.) unconformably overlying the irregular topography of the pre-existing surface created by LASS1, LASS2 and LASS3. Of the five facies units within LASS4, LASF7 dominates the sequence making up the large body of this material within the "Inner Loch" area (with the underlying LASF6) and the thin (maximum thickness 6 ms TWT) surface veneers, that sporadically cover the "Mouth Region" and the "Unnamed Strait". It is important to note that LASF6 and LASF7 do not occur on the inclined slopes of the loch margin and so are concentrated in the deeper parts of the pre-existing basin. By contrast LASF8 to LASF10 have a very restricted distribution, occurring as thin (maximum thickness 6.25 ms TWT) covers on the upper surfaces of shallow plateau areas and small depressions within the gentle sloping surfaces around the loch margins. Unlike the other three sequences both upper and basal reflectors can be clearly identified, with the seismic facies units of LASS4 unconformably resting on the underlying sequences.

The large (2.11 km^2) central body of LASS4 that occurs within the "Inner Loch" attains a maximum thickness of 22 ms TWT (Figure 6.23.). This large accumulation of LASS4 occurs south-west of the Luib inlet towards the north-western shoreline, with the sequence thinning out toward, and onlapping on to, the rising irregular topography of LASS1 that dominates the loch bed in the "Mouth Region" (See Figure 6.8.).

The upper sequence boundary of LASS4 represents the "time line" (See Section 6.2.3.) that is the current loch bed. As can be seen from all the seismic profiles presented within Chapter 6 the loch bed is characterised by a thin, prominent reflector with high lateral continuity and extent[8]. However, the nature of this boundary appears to have persistent properties irrespective of which seismic sequence actually outcrops on the loch bed. This conformity of acoustic style is almost certainly the product of the strong acoustic impedance contrast across the water - loch bed interface (See Section 6.2.1.) rather than a reflection of the material properties of the surficial materials in the survey area. It should be further noted that due to the reduced vertical resolution (0.3 m: See Section 2.3.3.3.) of this sub-bottom profiling

[8] See Figures 6.1, 6.10, 6.11, 6.12, 6.15, 6.16, 6.17, 6.20, 6.21, 6.22, 6.24, 6.25, 6.26.

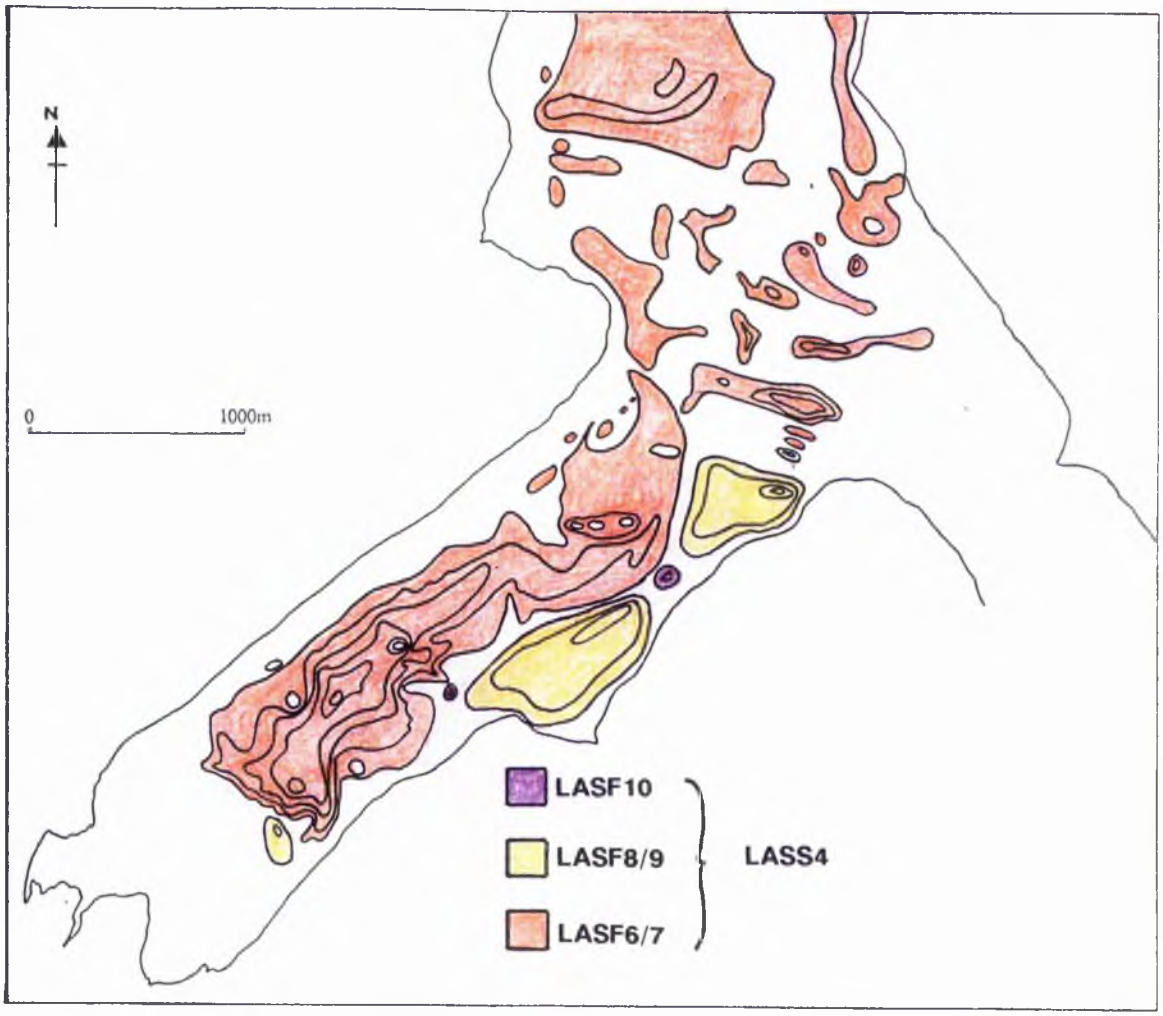

Figure 6.23. The spatial distribution of Seismic Sequence 4 (LASS4) including isopach contours in two-way travel time (Contour interval 4 milliseconds).

system and the thickness of this upper reflector (0.5 ms TWT ≈ 0.375 m)[9] it is unlikely that any coherent seismic data for the top 0.4 m of the survey area can be interpreted.

6.3.4.1. Seismic Facies Unit 6 (LASF6).

Seismic facies unit 6 has a low internal backscatter level and occasional weak, parallel, inclined internal reflectors with a high lateral continuity and extent (See Figure 6.24.). The lower sequence boundary to this unit again has high lateral continuity and extent, but the style of this basal reflector varies with the acoustic properties of the underlying sequence. Where LASF6 overlies the high internal backscatter material of LASS1 and LASS2 the sequence boundary can be clearly distinguished, however, where it rests upon LASS3 an arbitrary boundary has to be drawn. LASF6 has a conformable upper facies boundary with the ubiquitously overlying LASF7 (See Figure 6.24.). LASF6 attains a maximum thickness of 10 ms TWT.

This facies has a restricted distribution to areas south-west of the Luib inlet and north-east of the prominent slope that traverses the entire width of Loch Ainort at it's head (See Section 4.3.1.1.), occurring in the deepest parts of the pre-existing surface created from the underlying sequences within this region. This lower sequence boundary describes a broad basin form only being disrupted by the occasional topographic highs of LASS1 (See Section 6.3.1.1.). Where present the internal reflectors parallel the underlying sequence boundary with LASS1, LASS2 and LASS3 (See Figure 6.24.). At the margins of the "Inner Loch" palaeo-basin these internal reflectors onlaps on to the lower basal reflector.

6.3.4.2. Seismic Facies Unit 7 (LASF7).

Seismic facies unit 7 has a medium internal backscatter level and occasional weak, parallel, inclined internal reflectors with a high lateral continuity and extent (See Figure 6.24.). Again its lower boundary varies in style depending on the nature of the underlying material. In the "Mouth Region" and the outer part of the "Inner Loch" region LASF7 lies directly upon LASS1 material and so describes a prominent easily identifiable basal reflector (See Figure 6.10). Towards the head of the loch, where present, LASF7 has a conformable boundary with

[9] Value based on a compressional velocity value of 1500 ms^{-1}.

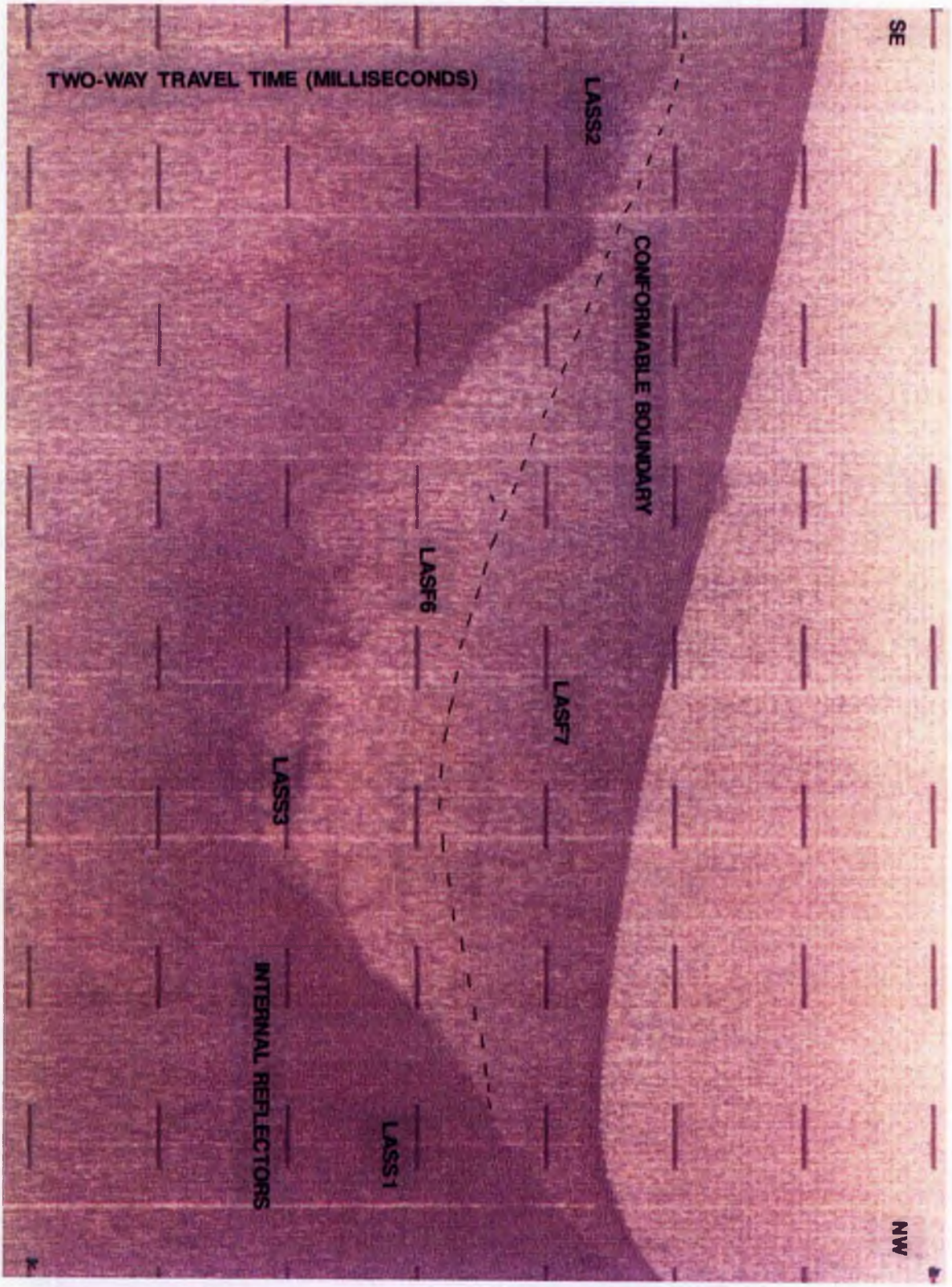

6.24. A pinger profile showing a characteristic image of LASF6 and LASF7 (Survey Line A1)

LASF6 (See Section 6.3.4.2.: Figure 6.24.) and elsewhere an arbitrary boundary against LASS3 (See Figure 6.20. or 6.21.). In a restricted number of traces, north-west of the Luib inlet, LASF7 lies directly up on LASS2 where it describes a diffuse and chaotic lower boundary (See Figure 6.15. or 6.16.). In the deeper parts of the "Unnamed Strait" LASF7 lies unconformably upon the prominent upper reflector characteristic of LASF5 (See Section 6.3.3.2.: Figure 6.22.). Again at the margins of this outer basin LASF7 onlaps on to the steeper loch margins composed of LASS1 material (See Figure 6.12. and 6.22.). LASF7 attains a maximum thickness of 12 ms TWT in the deepest part of the "Inner Loch" body compared to a maximum thickness of 6 ms TWT for the surface veneers of the "Unnamed Strait" and "Mouth Region".

As with LASF6 the internal reflectors parallel the broad basin topography of the underlying sequences and onlap the steeper slopes of the loch margins and topographic highs. The upper reflector to LASF7 coincides with the loch bed and describes a smooth form throughout (See Discussion Above).

6.3.4.3. Seismic Facies Unit 8 (LASF8).

Seismic facies unit 8 is a medium to high internal backscatter level with a chaotic, acoustically turbid texture with weak but thick and continuous internal reflectors (See Figure 6.25.). This seismic facies unit has a restricted distribution, occurring at two sites on the south-eastern shore of the "Inner Loch". It occurs beneath the gently inclined, shallow, surface of the Luib protrusion and the broad, shallow plateau area that extends from the lower slopes of Am Meall (See Figure 6.22.). At both these sites LASF8 has a chaotic, undulating and diffuse upper bounding reflector with LASF9 and a weak and diffuse unconformable basal reflector with LASS1. LASF8 attains a maximum thickness of 4.33 ms TWT.

6.3.4.3. Seismic Facies Unit 9 (LASF9).

Seismic facies unit 9 (See Figure 6.25.) is either acoustically transparent or displays a very low backscatter level, with no internal reflectors. LASF9 has a prominent bottom reflector which varies from being smooth and well defined where it unconformably overlies LASS1

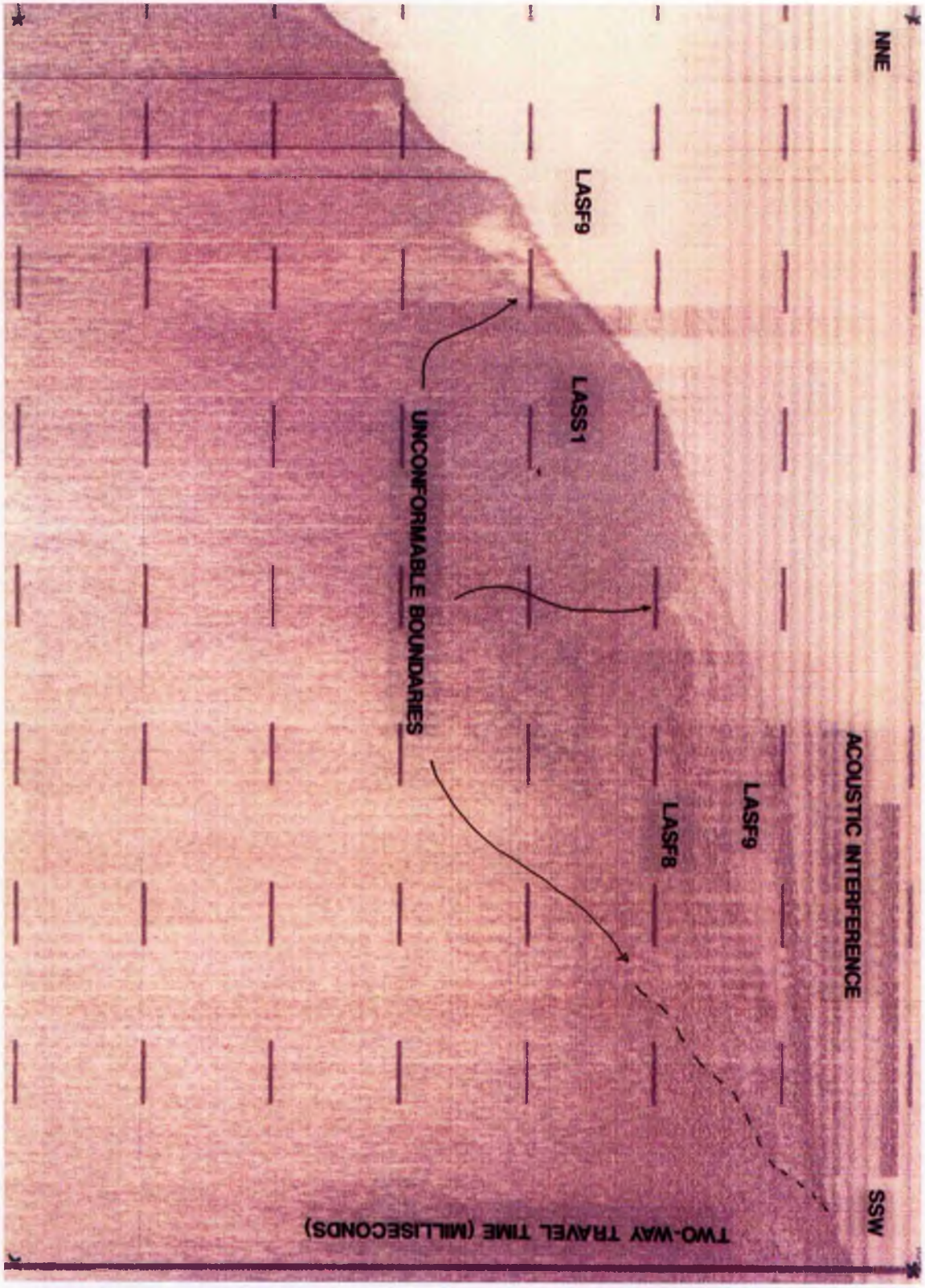

Figure 6.25. A pinger profile showing a characteristic image of LASF8 and LASF9 (Survey Line A13).

(See Section 6.3.1.) to diffuse and disturbed where it unconformably rests on LASF8 (See Section 6.3.4.4.). Due to it's intimate relationship with LASF8, LASF9 again has a limited distribution occurring as thin veneers on the upper surface of the shallow Luib protrusion, on the plateau of Am Meall and within a single small depression on the northern slope of the Am Meall plateau (See Figure 6.23.). The upper boundary of this seismic facies unit represents the current loch bed, however, as described for LASF7, its thin and strong appearance is a product of the system configuration rather than a true representation of the material properties of this unit (See Section 6.3.4.). LASF9 attains a maximum thickness of 6.25 ms TWT.

6.3.4.5. Seismic Facies Unit 10 (LASF10).

Seismic facies unit 10 has a low to medium internal backscatter level with strong internal reflectors which are parallel, inclined and have a high lateral continuity (See Figure 6.26.). Where present they have a diffuse and disturbed but concaved bottom reflector with the underlying LASF1. The strong internal reflectors parallel the concave nature of the basal reflector but terminate against the convex form of the upper reflector, which is coincident with the loch bed. Again this facies has a very restricted distribution (See Figure 6.23.) to shallow depressions on gently sloping plateau areas at the south-eastern margins of the "Inner Loch" region. In fact, LASF10 can be identified on only two survey lines, A5 and B1, so the three dimensional form of this seismic facies unit cannot be determined. LASF10 attains a maximum thickness of 4.16 ms TWT.

6.4. CONCLUSION.

Seismo-stratigraphic analysis of the sub-bottom profiles acquired from the Loch Ainort survey area has enabled the identification of 4 seismic sequences which can be further subdivided into ten seismic facies units (See Table 6.4.: Overleaf). The lowest sequence imaged is LASS1 (See Section 6.3.1.) which underlies the entire survey area. This sequence is typified by high internal backscatter level, numerous point hyperbolae and a dominantly strong upper boundary, particularly with LASS3 and LASS4. Within the "Mouth Region"

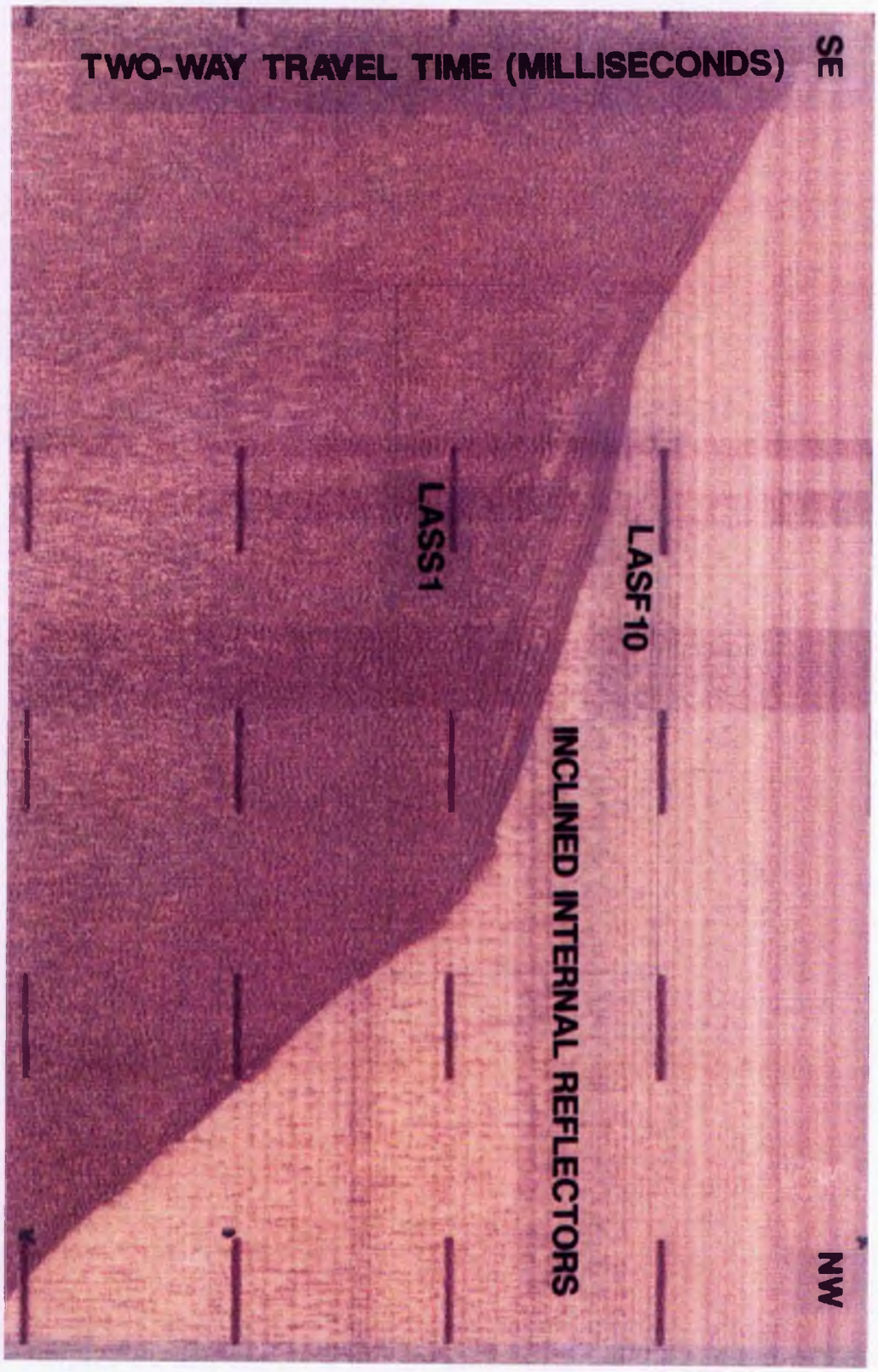

Figure 6.26. A pinger profile showing a characteristic image of LASF10 (Survey Line A5).

and at sporadic localities within the "Inner Loch" region, this upper reflector describes a marked relief, which is characterised by a series of asymmetric and occasionally symmetrical topographic highs. As discussed in Section 6.3.1.1. where overlap of survey lines occurs many of these topographic highs coincide with the ridges (AR1 - AR52b) identified from the side scan sonographs (See Section 5.3.). The "Unnamed Strait" is founded by a seismic facies unit (LASF2: See Section 6.3.1.2.) with similar acoustic properties but with an upper sequence boundary that lacks the extreme relief described in the remainder of the survey area.

Seismic Sequence	*Seismic Facies Units*		
LASS4	**LASF7:** medium internal backscatter level and occasional weak, parallel, inclined internal reflectors with a high lateral continuity and extent	**LASF9:** acoustically transparent or displays a very low backscatter level, with no internal reflectors.	**LASF10:** low to medium internal backscatter with strong internal reflectors which are parallel, inclined and have a high lateral continuity.
	LASF6: low internal backscatter and occasional weak, parallel, inclined internal reflectors with a high lateral continuity and extent.	**LASF8:** medium to high internal backscatter, with a chaotic, acoustically turbid texture with weak but thick and continuous internal reflectors.	
LASS3	**LASF4:** low to medium internal backscatter, with thick strong, discontinuous, horizontal to gently inclined, internal reflectors of high lateral extent.	**LASF5:** medium internal backscatter and thick, strong, parallel, internal reflectors with great lateral continuity. Thin but clearly marked upper reflector.	
LASS2	**LASF3:** very high internal backscatter, with a mottled appearance and no discrete internal reflectors. Upper bounding reflector irregular and chaotic describing a subdued topography.		
LASS1	**LASF1:** very high internal backscatter, with no discrete internal reflectors and a distinctive mottled appearance. Pronounced upper surface describes marked topographic highs.	**LASF2:** very high internal backscatter with no discrete internal reflectors and a distinctive mottled appearance. Upper boundary smooth, low relief, but laterally extensive.	

Table 6.5. A seismic para-stratigraphy, based on sub-bottom profiles, for the Loch Ainort field area.

Due to the similarity in acoustic properties between LASS2 and the underlying LASS1 discrimination of this sequence can be problematic, confident identification being only possible where reflectors within the bottom multiple are present. LASS2 is restricted to sites within the "Inner Loch" south-west of a transitional boundary north of the Luib inlet (See Figure 6.9.). This boundary coincides with the ridge complex identified from the side scan sonographs (See Section 5.3.3.) and centred on AR17. The upper reflecting boundary of this sequence is more diffuse and exhibits much more subdued relief than that described for LASS1.

LASS3 rests unconformably on the pre-existing surface described by the sequence boundaries with LASS1 and LASS2. This sequence is typified by a series of parallel, conformable, discontinuous internal reflectors with a high lateral extent and which onlap on to the underlying sequences. In the "Inner Loch" region this unit occurs at the lowest points within the pre-existing surface and has an arbitrary upper boundary with the seismic facies units LASF6 and LASF7 of seismic sequence 4. In the "Unnamed Strait" the internal reflectors, within the facies typifying this sequence, exhibit greater lateral continuity and onlap on to the simple basin form described by LASS1. Further the upper sequence boundary in this area is characterised by a single thin strong reflector with a gentle undulating relief.

LASS4 is the chrono-stratigraphically highest seismic sequence to be identified within the Loch Ainort survey area. Between the variable lower sequence boundary with LASS1, LASS2 and LASS3 and the current "time line" of the loch bed, occurs the a diverse group of five seismic facies units (LASF6 to LASF10). LASF6 and LASF7 dominate this sequence representing thick accumulation of low to medium internal backscatter material with weak internal reflectors. The maximum thickness of this material occurs towards the head of the "Inner Loch", with the "Mouth Region" and the "Unnamed Strait" being only partially covered by a thin veneer of LASF7. The remaining three facies identified have a very limited distribution, being restricted to the marginal slopes of the "Inner Loch" and in particular the shallow plateau areas off Luib and Am Meall.

CHAPTER 7

7. SEDIMENT ANALYSIS

7.1 INTRODUCTION

The geophysical investigations undertaken within Loch Ainort (See Chapters 5 and 6) can only provide comparative data on the vertical and spatial distribution of sediment types. In order to assign a lithological nomenclature to the seismic sequences and facies described in Sections 5.3. and 6.3. it is necessary to ground truth these sequences by direct sampling of the sediments present in the survey area. Ideally, the sampling stage should be undertaken as a post-seismic interpretational phase, so sites for the optimum retrieval of representative material of each seismic facies unit can be taken.

In addition to ascribing a sedimentological nomenclature to the seismic facies units, the analysis of core and surface sediments provides two other important components of palaeoenvironmental reconstruction. Firstly, when recorded on their own, the depths, thickness and dimensions of sequences and internal structures described in Section 6.3. can only be described in terms of two-way travel time (milliseconds: See Section 6.2.1.). This is because it is impossible to deduce the velocity of sound through each medium from the traces themselves. If the sediment type represented by a particular seismic facies unit is known, it is then possible to assign (by comparison with empirical studies) or calculate an average velocity value for each seismic facies unit or seismic sequence (See Section 7.2.6.). From this information the actual dimensions in metres for each sequence or feature can be calculated. Secondly, different sedimentary environments can be numerically characterised (Section 7.2.3.) by applying a variety of statistical calculations to the particle size distribution data collected at each site. It has therefore been possible to supplement the environmental inferences that can be deduced from the gross morphology described from the geophysical data (See Section 8.2.).

7.2. LOCH AINORT

A total of 14 cores were obtained from the Loch Ainort survey area (See Figure 7.1.) with a maximum core retrieval length of 1.28 m. At 7 sites surface sediment samples were collected. Extensive laboratory analysis has been undertaken on all the samples in order to both, assign a velocity value to the lithological units believed to be present within the area and to supplement the environmental reconstruction inferred from the compositional and morphological data obtained from the geophysical surveys. The following sections describe the rationale behind, and the reality of, the sampling program together with the methodology of, and the results from, a series of laboratory techniques. The information obtained from these analyses enables the identification and characterisation of four litho-facies for the Loch Ainort area. Each of these litho-facies are described and assigned an average velocity value.

7.2.1. CORE AND SURFACE SAMPLE LOCALITIES

Sediment sampling sites for the Loch Ainort field area were chosen to most effectively utilise the coring equipment available (See Section 2.4.). In this case the gravity corer at our disposal had a maximum operational core retrieval length of 3.5 m. Consequently the coring plan was constructed with the intention to access sites where all the seismic facies units identified from the sub-bottom (See Section 6.3.) and side scan sonar surveys (See Section 5.3.) were within 3.5 m of the surface. From 21 pre-determined sites, material was retrieved from a total of 19. Sediment was collected in the form of 14 cores (JC1 and JC2 collected at the same site) and 7 surface samples, one surface site duplicating the corresponding core site (JC1/JC2 and J1: See Figure 7.1.)[1]. The cores retained have a diameter of 5.7 cm and range in length from 18 cm (JC 4) to 128 cm (JC 1).

As described in Section 2.4., the positioning of the individual core sites was accomplished by the Magellan© GPS system. However, for reference in the text, the Magellan latitude and longitude co-ordinates have been converted to the OSGB36 grid co-ordinates using the Positron Navigation GEOGRID:GB co-ordinate converter. In addition, the water depth from

[1] The prefix JC for each core site and J for each surface sample shall be retained throughout.

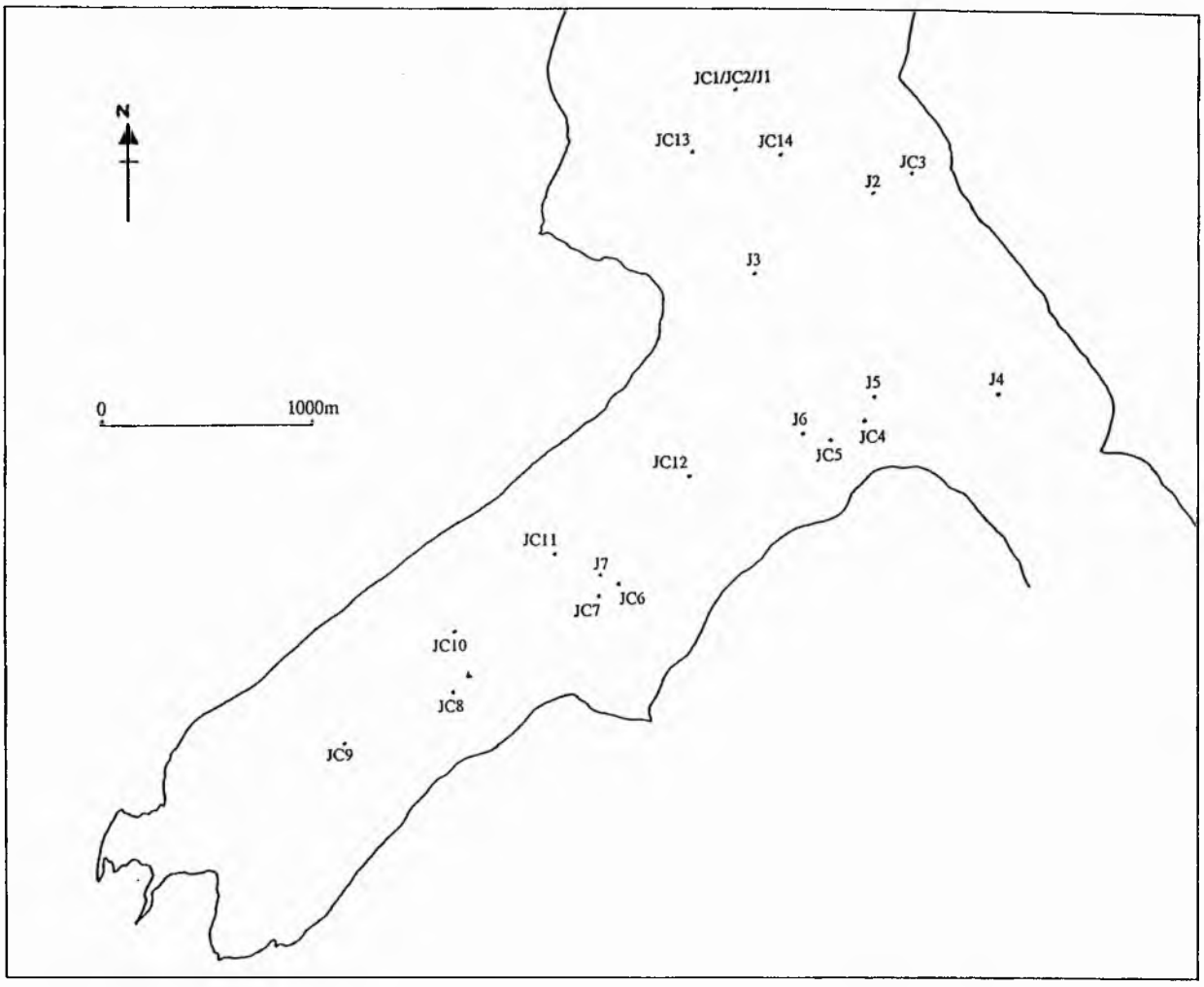

Figure 7.1. Locality of gravity cores and surface sediment samples taken from within Loch Ainort.

which each sample was taken was recorded on an echosounder trace obtained during each core drop (See Figure 7.2.). Using the tidal conversion method described in Section 4.2.3. these depths were converted to metres below Ordnance Datum Newlyn.

7.2.2. SEDIMENT ANALYSIS

Each core sample was X-rayed (for the non-destructive analysis of the material: See Section 7.2.2.1.), logged (See Section 7.2.2.2.), and sub-sampled at 10 cm intervals (or more frequently where boundaries were visible) to provide material for laboratory (See Section 7.2.2.3. and 7.2.2.4.) and X-Ray Diffraction analysis (See Section 7.2.2.5.). It should be noted that the verbal size grades used in the descriptive passages below are based on the Udden-Wentworth Grade Scale (Wentworth, 1922).

7.2.2.1. X-Ray Analysis.

A selected number of the cores (JC1, 2, 3, 5, 6, 7, 8, 9, 10 and 12) were subjected to X-Ray analysis to enable rapid, non-destructive investigation of sedimentary material and the identification of any structures invisible to visual inspection (Axelsson, 1983). The plastic liners containing the core material were cleaned and nominally subdivided into 40 cm sections, a measure which represents the maximum dimensions of the photographic plates. Each sub-divided section was numbered (increasing towards the bottom of the core) by adhering a lead painted number plate, which is opaque to X-rays, to the outer surface of the liner. The cores were analysed at 55 kV and 100 mA for 0.1 seconds by the staff of the Cottage Hospital, Radiological Unit, St.Andrews. Visual descriptions were made for each X-Ray photograph (See Below). It should be noted by the reader that all depth measurements quoted are approximations, as it is impossible to define the upper and lower margins of the core from the photographs alone. The grid co-ordinates (OSGB36) are given in square brackets for each sample site:

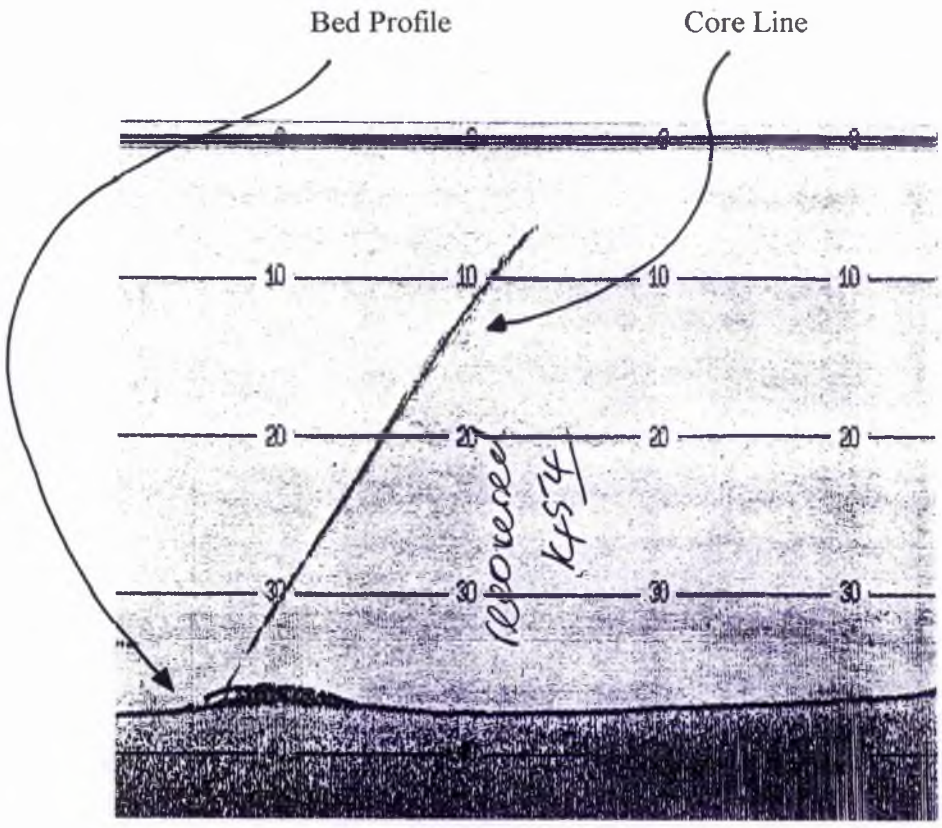

Figure 7.2. Example of echosounder trace taken during coring procedure.

JC1. [157088, 830922]. See Figure 7.3.: Between 0 and 21 cm is a fine light toned matrix (~70% of core) with numerous well distributed whole gastropod shells and occasional bivalve fragments. The gastropods are high spired forms (with a corresponding low apical angle), dextrally coiled, with no signs of internal ornaments but a well developed columella. The bivalve fragments are all sectioned perpendicular to the valve. Poorly defined layering between 14 and 20 cm is represented by slight, irregular colour variation (dark and light bands). The darker layers are ≤ 5 mm thick, whilst the intercalated lighter layers vary between 10 and 20 mm thick. All of the layers are concaved towards the top of the core. Between 21 and 28 cm a shell bed of the high spired gastropods is present. Both the upper and lower boundaries are well defined and concave towards the top of the core, which is almost certainly the consequence of deformation during the coring process.

Underlying the shell bed is a diamictic sediment (28-102 cm) with a dominant fine grained matrix (85% of core) and a large number of randomly dispersed, sub-angular to sub-rounded lithic fragments These lithic fragments vary in size from 2 to 65 mm, with the larger dimensions representing a number of well defined isolated pebbles and cobbles; two at the boundary with the shell bed, single pebbles at 41 cm, 47 cm, 62 cm and the largest (maximum dimension 65 mm) sub-rounded cobble between 75 and 81.5 cm. The concentration of lithic fragments increases gradually down core with a corresponding decrease in faunal content. No faunal fragments were identified below 39 cm. From 102 cm to the base of the core at 130 cm there is a marked increase in the proportion of lithic clasts relative to matrix (clasts 80% of core section). Clasts exhibit a range of sizes (3-30 mm) and grain shapes (sub-angular to sub-rounded). No layering could be identified below 28 cm.

JC2. [157088, 830922]: This core comprises a uniform fine grained material with numerous well distributed high spired gastropod fragments (See **JC1** for full description) and whole shells. A single, isolated, sub-angular trapezoid pebble (maximum dimension of 32 mm) occurs between 30.5 and 34 cm. Linear, occasionally amorphous, cross-cutting darker material (maximum width 3 mm) oriented parallel to the core margins probably represents a fractured section of the core.

JC3. [157883, 830471]: A uniform, fine grained material with numerous, whole, high spired gastropods (See **JC1**) and bivalve shells well dispersed through this core but

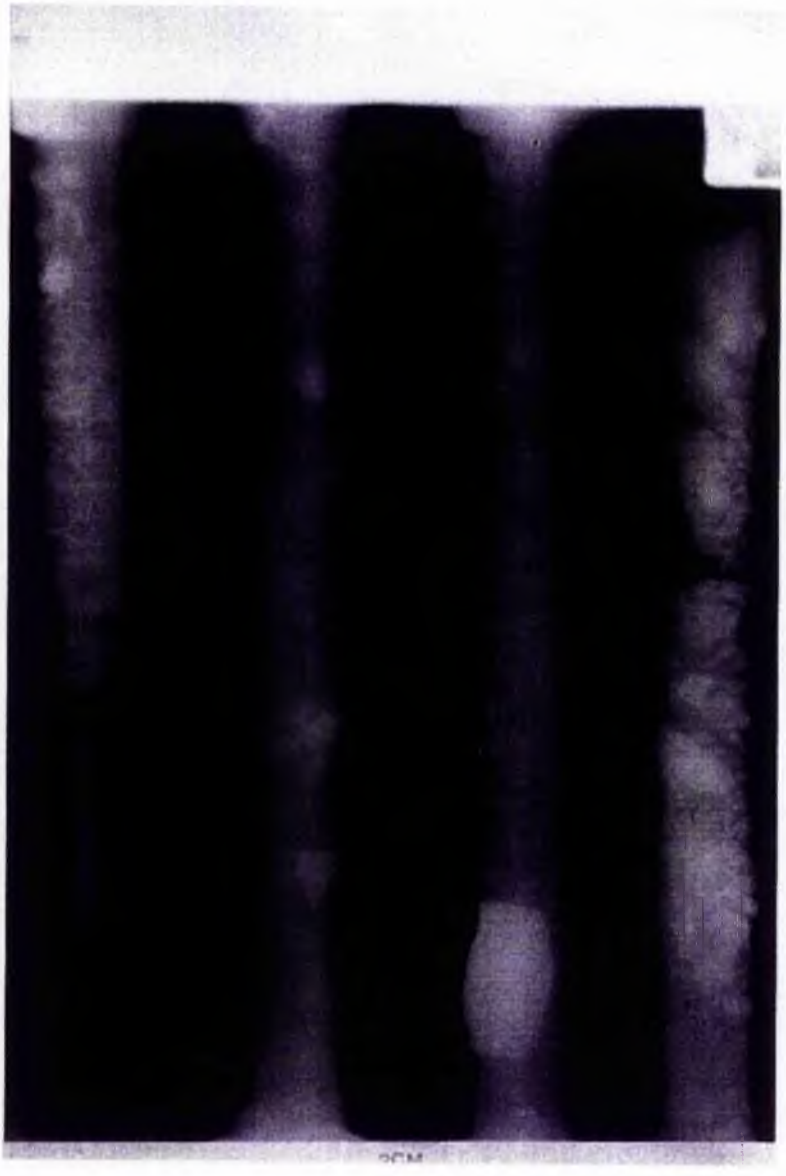

Figure 7.3. X-ray photograph of JC1

occasional shell clusters also occur. Below 42 cm the concentration of faunas increases and the first small (≤ 5 mm), sub-rounded to rounded lithic pebbles and granules appear.

JC5. [157438, 829233]: This is a core of uniform granular sediment with 60% of the core consisting of visible single and agglomerated (grains appear to be interconnected) grains between 1 and 2 mm in size. These grains lie within a fine subordinate matrix. There is no evidence of the presence of lithic or faunal fragments.

JC6. [156393, 828607]: The upper section of this core has a fine granular texture with a gradational boundary at approximately 23 cm with a fine grained, weakly laminated sediment. The laminae are represented by discontinuous, darker layers which pinch out towards one margin, decreasing from a thickness of 13 mm to 1 mm over a distance of 40 mm. The laminae are inclined and concave up core. A large, core parallel fracture occurs below 34 cm, offset towards one wall. Whole high spired gastropod (See **JC1**) and bivalve shells are distributed throughout the core but decrease in concentration with depth.

JC7. [156310, 828556]: Coarse grained, granular, well packed sediment between 0 and 6 cm is present. The maximum particle dimension varies between 2 and 15 mm with little evidence of a subordinate fine matrix. Individual clasts are sub-angular to sub-rounded in form. There is no sharp boundary at the base of this layer but a rapid gradational change to finer but still granular material. No fauna are present in the upper part of the core but high spired gastropods (See **JC1**) dominates the rest of the core. Between 51 and 53 cm three large (24 mm) globose, low spired (high apical angle) and large last whorl gastropods are present. A large inclined fracture at an oblique angle to the core wall occurs between 42 and 47 cm and which opens to a maximum of width of 4 mm. An associated en-echelon fracture pattern at an oblique angle to the main fracture is indicative of fine grained sediment dominating at depth. No large lithic clasts were identified below 6 cm.

JC8. [155579, 828135]: This core comprises of a fine grained sediment with identifiable discontinuous "wispy" layering throughout, but most clearly defined between 21 and 31 cm. The wispy layers are darker in tone and thinner (commonly ≤ 10 mm) than the predominant lighter (≥ 15 mm) layers. The darker layers tend to thin towards the centre of the core from a maximum margin width of 15 mm to a central width of 3 mm. Between 15 and 17 cm a

thicker darker layer (20 mm) is associated with a proto-shell bed composed of high spired gastropods (See **JC1**). At approximately 54 cm a single, isolated, tear-drop shaped rounded clast with a maximum dimension of 16 mm occurs within fine grained sediment. There is evidence of a darker layer at its up core pointing apex but it is only present on one side of the clast. There is no evidence of disturbance of the layering.

JC9. [155053, 827925]: This core comprises of a fine grained sediment with a high faunal content in the uppermost 20 cm. Below 20 cm the core has a lighter tonal coloration with poorly defined, discontinuous, dark wispy layers. Between 39 and 45 cm three large (≤ 30 mm) sinistrally coiled gastropod with a short spire, a large final whorl (giving a large apical angle) and a well developed siphonal canal are present. Occasional small (≤ 3 mm) angular fragments occur within the fine grained matrix but there is little morphological evidence to suggest either a lithic or faunal composition.

JC10. [155617, 828430]. See Figure 7.4.: Faint wispy laminae are present, sporadically distributed, throughout this core of fine grained sediment. A concentration of these wispy laminae occurs between 28 and 31 cm with three different layer types represented by dark, medium and light grey tonal variations. The latter lighter layer appears to be composed of layer parallel oriented shell fragments. Individual layers vary in thickness between 1 and 5 mm and do not appear to continue across the whole width of the core but taper towards the centre of the core. The majority of the layers are inclined and all are concave up core, some with pronounced central dips unlikely to be entirely due to core deformation during sampling. The faunal content is represented by small fragments of broken bivalve shells with occasional high spired gastropods and a single articulated bivalve shell. Between 4 and 19 cm a large, discontinuous, core parallel fracture offset towards the core margin opens to a maximum width of 4 mm.

JC12. [156765, 829106]: This core is characterised by uniform, fine grained material dominated by a high faunal content throughout. Whole, high spired gastropods and bivalve shell fragments are the only fauna identified. No layering is present and lithic content is low with a single, rounded pebble (maximum dimension 11 mm) at 38 cm.

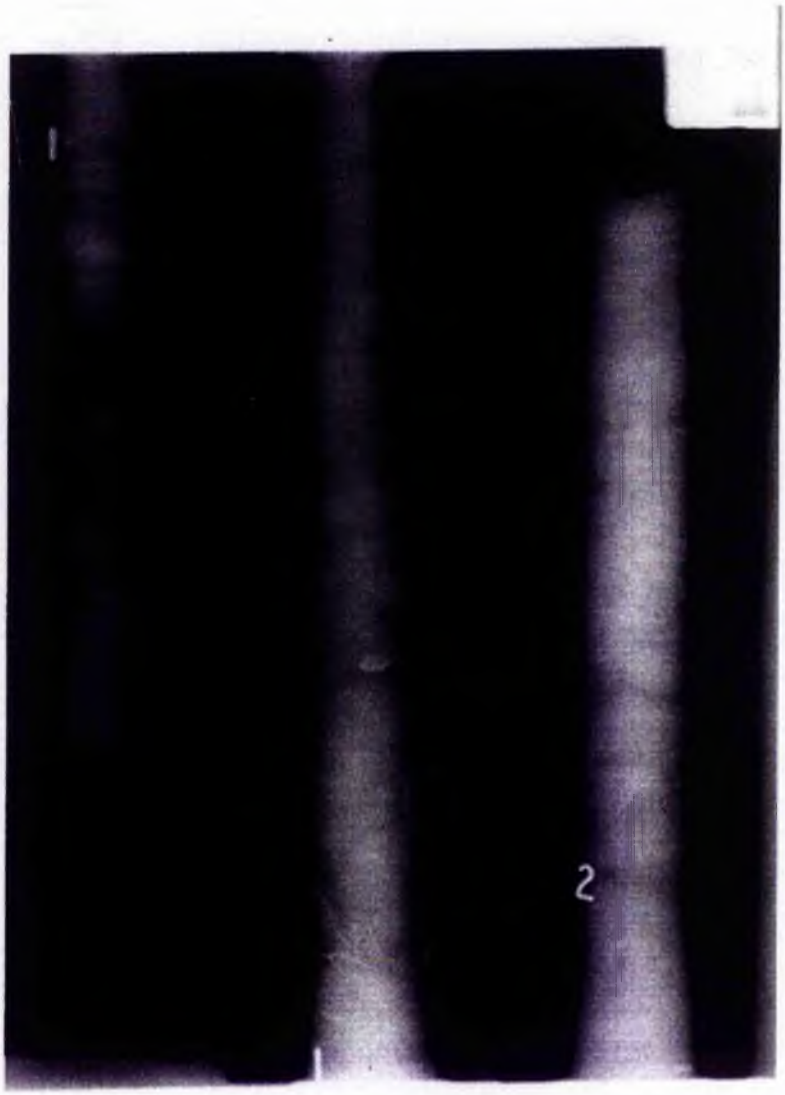

Figure 7.4. X-ray photograph of JC10

Collectively the X-Ray photographs enabled the identification of a number of different sediment types with their delimitation being most successful when strongly contrasting units are adjacent to each other. In general the majority of the boundaries between units are gradational making precise demarcation difficult from visual inspection alone. Internal structures are not prevalent in the cores, with the identification of only thin, indistinct, discontinuous wispy laminae in cores **JC1**, **JC6**, **JC8**, **JC9** and **JC10**. The X-Ray photographs have effectively identified the presence of large, isolated sub-angular to sub-rounded lithic fragments. It was also possible to identify the presence of a large faunal content in many of the cores, with a predominance of whole high spired gastropods and fragmented bivalve shells.

7.2.2.2. Core Descriptions.

Having undergone the non-destructive examination by X-Ray analysis (See Section 7.2.2.1.) all of the fourteen cores were split and visually analysed. To remove the sediment cores from their individual liners, each core was frozen and then the outer surface rapidly heated to create a low friction layer between the sediment and the liner. This enabled the sediment core to be forcibly extruded from the liner and into purposely cut "guttering" holders. Each core was then wrapped in strengthened polythene and returned to a cold store to thaw out at a controlled (5°C) temperature. Evidently such a process may lead to the destruction or creation of fine surface structures on each core and so care had to be taken in the interpretation of any surface features.

On completion of the whole core descriptions, each core was longitudinally split and re-examined in order to identify the presence of internal structures and lithological boundaries. The whole and sectioned core descriptions are as follows:

JC1. [157088, 8309221]. Total Length: 128 cm.

Whole Core Description: Within this core there is a gradational transition of colour from grey-green, to light grey and finally to light brown at approximately 110 cm. Faunal fragments present in the upper core section decrease in number below 28 cm. These

fragments are identified as being dominantly *Archimediella*[2] but with occasional bivalve fragments. All of the faunal fragments have dimensions of < 5 mm. The core fines rapidly at approximately 35 cm and this change is associated with an apparent increase in the water content of the core at this level. This oversaturated state is suggested by the presence of standing water within the core at this level and the fact that the core expanded between 35 and 51 cm. All these factors are indicative of an increase in clay content of the sediment at this section of the core. Occasionally, lithic pebbles and cobbles break the surface of the core throughout this section. From 101 cm to the base of the core the sediment has diamictic characteristics with a silty clayey matrix and a large increase in the number of visible lithic gravels, that range in size from 20-50 mm. No faunal fragments could be found in this lower section.

Sectioned Core Description: From 0-20 cm is a grey-green fine grained sediment, competent but easily parted, with no standing water and no obvious lithic fragments. Between 20 and 27 cm a shell bed is present with a concentration of whole, *Archimediella*. At the base of the shell bed there is a marked break with an underlying grey clayey homogeneous mud which is very cohesive and therefore difficult to part. Within this section no bedding structures could be identified and the faunal content is nil. The pebble concentration (average size 15 mm) increases down core with the section being dominated by three large isolated pebbles one at 68-74 cm and two at 103-109 cm. All these large grains have their long axes oriented parallel to the core margins. Lithic fragment size and morphology varies from discoid to equant forms with maximum dimensions from 65 to 32 mm (pebbles). The composition of these pebbles shows an equivalent variation including fine grained porphyritic dolerites, equigranular peridotites and leucocratic, fine grained granophyres. No obvious disturbance of the surrounding sediments is caused by the pebbles. A marked increase in the number of lithic gravels occurs at 115 cm, with the section becoming almost clast dominated. Again the section is dominated by two large pebbles between 114 and 122 cm. Form, composition and size of these larger pebbles again vary between a bladed, sub-angular, coarse

[2] This is the dominant fauna throughout the cores. It is a gastropod belonging to the Turritellidae family.

grained granodiorite (maximum dimension 63 mm) to an equant, sub-angular fine grained felsite (maximum dimension 30 mm.

JC2. [157088, 830922]. Total Length: 39 cm.

Whole Core Description: The core has a grey-green colour throughout. No lithological structures are present and there is no obvious particle size variation. The core represents a fine grained, homogeneous, cohesive and oversaturated (standing water present in upper section) clayey silt. Shell fragments are minimally dispersed throughout the core but at the base of the core there is an increased concentration of whole *Archimediella* .

Sectioned Core Description: This section reveals little more than that gleaned from the whole core description, the core being composed of a homogeneous grey-green clayey silt. At 34 cm two large (maximum dimension 40 mm), isolated, lithic pebbles of contrasting composition. One pebble is a sub-rounded fine grained ultrabasic rock whilst the other is composed of a fine grained microgranodiorite. Both pebbles were oriented parallel to the core walls. Poorly defined, fine (< 1 mm) bedding was identified in a section of sediment 1 cm thick, located at the apex of one of the isolated pebbles. At the base of the lower isolated pebble (36-39 cm) there is an apparent fining of particle size.

JC3 [157883, 830471]. Total Length: 60 cm.

Whole Core Description: A uniform, homogeneous, grey-green, fine sandy mud with no visible lithological variations. No identifiable siliciclastics are present but a large number of fragmented and entire shells, dominantly of *Archimediella*, do occur. A relatively dry and stiff core but still sufficiently cohesive to retain its shape in the core container. There is a possible increase in grain size at base (58-60 cm).

Sectioned Core Description: A grey-green core with uniform colour and structure throughout. The core has a high faunal (*Archimediella* and the articulated bivalve *Dosinia*) content which increases rapidly at a depth of 40 cm to represent 30 % of the total core section at this level. Fine grained basic pebbles and granules start to dominate the core at 58 cm.

JC4. [157594, 829317]. Total Length: 18 cm.

Whole Core Description: A grey-green fine grained, cohesive mud, with lithic fragments present throughout the core. All the lithic fragments are < 7 mm in diameter (pebbles to granules) with the greatest concentration being in the upper 10 cm. A high percentage (55%) of fresh, red and green coralline algae (Corallinaceae) is concentrated in uppermost centimetre of the core. The percentage and state of preservation of this algae decreases with depth.

Sectioned Core Description: The sectioned core reveals no structure, particle size variation or lithological boundaries. The high percentage of coralline algae (Corallinaceae) in the upper section of the core does however, decrease the cohesion of the sediment to give a more friable material.

JC5. [157438, 829233]. Total Length: 31 cm.

Whole Core Description: A grey-green fine grained, cohesive, mud with no obvious particle size variation along the length of the core. Red and white coralline algae (Corallinaceae) are the dominant fauna throughout with the greatest concentration being towards the top of the core.

Sectioned Core Description: The sediment in this core is more friable and granular than suggested by the whole core section. This granular texture is due to the pervasive presence of the algae. Lithic fragments are sporadically distributed throughout the core. The core becomes more cohesive with depth due to the decreasing percentage of coralline algae (Corallinaceae).

JC6. [156393, 828607]. Total Length: 44 cm.

Whole Core Description: The core is composed of grey-green (slight brown coloration on the outer surfaces), cohesive, fine grained silty sands which fine and become more cohesive with depth. Numerous small shell fragments (< 4 mm) are sporadically distributed along the barrel surfaces. Along the entire surface of the core are numerous small (< 1 mm) cubic

depressions, with a faint white coloration, interpreted as representing the growth and selective removal (probably during core retrieval) of halite crystals.

Sectioned Core Description: From this core it was not possible to identify any colour, structure or lithological changes. An inverse grading relationship is present in the core, with particle size decreasing from fine sands at the top of the core to silty muds at its base. Bivalve (*Chamlys*), *Archimediella* and globular gastropod (*Littorina littorea*) fragments are common throughout the core many of which exhibit bored and serpulid encrusted surfaces.

JC7. [156310, 828556]. Total Length: 57 cm.

Whole Core Description: The core has a grey-green coloration with a pronounced inverse grading relationship present in the upper section. The uppermost 5 cm is dominated by large (maximum dimension ≤ 32 mm), sub-angular to sub-rounded lithic pebbles (including fine grained felsitic and basaltic compositions) many with serpulid encrusted surfaces. The coarse upper section is followed by a rapid reduction in particle size between 10 and 20 cm from medium to fine sands and finally to the muds that dominate the remainder of the core section. The finer grained sediments at the base correlate with an increase in standing water, suggesting oversaturation of this part of the core.

Sectioned Core Description: A grey-green coloured core in which lithic clasts are concentrated in the uppermost 5 cm. The concentration of these clasts undergoes a rapid transitional decrease down core. No sharp lithological breaks are identified in the core. Between 0 and 40 cm the sediment is consolidated and easily parted, maintaining its shape on dissection. By contrast the sediment below 40 cm becomes more cohesive and is not easily separated. Shell fragments are concentrated between 41 and 43 cm with *Archimediella* and *Littorina littorea* dominating the faunal assemblage.

JC8. [155579, 828135]. Total Length: 85 cm.

Whole Core Description: the core is composed of grey-green soft, pliable, cohesive very fine clayey muds. No lithological, colour or particle size variations were observed down the

core. The oversaturated nature of the sediment results in standing water being present in the upper sections of the core.

Sectioned Core Description: The cohesive nature of the core (probably representing increased clay content) makes the sectioning of the core very difficult. No further evidence for lithological, colour or particle size changes within the core could be identified. At 51 cm a large (maximum dimension 20 mm), solitary pear shaped, sub-rounded granodioritic pebble is present. The core has a very low faunal content throughout.

JC9. [155053, 827925]. Total Length: 78 cm.

Whole Core Description: A generally grey-green coloured core of uniform, cohesive, oversaturated (standing water present throughout the core) fine grained muds. A slightly darker grey/grey-black coloration occurs towards the top of the section and an associated pungent odour of H_2S which may suggest a recent period of anoxic conditions Sporadic shell fragments (no entire shells present) which decrease in concentration with depth.

Sectioned Core Description: The sectioned provides very little additional information than that gleaned from the observations of the whole core. Dark coloration of sediment is restricted to the uppermost 10 cm with a gradational change to the more pervasive grey-green coloration. A slight, but identifiable transitional decrease in grain size and increase in cohesion does occur with depth. Three large, well preserved gastropods (*Buccinium undatum*) occur between 38 and 42 cm, all with well developed serpulid growths and borings.

JC10. [155617, 828430]. Total Length: 99 cm. Whole Core Description: A grey-green coloration is present throughout the core with no evident lithological boundaries. A down core decrease in particle size is present, with a variation from fine silt at the top to a finer more clay rich sediment at the base. Again there appears to be a corresponding increase in both the cohesive nature of the sediment and the water content of the core towards the base. Minor amounts of shell fragments (<5 %) between 0 and 60 cm with the total absence of fragments below 60 cm. No siliciclastic fragments are present.

Sectioned Core Description: The core is composed of a grey-green homogeneous silt with an inferred increase in clay content below 40 cm due to the increased cohesive nature of the sediment. The faunal content is < 5% throughout the core with the predominant fauna being *Dosinia* (bivalve) fragments.

JC11. [156111, 828773]. Total Length: 20 cm.

Whole Core Description: The core represents a fine to medium grained sand with a high percentage of both lithic and faunal fragments. Large individual pebbles (maximum dimension of 40 mm) of both gabbroic and granitic affinity are present. Sand content increases with depth but the core is still sufficiently competent to retain its shape on dissection. A shell bed is present at the base of the core (18-20 cm), which consists of whole and fragmented, bored *Archimediella* and occasional *Littorina littorea* shells.

Sectioned Core Description: Sectioning exposes no additional lithological boundaries. All three pebbles described from the whole core are angular, equant, coarse grained, leucocratic granitic clasts with maximum dimensions of between 25 and 35 mm.

JC12. [156765, 829106]. Total Length: 55 cm.

Whole Core Descriptions: A grey-green, competent fine muddy sand is present throughout the core with occasional, sporadically distributed lithics. The core appears to be over saturated throughout with standing water being present at all levels. The faunal content is high, with the greatest concentration of material between 0 and 18 cm. There is however a rapid decrease in faunal material beneath 18 cm. *Archimediella*, *Littorina littorea* (gastropods) and *Dosinia* (bivalve) fragments dominate the core.

Sectioned Core Description: The core section exposes no additional sedimentological information. In the sectioned core their is no decrease in faunal content beneath 18 cm.

JC13. [156877, 830643].Total Length: 43 cm.

Whole Core Description: The core represents a grey-green consolidated mud with numerous small (< 3 mm) shell fragments. A rapid coarsening of material occurs between 29 and 31 cm with a significant increase in the lithic gravel component.

Sectioned Core Description: A structurally homogeneous core of grey-green muds with a rapid gradational boundary at 29 cm being marked by a large lithic clast oriented perpendicular to the length of the core. This large (maximum dimension 55 mm), bladed, sub-angular felsitic pebble is again serpulid-encrusted.

JC14. [157287, 830600]. Total Length: 20 cm.

Whole Core Description: Within this short core there is a rapid change in particle size. The top section of the core is represented by a grey-green, fine, cohesive muddy sand, with numerous small lithic (< 3 mm) and shell (< 2 mm) fragments. A sharp lithological break occurs at a depth of 9.5 cm, with the lower half of the core consisting of a friable, poorly consolidated sediment. This lower sediment retains the grey-green coloration but is dominated by lithic pebbles (< 10 mm) within a muddy matrix.

Sectioned Core Description: Exposed between 0 and 1 cm is a large (maximum dimension 53 mm), isolated, fine grained, amygdaloidal basic igneous pebble which is covered by hexagonal serpulid growths. The sharp break at 9.5 cm is easily identifiable between the upper fine grained section and the lower diamictic sediment. The lower unit becomes more clast dominated towards the base of the core. Another isolated, fine grained, basic pebble (maximum dimension 25 mm), oriented perpendicular to the core walls, is exposed at 12.5 cm.

7.2.2.3. Water Content

Once the visual descriptions of the X-rayed and sectioned cores had been recorded (See Section 7.2.2.1. and 7.2.2.3.), sub-sampling of the wet sediment for water content, particle size (See Section 7.2.2.4.) and X-Ray Diffraction analysis (See Section 7.2.2.5.) was

undertaken. For the core material a standard sample interval of 10 cm was chosen to provide representative coverage of the cores. However, additional sub-samples were taken where specific lithological boundaries had been identified. This sampling strategy provided a total of 101 sub-samples. The 7 surface samples have been coned and quartered in order to obtain a representative sample with a bulk mass of between 20 and 30 g.

Following the methodology of Eilers (1981) each sample was weighed, in its natural state, to the nearest centigram and then oven dried at a temperature of 105°C for forty-eight hours. Whilst being maintained in a covered environment, the samples were allowed to cool to room temperature and re-weighed. Assuming the corresponding weight loss represents the removal of water from the sample, the water content for each sample could be calculated as a percentage by weight of the original bulk sample.

The water content values for all of the samples varies between 12% and 49% (See Figure 7.5.). In an attempt to identify any correlation between water content and other sediment parameters (depth and sand, silt and clay content)[3] the coefficient of determination (r^2) has been calculated for each pairing (See Table 7.1.).

Parameter	Water Content (%)
Depth (cm)	$r^2 = 0.005$
Sand (%)	$r^2 = 0.314$
Silt (%)	$r^2 = 0.411$
Clay (%)	$r^2 = 0.057$

Table 7.1. Loch Ainort: Coefficient of Determination Values (r^2) for sediment variables

As can be seen from this Table there is very poor correlation between water content and any of the four parameters tested. On the identification of the four litho-facies present in Loch Ainort re-plotting of the water content values for each litho-facies does show a good correlation ($r^2 = 0.963$) between litho-facies type (characterised by mean particle size) and water content (See Section 7.2.3.).

[3] Average particle size distribution figures calculated following the methodology described in Section 7.2.2.4.

Figure 7.5. Loch Ainort: Water Content (%) vs Depth of Sediment in Cores (cm).

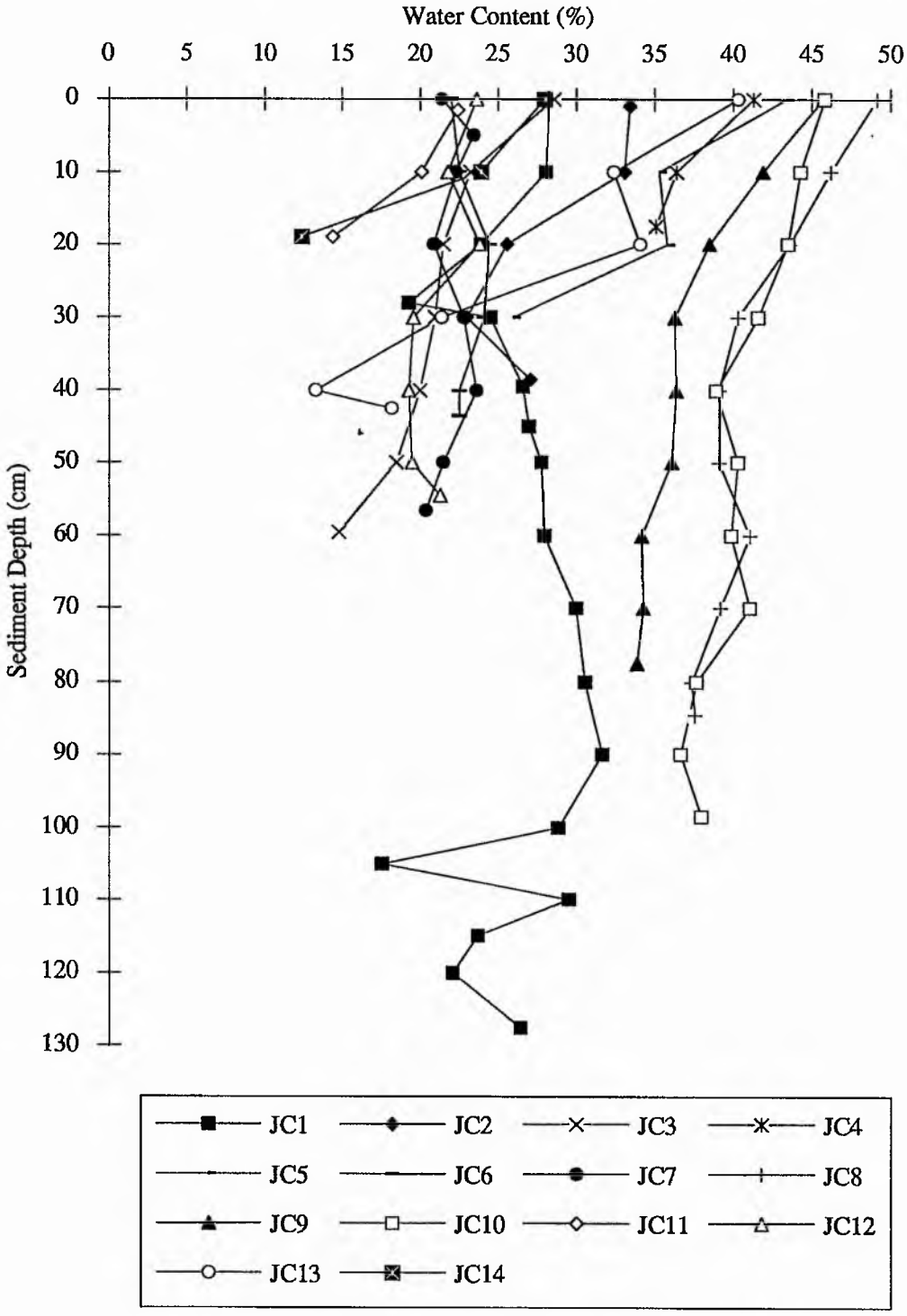

7.2.2.4. Particle Size Analysis

The 106, dried, sub-samples (See Section 7.2.2.3.) were all separated into two broad size fractions, < 250 μm and > 250 μm. The coarser fractions were weighed and then wet sieved for a period of ten minutes. The sieving stack was composed of 10 sieves representing whole phi intervals, between -4ϕ and -1ϕ and half phi intervals between -1ϕ and 2ϕ. The individual sieves were dried and the material in each sieve removed, weighed to the nearest decigram and recorded on purposefully designed sieving sheets. The difference between the original sample weight and the cumulative weight of each sieve fraction was assumed to represent the weight of the < 250 μm fraction that had not been removed during the initial separation of the sample. Also on these sieving sheets both the weight percent and the cumulative weight percent of each size fraction was recorded. The presence of a significant faunal content within any size fraction was also identified and described.

The faunal content (whole or fragmented) of each sample was retained as an integral part of the sediment. This decision was taken as the primary aim of the particle size analysis was to provide data for the calculation of the compressional velocity of sound waves through a sedimentary sequence (See Section 7.2.4.). Obviously the presence or absence of faunal material will effect the transmission of the pulse through the sediment. However, for the conventional use of particle size statistics in the environmental reconstruction of unconsolidated sediments the faunal fraction is removed (Cameron *pers. comm.*, 1990). Therefore whenever environmental interpretation is attempted (See Section 8.2.), it is always undertaken with reference to the visual core and sieving sheet (See Above) descriptions. This enables samples with significant faunal contents to be ignored or their statistical parameters adapted accordingly.

In order to assess the reproducibility of the wet sieving method, the surface sample J6 was coned and quartered and each quartered sample sieved using the standard procedure. The results from these four samples were found to have a maximum error of only ± 2.5%

For the < 250 μm fraction, particle size analysis for each sample was undertaken using a SediGraph 5100 analyser driven by a Zenith computer. Individual samples of 2-3 g in weight (the actual weight being recorded) were placed into a labelled 50 ml beaker with 40 ml of 2%

Calgon (Sodium metahexaphosphate) dispersing agent, in order to prevent particle aggregation. To enhance disarticulation of particulate aggregates the beakers were all placed in an ultrasonic bath for a minimum of five minutes. The SediGraph 5100 is a simple to operate, menu driven, instrument which once the initial parameters have been set (See Table 7.2.) the procedure simply requires; the creation of a sample ID and sample directory in which to store the results, the rinsing of the system and the entry of the sampled to be analysed.

Prior to each analysis session it is necessary to calibrate the SediGraph by collecting a "baseline" dataset. This is achieved by running just the pure 2% Calgon solution through the system. This procedure should be repeated on each occasion the Calgon supply is changed. Following calibration a prepared sample was removed from the ultrasonic bath and emptied in to the mixing chamber of the SediGraph, where it was kept constantly agitated by a magnetic stirrer. To ensure that all the sample was entered into the system the beaker was flushed with Calgon. The entire sample was then automatically loaded in to the X-Ray chamber and subjected to a high speed scan to determine the proportion of particle sizes between 250 μm and 50 μm.

Parameter	*Value*
Liquid Type	2% Calgon in Water
Run Type	High Speed
Sample Density	2.5 gcm^{-3}
Liquid Density	0.9946 gcm^{-3}
Liquid Viscosity	0.7441 cp

Table 7.2. Operational parameters for SediGraph 5100

The particle size distribution was initially presented visually as a log probability graph of equivalent spherical diameter vs % mass finer. This enabled the identification of either inconsistent or implausible data so any sample could be re-scanned to validate the original analysis. The accepted data was logged on disc and printed out as log probability graphs and as hard copy numerical data of the percentage cumulative mass finer from 250 μm and the percentage mass in each interval.

On the completion of these two forms of particle analysis the two data sets were combined to provide weight, weight % and cumulative weight % datasets at whole ϕ, half ϕ and a third ϕ intervals between -4ϕ and 12ϕ. The irregularity of the phi intervals is a product of the conversion (See ***Equation 7.1)***) between the μm interval scale that is recorded by the SediGraph and the ϕ interval required for the statistical analyses of the data. The irregularity of the phi scale interval does not affect the quality of the statistical data.

$$\phi = -\log_2 d \text{ (where d= particle size in mm)} \qquad \textit{Equation 7.1)}$$

Following the methodology of Stravers *et al.* (1991) the particle size data have been presented in three modes; moment statistics (Logarithmic mean particle size, logarithmic standard deviation, Skewness and Kurtosis), ternary diagrams of gravel-sand-mud and sand-silt-clay and cumulative frequency plots (with an arithmetic ordinate scale).

Moment statistics were calculated following the methodology set out in Lindholm (1987). The logarithmic mean and is taken to represent the theoretical average particle size for each sample. The logarithmic standard deviation measures the sorting or the uniformity of the particle size distribution and can be expressed both quantitatively (in ϕ units) and qualitatively (See Table 7.3.). The calculation of this parameter using the moments method with phi units allows comparison of sorting between materials of varying mean diameter (Lindholm, 1987). Skewness measures the asymmetry of the distribution, so if there is more material in the coarse tail, the skewness can be described as being negative. Conversely, if there is more material in the fine tail it can be described as positively skewed. Again this statistical parameter can be described both quantitatively (in ϕ units) and qualitatively (See Table 7.3.: Overleaf).

Finally, kurtosis is a measure of the ratio between the sorting of the tails of the distribution and the sorting in the central portion of the distribution. This parameter can identify between unimodal distributions with well sorted central portions (leptokurtic) to poorly sorted tails and distributions which are much flatter peaked with approximately equal levels of sorting between the centre and the tails (platykurtic). As kurtosis represents a ratio, it is expressed as a dimensionless quantity which has again been assigned with a verbal descriptive summary

(See Table 7.3.). In addition to the moment statistics calculated for each sample, "facies" moment statistics were determined for the averaged frequency distributions of all the samples assigned to an individual litho-facies (See Sections 7.2.3., 7.2.4., 7.3.2. and 7.3.3.).

The major fraction percentages for each sample were calculated using the Udden-Wentworth size classes (Wentworth, 1922: See Table 7.3.). In addition these weight % values were plotted on the two ternary diagrams (See Figures 7.6a and b.) of Folk (1980) to provide the nomenclature given in Section 7.2.3..

Classification	*Phi (ϕ) Interval*
Gravel	-12 to -1
Sand	-1 to 4
Silt	4 to 8.5
Clay	> 8.5

Table 7.3. Major sediment fractions based on Udden-Wentworth size classes.

Finally the cumulative frequency curves have been plotted on an arithmetic ordinate scale to provide a graphical representation of the particle size distribution for each sample. Each set of curves for the individual litho-facies has the range envelopes marked. As with all the particle size data the pictorial and numerical summaries are presented as statistical summaries of the litho-facies described in Section 7.2.3..

7.2.2.5. X-Ray Diffraction Analysis

In order to provide information on the mineralogical content of the silt (< 63 μm) and clay (< 2 μm) fraction of the Loch Ainort sediments X-Ray Diffraction analysis was undertaken on selected samples. Material for the < 63 μm analysis was separated from the < 250 μm fraction (obtained from the preparation for the particle size analysis) and back-packed into standard holders. The < 2 μm fraction was removed from within the < 63 μm fraction by firstly centrifuging an aqueous solution of the sediment at 2000 rpm for 40 seconds. This results in only the < 2 μm fraction remaining in suspension and so it can be readily decanted into another test tube. This solution is centrifuged again at 4000 rpm for 5 minutes to separate the < 2 μm fraction from the solution. This residue is removed by pipette and placed

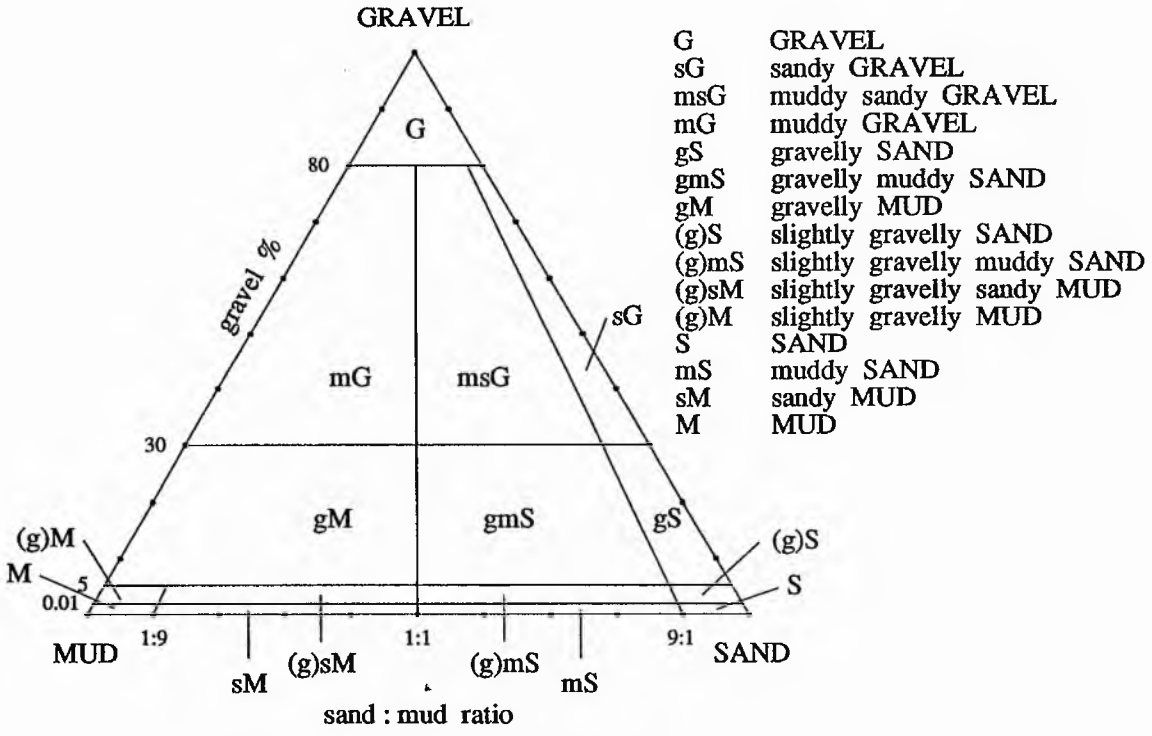

Figure 7.6a. Gravel : Sand : Mud Ratio

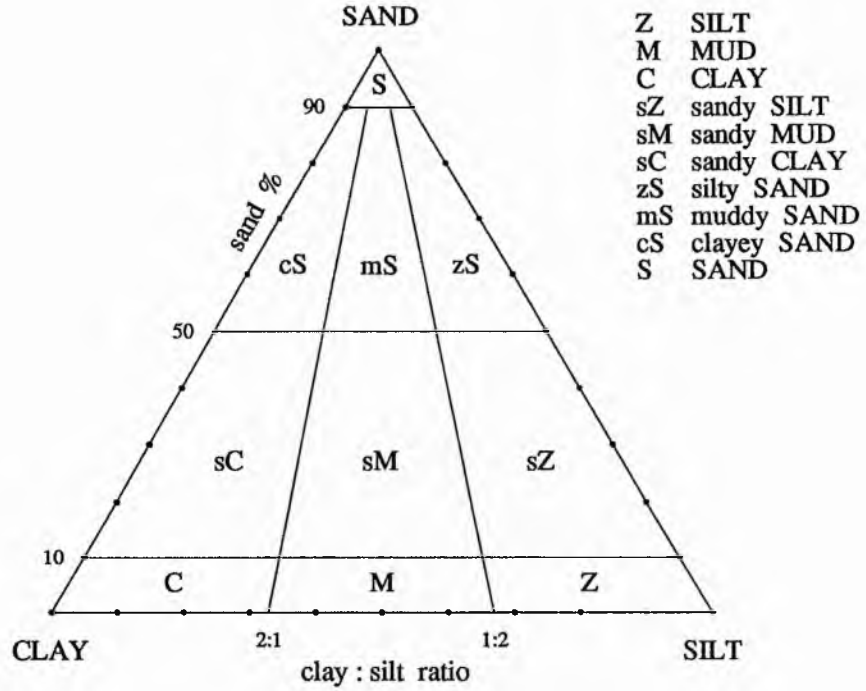

Figure 7.6b. Sand : Silt : Clay Ratio

Figures 7.6a & 7.6b. Ternary Diagrams Based on Major Fraction Percentages (After Folk, 1980)

onto glass slides where it is left to dry out at room temperature for 12 hours. The drying process results in the individual grains (predominantly sheet silicate minerals) being adhered to the slide with their 001 surfaces oriented perpendicular to the incoming rays.

Both the < 63 μm holders and < 2 μm slides have been irradiated by a copper anode with excitation conditions set at 40 kV and 30 mA. The samples were scanned at a rate of 0.02° per second between two theta values of 5 and 70 for the < 63 μm fraction and between two theta values of 5 and 40 for the < 2 μm fraction. The mineralogical data has been identified using the SIEMENS DIFFRAC-AT© v2. and presented in the litho-facies summary of Section 7.3.2..

7.2.3. LITHOLOGICAL FACIES DESCRIPTION AND DISTRIBUTION

By integrating the information obtained from X-Ray Diffraction analysis (See Section 7.2.2.1), visual descriptions (See Section 7.2.2.2.), water content (Section 7.2.2.3.) particle size distribution (major fraction percentages and moment statistics: See Section 7.2.2.4.) and the mineralogical composition of both the whole sample and the < 63 μm fraction (See Section 7.2.2.5.), it has been possible to identify four litho-facies. Due to the small number of sites and shallow penetration of the gravity corer the vertical and spatial distribution of the four litho-facies can only be generally surmised from core data alone (See Below). Despite the shallow maximum depths recorded by the cores taken from Loch Ainort (0.18 - 1.28 m) it has been possible to identify vertical lithological variations, particularly in the cores from the Unnamed Strait (See Section 4.3.1.5.).

The characteristics and broad distribution of the four Litho-facies are described in below with a summary diagram being presented in Figure 7.7. The prefix of ALF has been adopted for these litho-facies descriptions, it being an acronym for Ainort Litho-Facies, to emphasise the difference between these and the seismic facies units described in Section 6.3.:

ALF1.: Homogeneous grey-green to grey-black medium SILTS and MUDS with subordinate sandy SILTS (See Figure 7.8a) with the major fraction percentages of this litho-

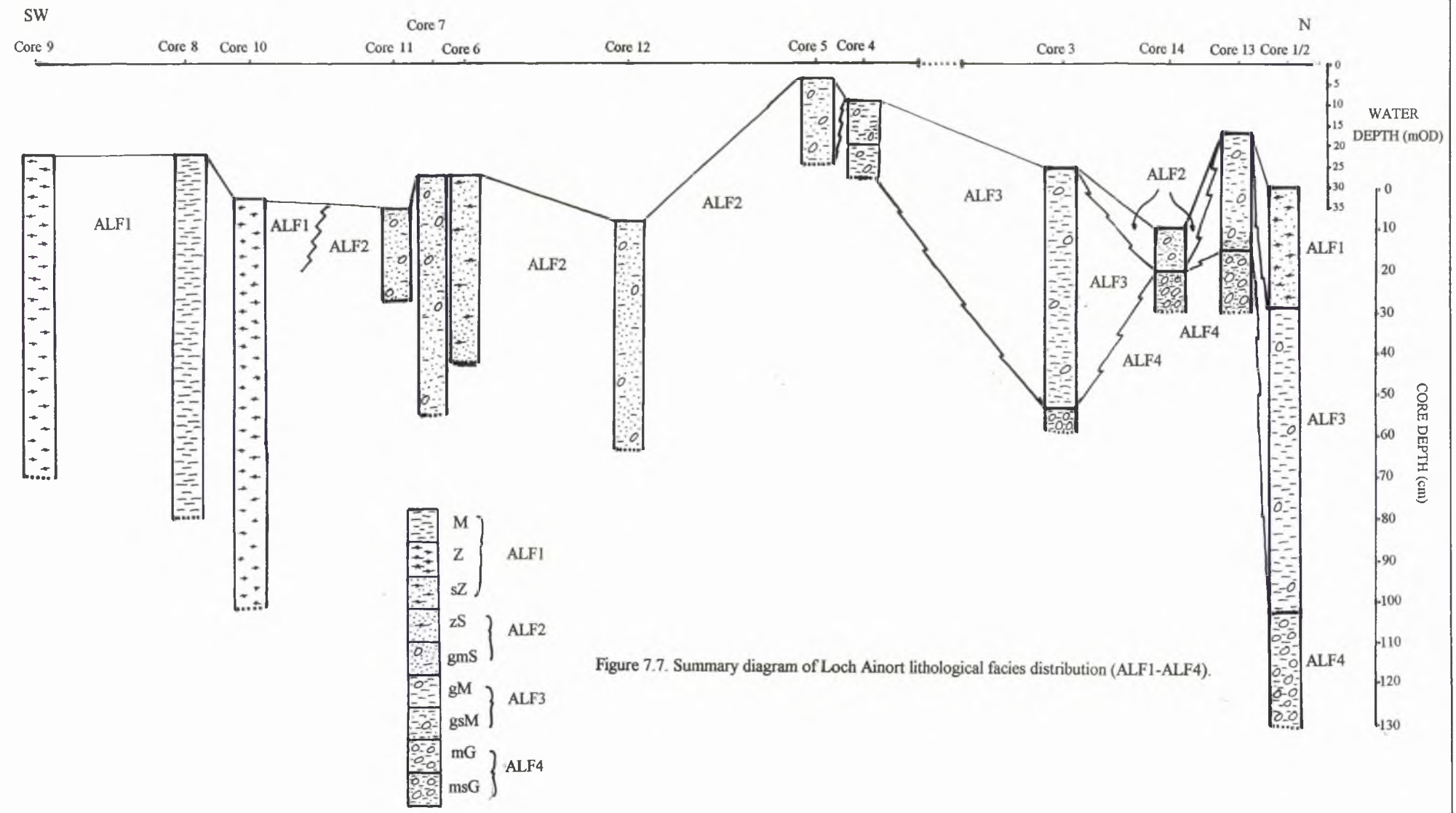

Figure 7.7. Summary diagram of Loch Ainort lithological facies distribution (ALF1-ALF4).

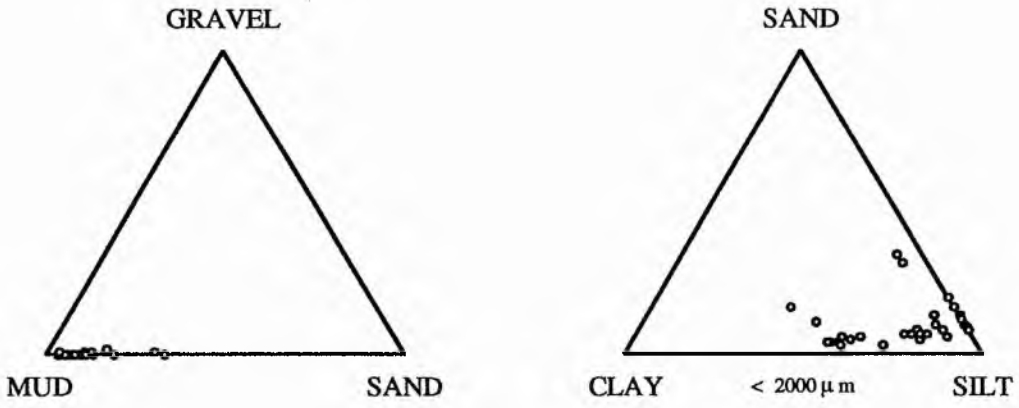

Figure 7.8a. Loch Ainort : ALF1

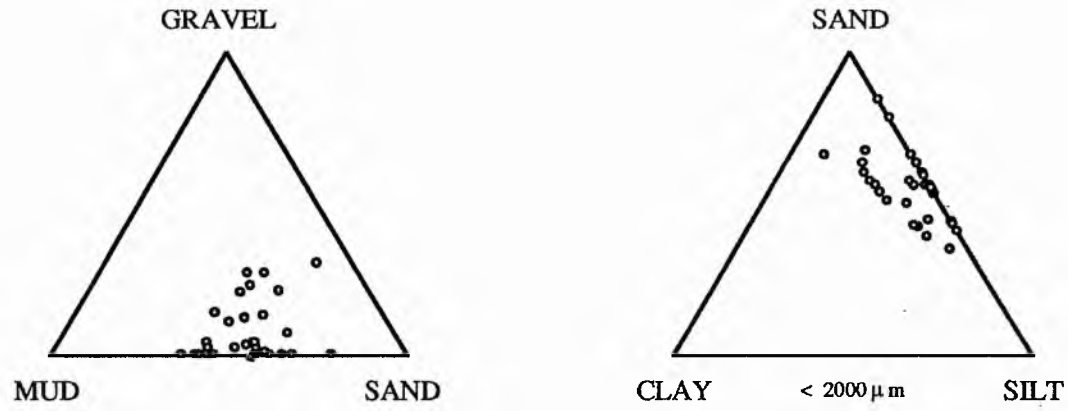

Figure 7.8b. Loch Ainort : ALF2

Figures 7.8a & 7.8b. Loch Ainort : Ternary Gravel-Mud-Sand and Sand-Silt-Clay Diagrams ALF1 and ALF2 (After Folk, 1980)

facies being Sand 10%, Silt 73% and Clay 17%. Discontinuous, dark, wispy, laminae are present in the upper most section of the cores (14 cm to 31 cm). These dark wispy layers, which tend to taper towards the centre of the core are thinner (≤ 10 mm) than the intercalated lighter layers (≥ 15 mm). In a single core (**JC10**: See Figure 7.4.) the lighter layers are associated with layer parallel oriented bivalve fragments. The inclined and up core concaved nature is attributed to the coring process and is therefore not considered as an environmental indicator. These laminae could only be identified in the X-Ray photographs there being no direct visual or statistically inferred indications of their existence.

The faunal content is commonly low (< 5%) and tends to decrease down core. However, high concentrations of whole *Archimediella* do occur in well defined shell beds (maximum thickness 7 cm). The concentration of lithics is low, being confined to a small number of isolated clasts (maximum dimension 40 mm) with lithological composition varying from granodioritic to ultrabasic. Water content (See Figure 7.9.) shows no significant variation with depth, with the majority of values ranging between 35 and 45% (the highest recorded in the area). A cluster of lower values (18 to 28%: See Figure 7.5.) is found associated with the slightly coarser sandy silts of **JC1**, **JC2** and **J1**.

Moment analysis gives a logarithmic mean particle size (**Mz**) for this sediment of 5.94ϕ (medium silt). The mean particle sizes of the individual samples making up this litho-facies vary from 3.82ϕ (very fine sand) to 7.84ϕ (Very fine silt). An average logarithmic σ value of 2.42ϕ suggests that the litho-facies as a whole is very poorly sorted. The individual moment analyses of each sample suggests the sediments of this litho-facies have logarithmic σ values ranging from 0.87ϕ (moderately sorted) to 4.69ϕ (extremely poorly sorted). An average skewness value for ALF1 of 0.49 suggests a very finely-skewed unit with a much larger percentage of material in the fine tail of this distribution. However, the samples in this litho-facies exhibit a wide range of skewness values, from -3.16 (very coarsely-skewed) to 0.51 (very-finely skewed). The kurtosis value of ALF1 is 3.83 (extremely leptokurtic) with the majority of the kurtosis values for each sample in this unit being within this category. Finally, Figure 7.10. is a graphical representation of the particle size distribution of the ALF1 sediments in the form of a cumulative weight % frequency curve. This graph shows that in excess of 90% of the particles in this litho-facies have a diameter less than 3ϕ (very fine sand).

Figure 7.9. ALF1: Water Content (%) vs Depth of Sediment in Cores (cm).

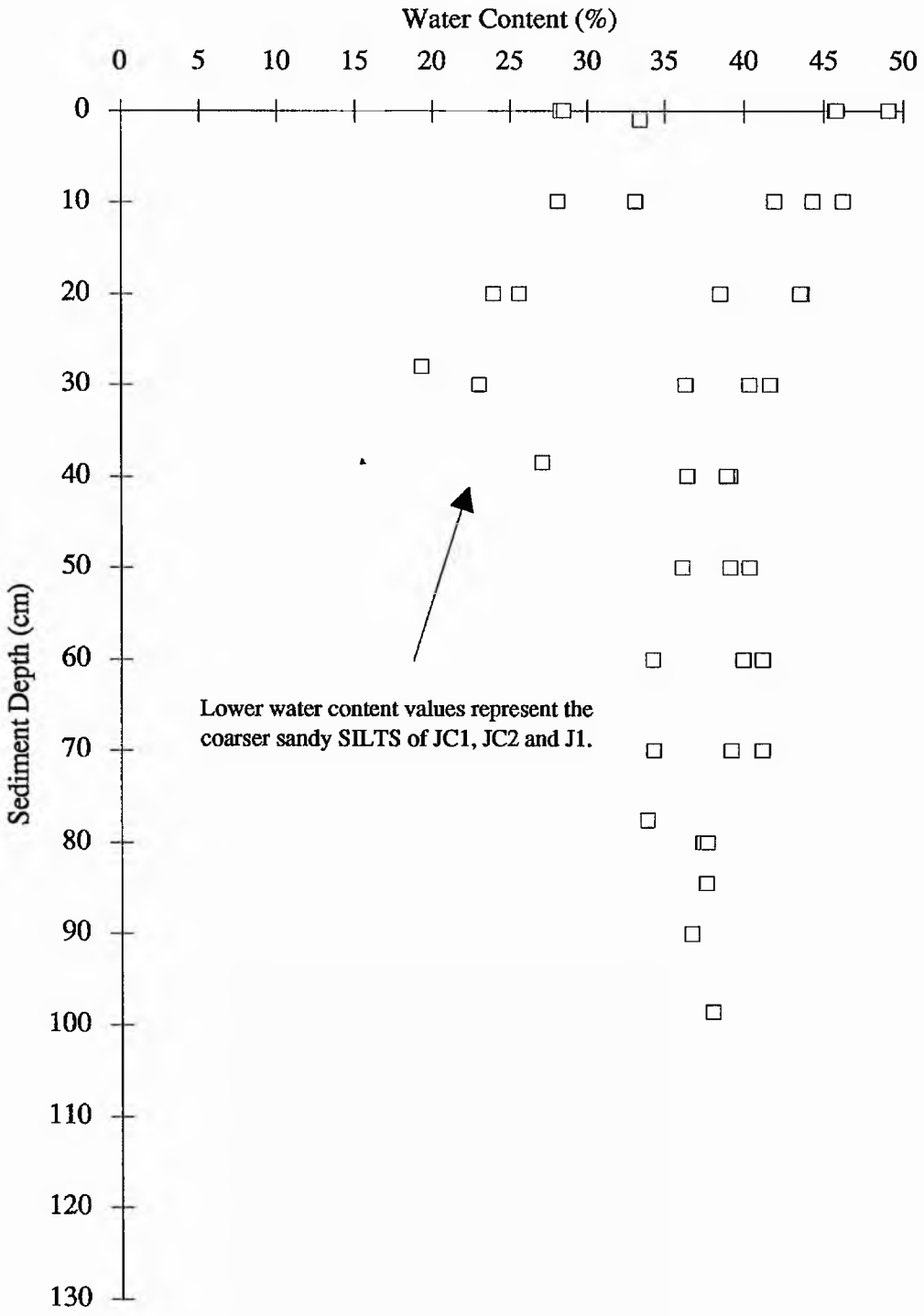

Figure 7.10. Cumulative Weight % Frequency Curve for ALF1

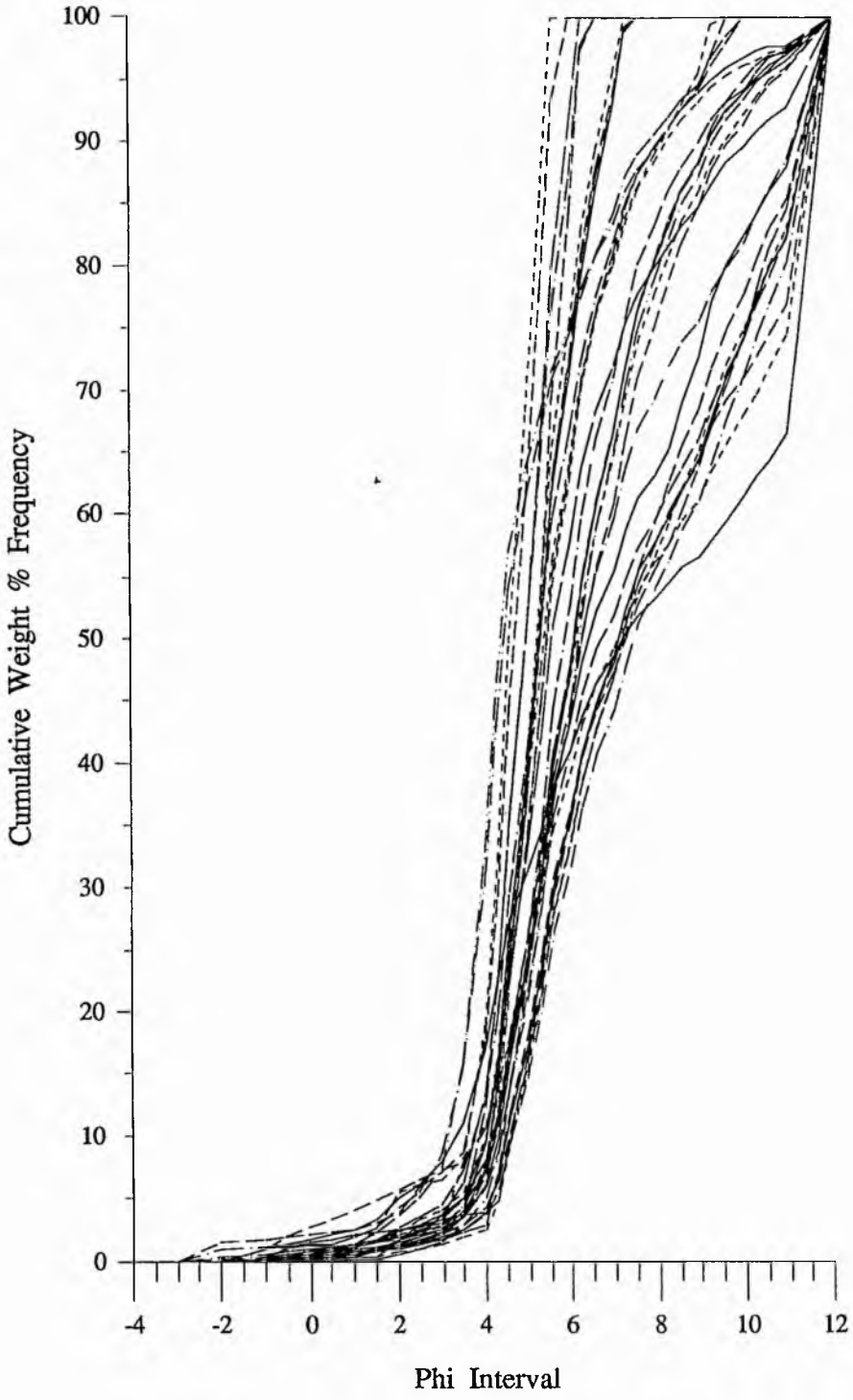

Equally it is possible to compare the restricted range of the coarser fraction of the material compared to the wide range of weight % values for the finer fractions.

ALF1 is found predominantly in the quieter and/or deeper waters of the inner and outer loch basins. The cores from within the loch are composed entirely of mud and silt with a maximum thickness of 99 cm being observed. In the outer, unnamed, basin ALF1 is represented by a thin veneer (0-28 cm: Core 1) of more sandy SILTS overlying ALF3 gravelly MUDS.

ALF2.: A grey-green slightly gravelly to gravelly, muddy to silty, very fine SAND (See Figure 7.8b) with major fraction percentages of Gravel 8%, Sand 52%, Silt 35% and Clay 5%. Occasional large individual clasts of both acidic and basic composition (maximum dimensions of 53 mm) and dispersed shells and shell fragments are also present. The individual clasts vary from angular to sub-rounded forms with the majority of them being covered in serpulid growths. In core **JC7** there is a concentration of larger lithic clasts (maximum dimensions $\leq$ 32 mm) in a single layer between 0 and 5 cm. Faunal content is dominated by *Archimediella*, *Littorina littorea* and *Dosinia*. Occasionally *Archimediella* concentrations are sufficiently significant to form well defined shell beds (**JC11**: between 18 and 20 cm). The main exception to this characteristic faunal assemblage is the abundant presence of red and white coralline algae (Corallinaceae) in **JC5**.

Figure 7.11. shows a good correlation of ALF2 sediments with water content, the majority of values ranging between 20 and 25%. The three significantly higher values (35-43%) are all associated with the concentration of coralline algae in **JC5**. This very fine sandy litho-facies (**Mz** = 3.23ϕ) exhibits a limited range of mean particle sizes from coarse sand (0.42ϕ) to coarse silt (4.60ϕ). The sediment is moderately (σ = 1.44ϕ) to very poorly sorted (σ = 4.69ϕ) and with a wide range of skewness values, from -1.51 to 1.16 (very fine to very coarse skewed). All the kurtosis values suggest a very, to extremely, leptokurtic distribution (1.58 to 5.54 with an average of 3.17) further emphasising the poorly sorted nature of these sediments. The cumulative frequency curve for this litho-facies is presented in Figure 7.12. and readily identifies the coarser nature of this sediment compared to ALF1 and the range of sizes represented in the fine tail of these sediments (coarse silt to clay).

Figure 7.11. ALF2: Water Content (%) vs Depth of Sediment in Cores (cm).

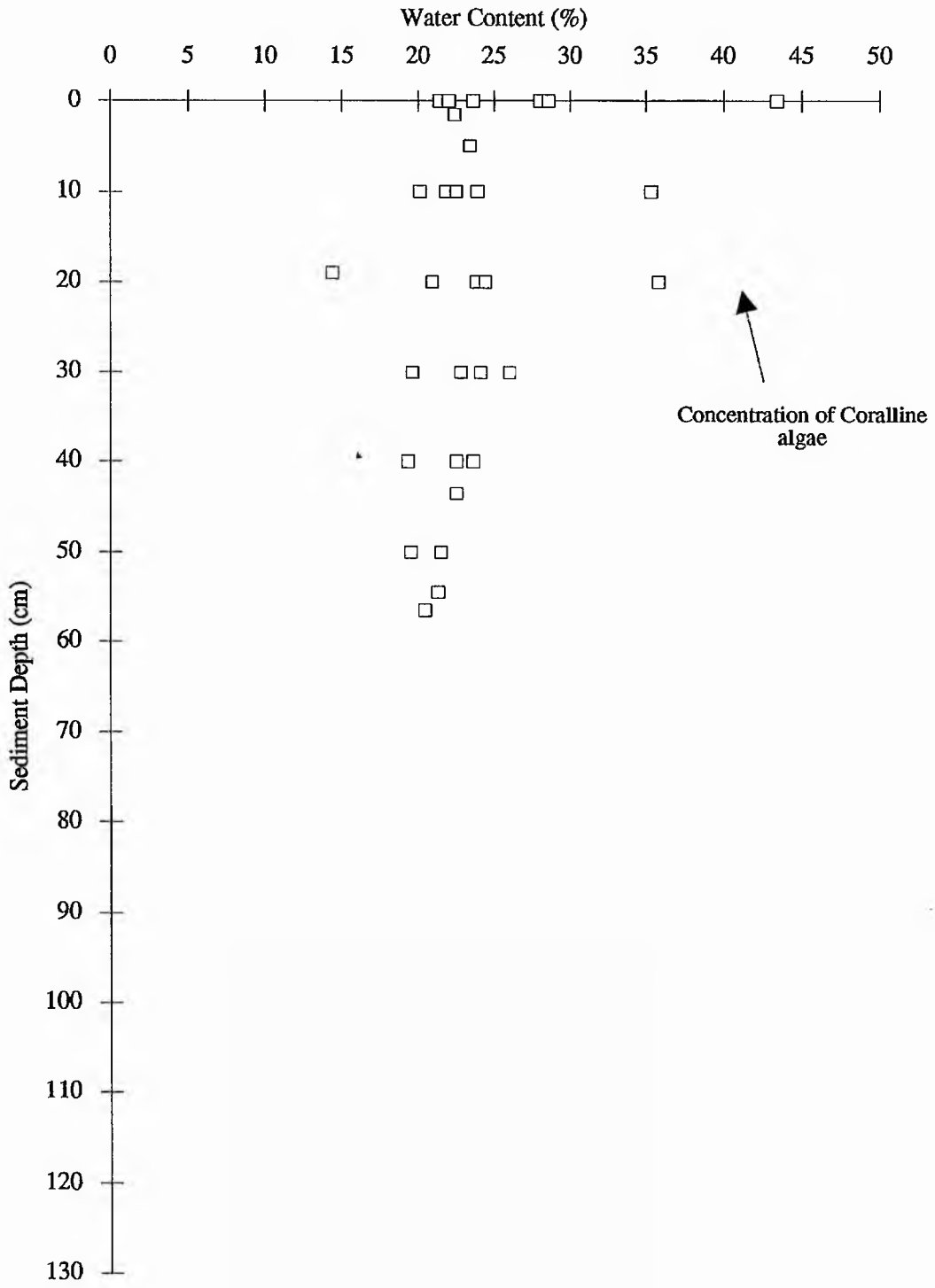

Figure 7.12. Cumulative Weight % Frequency Curve for ALF2

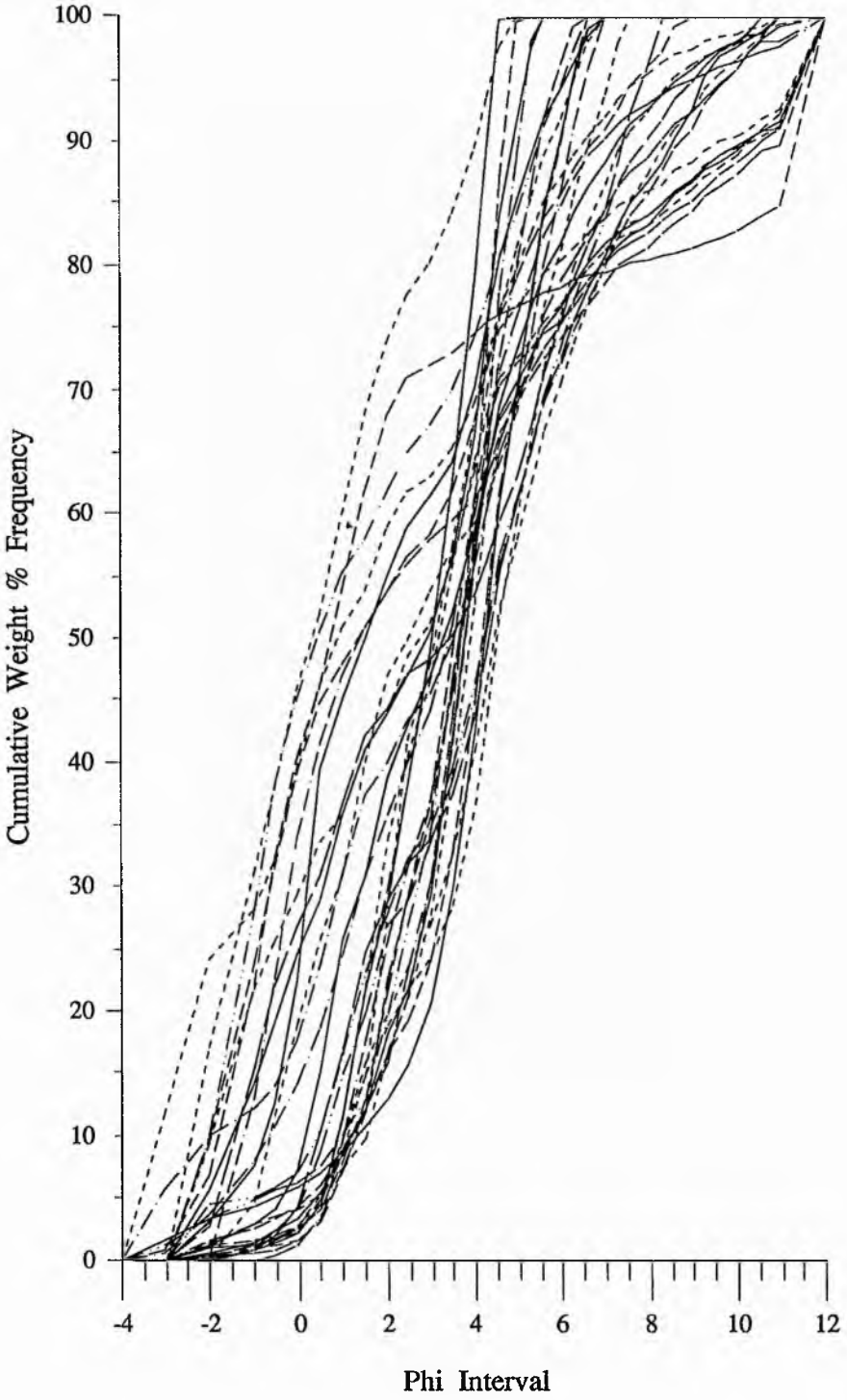

These coarser sediments are found in the cores to the north and north-east of the Luib protrusion and the gentle slopes of the south-eastern shore of Loch Ainort (See Figure 7.1.). In the outer basin, ALF2 is found in a single core (**JC14**) as a thin veneer (0-10 cm) overlying ALF4 sediments and from a single surface sample (**J3**) 450 m west of Maol Ban. There appears to be no apparent relationship with bathymetry as ALF2 is present in cores from water depths that range between 39.5 m (**JC14**) and 3 m (**JC 5**).

ALF3.: A grey-green slightly gravelly to gravelly, occasionally sandy MUD (See Figure 7.13a) with occasional large igneous pebbles and cobbles (maximum dimensions 65 mm) and dispersed shell fragments (*Archimedielleae* and *Dosinia*). Individual pebbles also vary dramatically in shape (discoid to compact) and composition (granophyric to peridotitic). Where the pebbles are more abundant (**JC4**) they tend to be smaller (≤ 7 mm) and concentrated in the upper 10 cm. The upper part of this core is also characterised by a high concentration of red coralline algae.

There is poor correlation between the sediments of ALF3 and water content, values varying between 17 and 42% irrespective of depth (See Figure 7.14.). The major fraction percentages for the litho-facies are Gravel 7%, Sand 27%, Silt 47% and Clay 19%. The litho-facies mean (**Mz**) is 5.09ϕ (medium silt) with a range from fine sand (2.28ϕ) to fine silt (7.44ϕ). This represents a similar size range as that described for ALF1, however, the sediments of ALF3 are characterised by an increased gravel content (1% and 7% respectively) which is reflected by the extremely poorly sorted nature of the sediment (σ = 3.72ϕ with a range from 2.55ϕ to 4.98ϕ) and its coarse-skewness (Skewness = -0.24 with a range from -1.16 to 0.65). A kurtosis value of 2.46 (range: 1.32 to 5.73) implies a very leptokurtic distribution. Comparison of the cumulative frequency curves for ALF1 and ALF3 (See Figure 7.15) readily identifies the relative dominance of a coarser fraction within the sediments of ALF3.

The core data suggest that its distribution is generally restricted to the outer basin, only a single surface sample (**J7**) being found within Loch Ainort, to the north-east of Luib. In the outer basin ALF3 material is found in all the cores except **JC14**. In **JC1**, **JC3** and **JC13** it rests up on ALF4 sediments and attains a maximum thickness of 75 cm (**JC1**). In the majority

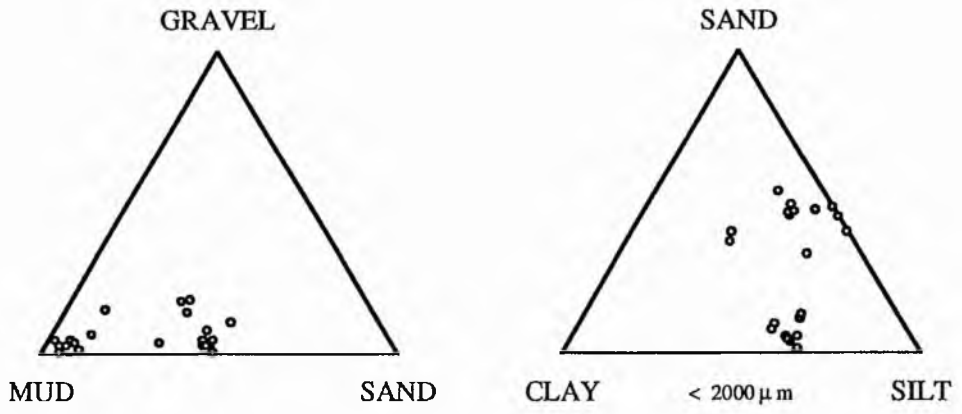

Figure 7.13a. Loch Ainort : ALF3

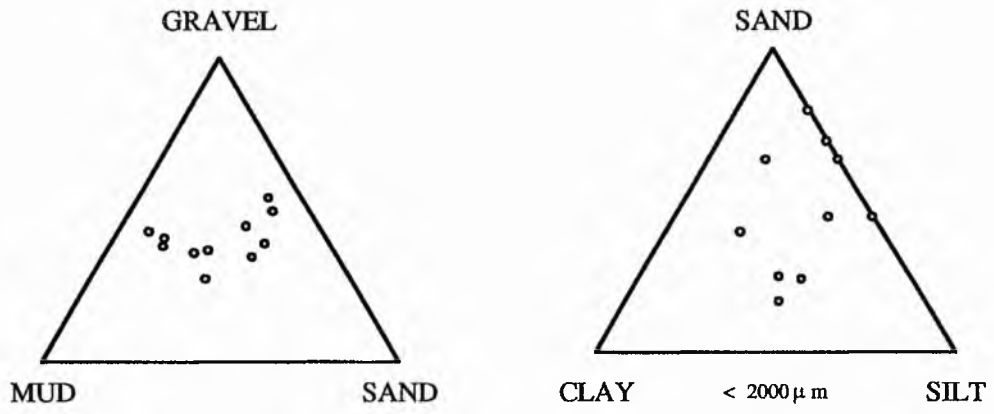

Figure 7.13b. Loch Ainort : ALF4

Figures 7.13a & 7.13b. Loch Ainort : Ternary Gravel-Sand-Mud and Sand-Silt-Clay Diagrams for ALF3 and ALF4 (After Folk, 1980)

Figure 7.14. ALF3: Water Content (%) vs Depth of Sediment in Cores (cm).

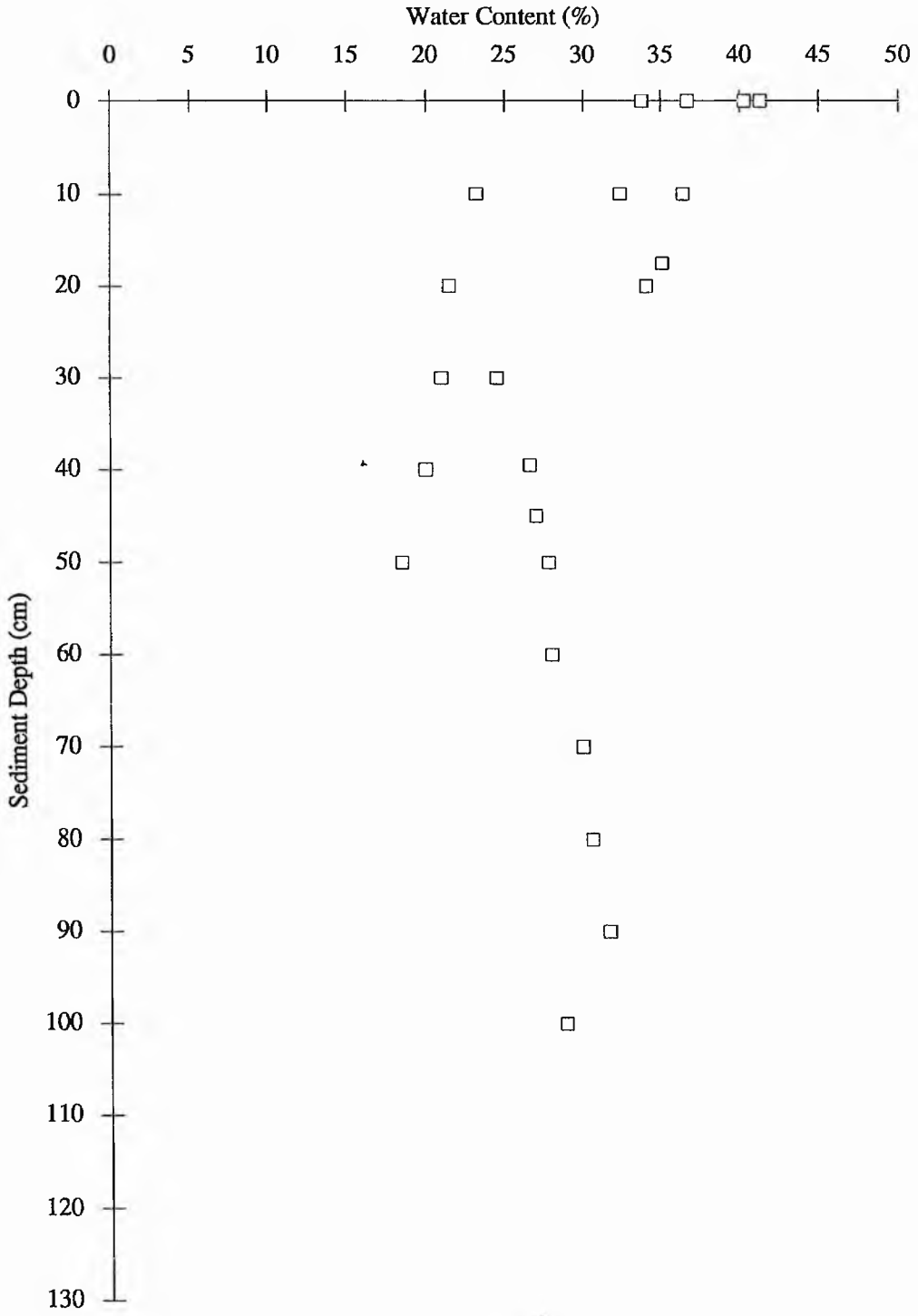

Figure 7.15. Cumulative Weight % Frequency Curve for ALF3

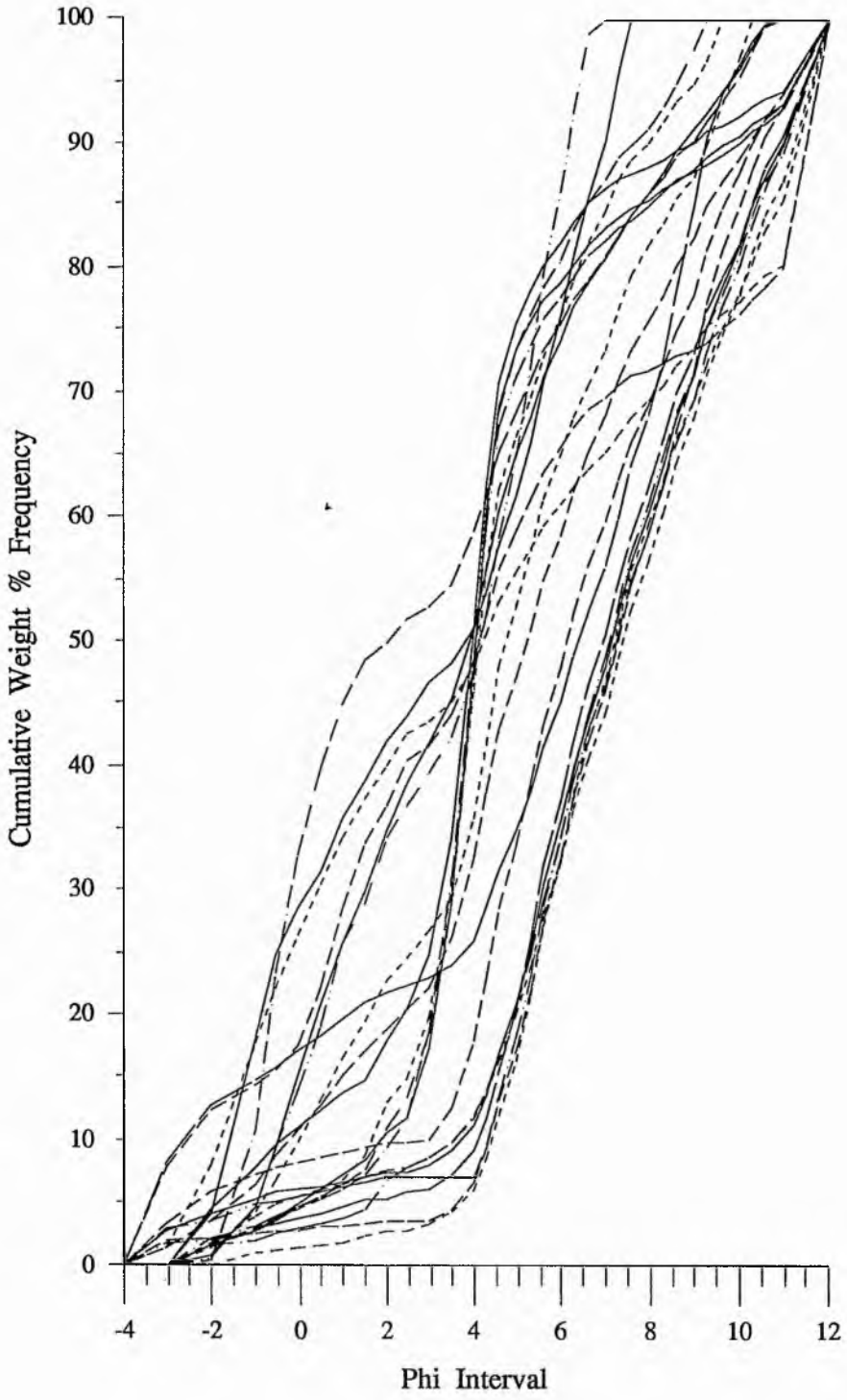

of the cores it is exposed at the surface of the loch bed, but within **JC1** it is overlain by 28 cm of ALF1 sediments.

ALF4.: Light brown to grey-green muddy to sandy muddy GRAVEL (See Figure 7.13b.) with occasional very large pebbles (maximum dimensions 63 mm). This litho-facies is commonly marked by a rapid gradational boundary with the overlying material. ALF4 is predominantly pebble dominated (up to 80% of the core section). The sub-angular to sub-rounded pebbles both vary in shape (bladed to equant) and composition (felsitic to basic). A small number of the larger pebbles are serpulid encrusted but otherwise the litho-facies is faunal free.

This litho-facies exhibits the lowest water content values (between 13 and 24%) but again there is little variation with depth (See Figure 7.16.). The major fraction percentages for the litho-facies are Gravel 41%, Sand 29%, Silt 19% and Clay 11%. The litho-facies mean particle size (**Mz**) value of 1.61ϕ (medium sand) with a range from -0.54ϕ (very coarse sand) to 3.20ϕ (very fine sand). ALF4 is extremely poorly sorted (σ = 4.44ϕ: range from 2.38ϕ to 5.55ϕ) with a strong positive skewness (Skewness = 0.83: range from 0.18 to 1.35) and a very leptokurtic distribution profile (Kurtosis = 2.50: range from 1.42 to 3.71). These averaged statistics reflect the 60:40 split between the > -1ϕ and the < -1ϕ fractions (the separation between the gravel and sand fractions). Consequently, the bimodal distribution of this sediment can be more clearly demonstrated by the cumulative frequency curve (See Figure 7.17.).

This litho-facies is found at depth in the cores taken from the outer basin where it is directly overlain by sediments of both Litho-facies 2 (**JC14**) and 3 (**JC1**, **JC3** and **JC13**). The only exposure of ALF4 material from the surface is at the mouth of Loch Ainort, 200 m north of Rubh' an Àirde Dhuirche (Samples **J5** and **J6**: See Figure 7.1.). It is also possible that **J4** (See Figure 7.1.) represent ALF4 material, however, this assumption is based up on descriptions from the field notes[4] taken at the time of coring as the cores yielded insufficient material for particle size analysis.

[4] At J4 the core head was split by a single leucocratic granitic boulder (55 mm x 50 mm) with the retention of small [31.55 g] sample of granular gravel (< 3 mm) in a very fine "clay" matrix.

Figure 7.16. ALF4: Water Content (%) vs Depth of Sediment in Cores (cm).

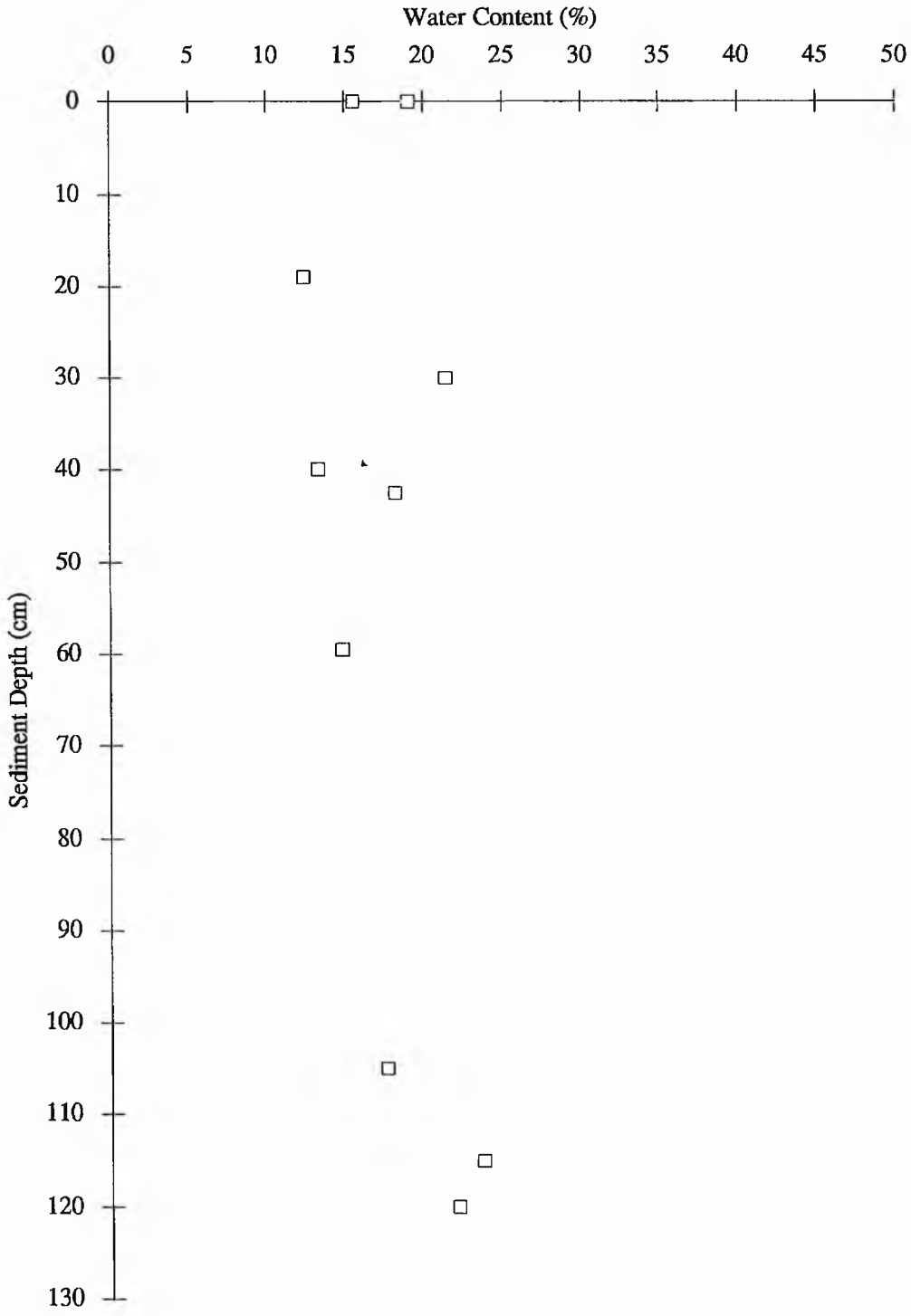

Figure 7.17. Cumulative Weight % Frequency Curve for ALF4

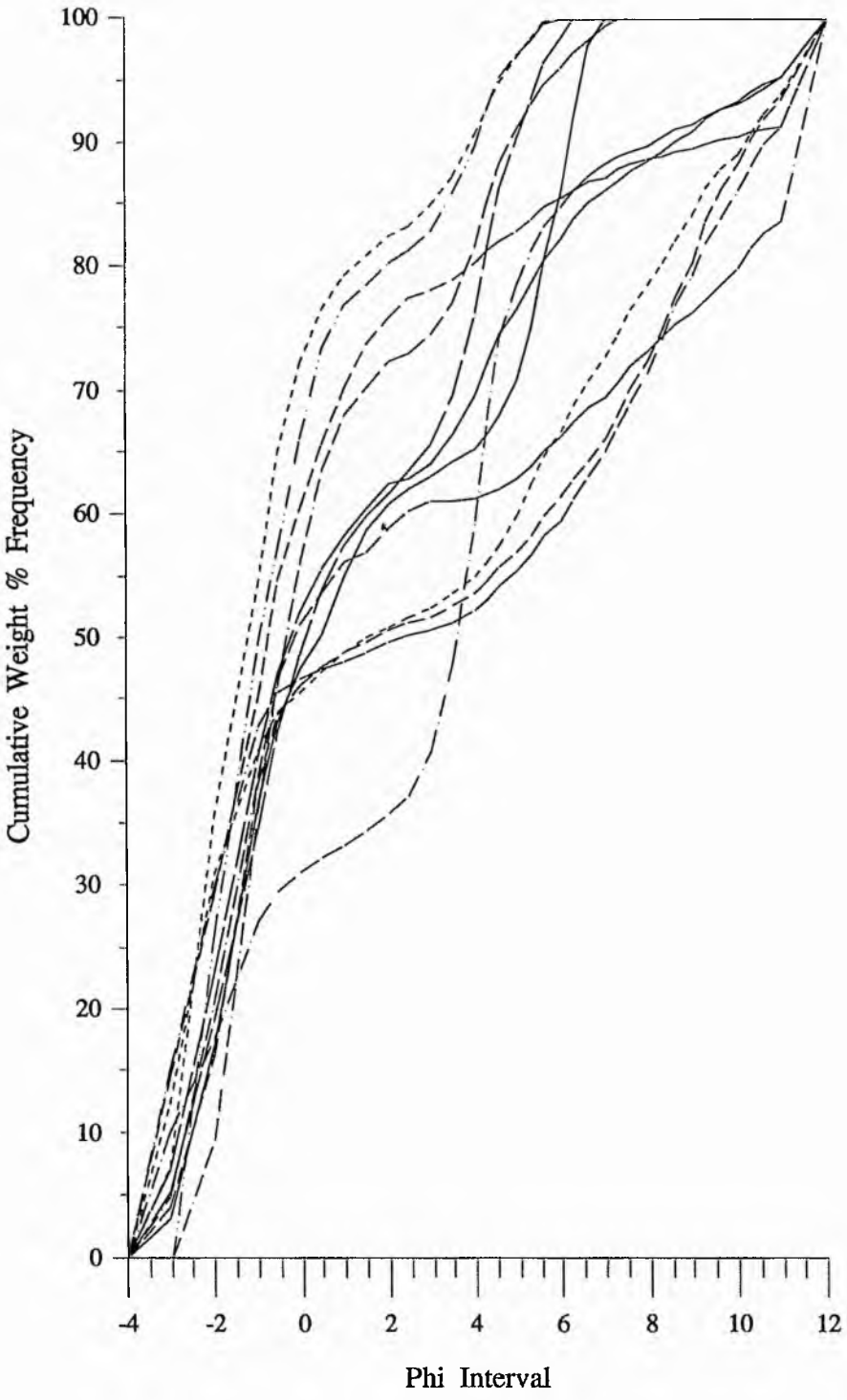

7.2.4. SEDIMENT VELOCITY MEASUREMENTS

Having identified the four litho-facies from sediment analysis (See Section 7.2.2. and 7.2.3.) an attempt was made to assign velocity values to each of them. This is an important property because where it has been possible to correlate the seismic facies units and sequences with the litho-facies, the calculation of a velocity value will enable the conversion of depths and thickness quoted in milliseconds to be converted to measurements in metres (See Section 8.2. and 8.3.).

This calculation of the velocity of propagation of sound through a sediment can be achieved by applying the regression equations of Orsi and Dunn (1991). These equations are based up on empirical studies of glaciomarine sediments taken from the Barents Sea. By the statistical analysis of laboratory-measured compressional wave (sound) velocity, porosity, wet bulk density and selected textural parameters Orsi and Dunn were able to identify the best indices with which to infer sound velocity.

Of the five parameters for which regression equations were calculated, the most appropriate one for the current study, was that relating compressional velocity (**Vp**) with mean particle size (**Mz**; $\mathbf{r^2} = 0.77$), where:

$$\mathbf{Vp = 1868.6 - 62.07Mz + 2.236Mz^2 \ (For\ Mz,\ 4\phi\ to\ 9\phi)} \qquad \textit{Equation 7.2)}$$

This equation is believed to provide reasonable estimates of compressional velocity (See Table 7.4.: Overleaf) for ALF1 and ALF3. However, the mean particle size values of ALF2 and ALF4 lie outside the recommended 4 to 9ϕ limits for this equation. Unfortunately the values of the other textural parameters for these litho-facies lie much further outside their corresponding limits (Orsi and Dunn, op cit.). In addition, the errors of these other regression equations are significantly higher ($\mathbf{r^2}$ varies from 0.74 to 0.67) than that for the mean particle size. It was therefore decided to calculate the ALF2 and ALF4 velocity values from the same equation but to present them with the caveat, that they can only be considered as the broadest estimates.

Litho-facies	*Sediment Type*	*Velocity (ms^{-1})*
ALF1	MUD	1582
ALF2	gravelly muddy SAND	1694
ALF3	gravelly sandy MUD	1616
ALF4	muddy GRAVEL	1775

Table 7.4. Loch Ainort Velocity values for litho-facies ALF1 - ALF4.

The values calculated from these equations correspond well with compressional velocities calculated for unconsolidated materials by a number of other authors (see Table 7.5.). The full significance of the velocity measurements for a variety of unconsolidated sediments is discussed in Section 8.3..

Sediment Type	*Velocity (ms^{-1})*
Mud	1540 (Howell, 1971)
Silt	1570 (MacAulay & Hobson, 1972)
Estuarine Sands & Silts	1530-1560 (D'Olier, 1979)
Sand-Silt-Clay	1582 (Hamilton & Bachman, 1982)
Sand	1734 (Orsi & Dunn, 1991)
Glacial Moraine	1600-2700 (McQuillin & Ardus, 1977)

Table 7.5. Propagation velocities of selected rock types.

7.3. CONCLUSION

From both the non-destructive and destructive investigation of sedimentary cores, including a range of laboratory analytical techniques, it has been possible to identify and characterise four litho-facies. Table 7.6. (Overleaf) summarises the diagnostic particle characteristics for each litho-facies. The statistics in this Table are based up on the averaged sediment distribution for each litho-facies, the cumulative frequency curves for these four hypothetical distributions are given in Figure 7.18.. Within Table 7.6., the velocity values for each litho-facies calculated from the averaged sediment parameters are also presented.

Figure 7.18. Summary Graph showing Cumulative Weight Frequency Curves for ALF1-4

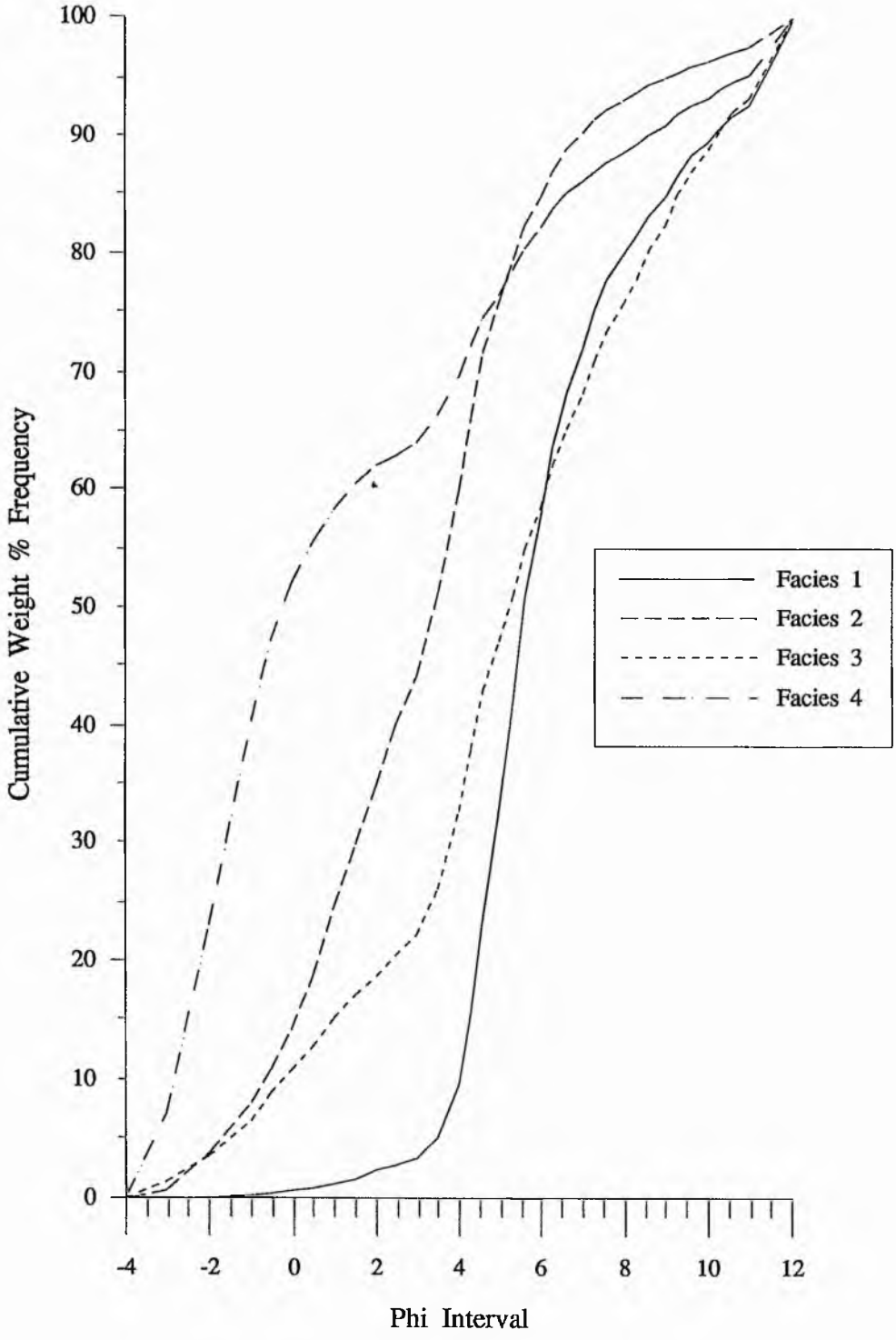

Litho-facies	*Gravel (%)*	*Sand (%)*	*Mud (%)*	*Silt (%)*	*Clay (%)*	*Mean (Mz: ϕ)*	*Sorting (σ: ϕ)*	*Skewness*	*Kurtosis*	*Velocity (ms^{-1})*
ALF1	1	13	86	72	14	5.94	2.42	0.49	3.83	1582
ALF2	8	52	40	35	5	3.23	3.09	0.38	3.17	1694
ALF3	7	27	66	47	19	5.09	3.72	-0.24	2.46	1616
ALF4	41	29	30	19	11	1.61	4.44	0.83	2.50	1775

Table 7.6. Loch Ainort Litho-facies Summary.

Figure 7.7. shows the distribution of the 4 litho-facies throughout the Loch Ainort field area. The SILTS and MUDS of ALF1 are found in the quiet water environments of inner Loch Ainort and in the deeper waters of the unnamed Outer Basin. ALF2, gravelly muddy SAND, appears to have no bathymetric control and is found between depths of 40 m in the Outer Basin and 3 m at the mouth of Loch Ainort. ALF3, gravelly MUD, have a similarly fine mean particle size as the sediments of ALF1 (5.09ϕ to 5.94ϕ respectively) but is distinguished by its higher gravel content (7% versus 1%). This litho-facies is generally restricted to the cores of the outer basin, a single surface sample (**J7**) being located to the north of the Luib protrusion. In cores **JC3** and **JC1** this litho-facies material is found at depth, being overlain by a thin (10 to 30 cm) veneer of ALF2 and ALF1 sediments respectively. Finally the coarsest litho-facies identified in the field area are the muddy GRAVELS of ALF4. They have been located at the base of all the cores in the outer basin and at the surface in a cluster of samples at the mouth of Loch Ainort.

CHAPTER 8

8. DISCUSSION

8.1. INTRODUCTION

King (1969) suggested the "Use of the combined [geophysical] techniques enables one to map to a high degree of detail, far beyond limits considered realistic if mapping were based on sample control alone.". Despite such early recognition of the need for a multi-disciplinary approach to the palaeo-environmental investigation of submerged environments, the use of such an integrated methodology is still conventionally overlooked or dismissed. For instance, Bishop & Jones (1979) acquired large volumes of side scan sonar data but paid scant attention to it when they attempted to both construct a seismic para-stratigraphy for the Skye-Shiant platform or more importantly present a palaeo-environmental interpretation of this area.

As described in Chapter 1 this project attempts to re-assess the suitability of such multi-instrument geophysical investigations for the interpretation of ancient, submerged, landscapes. In particular, emphasis has been placed on the investigation of nearshore sites that are suspected of having recently (< 20000 years) been glaciated. However, the ultimate aim of this work is to construct a single unifying investigative framework, which encompasses both the acquisition and the interpretation of a variety of geophysical and geological datasets, for use in nearshore palaeo-environmental reconstruction studies (See Chapter 9.).

Although it is hoped that the constructed framework is applicable to studies on a wide variety of scales, this project concentrates on high-frequency seismic reflection techniques that give a high-resolution record of both the loch bed and near-surface (< 30 m) units. During this project a 192 kHz echosounder (See Section 2.3.3.1.), a 400 kHz side scan sonar (See Section 2.3.3.2.) and a 3.5 kHz sub-bottom profiler (Pinger: See Section 2.3.3.3.) were deployed within the selected field area. Lithological calibration of the seismic data was provided by both a detailed review of the solid and drift geology of the surrounding area (See Chapter 3.) and the analysis of a series of 14 gravity cores and 7 surface sediment samples obtained from within the chosen loch (See Chapter 7.). For

the purposes of this assessment, all work was conducted in Loch Ainort and adjacent waters on the east coast of the Isle of Skye (See Section 3.1.). This site was carefully chosen (See Section 2.2.) to optimise both field time (a costly activity in offshore environments) and the beneficial extant onland data sets.

The data obtained from the echosounder survey (See Chapter 4.) was used to construct a bathymetric chart for the Loch Ainort field area (See Section 4.2. and Chart 4.2.). This chart was directly compared to the original Admiralty Chart (See Section 4.2.1. and Chart 4.1.), which was constructed from lead-line surveys conducted during the middle of the last century. Both charts were used to quantitatively describe the general morphology of the loch bed (See Section 4.3.). Analogue side scan sonographs were acquired through out Loch Ainort and were interpreted in detail to provide both qualitative and quantitative data on the topographic and material variations within the loch system (See Chapter 5.). The sub-bottom profiles obtained from this loch system enabled the high-resolution (< 0.3 m) study of the top 30 m of the loch bed stratigraphy. Detailed seismic sequence analysis (See Section 6.3.) of these profiles led to the identification and description of 4 seismic sequences and their further subdivision in to 10 seismic facies units.

The 14 cores and 7 surface samples obtained from within the Loch Ainort field area were analysed by a variety of laboratory techniques (See Section 7.2.2.) and on the basis of these results grouped in to a total of 4 lithological facies (See Section 7.2.3.). As described previously, with single channel profiling systems (*eg.* the 3.5 kHz Pinger) it is not possible to calculate velocity information directly from the acquired data, so that the conversion of reflection times into reflector depths has to utilise independent estimates of seismic velocity. (Kearey & Brooks, 1984). Consequently, the results of the particle size analysis conducted for all the acquired samples were used to calculate estimates for the compressional wave velocities for each lithological facies (See Section 7.2.4.).

Section 8.2. presents a reconstruction of the "recent" history of Loch Ainort based on the integration of the results from the four geophysical and geological data sets acquired and the extant onshore and offshore data summarised in Chapter 3. Due to the lack of any absolute dates obtained during this period of study only a relative reconstruction can

be confidently attempted. However, by closely justified inferences based primarily on the extant onland data an absolute sequence of events has been tentatively proposed. Section 8.3. uses this reconstruction to illustrate a critique of each of the acquisition and interpretation methodologies used during this survey. Each system is dealt with individually in Sections 8.3.1. to 8.3.4., with a discussion of the effective integration of all of these techniques being covered within Section 8.3.5..

Finally, Section 8.4. takes the composite para-stratigraphy interpreted for the Loch Ainort field area and attempts to compare it with the para-stratigraphies already constructed for the western seaboard of the Scottish Highlands (See Section 1.2.2.).

8.2. A PALAEO-ENVIRONMENTAL MODEL FOR LOCH AINORT, ISLE OF SKYE

Based on the evidence provided by the multi-disciplinary investigation of Loch Ainort and its surrounding catchment area, Section 8.2. attempts to present a hypothetical reconstruction of its recent geological past. This discussion has been subdivided into four Sections (Sections 8.2.1. to 8.2.4.) with the first three sections presenting a fully integrated stratigraphical interpretation of the sequences identified from the seismic para-stratigraphy presented in Section 6.4. (Table 6.5.). Section 8.2.4. presents an environmental synthesis for the Loch Ainort basin and is constructed on the basis of an inferred absolute chrono-stratigraphy.

8.2.1. SEISMIC SEQUENCES 1 AND 2

The basal section of Loch Ainort's stratigraphy, Seismic Sequences 1 and 2, are described together, as the general tonal characteristics of the seismic facies units of which they are composed (LASF1, LASF2 and LASF3) are considered to be almost identical (See Sections 6.3.1., 6.3.2. and 6.4.). These three seismic facies units having been distinguished purely on

the basis of the morphology of their upper boundaries and their spatial distribution. These variations will subsequently be discussed in relation to their chrono-stratigraphic association.

Acoustically LASF1 to 3 are typified by very high internal backscatter levels, no discrete internal reflectors, a distinctive mottled appearance (the product of small overlapping point hyperbolae) and occasional large individual point reflectors. Irrespective of the variable morphology they describe, their upper boundaries with the overlying seismic sequences 3 and 4 represent a large acoustic impedance contrast. Comparison with the local litho-stratigraphy, as described in Chapter 3, suggests that such strong, boundary and facies, characteristics could be produced by either a surficial sediment/bedrock interface or a loch sediment/glacial diamicton interface. Both of these hypotheses shall be considered here with reasoned arguments being presented for each.

The high acoustic internal backscatter level, lack of internal reflectors and their presence at the base of the imaged stratigraphy can all be considered as potential facies indicators of the "homogeneous" granite bedrock that underlies the Loch Ainort area (See Section 3.2.1.2. and 3.2.1.3.). As typified by the rounded hills of the Loch Ainort hinterland, granites typically erode to form relative smooth summits separated by broad cols and with gently undulating lower slopes (See Section 3.2.3.). Such a landscape could conceivably account for the low relief topography of LASF2 within the Unnamed Strait (See Section 6.3.1.2.) but it is difficult to reconcile such an erosional pattern with the pronounced and irregular topography of LASF1 (See Section 6.3.1.1.) or the subdued and chaotic upper surface of LASF3 (See Section 6.3.2.1.).

In order to persist with this interpretation it could be suggested that the Ainort Ridges, that are the surface correlatives of LASF1 (See Section 6.3.1.), could in fact represent differential erosion of the pervasive Skye Tertiary dyke swarm (See Section 3.2.1.4.). Indeed Bell and Harris (1986) suggests that these predominantly doleritic and tholeiitic intrusions do in fact erode to stand proud of the surrounding rocks. Yet the Loch Ainort field area is not characterised by the main Skye swarm but by the Scalpay subswarm in the eastern half of the area and an area of low dyke concentrations in the west (See Section 3.2.1.4.). Such an asymmetric distribution is broadly reflected in the distribution of the Ainort Ridges described from the side scan sonographs (See Section 5.3.) so supporting this general view point.

However, the average orientation of the subswarm (067.5°) is contrary to the mean axial orientation (127°) of the identified ridge complex. Equally if differential erosion was responsible for these features a change in the seismic signature would be anticipated between the topographic highs (basaltic rocks) and the intervening lows (granitic rocks) a variation that could not be identified in any of the sub-bottom profiles.

Further, the smoothed but asymmetric form of the Loch Ainort ridges, the large relief that they describe (160 m)[1] and the predominance of boulder clusters along their axes are not consistent with the lower relief (order of metres) and irregular features that characterise the terrestrially exposed dykes (Bell and Harris, op. cit.). No possible bedrock correlative for the chaotic and subdued upper surface for LASF3 could be determined by this author. Consequently, the body of evidence presented here does not support the hypothesis of a bedrock correlative for LASS1 and LASS2.

Section 3.2.2. clearly identifies the influence of glacial activity within the Loch Ainort field area, so the possibility of a glacially related origin for parts of the seismic para-stratigraphy is perfectly feasible. Glacial diamictons have previously been imaged by a variety of authors (*eg.* Johnson, 1980; Hutchinson *et al.*, 1981; Gilbert, 1985; King and Fader, 1986; King *et al.*, 1987) with these sediments being characterised acoustically by thick, uniformly dense patterns of unstratified facies with frequently abundant point reflectors and an upper reflector with pronounced positive relief. Such characteristics are clearly indicative of the three seismic facies identified at the base of the Loch Ainort seismic para-stratigraphy.

The majority of these authors also tend to go further with their interpretation using the genetically specific term "till" to describe these deposits, but these interpretations are frequently made without reference to any other geophysical or calibration data sets. The frequency of such sweeping and simple interpretations has recently come under considerable criticism (*eg.* Piper, 1988; Stewart and Stoker, 1990; Syvitski, 1991) as these latter authors argue that there would be little difference between the acoustic properties of till and a variety of either; ice-loaded glaciomarine, ice-contact or non-glacial debris flow deposits (For full

[1] Based on a compressional velocity value for Granite of 5500 ms^{-1} (Kearey and Brooks, 1991).

discussion see Syvitski, 1991). Such currently unresolved problems further emphasise the importance of presenting corroborative evidence for all genetic interpretations.

Despite the scepticism with which a number of authors view the validity of qualitative assessments of upper reflector relief for environmental interpretation, this author suggests such criticism is only relevant to interpretations based solely on two-dimensional seismic profiles. In Loch Ainort the ability to establish an inter-relationship between seismic facies LASF1 and the Ainort Ridges (See above and Section 6.3.1.) identified from the side scan sonographs, provides the opportunity for a more detailed and pertinent analysis of upper boundary morphology. As discussed in detail in Section 5.3. these sonographs suggest the loch floor is characterised by linear highs with asymmetric profiles, steeper down loch facing slopes (average angle 18.3°) and gentler (average angle 10.8°) up loch facing slopes. The ridges are predominantly concaved down loch with an average axial orientation of 127°, effectively perpendicular to the north-west and south-east margins of the loch. Their distribution throughout the region is uneven with the majority being concentrated in the "Mouth Region" (22 out of a total of 53) and towards the south-eastern margin of this area. In addition to this primary ridge cluster there are three other major ridge clusters at within loch sites (centred on AR14, AR17 and AR24) which span at least half the loch's width.

Comparison of the location and form of these ridges with the terrestrial limits established for the Loch Lomond Readvance glaciers (See Section 3.2.2.2.; Figures 3.5. and 3.6.) suggests a potential link between these two features. Firstly an inferred orientation for the Ainort Glacier terminus of 140°, a value based on terrestrial evidence, broadly concurs with the axial orientation (127°) described for the Ainort Ridges. Further the down loch concavity (*ie.* toward the proposed position of the Ainort Glacier) exhibited by many of the ridges is indicative of ice proximal activity (Price, 1983). The large cluster of moraines within the "Mouth Region" coincides with the maximum terrestrial extent of the Ainort Glacier defined by a chain of moraines south of Rubh' an Aird Duirche and potentially an intertidal spit on the northern shore (Benn, 1990). The two retreat positions, also identified from terrestrial evidence, again have offshore ridge equivalents albeit the marine record dictates a more complicated story of retreat (See Below). Consequently the, circumstantial, spatial and morphological evidence suggests a potentially intimate relationship between the Ainort Ridges

(and by association LASF1 and the acoustically similar LASF2 and LASF3) and glacial activity related to the Loch Lomond Readvance.

Such an inference of a glacial origin is also substantiated by material information obtained from both the side scan imagery and from core data. The side scan sonographs show that the majority of the Ainort Ridges are frequently encompassed by dark to very dark material reflector zones (potentially representing coarse sands to gravels: See Section 5.3., Table 5.1.). These images also suggest the presence of boulder and cobble clusters that have been identified on both the axes and the down loch margins of many of the ridges (See Section 5.3.). It is important to note that a number of the boulder clusters oriented parallel with the main ridge axes have also been found to be the surface expressions of buried ridges (See Section 6.3.1.1.).

Calibration of these acoustic textures has been possible through the coring programme undertaken in Loch Ainort with the ridge/dark material reflectors being identified as correlatives of ALF4 (See Section 7.2.3.). ALF4 is a light brown to grey-green, extremely poorly sorted, muddy to sandy muddy GRAVEL with occasional very large pebbles (maximum dimensions 63 mm) and so immediately supports the coarse nature of the material inferred directly from the sonographs and sub-bottom profiles. Statistical analysis of these sediments identifies a bimodal distribution with a split between the gravel and finer fractions (40% and 60% respectively). This bimodal distribution is clearly demonstrated by the cumulative frequency curve (See Figure 7.17.). Comparison with the work of Stravers *et al.* (1992) in Cambridge Fjord, northern Baffin Island, where they attempted to quantify the general characteristics of early to mid-Holocene fjordic glacial and marine sediments, shows good correlation of the grain size statistics of ALF4 with their Holocene Tills (See Table 8.1.)[2]. The major difference between the two litho-facies is the higher proportions of mud within LASF4. Stravers *et al.* (op. cit.) comment that other Baffin Island tills analysed by Andrews (1985) also exhibit a larger fine fraction, which they suggest is a result of these tills being exposed to post-depositional processes for longer periods than their early Holocene samples. It may therefore be inferred that

[2] Throughout this discussion it should be recognised that both sets of analyses are based on small sample numbers (N=12 and N=11, respectively).

ALF4 also has a longer depositional history than the Cambridge fjord tills (See Discussion Below).

In addition to these comparisons, the work of Vorren *et al.* (1983) and Schafer *et al.* (1989) also supports a glacial till origin, as they suggest that the glacial erosion of igneous terrain's commonly produces a multi-modal sediment [till] and frequently one with a subequal mixture of gravels, sands, silts and clays.

Litho-facies	*Gravel (%)*	*Sand (%)*	*Mud (%)*	*Silt (%)*	*Clay (%)*	*Mean (Mz: ϕ)*	*Sorting (σ: ϕ)*	*Skewness*	*Kurtosis*
ALF4	41	29	30	19	11	1.61	4.44	0.83	2.50
Till (Stravers *et al.*, 1992)	47.63	44.6	7.77	-	-	-0.31	2.76	1.19	3.81

Table 8.1. Comparison of the averaged grain size distributions (major fraction percentages and moment statistics) for ALF1 and a characteristic fjordic till.

The large individual clasts identified from the retained samples reflect the nature of the immediate hinterland with clast compositions varying from the leucocratic granites that dominate the Western Red Hills Centre within the field area (See Section 3.2.1.2.) to felsitc and basaltic fragments that can be identified from both the Western and Eastern Red Hills Centre at this site (See Sections 3.2.1.2. and 3.2.1.3.). The individual clasts vary from being sub-rounded to sub-angular with both bladed and equant forms being present. This variety of clast shapes is primarily controlled by lithology, however, the overall forms are indicative of a relatively immature sediment which has been transported for only short distances. Unfortunately due to the destructive nature of the gravity coring process and the small sample sizes retained, it is not possible to comment on the clast fabric within these obviously diamictic sediments. The lack of such information is critical as it is clast fabric that is frequently used for the accurate identification of the genetic history of a particular sediment (Drewry, 1986).

There is therefore no single piece of unequivocal evidence to suggest that LASS1 and LASS2 are in fact the seismic equivalents of glacial diamictons, however, the weight of

acoustic, morphological, material and spatial evidence all suggest such a relationship is probable. This interpretation for these sequences enables the assignment of a compressional velocity for all of these seismic facies units of 1775 ms^{-1} (See Section 7.2.4.: Table 7.4.). Being able to assign a velocity value to these units facilitates the conversion of the thickness and relief measurements from two-way travel time to metres. Using this value LASF1 can be seen to record a maximum thickness in excess of 55 m (no basal reflector is present to enable an absolute value to be quoted) with the topographic highs describing a maximum relief of 49 m. LASF2, which is restricted to the basal sections imaged in the "Unnamed Strait", attains a maximum thickness of 13.5 m but again as no basal reflector is present this is considered a minimum estimate. Finally LASF3, which has a restricted distribution to within the "Inner Loch", can be seen to attain an approximate maximum thickness of 10 m.

Having hypothesised that LASF1, LASF2 and LASF3 are glacial diamictons (probably till) which have formed in either a sub-glacial or pro-glacial environment it is possible to present a simple stratigraphical model for their formation. The close spatial correlation between the ridge topography of LASF1 and the terrestrial limits for the Ainort Glacier (Loch Lomond Stadial age) suggest that they are of equivalent age. It is therefore proposed that this seismic facies unit, and the Ainort Ridges its upper boundary describes, represents the offshore expression of the Ainort Glaciers advance and retreat stages *ie.* terminal and recessional moraines.

As discussed in Section 3.2.2.3. several lines of evidence suggest that during the Loch Lomond Stadial sea level in the area was at approximately the same level (± 5 m) as that of today. Even if the lowest possible limit is considered, reference to both bathymetric charts (See Chapter 4) suggests that the upper surfaces of LASS1 and LASS2 were still submerged except at marginal positions. Consequently, it can be inferred that the Ainort ridges were constructed in a sub-aqueous environment. Further, as the climatic conditions in North-West Europe during the Loch Lomond Stadial resulted in the development of temperate glaciers (Price, 1983), it can be hypothesised that the Ainort Glacier had to be grounded rather than having a floating termini, as the tensile strength of temperate ice is too low to advance by floating (Powell, 1984). If these conditions prevailed we can restrict the possible modes of

formation for these linear cross-valley moraines to three; either by glacial push, squeezing of till into basal crevasses or the coalescence of grounding line fans.

Push moraines are formed as the advancing glacier deforms the bed over which it rides to form large masses of material of largely sub-glacially deposited till. Previous authors (*eg.* Powell, 1981; Boulton, 1986; Larsen *et al.*, 1991), describing such moraines from a variety of fjordic glacial environments, suggest that they commonly have heights between 1 and 10 m high, inter-ridge distances of between 0 and 1000 m and axial lengths in the order of 10s to 1000s m's. These ridges also exhibit marked asymmetry, with steep distal slopes and shallow proximal slopes. Consequently, comparison with the dimensions of such features to those recorded for the Ainort ridges (See Sections 4.3.1., 5.3., and 6.3.1.)[3] show that the majority of the ridges have similar dimensions, however, it is difficult to reconcile the contrary asymmetry.

Similarly the squeezing of water-soaked ground moraine into a series of basal crevasses may also result in the formation of asymmetric ridges of fairly uniform coarse unsorted till (*eg.* Andrews, 1963; Beaudry and Prichonnet, 1991). Generally the dimensions and asymmetry of these features are similar to those created by glacial push and so when attempting a comparison with the Ainort ridges one encounters similar problems as described above. Due to their morphological similarity, these two types of moraine have been collectively grouped as De Geer moraines (Larsen *et al.*, 1991). De Geer moraines can be simply described as being:

> "..... a series of irregularly spaced ridges that are parallel to one another. They are found in glacial lakes or marine basins. The ridges are narrow and elongated, straight or sinuous, and some have minor appendages. Their profiles may be symmetrical or asymmetrical. The material forming the ridges usually consists of till..... Their axes are perpendicular to the ice flow....."
> Beaudry and Prichonnet (1991).

[3] Albeit values converted from TWT to m as presented in Table 6.4. are based on a velocity value of 1500 ms^{-1} and therefore represent underestimates.

The third possible mode of formation is the coalescence of ice-contact/grounding-line fans at a quasi-stable glacier margin. Ridges produced by this process have a composite nature with chaotic till masses interfingering with, and being overlain by, stratified sequences that fine with distance from the glacier (*eg.* Landmesser *et al.*, 1982; Dardis, 1985; Booth, 1986; Boulton, 1986; Powell, 1990). Evidently the Ainort ridges do exhibit the proximal asymmetry of these fans but they lack the composite morphology and the interdigitating relationships with the surrounding sediments that are so characteristic of such ridges.

Evidently the detailed descriptions of the three modes of moraine formation do not tally with LASS1 and LASS2 either in terms of morphology, in the case of the De Geer moraines, or complex lithology in the case of the coalescing fans. In the latter case it would be possible to invoke the argument that high-resolution seismic systems are incapable of identifying such acoustically subtle changes in lithology (See Piper, 1988 and Syvitski, 1991). However, neither the side scan sonographs nor the core material showed any evidence of any such cross-axis lithological changes. In addition, if the general description for the De Geer moraines presented by Beaudry and Prichonnet (1991) is taken at face value it is possible to account for the reverse asymmetry of the Ainort ridges (*ie.* the existence of steep proximal slopes). Therefore in the absence of any detailed cross-ridge lithological or clast fabric analysis these ridges are tentatively interpreted as being De Geer moraines.

The outer moraines within the "Mouth Region" extend significantly further into the loch than had been previously anticipated, occurring only 175 m from the western shore of Scalpay and 800 m beyond the limit inferred from the pre-existing terrestrial evidence (Ballantyne, 1989; Benn, 1990). This terminal limit is defined by a broken line of ridges, both buried and exposed and characterised by ABR12, AR49, BC22 and AR45 [157750 830450]. (See Figure 6.9.: Section 6.3.1.). As can be clearly seen from the isometric plot (See Figure 5.21.: Section 5.3.2.) between this terminal limit and the mouth of Loch Ainort a series of closely spaced (< 70 m) recessional positions are marked, terminating to the south-west with the major cross-valley ridge AR24 [156850 829300]. This ridge complex is 300 m to the south-west of the first major recessional limit inferred from the terrestrial exposures (See Figure 3.6.: Section 3.2.2.1.). This onshore limit in fact appears to coincide with a central "Mouth

Region" recessional position described by AR38 and AR44. To the knowledge of this author there is no terrestrial correlative of AR24.

The western margin of this maximal limit is evidently controlled by the dramatic change in loch bed bathymetry, as to the west of the "Mouth Region" the altitude of the upper boundary of LASS1 drops from approximately 10 mOD to 65 mOD at the base of the "Unnamed Strait" (over a distance of only 750 m). Due to the lack of penetration through LASS1 in the "Mouth Region" it is not possible to assess whether this change in relief is controlled by an underlying bedrock high, an accumulation of pre-existing glacial diamictons (See discussion below), deposition of purely Loch Lomond Readvance material or a combination of all three. As it is unlikely that Loch Lomond ice could be responsible for the deposition of such large volumes of material in a single location it is probable that this change in relief pre-dated the maximal position of the Ainort Glacier. Consequently, it is hypothesised that the maximal terminal position of the Ainort glacier occurred here as the Loch Lomond glacial system had insufficient energy to extend into this open deep of the "Unnamed Strait". Inevitably this dramatic change in bathymetry would promote iceberg calving as the tensile strength of the ice would be too low to advance into the deep by floating (Powell, 1984).

One point of note is the continued presence within the relief of the LASS1 upper boundary of the marked channel identified from the bathymetric data (See Sections 4.3.1.1., 4.3.1.2. and 4.3.1.3.). This prominent channel runs parallel to the north-western shore of the "Inner Loch", cuts the "Mouth Region" and turns through 90° as it opens out into the "Unnamed Strait". There is insufficient evidence to accurately account for the timing and mode of the channels formation, except to suggest a maximum Dimlington Stadial age as it is founded on LASS1 material (See Discussion Below). As it is difficult to comprehend a such laterally extensive area of non-deposition it is probable that the channel represents a localised erosive regime. It is therefore suggested that this area represents the location of a sub-glacial channel, inhibiting the development of the push-moraines along this northern shore. However, the author fully recognises that this interpretation is based on limited evidence particularly the lack of any signs of sub-glacial or sub-glacially related sedimentation (See Discussion in Section 8.2.2.).

Also of note are the two arcuate ridges, identified from both the bathymetric charts (ABR15 and ABR14) and the side scan sonographs (See Section 5.3.5.), located within Lùib na Moil

at the mouth of Coire Mòr, in the Moll peninsula. Albeit seismic evidence is poor, their association with "dark reflector" patches on the sonographs suggests a potential LASS1 composition (albeit which facies unit is not clear). Their location at the mouth of Coire Mòr would suggest that they are potentially related to the small (8.22 km²) Loch Lomond Stadial, Moll Glacier.

Albeit several ridges are identified within the "Inner Loch" (See Sections 5.3.1., 5.3.2., 5.3.3. and 6.3.1.) the next major "recessional" ridge complex is centred on AR17 [156550 828910]. This offshore complex coincides with a drift limit exposed on the north-western shore along the slopes of Leathhad Chrithinn, which is interpreted by Benn (1990) as being a recessional moraine. A third major "recessional" De Geer moraine (AR14) occurs to the north of Luib [156300 828650] but appears to have no terrestrial correlative. To the south-west of this feature the number of identifiable ridges (either buried or exposed on the loch bed) decreases markedly and no further major recessional features are seen (See Discussion Below).

Having established a hypothesis for an age and origin for LASF1 (De Geer moraines formed during the advance and recessional stages of a Loch Lomond Readvance glaciers) it is necessary to formulate hypotheses for the formation of LASF2 and LASS2 (LASF3). On the basis of seismo-stratigraphic analysis LASF2 is considered a lateral facies variation of LASF1. However, the interpretation of LASF2 as being a glacial diamicton (probably till) whilst having a restricted distribution to the "Unnamed Strait", and hence outside the Loch Lomond Readvance maximum identified within the "Mouth Region", presents an obvious chrono-stratigraphic dilemma. In order to deposit a glacial diamicton at this outer loch locality it is necessary to invoke a preceding period of glaciation. Section 3.2.2.1. describes the distribution of ice during the earlier Dimlington Stadial glacial maximum, from which it is clear that the entire Loch Ainort area was covered by both the Skye icefield and the north-westerly advancing mainland ice[4]. It is therefore proposed that LASF2 represents diamicton deposited during this earlier phase of glaciation. Although the terrestrial evidence suggests that a Dimlington Stadial age for this deposit is likely, the author recognises that the area has

[4] The confluence between these two having still not been identified (Benn *pers. comm.*, 1992).

undergone numerous earlier glaciations (See Sections 1.2.2. and 3.2.2.1.), so in the absence of *in situ* dates this quoted age should be considered equivocal.

This interpretation of an earlier age of deposition for LASF2 facilitates the revision of the formational hypothesis for LASF1. It can now be suggested that this facies actually represents the reworking of LASF2[5] with only a limited contribution from material deposited directly beneath or in front of the Loch Lomond glacier. This inference resolves the problem of the relatively small (3.023 km^3) Ainort Glacier being able to deposit, and subsequently deform, such a large (>55 m) thickness of LASF1. Indeed modern sediment-mass balance studies (*eg.* Syvitski, 1989) suggest that the flux of sediment from a modern analogue tidewater glacier is in fact dominated by glaciofluvial discharge (86%) with subordinate inputs from supraglacial dumping/ice-rafting (10%) and minimal subglacial deposition (4%). This "reworking" hypothesis may also account for the longer depositional history of the sampled till units as described from the averaged grain size distributions (See Discussion Above), particularly as the majority of samples analysed came from outwith the Loch Lomond Readvance limits.

The overlying LASS2 which is composed of the single facies LASF3 has also been identified as being a glacial diamicton but with restricted distribution to the inner part of the "Inner Loch" and with a subdued but chaotic upper bounding surface relief. Evidently it's stratigraphical position suggests that it is younger than the underlying LASS1 but in the absence of there being an additional Holocene glaciation it is likely that its formation is still related to Loch Lomond Stadial activity. Within the sub-aerial sections of the Loch Ainort basin, the unconsolidated glacial drift is characterised by numerous, low relief, isolated mounds and hummocks with little evidence of moraine orientation (See Section 3.2.2.2.). This characteristic "hummocky" relief pattern is interpreted as being the result of the mass dumping of diamicton from remnant glacier ice downwasting *in situ* (Benn *et al.*, 1992). It is therefore proposed that the similar morphology and inferred diamictic composition of LASF3 suggests is deposited by a similar offshore process.

[5] And potentially paraglacial and marine sediments deposited during the interval between the two glacial phases.

This interpretation is currently under debate, with a resurgence in the popularity of an active retreat hypothesis for the production of such landforms (For Summary See Bennett, 1994). Indeed the presence of the moraine complex AR14 [156300 828650], south-west of the maximal extent of the hummocky moraine terrain may lend credence to the active deglaciation model. However, there is insufficient evidence from this study to conclude if this feature was produced during active deglaciation or whether it represents a pre-existing ridge[6] that survived glacial advance. Further Benn *et al.* (1992) actually addressed the issue of active deglaciation versus stagnation concluding, on the basis of additional terrestrial evidence, that *in situ* downwasting was the dominant process acting in the Loch Ainort basin. Consequently, on the basis of spatial distribution (restricted to the inner loch) and upper bounding surface morphology (low relief and chaotic), it is hypothesised that LASS2 represents an equivalent offshore downwasting facies which is deposited upon LASS1 during the retreat phase of the Ainort Glacier.

8.2.2. SEISMIC SEQUENCE 3

An environmental interpretation of this seismic sequence inevitably has to be the most subjective as it stratigraphical position, in the centre of the sedimentary pile, negated both direct sampling or imaging by the non-penetrative geophysical methods. Consequently, this interpretation has to be based on acoustic comparison with facies units from LASS1 and LASS4, the stratigraphic styles of the internal reflectors and correlation with the sub-aerial drift stratigraphy. This sequence contains two facies LASF4 and LASF5 (See Sections 6.3.3.1. and 6.3.3.2. respectively) with the former restricted to the "Inner Loch" and the latter to the "Unnamed Strait". Albeit these two seismic facies have a similar acoustic signature and seismo-stratigraphical position it is proposed that they have two differing modes of formation and as such shall be discussed separately.

---

[6] Formed during either the Dimlington Stadial maximum or the advance stage of the Loch Lomond Stadial.

LASF4 occupies the deepest parts of the irregular relief described by the upper palaeo-surface of the glacial diamicton at the base of the imaged stratigraphy within the "Inner Loch". This facies has accumulated in three main bodies which are offset toward the axial region and north-western shore of the loch (See Figure 6.19.: Section 6.3.3.). Additional smaller (< 0.01 km^2) discrete bodies also occur sporadically distributed around the main accumulations. This facies is characterised by a low to medium internal backscatter level, with thick (1.4 ms TWT) strong, discontinuous, internal reflectors of high lateral extent. These irregular reflector packages have a horizontal to gently inclined orientation which terminate abruptly against the slopes of the underlying "till" units (See Figures 6.20. and 6.21.).

By comparison with the lithological interpretation of LASS1, LASS2 (See Section 8.2.1.) and LASF6 (See Section 8.2.3.) it is proposed that LASF4 represents a sediment with a strong bimodal grain size distribution. The strong discontinuous internal reflectors are considered to represent layers of muddy to sandy muddy GRAVELS similar to the underlying diamicton units. These discrete layers are contained within a poorly stratified (considering a vertical resolution limit of 0.3 m for the sub-bottom system) finer matrix of fine silts or clays comparable with the overlying LASF6 (See Section 8.2.3.). Albeit, this subjective interpretation is open to discussion it enables the assignment of an averaged velocity value for the unit of 1680 ms^{-1}. This gives a maximum thickness for this unit of 11.7 m with the individual "gravel" layers having an average thickness of 1.2 m.

Having presented a simple sedimentological description of this seismic facies unit it is necessary to form a hypothesis for it's mode of formation. It is suggested that this facies unit was deposited by debris flows induced by the influx of intermittent sedimentary gravity flows entering the loch from the steep slopes of Leathad Chrithinn along the northern shore of Loch Ainort. This hypothesis is based on four lines of evidence:

i) Stratigraphic style: Syvitski (1989) in a detailed discussion on the "...deposition of sediment within glacier-influenced fjords...." deconstructed the complex sedimentary structures identified within fjords into six simple stratigraphic styles. He further asserts that each style is primarily controlled by the dominant sedimentary process operating at the time of formation. Comparison of the internal reflector style identified in LASF4; and in particular the internal conformable layering, onlapping relationship with the underlying unit and the presence

of abrupt termination's; with his scheme suggest this facies unit represents a ponded style. Ponded sediments Syvitski suggests (op. cit.) are considered to be indicative of "sedimentary gravity flows" either entering the water body[7] from a sub-aerial source or via submarine slope failures. However, submarine slope failures tend to be associated with scoured and disturbed internal loch slopes (*eg.* Aarseth *et al.*, 1989) which have not been identified within any of the sub-bottom sections. Consequently, it is inferred that sub-aerially derived material is the dominant source for these flows (for additional evidence see *iv)*). The dimensions of the layering suggests that the influx of this material is sufficiently large to cause localised (both temporally and spatially) domination of the sedimentation processes operating in the loch during this period.

ii) Stratigraphic relationship: The location of this unit within the deepest parts of the "Inner Loch" basin and the filling of the irregular relief of underlying glacial diamicton surface is also indicative of debris flow deposits. In flowing, high concentration, debris flows would be significantly denser than the surrounding loch waters and so would enter the loch as hyperpycnal flows (or underflows: Leeder, 1982). These flows would travel along the loch bed, albeit with the insufficient energy to erode the underlying units, prior to deposition within the deepest depressions of the irregular loch bed. The non-erosive nature of the basal layer is again a characteristic of debris flows and can be identified in the Loch Ainort field area by the nature of the basal reflector of LASF4, particularly where it has an arbitrary/unconformable relationship with the underlying LASS2 (See Figure 6.21.). The steep slopes of the "Inner Loch" particularly along the northern shore (present day angles 12°: See Section 4.3.1.1.) would inhibit the immediate settling of in flowing material and hence the development of graded delta complexes.

iii) Sedimentology: Despite the equivocal nature for the inferred bimodal grain size distribution of LASF4 the poorly sorted mixture of muddy to sandy muddy GRAVELS within a fine silt matrix is indicative of debris flow deposits. Syvitski *et al.* (1987) suggest that debris flow deposits are characterised by poorly sorted pebbly muds. The individual clasts range from silt to boulder size grains, with these larger grains representing either syn-

[7] Utilising the arguments presented in Sections 3.2.2.3. and 8.2.1. it is assumed that the Loch Ainort field area has been continuously submerged throughout the Lateglacial and Holocene periods.

sedimentary clasts or autochthonous fragments. These coarser clasts float within a matrix of clay- and silt- grade material. Leeder (1982) further suggests that debris flow deposits exhibit poor sorting,. poor grading and no primary internal sedimentary structures. Debris flows tend to create deposits that range in thickness from decimetres to metres, comparable with the units described within LASF4. The dominance of the finer grained matrix material within this facies unit, and it's similarity with overlying LASF6 suggests periodicity of influx of this material enabling either the settling out of the finer fraction of the individual debris flows or the temporary return to conventional loch sedimentation patterns (See Section 8.2.3.1.).

iv) Spatial Distribution: Section 3.2.2.2. presents evidence that significant reworking of glacial drift occurred during the paraglacial period, with such activity being particularly prevalent on the steep slopes of Leathad Chrithinn to the north of Loch Ainort. Benn (1990) identified that Type I, II and III sedimentary gravity flows (After Lawson, 1982 and 1988) and landslides dominated this particular area. It is further suggested that this activity continued throughout the paraglacial, being dominant until the colonisation and stabilisation of these slopes by vegetation. Drewry (1986), identifies that all Lawson flow types are potential sources of gravel-sand-silt mixes with Types I, II and III having bulk mean grain sizes of -1ϕ to 2ϕ, 2ϕ to 3ϕ and -2.5ϕ to 2.5ϕ respectively.

The asymmetric distribution of LASF4 towards the north-western shore and the slopes of Leathad Chrithinn would therefore provide a suitable source for these sub-aqueous debris flow deposits. This interpretation therefore enables the source material for this facies unit to be identified as being reworked heterogeneous glacial diamicton of both pre- and syn-Loch Lomond age. Further, it enables the placement of LASF4 within the established Loch Ainort chrono-stratigraphy *ie.* during the paraglacial period and prior to a return to true inter stadial conditions during the early Holocene sedimentation conditions. In the case of Loch Ainort it is proposed that this activity would be initiated immediately following the sub-aerial exposure of these steep northerly slopes presumably at some time during Deglacial Phase II. It is difficult to assign an exact time to the start of the paraglacial period, however, the lack of interdigitation between LASF4 and the glacial diamictons of LASS2 clearly suggests that the

deposition of this material must have occurred after the last active readvance event[8]. Obviously such a stratigraphical relationship, overlying the "downwasted" LASS2 diamictons also negates the possibility of these flows being derived from a static glacier terminus position (See Section 8.2.1.).

As described in Section 6.3.3.1. and alluded to at the start of this section, acoustically LASF4 and LASF5 are very similar, with strong, laterally continuous, internal reflectors within a finer matrix of medium backscatter material. There are, however, several critical differences, firstly the individual internal reflectors are thinner (0.46 m *vs* 1.2 m for LASF4)[9] and secondly they describe a different stratigraphical style. In this region the strong internal reflectors have an apparent conformable relationship with the underlying unit in the deepest part of the "Unnamed Strait" but unconformably onlap on to the underlying LASS1 at the loch margins (See Figure 6.21. and 6.22.). The individual component reflectors of each laterally continuous layer also become more disrupted towards the loch margins. Comparison of this reflector configuration with the Syvitski (1989) stratigraphical style classification, shows they do not correspond with the ponded form indicative of sedimentary gravity flows but are in fact characteristic of an environment with decreasing current energy (wave or tidal) with depth.

In addition the "Unnamed Strait" is bounded by subdued lowland topography of both the Moll Peninsula in the west and the slopes of Scalpay to the east (See Section 3.2.3.) with neither of these areas having a thick veneer of drift, suggesting there is limited sub-aerial source material for debris flows. Similarly, both the bathymetric charts (See Sections 4.3.1.3. and 4.3.2.) and the isometric plot (See Section 5.3.4.) fail to identify any potential major source areas for submarine flows within the "Unnamed Strait", with only a small number (5) of ridges and gentle (< 4°) marginal loch slopes. The north-western edge of the "Mouth Region" could have been a possible southerly source of material but there is no evidence of, what would have to be extensive, downslope slumping on the numerous sub-bottom profiles that sectioned this slope. It is therefore necessary to identify a potential source for the

---

[8] Again this assumes that the boundaries between these seismic facies could actually be acoustically imaged (See Discussion in Section 8.2.1.).
[9] Using velocity conversion value of 1680 ms^{-1}.

heterogeneous coarse material which could have been deposited within a, depth controlled, variable energy environment.

Finally, the upper boundary of this facies unit with LASS4 is marked by a strong laterally continuous reflector against which LASF5 internal reflectors abruptly terminate (See Figure 6.22.). This boundary contrasts markedly with the gradational, "arbitrary boundary" described for the upper bounding reflector of LASF4. Finally, LASF5, as with LASF4, has a restricted spatial distribution being confined to a large (1.65 km^2), thick (average thickness 9.6 m and a maximum thickness of 11.7 m offset toward the mouth of the Luib na Moil inlet)[7] body within the "Unnamed Strait".

As a consequence of these marked differences it is not possible to apply the formational hypothesis presented above for LASF4. The broad grain size interpretations made for LASF4 can be retained with the bimodal nature of the sediment, layers of sandy muddy GRAVEL layers within a silt or clay grade matrix, still being evident in the backscatter levels of the unit. The absence of any low backscatter material does suggest that the matrix may represent the coarser end of this grade. Due to the location of ALF4 at depth within cores from the "Unnamed Strait" and underlying litho-facies units correlated with LASS4 reflectors, it could be suggested that ALF4 is in fact a correlative of LASF5 rather than LASF2 as discussed in Section 8.2.1.. It should therefore be highlighted that the absence of the pronounced erosive boundary between the corresponding litho-facies in core JC1[10] and the positive correlation of this litho-facies with the dark-reflector material identified from the sonograph requires the retention of a direct glacial origin for ALF4 is retained.

In the light of these problems three possible hypotheses for the formation of LASF5 are presented, however, with the limited corroborating evidence available none of them are considered by this author to be satisfactory.

i) Ice proximal discharge from maximal position of Loch Lomond Readvance glaciers: It is widely documented (*eg.* Powell, 1981; Boulton, 1986; Boulton, 1990; Powell, 1990) that

---

[10] Note cores JC13 and JC14 are too shallow to be within the resolution capability of the sub-bottom system.

deposition of glacier-contact fans is a common occurrence at temperate, grounded, tidewater fronts. Deposition, commonly in the form of a classic prograding sequence of distally fining sediments, occurs from hyperpycnal flows induced by the influx of subglacial (and occasionally englacial) waters. These fans tend to be compositionally and structurally complex being composed of direct marine outwash[11], *in situ* sedimentary gravity flows (instability being induced by the development of a continually steepening frontal slope) and the settling out of fines from the jet and plume of turbid meltwaters after it detaches from the loch bed.

Depending up on the relative contribution of these three factors the resulting sediments exhibit the classic deltaic topset-foreset-bottomset sequence. Initially the flow deposits coarse gravels and sands close to the efflux which grade into finer gravels and sands at distance. At the point of detachment of the flow (generally < 13.4D, where D is the tunnel diameter; Powell, 1990) a rising plume is created, stabilising either at mid-column or surface position. From this migrating plume silts and clays settle out to form laterally extensive frequently laminated sediments. This sedimentary sequence can be disturbed both by the redistribution of material through gravity flows or the migration of the efflux position along the grounding line. This latter control is particularly common at quasi-stable termini as active calving exposes the sinuosity of subglacial and basal tunnels, this movement being characterised by sheet or cut-and-fill geometry's within the sedimentary pile.

Evidently such a process operating at the maximal position of the Ainort Glacier could source the heterogeneous sequence identified in the "Unnamed Strait", however, there are several problems with this hypothesis. Firstly, as described previously the stratigraphic style exhibits neither foreset development, incision geometry's nor the disturbed or ponded layering anticipated for glacier-contact fans. In fact unless the environment of deposition of this facies unit was dominated by tidal/wind processes it is difficult to account for the onlapping reflectors that are actually identified. This is unlikely as the majority of LASF5 occurs between a depth of 25 mOD to 65 mOD. In open fjord conditions wave resuspension seldom extends below 30 m (Syvitski, 1989) and considering the sheltered locality of the area and the dominance of south-westerly winds during this period the "Unnamed Strait" would have been

[11] Defined as sediment deposited from a jet of submarine meltwater while it is in contact with the loch bed (Powell, 1990).

subject to a very limited fetch so negating the development of large waves. Tidal currents could have been sufficiently high to cause winnowing and erosion of the loch bed, but with maximal velocity values of 0.93 ms^{-1} (Calculated from Equation *3.1)* with a water depth of 60 m: See Section 3.3.) it is improbable that they could control deposition from a sub-glacial flow that could potentially exit the efflux at up to 6 ms^{-1} (Powell, 1990). The only way that tidal processes could become dominant would be to infer a significant drop in sea level, but the weight of evidence presented in Section 3.2.2.3. and 8.3.3. would appear to contradict this possibility.

Secondly, LASF5 appears to be relatively uniform in nature throughout the "Unnamed Strait" and exhibits no lateral grain size gradation. Considering we can identify the maximal position of the glacier snout within the "Mouth Region" (See Section 8.2.1.) it is difficult to comprehend how LASF5 could extend for over a 1000 m in to this area whilst still retaining a thickness of 3.5 m. Deposition on this scale would require the efflux of the channel to have a diameter in excess of 75 m (After Powell, 1990). Admittedly, if the internal structure of LASF5 and the unit is regarded as a whole, the northerly thinning of the unit from a maximum thickness of 11.7 m at the mouth of the Lùib na Moil inlet would confirm a potentially southerly source of material. Indeed, the location of this thick accumulation does coincide with a position proximal to both the terminal position of the Ainort and the smaller Moll Glacier snouts. Further, if we identify the prominent channel which cuts the mouth region and enters the "Unnamed Strait" at this locality as being founded on a previous location of a subglacial tunnel (See Section 8.2.1.) this would again account for a possible accumulation of LASF5 material here.

If it was assumed that deposition of this unit was related to Loch Lomond Stadial activity it is necessary to identify a sufficiently destructive process to account for the strong erosive upper boundary. Following the arguments presented above, it is evident that at such depths neither tidal or wind induced currents that may have existed during the Holocene could have been responsible. Further, if currents were a major control it would be necessary to account for the change from an environment where erosional processes dominated to one where the deposition of LASS4 was possible (See Section 8.2.3.1.). Localised increases in shallow water column velocities could have been induced with increased subglacial flow during the

retreat phases (Boulton, 1990), but again it is difficult to account for both the change from a depositing to an eroding flow and the erosion at distance of the LASF5 upper boundary (considering the rate of rise of the inflowing jet). The only other alternative this author can suggest is the erosion by a single or small number of catastrophic events, but in the absence of no supporting evidence this is rejected as a viable hypothesis.

Despite potential spatial evidence for a Loch Lomond Stadial ice-proximal discharge source for this facies unit, the questions raised over the stratigraphic style, sediment distribution and the origin of the erosive upper boundary are difficult to reconcile with this mode of origin.

ii) Iceberg rafting and sea ice deposition: Deposition of heterogeneous mixtures of coarse and fine grained material may also occur from either icebergs produced from an actively calving front or sea ice developed in front of the tidewater glacier. Depending upon the volume of subglacial, englacial and supraglacial material within individual bergs, sedimentation from these sources is frequently superimposed upon the more steady release of sediment from basal glacier and loch margin melt sources (Drewry, 1986). Consequently, Ice Rafted Debris (IRD) is characterised by the presence of dropstones, till pellets and conglomeratic lenses (Powell, 1984).

As has already been described in Section 8.2.1. it is probable that active calving occurred along the western margin of the tidewater front within the "Mouth Region". Assuming dominant tidal currents similar to those described for the present hydrodynamic regime (See Section 3.3.) it is reasonable to assume that the majority of icebergs would migrate northwards towards the Sound of Raasay and the Narrows of Raasay and to ultimately enter the Inner Sound. Further the study of sedimentation rates from icebergs in Spitsbergen by Dowdeswell and Dowdeswell (1989) suggests that bergs calved from tidewater valley glacier fronts predominantly release debris in relatively proximal locations with "... most deposition [being] likely to occur within the fjords, immediately beyond the parent glacier margins.". No estimates exist for the average volume of debris within Ainort Glacier ice, however, having already established (See Section 3.2.2.2.) that the glacier certainly overrode pre-existing Dimlington Stadial deposits and that sub-aerial gravity flows occurred throughout the area during the glacial and deglacial phases, it is proposed that there were several potential sources for material to have been incorporated in to Ainort Glacier ice. Consequently, appropriate

source materials, active calving processes and the presence of northerly flowing currents would all facilitate iceberg rafting proximal to the tidewater front.

Drewry (1986) states that sea ice develops when air temperature falls below the freezing point of seawater (-1.8°C at 34 psu). As described in Section 3.2.2.2., data for the Loch Lomond Stadial suggests that winter temperatures ranged from -15°C to -20°C whilst mean July sea-level temperature rose to approximately 6°C. Evidently sea ice would have developed within the exposed waters of the "Unnamed Strait" during the winter months but would have been seasonally controlled so providing a sporadic influx of dominantly supraglacial material in to the region.

Deposition from these two sources inevitably occurred within the "Unnamed Strait" and as this area was undergoing active tidal movements such currents would inevitably control the settling patterns of such deposits. Therefore a combination of constant background fine grained sedimentation from subglacial, supraglacial and terrestrial sources would be interspersed by localised accumulations of coarser debris from icebergs. There are, however, problems with this otherwise adequate analogue for LASF5. Firstly it is difficult to correlate the dominance of the internal reflectors (the inferred IRD) within LASF5 compared to the surrounding matrix (the inferred background sedimentation).

Studies by Dowdeswell and Dowdeswell (1989) on modern frozen based tidewater valley glaciers in Spitsbergen identify average iceberg sedimentation rates[12] of between 1-8 mm yr^{-1}. By comparison total sedimentation within these localities are generally an order of magnitude higher 30-100 mm yr-[1]. These authors also suggest that "..even where large icebergs are trapped for relatively extended periods close to the margins of tidewater glaciers, the enhanced ice rafted input is likely to be masked by more rapid sediment delivery from subglacially-derived meltwater." and that "This is similar to the situation for Alaskan [temperate] tidewater glacier-fjord systems".

[12] Calculations are dependant upon debris concentration by volume, basal melt out rate, glacier velocity, length of the tidewater front and size of the receptor basin

Compared to the Spitsbergen valley glaciers the Ainort and Moll Glaciers would have more numerous sources of debris supply (and so potentially greater debris concentrations), greater basal melt out rates due to higher summer sea temperatures and smaller receptor basin sizes, all of which would increase the potential berg sedimentation rate[13]. It is, however, considered unlikely that these factors would account for the qualitatively inferred discrepancy between iceberg sedimentation rate versus background sedimentation rate in the "Unnamed Strait". Even with additional material being provided by deposition from seasonal sea ice it is difficult to reconcile these differences. Equally, the thicknesses identified within this area may only represent minimal values as it cannot be known how much material was lost during the erosion of it's upper boundary. Finally, this particular model does not provide an control for the distribution of LASF5 and in particular the concentration of this facies unit toward the Lùib na Moil inlet.

As with the problems presented for a Loch Lomond maximum ice proximal source an ice-rafting hypothesis still fails to provide a process and more importantly the time for the erosion of the upper boundary of this facies unit to occur. Ice-rafting/sea ice activity related to the Loch Lomond Stadial may therefore be able to contribute to the formation of LASF5. However, it is difficult to envisage how it could be responsible for the entire unit and how such a time scale could accommodate the subsequent geological history of the area.

iii) Deposition from retreating Dimlington Stadial ice sheet: The final hypothesis presented for the formation of LASF5 effectively reiterates the arguments presented in the first two hypotheses. This theory suggests that the processes involved in the formation of LASF5 were either an amalgamation of ice-proximal and ice-rafting activity or a solely ice-rafting source but on a significantly larger scale. The major difference is the proposed timing of formation of this seismic facies unit. For hypotheses *i)* and *ii)* it has been casually assumed that, due to the similarity in location of LASF5 within the seismic para-stratigraphy as LASF4, it also represents Loch Lomond Stadial deposition. However, due to it's marginally remote position within the basin, it's unconformable lower boundary with LASS1, the lack of any direct samples and the absence of any independent dating leaves it's age open to interpretation.

---

[13] Note that there are no estimates for ice velocity for the Loch Lomond Readvance glaciers, and that the length of tidewater front in this area is shorter.

Section 8.2.1. has already proposed that in the "Unnamed Strait" the underlying LASF2 in fact represents glacial deposition related to the earlier Dimlington Stadial glaciation and that any direct Loch Lomond glacier influence terminated in the "Mouth Region". Section 3.2.2.1. suggests that glacial activity related to this Dimlington Stadial event reached a maximum at *c.* 18 ka BP or possibly slightly earlier, with retreat continuing until *c.* 12.5 ka BP. During this retreat phase the field area would have been influenced by the deglaciation of both the Skye ice cap and mainland ice. It is therefore probable that at some time during this deglacial phase glacial and paraglacial debris would have been flowing in to the "Unnamed Strait". Indeed toward the western shore of this area (*ie.* the Lùib na Moil inlet) a potentially complicated depositional environment could have existed as it represents the location of the confluent margin between the ice sheets (See Section 3.2.2.1.). Further the absence of any potential interglacial marine/glaciomarine deposits from the acoustic images between LASF2 and LASF5 would also support an immediate post Dimlington maximum phase. It is assumed that even if there was a relatively small period of exposure of the loch bed between Dimlington ice retreat and Loch Lomond Readvance, there would be significant interglacial paraglacial sedimentation in the "Unnamed Basin". Its absence, therefore presents additional negative evidence for hypotheses *i)* and *ii)*, albeit it is recognised that the arguments detailed in Section 8.2.1. for the identification of sediments that may have only subtle changes in acoustic impedance contrast also applies here.

This interpretation can be potentially supported by correlation, with the seismic para-stratigraphy for the north-western seaboard of Scotland, constructed by Davies *et al.* (1984). Albeit this para-stratigraphy is the subject of much debate (See Section 1.2.2.4.), the acoustic reflectors representing the transition from the Hebrides Fm. to the Barra Fm. are similar[14] to the acoustic transition from LASS1 (LASF2) to LASS3 (LASF5) in the "Unnamed Strait". On the basis of limited evidence Davies *et al.* (op. cit.) interpret this transition to represent "Late Devensian Glacial Maximum till", unconformably overlain by glaciomarine sediments deposited during ice-front recession during the deglacial phase of this ice sheet. Yet, Davies *et al.* (op. cit.) present minimal evidence to support their hypothesis, so this correlation should not be regarded as principal support for a Dimlington Stadial age for LASF5.

---

[14] Assuming allowance is made for the differing seismic systems used for data acquisition.

Seismo-Stratigraphy	*Seismic Signature*
Barra	Acoustically transparent with a low seismic background signal. Occasionally short randomly spaced internal reflectors. Unconformable upper and lower boundaries
Hebrides	Thin sequence of diffraction hyperbolae covering an extensive unconformable lower boundary.

Seismic Sequence	*Seismic Signature*
3	**LASF5:** medium internal backscatter and thick, disrupted, strong, parallel, internal reflectors with great lateral continuity. Thin but clearly marked upper unconformable reflector.
1	**LASF2:** very high internal backscatter with no discrete internal reflectors and a distinctive mottled appearance. Upper unconformable boundary smooth, low relief, but laterally extensive.

Table 8.2. Correlation of the Davies *et al.*'s (1984) "seismic para-stratigraphy" with part of that constructed for the "Unnamed Strait" (For full para-stratigraphy see Section 6.4.).

If an earlier age is assigned to this facies unit it does provide a potential process by which it's upper boundary can be eroded. With this hypothesis these deposits would have been exposed on the loch bed during the climatic deterioration at the end of the Dimlington Stadial and the subsequent advance of Loch Lomond Stadial glaciers. At the maximum extent of the glacier the tidewater front and any subglacial effluent would be proximal to the "Unnamed Strait". As described above the hyperpycnal flows that may have emanated during this period travel, in shallow water, at speeds up to 6 ms^{-1} (Powell, 1990: See Above) and certainly with the ability to erode a poorly consolidated/unconsolidated heterogeneous bed. Consequently such flows could be major agents of erosion in addition to being major sources of deposition.

An alternative hypothesis for loch bed erosion could be increased current induced activity at depth, due to the increased storm conditions that prevailed in north-west Scotland during this period (Dansgaard *et al.*, 1989: See Section 3.2.2.2.). However, as described previously at the maximum extent of the Loch Ainort and Moll glaciers the average fetch and hence average wave amplitude would be reduced. Consequently the period of time over which increased storminess could induce stronger bottom currents would be significantly shorter.

Evidently, there is still limited evidence to support this hypothesis and albeit it presents a potential solution to the unconformable upper boundary problem it still fails to account for all of the characteristics identified from seismo-stratigraphic analysis. Firstly, this process would still have difficulty in accounting for the lateral extent of the upper erosional surface (considering the limited distance of hyperpycnal flows) and the asymmetric accumulation pattern. Equally, if hyperpycnal flows did emanate from the Loch Lomond Glaciers why is

there no evidence of coarse ice-proximal deposition related to this event? Even if these glaciers were typified by low sediment concentrations some evidence of ice-proximal deposition is anticipated, as predicted by the model of Powell (1984) for warm ice, valley-outlet glaciers, with a melting/freezing base and which end as tidewater fronts.

In conclusion, there is insufficient corroborative evidence to be confident of any of the hypotheses presented for the formation of LASF5, all of them having conceptual drawbacks. However, in the absence of any additional evidence this author tentatively suggests that, of those presented here, hypothesis *iii)* is the most plausible.

8.2.3. SEISMIC SEQUENCE 4

Seismic sequence 4 is the highest sequence in the seismic para-stratigraphy constructed for the Loch Ainort field area. This sequence also exhibits the largest lateral and vertical seismic facies variation of all the sequences identified within the basin. The sequence is dominated by facies units LASF6 and LASF7 which cover the majority of the loch bed in both the "Inner Loch" and the "Unnamed Strait". These units dominate the deeper parts of the loch basin, occurring in shallower depths as thinner veneers on the marginal loch slopes[15] and small pockets of material within the lows of the ridge and basin topography of the "Mouth Region".

Within the "Inner Loch" these facies units unconformably overlie the irregular topography described by the pre-existing surface created by LASS1, LASS2 and LASS3, the sequence thinning out toward, and onlapping on to the internal and marginal topographic highs. Within the "Unnamed Strait" the same sequence is represented by LASF7 that creates a surface veneer which again is concentrated in the deepest parts of the basin. The remainder of the facies units identified within this sequence, LASF8 to LASF10, have a very restricted distribution, again occurring as thin covers on the upper surfaces of shallow plateau areas and small depressions within the gentle sloping surfaces around the loch margins.

---

[15] Identified purely from side scan sonographs being beyond the limit of resolution of the sub-bottom profiler.

For the majority of the area the upper sequence boundary to LASS4 represents the present loch bed thus providing evidence that, at least in part, this seismic sequence represents the product of modern sedimentation processes. Analysis of the four datasets enables the subdivision of the sequence in to three main sedimentary styles; General Loch Sedimentation, Deltaic Sedimentation and Mass Movement. This section will attempt to describe the processes and products identified within each of these sub-groups for the Loch Ainort region.

8.2.3.1. General Loch Sedimentation

As described above the principal seismic facies unit of LASS4 is LASF7. This unit has a medium internal backscatter level and occasional weak, parallel, inclined internal reflectors with a high lateral continuity and extent (See Section 6.3.4.2.). This unit rests on all of the seismic facies described previously with the style of it's lower boundary varying with the acoustic properties of the underlying material. Where it unconformably sits on LASS1 (both LASF1 and LASF2) the boundary is marked due to it's contrasting acoustic texture to the very dark tones of the "glacial tills" (See Section 8.2.1.). Within the "Inner Loch" accumulation of LASF7 frequently, totally or partially, obscures the irregular relief described by this lower boundary with LASS1. In the "Mouth Region" and the margins of the "Unnamed Strait" LASF7 occurs as a much thinner drape onlapping on to the underlying LASS1 surface. In the deeper parts of the "Unnamed Strait" the unit rests directly on the prominent upper erosive boundary of LASF5.

Towards the head of the "Inner Loch" the relationship between LASF7 and the remaining underlying seismic facies units can also be identified. South-west of the Luib inlet in the deep parts of the basin created by the basal sequences LASF7 has a conformable boundary with LASF6 (See Discussion Below). Where LASF6 pinches out (See Figure 6.20. or 6.21.) an arbitrary boundary between LASF7 and LASF5 can also be identified. Finally, to the north-west of the Luib inlet, LASF7 has a distinguishable unconformable lower boundary filling the diffuse and chaotic upper surface of LASS2. LASF7 attains a maximum thickness of 12 ms TWT in the deepest part of the "Inner Loch" body compared to a maximum thickness of 6 ms TWT for the surface veneers of the "Unnamed Strait" and the "Mouth Region".

In contrast to the general uniform nature of LASF7 the litho-facies interpreted from the core material and which are considered it's correlatives (ALF1-ALF3), suggests a greater degree of grain size variation for this unit. Consequently with the lack of acoustic variation in this facies unit, other than the presence of large scale reflectors indicating a decreasing energy environment with depth, environmental interpretation of this unit has to rely heavily on sedimentological analysis.

As can be seen from the summary diagram for the lithological facies identified in Loch Ainort (See Figure 7.7.: Section 7.2.3.), there is a general up loch and lateral coarsening sequence present in the upper part of LASS4. The sediments vary from medium SILTS and MUDS in the deep waters of the "Inner Loch", to very fine SANDS towards the "Mouth Region" and along marginal loch sites, to gravelly and sandy MUDS in the mouth region and along Scalpay's shores and finally a mixture of the finer fractions in the deeper parts of the "Unnamed Strait".

In the deeper parts of the "Inner Loch" between 1 and 2 km north-east of the prominent slope at the head of the loch the sediments are characterised by homogeneous grey-green to grey-black medium SILTS and MUDS. These sediments all have discontinuous, monochromatic, wispy layering with thinner darker layers (commonly $\leq$ 10 mm) and the more dominant and thicker lighter ($\geq$ 15 mm) layers. The concentration of lithics is low, being confined to a small number of isolated clasts (maximum dimension 40 mm) with lithological composition varying from granodioritic to ultrabasic. Faunal content is generally minimal (<5%) and tends to decrease with depth, with the highest concentrations (*Archimediella*) occurring in discrete shell beds.

These characteristics suggest relatively quiet water deposition of fine grained sediments within a fjordic system. The cores from this region (JC8, JC9 and JC10) all show a linear decrease in water content with depth (See Figure 7.5.: See Section 7.2.3.) which is inferred to represent conditions of normal consolidation under an approximately constant rate of sedimentation (Syvitski *et al.*, 1987). Potential sources of material would be from the inflowing streams predominantly entering the system via the Luib inlet and the headwater delta (See Section 8.2.3.2.) at Sròn Ard a' Mhullaich. The minimal *in situ* faunal content and the strong odour of H_2S from JC9 may also suggest periods (of what time-scale is unknown)

of anoxic conditions. It is hypothesised that such conditions will inevitably be promoted by the restriction of the tidal flow by the partial sill at the mouth of the loch (*ie.* the Loch Ainort ridge complex).

The sill obstruction will also significantly reduce tidal currents in this region to enable such fine grade sedimentation to preferentially occur at this "Inner Loch" locality. The inferred low level of current activity at the head of the loch will be further enhanced by the geographical location of this site. As westerly and south-westerly winds (*ie.* down loch) still dominate the west coast system, wind induced currents will be small due to the limited fetch in this area. The presence of occasional larger lithic clasts are difficult to reconcile with a persistent fine grained sedimentation pattern, but on the basis of only 3 clasts it is difficult to adequately identify a process for there deposition. Finally the presence of wispy layering may represent seasonal but more realistically (due to their dimensions and discrete distribution within the core) longer term fluctuations in source material but there is insufficient evidence to support a more detailed interpretation.

Between the Luib inlet and the "Mouth Region" and along the marginal slopes of the loch the litho-facies identified within the cores are dominated by sediments of ALF2. Despite the small number of cores acquired it has been possible to correlate this litho-facies with the "medium" to "medium-light" tones identified along the marginal loch slopes from the sonographs. This correlation enables the spatial extension of this unit to the marginal slopes of the Loch Ainort areas. This litho-facies represents a grey-green slightly gravelly to gravelly, muddy to silty, very fine SAND (**Mz** = 3.23ϕ). Within this fine grained matrix are occasional large individual, angular to sub-rounded, clasts of both acidic and basic composition.

There is no evidence of any fine scale sedimentary structures within the cores from these sediments, however, quantitative interpretation of the sonographs enables the identification of bedforms at several positions along the upper levels of these slopes. On the basis of comparisons with the dimensions (wavelength, amplitude and Ripple Index) of these features with ranges determined by both experimental and *in situ* studies, these bedforms can be

classified as megaripples[16]. It is interesting to note that this interpretation corroborates the grain size estimates for this litho-facies calculated from the grain size analysis as such bedforms are restricted to sediments with mean grain sizes > 4ϕ. This is particularly interesting when one considers the other litho-facies that are inferred to make up LASF7 have Mz values < 5ϕ. The orientation of these features suggests that they were formed by shore parallel currents.

This slightly coarser ALF2 (Including 52% Sand and 8% Gravels) occurs at depths ranging between 39.5 mOD to 3 mOD, suggesting there is no bathymetric control on deposition of this unit. It is therefore tentatively proposed that this reduction in the finer fraction of these sediments is due to a change in source material for ALF2 compared to ALF1. Firstly the majority (the exception being JC5) of the samples acquired were in proximity to the steep foreset slopes of the Luib delta and the discharge of the Allt na Lùibe. This suggests closer proximity to coarse fraction, alluvial and deltaic deposition, in this area. Further, these localities coincide with an increase in the number of the glacial ridges and associated lag deposits being exposed on the loch bed. Subsequent, reworking of both these sets of material could therefore be potential sources for the coarser fraction within the generally finer background sedimentation characterised by ALF1.

In marginal positions in the mouth region and the "Unnamed Strait" the surficial deposits (maximum thickness *c.* 0.55 m) are characterised by ALF3. This is a grey-green slightly gravelly to gravelly, occasionally sandy cohesive MUD (See Figure 7.13a) with occasional large igneous (granophyric to peridotitic) pebbles and cobbles and sizeable quantities of dispersed shell fragments (*Archimedielleae* and *Dosinia*). This facies is very similar to ALF1, however, these sediments exhibit an increased gravel content (7% vs 1% for ALF1) which is reflected by the extremely poorly sorted nature of the sediment (σ = 3.72ϕ with a range from 2.55ϕ to 4.98ϕ) and its coarse-skewness (Skewness = -0.24 with a range from -1.16 to 0.65).

[16] Leeder (1982) describes these bedforms as having wavelengths between 0.6 m - 100s m, amplitudes from 0.05 m to 10 m and ripple indices between 10 and 50.

The similarity of ALF3 to ALF1 suggests that fine grained deposition has recently been dominant in the Loch Ainort basin and again suggests that wind or tidal currents above the bed are relatively low throughout. Albeit the majority of faunal clasts are not deposited *in situ*, their abundance in the "Unnamed Strait" would suggest a persistence of oxic conditions, irrespective of the strength of the currents. The presence of the isolated lithic clasts is again difficult to account for by the modern processes inferred to be operating in this region. As with the ALF2 sediments described within the "Inner Loch" only a source for these clasts, in the exposed "till" sections of the mouth regions and at depth (note ALF4 occurs at the base of JC3 and JC13), can be proposed rather than a method of deposition.

This pattern of sedimentation is further confused by the presence of ALF1 and ALF2 deposits at surficial levels in central localities in adjacent central localities within the "Unnamed Strait". As with those described in marginal positions these cores identify a vertical stratigraphy with ALF4 being found at the base of each of them. In JC1, in a central loch locality, a three-fold stratigraphy is actually identified with *c.* 0.3 m of ALF1 conformably overlying 0.75 m of ALF3 and with unconformable lower boundary separating it from a basal sample of ALF4. Considering, the small areas over which these facies variations occur, the rapid changes in vertical stratigraphy, the lack of any obvious bathymetric control, and the inferred homogeneity of hydrodynamic conditions in the open basin (See Section 3.3.), it is considered inappropriate to construct a detailed interpretation of this environment.

Having described the litho-stratigraphic variations present within the single seismic facies unit LASF7, the lack of surface/near surface exposures of LASF6 presents the opposing interpretational problems. This facies unit is acoustically similar to the conformably overlying LASF7 but with lower internal backscatter levels, laterally extensive internal reflectors that actually parallel the underlying sequence boundary and a more restrictive distribution (to areas south-west of the Luib inlet and north-east of the prominent slope that traverses the entire width of Loch Ainort at it's head). Within this "Inner Loch" region LASF6 fills the deepest parts of the irregular surface created by the underlying units achieving a maximum thickness of 10 ms TWT.

The lower acoustic backscatter level would suggest that this facies unit represents a finer sediment than the overlying LASF7, however, considering the range of relatively fine grain

sizes described for this upper unit LASF6 is simply considered to be similar to the finer ALF1 (SILTS) found within this loch head area. In order to err on the side of caution a slightly lower velocity of 1540 ms^{-1} than that predicted for ALF1, this value being based on that of Howell (1971) for MUD (See Table 7.5.: Section 7.2.4.), this value giving a thickness of 7.7 m. As with all of the sequences described it is difficult to assign an absolute age, yet it's presence overlying facies of LASS2 and LASS3 in an inner loch locality suggests that it must post date Deglacial Phase II. In fact it's arbitrary boundary with LASF5 suggests an upward gradation from the bimodal debris flow deposits associated with mass movement on the poorly consolidated slopes of Leathad Chrithinn (See Section 8.2.2.), to more homogeneous fine grained sedimentation.

If it is hypothesised that seismic facies units LASF6 and LASF7 represent variable, post-glacial (presumably Holocene), fjordic sedimentation on the basis of its stratigraphic relationship with the underlying sequences it is difficult to reconcile the size of the sedimentary pile with a constant accumulation rate. If an averaged velocity value of 1630 ms^{-1} is assigned to LASF7 in order to accommodate the varied grain size distributions it represents, a maximum thickness of 9.8 m for the large inner loch body is recorded. This value is recorded from the same locality as the maximum thickness quoted for LASF6. These calculations give a total maximum thickness for the LASS4 sedimentary pile of 17.5 m.

As suggested above the arbitrary boundary between LASF6 and the underlying LASS3 represents a change from sedimentation related to active mass wasting to the input of fine grained homogeneous material. It is proposed that this gradational boundary is a result of the stabilisation of the exposed slopes by vegetation (See Section 3.2.2.2.). This transition may have occurred as late as 9600 yr BP where a sharp rise in the *Juniperus* peak in the Inner Hebrides pollen record is interpreted as representing the date of regional floral colonisation (Benn *et al.*, 1992). It should be noted that on Skye the timing of deglaciation was spatially variable and it is likely that colonisation started as soon as ice retreat began, with the eventual convergence of these floral communities producing the regional peak. However, samples from enclosed basins at Luib do not contain a full Flandrian pollen succession (Benn *et al.*, op. cit.) suggesting that ice was still present in this area at least during the early Flandrian.

Consequently if this date is used to represent the LASS3-LASF6 boundary it suggests an accumulation rate for the "Inner Loch" of 1.8 mm yr^{-1}.

There is limited independent data on accumulation rates for the fjordic coastline of the north-western seaboard of Scotland, with Syvitski *et al.* (1987) calculating a characteristic current accumulation rate of < 1 $mmyr^{-1}$ for the area and Wain Hobson (1976: *pers. comm.* in Boulton *et al.*, 1981) quoting an average rate for Loch Shiel of between 0.5 and 1 $mmyr^{-1}$. Yet if one assumes that under the present hydrodynamic regime one can look at the field area as a series of depocentres influenced by similar regional conditions, the "Inner Loch" rate is significantly greater than a calculated sedimentation rate for the "Unnamed Strait" of 0.5 mm yr^{-1}. The hypothesis that this variation in the rate of accumulation is simply the product of the constant accumulation of fine grained sediments within an "isolated" basin is considered fallacious. The present day inputs into the whole Ainort system are considered relatively uniform throughout except for the localised development of deltaic complexes (See Section 8.2.3.2.). Similarly despite the presence of occasional anoxic events the weight of evidence suggests that there is still significant tidal movement within the "Inner Loch" due to the partial nature of the sill (See Section 3.3.). Consequently active tidal activity would result in a more even distribution of material within the system. Finally, there is no evidence to suggest that the "Unnamed Strait" is undergoing significant removal of material.

It is therefore hypothesised that the accumulation of an anomalous thickness of LASS4 material in the "Inner Loch" is in fact a response to fine grained sedimentation during the latter phases of the paraglacial period. As has been identified above and in Sections 3.2.2.2., 8.2.1. and 8.2.3. deglaciation of the Loch Lomond Readvance glaciers has been a time transgressive process. The size of the hinterland and the identification of *in situ* downwasting would suggest that considerable volumes of ice would still have been present toward the head of the Ainort basin well in to the Flandrian. The melting of these final remnants of ice would result in enhanced volumes of sediment laden waters entering the loch at Sròn Ard a' Mhullaich and to a lesser extent at Luib. The finer fraction of this material was thus deposited within the basin, draping and ultimately burying the irregular topography created by the Ainort Glacier. On the final disappearance of glacier ice the system would return to ambient

fjordic sedimentation characterised by the deposition of fine grained material under tidal and fluvial influences.

8.2.3.2. Deltaic sedimentation

The locality, form and dimensions of the large protrusions identified at the mouth of the Luib embayment and at the head of the Loch Ainort clearly suggest they represent delta systems. The Luib delta extends 365 m into the loch but the shape and form of its outer margin is represented by contradictory forms in the two charts (See Discussion in Section 4.3.2.). The rhombic form described by the Admiralty chart is considered erroneous, as such an angularity is probably related to the interpolation process rather than natural processes (See Discussion in 4.3.1.1.). Chart 4.2. (See Section 4.3.2.) describes an arcuate form (concave to the south-east, towards Luib) for the delta which is dissected by a deep (maximum depth -32 mOD) central hollow. A prominent break in slope occurs at a depth of -10 mOD with a lower bounding contour of -26 mOD and a frontal slope angle of 7.8°. Side scan sonar imagery of the low lying, gently sloping (1°), delta top suggest this surface is covered by a chaotically distributed pebbles and boulders. in other parts of the delta top the upper surface is characterised by laterally extensive approximately shore parallel megaripple bedforms (suggesting that grain sizes at least exceed 4ϕ). The sonographs also suggest a material variation of the surface on which the larger clasts sit. However, it should be noted that due to the extreme angles of incidence recorded in this area it is difficult to assign a genetic significance to this variation (See Discussion in Section 5.3.2.).

Two related seismic facies units have been identified at shallow depths beneath the delta top surface. LASF8 has a medium to high internal backscatter level with a chaotic, acoustically turbid texture with weak but thick and continuous internal reflectors and a chaotic, undulating and diffuse upper bounding reflector with LASF9 and a weak and diffuse unconformable basal reflector with LASS1. Both LASF8 and LASF9 have a very restricted distribution being found only at this site and on the gentle slopes of Am Meall. LASF9 is an acoustically transparent unit with no internal reflectors. There is no independent lithological calibration available for this unit so only a tentative hypothesis can be presented for this site specific stratigraphy. The acoustic transparency of LASF9 is considered to be indicative of gas discharge from decomposition of biogenic material in deeper parts of the stratigraphy (Kearey

and Brookes, 1991). Similarly the chaotic lower boundary this facies unit has with LASF8 may suggest the lower facies unit may represented the source of such material the upper boundary being disturbed by the vertical movement of gas. This is not an improbable occurrence as fine grained biogenic rich sediments are considered characteristic of the upper surfaces of deltas (Leeder, 1982).

The identification of LASS1 (and assuming a Loch Lomond or earlier age for this unit: See Section 8.2.1.) at the base of the sequence and the thin overlying cover of LASF8 and LASF9 material may suggest a Holocene age for this deposit. However, considering a maximum relief of this feature of *c.* 16m it is difficult to reconcile the build of such large volumes of glacial material at this locality during a single phase of activity. It is therefore possible that the core of this feature was built over a longer time scale than predicted here. Indeed the marked change in orientation of the eastern end of AR14, to parallelism with the delta front, suggests that some kind of obstacle was present at this locality during ridge formation. Alternatively this lower unit may represent the accumulation of ice proximal sediments in relation to a separated glacier lobe that was known to have retreated up Srath Môr (See Section 3.2.2.2.). Again in the absence of any detailed seismic profiles or the presence of a lower bounding reflector to LASS1 it is impossible to confirm any of these hypothetical origins.

The most identifiable feature on the Luib delta slopes is the arcuate alluvial fan that has developed on the gentle (3°) northern slopes of the Luib delta (See Figure 5.20). The fan has a classic form with an axial length of 125 m, a maximum width of 90 m and an arcuate, raised (relief of 1.4 m), frontal edge. The surface of the mid-fan area is heavily sculpted by a ridge and furrow topography (with a crestal relief of 0.7 m to 0.8 m) which describes a radial flow pattern. There is an overall progressive tonal variation down the fan, from "very dark" at the fan head through "medium" tones to "light" tones for the mid- and distal sections of the fan lobe. Although independent calibration is not available comparison with the approximate scale relating tonal intensity with grain size (See Table 5.1.: Section 5.3.) shows the fan exhibits classic distal fining. With the coarsest material (sands and gravels) at the fan head through to sands in the mid-fan sections to silts at the distal margin of the fan lobe. The

dissection of this margin would suggest that radial flow has or is occurring and the fan is still active.

The delta at the head of the loch traverses its entire width at this point, a distance of 1200 m, and has a prominent eastwardly facing slope inclined at 7°. The base of the slope is defined by the -18 mOD with the upper break in slope occurring at -10 mOD. The upper plateau surface again slopes gently (3°) eastwards becoming permanently exposed 650 m to the south-west at Sròn Ard a'Mhullaich. Although little is known of the sedimentological make up of this unit its general form is characteristic of temperate fjord-head deltas, which are commonly sites of high sedimentation resulting in rapid progradation and accretion. The inferred size of the delta and the recognised low fluvial inputs entering the fjord system from up valley sites suggest that it is not purely the product of modern sedimentation processes. Considering the close proximity of the thick paraglacial deposits present in the "Inner Loch" (See Section 8.2.3.1.) it is probable that at least one major period of accretion was concomitant with the discharge of sediment laden meltwaters during this time. Further the relationship of the frontal slope and the ridges ABR3 and ABR4 identified from the Admiralty Chart may suggest that progradation in to the loch post dated the glacial advance. However, in the absence of any sub-bottom or lithological section through either of these localities make this a totally speculative assertion.

LASF10 has the most restricted distribution of any of the seismic facies units identified from the sub-bottom traces. In fact this unit is only identified in two survey lines (A5 and B1) that cut shallow plateau areas on the south-eastern slopes of the "Inner Loch" in two different localities. It is therefore impossible to make any statement on its three-dimensional expression particularly as no corroborative evidence for this unit could be provided by any of the other sampling methodologies. It can only be suggested that these striking inclined reflectors may represent incipient foresets relating to the development of small delta systems at the mouth of small streams that occur at both these localities.

8.2.3.3. Mass movement

Mass movement within the field area occurs in three discrete environments, downslope movement on the exposed slopes of the within loch ridges, small scale slumping on the

steeper submerged drift covered slopes and finally large scale debris fans related to terrestrial movements. Many of the linear ridge complexes identified at within loch localities have boulder clusters orientated perpendicular to their main axial orientations. These acute angles would suggest that these particular clusters do note represent surface expressions of buried ridge axes but the remobilisation of coarser material, probably from axial positions, under the influence of tidally or storm induced currents operating at these depths. Similar activity is seen to occur on the steeper foreslopes of the Luib delta front. In this locality instability inducing downslope movement maybe the result of foreslope oversteepening, the migration of coarse material known to be present on the delta top (See Section 8.2.3.3.) to a marginal position under the influence of extreme conditions or persistent current erosion.

Small scale slope failure is clearly evident on the north-western shore of the "Inner Loch" toward Maol Ban, on these steep offshore expressions of Leathad Chrithinn clusters of weak "scallop" shaped features with raised frontal/lower segments are observed (See Figure 5.15.). The dark acoustic texture described from both sonograph and the seismic profiles suggest that this slope is composed predominantly of glacial diamictons of unknown age. The arcuate nature of these features are indicative of small scale rotational slips as the result of localised dramatic failures. In a similar vein the shore-parallel benches that are found on both shores within the mouth of the "Inner Loch" may represent more uniform and slower downs slope failure or creep.

The most dramatic feature of mass movement in the surveyed region is a large boulder strewn fan that has developed from the north-western slopes of Am Meall and extends 185 m offshore. The fan attains a maximum width of 265 m and has a prominent dissected margin. This margin is probably the result of continued downslope failure induced by continued movement up slope or oversteepening of the steeper fan margins (Prior *et al.*, 1981). As can be seen in Figure 5.18. the dissected region occurs at the base of a strong arcuate reflector possibly representing a pre-existing topographic high over which downslope movement has occurred. Side scan imagery appears to suggest that these fan deposits rest unconformably on top of dark to very dark material similar to that, that dominates the "Mouth Region". As it lies within the Loch Lomond Stadial limits it is probable that this movement post-dates readvance activity and indeed Deglacial Phase II, however, the sharpness of the sonograph image would

suggest that the coarse fan deposits are not overlain by significant accumulations of fines suggesting an even later age of formation. A similar feature, with a chaotic distribution of boulder sized material and a dissected margin has also developed off the point of Maol Ban extending 80 m into the loch.

8.2.4. ENVIRONMENTAL SYNTHESIS

Having presented an environmental interpretation for all the seismic facies units identified in the seismic para-stratigraphy of the Loch Ainort area it is possible to present a summary of events, based on the available evidence:

I) The base of the sequence identified throughout the Loch Ainort basin and adjacent areas, represents diamicton deposited during the Dimlington Stadial (or potentially earlier) glacial phase. During the active retreat of both the mainland ice sheet and the Skye ice cap glacially related sedimentation occurred within the field area in the form of either ice-proximal grounding line fan deposition, iceberg/sea ice fallout or a combination of the two.

II) Climatic deterioration that began in 11.8 ka BP (Walker and Lowe, 1990) and which represented a return to full arctic conditions (Loch Lomond Stadial) during a period of overall Lateglacial amelioration, led to the development of a tidewater glacier in the Loch Ainort basin. As the Ainort Glacier advanced seaward it overrode and deformed the Dimlington Stadial diamictons, subsequent marine/glaciomarine deposits and the small volume of Loch Lomond Stadial ice-proximal deposits that founded the loch floor. The maximal limit of the Ainort Glacier is identified within the outer part of the "Mouth Region" with this entire region being characterised by a series of closely spaced De Geer moraines. To the west of the "Unnamed Strait" a smaller glacier occupying Coire Mòr in the Moll peninsula reached a maximal position at the mouth of Lùib na Moil.

Confirming the evidence from the poorly preserved terrestrial end and lateral moraines identified by Ballentyne (1989), the De Geer moraines are interpreted as representing a maximal advance position followed by an initial phase of deglaciation *ie.* active retreat

interrupted by periods of readvance and/or stillstands. This period of active retreat coincides with Deglacial Phase I which reflects decreased snow accumulation due to precipitation decline during the mid- to latter parts of the Stadial (See Section 3.2.2.2.). During the maximum stillstand position of the Ainort and Moll Glaciers subglacial meltwaters entering the "Unnamed Strait" resulted in strong hyperpycnal flows eroding the pre-existing loch bed in this area. Within the "Inner Loch" three major stillstand positions are identified suggesting periods of more sustained retreat with only occasional major readvance/stillstand events.

III) South-west of the recessional moraine complex AR17 [156550 828970] a change in style of deglaciation to a period of uninterrupted retreat and *in situ* downwasting is characterised by low "hummocky" relief and sporadic, small (< 175 m) diamictic cross-valley ridge features. This spatial transition in the style of glacial deposition coincides with the change to the uninterrupted retreat of Deglacial Phase II (See Section 3.2.2.2.). This Deglacial Phase is a response to increased ablation, which in turn is related to the rapid climatic amelioration that occurred at the very end of the Loch Lomond Stadial and the beginning of the early Flandrian (See Section 3.2.2.2.).

IV) On exposure to the wet and warming post-glacial environment the unvegetated and poorly consolidated drift covered slopes of the Loch Ainort basin were subject to extensive mass movement in the form of sedimentary gravity-flows, landslides and rockfalls. Such paraglacial activity dominated the slopes of the northern shore and provided a large source of material to the sub-aqueous environment. The periodic influxes of heterogeneous debris flows resulted in the deposition of ponded "turbidite" deposits in the lower parts of the irregular topography of the loch bed. Climatic amelioration would have also resulted in regional floral colonisation and ultimately the stabilisation of the terrestrial slopes bounding Loch Ainort. This would have reduced the input of coarse heterogeneous material in to the system and so initiating the final stage of paraglacial activity. This phase was characterised by the input in to the head waters of the Loch Ainort basin of sediment laden meltwaters emanating from the remnant stagnating ice masses that would have occupied the upper valley. This process resulted in the deposition of large accumulations of fine sediments draping the irregular topography of the post-glacial loch bed.

V) Modern fjordic sedimentation exhibits subtle variation throughout the loch. The major fluvial inputs at the head of the loch and at the Luib inlet have resulted in the accretion and progradation of deltas which may have been initiated during Deglacial Phase II or even earlier. The majority of the Ainort basin is undergoing slow 0.5 mm - 1 $mmyr^{-1}$ sediment accumulation from the redistribution of within loch sediment sources and small scale fluvial and tidal inputs. In situ mass wastage can also be identified at marginal positions within the loch system. Large scale debris fans are identified at plateau areas of both Am Meall and Maol Ban whilst small scale boulder clusters can be seen to have moved down both the oversteepened foreslopes of the Luib delta and unstable slopes of exposed De Geer moraines. In a small number of localities smaller scale rotational slippage and slow creep appear to effect steep drift covered slopes.

8.3. ASSESSMENT OF THE USE OF GEOPHYSICAL METHODS FOR SUBMERGED PALAEO-GLACIOMARINE ENVIRONMENTS.

On the basis of the experience gleaned during the acquisition, analysis and interpretation of seismic reflection and lithological data sets from the Loch Ainort field area, Section 8.3. presents an, illustrated, critical assessment of a variety of geophysical and geological methods. Arguments will be presented to suggest that multi-disciplinary investigations must become standard and that there is a need for a more rigorous scientific approach to all aspects of this form of field of research.

8.3.1. BATHYMETRIC DATA

Bathymetric charts have historically been the major source of morphological data used during the scientific investigation of any submerged aqueous environment (McQuillin & Ardus, 1977). Whether *in situ* data is acquired specifically for a site or if pre-existing

bathymetric charts (*ie.* Admiralty Charts) are consulted, the question of data quality must be considered, irrespective of it's source. This section therefore attempts to identify the specific problems encountered in the acquisition, analysis and interpretation of bathymetric data sets. In particular, the effectiveness of Admiralty Charts are discussed because of the frequency of their use by a number of glacial geomorphologists (*eg.* Ballantyne, 1989, Greene 1992, *etc.*).

The validity of both qualitative and quantitative morphological descriptions obtained from the processed bathymetric data, can easily be assessed by making inter-comparisons between the Admiralty and the Bathymetric Charts (See Charts 4.1. and 4.2. respectively) and, where appropriate, with the isometric plot constructed from the side scan sonographs (See Figure 5.21.). On large (100s m) scales, the qualitative descriptions of the morphological components of the Loch Ainort system , such as the asymmetric profile of Inner Loch Ainort (See Section 4.3.1.1.) or the deep symmetrical basin of the Unnamed Strait (See Section 4.3.1.3.), are clearly reproducible between the two surveys. However, at the same scale, an absolute quantitative comparison between the two datasets present a more equivocal picture, with depth errors between the two charts varying between $\pm$ 1 m and $\pm$ 4 m in the morphologically simple deep basins (See Section 4.3.2.). Although as absolute values these errors are small, they do represent a 10% variation in depth.

If an attempt is made to look at the detailed (10s m) morphology of the loch bed significant qualitative and quantitative discrepancies between the three plots are clearly present. Due to their recurring presence in all three of the geophysical datasets, it is apparent that the bed of Loch Ainort is characterised by a series of three-dimensional topographic highs or ridges[17]. However, the number, form and dimensions of these features varies considerably between each plot. From the isometric plot (See Figure 5.21.) a total of 53 linear or concave down-loch ridges can be identified, with average values for length height and orientation of 145 m, 3 m and 127° respectively. By

[17] These ridges actually represent a series of push moraines primarily related to the Loch Lomond Stadial Ainort Readvance Glacier (See Section 8.2.).

comparison a total of only 22 ridges can be identified from the two bathymetric charts (See Section 4.3.2.). The average dimensions of these ridges also varies compared to those described from the side scan sonographs with a recorded length of 290 m, height of 11 m and orientation of 126°.

Further, at this scale there are significant discrepancies between the spatial distribution of these ridge features within the field area. Of the 22 ridges identified from the Admiralty and Bathymetric Charts only 12 can be identified on both charts. These spatial discrepancies can be further emphasised by comparing the location of the topographic apex's determined from the sub-bottom profiles[18] and the ridges identified from the sonographs and Admiralty Chart (See Figures 5.24. and 6.9.). Out of a total of 48 topographic apex's present within the "Mouth Region" alone, only 22 coincide with a three-dimensional ridge.

These qualitative and quantitative discrepancies are the product of two major sources of errors. Firstly there are those associated with the acquisition of the original data and secondly those associated with the interpolation procedure integral to chart construction. As discussed in Section 2.3.2.1. position fixing for the echosounder surveys was provided by traversing, which gave a maximum positional error of ± 40 m in the central regions of the loch. Although this value compares favourably with surveys carried out using similar techniques (*eg.* Boulton *et al.*, 1981: error 30-100 m, Landmesser *et al.*, 1982: error ± 4 km) or alternative electronic navigation systems (*eg.* Decca: Bishop and Jones, 1979: error ± 460 m) such positional inaccuracies inevitably lead to significant analytical problems. The problems of positional errors can be clearly demonstrated by the irregular form of ABR1 (See Chart 4.2), which is the result of considerable depth inconsistencies between intersecting lines A16, B2 and B13 (See Section 4.3.1.1. and Figure 4.7.).

Frequently, locational inaccuracies are overlooked and the re-positioning of lines during analysis is common, "..... cross-over errors..., were generally insignificant except in the Inner

[18] This two-dimensional dataset can in this be considered a suitable proxy of the bathymetric data as it was run simultaneously with the echosounder surveys (See Section 6.3.).

Sound where the positions of some lines had to be shifted over distances up to about 0.5 km." (Bishop and Jones, 1979). In areas of simple or large-scale morphology (*eg.* the sub-marine end moraines on the Norwegian Shelf, which have axial lengths of 60 km, Holtedahl, 1989) such errors and practices will not significantly alter a palaeo-environmental interpretation. However, it is evident that in restricted areas, where individual bedforms may have dimensions of the order of 10s or 100s of metres (*ie.* Loch Ainort), positional errors of the magnitude quoted above are unacceptable.

To compound the errors inherent with poor positional data the density of traverse lines within the survey area will also have a major control on the integrity of the final chart. Section 4.2.2. discusses at length the compromises which have to be made between the density of coverage provided by the traverse lines and the expediency of the time frame in which to complete each survey. However, despite reaching a logistically viable traverse density of 5 lines/km^2 during this survey, analysis of the final charts clearly shows that, for the successful interpretation of a small scale complex topography, such a density is far from ideal. Again this can be clearly demonstrated by the number of potential ridge targets in the "Mouth Region" (identified from the sonographs) that failed to be cut by the echosounder traverse lines (See Figure 5.24.). It is probable that this poor traverse density is also the root cause of the quantitative discrepancy (±4 m) between the maximum depth recorded for the central deep from the two Charts.

Within this critical discussion of bathymetric data acquisition, emphasis has been placed up on survey methodology rather than the equipment deployed. It is considered outside the remit of this work to present a summary of the currently available instrumentation and their suitability to specific investigative tasks. Consequently, no assessment has been made of the relative merits of modern high-frequency echosounders and the traditional lead-line techniques.

Having identified potential errors inherent in the acquisition procedure it is also important to highlight those present in the analytical stage. Primarily problems are encountered in the interpolation stage of chart construction. If a chart is hand contoured it is essential that the location of the original survey lines are also presented as the three-dimensional form of many linear features frequently coincide with the orientation of the

original data points. For instance, the axes of ridges ABR18, ABR19 and ABR20 are coincidental with the traverse lines A9, A6 and A1 a relationship which suggests that they may be a product of this interpolation process rather than a true representation of the sea bed.

The interpolation problem can be partially overcome by the use of the three-dimensional images from the side scan sonar to aid the extrapolation between echosounder data sets. However, this does provide something of a chicken and egg situation, as the bathymetry is the only tool available to calculate bed angles, from which inclination distortion can be assessed and true isometric plots constructed (See Section 5.2.6.). Therefore, the side scan data must only be used to improve the educated guess rather than replace it. It is important to note that the problems associated with the interpolation process have not been solved by the introduction of computer based contouring packages. Such systems have similar procedural problems but these have been discussed in depth by other authors (*eg.* Keckler, 1994) and again are out of the remit of this project.

It is therefore evident that bathymetric charts rarely provide accurate ($< \pm$ 10 m) quantitative information for a three-dimensional plane. In environments where the loch or sea bed morphology is relatively simple and depths large this does not represent a problem. By contrast if such Charts are being used to make palaeo-environmental inferences for shallow areas with complex topographies little reliance can be placed up on these sources of information. This can be clearly demonstrated by discussion of the inferences made by Ballantyne (1989) for the location of the maximum position of the glacial termini of the Ainort Glacier and more importantly his estimates for the volumes of the Cuillin icefield tidewater glaciers. Ballantyne states that "Former ice volumes were calculated by measuring ice thickness (glacier surface altitude minus land surface altitude) at 30-80 regularly spaced points within each glacier, calculating the average thickness and multiplying by glacier area..... The lowest altitude of each former glacier was obtained from Ordnance Survey maps or estimated from bathymetric charts.".

As discussed above it has already been identified that a minimum depth error of 10% occurs between the two charts constructed for Loch Ainort. Further, as described in Section 8.2.1., the maximum position of the glacial terminus identified by Ballantyne from the Admiralty Chart bears only a passing resemblance to the actual limit as defined

from marine geophysical studies. The actual terminus identified from the current survey can be seen to extend a further 800 m into the outer loch. This represents a re-calculated volume estimate for the Ainort glacier of 20.52 km^3. If this 4% increase in ice volume is translated to all the tidewater glaciers of the Cuillin icefield it would represent an additional 0.96 km^3 of ice being present at the maximum advance position of Loch Lomond ice on Skye. It is also worth noting here that even these estimates are also widely inaccurate. This is because any data obtained solely from bathymetric charts takes no account of the potentially large quantities of para-glacial sediments that can accumulate on the palaeo-loch bed on which the glaciers originally sat (See Section 8.2.2. and 8.3.3.).

In summary it has been demonstrated that bathymetric charts have the potential to provide general qualitative and quantitative data particularly for the description of large scale topography. This technique does provide excellent background information, which can be particularly useful in the planning stages of any proposed survey. However, one should be circumspect when attempting to use any absolute values from these data. Equally, for the investigation of environments that are characterised by small scale topographic features bathymetric data is totally inappropriate. The exception to this would be the acquisition of bathymetric data from very small areas (size being time restricted) which could have been identified from previously conducted side scan sonar surveys. These small sites could be then surveyed using a very dense traverse grid (line spacing down to 5 or 10 m) and a high accuracy navigation system *eg.* Differential GPS (± 1 m)[19]. Under these conditions the bathymetric data would provide the best source of absolute dimensions for any particular sea bed feature as the accuracy of the dimensions calculated from side scan sonographs are notoriously poor (See Section 5.2.6.).

[19] The successor to the "stand-alone" GPS system described in Section 2.3.2.2. which, by the interrogation of a correction transmitted from a land based reference station, can account for errors produced by Selective Availability.

8.3.2. SIDE SCAN SONAR DATA

Side scan sonographs obtained from Loch Ainort provide a pseudo three-dimensional image of the sea bed which gives qualitative and quantitative information on both the material and topographic variations present. The wide vertical beam angle of the system results in a large (300 m) swath of the bed to be imaged per pulse and as a result large areas of the loch floor can be surveyed in a very short period of time. Again the accuracy of the plots produced from this system are dependant up on both the positioning system and traverse density employed during the survey (See Discussion in Section 8.3.1.). However, if distinctive topographical and material features can be identified on adjacent sonographs the process of "line shifting" can be accomplished with a greater degree of reliability.

In addition to topographic variations the side scan sonographs may yield speculative information on the material characteristics of the loch floor, with a simple relationship existing between tonal quality and grain size (See Section 5.2.2.). As discussed in Section 8.2. the calibration of the tonal scale identified for the Loch Ainort area is achieved by comparison with the grain size analysis conducted on the core and surface sample retrieved from the loch. Despite the ability to compare directly the tonal scale with grain size data, due to the possible reproduction of equivalent tonal variation from topographical changes as well, it must be re-emphasised that "....successful and accurate interpretation of side scan sonar records is an acquired skill that is based on experience and judgement as much as training. Training is required in the beginning to understand the physics of how the system functions but interpretations depends mostly on distinguishing between tonal intensities and relating target shapes to scaled down geological features." (Williams, 1982).

To complement the large volume of qualitative data, the side scan system provides the researcher with the opportunity to calculate quantitative information from the same source. Numerous workers (*eg.* Duck and McManus, 1985c; Klein, 1985; Le Bas, 1992; Voulgaris and Collins, 1991), have used a series of standard geometrical equations to calculate the height, true horizontal distances and ultimately isometric plots from the sonograph data. As has been discussed in Sections 5.2.3. and 5.2.6. much of these data, particularly height and depth calculations, must be considered suspect especially when dealing with Low Tonal

Colour Zones (**LTCZ's**) instead of true blank shadow zones. This is particularly important considering that, from this survey alone, the occurrence of **LTCZ's** appears to be much more common than that of shadow zones. However, having taken in to consideration the possible errors that may occur, the presence of such **LTCZ's** can be constructively used to provide estimates of distal (for positive targets) and proximal slope angles (for negative targets). To the author's knowledge the recognition of and calculations from **LTCZ's** have not been made before.

The combination of extensive quantitative and qualitative information from a single permanent paper record, and the ease at which extensive coverage of survey area can be made, make side scan sonar a very effective tool in the analysis of submerged glaciomarine environments (*eg.* Lowe, 1992). The main drawback of this geophysical technique is that the glaciomarine environment is characterised by an irregular and often high relief environment. This results in two main problems; firstly, due to the rapidly varying topography, it is difficult to decide on an optimum towing depth, because there is a continual trade off between loss of resolution at depth and grounding of the towfish. Due to the fragile nature of the towfish it is always deemed necessary to err on the side of caution and tow at shallow depths. Secondly, side scan sonar was originally established to survey flat bottomed marine environments (McQuillin and Ardus, 1977) and, as a consequence, distortion of both qualitative and quantitative data by reflection from inclined surfaces was not considered a major problem. Despite the series of corrections available for measurements from inclined surfaces it is still acknowledged that "...the complexity of distortions caused by sloping sea-beds is not fully understood" Flemming (1976). In order to compensate for this problem detailed bathymetry would have to be undertaken prior to a side scan survey, as has been done in this case. However, considering the drawbacks of bathymetric surveys as described in Sections 4.5. and 8.3.1., the prospect of completing highly accurate surveys is poor.

However, despite these drawbacks the amount and quality of qualitative knowledge that can be acquired from effective interpretation of side scan sonographs is extensive. The misconception that excessive post-glacial deposition will totally obscure glacially derived features is contradicted by the evidence obtained from Loch Ainort. As described in Section 5.3. and 8.2. push-moraine ridge systems can still be clearly identified and even where the

relief of these features is subdued due to post-depositional sedimentation the identification of boulder clusters can still be used to infer their presence. Consequently this author recommends that side scan sonar should be seen as an integral part of all offshore palaeo-environmental investigations (See Section 8.3.5.).

8.3.3. SUB-BOTTOM PROFILE DATA

The third geophysical technique to be used was the 3.5 kHz sub-bottom profiler or "Pinger" (See Section 2.3.3.3. and Chapter 6). The deployment of this instrument from a fixed transom mount and the singled focused beam emitted from its transducer, results in similar acquisition errors to those described for the echosounder system (See Section 8.3.2.). It is therefore considered unnecessary to reiterate the problems outlined above, suffice to state that without adequate positional control and a high traverse density the absolute dimensions and detailed morphology of interpreted palaeo-surfaces should be treated with caution.

Although assessment of the instrumentation is not within the general remit of project it is worth noting the inability of the 3.5 kHz system to be able to distinguish between subtle changes in grain size parameters. In particular there transpired to be little correlation between LASF7 (the dominant seismic facies unit of LASS4) and the sampled litho-facies ALF1, 2 and 3. Albeit representing a markedly different environment this conclusion does support the assertion that high-resolution seismic systems have difficulty in resolving boundaries across which there are minimal acoustic impedance contrasts (*eg.* Piper, 1988; Stewart and Stoker, 1990; Syvitski, 1991).

As alluded to in Section 1.2. the critical problem that requires to be addressed, prior to the successful use of sub-bottom profiling in palaeo-environmental studies, is the construction of a standard theory and nomenclature for the analysis of high-resolution profiles. Albeit that such a framework has long been established for the interpretation of deep seismic profiles this author can find no previous attempt to adapt conventional seismo-stratigraphic theory to the interpretation of shallow seismic data. The particular

problems faced by workers in this field are, firstly, the adoption of a standard nomenclature, secondly the indiscriminate mixing of seismo-stratigraphic descriptions with environmental interpretation and finally the problems of constructing a true chrono-stratigraphy.

Prior to the establishment of the conventional seismo-stratigraphical terms "Seismic Sequence" and "Seismic Facies Unit" (Vail and Mitchum, 1977)[20] it was unavoidable that a variety of terms (*eg.* "Formations" and "Acoustic Units") were in use. However, the persistence by some authors to introduce new terms into the literature (*eg.* "Layer", "Member" and "Type") for profile descriptions has continued to hinder the advancement of the science and reduce the impact of any conclusions made. It is also evident that a number of authors still have a problem with the concept of seismo-stratigraphic analysis. In particular previous workers have had considerable difficulty in accommodating similar or identical seismic facies units that may occur at more than one position within the seismo-stratigraphic column *ie.* within different seismic sequences.

The mis-use of the seismo-stratigraphic analytical technique can be clearly demonstrated by the inability of Bishop and Jones (1979) to fit their "sub-unit 3" into their seismic para-stratigraphy (See Sections 1.2.2.2.). Having identified reflector characteristics of "Seismic Sequence 3" passing laterally into and being overlain by "Seismic Sequence 1" they do not redefine their "Seismic Sequence 1" so as to contain a new facies with similar acoustic characteristics to the overlying sequence but contest that they "....are not able to speak of the four formations as time-stratigraphic units".

Similarly Boulton *et al.* (1981) evidently have problems stratigraphically locating their "Seismic Sequence 4". One theory identifies the sequence as having a stratigraphical position between Seismic Sequence 2 and 3 and representing proximal glaciomarine outwash related to Loch Lomond Readvance activity, a chronologically justifiable interpretation. The alternative hypothesis has the same sequence being formed by modern day processes. Evidently this inferred stratigraphical inversion cannot be accommodated

[20] Based on deep seismic profiles.

by the seismo-stratigraphical method and therefore requires reappraisal (See Section 8.4.).

This author therefore suggests a return to the standard nomenclature defined by the work of Mitchum and Vail, leading to the universal adoption of the terms "Seismic Sequence" and "Seismic Facies Unit". Further, the first two stages of seismo-stratigraphic analysis described by these two authors (Seismic Sequence Analysis and Seismic Facies Analysis; See Sections 6.2.3. and 6.2.4. respectively) should also be more closely adhered too. As an integral part of both these analytical techniques it is considered essential that particular emphasis is placed on the detailed description of the morphology of the upper and lower bounding reflectors. Albeit the form of internal reflectors has the potential of giving the scientist insight into the small scale processes that may have occurred within an environment, the morphology of the bounding reflectors gives one critical evidence for large scale environmental changes with time. This again can be clearly demonstrated by the Loch Ainort model where the difference between the acoustically similar Seismic Sequences 1 and 2 are purely distinguished by the nature of their bounding reflectors (See Sections 6.3.1. and 6.3.2. respectively). The contrasting nature of these boundaries is interpreted as representing a critical change in the processes of deglaciation, namely the transition between a period of active glacier advance and retreat versus *in situ* ice stagnation (See Section 8.2.1.).

The major adaptation to the analytical methodology of Mitchum and Vail (1977), for use in the interpretation of high resolution sub-bottom profiles, has to be on phase 3 of the seismo-stratigraphic process (See Section 6.2.). As described in Section 6.2., conventionally this phase represents the interpretation of the seismic para-stratigraphy based on sea level analysis. However, due to the shallow penetrative capability of these instruments and the high rates of deposition and erosion indicative of nearshore glaciomarine environments (Drewry, 1986) and hence the relatively short geological time scales being dealt with, it is unlikely that such profiles will record a large number of transgressive and regressive events. It is therefore suggested that this phase should in fact provide what this author terms a "composite para-stratigraphy". This should represent a process based, litho-stratigraphic interpretation that, by virtue of the detailed spatial

extent afforded it by geophysical data, can be placed in a wider environmental context[21]. The term para-stratigraphy (Krumbein and Sloss, 1951) has been retained, as even with the inclusion of a lithological component to the interpretational process the majority of the inferences still rely heavily up on objective criteria that merely reflect lithology. It is not this author's wish to introduce new terms in to a field of research which already has an excessively large nomenclature, but it seems necessary for a distinction to be made between a seismic para-stratigraphy based purely on acoustic imagery (See Section 6.2.) and an integrated interpretation of an environment.

This process can be successfully achieved by the correlation of the developed seismic para-stratigraphy with an acquired litho-stratigraphy. As shall be described in detail in Section 8.3.4. for effective environmental reconstruction of nearshore sites, the litho-stratigraphy should be constructed from both the analysis of samples taken from within the field area and, where available, data acquired from terrestrial mapping of both the solid and drift geology. The importance of this latter source of data and in particular its usefulness in the assignment of a simple absolute time scale, is clearly demonstrated by using an example from the Loch Ainort model.

The composite para-stratigraphy of the Loch Ainort palaeo-environmental model (See Sections 8.2.4. and 8.4.) does not conform with the initial seismic para-stratigraphy on which it is based (See Section 6.4.). For instance, Seismic Sequence 1 of the Loch Ainort seismic para-stratigraphy (See Section 8.2.1.) is constructed from two very similar facies (LASF1 and LASF2) only being distinguished on their contrasting upper boundary styles and their spatial distribution. In fact the facies boundary that separates them is purely arbitrary as their bulk acoustic properties merge in to each other. However, when the sub-bottom profile data is integrated with the other three datasets it is hypothesised that these facies units represent two distinct rather than related phases of glacial deposition (Loch Lomond Readvance and Dimlington Maximum respectively). A similar contradiction is present with the interpretation of overlying Sequence 3 (LASF4 *vs* LASF5: See Section 8.2.2.) which contains facies that again are interpreted as glacially

[21] For the Loch Ainort model this is effectively the Environmental Synthesis presented in Section 8.2.4.

related deposition during the Loch Lomond Stadial and the deglacial period following the Dimlington Maximum respectively.

This scenario brings in to question the validity of the assumption that a seismic sequence boundary is in fact a "time line" as described by Bally (1987: See Section 6.2.3.). From a study of the complete dataset the actual "time" boundary would separate LASF1, LASF3 and LASF4 of the "Inner Loch" and "Mouth Region" from LASF2 and LASF5 of the "Unnamed Strait". Evidently from the discussion in Section 8.2.2. it would have been impossible to make this division on the basis of acoustic imagery alone. However, this does not negate the use of seismo-stratigraphic analysis it just reiterates the importance of seeing the seismic para-stratigraphy as representing a single stage within the construction of a composite para-stratigraphy.

Having identified the importance of phase 3 to effective seismo-stratigraphic analysis it is important to re-iterate that, when presenting data from a survey area, it is essential not to inter-weave the three phases within a single text document. The effective replacement of simple reflector description by environmental interpretation inhibits the continued use of any such data set by subsequent authors, as such a procedure facilitates an inductive rather than a deductive approach to model development. This is clearly demonstrated by the inherent weaknesses evident in the current supposed seismic para-stratigraphy presented for the north-western seaboard of the Scottish Highlands (See Section 1.2.2. and 8.4.). It is therefore proposed that for any high-resolution data set phases 1 and 2 of the seismo-stratigraphic method should be presented separately from the interpretational composite para-stratigraphy of phase 3.

Having dealt with the theory of seismo-stratigraphic analysis it is important to stress the particular importance of this technique to the investigation of submerged palaeo-glaciomarine environments. As temperate, palaeo-glaciomarine environments are characterised by large scale rapid sedimentation processes (Drewry, 1986), it is inevitable that many of the indicators of past glacial activity are buried beneath large volumes of syn- and para-glacial sediments. It is therefore self-evident that in order to reconstruct such environments, sections through these sub-surface units should be acquired. This conclusion should not, however, be seen as a contradiction of the statements made in

Section 8.3.2., where it is inferred that many features are in fact still exposed and so can therefore be imaged by non-penetrative devices such as the side scan sonar. As can be clearly seen from the isopach diagrams constructed for Seismic Sequences 2, 3 and 4 (See Section 6.3.; Figures 6.14., 6.19. and 6.23.), the post-glacial maximum sedimentary fill of which they are interpreted as being correllatories (See Section 8.2.2. and 8.2.3.) has in fact a restricted spatial distribution. The thickest and most extensive deposits are identified within the "Inner Loch" whilst only a thin and sporadic cover is present within the "Mouth Region". It is therefore not surprising that if we compare this distribution with the distribution of ridges identified on the isometric plot (See Figures 5.21.) that an inverse spatial relationship is seen *ie.* the greatest number of ridges are identified in the "Mouth Region".

Where thick deposits of material are identified the sub-bottom profiles enable the reconstruction of events since the deposition of the lowest seismic sequence imaged. In the example of Loch Ainort (Section 8.2.) the identification of the two phased deglacial cycle; the occurrence of debris flow deposits related to both discharge at the glacial maximum position and excessive mass movement during the deglacial phase; and finally the extent of para-glacial sedimentation that occurred within the loch could not have been inferred from the non-penetrative techniques. In addition to the detail such systems provide for the palaeo-environmental model, they further bring into question ice volume calculations and geomorphic interpretations made on the basis of bathymetric data alone.

As described in Section 8.3.1., the errors that are present in the absolute values obtained from the Loch Ainort bathymetric charts altered the volume calculations of Ballantyne (1989) by 0.96 km^3. The sub-bottom profiles and their subsequent calibration by core samples suggest that the Ainort Glacier in fact over rode a surface that was at a minimum of 30 m below the lowest altitude (-20 m) quoted by Ballantyne. If the ice volume for the glacier is re-calculated with this lower base level (using the same procedure as described by Ballantyne, op cit.) a 20% increase in ice volume is recorded (*ie.* 3.615 km^3 vs 3.023 km^3). If we infer a similar sedimentary pile to be present in all the sea lochs that were once occupied by Loch Lomond ice, it can be estimated that the Cuillin Icefield would gain an additional 2.7 km^3 of ice compared to Ballantyne's figures.

This would represent an overall 10% increase in size of the Loch Lomond Readvance Glacier complex of Skye. If we extrapolated such figures for all the west coast Loch Lomond Readvance glaciers along the western seaboard and all the inland lake glacial systems this would represent a significant impact up on the Scottish land mass.

The author fully recognises that due to varying; sediment supplies, related to both the nature of the catchment area and ice rheology; para-glacial sedimentary histories and hydrodynamic regimes; the assumption that the base level for such calculations should be dropped by a single standard figure is fallacious. However, this example clearly shows that without a full appreciation of the thickness of the sedimentary pile that may be present within both enclosed and open lochs, conventional ice volume calculations may represent significant under estimates. The author would also like to cite in favour of this hypothesis that the only other loch systems that have been geophysically surveyed in the north-west Highlands (Loch's Nevis and Ailort, Boulton *et al.*, 1981; Loch Callater, Muick and Lee, Lowe, 1992) have all contained a post-Loch Lomond sedimentary fill, albeit no absolute values for its thickness have been quoted.

This discrepancy in inferred ice volumes has implications for current studies in to the sea-level record for north-west Scotland. Recent research in this area is being approached by two different methods; the study of pollen, diatom, radiocarbon and lithostratigraphical data from selected isolation basins (*eg.* Shennan, 1992; Shennan *et al.*, 1993 and 1994); and high-precision rebound models (*eg.* Lambeck, 1993a and b; Lambeck, 1995). The conclusions drawn from these works suggest that the relative sea-level curves produced from the field data are consistent with the general trends predicted by the models. However, the recorded absolute values require a greater thickness of ice than those currently adopted in the ice reconstruction's for both the glacial maximum and the Loch Lomond Readvance. In the current models a maximum ice thickness for central Scotland of 1500 m and 400 m for the Dimlington and Loch Lomond maximums respectively have been used. Lambeck (1995) further suggests that for improved correlation, ice thicknesses over northern Scotland, north of the Great Glen, need to be increased by at least 15%.

On the basis of data acquired from a single loch and a literature review it would be presumptuous to assume that the inaccurate calculation of the base levels of sub-aqueous glaciers could be entirely responsible for two-thirds of this discrepancy. However, future investigations of a small number of representative loch's could potentially resolve this issue.

8.3.4. LITHOLOGICAL CALIBRATION DATA

As has been described on several occasions within this thesis (See Chapters 2, 5 and 6), the descriptions of the seismic facies and sequences identified from both the side scan sonographs and the sub-bottom profiles are not direct correlatives of lithological sequences. Albeit simple interpretations can be made on the basis of tonal intensity (*eg.* See Table 5.1. "The categories of tonal coloration and the approximated corresponding material characteristics, employed during sonograph interpretation") or type acoustic signatures (*eg.* the high backscatter and abundant point hyperbolae indicative of diamictic sediments; See Section 8.2.1.), these images cannot be considered reliable indicators of either material properties or specific depositional processes (See Section 2.3.3.). The inconsistencies between sedimentary models constructed purely on the basis of "seismic facies analysis [sic]" and those that reference *in situ* borehole data having been previously identified Stewart and Stoker (1990).

It is therefore evident that the calibration of both surficial and sub-bottom seismic facies units is essential to the effective interpretation of any submerged environment. The process of calibration not only enables one to assign a lithological term and hence infer potential genetic processes involved in the formation of each sequence, but to convert the sub-bottom profiles from a millisecond scale to a metric scale. This procedure is essential to the effective quantification of unit dimensions but also to the construction of a true geometry for the topography of the system. Considering the importance of the thickness of the para-glacial sedimentary pile when considering the reconstruction of a submerged environment (See Section 8.3.3. and 8.5.) the use of an appropriate velocity value is critical. For instance, numerous authors fail to quote a conversion velocity, but that most

consistently used is the value for sound in water (1500 ms^{-1}). However, the Loch Ainort litho-facies have compressional wave velocities that range between 1582 ms^{-1} to 1775 ms^{-1} (See Table 7.4.; Section 7.2.4.) with an average value for the sedimentary pile of 1650 ms^{-1}. With a maximum penetration for this system being recorded at 40 ms TWT the use of an inappropriate velocity value will represent an underestimate of the absolute thickness by 3 m (*ie.* penetration of 30 m *vs* 33 m). As an absolute value this represents a small error and potentially well within many of the inherent procedural errors quoted to date, but as a relative value this represents a significant 9% depth error.

In addition to the calibration of seismic sequences, effective laboratory analysis of any lithological samples acquired from a surveyed area can provide a substantial source of corroborative information for the production of any environmental model. In particular the use of detailed grain size statistics and graphic representations can be used to supplement the gross morphological data obtained from the geophysical surveys. For example, the average grain size distributions derived for the four Loch Ainort lithological facies compare favourably with similar distributions identified from modern glaciomarine environments (Stravers *et al.*, 1992; See Discussion in Section 8.2.3.). This argument has to be somewhat tempered by the comments of Lindholm (1987) who suggests that the "....results [grain-size parameters as a guide to interpreting palaeo-environments] have been disappointing and disproportionately small relative to the effort expended". Indeed where it has been necessary to rely almost entirely up on sedimentological data within the Loch Ainort model, such as the interpretation of the General sedimentation processes within the loch inferences are somewhat suspect (See Section 8.2.3.1.).

In addition to the acquisition of *in situ* data, this thesis has attempted to emphasise the necessity for the effective use of detailed, on-land, geomorphological and geological (both solid and drift) data sets during phase 3 of seismo-stratigraphic analysis. For the nearshore environments such information may not only provide additional information pertinent to the interpretation of offshore seismic sequences (*eg.* the dismissal of a hard rock origin for the ridge features identified on both the side scan sonographs and the sub-bottom profiles; See Section 8.2.1.), but also facilitates the conversion of the seismic para-stratigraphy into a composite para-stratigraphy with an inferred absolute time-scale.

In the Loch Ainort model presented in Section 8.2. there is a wealth of evidence to justify the hypothesis that LASF1 and LASF3 represent Loch Lomond Readvance glacial activity on what are almost certainly pre-existing glacial and non-glacial sediments. On the basis of this interpretation it is then possible to place the rest of the stratigraphy in a Lateglacial to present chrono-stratigraphic sequence. The author does, however, recognise that such inferences can never replace the necessity of obtaining suitable *in situ* samples for absolute dating techniques. Further, it is important to re-iterate that one should be extremely careful when using land based studies as an additional dataset as interpretational objectivity may be lost and inductive rather than deductive reasoning applied.

8.3.5. MULTI-DISCIPLINARY SURVEYS

Having discussed in detail the performance of the four techniques deployed during the investigation of the Loch Ainort surveys it is necessary to surmise the success of this methodological approach. Unsurprisingly it is evident that the multi-disciplinary approach invoked by earlier scientists (*eg.* King, 1969; See Section 8.1.) is the most appropriate for the investigation of submerged glaciomarine environments. However, the detailed analysis presented here suggests for this approach to be effective considerable thought and consideration has to be undertaken during the pre-, syn- and post-survey stages. Prior to the start of any survey it is prudent to get an impression of the proposed survey area from extant data sets such as the Admiralty Chart series. Such information can help plan the structure of the survey, as they enable the identification of sites of potential interest *ie.* sills or ridge complexes within the system (depending up on the scale of the chart), overall water depths (useful for predicting appropriate towing depths), the location of any land based navigational stations if so required and most importantly the location of launching and landing sites.

The worked presented here though suggests that caution should be taken to avoid over interpretation of what may be a flawed data set. The Loch Ainort Admiralty Chart, as with many of those available for the western seaboard of Scotland, is in fact based on a

19th Century lead-line survey which has been shown to be incapable of both identifying small scale features indicative of palaeo-glaciomarine environments, and presenting reliable absolute data values. Further, the evidence from the sub-bottom profiles suggests that considerable post-glacial maximum fill results in the current bathymetry being a poor representation of the surface on which any glacier system may have sat. It is therefore suggested that one must be careful when interpreting the development of tidewater glaciers on the basis of such data sets alone.

In addition to the potentially erroneous ice volume calculations made by Ballentyne (See Section 8.3.4.), a further example of a potential mis-interpretations based on Admiralty Charts are the inferences made by Greene (1992). Greene attempted to identify both the controls on tidewater glaciers in Scottish sea lochs and the nature of the growth and decay of the Loch Lomond Stadial glaciers. From an analysis of the published literature concerning on land evidence for the glacial limits in a total of 25 Scottish sea lochs and the interpretation of Admiralty charts Greene concluded that:

i) "The geomorphological evidence for glacial stillstand locations in Scottish Sea lochs indicates that they coincide with pinning points, as do many other glacial limits."

ii) "Available evidence from Scottish sea lochs thus supports [a] pattern of slow glacial advance and rapid retreat [as proposed for Alaskan tidewater glaciers by Mercer, 1961]."

iii) these findings supported the hypothesis of Mann (1986) that "...the climatic change has little control over their [tidewater glaciers] short-term fluctuations." and further that "there were probably topographic thresholds which produced a stepped, episodic pattern of glacier growth and decay in response to smooth climatic forcing.".

Although Loch Ainort was not one of the 25 lochs identified from Greene's study[22] it is evident that the detailed results from this current survey contradict many of these points. Firstly evidence from both the isometric plot (See Figure 5.21.; Section 5.3.2.) and the

[22] The morphologically similar glacier occupying Loch Sligachan, 7 km to the north is actually referenced.

apex location of the sub-bottom ridges (See Figure 6.9.; Section 6.3.1.) suggest that the position of the Loch Lomond Readvance glacial maxima occurs approximately 1 km outside the nearest pinning point *ie.* the mouth of Loch Ainort. Further the presence of the ridge complex AR17[23] suggesting a subsequent stillstand position, which albeit spatially concurs with the on land limit of Benn (1990; See Section 8.2.1.), does not coincide with any identifiable topographic pinning points. It is interesting to note that the out of loch location of the Ainort readvance maxima does support Mercer's (1961) theory, quoted in Greene (1992), that "...in certain sea lochs, the maximum extent of ice cover during the L.L.S. may have been greater than is currently accepted.".

Secondly, the concentration of inferred push moraines (See Section 8.2.1.) in the "Mouth Region" suggests a fluctuating ice margin which underwent a retreat phase interrupted by one or two stillstand periods. This was followed by rapid climatic amelioration, the Deglacial Phase II of Benn (1990), resulting in the uninterrupted retreat and possibly the *in situ* stagnation of isolated ice bodies leading to the deposition of Seismic Sequence 2. This irregular pattern of retreat is not easily accountable by the proposed "....pattern of slow glacial advance and rapid retreat" described by Greene. However, this author does recognise this thesis has provided no evidence on the nature of the glacial advance phase.

Finally the correlation of the stepped retreat pattern, inferred from both terrestrial and submerged evidence, with the rapid climatic amelioration identified independently from ice cores (Bard *et al.* (1987) and Dansgaard *et al.* (1989); See Section 3.2.2.2.), suggests that ice decay was controlled, in Loch Ainort at least, by climatic change and not the presence of topographic thresholds. In fact all the evidence presented here suggests that during the latter part of the Loch Lomond Stadial climatic amelioration was far from smooth.

Having undertaken a preliminary but restricted review of extant datasets it is suggested that side scan sonar sonographs are obtained initially from the survey area. Due to the

---

[23] Ridge complex AR14, may also represent a secondary stillstand position see full discussion in Section 8.2..

wide swathe widths obtainable with this system large areas of the loch or sea bed can be imaged rapidly and at a high resolution. As with all the geophysical techniques described here, it is regarded as essential that they are operated in conjunction with as high accuracy positional techniques as available to the operators. Further traverse densities for such a particular survey should be chosen so as to facilitate at least a 50 m overlap between traces.

Following the acquisition and processing of the side scan sonar data to produce a pseudo-three-dimensional image of the loch bed it is suggested that sub-bottom profiles should be acquired in order to give the "fourth dimension". Again as high an accuracy position fixing system should be used, but on this occasion with the largest traverse density survey time will allow. With the systems deployed during this survey interference negates the possibility of deploying both the side-scan sonar and the sub-bottom profiler simultaneously. Modern technology does now enable the simultaneous acquisition of both datasets thus facilitating the correlation between seismic facies units identified from the two systems. It is however important to recognise that if dual-acquisition systems are deployed, real-time interpretation is desirable as the ideal traverse densities for the two techniques are still incompatible.

The results from this work suggest that high-frequency echosounding should ideally be restricted to very closely spaced surveys (5 - 10 m line spacing) of small but topographically irregular areas identified from the side scan sonographs. For instance a small scale, but high traverse density, survey of the "Mouth Region" would have provided invaluable quantitative data on the three-dimensional form of the glacial terminus ridge complex. The only exception to this proposed survey programme is the acquisition of a low traverse density echosounder survey for areas in which no Admiralty Chart or similar extant depth data set are available.

Having acquired the geophysical data this author considers it essential that complete seismo-stratigraphical analysis of the side scan sonographs, the sub-bottom profiles and the inclusion where appropriate the quantitative bathymetric data, is undertaken. The production of isometric plots, seismic para-stratigraphies and isopach diagrams enables the accurate location of lithological sampling sites so as to expediently utilise what is

frequently restricted sampling time. A discussion on the suitability of the gravity coring technique employed during this research is considered to be outwith the remit of this work. However, if short barrel (< 3 m) samplers are used, irrespective of the actual coring technique, the pre-identification of suitable sampling sites is considered by this author to be an essential pre-requisite. In addition to the *in situ* sampling this is also an appropriate point in the programme at which to fully undertake a desk based (or if necessary field) review of the terrestrial geology of the adjacent coastline and hinterland.

Finally on completion of the survey programme and the analysis of the retrieved sediment samples (See Section 8.3.4.) it is essential that the three phase procedure of seismo-stratigraphic analysis, as presented in Section 8.3.4., is adhered to. Consequently, the seismic para-stratigraphies, litho-stratigraphies and the final composite para-stratigraphy (complete with cross-referenced justification) for the area should all be presented separately.

8.4. A REVISED OFFSHORE PARA-STRATIGRAPHY FOR NORTH-WEST SCOTLAND

One of the primary objectives of this thesis was to:

> "To construct a seismic para-stratigraphy (based on all three seismic reflection techniques) for the chosen survey areas and to attempt to correlate this with the extant seismic para-stratigraphies developed for the western seaboard of the Scottish Highlands."

The outcome of this work suggests that it is no longer sufficient to present a mixture of description and interpretation under the title of a "seismic para-stratigraphy" as has been done by previous authors (See Section 1.2.2.). Indeed evidence has been presented in Section 8.3.3. to suggest that a true "seismic para-stratigraphy" represents only an intermediate stage in the production of a complete "composite para-stratigraphy". The former stratigraphy must still be retained and presented to the community as it represents

effectively a synthesis of the first stage interpretation of high-resolution seismic profiles. This is in fact of most benefit to the scientific community as, if constructed within the strict guidelines of the seismo-stratigraphic analysis technique (and using the correct nomenclature), it provides an objective description of the Sequences and facies units present within the area. The composite para-stratigraphy can then be presented as a subjective hypothesis which can be accepted or discarded by the reader depending up on the quality of the supporting evidence presented. This Section will therefore present both a seismic para-stratigraphy and a composite para-stratigraphy for the Loch Ainort Basin. Evidently, comparisons with the established "para-stratigraphies" will be made on the basis of the composite para-stratigraphy.

Table 8.3. (See Overleaf) represents the "seismic para-stratigraphy" constructed primarily on the basis of the sub-bottom profile data but with additional geophysical information being included from the side scan sonographs where appropriate. Individual features that are only imaged on the sonographs (*eg.* the alluvial fan and debris fan identified along the south-eastern shore: See Sections 8.2.3.2. and 8.2.3.3. respectively) have not been included within the seismic para-stratigraphy as they are considered too site specific. This stratigraphy has broad chronological significance but as has been detailed in Section 8.2. and 8.3.3. significant revisions have been made during the interpretational phase.

As discussed in Section 8.3.3. correlation of the seismic para-stratigraphy with the terrestrial stratigraphy and the information gleaned from lithological analysis of within loch samples resulted in the adaptation of the chronology of the para-stratigraphy. In particular, during this phase it was possible to resolve the inter-relationship between LASF1 and LASF2 and similarly LASF3 and LASF4. It is useful to note that the only adaptations that had to be made were on units where either an arbitrary boundary separated them (*eg.* that between LASF1 and LASF2 in the "Unnamed Strait") or that facies units were spatially remote. In the latter case correlation was possible only on the basis of the facies units relative association with their bounding facies units (*eg.* LASF4 and LASF5). It is probable that additional acoustic imagery within this or an adjacent area could have resolved these discrepancies at the facies analysis stage.

Seismic Sequence	*Seismic Facies Units*		
LASS4	**LASF7:** medium internal backscatter level and occasional weak, parallel, inclined internal reflectors with a high lateral continuity and extent. Upper surface characterised by medium to medium/light backscatter levels. Occasional small scale (1-10 m) linear, parallel, topographic highs with small amplitudes (< 1 m).	**LASF9:** acoustically transparent or displays a very low backscatter level, with no internal reflectors.	**LASF10:** low to medium internal backscatter with strong internal reflectors which are parallel, inclined and have a high lateral continuity.
	LASF6: low internal backscatter and occasional weak, parallel, inclined internal reflectors with a high lateral continuity and extent.	**LASF8:** medium to high internal backscatter, with a chaotic, acoustically turbid texture with weak but thick and continuous internal reflectors.	
LASS3	**LASF4:** low to medium internal backscatter, with thick strong, discontinuous, horizontal to gently inclined, internal reflectors of high lateral extent.	**LASF5:** medium internal backscatter and thick, strong, parallel, internal reflectors with great lateral continuity. Thin but clearly marked upper reflector.	
LASS2	**LASF3:** very high internal backscatter, with a mottled appearance and no discrete internal reflectors. Upper bounding reflector irregular and chaotic describing a subdued topography.		
LASS1	**LASF1:** very high internal backscatter, with no discrete internal reflectors and a distinctive mottled appearance. Pronounced upper surface describes marked topographic highs. Topographic highs correlates with large scale (10's - 100's m) linear positive targets, frequently with asymmetric slopes. Targets associated with large dark reflector material zones and concentrations of point reflector targets in axial locations.	**LASF2:** very high internal backscatter with no discrete internal reflectors and a distinctive mottled appearance. Upper boundary smooth, low relief, but laterally extensive.	

Table 8.3. A seismic para-stratigraphy for the Loch Ainort field area.

Table 8.4. (See Overleaf) represents the composite para-stratigraphy constructed for Loch Ainort. It was not felt necessary to name each sequence with a locationally spaced term instead the simple prefix CAS (Composite Ainort Sequence) has been utilised. Each sequence is presented with a short description of the known or proposed sediment types and an environmental interpretation. It should be noted that LASS4 has not been subdivided during this stage in to the two sequences representing fine grained paraglacial sedimentation and modern fjord sedimentation respectively. This is because there is neither seismic nor lithological evidence to support this hypothesis, the interpretation being based on what is regarded as being an anomalous accumulation rate calculation. Again it is necessary to re-iterate that due to the nature of the seismo-stratigraphic method it is always necessary to present a detailed justification of each inference made so this para-stratigraphy should never be presented in isolation.

Finally it is necessary to present a comparison between the "seismic para-stratigraphies" of previous authors (See Section 1.2.2.) and the composite para-stratigraphy constructed for the Loch Ainort region. As significant re-interpretation of the early para-stratigraphies has already been undertaken by subsequent authors and as they are primarily based on shelf deposits with minimal reference to Loch Lomond Stadial events emphasis shall be placed on the seismic para-stratigraphies of Boulton *et al.* (1981) and Davies *et al.* (1984). As can be seen from Table 8.5. (Overleaf) CAS1 is comparable to the Hebrides and Minches Formations of Boulton *et al.* and Davies *et al.*. Unfortunately, having only an inferred age for CAS1 this correlation cannot provide any additional evidence for the re-interpretation of Binns *et al.*'s (1974a and b) Seismic Sequence 1 as being related to pre-Devensian glacial activity (See Section 1.2.2.4.).

On the basis of seismo-stratigraphical position, reflector style and hypothesised mode of formation CAS2 is correlated with the Muck Formation (2a) of Boulton *et al.* and the Barra Formation of Davies *et al.* (See Section 8.2.2.). This correlation further brings in to question the attempt of Davies *et al.* to compare this unit with their own "Muck Member", part of the stratigraphically higher Jura Formation (See Discussion in Section 1.2.2.4.). It is worth noting that the absence of a correlative to the overlying Muck Formation (2b) (or Muck/Rhum Members) may suggest that a return to true marine

conditions in the Loch Ainort region during the interstadial period never occurred. Although negative evidence is always suspect this hypothesis may support the theory of Sutherland (1984) that total deglaciation did not occur. . However, due to the nature of

Composite Sequence	*Seismic Sequence or Facies Unit*	*Proposed Sediment Type*	*Environmental Interpretation*
CAS6	**LASS4**	A variety of sediment types dominated by MUD and SILT deposits with coarser deltaic and debris flow material in marginal positions	Represents transition from the final stages of paraglacial activity (fine grained sedimentation from valley head sediment laden meltwaters) to ambient fjordic sedimentation patterns.
CAS5	**LASF4**	Bimodal deposits with poorly sorted layers of ponded sandy muddy GRAVELS within a fine silt matrix	Periodic influxes of heterogeneous debris flows induced by extensive mass movement on the exposed poorly consolidated drift covered slopes of the Loch Ainort basin. Such paraglacial activity was initiated during initial stages of ice retreat and continued until stabilisation of the slopes during the early Flandrian.
CAS4	**LASS2**	Glacial Diamictons	*In situ* downwasting results in low "hummocky" relief and sporadic, small cross-valley ridge features composed of diamicton. This deglacial phase relates to rapid climatic amelioration during the end of the Loch Lomond Stadial and the beginning of the early Flandrian.
CAS3	**LASF1**	Glacial Diamictons	A combination of direct subglacial deposition of glacial till and the deformation of Dimlington Stadial diamictons, subsequent marine/glaciomarine deposits by overriding Loch Lomond Readvance ice. Maximal extent of ice advance characterised by closely spaced De Geer moraines suggesting initial phase of active retreat. At within loch positions retreat positions also identified.
CAS2	**LASF5**	Bimodal deposits with stratified but discontinuous layers of sandy muddy Gravels within a SILT or MUD matrix	Proglacial sedimentation, under the influence of a decreasing energy environment, in the form of either ice-proximal grounding line fan deposition, iceberg/sea ice fallout or a combination of the two, during the retreat phase of the Dimlington Stadial ice sheet.
CAS1	**LASF2**	Glacial Diamicton	Till deposited beneath a Dimlington Stadial (or potentially earlier) ice sheet.

Table 8.4. A composite para-stratigraphy for the Loch Ainort Field area.

Table 8.5. Comparison of the Loch Ainort composite para-stratigraphy with the "seismic para-stratigraphies" previosly constructed for North-West Scotland.

nature of the marked unconformable upper boundary to this sequence and the arguments for relatively low rates of accumulation during temperate conditions (See Section 8.2.3.1.) make it more probable that evidence for any true marine deposit would have been removed.

CAS3, CAS4 and CAS5 are all believed to be related to glacial activity during the Loch Lomond Stadial. Evidently, the limited attention paid to this period by Davies et al., makes correlation difficult. Indeed as these authors concentrated primarily on open sea shelf environments rather than on nearshore fjord systems (the notable exception being the Firth of Lorne) successful comparison between these sequences and the age equivalent Jura Formation is unlikely. This is also true of the earlier work of Binns *et al.* (1974a and b) and Bishop and Jones (1979). Conversely the data acquired in the sea-lochs Nevis and Ailort by Boulton *et al.* and the subsequent para-stratigraphy they created allows the most direct and accurate comparisons to be made. Comparison of Table 1.3. and Section 8.2.1. clearly shows the a good correlation between CAS3 and the Mallaig Formation, this sequence also being inferred to be the product of sub-glacial deformation under advancing Loch Lomond Readvance glaciers. Boulton *et al.* do not describe any sequence that exhibits properties comparable with CAS4. As this latter unit represents a change in style of subglacial deposition during the deglacial phase it is possible that these authors either failed to identify this change or the deglacial history of their field areas was simpler.

The seismic characteristics and stratigraphic location of CAS5 would suggest it represents a similar sequence to Boulton *et al.*'s "Seismic Sequence 4". Indeed the correlation is so good that it is suggested that it could be used to support the retention of "Seismic Sequence 4" stratigraphical position between the Mallaig and Arisaig Formations (See Discussions in Section 1.2.2.3. and 8.3.3.). However, it is difficult to comment up on the validity of the environmental interpretation for the sequence given by Boulton *et al.*. They suggest the sequence represents "proximal glaciomarine outwash" but present no evidence to support this hypothesis. These authors do in fact the describe the "closely spaced, irregular strong reflectors..... infill basins rather than drape the substratum" and the line interpretations they present show these reflectors to possess a

style indicative of sediment ponding. Obviously on the basis of stratigraphic style alone it would not be possible to reinterpret the mode of formation of this unit. However, there is sufficient evidence (or lack of it) to suggest a reappraisal of this formational hypothesis.

Finally, the upper sections CAS6 is evidently a correlative of the Davies et al.'s Lorne Formation and the Seismic Sequence 4 of Binns *et al.* (1974a and b) and Bishop and Jones (1979), *ie.* modern sedimentation processes. Of particular interest, however, is the similarity between the Arisaig Formation of Boulton et al. and the lower part of CAS6, namely LASF6 and LASF7. Both of these are interpreted as representing distal deposition of sediment laden meltwaters from the final stages of deglaciation. The major difference is the inferred age of deposition with the upper surface of the Arisaig Formation being dated as early Flandrian and representing a return to full marine conditions whereas CAS6 sedimentation is believed to have been initiated during this period. Without independent dating of either sequence it will not be possible to resolve this dichotomy. Albeit Davies et al. attempt to correlate the Arisaig Formation with their Arisaig and Sleat Members but yet again present no evidence to support this statement. These authors also have difficult in chronologically separating the individual members suffice to say that the top of the sequence is "placed somewhere in the Holocene". With the minimal nature of their descriptions of the acoustic properties of these sequences it is not possible to present any reasoned correlation. It can only be hypothesised that a correlative of the base of CAS6 occurs somewhere in the upper part of the Jura Formation.

CHAPTER 9

9. CONCLUSIONS

Over the last thirty years high resolution marine geophysical techniques have been deployed in a variety of both ancient and modern glacial environments. Despite the fact that the earliest workers recognised the importance of a multi-disciplinary approach, the majority of these studies have still been restricted to single system surveys, be they penetrative or non-penetrative systems. Similarly seismo-stratigraphic analysis, a theory originally proposed for the objective study of deep seismic profiles, has been available to high-resolution geophysicists. This technique, albeit requiring slight modification, provides a unifying framework in which the description and interpretation of raw seismic data can be placed. Only through the application of a strict analytical procedure is it truly possible for the science to develop and a constructive body of work to be produced. Yet the majority of authors have failed to adhere to any such procedure at all and have persisted in creating new nomenclatures and descriptive styles at every opportunity. The results of this work are therefore frequently presented as environmental models composed of an ad hoc mixture of data description and interpretation.

The aim of this project was therefore to critically assess the use of high resolution geophysical acquisition and seismo-stratigraphic analytical techniques for the investigation of submerged palaeo-glaciomarine environments. This has been achieved through the construction of a detailed palaeo-environmental model for a fjordic system off the north-western seaboard of the Scottish Highlands. The field site chosen was Loch Ainort on the eastern coast of the Isle of Skye. This presented itself as an ideal site in both operational and scientific terms. The combination of a well constrained late Quaternary history with a lack of information from any of the nearshore environments adjacent to the island provided an ideal test bed for this research. A detailed discussion of all the points raised has been presented in Chapter 8 so only a brief synthesis of the major results is given here.

The final palaeo-environmental model for Loch Ainort was produced by combining data acquired from three seismic devices (echosounder, side scan sonar and sub-bottom profiler) with *in situ* sediment samples and a synthesised account of the extant lithological datasets. During the course of this research it has been possible to identify the suitability of each of these techniques to the investigation of these palaeo-glaciomarine deposits. As a result recommendations have been made regarding the most effective way to undertake a multi-disciplinary investigation of what is a complex morphological and sedimentological environment. Particular emphasis has been placed on the modification of the seismo-stratigraphical analytical technique for use with any shallow penetration datasets. In addition, to the methodological assessment it has also been possible to provide additional new data to both our knowledge of the late Quaternary environment of north-west Scotland.

Bathymetric data is considered to be useful on two scales, firstly to provide a basic understanding of the gross morphology of any area. This information is useful for both the successful deployment of towed devices and the identification of areas of requiring more detailed survey work *eg.* topographic highs and lows or areas of rapid changes in relief. This information can be successfully gleaned from Admiralty charts or rapid broad scale surveys. The limitation of these datasets is their accuracy. Where either navigation is poor or traverse density is low it is not possible to use these charts as sources of reliable quantitative information. This is particularly true of glaciomarine environments as loch bed features may frequently have dimensions in the range of only 10's of metres which is outwith the accuracy of some of the navigation techniques and the majority of feasible traverse densities on a sea loch scale. Further, as has been identified in Loch Ainort tidewater glaciomarine environments can be characterised by large accumulations of paraglacial sediments, which may obscure pertinent features. Consequently inferences made for glacier form and dimensions purely on the basis of bathymetric data have to be considered suspect. In particular both the location of terminal tidewater front positions and maximum ice thicknesses can both be underestimated on the basis of this data alone.

Accurate bathymetric data should not, however, be dismissed as an impractical source of useful information. The simultaneous logging of high resolution (± 1 m) navigation data with high accuracy echosounders, will improve the quality of the raw depth data. Similarly by the use of helmsman packages it is possible to plan gridded surveys well in advance and to display them in real time so as to ensure complete coverage whilst in the field. The problem of traverse density is not as easy to reconcile as depth contouring is still a process of interpolation wether achieved by hand or computer package. A practical solution is to restrict the areas from which detailed quantitative information is required, so allowing a localised increase in traverse density. Targets for further research could be potentially identified from the rapid assessment of side scan sonar data either in the field or from a previous survey.

Side scan sonar imagery proved to be an ideal system for the investigation of this particular type of environment. The system was able to provide both material and topographic information from large areas of the loch bed during a very short survey period. As with the echosounder data navigational control is again important, however, as long as overlap between traverses is ensured it is possible to adequately locate features even with the poorest navigational systems. The resolution of the system was capable of identifying a large number of small scale features missed by the low traverse density echosounder runs. Isometric plots constructed from the pseudo-three dimensional sonographs provided more reliable qualitative information on target form than could be inferred from the interpolated bathymetric charts. The isometric plots also enabled the individual targets to be spatially located relative to both themselves and key terrestrial features thus aiding correlation.

Calibration of the material properties hypothesised from the sonographs with both the seismic facies units identified from the sub-bottom traces and the litho-facies calculated from surficial sediment samples was successful. It is possible to obtain quantitative information from the sonographs, including the new application of Low Tonal Colour Zones (LTCZ's) for the constraint of slopes angles and improved height estimates. Yet due to the number of

assumptions that have to be made when calculating dimensions from the simple standard equations, they should be regarded as relative estimates rather than reliable absolute values.

The third of the geophysical techniques, sub-bottom profiling, was evidently the most useful of the techniques as it provided an additional fourth dimension, time. On the basis of this work the 3.5 kHz system was capable of resolving a *c.* 20000 year stratigraphy in some detail, with the environmental changes related to two glacial to interglacial transitions being documented. It was also possible to resolve spatial variations in sedimentary style over an area of only a few kilometres. The lack of penetration and consequent identification of the bedrock reflector results in arbitrary lower boundaries having to be constructed for the basal sequences. However, the adoption of a lower frequency system to ensure penetration would inevitably have resulted in an undesirable loss of detail. Equally, subtle vertical and lateral changes in grain sizes did not provide sufficient acoustic impedance contrast to be imaged. Consequently there are inherent system constraints placed up on the use of these low frequency devices. As a narrow beam system this technique has similar operational inaccuracies, related to the quality of the navigational control and the traverse density, to the high frequency echosounder.

The most critical control on the successful use of high-resolution geophysical datasets is the appropriate use of both a standard nomenclature and a single unifying investigative framework for the objective description of seismic profiles from both penetrative and non-penetrative systems. The original analytical technique devised by Mitchum and Vail (1977) for the description of deep seismic sections has been adapted for use with shallow penetration, high resolution data. The basic subdivision into large scale seismic sequences and component seismic facies units on the basis of seismic sequence analysis and seismic facies analysis has been retained. For both analytical techniques the adoption of a standardised descriptive nomenclature is deemed essential. Contrary to previous work, the importance of adequately describing both bounding reflector morphology and the spatial distribution of both facies units and sequences, was shown to be vital. This latter procedure is considered particularly important for surveys in nearshore localities.

The identification of seismic sequences and seismic facies units enables the construction of a true seismic para-stratigraphy. This should represent a chronologically simple sequence of events defined purely on the basis of changing acoustic character. With a multi-disciplinary survey the inclusion of side scan sonar data in to the description for units that outcrop on the loch bed should always be included. On completion of the seismic para-stratigraphy an equivalent litho-stratigraphy should be established for the survey area. This should include data from cores obtained *in situ*, preferably taken at sites pre-determined by the seismic para-stratigraphy so optimising the opportunities for effective calibration. For nearshore environments it is imperative that either a detailed synthesis of extant terrestrial datasets are made or that independent onland mapping is undertaken. Under these circumstances it is important to ensure that these potentially more detailed datasets do not lead the interpretation of the offshore deposits but provide sources of independent evidence. Correlation with terrestrial data is particularly useful when there is an absence of any absolute dates from within the survey area, as established chrono-stratigraphies for the onshore sequence can be used to place the relative chronology of the seismic para-stratigraphy in to a regional context.

The final product of this three stage process is the production of, what is termed by this author, a composite para-stratigraphy. This represents a true multi-component interpretation but in order to be effective the details of the preliminary phases should always be presented or at least made available. This is particularly important as the chronostratigraphic relationships between on both facies and sequence scale may change between stages. Similarly, as the composite para-stratigraphy effectively represents a single or multiple hypothesis for environmental change it should always be supported by detailed and cross-referenced justification.

It is therefore evident from the detailed palaeo-environmental model presented for Loch Ainort that a fully integrated multi-disciplinary approach is ideal for the investigation of submerged glaciomarine environments, as long as the constraints proposed here are adhered

to. It is in fact proposed that these acquisition and analytical methodologies are in fact applicable to all nearshore environments.

In addition to the general methodological conclusions presented above it is also necessary to summarise the site specific information gleaned during this research project. It has been possible to propose a hypothesis for the evolution of the Ainort Basin since the Dimlington Stadial maximum. The sedimentary record in this area is dominated by a Loch Lomond Stadial readvance glacier that occupied the entire "Inner Loch" basin extending well into the "Mouth Region" and reaching a terminal position within 175 m of the western shore of Scalpay. This region is characterised by a series of closely spaced De Geer moraines believed to represent a fluctuating ice margin that moved in response to an initial phase of deglaciation (Deglacial Phase I). Within the loch the frequency of these cross-valley ridge systems decreases with three major stillstand/readvance positions being identified (two of these positions have no terrestrial correlatives). Towards the head of the loch hummocky moraine dominates the glacial sequence, this being inferred to represent *in situ* downwasting of stagnating ice in response to rapid climatic amelioration at the end of the stadial (Deglacial Phase II). This glacial stratigraphy correlates well with the detailed terrestrial evidence and in fact provides clear supporting evidence for a stepped mode of glacial retreat.

Within the "Inner Loch" the overlying sequences are dominated by paraglacial sedimentation. Firstly, by debris flow and turbidite deposits, induced by mass movement of the unstable drift covered slopes of the north-western shore. This process was initiated as the glacier retreated and exposed the slopes to the late Stadial - early Flandrian environment. As floral colonisation stabilised these slopes the influence of these bimodal deposits reduced and sedimentation was dominated by the settling out of fine material from sediment laden meltwaters emanating from remnant glacial ice at the head of the valley. Once the final remnants of ice had disappeared and the climate returned to true inter-stadial conditions modern fjord sedimentation patterns prevailed. This environmental transition complements the perceived development of Eastern Skye during this period, as hypothesised from the

terrestrial evidence. To the authors knowledge, however, this is the first time that such a detailed palaeo-environmental model has been produced for a Scottish sea loch.

On a process level this work has provided evidence to enable comment on theories for both sea-level fluctuation and glacial retreat. Firstly, current sea-level research in North-West Scotland is attempting to identify a cause for greater thicknesses of Dimlington Stadial and Loch Lomond Stadial ice. This they believe would account for the discrepancies between sea-level curves calculated from high-precision rebound models and constructed from the most recent *in situ* sampling. As stated above there is evidence to suggest that underestimates for ice volumes of loch glaciers are frequently made due to a lack of appreciation of post-glacial accumulation rates and the controls on terminal snout positions. Simple recalculations for the Ainort Basin and by extrapolation the Cuillin icefield, suggest a 20% and 10% underestimate in ice volume respectively. It is therefore considered that a reappraisal of selected offshore sites may be able to identify if the Loch Ainort environment and the associated mis-calculations is a common situation. Secondly, the location of terminal moraines and associated De Geer moraines towards the Scalpay shoreline and cross-valley ridges at within loch sites brings into question the importance of topographical pinning points to stillstand locations. None of these glacial features appear to be topographically controlled indeed the weight of both submarine and terrestrial evidence for the Loch Ainort region at least suggests that the style of ice decay was closely controlled by climatic change.

Finally, through the comparison of the composite para-stratigraphy constructed for the Loch Ainort basin with the supposed "seismic para-stratigraphies" of a number of previous authors working along the western seaboard of Scotland it is evident that a significant review of the available data should be undertaken. In simple terms adequate correlations can be made with the para-stratigraphies of both Boulton *et al.* (1981) and Davies *et al.* (1984). However, the questions raised by the clear discrepancies both between and within these earlier para-stratigraphies clearly emphasises the requirement for, or more accurately the

adherence to a standardised seismo-analytical framework. It is hoped that the work presented here will fulfil this requirement.

CHAPTER 10

10. REFERENCES

Aarseth, I., 1987. Seismic stratigraphy of Subrecent Ice-margin Outwash Deltas in Nordfjord, Norway. In: Nemec, W. (Ed.). Fan Deltas. Int. Symp. Abst., *Univ. Bergen*: 109-111.

Aaresth, I., Lønne, Ø and Giskødegaard, O, 1989. Submarine slides in glaciomarine sediments in some western Norwegian Fjords. *Mar. Geol.*, **88**: 1-21.

Al-Ansari, N.A. and McManus, J., 1980. A reinvestigation of the bathymetry of Loch Earn. *Scot. Geog. Mag.*, **96**: 105-113.

Amman, B. and Lotter, A.F., 1989. Late-Glacial radiocarbon- and Palyno-stratigraphy on the Swiss Plateau. *Boreas*, **18**: 109-126.

Anderson, F.W. and Dunham, K.C., 1966. The Geology of Northern Skye. *Mem. Geol. Surv. G.B.*.

Anderton, R., Bridges, P.H., Leeder, M.R. and Sellwood, B.W., 1979. A Dynamic Stratigraphy of the British Isles. A Study in Crustal Evolution. *George Allen & Unwin*, London: 301 pp.

Andrews, J.T., 1963. The cross-valley moraines of Rimrock and Isortoq river valleys, Baffin Island, N.W.T.: a descriptive analysis. *Geog. Bull.*, **19**: 49-77.

Andrews, J.T., 1985. Grain size characteristics of Quaternary sediments, Baffin Island region. In: Andrews, J.T. (Ed.). Quaternary environments: Eastern Canadian Arctic, Baffin Bay, and Western Greenland. *Allen and Unwin*, Boston: 124-153.

Anon., 1990. Tide Time and Distance Tables 1990. Dundee Port Authority, Dock Street, Dundee. *Munro & Co. Ltd.*, Glasgow: 192 pp.

Atkinson, T.C., Briffa, K.R. and Coope, G.R., 1987. Seasonal temperatures in Britain during the past 22,000 years, reconstructed using beetle remains. *Nature*, **325**: 587-593.

Axelsson, V., 1983. The use of X-ray radiographic methods in studying sedimentary properties and rate of sediment accumulation. *Hydrobiol.*, **103**: 65-69

Ballantyne, C.K., 1984. The Late Devensian periglaciation of upland Scotland. *Quat. Sci. Rev.*, **3**: 311-343.

Ballantyne, C.K., 1988. Ice-sheet moraines in southern Skye. *Scott. J. Geol.*, **24**: 301304.

Ballantyne, C.K., 1989. The Loch Lomond Readvance on the Isle of Skye, Scotland: Glacier Reconstruction and Palaeoclimatic Implications. *J. Quat. Sci.*, **4**: 95-108.

Ballantyne, C.K., 1990. The Late Quaternary glacial history of the Trotternish Escarpment, Isle of Skye, Scotland, and its implications for ice-sheet reconstruction. *Proc. Geol. Assoc.*, **101**: 171-186.

Ballantyne, C.K. and Benn, D.I., 1991. The glacial history of the Isle of Skye. In: Ballantyne, C.K., Benn, D.I., Lowe, J.J. and Walker, M.J.C. (Eds.). The Quaternary of the Isle of Skye: Field Guide. *Quat. Res. Assoc.*, Cambridge: 11-34.

Bally, A.W., 1987. Atlas of Seismic Stratigraphy, Volume 1. *AAPG Studies in Geology*, **27**. 124 pp.

Bard, E., Arnold, M., Maurice, P., Duprat, J., Moyes, J. and Duplessy, J., 1987. Retreat velocity of the North Atlantic polar front during the last deglaciation determined by ^{14}C accelerator mass spectrometry. *Nature*, **328**: 791-794.

Bearman, G., 1989. Waves, Tides and Shallow-water processes. *Open University, Oceanography Course Team*: 187 pp.

Beaudry, L.M. and Prichonnet, G., 1991. Late Glacial De Geer moraines with glaciofluvial sediment in the Chapais area, Québec (Canada). *Boreas*, **20**: 377-394.

Belderson, R.H., Kenyon, N.H., Stride, A.H. and Stubbs, A.R., 1972. Sonographs of the Seafloor. A Picture Atlas. *Elsevier*, Amsterdam: 183 pp.

Bell, B.R., 1984. The basic lavas of the Eastern Red Hills district, Isle of Skye. *Scott. J. Geol.*, **20**: 73-86.

Bell, B.R. and Harris, J.W., 1986. An excursion guide to the Geology of the Isle of Skye. *Geol. Soc. Glasgow*: 317 pp.

Bell, J.D., 1976. The Tertiary intrusive complex on the Isle of Skye. *Proc. Geol. Assoc.*, **87**: 247-271.

Bellaiche, G.V., Coutellier, M. and Droz, L., 1986. Seismic evidence of widespread mass transport deposits in the Rhône deep sea fan: their role in fan construction. *Mar. Geol.*, **71**: 327-340.

Ben-Avraham, Z., Shaliv, G. and Nur, A., 1986. Acoustic reflectivity and shallow sedimentary structures in the Sea of Galilee, Jordan Valley. *Mar. Geol.*, **70**: 175-189.

Benn, D.I., 1989. Debris transport by Loch Lomond Readvance glaciers in Northern Scotland: basin form and the within-valley asymmetry of lateral moraines. *J. Quat. Sci.*, **4**: 243-254.

Benn, D.I., 1990. Debris transport by Loch Lomond Readvance glaciers in Northern Scotland: basin form and the within-valley asymmetry of lateral moraines. Unpublished Ph.D. Thesis, *University of St. Andrews*.

Benn, D.I., 1991a. Glacial landforms and sediments on Skye. In: Ballantyne, C.K., Benn, D.I., Lowe, J.J. and Walker, M.J.C. (Eds.). The Quaternary of the Isle of Skye: Field Guide. *Quat. Res. Assoc.*, Cambridge: 35-67.

Benn, D.I., 1991b. Raised Shorelines on Skye. In: Ballantyne, C.K., Benn, D.I., Lowe, J.J. and Walker, M.J.C. (Eds.). The Quaternary of the Isle of Skye: Field Guide. *Quat. Res. Assoc.*, Cambridge: 90-97.

Benn, D.I., Lowe J.J. and Walker, M.J.C., 1992. Glacier response to climatic change during the Loch Lomond Stadial and early Flandrian: geomorphological and palynological evidence from the Isle of Skye, Scotland. *J. Quat. Sci.*, **7**: 125-144.

Bennett, M.R., 1994. Morphological evidence as a guide to deglaciation following the Loch Lomond Readvance: a review of research approaches and models. *Scot. Geog. Mag.*, **110**: pp 24-32.

Bennett, M.R. and Boulton, G.S., 1993. Deglaciation of the Younger Dryas or Loch Lomond Stadial ice-field in the northern Highlands, Scotland. *J. Quat. Sci.*, **8**: 133-145.

Binns, P.E., Harland, R. and Hughes, M.J., 1974a. Glacial and postglacial sedimentation in the Sea of the Hebrides. *Nature*, **248**: 751-754.

Binns, P.E., McQuillin, R. and Kenolty, N., 1974b. The Geology of the Sea of the Hebrides. *Rep. Inst. Geol. Sci.*, **73/14**: 43 pp.

Birse, E.L. and Dry, F.T., 1970. Soil Survey of Scotland. Assessment of climatic conditions in Scotland based on accumulated temperature and potential water deficit. *Macaulay Inst. Soil Res.*: 25 pp.

Bishop, P., 1975. The Palaeomagnetism of muddy sediment cores from the Inner Sound, Northwest Scotland, and the glacial and Post-glacial History of sedimentation in the area. *E.P.S.L.*, **27**: 51-56.

Bishop, P., 1977. Glacial and Post-glacial Sedimentation in the Minches, North-west Scotland. Unpublished Ph.D. Thesis, *University College, London.*

Bishop, P. and Jones, E.J.W., 1979. Patterns of Glacial and Post-Glacial Sedimentation in the Minches, North-West Scotland. In: Banner, F.T., Collins, M.B. and Massie, K.S. (Eds.). The North-West European Shelf Seas: the Sea Bed and the Sea in Motion 1. Geology and Sedimentology. *Elsevier Oceanography Series* **24A**, Oxford: 89-194.

Bishop, W.W. and Coope, G.R., 1977. Stratigraphical and faunal evidence for Lateglacial and early Flandrian environments in south-west Scotland. In: Gray, J.M. and Lowe, J.J. (Eds.). Studies in the Scottish Lateglacial Environment. *Pergamon*, Oxford: 61-88.

Booth, D.B., 1986. The formation of ice-marginal embankments into ice-dammed lakes in the eastern Puget Lowland, Washington, U.S.A., during the late Pleistocene. *Boreas*, **15**: 247-263

Boulton G.S., 1974. Processes and Patterns of Glacial Erosion. In: Coates, D.R. (Ed.). Glacial Geomorphology. *New York State Univ.*, Binghamton.

Boulton, G.S., 1986. Push-moraines and glacier-contact fans in marine and terrestrial environments. *Sedimentology*, **33**: 677-698.

Boulton, G.S. and Jones, A.S., 1975. Stability of temperate ice-caps and ice-sheets resting on beds of deformable sediment. *J. Glaciol.*, **24**: 29-43.

Boulton, G.S., Jones, A.S., Clayton, K.M. and Kenning, M.J., 1977. A British ice-sheet model and patterns of glacial erosion in Britain. In: Shotton, F.W. (Ed.). British Quaternary Studies: Recent advances. *Clarendon Press*, Oxford: 231- 246.

Boulton, G.S., Chroston, P.N. and Jarvis, J., 1981. A marine seismic study of late Quaternary sedimentation and inferred glacier fluctuations along western Inverness-shire, Scotland. *Boreas*, **10**: 39-51.

Boulton, G.S., Peacock, J.D. and Sutherland, D.G., 1991. Quaternary. In: Craig, G.Y. (Ed.). Geology of Scotland 3rd Edition. *Geol. Soc.*, London: 503-543.

Bowen, D.Q. and Sykes, G.A., 1988. Correlation of marine events and glaciations on the northeast Atlantic margin. *Phil. Trans. Roy. Soc. Lond.*, **B318**: 619-635.

Boyle, E.A. and Keigwin, L., 1987. North Atlantic thermohaline circulation during the past 20,000 years linked to high-latitude surface temperature. *Nature*, **330**: 35-40.

British Geological Survey, 1984. Kintail, Scotland Sheet 72 (W), Solid Edition. Natural Environment Research Council, © *Crown Copyright*:: 1:50000 Series.

Broecker, W.S. and Denton, G.H., 1989. The role of ocean-atmosphere reorganisations in glacial cycles. *Geochem. Cosmochim. Acta*, **53**: 2465-2501.

Broecker, W.S. and Denton, G.H., 1990. What Drives Glacial Cycles? *Sci. Am.*, **Jan**: 4350.

Bryant, R.S., 1975. Side Scan Sonar for Hydrography: An evaluation by the Canadian Hydrographic Service. *Int. Hydrograph. Rev.*, **52**: 43-56.

Canals, M., Catafau, E. and Serra, J., 1988. Sedimentary structure and seismic facies of the inner continental shelf north of the Ebro Delta (Northwestern Mediterranean Sea). *Cont. Shelf Res.*, **8**: 961-977.

Carlson, P.R., 1989. Seismic reflection characteristics of glacial and glacimarine sediment in the Gulf of Alaska and adjacent fjords. *Mar. Geol.*, **85**: 391-416.

Carlson, P.R., Powell, R.D. and Phillips, A.C., 1992. Submarine sedimentary features on a fjord delta front, Queen Inlet, Glacier Bay, Alaska. *Can. J. Earth Sci.*, **29**: 565-573.

Church, M. and Ryder, R.M., 1972. Paraglacial sedimentation: A consideration of fluvial processes conditioned by Glaciation. *Geol. Soc. Am.*, **83**: 3059-3072.

CLIMAP Project Members, 1981. Seasonal reconstruction of the Earth's surface at the last glacial maximum. *Geol. Soc. Am.; Map and Chart Series*, **136**.

Clough, C.T. and Harker, A., 1904. The geology of west-central Skye with Soay. *Mem. Geol. Surv. U.K.*.

Cook, D.O., 1982. Nearshore bedfrom patterns along Rhode Island from side-scan sonar surveys - discussion. *J. Sed. Pet.*, **52**: 677-679.

Dansgaard, W., White, J.W.C and Johnsen, S.J., 1989. The abrupt termination of the Younger Dryas climate event. *Nature*, **339**: 532-534.

Dardis, G.F., 1985. Genesis of Late Pleistocene cross-valley moraine ridges, south-central Ulster, Northern Ireland. *E.S.P.L.*, **10**: 483-495.

Davies, H.C., Dobson, M.R. and Whittington, R.J., 1984. A revised seismic stratigraphy for Quaternary deposits on the inner continental shelf west of Scotland between 55°30'N and 57°30'N. *Boreas*, **13**: 49-66.

Dawson, A.G., 1980. The Low Rock Platform in Western Scotland. *Proc. Geol. Assoc.*, **91**: 339-344.

Dawson, A.G., 1984. Quaternary Sea-level changes in Western Scotland. *Quat. Sci. Rev.*, **3**: 345-368.

Dawson, A.G., 1988. The Main Rock Platform (Main Lateglacial Shoreline) in Ardnamurchan and Moidart, western Scotland. *Scott. J. Geol.*, **24**: 163-174.

Dawson, A.G., 1989. Distribution and development of the Main Rock Platform, Western Scotland: Comment. *Scott. J. Geol.*, **25**: 227-231.

Dawson, A.G., 1992. Ice Age Earth: Late Quaternary geology and climate. *Routledge*, London: 293 pp.

Dawson, L.S., 1969. Memoirs of Hydrography. Part II (1830-1885). *Cornmarket Press*, London: 209 pp.

Denton, G.H. and Hughes, T.J., 1981. The last great ice sheets. *J. Wiley & Sons*, New York: 484 pp.

Derbyshire, E., 1974. The bathymetry of Jokulsarlon, southeast Iceland. *Geogr. J.*, **140**: 269-274.

D'Olier, B., 1979. Side-scan sonar and seismic reflection profiling. In: Dyer, E.K. (Ed.). Estuarine hydrography and sedimentation. Estuarine and brackish-water sciences association handbook. *Camdridge University Press*, Cambridge: 57-86.

Doodson, A and Warburg, S, 1941. Admiralty Manual of Tides. *H.M.S.O.*. London: 270 pp.

Dowdeswell, J.A. and Dowdeswell, E.K., 1989. Debris in icebergs and rates of glaci-marine sedimentation: observations from Spitsbergen and a simple model. *J. Geol.*, **97**: 221-231.

Drewry, D., 1986. Glacial Geologic Processes. *Edward Arnold*, London: 276 pp.

Duck, R.W. and McManus, J., 1985a. Short-term bathymetric changes in an ice-contact proglacial lake. *Norsk. geogr. Tidsskr.*, **39**: 39-45.

Duck, R.W. and McManus, J., 1985b. Bathymetric charts of ten Scottish Lochs. Tay Estuary Research Centre, Report No.9. *Dundee University*.

Duck, R.W. and McManus, J., 1985c. A sidescan sonar survey of a previously drawndown reservoir : a control experiment. *Int. J. Rem. Sens.*, **6**: 601-609.

Duck, R.W. and McManus, J., 1990. Uses of sidescan sonar in lakes and reservoirs. In: Price, D.G., (Ed.) Proc. Sixth Int. IAEG Congress. *Balkema*, Amsterdam: 1081-1085.

Duplessy, J., Delibrias, G., Turon, J.L., Pujol, C. and Duprat, J., 1981. Deglacial warming of the Northeastern Atlantic Ocean: correlation with the palaeoclimatic evolution of the European continent. *Palaeogeog., Palaeoclim., Palaeoecol.*, **35**: 121-144.

Duplessy, J.C., Shackleton, N.J., Fairbanks, R.G., Labeyrie, L., Oppo, D. and Kallel, N., 1988. Deepwater source variations during the last climatic cycle and their impact on the global deep-water circulation. *Palaeoceano.*, **3**: 343-360.

Edwards, A. and Sharples, F., 1991. Scottish Sea Lochs: A Catalogue. *Nature Conservancy Council/Dunstaffinage Marine Laboratory*: 151 pp.

Eilers, R.G., 1981. Water Content and Retention (Porosity). In: McKeague, J.A. (Ed.). Manual on soil sampling and methods of analysis. 2nd Ed. *Canadian Society of Soil Science*: 41-42.

Ellett, D.J. and Edwards, A., 1983. Oceanography and inshore hydrography of the Inner Hebrides. *Proc. Roy. Soc. Edinb.*, **83B**: 143-160.

Finckh, P., Kelts, K. and Lambert, A., 1984. Seismic stratigraphy and bedrock forms in perialpine lakes. *Geol. Soc. Am. Bull.*, **95**: 1118-1128.

Fish, J.P. and Carr, H.A., 1990. Sound Underwater Images. A Guide to the Generation and Interpretation of Side Scan Sonar Data. *Lower Cape Publications*, Orleans: pp 190.

Fish, J.P. and Klein, M., 1984. The Use of Reconnaissance Hydrographic Surveys for Establishment of Essential Navigation Bathymetric Data in the Third World Countries. In: *Papers of the 2nd International Hydrographic Technical Conference*.

Flemming, B.W., 1976. Side-scan sonar: A practical guide. *Int. Hydrograph. Rev*, **53**: 6591

Folk, R.L., 1980. Petrology of Sedimentary Rocks. *Hemphill*, Austin Texas: pp 225

Forbes, D.L., Boyd, R. and Shaw, J., 1991. Late Quaternary sedimentation and sea level changes on the inner Scotian Shelf. *Cont. Shelf Res.*, **11**: 1155-1179.

Gerken, B., 1974. New method for the reduction of soundings in the tidal area of the German Bight and in tidal flats, with the Outer Elbe serving as example. In: *14th Coastal Engineering Conference*, Vol II. Copenhagen, Denmark: 1009-1024.

Gilbert, R., 1985. Quaternary Glaciomarine Sedimentation Interpreted from Seismic Surveys of Fiords on Baffin Island, N.W.T.. *Arctic*, **38**: 271-280.

Gray, J.M., 1974. The Main Rock Platform of the Firth of Lorn, western Scotland. *Trans. Inst. Brit. Geog.*, **61**: 81-99.

Gray, J.M., 1978. Low-level shore platforms in the south-west Scottish Highlands: altitude, age and correlation. *Trans. Inst. Brit. Geog,.N.S.*, **3**: 151-164.

Gray, J.M., 1989. Distribution and development of the Main Rock Platform: Reply. *Scott. J. Geol.*, **25**: 233-238.

Gray, J.M. and Ivanovich, M., 1988. Age of the Main Rock Platform western Scotland. *Palaeogeog., Palaeoclim. Palaeoecol.*, **68**: 337-345.

Griffith, T.W. and Anderson, J.B., 1989. Climatic control of sedimentation in bays and fjords of the northern Antarctic Peninsula. *Mar. Geol.*, **85**: 181-204.

Greene, D., 1992. Topography and former Scottish tidewater glaciers. *Scott. Geog. Mag.*, **108**: 164-171.

Gustavson, T.C., 1975. Bathymetry and sediment distribution in proglacial Malaspina Lake, Alaska. *J. Sed. Pet.*, **45**: 450-461.

Hall, Rear-Admiral G.P.D., Hydrographer of the Navy, 1989. Admiralty Chart **2209**, Scotland - West Coast, Inner Sound, ©*Crown Copyright.*: 1:50000 Series.

Hamilton, E.L. and Bachman, R.T., 1982. Sound velocity and related properties of marine sediments. *J. Acoust. Soc. Am.*, **72**: 1891-1904.

Harker, A., 1901. Ice erosion in the Cuillin Skye. *Trans. Roy. Soc. Edin.*, **40**: 221-252.

Harvey, L.D.D., 1989. Modelling the Younger Dryas. *Quat. Sci. Rev.*, **8**: 137-149.

Hequette, A. and Hill, P.R., 1989. Late Quaternary seismic stratigraphy of the inner shelf seaward of the Tuktoyaktuk Peninsula, Canadian Beaufort Sea. *Can. J. Earth Sci.*, **26**: 1990-2002.

Holtedahl, H., 1989. Submarine end moraines and associated deposits off the south coast of Norway. *Mar. Geol.*, **88**: 23-48.

Howell, F.T., 1971. A continuous seismic profile survey of Windermere. *Geol. J.*, 7: 329-334.

Hutchinson, D.R., Ferrebee, W.M., Knebel, H.J. and Wold, R.J., 1981. The Sedimentary Framework of the Southern Basin of Lake George, New York. *Quat. Res.*, **15**: 44-61.

Jansen, J.H.F., 1976. Late Pleistocene and Holocene history of the northern North Sea, based on acoustic reflection records. *Neth. J. Sea Res.*, **10**: 1-43.

Johnson, T.C., 1980. Late-glacial and postglacial sedimentation in Lake Superior based on acoustic reflection records. *Quat. Res.*, **13**: 380-391.

Kearey, P. and Brooks, M., 1991. An Introduction to Geophysical Exploration (Second Edition). *Geoscience Texts, Blackwell Scientific Publications*: 254 pp.

Keckler, D., 1994. SURFER for Windows. Contouring and 3D Surface Mapping. *Golden Software, Inc.*, Colarado: 225 pp.

King, L.H., 1969. Submarine End Moraines and Associated Deposits on the Scotian Shelf. *Geol. Soc. Am. Bull.*, **80**: 83-96.

King, L.H. and Fader, G.B.J., 1986. Wisconsian glaciation of the Atlantic continental shelf of southeast Canda. *Geol. Surv. Can. Bull.*, **363**: 72 pp.

King, L.H., Rokoengen, K. and Gunleiksrud, T., 1987. Quaternary seismostratigraphy of the mid Norwegian Shelf 65° - 67°30'N - a till tongue stratigraphy. *IKU Publicat.*, **114**: 58 pp.

Kjemperud, A., 1986. Late Weichselian and Holocene shoreline displacement in the Trondheimsfjord area, central Norway. *Boreas*, **15**: 61-82.

Klein, M., 1985. Side Scan Sonar Record Interpretation. *Klein Associates Training Manual*: 150 pp.

Krumbein, W.C., and Sloss, L.L., 1963. Stratigraphy and Sedimentation. *Freeman*, San Francisco:

Larsen, E, Oddvar, L. and Follestad, B.A., 1991. Formation of De Geer moraines and implications for deglaciation dynamics. *J. Quat. Sci.*, **6**: 263-277.

Lambeck, K., 1993a. Glacial rebound of the British Isles - I. Preliminary model results. *Geophys. J. Int.*, **115**: 941-959.

Lambeck, K., 1993b. Glacial rebound of the British Isles - II. A high-resolution, high-precision model. *Geophys. J. Int.*, **115**: 960-990.

Lambeck, K., 1995. Late Devensian and Holocene shorelines of the British Isles and North Sea from models of glacio-hydro-isostatic rebound. *J. Geol. Soc. Lond.*, **152**: 437-448.

Landmesser, C.W., Johnson, T.C. and Wold, R.J., 1982. Seismic reflection study of recessional moraines beneath Lake Superior and their relationship to regional deglaciation. *Quat. Res.*, **17**: 173-190.

Larsen, E., Longva, O. and Follestad, B.A., 1991. Formation of De Geer moraines and implications for deglaciation dynamics. *J. Quat. Sci.*, **6**: 263-277.

Lawson, D.E., 1982. Mobilization, movement and deposition of active subaerial sediment flows, Matanuska Glacier, Alaska. *J. Geol.*, **90**: 279-300.

Le Bas, T., 1992. TOBI discovers World War II Shipwrecks. *NERC news.*, **April**: 3031.

Leeder, M.R., 1982. Sedimentology: Process and Product. *Unwin Hyman*, London: 344 pp.

Lindholm, R.C., 1987. A Practical Approach to Sedimentology *Allen & Unwin*. London: 276 pp.

Lineback, J.A., Gross, D.L. and Meyer, R.P., 1971. High-resolution Seismic Profiles and Gravity Cores in Southern Lake Michigan. *Illinois State Geol. Surv.*, Env. Geol. Notes, **54**.

Lisle, R.J., 1988. Geological Structures and Maps. A Practical Guide. *Pergamon Press*, Oxford: 150 pp.

Long, D. The Quaternary, 1991. Preliminary draft of the Malin-Hebrides Regional Report. Unpublished version, *B.G.S.*: 1-18.

Lord, J., 1991. The Physical Limnology of the Upper Glendevon Reservoir, Central Scotland. Unpublished Unergraduate Thesis, *University of St. Andrews.*

Lowe, J.J., 1991. Stratigraphic resolution and radiocarbon dating of Devensian Lateglacial sediments. In: Lowe, J.J. (Ed) Radiocarbon dating: Recent applications and future potential. *Quat. Proc.* **1**, QRA, Cambridge: 19-25.

Lowe, J.J. and Walker, M.J.C., 1984. Reconstructing Quaternary Environments. *Longman*, London: 389 pp.

Lowe, P.A., Duck, R.W. and McManus, J., 1991. A bathymetric reappraisal of Loch Muick, Aberdeenshire. *Scot. Geog. Mag.*, **107**: 110-115.

Lowe, P.A., 1992. The Seismic Investigation of Loch Lomond Glacier Limits: Evidence from Scottish Lochs. Unpublished Postgraduate Thesis, *University of St.Andrews*: 436 pp.

MacAulay, H.A. and Hobson, G.D., 1972. A seismic refraction survey of the North Okanagan and South Shuswap valleys. *Geol. Surv. Cand.*, Paper **72-8**, Part A: 1-8.

Manley, G., 1949. The snowline in Britain. *Geografisk. Ann.*, **31**: 179-193.

Manley, G., 1971. The mountain snows of Britain. *Weather*, **26**: 192-200.

Mann, D.H., 1986. Reliability of a fjord glacier's fluctuations for palaeoclimatic reconstructions. *Quat. Res.*, **25**: 10-14.

McCann, S.B., 1968. Raised shore platforms in the Western Isles of Scotland. In: Bowen, E.G., Carter, H. and Taylor, J.A. (Eds.). Geography at Aberystwyth. *Univ. of Wales Press*, Cardiff: 22-34.

McManus, J., 1985. Scottish Lochs: Physical and sedimentological investigations. *Forth Nat. and Hist.*, **7**: 22-29.

McManus, J. and Duck, R.W., 1983. Sidescan sonar recognition of subaqueous landforms in Loch Earn, Scotland. *Nature*, **303**: 161-162.

McQuillin, R. and Ardus, D.A., 1977. Exploring the geology of shelf seas. *Graham and Trotman*, London: 234 pp.

Mercer, J.H., 1961. The response of fjord glaciers to changes in the firn limit. *J. Glaciol.*, **10**: 850-858.

Milne, P.H., 1972. Hydrography of Scottish west coast sea lochs. *Marine Res.*, **3**. Dept. Agri. and Fish. for Scot.: pp 50.

Mitchum, R.M., Vail, P.R. and Sangree, J.B., 1977a. Stratigraphic interpretation of seismic reflection patterns in depositional sequences. In: Payton, C.E. (Ed.). Seismic-stratigraphy - applications to hydrocarbon exploration. *AAPG Mem.*, **26**: 117-133.

Mitchum, R.M., Vail, P.R. and Thompson, S. III., 1977b. Seismic stratigraphy and global changes of sea level: depositional sequence as a basic unit for stratigraphical analysis. In: Payton, C.E. (Ed.). Seismic-stratigraphy - applications to hydrocarbon exploration. *AAPG Mem.*, **26**: 53-62.

Mitchum, R.M. and Vail, P.R., 1977. In: Payton, C.E. (Ed.). Seismic-stratigraphy - applications to hydrocarbon exploration. *AAPG Mem.*, **26**:

Mix, A.C. and Ruddiman, W.F., 1985. Structure and timing of the last deglacition, oxygen-isotope. *J. Quat. Sci.*, **4**: 125-144.

Morang, A. and McMaster, R.L., 1980. Nearshore bedform patterns along Rhode Island from side-scan sonar surveys. *J. Sed. Pet.*, **50**: 831-839.

Mullins, H.T., Eyles, N. and Hinchey, E.J., 1990. Seismic reflection investigation of Kalamalka Lake: a "fiord lake" on the Interior Plateau of southern British Columbia. *Can. J. Earth Sci.*, **27**: 1225-1235.

Officer, C.B. , 1976. Physical Oceanography of Estuaries and Associated Coastal Waters. *Wiley*, New York.

Orheim, O, 1988. Glaciology, Hydrology and Glacial Geology around Jostedalsbreen. *Norsk Polarinstutt, Norwegian Water Resources & Energy Administration*: 46-56.

Orsi, T.H. and Dunn, D.A., 1991. Correlations between Sound Velocity and Related Properties of Glacio-marine Sediments: Barents Sea. *Geo-marine Letts.*, **11**: 79-83.

Peach, B.N., Horne, J., Woodward, H.B., Clough, C.T. and Harker, A., 1910. The geology of Glenelg, Lochalsh and south-east part of Skye. *Mem. Geol. Surv. U.K.*.

Peacock, J.D., 1970. Some aspects of the glacial geology of west Inverness-shire. *Geol. Surv. G.B. Bull.*, **33**: 43-56.

Peacock, J.D., 1981. Scottish Lateglacial marine deposits and their environmental signature. In: Neale, J. and Fenley, J. (Eds.). The Quaternary in Britain. *Pergamon Press*, Oxford: 222-236.

Pilcher, J.R., 1991. Radiocarbon Dating for the Quaternary Scientist. In: Lowe, J.J. (Ed.). Radiocarbon Dating: Recent Applications and Future Potential. *Quat. Proc.*, **1**: 27-33.

Piper, D.J.W., 1988. Glaciomarine sedimentation on the continental slope off eastern Canada. *Geosciences Canada*, **15**: 23-28.

Powell, R.D., 1981. A model for sedimentation by tidewater glaciers. *Ann. Glacio.*, **2**: 129-134.

Powell, R.D., 1984. Glacimarine processes and lithofacies modelling of ice shelf and temperate tidewater glacier sediments based on Quaternary examples. *Mar. Geol.*, **57**: 1-52.

Powell, R.D., 1990. Glacimarine processes at grounding-line fans and their growth to ice-contact deltas. In: Dowdeswell, J.A. and Scourse, J.D. (Ed.). Glacimarine Environments: Processes and Sediments. *Geol. Soc. Spec. Publ.*, **53**: 53-73.

Price, R.J., 1983.Scotland's Environment during the last 30000 years. *Scott. Academ. Press*, Edinburgh: 224 pp.

Prior, D.B., Wiseman Jr, Wm J. and Bryant, W.R., 1981. Submarine chutes on the slopes of fjord deltas. *Nature*, **290**: 326-328.

Prior, D.B. and Bornhold, B.D., 1989. Submarine sedimentation on a developing Holocene fan delta. *Sedimentology*, **36**: 1053-1076.

Ravenne, C., 1978. Étude Bibliographique des Publications d'Exxon Concernant L'Interpretation Stratigraphique que des Sections Sismiques. *Rev. I.F.P.*, **26**: 179pp.

Richards, A., 1969. Some aspects of the evolution of the coastline of north east Skye. *Scot. Geog. Mag.*, **85**: 122-131.

Richards, A., 1971. The evolution of marine cliffs and related landforms in the Inner Hebrides. Unpublished Postgraduate Thesis, *University of Wales.*

Rind, D., Peteet, D., Broecker, W., McIntyre, A. and Ruddiman, W., 1986. The impact of cold North Atlantic sea surface temperatures on climate: implications for the Younger Dryas cooling (11-10k). *Clim. Dyn.*, **1**: 3-33.

Robinson, M. and Ballantyne, C.K., 1979. Evidence for a glacial readvance pre-dating the Loch Lomond Advance in Wester Ross. *Scott. J. Geol.*, **15**: 271-277.

Rose, J., 1985. The Dimlington Stadial/Dimlington Chronozone: a proposal for naming the main glacial episode of the Late Devensian in Britain. *Boreas*, **14**: 225-230.

Ruddiman, W.F. and McIntyre, A., 1973. Time-transgressive deglacial retreat of Polar waters from the North Atlantic. *Quat. Res.*, **3**: 117-130.

Ruddiman, W.F. and McIntyre, A., 1981. The North Atlantic Ocean during the last deglaciation. *Palaeogeog., Palaeoclim., Palaeoecol.*, **35**: 121-144.

Ruddiman, W.F., Sancetta, C.D. and McIntyre, A., 1977. Glacial/Interglacial response rate of subpolar North Atlantic water to climatic change: the record in ocean sediments. *Phil. Trans. R. Soc.*, **B280**: 119-142.

Schafer, C.T., Cole, F.E. and Syvitski, J.P.M., 1989. Bio- and Lithofacies of modern sediments in Knight and Butte Inlets, British Columbia. *Palaios*, **4**: 107-126.

Shennan, I., 1992. Late Devensian and Holocene relative sea-level changes and crustal movements in western Scotland: new data to test old models. In: Berryman, K. (Ed.). Int.

Symposium on Diversity in Coastal Evolution in the Quaternary: Programme and Abstracts. *Geol. Soc. NZ. Misc. Publ.*, **65A**: 51.

Shennan, I., Innes, J.B., Long, A.J. and Zong, Y., 1993. Late Devensian and Holocene relative sea-level changes at Rumach, near Arisaig, northwest Scotland. *Norsk Geol. Tidss.*, **73**: 161-174.

Shennan, I., Innes, J.B., Long, A.J. and Zong, Y., 1994. Late Devensian and Holocene relative sea-level changes at Loch nan Eala, near Arisaig, northwest Scotland. *J. Quat. Sci.*, **9**: 261-283.

Sissons, J.B., 1974a. Late-glacial marine erosion in Scotland. *Boreas*, **3**: 41-48.

Sissons, J.B., 1974b. The Quaternary in Scotland: a review. *Scot. J. Geol.*, **10**: 311-337.

Sissons, J.B., 1977. The Loch Lomond Advance in southern Skye and some palaeoclimatic implications. *Scott. J. Geol.*, **13**: 23-36.

Sissons, J.B., 1979a. The Loch Lomond Stadial in the British Isles. *Nature*, **280**: 199-203.

Sissons, J.B., 1979b. Palaeoclimatic inferences from former glaciers in Scotland and the Lake District. *Nature*, **278**: 518-521.

Sissons, J.B., 1980. Palaeoclimatic inferences from former Loch Lomond Advance glaciers.In: Lowe, J.J., Gray, J.M. and Robinson, J.E. (Eds.). Studies in the Lateglacial of North-west Europe. *Pergamon Press*, Oxford: 31-43.

Sissons, J.B., 1981a. A former ice-dammed lake and associated glacier limits in the Achnasheen area, central Ross-shire. *Trans. Inst. Br. Geogr. N.S.* 7: 98-116.

Sissons, J.B., 1981b. The last Scottish ice-sheet: facts and speculative discussion. *Boreas*, **10**: 1-17.

Sissons, J.B., 1983a. Shorelines and isostasy in Scotland. In: Smith, D.E. and Dawson, A.G. (Eds.). Shorelines and Isostasy. *Academic Press*, London: 209-226.

Sissons, J.B., 1983b. The Quaternary geomorphology of the Inner Hebrides: a review and reassessment. *Proc. Geol. Assoc.*, **94**: 165-175.

Sissons, J.B. and Dawson, A.G., 1981. Former sea-levels and ice limits in part of Wester Ross, northwest Scotland. *Proc. Geol. Assoc.*, **92**: 115-124.

Sloss, L.L., 1963. Sequences in the cratonic interior of North America. *Geol. Soc. Am. Bull.*, **74**: 93-113.

Sly, P.G., 1981. Equipment and techniques for offshore survey and site investigations. *Can. Geotech. J.*, **18**: 230-249.

Speight, J.M., Skelhorn, R.R., Sloan, T. and Knaap, R.J., 1982. The dyke swarms of Scotland. In: Sutherland, D.S. (Ed.). Igneous Rocks of the British Isles. *John Wiley & Sons Ltd.*, London: 449-459.

Stewart, F.S. and Stoker, M.S., 1990. Problems Associated with Seismic Facies Analysis of Diamicton Dominated, Shelf Glacigenic Sequences. *Geo-Mar. Letts.*, **10**: 151-156.

Stoker, M.S., 1988. Pleistocene ice-proximal glaciomarine sediments in boreholes from the Hebrides Shelf and Wyville-Thomson Ridge, NW UK Continetal Shelf. *Scot. J. Geol.*, **24**: 249-262.

Stravers, J.A., Syvitski, J.P.M. and Praeg, D.B., 1992. Application of size sequence data to glacial-paraglacial sediment transport and sediment partitioning. In: Syvitski, J.P.M. (Ed.). Principles, methods and applications of particle size analysis. *Cambridge Univ. Press*: 368 pp.

Sutherland, D.G., 1984. The Quaternary deposits and landforms of Scotland and the neighbouring shelves: a review. *Quat. Sci. Rev.*, **3**: 157-254.

Sutherland, D.G., 1991. Loch Lomond stage ice cap limit. In: Craig, G.Y. (Ed.). Geology of Scotland 3rd Edition. *Geol. Soc.*, London: Figure 15.17, p.523.

Swan, D., Clayne, J.J. and Luternauer, 1979. Grain-size statistics II: Evaluation of grouped moment measures. *J. Sed. Pet.*, **49**: 487-500.

Syvitski, J.P.M., Burrell, D.C. and Skei, J.M., 1987. Fjords. Processes and Products. *Springer-Verlag*, New York Inc.: 379 pp.

Syvitski, J.P.M., 1989. On the deposition of sediment within glacier-influenced fjords: oceanographic controls. *Mar. Geol.*, **85**: 301-330.

Syvitski, J.P.M., 1991. Sediment deposition on glaciated continental shelves. *Cont. Shelf Res.*, **11**: 897-937.

Telford, W.M., Geldart, L.P., Sheriff, R.E. and Keys, D.A., 1976. Applied Geophysics. *Cambridge Univ. Press*, Cambridge.

T.E.R.C., 1991. Chart of the Upper Forth Estuary Alloa to Kincardine Bridge. Unpublished Bathymetric Chart, *Tay Estuary Research Centre*.

Thompson, J.E., 1931. Trigonometry For the Practical Man. *Routledge and Sons Ltd.*, London: 204 pp.

Vail, P.R., 1987. Seismic stratigraphy interpretation procedure. In Bally, A.W. (Ed.). Atlas of Seismic Stratigraphy, Volume 1. *AAPG Studies in Geology*, **27**.: 1-11.

Vail, P.R. and Mitchum, R.M., 1977. Seismic stratigraphy and global changes of sea level. In: Payton, C.E. (Ed.). Seismic-stratigraphy - applications to hydrocarbon exploration. *A.A.P.G. Mem.*, **26**: 145-163.

Vorren, T.O., Hald, M., Edvardsen, :M and Lind-Hansen, O.-W., 1983. Glacigenic sediments and sedimentary environments on continental shelves: General principles with a case study from the Norwegian shelf. In: Ehlers, J. (Ed.) Glacial deposits in the north-east Europe. *Balkema Publ.*; Rotterdam. 61-73.

Voulgaris, G. and Collins, M.B., 1991. Linear features on side-scan sonar images: An algorithm for the correction of angular distortion. *Mar. Geol.*, **96**: 187-190.

Walker, M.J.C., Ballantyne, C.K., Lowe, J.J. and Sutherland, D.G., 1988. A reinterpretation of the lateglacial environmental history of the Isle of Skye, Inner Hebrides, Scotland. *J. Quat. Sci.*, **3**: 135-146.

Walker, M.J.C. and Lowe, J.J., 1990. Reconstructing the environmental history of the last glacial-interglacial transition: evidence from the Isle of Skye, Inner Hebrides, Scotland. *Quat. Sci. Rev.*, **9**: 15-49.

Weaver, P.P.E. and Schultheiss, P.J., 1983. Detection of repenetration and sediment disturbance in open-barrel gravity cores. *J.Sed.Pet.*, **53**: 0649-0678.

Weaver, P.P.E. and Schultheiss, P.J., 1990. Current methods for obtaining, logging and splitting marine sediment cores. *Mar. Geophy. Res.*, **12**: 85-100.

Wentworth, C.K., 1922. A scale of grade and class terms for clastic sediments. *J. Geol.*, **30**: 377-92.

Werner, F., 1982. Nearshore bedfrom patterns along Rhode Island from side-scan sonar surveys - discussion. *J. Sed. Pet.*, **52**: 674-677.

von Weymarn, J. and Edwards, K.J., 1973. Interstadial site on the Island of Lewis, Scotland. *Nature*, **246**: 473-474.

Williams, S.J., 1982. Use of high resolution seismic reflection and side-scan sonar equipment for offshore surveys. *U.S. Army Corps of Engineers, Coastal Engineering Tech. Aid Rept. No.* **82-5**: 22 pp.

Wingfield, R.T.R., 1990. The origin of major incisions within the Pleistocene deposits of the North Sea. *Mar. Geol.*, : 31-52.

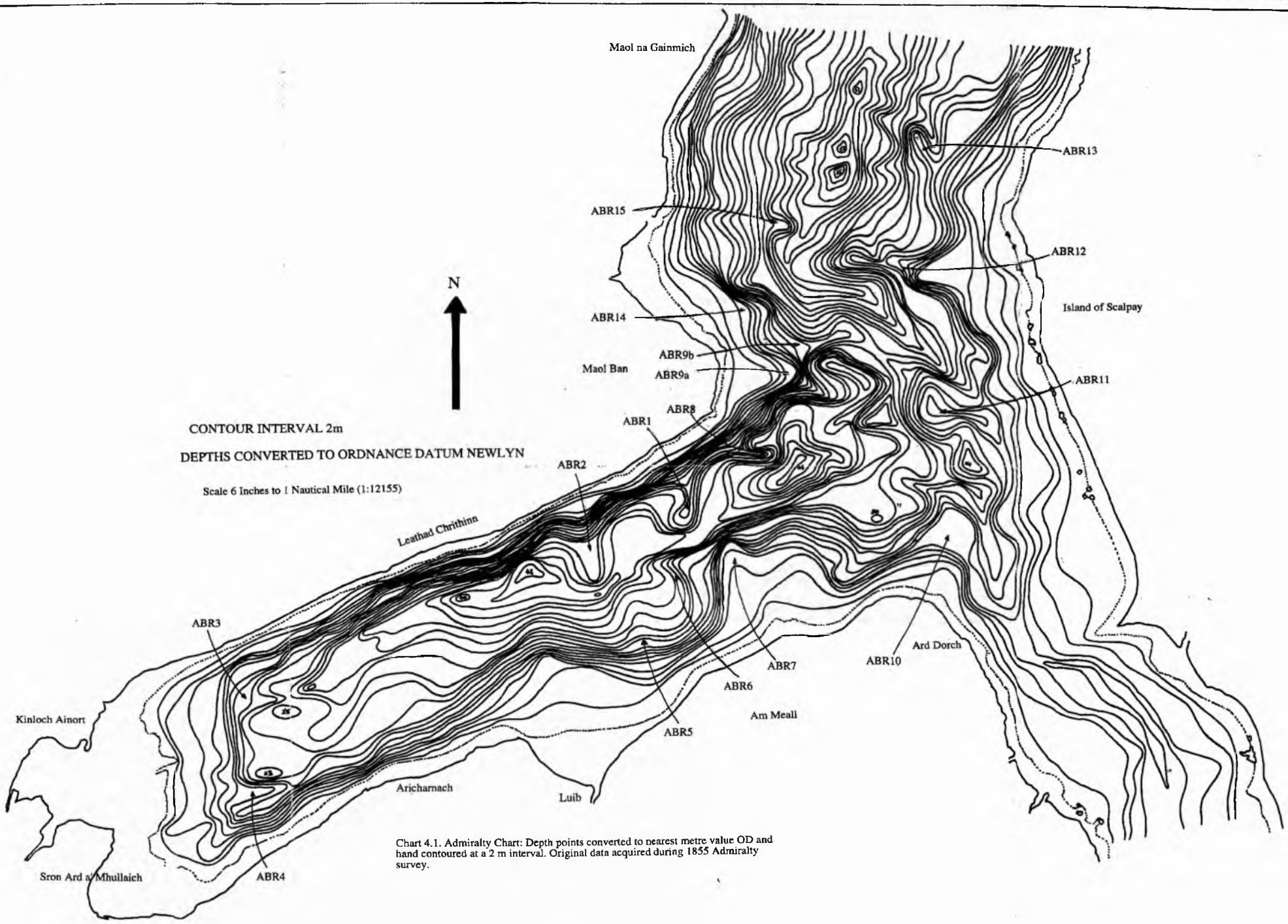

Chart 4.1. Admiralty Chart: Depth points converted to nearest metre value OD and hand contoured at a 2 m interval. Original data acquired during 1855 Admiralty survey.